# Brain Structural Correlates of Cognitive and Emotional Differences Comparing Youth With and Without An Asthma History in a Large Periadolescent Cohort

by

Claire M. Laubacher

A dissertation submitted in partial fulfillment of

the requirements for the degree of

Doctor of Philosophy

(Psychology)

at the

UNIVERSITY OF WISCONSIN-MADISON

2024

Date of final oral examination: 05/17/2024

The dissertation is approved by the following members of the Final Examination Committee:

Melissa Rosenkranz, Assistant Professor, Psychiatry, Center for Healthy Minds
John-Paul (JP) Yu, Assistant Professor, Neuroradiology
Lyn Abramson, Professor, Psychology
John J. Curtin, Professor, Psychology
James J. Li Associate Professor, Psychology

# ACKNOWLEDGMENTS

I would like to thank my committee members for their guidance and mentorship. I would like to thank Lyn Abramson, John J. Curtin, and James J. Li for challenging me and pushing me to grow both in class in outside of class. Your perspectives have each left a lasting mark on my scientific perspective.

I would especially like to thank Melissa Rosenkranz and JP Yu for finding me a new scientific home when I was not sure if I would still be able to pursue my dream. I would especially like to thank Melissa for introducing me to the world of contemplative science as well as psychoneuroimmunology and modeling that being an exceptionally rigorous scientist and bringing your true self to work can coexist.

I would like to thank Doug Dean, the members of the UW Center or High Throughput Computing and the members of the Center for Healthy Minds Research Support Core for technical support for their help with the challenging technical components of this project.
I would like to thank the members of the Rosenkranz group, particularly Estelle Higgins, for helping me to articulate my ideas more clearly. I would like to thank the members of the UW Medical Scientist Training Program, especially Chelsea Hanewall, for guiding me through this process. I thank Robin Goldman, Jennifer Conrad, Ellen-Cecil-Lemkin, and Thranh Ngo for helping me build the skills to persevere. I would also like to thank Hadley Rahrig, Emily Hamm, Monica Cho, Bo Peng, Erin Wiegert, Mary Clare Roche, Michelle Kendler-Kretch, Deanna Bennet, Kevin Bennet, Karl Laubacher, Mark Laubacher, and Martha Laubacher for always believing in me. I could not have done this without every one of you.

## ABSTRACT

The developmental trajectories of neural circuits that support cognitive and affective processes are involved in transdiagnostic psychopathology. Systemic inflammation can influence the development of this neurocircuitry. Interactions between brain structure and systemic inflammation are a potential mechanism by which youth with chronic inflammatory disease are at greater risk for poor neuropsychological outcomes. In youth with asthma, the most prevalent chronic childhood disease, there are well-documented increases in rates of anxiety and depressive disorders and lower academic achievement. To date, there has been no investigation of whether these cognitive and emotional changes are reflected in differences in brain structure between youth with and without an asthma history. These relationships are particularly important to understand in the transition to adolescence, a critical window of plasticity when the development of these circuits may be shifted.

The current project uses the peri-adolescent Adolescent Brain and Cognitive Development (ABCD) Study to examine associations between asthma history, cognitive function, psychological symptoms, brain morphology, and brain microstructure in the early adolescent period ($N$ = 6,488; ages 11 to 13 years old). Youth with an asthma history had lower language, memory, and executive functioning scores, and higher numbers of parent-reported total problems than their peers without an asthma history. Youth with an asthma history also had slower increases in memory scores from 9-11 to 11-13, which was more pronounced in youth with more lifetime asthma attacks. Youth with an asthma history had lower cortical thickness in important regions involved in sensing and regulating inflammation (anterior insula, anterior cingulate) and smaller subcortical volumes in structures related to memory and cognitive control

(caudate and hippocampus). These structural changes partially mediate cognitive differences between youth with and without an asthma history.

These findings support the idea that, in asthma, brain-related changes may contribute to differences in cognitive and emotional function, and they suggest that brain structural changes previously observed in adults with asthma may begin earlier in life. These data also highlight the importance of considering asthma as a systemic inflammatory condition and calls for future work to derive a mechanistic understanding of brain-immune interactions in youth with asthma.

TABLE OF CONTENTS

# LIST OF TABLES

# LIST OF FIGURES

# LIST OF ABBREVIATIONS

| | |
|---|---|
| ADHD | Attention-deficit/hyperactivity disorder |
| PET | Positron Emission Tomography |

# CHAPTER ONE: NEURAL CONSEQUENCES OF CHRONIC INFLAMMATION: IMPLICATIONS FOR PSYCHOPATHOLOGY IN YOUTH WITH ASTHMA

Adolescence is an important turning point for psychopathology risk across the life course. Worldwide, only 3% of mood disorders, psychotic disorders, and substance use disorders onset before age 14. This number triples between ages 14 and 18 (Solmi et al., 2022). One explanation for this timing is that certain cognitive and emotional skills that mature during late childhood and early adolescence are disrupted across a range of transdiagnostic mental health problems, including thought disorders (like psychotic disorders), internalizing disorders (like depression, anxiety, and PTSD) and externalizing behaviors (disinhibited, impulsive, and antagonistic behaviors; Beauchaine & Cicchetti, 2019; Caspi et al., 2014). These transdiagnostic cognitive and emotional skills, such as executive functions or affective control, depend on the maturation of a group of interdependent circuits in the adolescent brain. Therefore, alterations in the adolescent development of the circuits that support the acquisition of these skills (including the prefrontal cortex, the reward network, and the salience network) represent transdiagnostic risk factors for psychopathology.

The adolescent development of these interdependent neural circuits is especially sensitive to influences from life experience and the environment (Bilbo & Schwarz, 2009; Brenhouse & Schwarz, 2016; Casey et al., 2008; Thompson & Steinbeis, 2020). Perhaps the best known example of an environmental risk factor related to elevated transdiagnostic risk for psychopathology is chronic early life stress (Arnsten et al., 2014; Bilbo & Schwarz, 2009; Gunnar & Quevedo, 2007; Heleniak et al., 2016). Links between early life stress and adult psychopathology are related to changes in the function of the prefrontal cortex, the reward network, and the salience network (McLaughlin et al., 2019). In addition, early life stress

increases peripheral inflammation, and inflammation appears to play a significant role in many of the neural and behavioral consequences of early life stress (Bilbo & Schwarz, 2009; Brenhouse & Schwarz, 2016; Catale et al., 2020; Chiang et al., 2022). Indeed, several theories have proposed that elevated levels of pro-inflammatory markers partially *mediate* the relationship between brain structural or functional alterations and elevated risk of transdiagnostic psychopathology associated with early life stress (Bilbo & Schwarz, 2009; Nusslock et al., 2024). Further, experimental evidence shows that peripheral inflammatory signaling alone can alter circuit function including the prefrontal cortex, the reward network, and the salience network.

Exposure to chronic inflammation during development is an overlooked risk factor for transdiagnostic psychopathology. Because adolescence is a critical period of cognitive and emotional skill development and a period of heightened sensitivity to environmental influences in the prefrontal cortex, the reward network, and the salience network**,** youth with chronic inflammatory disease may be at increased risk of transdiagnostic psychopathology in part through alterations in these circuits.

As delineated in the review below, more research is needed to explore potential differences in brain structure and function in youth exposed to chronic inflammation and inflammatory disease that may correspond with an elevated risk for psychopathology. After a brief primer on relevant immune signaling, I will review key inflammation-sensitive regions of the brain that have been implicated in the adolescent acquisition of cognitive and emotional abilities related to the risk of transdiagnostic psychopathology. I will present evidence that the function of these regions is altered by elevated levels of circulating inflammatory markers, and that inflammation exposure is related to elevated risk for psychopathology. Finally, I will explore

the existing evidence that these inflammation-sensitive circuits may be vulnerable in youth exposed to chronic inflammatory disease, using the most prevalent chronic disease of childhood (i.e. asthma) as an example.

## An Immune System Primer: The Role of Circulating Cytokines

The immune system is generally divided into two branches: the innate immune system, which can respond to novel pathogens, and the adaptive immune system, which responds to antigens that have been encountered previously. The behavior of immune cells in both branches is governed by signaling molecules called cytokines, which are primarily released by other immune cells. Several cytokines are released by innate immune cells in response to a broad range of inflammatory stimuli including bacteria, viruses, injuries to the epithelium (e.g. wounds), tumors, and during autoimmune reactions. These include IL-1, IL-6, tumor necrosis factor (TNF-a), and interferon-alpha (INF-a). When these cytokines are released into systemic circulation, they trigger the production of proteins from the liver, notably C-reactive protein (CRP). Both cytokines and CRP increase in proportion to the intensity of the immune response (Markanday, 2015) and are measured in peripheral blood as an index systemic inflammation. I will be broadly referring to these domain-general inflammatory cytokines and CRP measured in serum as "circulating inflammatory markers."

## Neuroanatomy of Cognitive and Emotional Function in Adolescence

### The Prefrontal Cortex

During adolescence, the cortical maturation process that began in sensory-motor cortices in childhood reaches prefrontal areas (Moura et al., 2017). The structural and functional maturation of the prefrontal cortex and of cortical-subcortical circuits correspond to improvements in a broad group of abilities that have been conceptualized as cognitive control,

executive functioning, inhibitory control, emotion regulation, and affective control (Cohen et al., 2016; McLaughlin et al., 2015; Schweizer, Gotlib, et al., 2020). Although some of these skills can be dissociated, and have neuroanatomical correlates within distinct prefrontal subregions, they are interdependent and share important commonalities. All of these constructs include an ability to voluntarily engage attention to pursue goal-directed, future-oriented behavior and self-regulation even in the presence of competing, immediate goals, previously learned behaviors, or involuntary, reflexive responses. The disruption of the neurodevelopment underlying these broad processes is thought to be at the heart of commonalities between manifestations of psychopathology across the diagnostic spectrum that emerge in adolescence (Casey et al., 2008; Luna et al., 2010; Somerville and Casey, 2010; Somerville et al., 2010). In turn, better affective control, emotional regulation, and executive functioning in late childhood and early adolescence longitudinally predict better mental health outcomes across a range of internalizing and externalizing symptoms (McLaughlin et al., 2011; Schweizer, Gotlib, et al., 2020; Yang et al., 2022).

## The Immature Prefrontal Cortex Is Sensitive to Inflammation

Prefrontal cortical development is driven by experience-dependent dendritic pruning and experience-dependent myelination. Circuits become more efficient as active neurons refine their synaptic connections through dendritic pruning and increase the speed of signal transmission by myelinating axons. Both of these processes depend heavily on the function of a group of cells called microglia. Microglia (and astrocytes) are considered the brain's resident immune cells, and their function can be altered in response to peripheral inflammatory signals through a variety of mechanisms (Catale et al., 2020; Colonna & Butovsky, 2017; Schalbetter et al., n.d.; Schramm & Waisman, 2022; Woodburn et al., 2021). Adolescent dendritic pruning by microglia in the

prefrontal cortex is needed for normal cognitive development (B. L. Smith et al., 2020). Thus, the processes of experience-dependent synaptic pruning and experience-dependent myelination can be disrupted by early life inductions of peripheral inflammation (Brenhouse, 2023; Schalbetter et al., n.d.). For example, in a recent study, mice had a potent induction of the innate immune response shortly after birth (via lipopolysaccharide (LPS) injection). In responses to adolescent stress, the behavior of microglia changed in mice exposed to LPS. The microglia reduced their pruning of neuronal dendritic spines in response to adolescent stress, which was associated with depressive behaviors in response to stress. When microglia were deleted or chemically inhibited, the mice did not show depressive-like behaviors in response to adolescent stress (Cao et al., 2021).

Therefore, systemic immune activation has the ability to fundamentally alter the cellular processes that govern the maturation of the prefrontal cortex, which is necessary for a range of skills known to be related to the emergence of transdiagnostic psychopathology. There is still much to be learned about the complex ways in which the peripheral immune system communicates with the central nervous system. For instance, the degree to which the brain receives systemic immune signaling can be moderated by context. The permeability of the blood-brain barrier, and thus the degree to which microglia are exposed to circulating inflammatory signals, can be altered by, for instance, a history of repeated social defeat stress in rodents (Nusslock et al., 2024; Weber et al., 2017). This may help to explain why more intense or repeated immune activation may have more lasting effects on the brain than transient immune activation like childhood illnesses and infections. However, a full discussion of the diverse mechanisms of brain-immune signaling is beyond the scope of this review (Dantzer, 2018). These early examples illustrate that immune activation alone is sufficient to alter prefrontal

dendritic pruning during the sensitive adolescent period and that immune signaling may have a more fundamental role in regulating experience-dependent plasticity than is typically considered. Next, I will explore specific cortical-subcortical connections that mature during adolescence, that have been linked to immune-sensitivity and psychopathology more specifically in human studies.

Dopamine and Striatum-to-Prefrontal Connectivity

The connectivity between the ventral striatum and the medial prefrontal cortex specifically is often referred to as the core of the "reward network." The ventral striatum, also referred to as the nucleus accumbens, is a subcortical region that represents the value of reward (A. P. Chen et al., 2021). The ventral striatum is part of a larger group of structures called the basal ganglia that are critical for motivation and motor control, and whose function is closely associated with dopaminergic input from the midbrain. Traditionally, striatal areas have been studied in the context of reward processing, approach behavior, and externalizing psychopathology (like substance use disorders, impulsive behaviors; Beauchaine & Cicchetti, 2019). Both decreased reward sensitivity and increased reward sensitivity can be predictors of the onset and the disease course of unipolar and bipolar depression (Alloy et al., 2016) and have been related to schizophrenia and addiction risk (Nusslock & Alloy, 2017).

Maturation of the connectivity between the striatum and dorsolateral prefrontal cortex is critical for age-related increases in inhibitory control in the context of reward (Larsen et al., 2018). While both children and adults have the ability to accurately perform inhibitory control tasks, the consistency with which youth engage the prefrontal cortical activity needed for effective response inhibition improves over adolescence. In adolescence, whether the dorsolateral PFC will be engaged during inhibitory control is more dependent on the presence of a reward and more highly correlated with the activation of the nucleus accumbens than it is in

adults (For review, see Constantinidis and Luna, 2019). Structural maturation of prefrontal-striatal white matter is associated with age-related increases in performance improvement in the context of reward (Larsen et al., 2018).

Inflammation and the Striatum

Circulating inflammatory cytokines impact basal ganglia and cortical reward and motor circuitry in both animal models and human experiments (Felger, 2018). The most commonly studied transdiagnostic clinical correlate of inflammation-related changes in reward signaling is anhedonia, which is most prominent in mood and depressive disorders, but can also be prominent in schizophrenia (Zhang 2016) and PTSD (Mehta et al., 2020; Nawijn et al., 2015). In humans, decreased fMRI activation of the ventral striatum during a reward task has been observed after a single vaccine administration in healthy volunteers, as well as in patients chronically treated with IFN-alpha for chronic hepatitis C. Further, in the IFN-alpha-treated patients, decrease in reward-related activity in the ventral striatum was correlated with decreased motivation and increased fatigue (Capuron et al., 2012; Felger, 2018). Decreased activity in the ventral striatum in response to inflammation has been linked to a decrease in dopamine synthesis and turnover (Capuron et al., 2012; Felger, 2018; Nusslock et al., 2024). The connectivity of the ventral striatum and the medial prefrontal cortex has repeatedly been shown to be altered in a specific subset of patients with depression with CPR at clinically elevated levels ( > 3 mg/dL) (Felger, 2018). In a recent study, an acute challenge with a dopamine precursor compared to a placebo increased resting state functional connectivity between the ventral striatum and the ventromedial prefrontal cortex only in depressed patients with higher CRP and not patients with low CRP. The increase in functional connectivity was further associated with improvements in symptoms of anhedonia (Bekhbat et al., 2022).

Although classically, the most prominent feature of anhedonia in depression is a decreased experience of pleasure, the specific behavioral correlate of reduced dopaminergic signaling seems to be deficits in motivation. Inflammation-induced decreases in dopamine in the dorsal striatum are most specifically associated with reduced willingness to expend effort for monetary rewards (Boyle et al., 2019; Nusslock et al., 2024; Vichaya & Dantzer, 2018). Striatal dopamine is also critical to exert the cognitive effort required to correctly perform executive functioning tasks like working memory tasks (Westbrook et al., 2020). Notably, deficits in executive functioning are another core symptom of disorders characterized by anhedonia including major depressive disorder and schizophrenia (Snyder, 2013; Y. Zhu et al., 2019). Future work is needed to more directly investigate whether inflammation-related changes to dopamine availability are related to reduced executive functioning performance in individuals with high levels of circulating inflammatory markers.

The Salience Network

The amygdala, located in the medial temporal lobe, is closely connected to the cortical areas of the anterior insula and anterior cingulate cortex (ACC). In psychopathology research, these regions working together are often called the salience network, and are known for their role in fear, avoidance behavior, and internalizing disorders (anxiety, depression, PTSD; Beauchaine & Cicchetti, 2019).The anterior insula and ACC are involved in a diverse array of cognitive and emotional tasks including interoceptive awareness, emotion regulation, and cognitive control (Menon & D'Esposito, 2022; Seeley, 2019; Shackman et al., 2011). Notably, they have a role in both ascending perception of sensory information from the periphery–including information about both autonomic and immune functions–and descending regulation of these systems. Resting state connectivity between the amygdala and salience network increases during

adolescence, and increasingly stronger connectivity has been associated with higher levels of transdiagnostic psychopathology (Brieant et al., 2021; Poon et al., 2022). There is additional preliminary evidence that more difficulties with emotion regulation mediate the longitudinal relationship between increasing functional connectivity while viewing emotional images and increased psychopathology (Poon et al., 2022).

In cognitive neuroscience research, the anterior insula and ACC are often labeled the cingulo-opercular network, especially when they are involved in sustained attention during executive tasks. The labels “salience network” and “cingulo opercular network” are often used interchangeably. Notably, the anterior insula and ACC are more closely tied to executive function performance in inhibitory control and working memory tasks in youth than they are in adults (for review, see Constantinidis and Luna 2019). While the activity of most cortical networks becomes more segregated from age 10 to 26, the function of the anterior insula and anterior cingulate becomes increasingly integrated with other regions. The increased integration significantly moderates the age-related increase in inhibitory control task performance (Marek et al., 2015). Difficulties with inhibitory control or applying inhibitory control in the presence of emotional information (affective inhibitory control) are a feature of common impairing symptoms in a range of psychiatric conditions and can predict the emergence of future health problems. For example, in 11-14 year olds, better performance on an inhibitory control task in the presence of emotional information was 1) associated with fewer mental health difficulties, 2) associated with better self-reported emotion regulation, and 3) partially mediated slower longitudinal age-related increases in mental health problems in older adolescents (Schweizer, Gotlib, et al., 2020; Schweizer, Parker, et al., 2020).

Inflammation and the Salience Network

Many of the same human studies that show circulating inflammatory cytokines impact reward circuitry also show changes in these key salience network regions (Felger, 2018). When high levels of circulating inflammatory cytokines are experimentally induced in healthy humans (e.g. endotoxin or vaccination), there are consistent activity changes in the amygdala, insula, and anterior cingulate cortex (ACC) pre- to post-induction in PET and fMRI studies (for review see Felger 2019). This is also the case for patients with Hepatitis C who are chronically administered IFN-α (Goldsmith et al., 2023) as well as patients with asthma who are exposed to allergen challenge (Dill-McFarland et al., 2024; Rosenkranz et al., 2005, 2012, 2018; Rosenkranz, Esnault, et al., 2022). In animal studies, peripheral inflammatory stimuli increase amygdala activation, and this change in activity is associated with anxiety-like behaviors (Goldsmith et al., 2023; Munshi & Rosenkranz, 2018).

In human imaging work, there has been less precision in identifying behavioral changes associated with changes in anterior cingulate and anterior insula activity during inflammation. In inflammatory paradigms, salience network changes have been most studied in the context of anxiety symptoms (Labrenz et al., 2019) and depressed mood. While both acutely increased and amygdala activation in response to emotional stimuli has been related to increased depressive symptoms (Davies et al., 2021; Harrison et al., 2009), a failure to mobilize the cortical regions of the salience network in respond to inflammatory may be associated with negative mood. For example, in response to an experimentally induced immune challenge, healthy adults who reported the greatest decrease in mood showed the greatest reduction in functional connectivity between the right amygdala and subgenual ACC (Harrison et al., 2009). Within depressed adults, individuals with clinically elevated levels of serum CRP have been found to have reduced

response to reward anticipation in the insula (Burrows et al., 2021). It is possible that loss of coordination between the amygdala and prefrontal regions in the salience network is an important component of mood-related changes, but this is an active area of investigation.

Summary

In summary, patterns of adolescent brain maturation, particularly in cortico-striatal and salience network circuitry, support the development of executive functioning and emotion regulation capabilities (Baron Nelson et al., 2019). These circuits are sensitive to inflammation initiated in the periphery that can affect the behavior of brain microglia, which can disrupt cellular processes necessary for experience-dependent plasticity. Changes in these circuits and deficits in these functions are linked to the emergence of many adolescent- and adult-onset psychiatric disorders (Halse et al., 2022; Yang et al., 2022). It is further interesting to note that few studies have examined whether changes in "reward" and "threat" circuitry in the context of inflammation can occur independently or if they influence one another. There has also been limited research on the potential associated cognitive consequences of disrupting this "affective" circuitry. Particularly in the context of adolescent development, the interdependence or independence of these processes is important to assess. If exposure to inflammation affects whichever circuits are currently developing, this could result in different inflammation-related phenotypes depending on the timing of exposure. The sequential emergence of certain phenotypes could change strategies for screening at-risk youth as well as strategies for intervening as targeting a critical window of plasticity may be more viable targets for intervention.

## Are the Brains of Youth With Chronic Inflammatory Disease At High Risk?

### The Example of Asthma

In adults, elevated psychiatric symptoms and elevated levels of systemic inflammation often co-occur. A significant subpopulation of adult patients with a variety of psychiatric diagnoses show elevations in peripheral inflammatory cytokines and acute phases reactants, including major depressive disorder, generalized anxiety disorder, panic disorder, and post-traumatic stress (For review Felger et al., 2018). Further, there is elevated comorbidity between immune-mediated chronic diseases (including inflammatory bowel disease, rheumatoid arthritis, and asthma) and a variety of psychiatric conditions including depression, anxiety disorders, and bipolar disorder (Marrie & Bernstein, 2021). In these psychiatric populations, markers of elevated peripheral inflammation are related to both more severe symptoms and a higher likelihood of treatment resistance (For review see Felger et al.,2018). These core population-level observations motivate some of the proposed theories that elevated levels of proinflammatory markers mediate the elevated risk of transdiagnostic psychopathology associated with certain early environmental exposures (Beumer et al., 2012; Fagundes et al., 2013; Nusslock and Miller, 2016).

Similar patterns have been observed in youth. A recent meta-analysis of case-control studies of pediatric anxiety and depressive disorders found that in general, peripheral cytokine levels were elevated in youth with internalizing psychopathology (Howe & Lynch, 2022). There have been fewer investigations of cytokines in youth with other kinds of psychopathology, but these elevations may not be unique to internalizing disorders. In a recent meta-analysis of 8 case-control studies, youth with ADHD tended to show elevated levels of IL-6 and reduced levels of TNF-α compared to the healthy control group (Misiak et al., 2022). As for the other direction,

rates of psychopathology in youth with chronic inflammatory disease, most of the chronic inflammatory conditions that have been investigated within the neuroimmune network hypotheses onset in middle age. One exception is asthma, where most youth have symptoms of wheezing before 5 years old (Yang, 2013). It is also the most common chronic disease of childhood (G. F. Miller et al., 2016). In youth with asthma, depressive and anxiety disorders are observed at twice the rate of the general population (Dudeney et al., 2017; Y. Lu et al., 2012; Määttä et al., 2022), matching the elevated rates of these conditions in adults with asthma. Further, as a group, youth with asthma show signs of compromised executive functioning. Youth with asthma and similar allergic diseases have higher rates of inattentive symptoms and ADHD (Kaas et al., 2021) and lower levels of academic achievement (Irani et al., 2017).

There are also experimental animal models that suggest that chronic airway inflammation can lead to similar brain changes to those that have been induced in models with non-allergic inflammatory provocation. Early exposure to allergic inflammation can alter brain microglial behavior like more traditional inflammatory stimuli. For instance, early exposure to allergic inflammation can alter the morphology pruning ability of hippocampal microglia in mice (Saitoh et al., 2021). Notably, in this allergic-sensitization model, exposure to immune challenge was initiated with similar timing (within 2 days) in the same mouse line as the study where LPS exposure reduced microglial pruning of dendritic spines in the ACC and depressive behaviors in response to adolescent stress (Cao et al., 2021). Similarly, in an asthma-specific mouse model, exposure to bronchoconstriction in the adolescent period led to increased anxiety-like behaviors, changes in hippocampal gene expression, (Caulfield et al., 2017), and marginal changes in hippocampal microglia (Caulfield et al., 2021).

Finally, structural brain imaging in adults with asthma suggests that over the life course, asthma is related to accelerated degenerative brain structural changes, including in these critical fronto-striatal and salience network regions. In older adults, asthma is associated with an elevated risk of Alzheimer's disease (Bartels et al., 2024). Further, people with severe asthma have shown a stronger relationship between cognitive decline and common Alzheimer's disease risk factors like cardiovascular risk, genetic risk, and cerebral spinal fluid amyloid and tau markers (Nair et al., 2022). While all adults show some cognitive decline and decreases in brain integrity with aging, the relationship between older age and decreased white matter integrity has been shown to be stronger in people with asthma. In the same sample, with a mean age of 65 years, lower white matter integrity was also associated with accelerated cognitive decline in people with asthma, but not in health controls (Nair et al., 2023). However, there is also evidence that asthma-related changes in brain integrity may start even earlier in life. Evidence of negative relationships between asthma severity and brain integrity have been detected in a sample of participants with asthma ranged 25 to 66 years-old with a mean age of 44. Compared to healthy controls, participants with asthma had widespread decreases in white matter integrity across the brain. Greater asthma severity was associated with reduced white matter integrity specifically in tracts that link the prefrontal cortex and temporal lobe (important for salience network function), and fronto-parietal tracts critical for executive functioning. Greater asthma severity was also correlated with higher serum markers of neuroinflammation, glial fibrillary acidic protein (GFAP). Finally, in people with asthma, decreased white matter integrity was associated with slower cognitive processing speed. These results are consistent with the possibility that asthma is related to accelerated brain degeneration, that the acerated degeneration is related to inflammatory processes, and that the neuroimaging findings have relevance for functional

outcomes in people with asthma (Rosenkranz, Dean, et al., 2022). If these changes are widespread at age 44, the question becomes, how young do these changes start, given asthma often onsets before 10 years old?

Adolescence as an Ideal Time to Shift Trajectories

Developing mental disorders in adolescence compared to later in life is associated with increased disease severity, increased treatment resistance, and increased morbidity (Copeland et al., 2015; Kessler et al., 2005; Ravens-Sieberer et al., 2015). Related problems with executive functioning are also related to reduced educational attainment (Cortés Pascual et al., 2019; Deer et al., 2020; Usán Supervía & Quílez Robres, 2021) and lower quality of life in adulthood (Davis et al., 2010). However, increased prefrontal plasticity in adolescence has led some to theorize that this may be a unique window when intervention can shift life course trajectories in a more positive direction.

The structural brain changes observed in adults with asthma are very likely to be multifactorial (Kroll & Ritz, 2023) and not exclusively related to elevated levels of circulating inflammatory cytokines. However, given that uncontrolled airway inflammation is associated with systemic inflammation including elevated levels of circulating cytokines (Tattersall et al., 2024), if these systemic inflammatory processes contribute to brain dysfunction, youth with asthma are often more highly exposed, especially adolescents. Indeed, asthma morbidity often increases during adolescence as treatment adherence decreases when primary responsibility for medical care transitions from caregivers to youth (Kaplan & Price, 2020). Asthma affects 1 of every 12 youth aged 12 to 14, 40% of whom have uncontrolled disease, which suggests they are exposed to higher levels of airway inflammation (AsthmaStats Uncontrolled Asthma among

Children, 2012–2014). Indeed, it has been estimated that only ~50% of youth are taking medication as prescribed (Kaplan & Price, 2020).

Because youth with uncontrolled asthma may be exposing sensitive circuitry to elevated inflammation at a critical age, uncontrolled asthma may be contributing to higher risk of psychopathology emerging earlier in life. If there is indeed a relationship between asthma control and brain structural integrity in youth, achieving better asthma control may support the normal acquisition of important cognitive and emotional skills and decrease the risk of developing early onset psychopathology. Tantalizingly, better early disease control may even protect the brain from accelerated aging. Preventing psychopathology in youth can have cascading positive consequences throughout the life course. Therefore, it is important to identify whether elevations of psychopathology in youth with asthma are related to the asthma disease process and associated brain changes. Given the important role that motivation plays in medication adherence in adolescent asthma management, identifying and disseminating information about the connection between disease control and brain health has the potential for a wide reaching public health impact (Kaplan & Price, 2020).

# CHAPTER TWO: DIFFERENCES IN COGNITIVE AND EMOTIONAL FUNCTION BETWEEN YOUTH WITH AND WITHOUT ASTHMA IN A LARGE PERIADOLESCENT COHORT

## Introduction

Chronic inflammatory disease is a common comorbidity for several debilitating brain-related conditions, including major depressive disorder and Alzheimer's disease (Marrie & Bernstein, 2021; Newcombe et al., 2018). For instance, asthma is associated with an elevated risk of both of these problems (Bartels et al., 2024; Z. Lu et al., 2018) and, further, more severe asthma is associated with more severe depression and more severe neurodegeneration (Nair et al., 2023; Rosenkranz, Dean, et al., 2022). While chronic inflammatory disease is often synonymous with aging, the association between chronic inflammation and difficulties with cognitive and emotional functioning are evident much earlier in life. Because two-thirds of adults with asthma first have symptoms as children (Trivedi & Denton, 2019), it is possible that the neurobiological and behavioral alterations observed in adults with asthma begin in childhood.

Youth with asthma are at an increased risk for depression (Y. Lu et al., 2012; Z. Lu et al., 2018), anxiety disorders (Dudeney et al., 2017; Y. Lu et al., 2012), ADHD (Kaas et al., 2021), inattentive symptoms (Chuang et al., 2022), lower academic achievement, and problems with language, memory, and executive functioning (Irani et al., 2017). If the development of normal cognitive and emotional function early in life provides some protection from conditions like depression or Alzheimer's disease, understanding the biopsychosocial processes that underpin the link between asthma and altered cognitive and emotional function in youth may provide an opportunity to reduce the long-term increased risk for these conditions in adults with asthma. This has the potential to have a substantial public health impact as youth with asthma represent a

substantial portion of the population, with 9.9% of youth reporting an asthma diagnosis at some point before age 18 (CDC asthma fast stats). Adolescence specifically is a period when youth experience rapid gains in complex cognitive abilities, including increases in working memory, executive function, and emotional regulation skills (Cohen et al., 2016; McLaughlin et al., 2015; Schweizer, Gotlib, et al., 2020). The development of these skills is sensitive to environmental influences (Bilbo & Schwarz, 2009; Brenhouse & Schwarz, 2016; Casey et al., 2008; Thompson & Steinbeis, 2020) and having low levels of skills increases the risk of developing mental health problems in adolescence (McLaughlin et al., 2011; Schweizer, Gotlib, et al., 2020; Yang et al., 2022). Further, characterizing alterations in cognitive and emotional function in youth with asthma is important for developing strategies to support this vulnerable population.

Although several meta-analyses suggest youth with asthma are at a heightened risk for a range of poor cognitive and emotional outcomes, important gaps remain. Of the few prior studies of asthma and cognition that include more than 30 children with asthma and a comparison group unaffected by asthma, most used global assessments of academic achievement and included youth across a 5 to 10 year age span (Mitchell et al., 2022; Senter et al., 2021). This large age range and non-specific performance metric make it difficult to identify any specific underlying cognitive functions that may be affected or the developmental window when they may arise. Further, most of the existing studies of difficulties in psychological functioning among youth with chronic illness have either been in small samples with poor generalizability or have examined the relative risk of specific diagnoses in youth with and without asthma (Määttä et al., 2022). However, it is unclear to what extent the increased risk in youth with asthma for depression (Y. Lu et al., 2012; Z. Lu et al., 2018), anxiety disorders (Dudeney et al., 2017; Y. Lu et al., 2012), ADHD (Kaas et al., 2021), and future schizophrenia and bipolar disorder (Wu et al.,

2019, p. 201) stem from shared or independent alterations in cognitive and emotional processes. Given that both asthma and the associated mental health conditions have a large amount of heterogeneity in both symptom expression and underlying biopsychosocial drivers, it is unlikely that all youth diagnosed with asthma are at equally increased risk for all associated conditions. Further, although they are often studied independently, cognition and emotion fundamentally influence one another throughout development (Donati et al., 2021). Externalizing problems, internalizing problems, and cognitive ability each longitudinally predict changes in one another throughout childhood into early adolescence (Flouri et al., 2019). Instead of looking at the associations between asthma and a variety of specific mental health conditions, it would be more useful to understand the underlying cognitive and emotional processes that differ in youth with asthma that increase risk for specific comorbidities. Elucidating the relationship between dimensions of cognitive and emotional functioning and individual-level clinical asthma characteristics is a critical next step towards an understanding of the biopsychosocial systems that underpin these relationships.

Specifically, the age of onset, severity, and degree of control over asthma symptoms may be critical moderators of the relationships between asthma and negative cognitive and emotional outcomes. While some studies have detected a greater number of cognitive or emotional problems in youth with asthma as early as preschool (Husain et al., 2024), others have only seen differences emerge after middle childhood. For instance, a large Finnish study found that a diagnosis of atopic dermatitis, allergic rhinitis, and/or asthma at 7 years old was related to higher risk of internalizing problems, somatic complaints, and delinquent behaviors at 16 years old, but only youth who developed chronic disease after age 7 had higher risk of depression-related problems (Määttä et al., 2022). An increased risk of bipolar disorder was only detected in youth

hospitalized for asthma after 11 years old (Wu et al., 2019). These findings suggest that the increased risk of severe asthma on poor mental health outcomes may depend on the age that youth develop severe asthma. Asthma-related differences in school performance at 15–16 years old were not evident at 12-14 years old (Lundholm et al., 2020). Additionally, both asthma severity and asthma control appear to be important moderator of the relationship between asthma and cognition. For example, a recent large Swedish population-based cohort study found that overall, youth with asthma had slightly better school performance than youth without asthma. The degree of uncontrolled asthma, regardless of severity, was associated with worse school performance, above and beyond a sibling comparison for unmeasured environmental factors (Lundholm et al., 2020). Failure to measure severity or control may also explain why not all studies find consistent differences in cognitive function between youth with and without asthma (Cohen et al., 2016). Indeed, a recent meta-analysis of cognitive function in asthma noted that only 7 of 18 existing studies included information related to severity (Irani et al., 2017).

Higher activity of certain inflammatory pathways may help to explain why more uncontrolled asthma symptoms are associated with greater differences in cognitive and emotional function. Asthma severity and asthma control are also integrally tied to peripheral inflammation as more severe asthma and uncontrolled asthma are both related to elevated levels of inflammatory markers in the lung. These findings are accompanied by animal models that show chronic peripheral inflammation can influence brain structure and behavior (Caulfield et al., 2017; Dantzer, 2018). Understanding the specific role of chronic peripheral inflammation would be useful to monitor and, ultimately, prevent the increased risk for comorbidities. However, only a few small clinical studies have examined how asthma-related inflammatory

markers may be related to differences in cognitive or emotional outcomes in youth (Ehrlich et al., 2015; Kang et al., 1997).

The current investigation will examine the relationship between characteristics of asthma (asthma history, asthma severity, and peripheral inflammation) and cognitive and emotional function in the longitudinal, United States, peri-adolescent community sample, the Adolescent Brain Cognitive Development (ABCD) Study. Youth were recruited between 9 and 11 years-old and will be assessed every two years for a decade. I will compare cognitive and emotional functioning in youth with an asthma history to youth with no asthma history. I hypothesize that I will see elevations in inattentive, anxiety, and depressive symptoms, as well as lower levels of executive functioning in youth with, relative to youth without, an asthma history. While I focus on the year-two follow-up data (ages 11-13), I will also examine group differences in longitudinal trends in these metrics from baseline to year-two follow-up. Additionally, I will examine how these metrics are influenced by asthma-related moderators, including asthma severity and markers of peripheral inflammation. I hypothesize that gaps in cognitive and emotional performance between youth with and without asthma will be exacerbated in youth with higher asthma severity and in youth with greater elevations in peripheral inflammatory markers. Examining the relationship between markers of candidate biopsychosocial mechanisms and dimensional cognitive and emotional outcomes in youth with asthma will advance our ability to address the risk for negative outcomes in this vulnerable population.

## Methods

### Population

The Adolescent Brain Cognitive Development (ABCD) Study is a 21-site, nationally representative sample (Garavan et al., 2018) that recruited 10,000 9- and 10-year-olds between

2016 and 2018 with plans for a 10 years follow up. The ABCD 4.0 dataset includes longitudinal data from baseline (when youth are 9-11 years old), a year-1, year-2, and partially released year-3 follow up data. Participants were not enrolled if they had a major medical or neurological condition, a gestational age < 28 weeks, a history of traumatic brain injury, or a current diagnosis of schizophrenia, moderate to severe autism spectrum disorder, intellectual disability, substance use disorder, or alcohol use disorder (Garavan et al., 2018). Additionally, participants were not included in the analyses reported here if they endorsed history of one of the following health issues at any point during the study: brain injury, knocked unconscious, cancer, cerebral palsy, diabetes, epilepsy, seizure disorder, kidney disease, lead poisoning, muscular dystrophy, multiple sclerosis, heart problems, or sickle cell disease.

Additionally, youth who did not meet criteria for having a history of asthma (described below) were excluded if they were missing medical history either at baseline or at the 2-year follow up. Finally, youth who did not otherwise meet criteria for an asthma history but did meet either of two criteria for an ambiguous inflammatory disease status were excluded. Youth were excluded if they had biomarkers consistent with elevated inflammation (absolute eosinophil count > 500 cells per cubic millimeter or neutrophil to lymphocyte ratio (NLR) > 3). Youth who were taking leukotriene receptor antagonists (a medication that can be prescribed for asthma and allergies) and no other asthma medication (e.g. beta-agonist rescue inhaler) were also excluded.

Asthma History Classification

Parents reported on their child's medical history during baseline, 1-year follow up, and 2-year follow up time points. Youth were classified as having an asthma history if they met one of the following criteria: child had seen a doctor for asthma during their lifetime, child received medical attention because of an asthma attack, or child was taking medications consistent with

an asthma diagnosis at a study collection time point (e.g. daily inhaled corticosteroids, short-acting beta agonists (SABAs), anticholinergics, long-acting beta-agonists, theophylline, or leukotriene receptor antagonists (LTRAs)). The specific medications classification protocol is detailed in Appendix A.

Asthma Severity Classification

Asthma severity was classified in two ways: reported lifetime asthma attacks and a categorical label of asthma severity based on a combination of reported medication usage and recent asthma attacks (Asthma Care Quick Reference, 2002; Pocket Guide for Asthma Management and Prevention for Adults and Children Older than 5 Years, 2022). To be eligible for the severity analysis, youth needed to have a positive asthma history classification and have enough data to be classified with a categorical label both at the baseline and year 2 follow up time points. The categorical cumulative severity labels were assigned using a stepwise approach in consultation with collaborating physician asthma experts. Medication-based severity classification has been successfully used to detect asthma-related brain changes in older adults where similar medical history was available (Nair et al., 2022, 2023) and to detect differences in school performance in youth from large population samples (Lundholm et al., 2020).

The severity classification approach proceeded in two steps. First, the daily controller medication profile was evaluated per 2020 National Asthma Education and Prevention Program guidelines (Shero et al., 2023). Youth were classified Level 1 “mild intermittent” if they reported using a rescue inhaler (SABAs) and no other asthma-related medications; Level 2 “mild persistent” if their only asthma controller medications were daily leukotriene receptor antagonists, daily theophylline, or daily mast cell stabilizers; Level 3 “persistent unknown” if they reported taking daily inhaled corticosteroids with insufficient information to classify dose;

Level 4 “persistent moderate” if they were taking both an inhaled corticosteroid and a second daily controller medication (e.g. LABA, LTRA, theophylline); or Level 5: “persistent severe” if they reported using daily high-dose corticosteroids and/or monoclonal antibodies.

In the second step, these classifications were adjusted to ensure that youth with undertreated asthma would not be classified as having mild disease. Youth were moved to a higher level if their reported rescue inhaler use exceeded their controller-related classification. If youth reported using their rescue inhaler 2 to 6 days per week, they were eligible for Level 2 “mild persistent,” daily use was consistent with Level 4 “persistent moderate,” and more than once daily was classified as Level 5 “persistent severe.” Youth who reported greater than or equal to two asthma attacks between any two study time points were reclassified as Level 4 “persistent moderate” if their controller medication use did not put them in the Level 5 “persistent severe” category.

To include information from youth who had varying numbers of timepoints when their asthma severity could be classified, the final cumulative severity score was an average of the classification levels at each of the time points where information was available.

Peripheral Inflammatory Biomarkers

During the 2-year follow up time point, $N = 604$ youth provided a peripheral blood sample, on which a complete blood count (CBC) with differential was performed. This was used to calculate two metrics to approximate circulating inflammation: a blood eosinophil count and neutrophil-to-lymphocyte ratio (NLR). In the predominant asthma endotype (Fahy, 2015), asthma symptoms are accompanied by eosinophils migrating into the airway (Busse et al., 2021). Thus, peripheral eosinophil count is sometimes used clinically to approximate asthma severity in youth (Licari et al., 2018).

However, a minority of youth with asthma present with low levels of eosinophils and predominantly neutrophilic inflammation in the airway. Neutrophilic asthma is important to identify because it is associated with severe, treatment-resistant disease (Yamasaki et al., 2022). Although NLR has not been explicitly used to differentiate eosinophilic from neutrophilic asthma, it is likely a clinically relevant marker of circulating inflammation. NLR is elevated in patients with asthma relative to healthy controls (Huang et al., 2020) and is widely used as an indicator of systemic inflammation in a variety of other chronic diseases (Afari & Bhat, 2016; W. Chen et al., 2021). NLR can also be related to asthma control. Among people with asthma, NLR is elevated in patients with recent asthma exacerbations compared to those with well-controlled asthma (Esmaeilzadeh et al., 2021).

Cognitive Functioning

The National Institutes of Health Toolbox Cognition Battery (NIH Toolbox) uses seven tests to assess a range of cognitive abilities including episodic memory, executive function, attention, working memory, processing speed, and language abilities (Weintraub et al., 2013). This measure was administered during the baseline and 2-year follow up time points. Because most of the two-year follow-up data was administered remotely during COVID-19 pandemic, some tasks, like the Dimensional Change Card Sort Task, were not administered. Therefore, typical NIH global cognitive composite scores could not be calculated. Replicating a published confirmatory factor analysis on the two year follow up data, (Chaku et al., 2022; Pat, Riglin, et al., 2022; Pat, Wang, et al., 2022), I used a bifactor model to generate four latent variable scores: a general intelligence factor (*g*), executive functioning (Flanker Inhibitory Control and Attention Test, Pattern Comparison Processing Speed Test), memory (Picture Sequence Memory Test, Rey Auditory Verbal Learning Test), and language (Picture Vocabulary Test, Oral Reading

Recognition Test). The model fit the data adequately (CFWE = 0.991, TLI = 0.976, 95% CI RMSE [0.032 -0.049]). Latent factor scores were transformed to standard scores with a mean of 0 and standard deviation of 1 to improve interpretability.

Emotional Functioning

Using the Child Behavior Checklist (CBCL), parents rate 113 items related to their child's behavior in the last 6 months, on a three-point scale (not true, somewhat/sometimes true, very often/always true). CBCL generates a raw score as well as age- and sex-adjusted *t*-scores which are well-validated to identify clinically significant problems in 6-18 year olds (Achenbach & Rescorla, 2001). The CBCL scales have a hierarchical organization, with 3 summary scales and 8 core scales. The Total Problems score is a sum of Social Problems, Thought Problems, Attention Problems, Internalizing Problems (which is a sum of Anxiety/Depressed Problems, Withdrawn/Depressed, and Somatic Complaints), and Externalizing Problems (which includes Delinquent Behavior and Aggressive Behaviors). This measure was administered during the baseline, 1-year, 2-year, and 3-year time points. The current investigation focuses on the Total Problems score, the Anxious/Depressed score, and the Attention Problems score.

Statistical Modeling

Because ABCD is a multi-site study and enrolled some groups of siblings, random effects were needed to appropriately model non-independence introduced by this grouping structure. In some analyses, models would not converge with this complicated random effects structure. To allow model convergence in these cases (described in detail below), one sibling from each family was selected to be included in analyses, prioritizing youth with asthma in discordant families.

Statistical Modeling of Cognitive Function

Cross-sectional analyses used outcome variables from the two-year follow-up data when youth were 11 – 13 years old. Using the lmer package in R (Version 4.2.1), I created a series of linear mixed effects models where I regressed asthma lifetime asthma history (0.5 = asthma history, -0.5 = no asthma history), age (in months) and sex at birth onto the outcome measures of interest and included a by-data-collection-site random intercept and a by-family random intercept to account for non-independence introduced by the nested data structure (i.e. Outcome ~ asthma history + age + sex + (1 | site) + (1 | family)).

Analyses were repeated including each of the four asthma-related moderators: lifetime attacks, cumulative severity, eosinophil count, and NLR. Cumulative severity and lifetime asthma attacks were modeled only in youth with an asthma history. Serum analyses additionally controlled for the mean group difference in inflammatory markers with youth with and without an asthma history. In cumulative severity and biomarker models, one sibling per family was included as previously described, eliminating the need to model the random effect of family, which allowed models to converge. In these analyses with a more limited sample size, models were tested with and without outliers at a cutoff of cook's $d > 4/N$.

In longitudinal analyses, data collection time point was coded (0-3), and analyses were repeated as described with an asthma predictor * time interaction and a random by-subject intercept. These predictors included asthma history and lifetime asthma attacks. (e.g. Outcome ~ asthma-related moderator*time + age + sex + (1 + time | subject) + (1 | site) + (1 | family)). When models did not converge, the correlation between the random by-subject slope and random by-subject intercept were removed.

Statistical Modeling of Emotional Function

Preregistered analyses of emotional functioning proposed using the linear mixed effects models approach as with cognitive functioning, with age and sex-adjusted CBCL t-scores as outcome measures. However, when visually inspected, these scores were bimodally distributed with a peak both at the expected mean and a second peak around 0 reported symptoms. Raw scores of 0 represented 19% (N = 1366) of reported internalizing scores, 35% (N = 2447) of anxiety/depressive scores, and 36% (N = 2551) of attentional scores at year 2 follow-up. Therefore, zero-inflated negative binomial models using the raw scores as an outcome measure were calculated, using the mixed_model function from the GLMMadaptive package (Rizopoulos, 2023) in R. This package can only account for one source of random effects. That combined with convergence difficulties, meant that for cross-sectional models, I used the strategy of retaining one sibling per family and modeling site as the random effect. When models containing random effects could not estimate all parameters, the zeroinfl function from the pscl package (Jackman et al., 2024) was used instead.

To examine longitudinal changes over time in each participant, the longitudinal models included a by-time slope and random intercept for each subject. These parameters were allowed to correlate. Although mean CBCL scores are not identical across sites, it is reasonable to assume that this can be explained by covariates that can be modeled to reflect broad demographic differences between sites rather than reflecting true non-independence due to factors like equipment or experimenter training. I considered including site as a fixed effect, but it was not feasible because of model convergence difficulties.

Additional Statistical Modeling Concerns

Group-level demographic differences between youth with and without asthma cannot accurately be accounted for simply by adding these factors as additional covariates of interest in linear models (G. A. Miller & Chapman, 2001). However, as results in the literature often report analyses using these covariates, I repeated the analyses controlling for several demographic factors that are included in Appendix C. These factors were highest educational attainment of the two caregivers reported on (four levels - no high school diploma, high school diploma or equivalent, some college, college or advanced degree), family income (10 levels), and Black/African American race, and birthweight. Asthma is more prevalent, severe, and uncontrolled in low income, urban populations, particularly in Black/African-American and Puerto Rican populations (Perez & Coutinho, 2021). Parents were asked "What race do you consider your child to be?" and were encouraged to select all racial groups that apply. If Black/African American was one of the race categories chosen, it was coded as present. Birthweight was also included as a covariate of interest as low birthweight can be influenced by several social determinants of health (Lorch & Enlow, 2016) and has a hypothesized causal relationship with asthma, as low birthweight is associated with a higher risk of respiratory problems beginning shortly after birth (Xu et al., 2014).

## Results

Descriptive Statistics

Compared to youth without an asthma history, youth with asthma were more likely to be male ($X^2(1) = 191.29$, $p < 2.20e^{-16}$), more likely to be from a family with a lower total income, ($X^2(9) = 229.27$, $p < 2.20e^{-16}$), less likely to have a parent with a college education or advanced degree ($X^2(3) = 29.12$, $p = 2.11e^{-6}$; $X^2(1) = 26.11$, $p = 3.22e^{-07}$), and more likely to be

Black/African American ($X^2(1) = 16.62$, $p = 0.0000456$). Notably 30.2% of youth with an asthma history were Black/African American compared to 14.8% of youth without an asthma history. Youth with asthma had higher peripheral eosinophil counts ($b = 105$, $F(1, 555.21) = 48.34$, $p = 1.01e^{-11}$) and higher neutrophil to lymphocyte ratios (NLR; $b = 0.15$, $F(1, 556.98) = 5.47$, $p = 0.020$; Table 2.1).

**Table 2.1 Demographic differences between youth with and without an asthma history at year 2 follow up time point in the ABCD**

| | **Asthma history** | **No asthma history** |
|---|---|---|
| | *N* = 1250 | *N* = 5238 |
| Age (months) | 143.3 | 143.2 |
| Sex (% Female) | 40.0 % | 49.5 % |
| **Family Income** | | |
| < $5,000 | 37 (3.25%) | 109 (2.29%) |
| $5,000 - $24,999 | 135 (11.88%) | 366 (7.49%) |
| $25,000 - $49,999 | 179 (15.75%) | 567 (11.60%) |
| $50,000 - $74,999 | 175 (15.40%) | 637 (13.03%) |
| $75,000 - $99,999 | 175 (15.40%) | 681 (14.93%) |
| $100,000 - $199,999 | 331 (29.13%) | 1750 (35.79%) |
| $200,000+ | 104 (9.15%) | 779 (15.93%) |
| **Parents' highest education** | | |
| No high school diploma | 30 (2.3%) | 224 (4.28%) |
| HS diploma or equivalent | 171 (13.38%) | 405 (7.75%) |
| Some college | 192 (15.02%) | 626 (11.98%) |
| College or advanced degree | 885 (69.25%) | 3971 (75.98%) |
| Birthweight (oz) | 83.65 ± 18.42 | 86.05 ± 17.89 |
| % Black/African American | 30.2 % | 14.8 % |
| **Serum measures** | ***N* = 123** | ***N* = 408** |
| Serum eosinophil count | 280 ± 240 | 200 ± 200 |
| Neutrophil to lymphocyte ratio | 1.5 ± 0.83 | 1.3 ± 0.71 |

**Table 2.2 Outcome measures in youth with and without an asthma history**

| | **Asthma history** | **No asthma history** |
|---|---|---|
| **NIH Toolbox outcome measures** | ***N* = 1250** | ***N* = 5147** |
| Picture Vocabulary Test | 87.83 ± 8.61 | 89.34 ± 8.34 |
| Oral Reading Recognition Test | 94.14 ± 6.82 | 95.03 ± 6.57 |
| Flanker Inhibitory Control and Attention Test | 99.36 ± 8.22 | 100.33 ± 7.43 |
| Pattern Comparison Processing Speed Test | 101.72 ± 15.27 | 103.74 ± 15.06 |
| Picture Sequence Memory Test | 107.78 ± 12.52 | 109.76 ± 11.95 |
| Rey Auditory Verbal Learning Test | 8.81 ± 3.00 | 9.32 ± 2.84 |
| **CBCL scales raw scores** | ***N* = 1383** | ***N* = 5644** |
| Total problems | 18.49 ± 18.12 | 15.38 ± 16.17 |
| Internalizing problems | 5.42 ± 5.88 | 4.66 ± 5.36 |
| Anxiety/depressive problems | 2.43 ± 3.01 | 2.22 ± 2.86 |
| Depressive/withdrawn problems | 1.33 ± 1.99 | 1.17 ± 1.85 |
| Somatic problems | 1.67 ± 2.12 | 1.28 ± 1.80 |
| Externalizing problems | 4.49 ± 6.00 | 3.66 ± 5.19 |
| Attention problems | 3.13 ± 3.44 | 2.53 ± 3.21 |
| Thought problems | 1.55 ± 2.20 | 1.34 ± 1.20 |
| Social problems | 1.50 ± 2.14 | 1.21 ± 1.98 |

Differences in Cognitive Function Between Youth With and Without an Asthma History at 11 to 13 Years Old

When controlling for age and sex, youth with a history of asthma had lower scores in all cognitive domains tested including the general intelligence factor ($b$ = -0.16, $F(1, 6120.9)$ = 34.12, $p < 0.0001$), memory ($b$ = -0.16, $F(1, 6303.7)$ = 33.46, $p < 0.0001$), language ($b$ = -0.14,

$F(1, 6120.9) = 34.12$, $p = 5.45e^{-9}$), and executive functioning ($b = -0.12$, $F(1, 6377.5) = 23.45$, $p < 0.0001$; Figure 2.1).

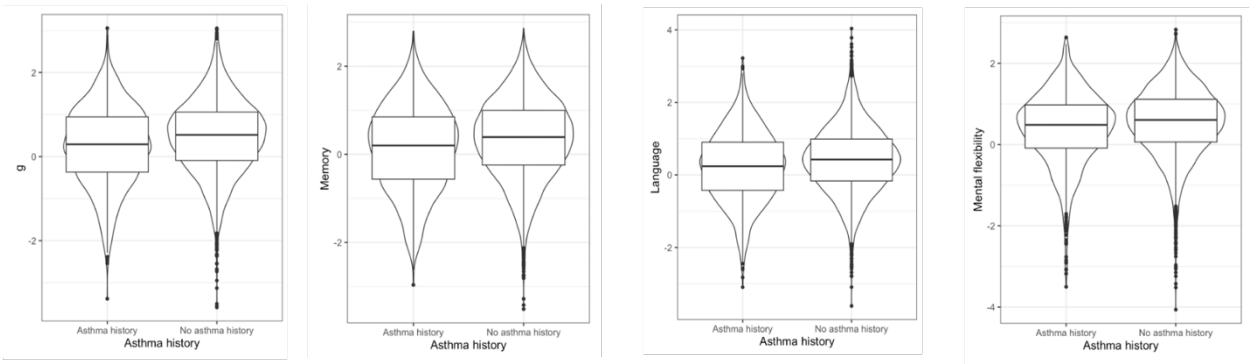


**Figure 2.1 Differences in Cognitive Function Between Youth With and Without an Asthma History at 11 to 13 Years Old**

Plot displays age and sex adjusted cognitive scores derived from bifactor model of NIH Toolbox performance of ABCD year 2 follow-up data; Youth with a history of asthma had lower scores in all cognitive domains tested including (from left to right) *g*, memory, language, and mental flexibility scores.

Differences in Cognitive Function and Asthma-Related Moderators

Among youth with asthma ($N = 306$), lifetime asthma attacks were not related to *g* ($b = -0.003$, $F(1, 286.91) = 0.05$, $p = 0.821$), executive functioning ($b = 0.003$, $F(1, 282.39) = 0.08$, $p = 0.778$), memory ($b = -0.001$, $F(1, 287.51) = 0.01$, $p = 0.913$) or language scores ($b = -0.006$, $F(1, 287.22) = 0.22$, $p = 0.638$). However, within youth with asthma who had adequate information to categorize longitudinal severity ($N = 144$), asthma severity score related to lower general intelligence ($b = -0.16$, $F(1, 137.06) = 4.24$, $p = 0.041$), memory ($b = -0.18$, $F(1, 138.59) = 4.52$, $p = 0.035$) and executive function scores ($b = -0.15$, $F(1, 137.65) = 4.26$, $p = 0.041$), but not language scores ($b = -0.12$, $F(1, 136.90) = 1.97$, $p = 0.163$; Figure 2.2).

Across all individuals, eosinophils counts were trending towards a relationship with cognition for *g* ($N = 531$, $b = -0.33$, $F(1, 434.36) = 1.86$, $p = 0.174$), executive function ($b = -0.32$, $F(1, 521.18) = 1.79$, $p = 0.182$), and language ($b = -0.42$, $F(1, 481.99) = 2.8696$ p = 0.091),

but not memory scores ($b$ = -0.09, $F$(1, 408.02) = 0.13, $p$ = 0.715). However, these relationships were less robust when outliers were dropped ($g$: $N$ = 498, $b$ = -0.33, $F$(1, 317.72) = 1.64, $p$ = 0.201; executive function $N$ = 506, $b$ = -0.13, $F$ (1, 462.24) = 0.29, $p$ = 0.592; language $N$ = 497, $b$ = -0.22, $F$(1, 365.74) = 0.67, $p$ = 0.411; memory $N$ = 505, $b$ = -0.23, $F$(1, 419.92) = 0.70, $p$ = 0.404). There was also no relationship between NLR and any of the outcomes tested (Appendix B).

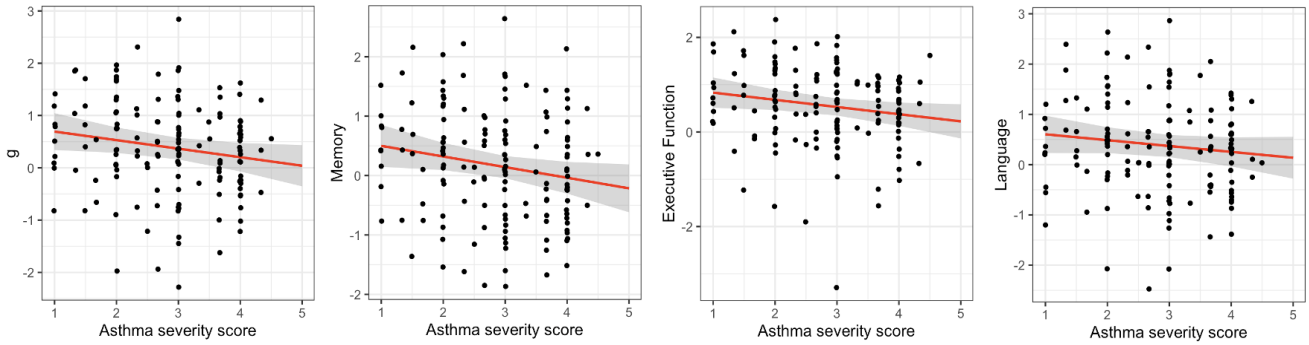


**Figure 2.2 Relationship Between Asthma Severity and Cognitive Function at 11 to 13 Years Old**

Youth with asthma ($N$ = 144) were assigned a severity score at each time point based on their reported use of asthma controller medication, asthma rescue medication, and frequent asthma exacerbations. Plot displays the relationship between average severity score and age- and sex-adjusted cognitive scores derived from bifactor model of NIH Toolbox performance of ABCD year 2 follow-up data. Higher cumulative severity scores were related to lower general intelligence, memory, and executive function scores, but not language scores.

Differences in Emotional Function Between Youth With and Without an Asthma History at 11 to 13 Years Old

Among youth reporting at least one symptom, youth with asthma had higher rates of total parent reported problems ($b$ = 2.81, $SE$ = 0.03, $Z$ =84.55, $p$ < 0.0001), higher rates of attentional problems ($b$ = 0.08, $Z$ = 0.04, $SE$ = 2.08, $p$ = 0.040), and higher rates of internalizing problems ($b$ = 0.10, $SE$ = 0.04, $Z$ = 2.62, $p$ = 0.009), although this was not reflected in higher anxiety-depressive symptoms ($b$ = 0.03, $SE$ = 0.04, $Z$ = 0.60, $p$ = 0.550) (Figure 2.3). Exploratory analyses of other CBCL internalizing scales suggested that youth with asthma had increased

somatic problems (*b* = 0.17, Z= 3.32, p = 0.000914), but no difference in withdrawn-depressed problems (b = 0.09, SE=0.06, Z=1.50, *p* = 0.134). Further exploratory analyses found no evidence of sex differences in the relationship between asthma and total problems (*b* = -0.06, SE = 0.06, Z = -1.00, *p* = 0.318), internalizing problems (*b* = -0.11, SE = 0.07, Z = -1.53, *p* = 0.125), anxiety and depressive problems (*b* =-0.01, SE = 0.09, Z = -0.14, *p* = 0.885), or attention problems (*b* = -0.12, SE = 0.08, Z = -1.48, p = 0.140).

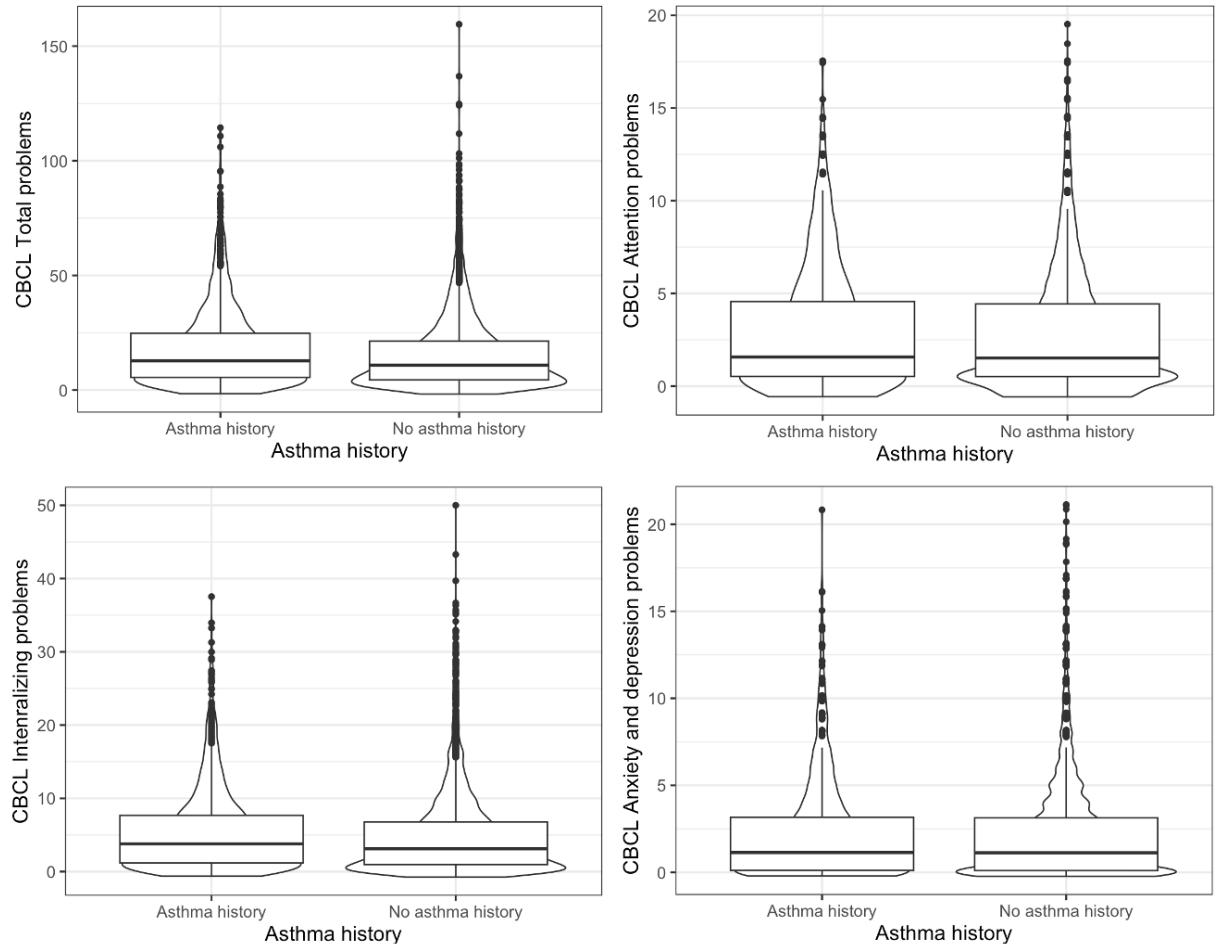


**Figure 2.3 Differences in Emotional Function Between Youth With and Without an Asthma History at 11 to 13 Years Old**

Plot displays age- and sex-adjusted scores on the Child Behavior Checklist. Youth with a history of asthma higher parent-reported total problems (top left), attentional problems (top right), and internalizing problems (bottom left), but no difference in anxiety and depression problems (bottom right).

Differences in Emotional Function and Asthma-Related Moderators

Among youth with asthma, a higher number of lifetime asthma attacks was associated with higher number of total problems ($N$ = 5814; $b$ = 0.02, $SE$ = 0.01, $Z$ = 2.44, $p$ = 0.015), more internalizing problems ($b$ = 0.02, $SE$ = 0.01, $Z$ =1.98, $p$ = 0.047), more anxiety and depressive problems ($b$ = 0.02, $SE$ = 0.01, $Z$ = 2.02, $p$ = 0.044), but not more attentional problems ($b$ = 0.01, $SE$ = 0.01, $Z$ = 1.34, $p$ = 0.180; Figure 2.4).

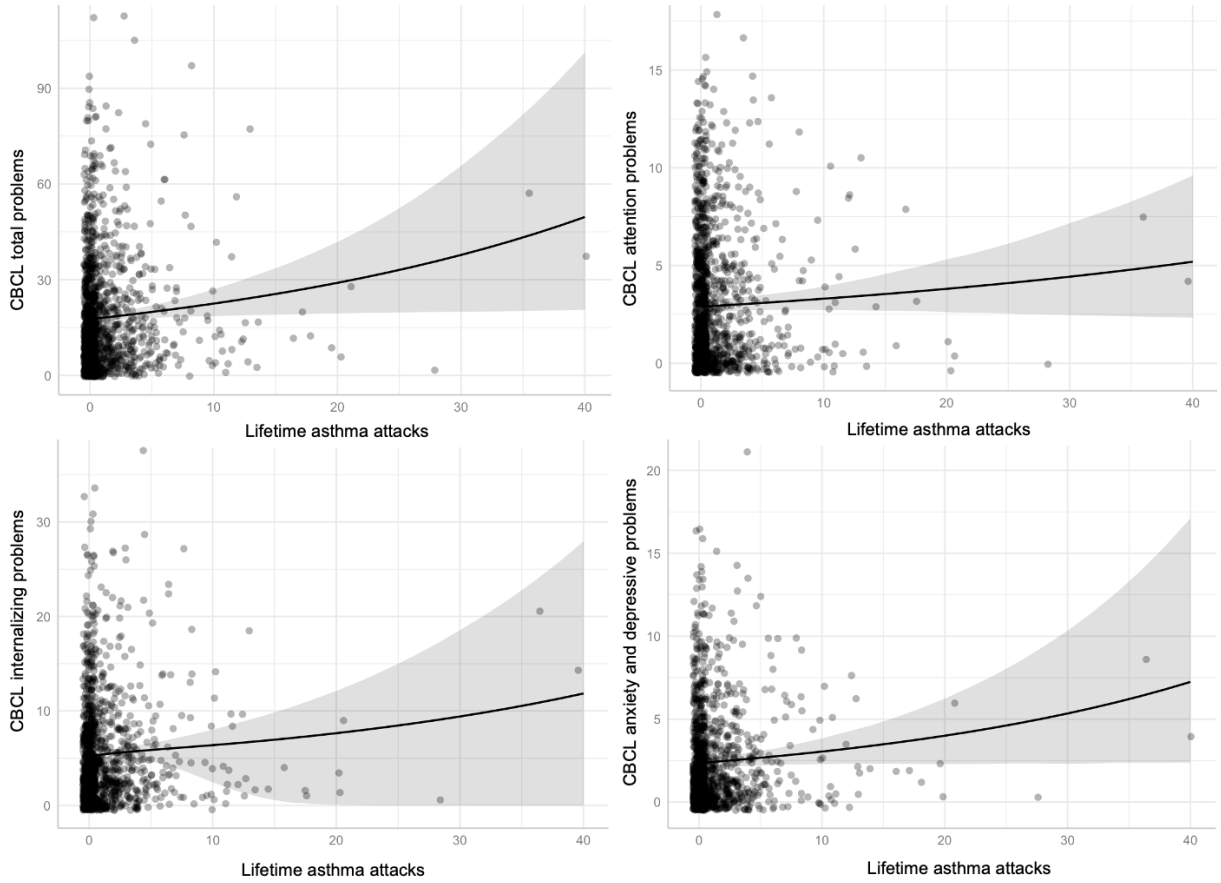


**Figure 2.4 Relationship between lifetime attacks and emotional function at 11-13 years old**

Plot displays raw scores on Child Behavior Checklist and model predictions conditioned on mean age, sex, and the model's zero-inflated component. A greater number of lifetime asthma attacks were associated with more parent-reported total problems (top left), no difference in attentional problems (top right), more internalizing problems (bottom left), and more anxiety and depression problems (bottom right).

Given the model complexity and relatively small sample size for severity analyses ($N$ = 148), not all parameters could be reliably estimated with the random effect of site. Omitting the random effect of site changed the magnitude of some beta-values, but the overall pattern, significance, and direction of findings was unchanged. Youth with higher asthma severity had *lower* levels of internalizing problems ($b$ = -0.21, SE = 0.09, $Z$ = -2.43, $p$ = 0.015) and *lower* levels of anxiety and depressive problems ($b$ = -0.28, SE = 0.12, $Z$ = -2.34, $p$ = 0.019), but no differences in total problems ($b$ = -0.06, SE = 0.07, $Z$ = -0.825, $p$ = 0.409) or attention problems ($b$ = 0.07, SE = 0.09, $Z$ = 0.81, p = 0.420; Figure 2.5).

There were no relationships between eosinophils and emotional metrics or between NLR and emotional metrics (Appendix B).

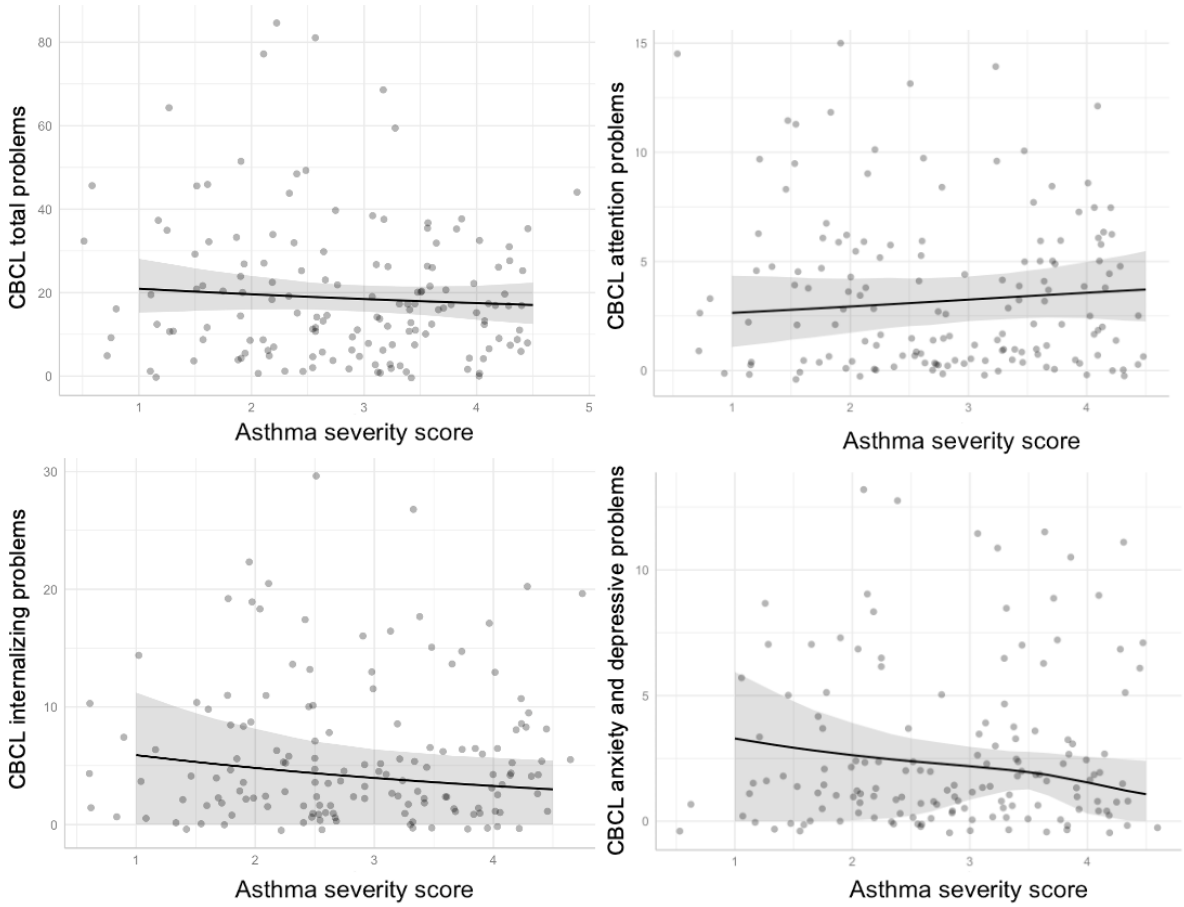


**Figure 2.5 Relationship between asthma severity and emotional function at 11-13 years old**

Plot displays raw scores on Child Behavior Checklist and model predictions conditioned on mean age, sex, and the model's zero-inflated component. Greater asthma severity (estimated with medication use and recent attack frequency) was associated with more parent-reported total problems (top left), no difference in attentional problems (top right), fewer internalizing problems (bottom left), and fewer anxiety and depression problems (bottom right).

Differences in Longitudinal Change in Cognitive and Emotional Function

Youth with asthma showed marginally slower increases in memory scores ($b$ = -0.020, $F(1, 6932.7) = 3.33$, $p = 0.068$), but no differences in change in general cognitive function ($b$ = -0.01, $F(1, 6721.6) = 2.00$, $p = 0.157$), language ($b$ = -0.004, $F(1, 6626.1) = 0.26$, $p = 0.609$), or executive function ($b$ = -0.01, $F(1, 7182.0) = 1.05$, $p = 0.306$) from ages 9 to 11 to ages 13 to 15. In a similar pattern, among youth with asthama, higher numbers of lifetime asthma attacks were

associated with slower increases in memory scores ($b$ = -0.0077, $F$(1, 7013.9) = 5.50, $p$ = 0.019), marginally slower increases in general cognitive function ($b$ = -0.004, $F$(1, 6700.2) = 2.76, $p$ = 0.096), but not with changes in language ($b$ = -0.0018, $F$(1, 6605.2) = 0.50, $p$ = 0.480) or executive function ($b$ = -0.002, $F$(1, 7256.6) = 0.26, $p$ = 0.608).

On average, youth in the study had a decrease in parent-reported total problems over the two years ($b$ = -0.05, SE = 0.005, $Z$ = -10.72, $p$ < 0.0001), but in youth with asthma, these decreases were slower ($b$ = -0.02, SE = 0.0091, $Z$ = -2.20, $p$ = 0.028). Youth with asthma also showed decreases in internalizing symptoms (asthma x time: $b$ = -0.02, SE = 0.01, $Z$ = -2.29, $p$ = 0.022), although there was no change in internalizing symptoms over time in the overall population ($b$ = -0.007, SE = 0.007, $Z$ = -0.96, $p$ = 0.336). Models with attention and anxiety did not converge.

## Discussion

The current study is one of the largest U.S. population samples to examine the relationship between characteristics of asthma and a range of cognitive and emotional outcomes. I found that on average youth with a history of asthma had lower cognitive performance than youth with no asthma history at 11 to 13 years old, ranging from a gap of 0.14 to 0.16 standard deviations. When compared against the effect of age on these scores, the performance of youth with asthma trailed their unaffected peers by an equivalent of 4.7 months for language scores to 9.1 months for memory scores. Youth with asthma also had higher numbers of parent-reported total problems, including more attentional problems, but showed no differences in frequency of anxiety and depressive problems. Importantly, many of the group differences in cognitive and emotional functioning were exacerbated by more severe asthma. Youth with higher levels of lifetime asthma attacks had more anxiety and depressive problems. Within youth with asthma, a

history of more severe asthma was related to lower general intelligence, memory, and executive functioning. Surprisingly, higher asthma severity was related to fewer internalizing and anxiety/depressive problems. There were no strong relationships between markers of peripheral inflammation and cognitive or emotional outcomes. Finally, there was a relationship between asthma history and longitudinal change in cognitive scores such that youth with asthma had slower longitudinal increases in memory scores from 9-11 to 11-13 which was more pronounced in youth with more lifetime asthma attacks. Youth with asthma also showed slower longitudinal decreases in total problem and a decrease in internalizing problems compared to youth without an asthma history. The implications of these findings will be explored in the following sections.

Group Differences in Cognitive Functioning, But Not Depressive Symptoms at 12 Years Old

An important step towards understanding how and whether we can interrupt the relationship between asthma and chronic psychiatric and neurological conditions is to determine when in development differences in cognitive and emotional functioning emerge. Here I detect lower levels of global cognitive functioning at 12 years old. This contrasts with a recent longitudinal cohort study which found no asthma-related differences in school performance at 13 years old; instead performance differences emerged at 15 to 16 years old (Lundholm et al., 2020). The NIH toolbox may be more sensitive to detect subtle differences in cognitive function than a more global metric like exam pass rates. It is also possible that the effects of subtle differences in cognition evident earlier in life may accumulate over time and become detectable in metrics like test scores later in teen years. Indeed, in the current study, youth with asthma showed slower increases in memory scores from 9 to11 years old to 11 to 13 years old, a pattern that was exacerbated by a history of more lifetime asthma attacks. However, no longitudinal pattern was evident in the other metrics, which could be consistent with group differences

established earlier in life than the study period, rather than increasing over adolescence. The current investigation did not have information about asthma age of onset or whether youth were exposed to asthma during gestation. In a recent longitudinal study, maternal asthma symptoms during pregnancy were associated with higher internalizing symptoms and lower executive functioning at age 7, but there were no differences related to preschool asthma symptoms (Husain et al., 2024). This dissociation underscores the importance of a life-course, developmental approach to understanding the relationship between asthma and cognition as associated risks for specific cognitive and emotional problems may not be uniform across childhood.

Although there is an extensively documented link between asthma, anxiety, and depressive symptoms, including in youth (Dudeney et al., 2017; Y. Lu et al., 2012; Z. Lu et al., 2018, p. 20), I did not find hypothesized group differences in anxiety and depressive symptoms between youth with and without asthma. Detecting differences in attentional problems and without differences in anxiety and depressive symptoms in youth with asthma is not unprecedented. A recent longitudinal Finnish study found 16-year old youth with asthma had higher levels of self-reported internalizing problems, somatic complaints and delinquent behaviors, but not significantly higher levels of anxiety and depressive problems (Määttä et al., 2022). Similarly, a large longitudinal cohort study of Canadian youth found that children with chronic disease (65% with asthma) showed no difference in depressive symptoms at age 12, but a faster increase from 12 to 16, and then steady elevations in depressive symptoms that followed the same trajectory of adolescents without chronic disease through age 25 (Ferro et al., 2015). Notably, the Canadian study found that depressive symptoms followed a complex non-linear

trajectory until age 16. In contrast, I only modeled a linear trend in symptoms from 9 to 15 years old, which may not appropriately reflect changes in internalizing symptoms during this period.

The difference in cognitive function and attentional problems, but not anxiety and depressive symptoms at this specific age raises the intriguing possibility that elevated internalizing problems in youth with asthma onset at later ages than problems with attention and cognitive function. This would match population level patterns where the most common symptoms in childhood are externalizing problems and ADHD, while the prevalence of internalizing problems increases in puberty, especially in girls. If these phenotypes are indeed arising at different points in development, it will be important to establish if these are happening in two distinct populations of individuals or if cognitive and/or attention problems predict later internalizing problems. For instance, it could be that exposure to asthma starting in preschool is related to attentional difficulties and asthma exposure starting in adolescence is related to internalizing difficulties. This would be consistent with what was observed in a longitudinal study of children with a range of chronic diseases, where children with disease onset before age 7 had a higher risk of externalizing and attentional problems at age 16, while youth with active chronic disease at age 16 had higher levels of internalizing problems regardless of disease status at age 7 (Määttä et al., 2022). Alternatively, early cognitive or attentional problems could be a precursor to later internalizing problems within the same individual. While they are often studied independently, externalizing problems, internalizing problems, and cognitive ability are longitudinally predictive of each other throughout development (Flouri et al., 2019). For example, in a longitudinal study of youth with ADHD, symptoms of impulsivity and hyperactivity declined from ages 10 to 18 while depressive symptoms rose especially in girls (Eng et al., 2023). This pattern has also been observed in symptoms correlated with early life

exposure to elevated levels of inflammation. In a longitudinal study, externalizing symptoms in childhood mediated the relationship between maternal IL-6 in pregnancy and adolescent depression symptoms in boys (Lipner et al., 2024). Further longitudinal work, and further work elucidating the neurobiological basis of both phenotypes will be helpful to disentangle these possibilities. Although there was no evidence for sex differences in the relationship between asthma status and emotional outcomes in the current sample, future work should continue to explore the potential role of sex as a moderator given the increased prevalence of both internalizing symptoms and asthma diagnoses in females beginning in adolescence (*Most Recent National Asthma Data | CDC*, 2021; Murray et al., 2022).

The speculation comparing cognitive and emotional outcomes directly should be tempered by methodological limitations. Specifically, while the NIH toolbox is designed to measure cognition across the normal range, the CBCL asks parents to endorse the presence of problems. Although a certain number of problems is considered normal, there are generally floor effects. In this sample, an unexpected number of parents reported zero problems, which required adjusting my analytic strategy. It is possible that either the parent reported CBCL or my statistical models are simply less sensitive to detect variation in emotional function.

Variations in Cognitive and Emotional Functioning Related to Lifetime Asthma Attacks, Cumulative Asthma Severity, and Eosinophil Count

One of my investigation's strengths is that it examines how cognitive and emotional outcomes are related to characteristics of asthma. My study includes three asthma-related moderators: the number of lifetime asthma attacks, an estimation of cumulative asthma severity during the study period for youth with asthma (using rescue medication use, controller medication use, and asthma attack frequency at each time point), and a peripheral eosinophil

count (which was collected for a subset of participants with and without asthma). For cognitive metrics, lower cognitive performance was associated with higher asthma severity, in line with the direction of my hypothesis. However, results were in mixed support of my hypothesis for emotional outcomes. More internalizing problems and higher anxiety and depressive problems were related to higher number of lifetime asthma attacks but were unexpectedly related to lower severity scores.

Differences in the relationships with cognitive and emotional outcomes may be in part because lifetime attacks, the cumulative severity score, and eosinophil counts are all influenced to different extents by several components: the severity of the underlying disease, the frequency and severity of symptoms experienced, and the medications needed to manage symptoms. These can be difficult to disentangle as more severe, more frequent symptoms are often the consequence of more severe underlying disease. Although caution should be taken in directly comparing the patterns of different metrics given their differences in statistical power, chronicity of asthma exposure compared to current disease activity is an interesting continuum to examine. For example, the number lifetime of asthma attacks is most influenced by asthma severity and control before the study started, cumulative asthma severity relies on medical contact related to asthma *during* the study periods, and peripheral biomarkers index inflammation *on the day* blood was drawn.

Lower cognitive scores were associated with higher study period asthma severity, while more lifetime attacks predicted slower longitudinal increases in general intelligence and memory scores. Within the timing framework, this suggests that there may be a combination of acute and chronic influences of asthma on cognitive task performance. In contrast, more internalizing problems and higher anxiety and depressive problems were each related to higher number of

lifetime asthma attacks, but unexpectedly lower cumulative severity scores. Because the cumulative severity scores were heavily influenced by medication use, one potential explanation is that youth with anxiety or depressive symptoms are using less medication regardless of true underlying disease severity. More detailed exploration of inflammatory status and lung function would be helpful to resolve whether this is indeed an unexpected finding or a complex relationship between anxiety, healthcare usage, and inflammatory biology.

This study broadly conceptualized asthma history as a cumulative exposure, implicitly hypothesizing that asthma severity and duration would be more important for cognitive and emotional outcomes than the specific timing. This was informed by work in adults with asthma where severe asthma is most consistently associated with negative outcomes (Nair et al., 2023; Rosenkranz, Dean, et al., 2022). However, it is also possible that active disease is most important for cognitive performance at this age. One example mechanism would be if the presence of elevated circulating levels of inflammatory cytokines mediated the difference in cognitive performance. For instance, one longitudinal cohort study measured both inattentive symptoms and asthma diagnosis at ages 11, 18 and 22. They found that early inattentive symptoms did not predict later asthma diagnosis and asthma diagnosis did not predict later inattentive symptoms. Instead, at any time point, when people had an active asthma diagnosis they were more likely to meet diagnostic criteria for ADHD. Further, elevated levels of the proinflammatory cytokine IL-6 were detected only in people with both current asthma and ADHD (Leffa et al., 2021). If asthma history generated a cumulative risk for cognitive dysfunction, I would expect asthma at younger ages to predict ADHD later in life. Instead, this pattern is consistent with a model where something about active asthma is related to attention problems, such as inflammatory signaling or effect of asthma symptoms like sleep disturbance, nocturnal awakenings, sleep disordered

breathing, activity limitations, or missed days of school. A state dependent-relationship between asthma and ADHD also raises the potential influence of cognitive and emotional problems on asthma outcomes. For instance, youth with more difficulties in executive functioning and higher depressive symptoms are less able to manage their controller medications and thus may experience higher levels of asthma symptoms (Leonard et al., 2022).

To date, the potential role of ongoing peripheral inflammation in cognitive and emotional dysfunction has been largely neglected in youth with asthma. To my knowledge, this is the first study to explore the relationship between a biomarker of Type 2 inflammation and cognition in a large youth cohort. I initially expected an interaction between asthma history and eosinophil count, such that disease-relevant inflammatory markers would be related to cognition in youth with asthma, but not in youth with no asthma history. Instead, I found marginal, trend-level relationships between higher levels of peripheral eosinophils and reduced cognitive functioning across all youth. Consistent with the overall lack of relationship between asthma and emotional outcomes, I did not see relationships between eosinophils and CBCL scores. The relationship with Type 2 inflammation and lower cognitive performance is consistent with previous work that has found higher rates of neurodevelopmental disorders across the continuum of common childhood atopic disease (eczema, allergic rhinitis, and asthma). For instance, there is a meta-analytic association between atopic dermatitis and developmental delays (Jackson-Cowan et al., 2021), as well as atopic disease broadly and ADHD (Chuang et al., 2022, p. 2). The observed relationships between cognition and peripheral inflammatory markers consistent with the notion that active disease, in addition to disease history, is an important consideration.

I also did not detect a relationship between my outcomes of interest and the neutrophil to lymphocyte ratio (NLR). The null finding in this study could easily be due to the limited number

of participants with high NLRs. NLR between 1 and 2 is normal, and above 3 is considered clinically elevated (Afari & Bhat, 2016). In my sample, only 15% of samples were above the normal range and only 3% were clinically elevated. NLR may be a more useful biomarker in samples with a higher proportion of patients with uncontrolled disease.

Limitations and Future Directions

As previously mentioned, the observational nature of the study means that we cannot test to what extent asthma has a causal effect on cognitive or emotional outcomes, as there are many biopsychosocial factors that influence both asthma and these outcomes, as well as bidirectional relationships between cognitive and emotional function and asthma symptoms (e.g. disease management, response to stressful life events). Notably, in this study, as in the United States more generally, the relationship between asthma status and cognitive and emotional outcomes is confounded by social processes and structural factors. In this sample, youth with asthma were more likely to be of lower SES (often proxied by income and parental education) and more likely to identify as Black/African American, and therefore more likely to be exposed to the consequences of structural racism in the United States that has historically excluded Black/African American families. Low SES is a well-known predictor of cognitive and emotional difficulties (Noble & Giebler, 2020). Low SES and structural racism can increase exposure to chronic stressors and decreases access to resources (e.g. high-quality housing, high quality education). These exposures can increase the likelihood that an individual develops asthma, impede asthma control (e.g. through reducing access to healthcare), and can modify inflammatory biology such that individuals have more extreme inflammatory reactions when encountering an allergen (Elwenspoek et al., 2017; G. E. Miller et al., 2011). This potentially

places low SES as a simultaneous upstream cause and a moderator of the relationship between asthma and cognitive and emotional outcomes.

The current study is not designed to assess the relationships between asthma, structural factors, and cognitive or emotional outcomes. Future work with a matched-control design would be better able to isolate the role of asthma above and beyond other factors, but it would not be well-suited to explore more complex, interactive relationships. Moving toward a biopsychosocial mechanistic understanding of these relationships will allow the field to more accurately quantify these relationships and to understand which interventions would be best suited to address the correlation between asthma history and cognition. Understanding the relationship between asthma and cognitive and emotional outcomes will have a greater impact on minority populations because they bear the brunt of the public health burden of asthma. As a mechanistic understanding grows, developing interventions to close gaps in cognitive and emotional outcomes between youth with and without asthma, should continue to consider the specific needs of the communities disproportionately affected by asthma.

Because the ABCD study was not designed to examine asthma-specific outcomes, the advantages of comparing youth with asthma to a large population cohort sample come with limitations in my ability to characterize asthma history and asthma-related biology compared to the detail available in a small clinical study. Most notably, this adds a level of uncertainty to the asthma history classification employed, in the absence of a physician's diagnosis of asthma with pulmonary testing. Further, my three asthma-related moderators are all imprecise methods to distinguish the relative contribution of current asthma severity, asthma control, the activity of specific inflammatory pathways, and asthma-specific symptoms experienced. Similarly, knowing the age of asthma onset, number of lifetime hospitalizations for asthma, and number of lifetime

asthma exacerbations, would all improve my ability to identify individual differences among youth with asthma that are most relevant for differences in cognitive and emotional outcomes. These individual factors are likely most evident in youth with the most severe, uncontrolled disease, who are not common in this sample. Previous work in adults suggests that the negative cognitive and emotional outcomes associated with asthma may not be linearly related to severity, and instead may be concentrated in people with severe disease (Nair et al., 2023). Further, we cannot establish which aspects of more severe asthma may be driving the observed asscoaitons (e.g inflammatory signaling, sleep disturbance, nocturnal awakenings, sleep disordered breathing, activity limitations, missed days of school).

Other limitations of the study include limitations in the outcome measures I chose. The parent-reported CBCL is the most comprehensive longitudinal measure of emotional function currently available in ABCD, but parent-reported and child-reported internalizing symptoms diverge as youth age. For cognitive outcomes, bifactor modeling may not reliably replicate in other studies. Data collection for this wave was interrupted by the COVID-19 pandemic which likely contributed to a low *N* for serum samples, and decreased the NIH Toolbox measures available at the year 2 follow up. Reliability of NIH Toolbox when done on the iPad is still being explored (Brearly et al., 2019).

Despite the limitations, this investigation still represents an important contribution by examining the relationship between asthma, cognition, and mental health within a shared biopsychosocial framework. Asthma is the most common chronic condition in children, affecting 1 in 12 US children aged 12 to 14, 40% of whom have uncontrolled disease (G. F. Miller et al., 2016; *Most Recent National Asthma Data | CDC*, 2021), but it is still primarily viewed as a transient issue that will resolve with age and is only important when active symptoms are

impairing daily functioning. On the contrary, evidence is growing that asthma is a systemic condition with effects on the brain and vasculature, in addition to the lungs (Nair et al., 2022; Tattersall, 2023). Identifying the precise developmental period when differences in cognitive and emotional function emerge in youth with asthma, how cognitive and emotional function are related to one another in youth with asthma, and how or whether these group differences detected in childhood may compound throughout life are important next steps.

Although the links between asthma and differences in cognitive and emotional function are certainly complex and multifactorial, the effect of chronic inflammatory signaling on brain function is one worrying potential contributor. For example, animal models of asthma demonstrate that depressive behaviors are mediated by brain structural changes, and that both structural and behavioral change can be prevented with corticosteroid treatment, the mainstay of asthma management (Dehdar & Raoufy, 2023b). If inflammatory signaling is making a similar contribution in human adolescents, controlling asthma-related inflammation may serve as a leverage point to shift the increased risk for negative outcomes. The transition from childhood to adolescence is particularly ripe for intervention as youth are growing in autonomy and taking more control of their healthcare (Kaplan & Price, 2020). This line of inquiry has the potential to especially benefit marginalized communities where asthma is most prevalent, severe, and undertreated. As the field moves to a more comprehensive biopsychosocial understanding of the relationship between asthma and high rates of comorbid major depressive disorder and Alzheimer's disease, it will be important to continue to define and measure more specific characteristics of asthma, more specific behavioral dimensions, and more specific biological processes involved rather than simply documenting the rates of co-occurrence of asthma broadly with other conditions.

# CHAPTER THREE: DIFFERENCES IN BRAIN STRUCTURE BETWEEN YOUTH WITH AND WITHOUT AN ASTHMA HISTORY IN A LARGE PERIADOLSCENT COHORT

## Introduction

It is well recognized that many biopsychosocial factors can influence the course of adolescent brain development to influence adult outcomes. Patterns of adolescent brain maturation, particularly in frontal-parietal and cortico-striatal circuitry, support the development of executive functioning and emotion regulation capabilities (Baron Nelson et al., 2019). Deficits in these functions are linked to the emergence of many adolescent- and adult-onset psychiatric diseases (Halse et al., 2022; Yang et al., 2022), reduced educational attainment (Cortés Pascual et al., 2019; Deer et al., 2020; Usán Supervía & Quílez Robres, 2021), and lower quality of life in adulthood (Davis et al., 2010). One component of the biopsychosocial environment, exposure to chronic systemic inflammation, has been increasingly recognized as a powerful modulator of brain structure during infancy (Bilbo & Schwarz, 2009) and aging (Furman et al., 2019; Newcombe et al., 2018). In adults, brain structural changes have been associated with peripheral inflammatory markers in individuals with major depressive disorder, schizophrenia, cognitive impairment, and Alzheimer's disease (Frodl & Amico, 2014). However, there have been remarkably few investigations of the relationship between brain structure and exposure to chronic inflammation in human adolescents.

Large neuroimaging cohort studies that include youth with a history of asthma provide an excellent opportunity to ask whether chronic inflammatory disease influences adolescent brain structure. Asthma is a prevalent chronic inflammatory disease of the airways, affecting 1 of every 12 youth aged 12 to 14, 40% of whom have uncontrolled disease (AsthmaStats, 2019). Adolescents with asthma are at an increased risk for depression (Z. Lu et al., 2018), anxiety

disorders (Dudeney et al., 2017), inattentive symptoms (Chuang et al., 2022), and deficits in executive functioning (Irani et al., 2017). In adults with asthma, loss of microstructural integrity in cortico-striatal white matter tracts is associated with cognitive decline, and these relationships are exacerbated with increasing asthma severity (Nair et al., 2022; Rosenkranz, Dean, et al., 2022). Further, higher serum markers of white matter injury are associated with lower cognitive scores in adults with both asthma and depression (Y. Lu et al., 2022). However, no previous studies have examined whether differences in cognitive and emotional functioning between youth with and without asthma are related to differences in grey matter (GM) or white matter (WM) brain structure.

Three neural systems that are actively developing during adolescence may be particularly relevant for understanding elevated risk for psychopathology in youth with asthma. The first is the fronto-parietal network (FPN) which is important for the typical development of cognitive control and emotion regulation skills that are necessary for healthy psychological functioning. During typical development, adolescent structural changes in frontoparietal regions that support more efficient multi-sensory integration also enable the increase in working memory capacity and executive functioning (Sydnor et al., 2021). Patterns of increasing microstructural maturity in both GM and WM fronto-parietal structures have been shown to partially mediate the association between increased age and improved executive functioning during childhood and adolescence (Baron Nelson et al., 2019; Goddings et al., 2021). During typical development, GM changes in lateral temporal, lateral parietal, and dorsal/medial prefrontal cortices (Sydnor et al., 2021) are accompanied by increases in WM volume and integrity (Moura et al., 2017; Sydnor et al., 2021) in inter-lobar tracts (inferior fronto-occipital fasciculi, inferior longitudinal fasciculi, and superior longitudinal fasciculi; Sydnor et al., 2021). Further, these are the WM tracts where

robust differences in middle aged-adults with asthma have been related to accelerated cognitive slowing (Nair et al., 2022; Rosenkranz, Dean, et al., 2022).

The second system of particular interest for understanding adolescent brain development in youth with asthma is the cortico-striatal reward system. Reward processing regions in the basal ganglia have unique changes in sensitivity during adolescence (Gee et al., 2018), and changes in striatal function are known to mediate increased depressive symptoms in the presence of acute inflammatory provocation (Felger, 2018). During typical development, microstructural developmental changes in adolescence have been observed in basal ganglia nuclei more broadly, including the striatum, globus pallidus and putamen (Mah et al., 2017; Palmer et al., 2022).
The third system includes the integration of prefrontal regions with medial temporal lobe structures and striatal structures. Increased connectivity between the orbital frontal cortex and the cingulate cortex with medial temporal lobe structures is facilitated by increased volume and integrity of the WM tracts of the uncinate fasciculus and cingulum bundle. The connectivity between these groups of structures is associated with improvements in regulating emotion and in regulating reward-based behavior (Park et al., 2021, Pederson et al., 2021).

The integrity of these tracts may be vulnerable in youth with asthma, as the integrity appears to be related to circulating inflammatory markers. In adults, several studies have shown that higher levels of peripheral systemic inflammatory markers are correlated with reduced microstructural integrity in the cingulum bundle in adults with major depressive disorder (L. Chen et al., 2022; Lim et al., 2021, p. 20; Sugimoto et al., 2018; Thomas et al., 2021).

The current study will examine the association between asthma, brain microstructure, and important neurocognitive and behavioral outcomes in the early adolescent period using diffusion-weighted magnetic resonance imaging, behavioral, and medical history data from the

Adolescent Brain and Cognitive Development (ABCD) study 4.0 release, primarily the two-year follow-up data when youth range from 11 to 13 years old. I hypothesize that adolescents with a history of asthma will have reduced WM integrity compared to youth without asthma in a pattern consistent with less maturity. I hypothesize that group WM differences will be most pronounced in the frontal lobe, fronto-parietal and frontal-subcortical WM tracts (inferior fronto-occipital fasciculi, superior longitudinal fasciculi, inferior longitudinal fasciculi, anterior corpus collosum, internal capsule). I hypothesize that, in GM regions that are actively maturing during early adolescence (thalamus, basal ganglia, anterior cingulate, orbital frontal cortex, fronto-parietal network), youth with an asthma history will have less mature patterns of microstructure, as measured by diffusion-weighted imaging than youth without an asthma history. I hypothesize that group differences in brain microstructural integrity will be moderated by asthma severity, where youth with more severe asthma will show greater deviation from youth without asthma compared to youth with more mild asthma. Finally, I will test both cross-sectional and longitudinal statistical meditation models. I hypothesize that the data will be consistent with a statistical model where brain structure partially mediates the relationship between asthma history and behavioral outcomes at the two-year follow-up and that microstructural differences at 11 to 13 years old partially mediate deficits in cognitive functioning and elevations in psychopathology at age 12 to 14 years old between the youth with and without an asthma history measured at baseline ages 9 to 11.

These hypotheses and analytic plan were pre-registered with the Open Science Framework (OSF) to be tested with specific voxelwise metrics of diffusion weighted imaging, in both GM and WM described further in the methods. However, due to computational constraints, I primarily pursued a region-of-interest (ROI) based-approach using the publicly available

ABCD metrics. Because the ABCD releases multi-modal data using the same set of ROIs, this allowed me to expand the scope of the investigation by including GM volume and cortical thickness metrics. Thus, the interpretation of GM volume and thickness, especially in GM, should be considered more exploratory.

## Methods

Building on the analyses described in Chapter 2, briefly, I used data from the Adolescent Brain Cognitive Development (ABCD) Study (Release 4.0), focusing on the year-2 follow up data when youth were 11 to 13 years of age. I classified individuals as in Chapter 2, as having a positive or negative asthma history using parent-reported medical history, lifetime asthma attacks, and medication usage where available. A subset of youth had blood eosinophil counts, an index of Type-2 allergic inflammation associated with asthma. These data were used to create three asthma-related moderators: lifetime attacks, cumulative asthma severity, and blood eosinophil count. Neutrophil-to-lymphocyte ratio (NLR) was also explored as a non-asthma specific inflammatory biomarker.

Behavioral outcome measures included metrics of cognitive functioning and emotional functioning, as described in the previous chapter. Four metrics of cognitive functioning (g, executive functioning, language, and memory) were derived from a replication of a bi-factor confirmatory factor analysis model on the National Institutes of Health Toolbox (NIHT) Cognition Battery. Emotional functioning was operationalized using the Child Behavior Checklist (CBCL) Total Problems score, the Anxious/Depressed score, and the Attention Problems score. CBCL scores were available for the baseline, year 1, year 2 and year 3; NIHT scores were collected at baseline and year 2 time points only.

ABCD Structural Region of Interest (ROI) Metrics

For the majority of analyses presented, I used both structural morphometry and diffusion-weighted imaging metrics averaged across regions of interest (ROIs) processed by the ABCD pipeline. These analyses were not initially included in the OSF preregistration and were conducted after encountering difficulties with the planned voxelwise analyses described below. The pivot to ROIs allowed me to include structural morphology parameters in addition to the preregistered diffusion weighted parameters, including more exploratory analyses of volume and cortical thickness metrics.

A comprehensive description of the ABCD acquisition parameters and processing pipeline has been published (Hagler et al., 2019). Briefly, average subcortical GM volume, average cortical GM volume, and average cortical GM thickness estimates were generated from each subject's T1-weighted structural MRI scan using an automated, atlas-based, volumetric segmentation tool from FreeSurfer v5.3 (Fischl et al., 2002). For cortical regions, average cortical thickness (Fischl & Dale, 2000) and volume (Fischl et al., 1999) were calculated for each parcel in the Destrieux atlas (Destrieux et al., 2010) from unsmoothed, surface-based maps of morphometric measures. For cortical thickness, FreeSurfer calculates the distance between the pial and white surface and cortical volume represents a product of cortical thickness and surface area (Backhausen et al., 2022). This results in 14 subcortical GM volumes (bilateral thalamus, caudate, putamen, pallidum, hippocampus, amygdala and accumbens areas) and 148 cortical GM ROIs.

To generate WM ROIs, major WM tracts were labeled using AtlasTrack, a probabilistic atlas-based method for automated segmentation of WM fiber tracts. FreeSurfer's automated brain segmentation was used to identify and exclude voxels containing primarily gray matter or

cerebral spinal fluid from tract related calculations (Hagler et al., 2009, p. 300). This program generates 31WM tracts: the forceps major, forceps minor, corpus callosum bilateral fornix, cingulum bundles (cingulate and parahippocampal regions), corticospinal-pyramidal tracts, anterior thalamic radiations, uncinate fasciculi, inferior longitudinal fasciculi, inferior frontooccipital fasciculi, superior longitudinal fasciculi (temporal and parietal proportions), superior corticostriate, striatal inferior frontal cortex, and inferior frontal superior frontal cortex. The values for diffusion tensor parameters within each ROI are an average of voxelwise estimates. An ellipsoid tensor model is fit in each voxel to estimate the movement of water molecules in three orthogonal directions. The degree of water movement can be used to estimate the surrounding microstructure which constrains that movement (Vorona & Berman, 2015). In the ABCD study, four diffusion tensor parameters, mean diffusivity (MD), axial diffusivity (AD), radial diffusivity (RD), and fractional anisotropy (FA) were calculated using a standard, linear estimation approach with log-transformed diffusion-weighted signals (Basser et al., 1994). Each of these parameters gives summary information about water's motion in three orthogonal directions. MD is the average amount of movement in all three directions. AD is the amount of movement parallel to the principal axis of water diffusion. RD is the amount of movement perpendicular to the principal axis of diffusion. Finally fractional anisotropy (FA) is the extent the water travels in primarily one direction (FA=1) compared to water freely diffusing with no constraints (FA = 0).

The interpretation of DTI metrics in WM is relatively well-established. In WM, the structures constraining water movement are primarily bundles of myelinated axons. Water cannot diffuse through the hydrophobic myelination layer, so water travels primarily parallel to coherent, intact, WM tracts with very little perpendicular movement, which results in high FA,

low MD, AD, and RD. As tracts mature, WM tracts increase in volume, packing density, and myelination. This results in greater FA, lower MD, and lower RD (Sousa et al., 2018). AD increases in the setting of axonal damage and RD increases with demyelination, and therefore, AD and RD are often interpreted as proxies of axonal and myelin integrity receptively, although neither is specific to these processes (Vorona & Berman, 2015).

The biological interpretation of DTI metrics in GM is less clear. The 1 $mm^3$ resolution of GM tissue contains neuronal cell bodies, dendritic arbor, glia, blood vessels and both myelinated and unmyelinated axons (Backhausen et al., 2022). These structures have a less uniform orientation than myelinated axons in major tracts, and the ellipsoid tensor model is not a reliable reflection of spatial organization of cells in the voxel. In GM, DTI metrics are sensitive to many factors including glial number, axonal number, myelination, membrane permeability, glial morphology, dendritic architecture within the voxel, and partial volume effects (Nair et al., 2023). Normative developmental changes in GM microstructure have been less studied, but subcortical GM structures do appear to have reliable patterns of age-related change where FA increases and MD decreases with age (Baron Nelson et al., 2019; Mah et al., 2017) perhaps due to increased myelination in maturing nuclei (Ouyang et al., 2019).

Voxelwise Neurite Orientation Dispersion and Density Imaging (NODDI*)*

Additional metrics have been developed to improve the specificity and interpretability of the traditional diffusion weighted imaging. Specifically, the neurite orientation dispersion and density imaging (NODDI) model (Zhang et al., 2012) estimates the movement of water within a biophysical model, rather than an ellipsoid tensor. The NODDI model estimates to what extent water movement is consistent with three potential compartments: a cerebral spinal fluid compartment, an intra-neurite compartment (within axons or dendrites), or an extra-cellular

compartment (around cell bodies and glia). These estimates generate additional parameter maps including an intercelluar volume fraction (ICVF), an orientation and dispersion index (ODI), and a fraction of isotropic diffusion compartment (FISO). I hypothesized that less WM maturity in adolescents with an asthma history would be indicated by reduced neurite density (NDI; indexed by ICVF) in addition to reduced FA and increased MD, and that GM regions would show reduced NDI and changes in ODI in an unknown direction. Because this is a relatively novel technique, NODDI metrics are not available in the pre-tabulated ABCD data. Therefore, for each child, I calculated 7 whole-brain voxel-wise parameter maps; four metrics from a DTI model as previously described (FA, MD, RD, AD) and the three additional NODDI metrics (ICVF, ODI, FISO).

Whole-brain analyses used minimally processed year two follow-up ABCD images which have undergone eddy-current correction, head motion correction, B0 field inhomogeneity correction, gradient unwarping, replacement of bad slice-frames, between-scan motion correction and resampling to a standard orientation with 1.7 mm isotropic resolution (Hagler et al., 2019). Only images that passed the ABCD workgroup recommended quality control standards were included.

For each child, I calculated 7 whole-brain voxel-wise parameter maps; four metrics using a DTI model as previously described (FA, MD, RD, AD) and the three additional NODDI (ICVF, ODI, FISO). Brain tissue was extracted from the surrounding skull using the FMRIB Software Library (FSL) Brain Extraction Tool (BET) (S. M. Smith, 2002), and then a tensor was fitted at each voxel using the DIPY Python library and a weighted least squares model. The NODDI model was fit in Python using a Watson distribution (Zhang, et al., 2012). This pipeline

was successfully completed for $N = 6153$ participants who had adequate asthma-related data and met NIH quality standards.

Group analyses used Gray-matter Based Spatial Statistics (GBSS), a statistical technique that adapts the tract-based spatial statistics (S. M. Smith et al., 2006) framework in order to allow voxelwise analysis of NODDI metrics in gray matter (Nazeri et al., 2015, 2017). For consistency, I used GBSS for both white and grey matter. Briefly, the *Atropos* segmentation tool (Avants et al., 2011) in Advanced Normalization Tools (ANTs) was used to generate WM fraction maps from FA maps in each subject. Then GM fraction maps were generated by subtracting WM fraction maps and CSF fraction maps (NODDI FISO parameter maps) from the subject's FA map.

The 7 native diffusion space parameter maps (FA, RD, AD, MD, ICVF, ODI and FISO), gray matter fraction maps, and WM fraction maps were nonlinearly warped to the FSL HCP1065 FA template, resampled to the ABCD resolution (1.7 $mm^3$). Standard-space gray matter fraction maps and WM fraction maps were averaged to create mean gray and WM images, which were skeletonized using the *tbss_skeleton* tool in FSL. Finally, the parameter maps were projected onto the population skeletons from the subjects' local maxima. Initial feasibility group analyses were run which took several weeks of computation time to complete. Upon encountering additional technical difficulties, I pivoted to the previously described ROI approach.

Statistical Modeling

Group level statistics were generated using FSL's permutation analysis of linear models (PALM) (Winkler et al., 2014) with 500 permutations. Random effects of site and family relationship were modeled using exchangeability blocks (Winkler et al., 2015). PALM can simultaneously test a statistical model using multiple imaging metrics calculated from the same

ROIs (or voxels). For WM ROI analyses, the metrics included in the omnibus analysis were FA, MD, AD, RD, and tract volume. For subcortical GM ROIs, MD, AD, RD, and structure volume were included. Cortical GM ROIs analyses included MD, AD, RD, volume, and thickness. PALM implements two levels of family-wise error correction, controlling type I error inflation when testing multiple ROIs with the same metric (FWE) and controlling type I error when testing multiple ROIs across multiple metrics (mFWE).

Group Difference ROI Analyses

To test for group differences, three PALM linear models (WM ROIs, GM subcortical ROIs, GM cortical ROIs) were fit with asthma history (present or absent) as the regressor of interest and age, sex, and mean head motion were included as the OSF pre-registered covariates of no interest. I report both ROIs with a significant omnibus Fisher F test as well as individual metrics that survive multiple comparison correction for both regions and metrics (mFWE).

Asthma-Related Moderators ROI Analyses

For youth with asthma, three PALM linear models were fit as described above with number of lifetime asthma attacks as the regressor of interest. Similarly, three PALM linear models were fit for youth with asthma severity scores, with examining cumulative severity as the regressor of interest.

Whole-brain Correlations with Serum Markers

For both the serum eosinophil count and the neutrophil to lymphocyte ratio, a PALM linear model was fit for the interaction between group and serum markers. This included the ability to test for relationships between serum markers and brain structure in each group individually. These analyses were repeated for both GM and WM.

Mediation Analyses

To test whether the data is consistent with a statistical model where changes in brain metrics mediate the relationship between asthma history and negative cognitive and emotional outcomes, I tested two types of mediation analyses. First, I performed cross-sectional mediation analyses where I tested whether microstructure mediated the relationship between cumulative asthma history and CBCL and NIH Toolbox outcomes. For the CBCL outcomes, I additionally tested whether the data fit longitudinal mediation models; in other words, whether the relationship between asthma history at baseline and CBCL scores at year 3 were mediated by year 2 microstructure.

Data was considered consistent with a mediation model if, within a single anatomical region, there was evidence of four criteria: 1) a relationship between microstructure and asthma history, 2) a relationship between microstructure and a behavioral outcome, 3) a relationship between the behavioral outcomes and asthma history, and 4) the estimated confidence interval around the size of the indirect effect of baseline asthma history on behavior did not include zero.

Criterion 1 was tested in the PALM ROI analyses described above. Criterion 2 was tested in Chapter 2. To rigorously test Criterion 3, I ran a PALM analysis where I fit a linear model with the behavioral outcome of interest as the regressor of interest and age, sex, and mean head motion were included as covariates of no interest. For ROIs that met Criteria 1-4, I estimated a confidence interval around the indirect effect using a bootstrapping procedure with the laavan package in R version 0.6.16 (Rosseel, 2012). Because the laavan package does not support random effects, bootstrapping analyses were performed with one child per family, prioritizing youth with an asthma history in discordant sibling pairs as described in Chapter 2. When estimating the indirect effect, the model of the effect of asthma on outcomes included age, sex,

and site as covariates of no interest. The model of the effect of asthma on volume included age, sex, site, and mean head motion as covariates of no interest.

## Results

### Group Difference ROI Analyses

#### White Matter Microstructure and Morphology

In the omnibus Fisher test, there were no significant differences in structure between youth with and without an asthma history in any of the 31 tracts tested. However, the volume of the left fornix was significantly lower in youth with an asthma history than youth without an asthma history (mFWE $p = 0.0178$; Figure 3.1; Table 3.1).

Although these findings did not survive the most conservative FWE $p < 0.05$ correction across multiple modalities, when correcting within modalities, youth with an asthma history showed lower FA in the left superior longitudinal (FWE $p = 0.0073$) and temporal (FWE $p = 0.0053$) fasciculi, trending in that direction for the left parietal superior longitudinal fasciculus (FWE $p = 0.0637$). Youth with an asthma history also showed lower AD in these same tracts (e.g. left superior longitudinal fasciculus: FWE $p = 0.001$, left temporal longitudinal fasciculus: FWE $p = 0.0012$; left parietal superior longitudinal fasciculus: FWE $p = 0.0130$), as well as lower AD in white matter of the left inferior superior frontal cortex (FWE $p = 0.0136$).

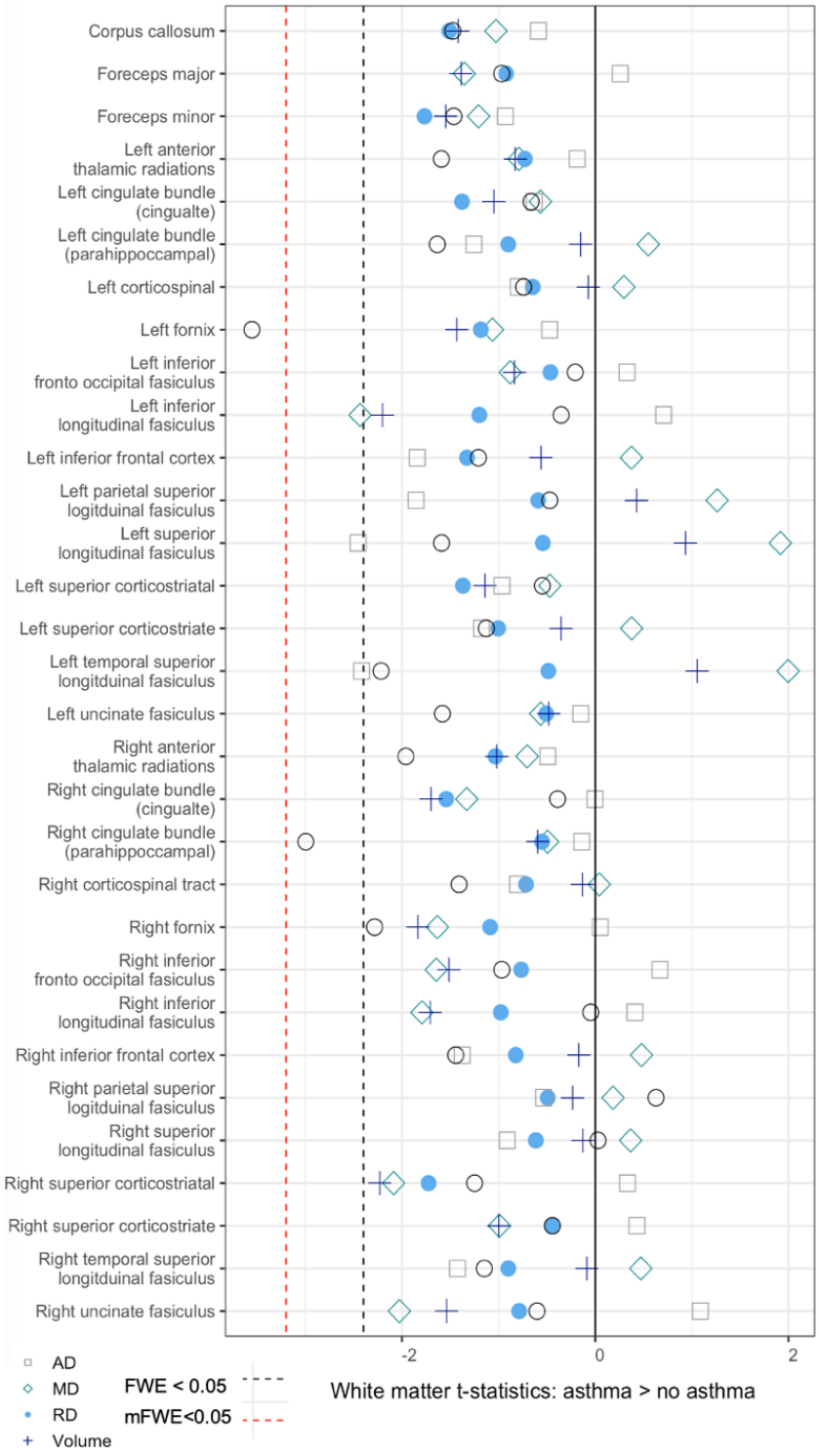


**Figure 3.1 Group differences in white matter structure**

T-statistics from FSL's permutation analysis of linear models (PALM) testing for differences between youth with and without an asthma history in five metrics: axial diffusivity (AD), fractional anisotropy (FA), mean diffusivity (MD), radial diffusivity (RD), and tract volume. Models corrected for age, sex, mean head motion, imaging site and family membership. Dashed

lines indicate regions that survived family-wise error correction controlling for multiple tracts (FWE, black) or controlling for multiple modalities (mFWE, red).

Subcortical Grey Matter Microstructure and Morphology

In the omnibus Fisher test, the right caudate nucleus showed significant group differences in microstructure ($F = 19.77$, $p = 0.011$; Figure 3.2, Table 3.2). This was driven by smaller GM volume in the right caudate for youth with asthma (mFWE $p = 0.0028$). No other structures had significantly different Fisher tests (Table 2.2). Although the whole region did not have a significant Fisher F test, even when stringently correcting for multiple ROI comparisons across modalities, youth with an asthma history had smaller GM volumes in the right hippocampus (mFWE $p = 0.0061$). Youth with an asthma history trended towards having smaller GM volumes in the left hippocampus (FWE $p = 0.048$, mFWE $p = 0.062$), left caudate nucleus (FWE $p = 0.071$, mFWE $p = 0.0973$), left amygdala (FWE $p = 0.0492$, mFWE $p = 0.0635$), right amygdala (FWE $p = 0.0541$, mFWE $p = 0.071$), and left accumbens (FWE $p = 0.0523$, mFWE $p = 0.0681$).

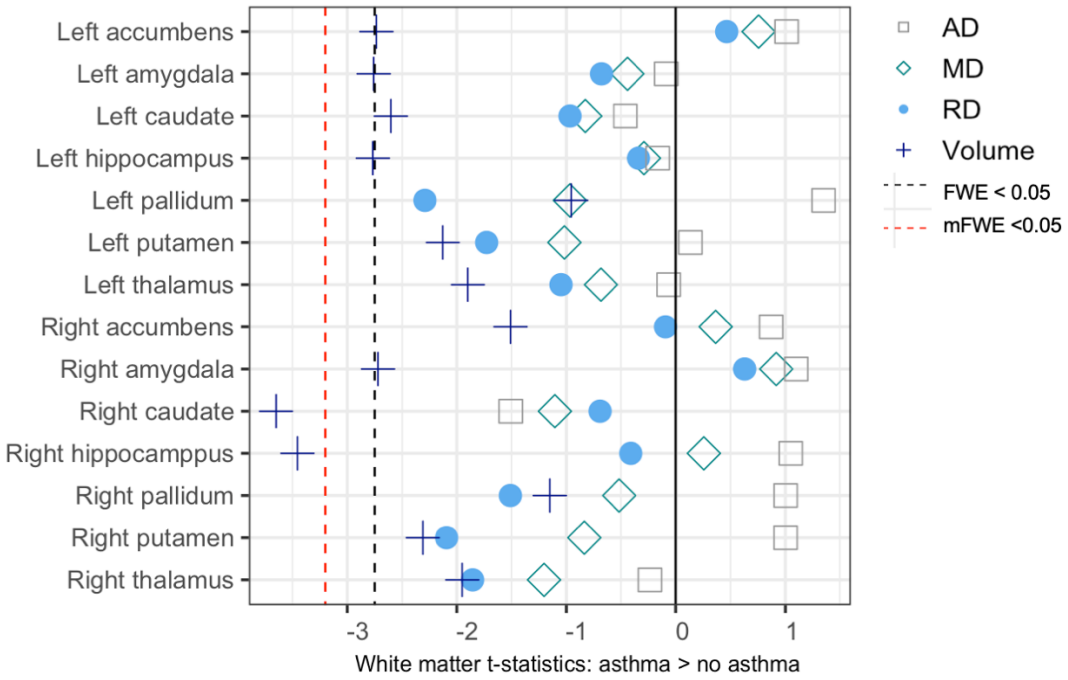


**Figure 3.2 Group differences in subcortical grey matter structure**

T-statistics from FSL's permutation analysis of linear models (PALM) testing for differences between youth with and without an asthma history in four metrics: axial diffusivity (AD), fractional anisotropy (FA), mean diffusivity (MD), radial diffusivity (RD), and tract volume. Models corrected for age, sex, mean head motion, imaging site and family membership. Dashed line indicates the region survived family-wise error correction controlling for multiple tracts (FWE, black) or additionally controlling for multiple modalities (mFWE, red).

Cortical Grey Matter Microstructure and Morphology

Only the left parieto-occipital sulcus had a significant group difference in morphology by the omnibus test ($F = 51.83$ , $p = 0.015$). However, when stringently correcting for multiple comparisons across modalities, youth with an asthma history had lower cortical thickness and lower volume than youth without an asthma history in several additional regions. Regions of lower thickness included key regions of the salience network, such as the circular sulcus of the left anterior insula (mFWE $p = 0.0028$) and the right middle anterior part of the cingulate gyrus and sulcus (mFWE $p = 0.028$). Further, youth with an asthma history had lower thickness in the left orbital gyrus (mFWE $p = 0.020$), right parahippocampal gyrus (mFWE $p = 0.036$), somatomotor areas including the left central sulcus (mFWE $p = 0.026$), left postcentral gyrus

(mFWE p = 0.0119), left paracentral lobule and sulcus (mFWE p = p 0.038). Finally youth with asthma had lower cortical thickness in several areas of the occipital lobe, including the right occipital pole (mFWE p = 0.0401), right posterior transverse collateral sulcus (mFWE p = 0.027), bilateral lateral occipito-temporal gyri (L mFWE p = 0.0099, R mFWE p = 0.0077), bilateral parieto-occipital sulci (L mFWE p < 0.0001, R mFWE p = 0.0087), and bilateral medial occipito-temporal/lingual sulci (L mFWE p = 0.0012, R mFWE p = 0.0014).

In addition to lower cortical thickness, youth with an asthma history had smaller cortical GM volumes in the left anterior insula (mFWE p = 0.0217), left orbital gyri (mFWE p = 0.0201), left postcentral gyrus (mFWE p = 0.0007), and left temporal pole (mFWE p = 0.0173). Smaller GM volumes in youth with an asthma history were also observed in the bilateral superior parietal lobules (L mFWE p = 0.0264 , R mFWE p = 0.0215) and left precuneus (mFWE p = 0.0418).

Asthma Related Moderators

Higher number of lifetime asthma attacks ($N$ = 1193) was associated with a smaller volume of the right insula (t = 4.16, mFWE $p$ = 0.002), left insula (t = 3.49, mFWE $p$ = 0.025), the right interparietal/transverse parietal sulci (t = 3.71, mFWE p =0.012), and marginally related to a smaller right superior parietal lobule volume (t = 3.09, mFWE p= 0.083). There were no associations between lifetime asthma attacks and either WM or subcortical GM metrics. There were also no relationships detected between asthma severity ($N$ = 238) and WM, subcortical GM, or cortical GM (Appendix B).

Whole Brain Voxelwise Analyses

I tested four models looking for group differences in the voxelwise association between brain microstructure and serum markers for the 497 youth with both serum data and quality diffusion weighted data. I examined differences in the relationship between NLR and eosinophils

in both GM and WM. In the omnibus Fisher tests, no voxels survived the $p < 0.05$ FWE correction for any of the contrasts tested, detecting no group by inflammatory marker interactions and no relationship between microstructure and inflammatory markers in either group individually.

Mediation Analyses

To identify regions that may mediate the relationship between group differences in brain microstructure and cognitive and emotional outcomes, I ran PALM analyses to determine if there were regions where brain structural metrics were associated with outcomes of interest. For a comprehensive description of associations beyond those described in subsequent mediation analyses, see Tables B1 to B24. Briefly, across groups, poorer performance on all NIH Toolbox metrics tested (*g*, executive functioning, language, memory) was associated with smaller WM tract volumes in all tracts tested, smaller GM volumes in all subcortical structures tested, and widespread decreases in cortical GM volume and decreases in cortical thickness. For relationships between brain metrics and CBCL scores, higher total problems and higher attentional problems were associated with lower GM volumes across all subcortical structures tested. Only a few structures were associated with internalizing symptoms (Appendix B).

Regions that showed correlations between cortical volume and behavioral scores and also showed group differences in the analyses described above included the left anterior insula, left orbital gyri, left central sulcus, left postcentral gyrus, bilateral precuneus, bilateral superior parietal lobule, left temporal pole. Regions that showed correlations between with cortical thickness and one or more behavioral scores included the left anterior insula, right anterior midcingulate cortex, left orbital gyri, left orbital part of the inferior frontal gyrus, left central sulcus, left postcentral gyrus, left paracentral lobule and sulcus, left sulcus intermedius primus,

right superior temporal sulcus, left temporal pole, bilateral parahippocampal gyrus, right posterior transverse collateral sulcus, bilateral parietooccipital sulcus, bilateral lateral occipito temporal gyrus, bilateral medial occipito temporal sulcus and lingual sulcus, left middle occipital gyrus, and right occipital pole.

Given the larger than expected number of regions that showed associations with cognitive metrics and the more exploratory nature of the cortical GM ROI analysis, I focused on testing mediation in regions where I had a-priori hypotheses including the WM volume of the left fornix, fractional anisotropy (FA) in the superior longitudinal fasciculus (SLF), GM volume of the right caudate, right hippocampus, and left anterior insula, as well as GM thickness of the left anterior insula and right anterior mid cingulate cortex were further explored for evidence of statistical mediation. The results of the mediation analyses are reported below.

Although group differences in WM metrics were identified in the permutation testing describe in previous sections, when estimated with the bootstrapping procedure to test mediation models, the relationship between asthma and fornix volume (95% CI [-0.114, 0.016]), the relationship between asthma and SLF FA (95% CI [-0.091, 0.026]), and the relationship between asthma and cortical thickness of the anterior cingulate 95% CI [-0.114, 0.065] were not significant. Thus, the conditions to test mediation further were not met.

GM volume of right caudate and right hippocampus

Data was consistent with a statistical model where smaller GM volume of both the right caudate and the right hippocampus mediated the relationship between asthma history and reductions in memory (6.41%, 5.93%), general cognition (8.43%. 7.22%), executive functioning (7.51%, 6.35%), language (10.41%, 8.71%), and higher CBCL attention problems (5.80%, 4.04%), and CBCL total problem scores (5.14%, 4.55%; Table 3.4). Longitudinally, the volume

of right caudate mediated 3.36% the relationships between asthma status at 9-10 years old and lower attention scores at 12-14 years old. Longitudinally, asthma status at 9-10 years old was not related to right hippocampal volumes at 11- 13 95% CI [-0.145, 0.016] and thus did not meet criteria to test for mediation.

Cortical GM in Left Anterior Insula and Anterior Midcingulate

Data was consistent with a statistical model where smaller GM volume and smaller thickness of the left anterior insula mediated a relationship between asthma history and lower general cognitive scores (4.67%, 4.67%), executive function scores (3.42%, 5.13%), memory scores (2.76%, 4.15%), language scores (6.57%, 4.69%). Only smaller GM left anterior insula volumes mediated higher total problems (3.52%) and more inattentive symptoms (4.56%; Table 3.5). Asthma at age 9-11 years old was not related to lower anterior insula cortical thickness at 11-13 95% CI [-0.164, 0.094]. Thus, the conditions to test for mediation longitudinally were not met.

## Discussion

The current study is the largest analysis of brain structure in youth with asthma to date. I hypothesized that WM microstructural differences between youth with and without asthma would be localized to the fronto-parietal network (FPN) and the fronto-striatal/fronto-limbic reward network. I further hypothesized that structural changes would be correlated with asthma-related moderators in youth with asthma and that structural changes would mediate the relationship between asthma history and both lower NIH Toolbox scores and higher numbers of CBCL parent-reported problems.

Across WM, cortical GM, and subcortical GM, the localization of group differences was partially consistent with my hypothesis. I found youth with asthma had trending lower FA in one

key FPN tract, the superior longitudinal fasciculus. In GM metrics, I did not see differences in the thalamus or FPN as I expected, but I did observe group differences in striatal regions (caudate nucleus of basal ganglia), salience network regions (anterior cingulate, anterior insula), and the orbital frontal cortex. Further, reductions in GM volume of the left anterior insula were more pronounced in youth with higher number of lifetime asthma attacks. Notably, I found evidence that the data were consistent with a statistical model where smaller GM volumes in right caudate partially mediated the cross-sectional relationship between asthma history and lower general cognition, memory, language and executive functioning, as well as higher attention problems. A smaller volume of right caudate also partially mediated the relationships between asthma status at 9-10 years old and lower attention scores at 12-14 years old.

Are Differences Between Youth With and Without Asthma Consistent With Differences in Structural Maturity?

I hypothesized that youth with asthma would have less mature brain structural metrics, consistent with a disruption in typical development. These hypotheses were based on WM microstructural metrics, which have a well-defined developmental trajectory where FA, NDI, and WM volume reliably increase with age (DiPiero et al., 2022; Goddings et al., 2021; Mukherjee et al., 2002). When I did find group differences, youth with an asthma history consistently had smaller WM volumes, smaller cortical and subcortical GM volumes, and lower cortical thickness than youth with no asthma history. Cross-sectional GM morphometry metrics are more difficult to interpret in developmental terms because cross-sectional and longitudinal predictions can go in opposite directions. Within individuals, GM thinning is related to increase maturity and better cognitive performance. This is driven by a combination of decreased synaptic density, increased pruning of dendritic spines, reductions in glial cells, and increased myelination

within the cortex (Backhausen et al., 2022; Norbom et al., 2021). However, between individuals, higher cortical GM volumes are correlated with positive cognitive and emotional outcomes across development (Barch et al., 2022). This was consistent with the results of my correlational analyses where between subjects, larger cortical GM volumes and greater cortical GM thickness were associated with better performance on cognitive tasks. The direction of cross-sectional group differences in subcortical grey matter volumes can also be difficult to interpret in developmental terms. The normal developmental growth trajectory varies between subcortical structures. Within individuals, there will sometimes even be bilateral differences in the directions that structures change volume with age (Mills & Tamnes, 2014). When averaged over larger populations, subcortical volumes tend to increase with age and larger volumes tend to be correlated with positive cognitive and emotional outcomes (Barch et al., 2022), which was consistent with my correlational findings where larger subcortical GM volumes were associated with better cognition and fewer parent-reported problems.

Thus, while I cannot definitively say that one group's profile is "more mature," the associations with NIH Toolbox and CBCL scores consistently suggested that higher GM volume, greater WM volumes, and greater cortical thickness were associated with salubrious outcomes while lower GM volumes, lower WM volumes, and smaller cortical thickness were associated with deleterious outcomes. Whether the pattern of findings represents accelerated maturity, delayed maturity, or a process of volume loss (e.g. like atrophy), they still appear to be associated with poor outcomes. I will discuss the implications of the regions affected on brain function and behavior, and then I will return to consider the potential cellular basis underlying the direction of the observed group differences.

Key Salience Network Nodes Mediate Cognitive Differences Between Youth With and Without an Asthma History

I hypothesized that cognition-related structural differences between youth with asthma would be localized to the developing frontoparietal network (FPN), including lower WM microstructural integrity in interlobar fronto-parietal tracts. This hypothesis was partially supported. Youth with asthma had trending lower FA in the SLF, although this did not survive the most stringent multi-modality FWE correction. In the overall sample, reduced FA in SLF was related lower language scores and trended towards lower *g* and lower memory scores. This is consistent with previous studies of youth brain microstructure that have found relationships between lower FA in the SLF and lower cognitive abilities (Goddings et al., 2021). However, reduced FA in the SLF did not statistically mediate the relationship between asthma history and cognitive outcomes, nor was it related to asthma severity or inflammatory characteristics.

I also hypothesized that GM differences between youth with and without asthma would be localized to canonical FPN nodes, such as the middle frontal gyrus and inferior parietal lobule (Marek & Dosenbach, 2018). Instead, I found that youth with asthma had lower cortical thickness within key GM regions of the salience network, and that these changes were consistent with statistical mediation between asthma history and lower cognitive performance. Specifically, the anterior insula, anterior midcingulate cortex, and the amygdala are the core regions of the salience network, important for both cognitive control and the regulation of inflammation (Menon & D'Esposito, 2022; Seeley, 2019; Shackman et al., 2011). Lower GM volume and lower cortical thickness of the left anterior insula partially mediated the relationship between asthma history and all four cognitive metrics. Strikingly, volume decreases in the bilateral anterior insula were proportional to the number of lifetime asthma attacks.

Both salience network regions and FPN regions are critical for executive functioning, especially in youth. The anterior insula and anterior cingulate cortex (ACC) are more strongly recruited in tasks that classically rely on FPN function, like working memory tasks, in youth compared to adults (Andre et al., 2016; Simmonds et al., 2017), and the activation of these salience network regions is more closely related to task performance in youth compared to adults (Rosenberg et al., 2020; Yaple & Arsalidou, 2018). A recent PET imaging study also suggests that the timing of salience network and FPN development differs, and the timing of the development may be relevant to youth cognition. In a sample of youth 9-12 years old, age-related improvements in performance on executive function tests were mediated not only by increased structural maturity in the frontal cortex and the cingulate (increased FA), but in changes in metabolism. A marker of energy metabolism (*N*-acetyl-l-aspartate), interpreted as an indicator of structural growth, increased in salience network regions (insula and ACC) while it decreased in the parietal cortices, which are more traditional FPN members (Baron Nelson et al., 2019). This suggests that decreases in salience network regions' abilities to contribute to cognitive control might have larger effect in this age rage than has been observed in adults.

Unlike FPN, salience network regions have a special relationship with inflammation. In addition to their role in autonomic processing and implicit emotion regulation (Menon & D'Esposito, 2022; Seeley, 2019), salience network regions, and the insula specifically, are involved in sensing and regulating peripheral inflammation (Koren et al., 2021; Rolls, 2019). In asthma specifically, acute increases in anterior cingulate cortex (ACC) and insula activity in response to emotional stimuli (social stress and unpleasant emotional stimuli) have been associated with greater increases in airway inflammation in people with asthma (Ritz et al., 2019; Rosenkranz, Esnault, et al., 2022; Rosenkranz et al., 2005, 2018). The observation that structural

changes with youth with asthma scale with lifetifme attack could theoretically either be a consequence of higher exposure to inflammation, or a marker of difficulty regulating inflammation. Indeed, one could imagine a feedback loop, like the process that has been documented in stress-related hippocampal volume reduction, where cortical changes associated with elevated inflammation subsequently increase the propensity for future inflammation. However, more work needs to be done to establish to what extent the insula's inflammation regulation functions and cognitive control of attentional functions rely on interdependent cells and circuits.

Differences in Cognitive Performance Between Youth With and Without Asthma Mediated by Fronto-Striatal Circuitry

I also hypothesized that there would be group differences in brain structure between youth with and without an asthma history in the striatum and the orbital frontal cortex. This was partially supported as group differences were localized slightly differently than I expected. A large body of work, particularly work focused on the relationships between circuiting inflammation and depression, has found effects of inflammation on the connectivity between the nucleus accumbens of the basal ganglia and the medial orbital frontal cortex (Bekhbat et al., 2022; Nusslock et al., 2024). Instead of microstructural differences in the accumbens, I found that youth with an asthma history had lower GM volumes in the right caudate nucleus, a more dorsal region of the striatum. Lower GM volume of the right caudate nucleus statistically mediated the relationship between asthma history and lower scores on the four cognitive metrics, as well as more total parent-reported problems and more attention problems. Finally, lower volume of the right caudate statistically mediated the relationships between asthma status at 9-10 years old and lower attention scores at 12-14 years old. Interestingly, there were also group

differences in morphology in a prefrontal cortical area that is suturally connected to the caudate, a more lateral part of the orbital frontal cortex. Specicially, youth with asthma had smaller GM volumes in the left orbital gyrus and left orbital portion of the inferior frontal gyrus. Further, youth with asthma had reduced FA and increased AD in the adjacent WM of the left inferior superior frontal cortex, consistent with reduced structural connectivity between the prefrontal cortex and striatum. The co-localized findings across multiple metrics could be consistent with a change in the functional circuit.

While much of the work on the role of inflammation in depression has focused on the relationship between inflammation in the ventral striatum and reduced reward sensitivity (Nusslock et al., 2024), the caudate is also sensitive to inflammatory cues. The effects of inflammation on caudate function are thought to be related to the motor slowing in inflammatory states (Felger & Treadway, 2017). For example, in patients chronically treated with TNF-a, decreased dopamine uptake and turnover was observed in the caudate and putamen, in addition to the ventral striatum (Capuron et al., 2012). When their functions are carefully segregated, the ventral striatum is more involved in representing hedonic value, while the dorsal striatum has a greater role in action selection, but they work together during reward learning, and flexible, goal-directed behavior (A. P. Chen et al., 2021). The associations found in this study between caudate volume and cognitive abilities is consistent with the known role of the caudate in action selection during more classically cognitive related processes like inhibitory control (Schmidt et al., 2012; Westbrook et al., 2020). Indeed, the caudate nucleus works with the inferior frontal gyrus, anterior insula and anterior cingulate during inhibitory control and motivational control of goal-directed action (Oyama et al., 2022).

Inhibitory control is one of the executive control functions that matures markedly during adolescence (Cohen-Gilbert & Thomas, 2013; Parr et al., 2022). Microstructural maturation in the caudate has been previously linked to improving inhibitory control in this age range, as well as improvements in attention (Baron Nelson et al., 2019). The relationship lower volume and thickness the caudate and lateral orbital frontal cortex may reflect youth with asthma having more difficulty with inhibitory control. In our analyses, the structure of the caudate correlated with cognitive performances more broadly, rather than inhibitory control specifically, but future work on the functional consequences of chronic inflammation should continue to investigate the more dorsal-lateral fronto-striatal circuits in addition to the medial circuits.

Differences in Cognitive Performance Between Youth With and Without Asthma Mediated By Hippocampal Volume

Across multiple metrics, youth with asthma showed structural changes in key memory-related structures in the temporal lobe. Youth with an asthma history had smaller GM volumes of the right hippocampus (trending bilaterally), lower WM volumes of the left fornix, a key WM tract connecting the hippocampus to the nucleus accumbens and medial prefrontal cortex (Benear et al., 2020), reduced GM thickness in the left parahippocampal gyrus, bilateral lateral occipitotemporal, medial occipitotemporal, and lingual sulci, and reduced GM volume in the left temporal pole. Further, smaller volume of the right hippocampus was consistent with a cross-sectional mediation model between asthma history and lower general cognition, memory, language and executive functioning, as well as higher attention problems.

The hippocampus and medial temporal lobes have important roles in both cognition and emotion. The best-known function of the hippocampus is in episodic memory, and there have been studies linking reduced hippocampal volume to worse memory performance. Indeed, larger

hippocampal GM volume has been related to better out of scanner working memory performance in ABCD sample (Assari et al., 2021). Reductions in hippocampal volumes is associated with early life chronic stress in populations with a range of psychiatric symptoms (Besteher et al., 2019; Calem et al., 2017).

Early life stress also has proinflammatory effects (Chiang et al., 2022), and structural differences in the medial temporal lobe have previously been related to elevated peripheral inflammation in adults. Specifically, smaller hippocampal volumes have previously been observed in men with asthma compared to healthy controls (Carlson et al., 2017), higher circulating levels of IL-6 have been associated with smaller hippocampal GM volumes in healthy adults (Marsland et al., 2008), and higher levels of circulating inflammatory cytokines have been correlated with reduced microstructural integrity in the fornix in adults with major depressive disorder (L. Chen et al., 2022; Lim et al., 2021; Sugimoto et al., 2018; Thomas et al., 2021). Rodent work suggests that asthma-related inflammation can cause hippocampal volume reductions. In a rat model of asthma, the asthma group had smaller hippocampal volumes than the unexposed group, and more neuroinflammation indexed by increased labeling of astrocytes (GFAP) and microglia (IbA1). Within the asthma group, smaller hippocampal volumes were correlated with higher indices of depression-like behavior (Dehdar & Raoufy, 2023a). Further, both behavioral changes and hippocampal volume reductions were prevented by pre-treatment with corticosteroids, suggesting that inflammation is involved in the volume reduction process (Dehdar & Raoufy, 2023b).

A few longitudinal studies have found that smaller hippocampal volumes in childhood predict the later emergence of depressive symptoms (Barch et al., 2019a; Jones et al., 2017; Whittle et al., 2017). In one notable longitudinal investigation, both smaller hippocampal

volumes and smaller increases in hippocampal volumes over four years were associated with reduced episodic memory scores at 10-15 years old. While the study found only modest relationships between depressive symptoms and hippocampal volumes, smaller hippocampal volumes were robustly related to more emotion dysregulation and higher life-stress (Barch et al., 2019b). Inflammation from asthma may act similarly to a chronic stressor or exacerbate the effects of pre-existing stress-related inflammation. Hippocampal volumes may be a marker of future risk for emotional problems in youth with asthma, as well as risk that may be mitigated by early intervention.

Potential Cellular Underpinnings of Observed Structural Differences

The cellular basis of GM volume changes is uncertain, and this correlational study cannot establish if the biology of asthma has a causal impact on brain structure; nonetheless, I would like to introduce two mechanistic models by which asthma-related biology could affect brain structure.

One mechanism is that asthma could alter the normal process of brain maturation. For instance, in animal models, peripheral allergic inflammation can change the synaptic pruning activity of microglia (Caulfield et al., 2021; Saitoh et al., 2021). Synaptic pruning, along with experience-dependent myelination, are key cellular processes driving normative developmental changes in GM and WM structure. While it has been less explored in allergic asthma, peripheral inflammation-related changes in microglial function can also alter experience-dependent synaptic pruning (Brenhouse, 2023) which is critical for the development of the prefrontal cortex. In this case, the smaller volumes observed in the study would be a result of disrupted maturation process and correspond with hype-ramified, under-myelinated neurons. If the

microglia processes that support brain maturation are altered in youth with asthma, the timing and duration of exposure to peripheral inflammation may be critical to the neural sequelae.

Another mechanism by which asthma could alter brain structure is through a neurotoxic, neurodegenerative mechanism. A recent rodent model that examined the relationship between chronic lung inflammation and GM volume found that the group exposed to inflammation had reduced GM volumes in many of the same areas as the current study including the hippocampus, caudate/putamen, insula, cingulate cortex and somatosensory cortex, auditory cortex, visual cortex, and superior colliculus. In these areas, decreased GM volume was associated with reduced neuronal density and abnormal morphology. In the hippocampus, caudate/putamen, and insula, GM volumes were associated with pro-inflammatory cytokines of IL-1β, IL-6, TNF-α. In the insula, the levels of cytokines were further correlated with a marker of cell injury (FIPA of Nogo-A(J. Chen et al., 2019). In a recent analysis from our group, adults with high severity asthma (mean age 44), lower insula thickness was associated with higher serum levels of glial fibrillary acidic protein (GFAP), an index of reactive astrocytes indicative of neuroinflammation (Carrol et al, in prep). In this same sample, asthma was related to widespread increases in MD and RD in WM, consistent with myelin injury, and increased MD and RD were further associated with higher asthma severity and higher levels of serum GFAP (Rosenkranz, Dean, et al., 2022). Therefore, the findings in the current study could be consistent with early signs of neural injury. If this mechanism is at work in youth with asthma, we might expect the effects of exposure to asthma-related inflammation to be more cumulative and less specific to particular developmental windows.

Both altered development and neural injury mechanisms would predict similar directions of change in diffusion-weighted and morphological metrics. In this sample, we do not see

widespread increases in WM RD that might be more likely to occur more specifically with neurodegenerative processes. Further, one might expect changes secondary to an altered developmental process might be localized to specific, actively developing circuits, while a degenerative process might be more diffuse or localized based on a non-specific functional process like metabolic demand. The pattern of spatial findings in the current project included important developing regions consistent with my hypotheses, as well as unexpected, widespread cortical GM changes in the superior-medial parietal lobe and the occipital lobe that are not clearly consistent with specific developmental timing or with specific patterns of degenerative disease. Longitudinal work, more sophisticated imaging metrics like NODDI imaging, and targeted animal experiments may be able to adjudicate between one process over another. In contrast, both processes could be happening simultaneously or could influence one another. Serum biomarkers of degeneration might help provide clarity, as lumbar punctures to obtain cerebral spinal fluid have additional ethical drawbacks in youth. However, both compromised development and accelerated degeneration have the potential to be detrimental to developing cognitive ability and learning to regulate emotions, which improve markedly in typically developing youth from middle childhood to late adolescence (McLaughlin et al., 2011, 2015). These two processes may require different intervention strategies depending on the underlying cellular mechanisms and relevant signaling pathways involved. An important next step will be to more clearly identify whether elevated peripheral inflammation has a specific role in the observed structural changes in humans, and to determine whether the available inflammation-targeted treatments can interrupt negative cognitive and emotional sequelae.

Limitations

Some of the limitations of this investigation were explored in Chapter 2, notably, the uncertainty in the classification of asthma and asthma-related moderators as well as limitations in the outcome measures that I chose. This also relates to the problem of heterogeneity in asthma phenotypes and the variety of potential mechanisms by which asthma interacts with the central nervous system. Each individual with asthma will have a different combination of these mechanisms contributing to brain-behavior associations. Grouping all individuals with asthma together as having the same exposure cannot capture important individual differences in the peripheral inflammatory processes that may alter or be altered by brain-structure. While I speculated about the role of inflammation in asthma specifically, there are a variety of other disease relevant processes that could contribute or interact with effects of inflammation on brain structure, including potential vascular effects of asthma (Tattersall et al., 2018). The role of other factors known to impact inflammatory status that may serve as moderators, such as SES, race, and sex differences were not thoroughly explored.

There are additional limitations to ABCD neuroimaging metrics. I have discussed limitations in determining the cellular mechanisms associated with differences in these metrics. Further, regions that show cross-sectional differences at this age range may not be the regions changing most quickly with development. The originally planned voxelwise analyses have additional sensitivity in their spatial resolution and the planned NODDI metrics are more sensitive to age-related changes than traditional DTI measures. Further, the broad behavioral correlates I chose (latent NIH Toolbox scores and parent CBCL scores) likely are not the most precise estimation of the functional significance of the brain changes observed. While these

provide behavioral correlates to guide the functional significance of the interpretation of findings, but there is also a degree of reverse inference.

Additionally, there are limitations to statistical mediation. If any unmeasured factor could both cause asthma history and changes in brain structure, it could bias the size and potentially even the direction of estimated mediating effect. For example, any shared genetic factors that both increase propensity to develop asthma and influence neuronal development may qualify as an unmeasured factor (Z. Zhu et al., 2019). There is still much that is not known about the precise causal factors that lead to asthma and that drive brain structural development. There are also many social determinants of health that influence asthma risk and psychopathology expression, which make it unlikely that the simplified mediation model tested estimates the magnitude of the mediated effect without bias. Further, the mediation model assumes that both the relationship between asthma and brain function and the relationship between asthma and behavior change are unidirectional. Bidirectional effects are likely occurring where brain function and behavior influence also asthma management and increases asthma symptoms. However, this preliminary investigation justifies future more nuanced exploration of the interactions between asthma, brain structure, and behavioral changes.

Future Directions

Immediate future directions include completing the planned voxelwise analyses with NODDI metrics, which may increase the interpretability of some of the GM findings. Voxelwise analyses may have superior sensitivity to detect group differences in regions that do not align precisely with atlas-based parcellations or are further localized than the ROI average can detect. Going forward, instead of looking at GM and WM ROIs as independent tests, I would like to use more sophisticated clustering techniques to identify groups of metrics that tend to change

together. This would help to clarify whether the changes in the "salience network" and "cortico-striatal regions" are indeed two dissociable systems that can change independently, or if there is a different label that better classifies the underlying shared functions of the wide range of brain structural differences between youth with and without asthma.

I would also like test longitudinal neuroimaging models to see if asthma history or asthma-related moderators alter trajectories of structural change over time. It will also be important to examine the functional consequences of any group differences in structural trajectories. There are not high rates of depressive symptoms at the two-year assessment point, but this may provide an opportunity to explore whether group differences in brain microstructure predict risk for future anxiety and depressive symptoms that have been documented as more common in youth with asthma in the literature. Specifically, monitoring whether changes in structure are dynamic based on changes in asthma control over time will be an important clue about whether the current findings are related to asthma management.

These further investigations should be complemented by clinical studies that can more closely examine the relationship between brain microstructure and more specific phenotypic characteristics of asthma. Careful clinical phenotyping will be an important way to establish the characteristics of asthma that are most closely associated with brain changes (e.g. asthma control, lung function) and to examine whether there are individual differences in the biological drivers of brain structural alterations in youth with asthma. Together, population studies and clinical studies can generate more specific hypotheses that can be tested for a causal contribution in experimental settings and in animal models.

**Table 3.1 Group differences in white matter microstructure**

The table displays metrics generated from the two-tailed test of group differences across white matter ROIs with PALM. Each of the five metrics included in the omnibus test has a t-value, a *p* value corrected for multiple comparisons across ROIs (FWE), and a *p* value corrected for multiple comparisons across ROIs and modalities (mFWE *p*).
FA = fractional anisotropy; MD = mean diffusivity, RD = radial diffusivity; AD = axial diffusivity; * $p < 0.05$; $^{+}$ $p < 0.10$

| | Right fornix | Left fornix | Right cingulate bundle (cingualte) | Left cingulate bundle (cingualte) | Right cingulate bundle (parahippoccampal) | Left cingulate bundle (parahippoccampal) | Right corticospinal tract | Left corticospinal tract | Right anterior thalamic radiations | Left anterior thalamic radiations | Right uncinate fasciculus | Left uncinate fasciculus | Right inferior longitudinal fasciculus | Left inferior longitudinal fasciculus |
|---|---|---|---|---|---|---|---|---|---|---|---|---|---|---|
| **Asthma > No asthma** | | | | | | | | | | | | | | |
| **Fisher F** | **18.04** | **15.61** | **18.83** | **14.56** | **9.01** | **10.34** | **9.10** | **8.79** | **12.76** | **10.99** | **17.27** | **8.94** | **18.64** | **24.12** |
| **Fisher FWE p** | **0.658** | **0.778** | **0.618** | **0.825** | **0.978** | **0.957** | **0.977** | **0.981** | **0.893** | **0.943** | **0.698** | **0.979** | **0.627** | **0.362** |
| FA | -1.63 | -1.06 | -1.33 | -0.57 | -0.49 | 0.55 | 0.04 | 0.3 | -0.7 | -0.79 | -2.03 | -0.57 | -1.79 | -2.43 |
| FA FWE p | 0.898 | 0.992 | 0.969 | 0.999 | 0.999 | 0.999 | 0.999 | 0.999 | 0.999 | 0.999 | 0.702 | 0.999 | 0.833 | 0.42 |
| FA mFWE p | 0.909 | 0.993 | 0.972 | 0.999 | 0.999 | 0.999 | 0.999 | 0.999 | 0.999 | 0.999 | 0.728 | 0.999 | 0.85 | 0.451 |
| MD | 1.09 | 1.19 | 1.54 | 1.38 | 0.55 | 0.90 | 0.72 | 0.65 | 1.03 | 0.73 | 0.79 | 0.51 | 0.98 | 1.20 |
| MD FWE p | 0.454 | 0.402 | 0.234 | 0.306 | 0.727 | 0.553 | 0.648 | 0.682 | 0.482 | 0.642 | 0.612 | 0.745 | 0.512 | 0.395 |
| MD mFWE p | 0.992 | 0.986 | 0.934 | 0.966 | 0.999 | 0.997 | 0.999 | 0.999 | 0.994 | 0.999 | 0.999 | 0.999 | 0.995 | 0.985 |
| RD | 1.84 | 1.43 | 1.70 | 1.05 | 0.60 | 0.15 | 0.13 | 0.07 | 1.02 | 0.83 | 1.54 | 0.48 | 1.71 | 2.20 |
| RD FWE p | 0.458 | 0.681 | 0.536 | 0.846 | 0.952 | 0.989 | 0.99 | 0.992 | 0.856 | 0.909 | 0.626 | 0.966 | 0.531 | 0.263 |
| RD mFWE p | 0.831 | 0.957 | 0.887 | 0.993 | 0.999 | 0.999 | 0.999 | 0.999 | 0.994 | 0.998 | 0.935 | 0.999 | 0.884 | 0.614 |
| AD | -0.05 | 0.47 | 0.00 | 0.63 | 0.14 | 1.26 | 0.81 | 0.80 | 0.49 | 0.19 | -1.09 | 0.15 | -0.41 | -0.71 |
| AD FWE p | 0.704 | 0.411 | 0.675 | 0.324 | 0.601 | 0.087 | 0.24 | 0.243 | 0.40 | 0.575 | 0.979 | 0.595 | 0.854 | 0.931 |
| AD mFWE p | 0.999 | 0.999 | 0.999 | 0.999 | 0.999 | 0.98 | 0.998 | 0.999 | 0.999 | 0.999 | 0.999 | 0.999 | 0.999 | 0.999 |
| Volume | -2.28 | -3.55 | -0.39 | -0.66 | -3.00 | -1.64 | -1.41 | -0.74 | -1.96 | -1.59 | -0.60 | -1.58 | -0.05 | -0.35 |
| Volume FWE p | 0.200 | 0.012* | 0.924 | 0.862 | $0.050^{+}$ | 0.466 | 0.573 | 0.840 | 0.320 | 0.486 | 0.878 | 0.491 | 0.969 | 0.930 |
| Volume mFWE p | 0.601 | 0.018* | 0.999 | 0.999 | 0.135 | 0.944 | 0.981 | 0.999 | 0.818 | 0.954 | 0.999 | 0.956 | 0.999 | 0.999 |

Table 3.1 continued

| | Right inferior fronto occipital fasciculus | Left inferior fronto occipital fasciculus | Foreceps major | Foreceps minor | Corpus callosum | Right superior longitudinal fasciculus | Left superior longitudinal fasciculus | Right temporal superior longitduinal fasciculus | Left temporal superior longitduinal fasciculus | Right parietal superior logitduinal fasciculus | Left parietal superior logitduinal fasciculus | Right superior corticostriate | Left superior corticostriate | Right superior corticostriatal | Left superior corticostriatal | Right inferior frontal cortex | Left inferior frontal cortex |
|---|---|---|---|---|---|---|---|---|---|---|---|---|---|---|---|---|---|
| **Asthma > No asthma** | | | | | | | | | | | | | | | | | |
| **Fisher** | **15.42** | **10.82** | **14.69** | **20.08** | **17.03** | **9.96** | **12.91** | **11.08** | **12.42** | **10.34** | **11.26** | **11.18** | **11.13** | **24.16** | **15.61** | **10.71** | **15.23** |
| **Fisher FWE p** | **0.787** | **0.947** | **0.819** | **0.553** | **0.709** | **0.964** | **0.888** | **0.941** | **0.904** | **0.957** | **0.937** | **0.939** | **0.94** | **0.36** | **0.778** | **0.95** | **0.795** |
| FA | -1.65 | -0.88 | -1.36 | -1.21 | -1.03 | 0.37 | 1.92 | 0.47 | 2.00 | 0.18 | 1.26 | -0.99 | 0.38 | -2.09 | -0.47 | 0.48 | 0.37 |
| FA FWE p | 0.894 | 0.997 | 0.965 | 0.983 | 0.993 | 0.999 | 0.999 | 0.999 | 0.999 | 0.999 | 0.999 | 0.995 | 0.999 | 0.664 | 0.999 | 0.999 | 0.999 |
| FA mFWE p | 0.905 | 0.998 | 0.969 | 0.984 | 0.994 | 0.999 | 0.999 | 0.999 | 0.999 | 0.999 | 0.999 | 0.995 | 0.999 | 0.691 | 0.999 | 0.999 | 0.999 |
| MD | 0.77 | 0.46 | 0.92 | 1.77 | 1.51 | 0.62 | 0.54 | 0.9 | 0.49 | 0.49 | 0.59 | 0.45 | 1.01 | 1.73 | 1.37 | 0.82 | 1.33 |
| MD FWE p | 0.623 | 0.763 | 0.542 | 0.152 | 0.247 | 0.697 | 0.73 | 0.553 | 0.754 | 0.752 | 0.708 | 0.769 | 0.498 | 0.166 | 0.311 | 0.594 | 0.330 |
| MD mFWE p | 0.999 | 0.999 | 0.997 | 0.861 | 0.941 | 0.999 | 0.999 | 0.997 | 0.999 | 0.999 | 0.999 | 0.999 | 0.995 | 0.877 | 0.967 | 0.998 | 0.972 |
| RD | 1.51 | 0.84 | 1.39 | 1.55 | 1.42 | 0.13 | -0.93 | 0.09 | -1.05 | 0.24 | -0.43 | 0.999 | 0.35 | 2.23 | 1.14 | 0.17 | 0.56 |
| RD FWE p | 0.640 | 0.907 | 0.704 | 0.621 | 0.688 | 0.990 | 0.999 | 0.991 | 0.999 | 0.985 | 0.999 | 0.863 | 0.977 | 0.250 | 0.813 | 0.988 | 0.956 |
| RD mFWE p | 0.941 | 0.998 | 0.964 | 0.933 | 0.959 | 0.999 | 0.999 | 0.999 | 0.999 | 0.999 | 0.999 | 0.995 | 0.999 | 0.594 | 0.989 | 0.999 | 0.999 |
| AD | -0.67 | -0.33 | -0.26 | 0.93 | 0.59 | 0.91 | 2.45 | 1.43 | 2.42 | 0.54 | 1.86 | -0.43 | 1.18 | -0.33 | 0.97 | 1.38 | 1.84 |
| AD FWE p | 0.923 | 0.825 | 0.798 | 0.188 | 0.348 | 0.195 | 0.001* | 0.054$^{+}$ | 0.001* | 0.376 | 0.013* | 0.861 | 0.106 | 0.827 | 0.174 | 0.063$^{+}$ | 0.014* |
| AD mFWE p | 0.999 | 0.999 | 0.999 | 0.997 | 0.999 | 0.997 | 0.437 | 0.958 | 0.462 | 0.999 | 0.822 | 0.999 | 0.986 | 0.999 | 0.996 | 0.966 | 0.827 |
| Volume | -0.97 | -0.21 | -0.97 | -1.46 | -1.48 | 0.03 | -1.59 | -1.15 | -2.22 | 0.63 | -0.47 | -0.44 | -1.13 | -1.25 | -0.55 | -1.44 | -1.21 |
| Volume FWE p | 0.763 | 0.952 | 0.762 | 0.547 | 0.541 | 0.975 | 0.487 | 0.690 | 0.223 | 0.997 | 0.908 | 0.914 | 0.699 | 0.647 | 0.891 | 0.556 | 0.664 |
| Volume mFWE p | 0.999 | 0.999 | 0.999 | 0.975 | 0.974 | 0.999 | 0.954 | 0.996 | 0.651 | 0.999 | 0.999 | 0.999 | 0.997 | 0.993 | 0.999 | 0.977 | 0.994 |

**Table 3.2 Group differences in subcortical grey matter microstructure**

The table displays metrics generated from the two-tailed test of group differences across subcortical grey matter ROIs with PALM. For each of the four individual metrics included in the omnibus test, there are three additional statistics: a *t*-value, a *p* value corrected for multiple comparisons across ROIs (FWE), and a *p* value corrected for multiple comparisons across ROIs and modalities (mFWE). FWE = Familywise error, MD = mean diffusivity, RD = radial diffusivity; AD = axial diffusivity; * $p < 0.05$; $^{+}$ $p < 0.10$

| | Left thalamus | Left caudate | Left putamen | Left pallidum | Left hippocampus | Left amygdala | Left accumbens |
|---|---|---|---|---|---|---|---|
| **Fisher F Asthma < No asthma** | **15.21** | **19.77** | **19.44** | **16.34** | **17.3** | **18.22** | **13.15** |
| **Fisher F p** | **0.690** | **0.870** | **0.860** | **0.740** | **0.790** | **0.820** | **0.560** |
| MD | 0.68 | 0.83 | 1.02 | 0.97 | 0.29 | 0.44 | -0.76 |
| MD FWE p | 0.548 | 0.464 | 0.356 | 0.383 | 0.765 | 0.687 | 0.993 |
| MD mFWE p | 0.970 | 0.947 | 0.898 | 0.913 | 0.996 | 0.991 | 0.999 |
| RD | 1.05 | 0.97 | 1.73 | 2.29 | 0.34 | 0.68 | -0.47 |
| RD FWE p | 0.600 | 0.645 | 0.240 | 0.068 | 0.900 | 0.784 | 0.993 |
| RD mFWE p | 0.888 | 0.914 | 0.526 | 0.204 | 0.995 | 0.971 | 0.999 |
| AD | 0.06 | 0.46 | -0.13 | -1.35 | 0.16 | 0.09 | -1.01 |
| AD FWE p | 0.736 | 0.504 | 0.828 | 0.999 | 0.681 | 0.724 | 0.992 |
| AD mFWE p | 0.999 | 0.99 | 0.999 | 0.999 | 0.998 | 0.999 | 0.999 |
| Volume | 1.90 | 2.60 | 2.13 | 0.96 | 2.77 | 2.76 | 2.73 |
| Volume FWE p | 0.270 | $0.071^{+}$ | 0.186 | 0.714 | $0.048^{+}$ | $0.049^{+}$ | $0.052^{+}$ |
| Volume mFWE p | 0.416 | 0.097 | 0.283 | 0.917 | $0.062^{+}$ | $0.064^{+}$ | $0.068^{+}$ |

Table 3.2 Continued

| | Right thalamus | Right caudate | Right putamen | Right pallidum | Right hippocampus | Right amygdala | Right accumbens |
|---|---|---|---|---|---|---|---|
| **Fisher F Asthma < No asthma** | **20.35** | **30.13** | **20.69** | **12.34** | **19.87** | **12.75** | **8.30** |
| **Fisher F p** | **0.890** | **0.990** | **0.890** | **0.500** | **0.870** | **0.530** | **0.190** |
| MD | 1.20 | 1.10 | 0.84 | 0.52 | -0.26 | -0.92 | -0.36 |
| MD FWE p | 0.262 | 0.311 | 0.458 | 0.645 | 0.944 | 0.997 | 0.962 |
| MD mFWE p | 0.828 | 0.869 | 0.945 | 0.986 | 0.999 | 0.999 | 0.999 |
| RD | 1.85 | 0.69 | 2.09 | 1.51 | 0.41 | -0.63 | 0.09 |
| RD FWE p | 0.188 | 0.778 | 0.111 | 0.343 | 0.881 | 0.997 | 0.950 |
| RD mFWE p | 0.444 | 0.969 | 0.301 | 0.664 | 0.992 | 0.999 | 0.999 |
| AD | 0.23 | 1.51 | -1.00 | -1.00 | -1.05 | -1.10 | -0.87 |
| AD FWE p | 0.641 | 0.060 | 0.991 | 0.991 | 0.993 | 0.995 | 0.985 |
| AD mFWE p | 0.997 | 0.666 | 0.999 | 0.999 | 0.999 | 0.999 | 0.999 |
| Volume | 1.95 | 3.65 | 2.31 | 1.15 | 3.45 | 2.72 | 1.51 |
| Volume FWE p | 0.250 | 0.003* | 0.132 | 0.625 | 0.007* | $0.054^{+}$ | 0.448 |
| Volume mFWE p | 0.384 | 0.003* | 0.196 | 0.850 | 0.006* | $0.071^{+}$ | 0.664 |

**Table 3.3 Group differences in cortical grey matter microstructure and morphology**

The table displays metrics generated from the two-tailed test of group differences across grey matter ROIs with PALM. FWE = family-wise error corrected for multiple ROIs; mFWE = family-wise error corrected for multiple ROIs and multiple modalities; MD = mean diffusivity, RD = radial diffusivity; AD = axial diffusivity; * $p < 0.05$; $^{+}$ $p < 0.10$

| | Left fronto marginal gyrus and sulcus | Left inferior occipital gyrus and sulcus | Left paracentral lobule and sulcus | Left subcentral gyrus and sulci | Left transverse frontopolar gyri and sulci | Left anterior part of the cingulate gyrus and sulcus | Left middle anterior part of the cingulate gyrus and | Left middle posterior part of the cingulate gyrus and | Left posterior dorsal part of the cingulate gyrus | Left posterior ventral part of the cingulate gyrus | Left cuneus | Left opercular part of the inferior frontal gyrus | Left orbital part of the inferior frontal gyrus | Left triangular part of the inferior frontal gyrus | Left middle frontal gyrus |
|---|---|---|---|---|---|---|---|---|---|---|---|---|---|---|---|
| **Fisher F** | **7.74** | **11.28** | **40.33** | **10.39** | **6.38** | **2.38** | **14.89** | **16.84** | **15.68** | **14.34** | **11.81** | **3.41** | **22.32** | **6.4** | **12.17** |
| **Fisher FWE p** | **0.999** | **0.999** | **0.110** | **0.999** | **0.999** | **0.999** | **0.985** | **0.959** | **0.976** | **0.989** | **0.999** | **0.999** | **0.785** | **0.999** | **0.998** |
| MD | -1.17 | -0.7 | 1.95 | 0.41 | -0.61 | -0.97 | -0.45 | 0.25 | -0.25 | 0.66 | 0.35 | -0.47 | 0.15 | -0.59 | -0.92 |
| MD FWE p | 0.999 | 0.999 | 0.582 | 0.998 | 0.999 | 0.999 | 0.999 | 0.999 | 0.999 | 0.992 | 0.998 | 0.999 | 0.999 | 0.999 | 0.999 |
| MD mFWE p | 0.999 | 0.999 | 0.989 | 0.999 | 0.999 | 0.999 | 0.999 | 0.999 | 0.999 | 0.999 | 0.999 | 0.999 | 0.999 | 0.999 | 0.999 |
| RD | -1.42 | -0.98 | 2.06 | 0.57 | -0.56 | -1.28 | -0.41 | 0.48 | -0.22 | 0.77 | 0.27 | -0.66 | 0.16 | -0.42 | -0.89 |
| RD FWE p | 0.999 | 0.999 | 0.554 | 0.997 | 0.999 | 0.999 | 0.999 | 0.998 | 0.999 | 0.992 | 0.999 | 0.999 | 0.999 | 0.999 | 0.999 |
| RD mFWE p | 0.999 | 0.999 | 0.969 | 0.999 | 0.999 | 0.999 | 0.999 | 0.999 | 0.999 | 0.999 | 0.999 | 0.999 | 0.999 | 0.999 | 0.999 |
| AD | -0.56 | -0.11 | 1.53 | 0.05 | -0.58 | -0.26 | -0.45 | -0.26 | -0.25 | 0.36 | 0.47 | -0.05 | 0.11 | -0.84 | -0.87 |
| AD FWE p | 0.999 | 0.999 | 0.797 | 0.999 | 0.999 | 0.999 | 0.999 | 0.999 | 0.999 | 0.998 | 0.997 | 0.999 | 0.999 | 0.999 | 0.999 |
| AD mFWE p | 0.999 | 0.999 | 0.999 | 0.999 | 0.999 | 0.999 | 0.999 | 0.999 | 0.999 | 0.999 | 0.999 | 0.999 | 0.999 | 0.999 | 0.999 |
| Volume | -1.45 | -2.16 | -2.88 | -2.91 | -2.68 | -1.20 | -1.21 | -2.24 | -1.67 | 0.25 | -1.15 | -1.74 | -2.93 | -3.19 | -1.36 |
| Volume FWE p | 0.976 | 0.781 | 0.343 | 0.326 | 0.471 | 0.992 | 0.991 | 0.743 | 0.946 | 0.999 | 0.994 | 0.933 | 0.314 | 0.179 | 0.984 |
| Volume mFWE p | 0.999 | 0.977 | 0.605 | 0.580 | 0.764 | 0.999 | 0.999 | 0.964 | 0.999 | 0.999 | 0.999 | 0.999 | 0.563 | 0.342 | 0.999 |
| Thickness | -1.76 | -2.31 | -3.87 | -1.18 | -1.22 | 0.70 | -2.85 | -2.76 | -2.88 | -1.32 | -1.49 | 0.59 | -3.60 | -1.24 | -2.60 |
| Thickness FWE p | 0.926 | 0.643 | 0.026* | 0.998 | 0.998 | 0.999 | 0.300 | 0.351 | 0.281 | 0.995 | 0.981 | 0.999 | 0.056 | 0.997 | 0.446 |
| Thickness mFWE p | 0.999 | 0.862 | 0.038* | 0.999 | 0.999 | 0.999 | 0.444 | 0.517 | 0.417 | 0.999 | 0.999 | 0.999 | 0.082 | 0.999 | 0.644 |

Table 3.3 continued

| | Left long insular gyrus and central sulcus of the insula | Left short insular gyri | Left middle occipital gyrus | Left superior occipital gyrus | Left lateral occipito temporal gyrus | Left lingual gyrus | Left parahippocampal gyrus | Left orbital gyri | Left angular gyrus | Left supramarginal gyrus | Left superior parietal lobule | Left postcentral gyrus | Left precentral gyrus | Left precuneus |
|---|---|---|---|---|---|---|---|---|---|---|---|---|---|---|
| **Fisher F** | **14.26** | **23.18** | **19.3** | **15.19** | **34.8** | **17.5** | **26.46** | **28.63** | **10.08** | **11.69** | **11.58** | **32.17** | **16.94** | **15.71** |
| **Fisher FWE p** | **0.99** | **0.747** | **0.899** | **0.982** | **0.24** | **0.946** | **0.589** | **0.484** | **0.999** | **0.999** | **0.999** | **0.331** | **0.957** | **0.976** |
| MD | 0.40 | 1.02 | -1.00 | 0.44 | 1.15 | -0.34 | 0.63 | 0.52 | -0.18 | 0.11 | -0.79 | 0.84 | 0.46 | 0.42 |
| MD FWE p | 0.998 | 0.963 | 0.999 | 0.997 | 0.94 | 0.999 | 0.993 | 0.996 | 0.999 | 0.999 | 0.999 | 0.981 | 0.997 | 0.997 |
| MD mFWE p | 0.999 | 0.999 | 0.999 | 0.999 | 0.999 | 0.999 | 0.999 | 0.999 | 0.999 | 0.999 | 0.999 | 0.999 | 0.999 | 0.999 |
| RD | 0.47 | 1.02 | -0.35 | 0.59 | 1.42 | -0.47 | 0.76 | 0.33 | 0.04 | 0.26 | -0.64 | 1.01 | 0.43 | 0.31 |
| RD FWE p | 0.999 | 0.975 | 0.999 | 0.997 | 0.894 | 0.999 | 0.993 | 0.999 | 0.999 | 0.999 | 0.999 | 0.977 | 0.999 | 0.999 |
| RD mFWE p | 0.999 | 0.999 | 0.999 | 0.999 | 0.999 | 0.999 | 0.999 | 0.999 | 0.999 | 0.999 | 0.999 | 0.999 | 0.999 | 0.999 |
| AD | 0.19 | 0.83 | -1.67 | 0.17 | 0.39 | -0.1 | 0.31 | 0.7 | -0.52 | -0.21 | -0.99 | 0.51 | 0.47 | 0.6 |
| AD FWE p | 0.999 | 0.98 | 0.999 | 0.999 | 0.998 | 0.999 | 0.999 | 0.989 | 0.999 | 0.999 | 0.999 | 0.996 | 0.997 | 0.993 |
| AD mFWE p | 0.999 | 0.999 | 0.999 | 0.999 | 0.999 | 0.999 | 0.999 | 0.999 | 0.999 | 0.999 | 0.999 | 0.999 | 0.999 | 0.999 |
| Volume | -2.13 | -3.04 | -3.08 | -2.49 | -2.25 | -0.32 | -3.07 | -4.85 | 0.15 | -2.48 | -4.00 | -4.76 | -3.38 | -3.89 |
| Volume FWE p | 0.799 | 0.250 | 0.233 | 0.590 | 0.735 | 0.999 | 0.235 | <0.001* | 0.999 | 0.597 | 0.013* | < 0.001* | 0.111 | 0.021* |
| Volume mFWE p | 0.982 | 0.464 | 0.436 | 0.876 | 0.961 | 0.999 | 0.438 | <0.001* | 0.999 | 0.882 | 0.026* | 0.001* | 0.218 | 0.042* |
| Thickness | -2.11 | -2.89 | -3.66 | -2.23 | -4.31 | -3.07 | -3.78 | -4.08 | -1.43 | -1.92 | -2.5 | -4.25 | -2.51 | -2.28 |
| Thickness FWE p | 0.770 | 0.277 | 0.047* | 0.694 | 0.007* | 0.197 | 0.034* | 0.014* | 0.987 | 0.867 | 0.517 | 0.008* | 0.511 | 0.660 |
| Thickness mFWE p | 0.955 | 0.412 | 0.069$^{+}$ | 0.904 | 0.010$^{+}$ | 0.294 | 0.050$^{+}$ | 0.020* | 0.999 | 0.992 | 0.731 | 0.012* | 0.724 | 0.877 |

Table 3.3 continued

| | Left subcallosal gyrus | Left anterior transverse temporal gyrus | Left lateral aspect of the superior temporal gyrus | Left planum polare of the superior temporal gyrus | Left planum temporale | Left inferior temporal gyrus | Left middle temporal gyrus | Left horizontal ramus of the anterior segment of the lateral sulcus | Left vertical ramus of the anterior segment of the lateral sulcus | Left posterior ramus of the lateral sulcus | Left occipital pole | Left temporal pole | Left calcarine sulcus | Left central sulcus |
|---|---|---|---|---|---|---|---|---|---|---|---|---|---|---|
| **Fisher F** | **4.44** | **33.96** | **12.03** | **1.19** | **4.16** | **8.90** | **6.47** | **10.24** | **4.44** | **19.06** | **8.43** | **19.51** | **17.04** | **23.48** |
| **Fisher FWE p** | **0.999** | **0.267** | **0.999** | **0.999** | **0.999** | **0.999** | **0.999** | **0.999** | **0.999** | **0.906** | **0.999** | **0.892** | **0.955** | **0.733** |
| MD | -0.30 | 2.29 | -0.43 | -1.29 | -0.90 | -1.76 | -0.98 | 0.25 | -0.25 | 0.57 | -1.63 | -0.67 | 0.36 | -0.33 |
| MD FWE p | 0.999 | 0.359 | 0.999 | 0.999 | 0.999 | 0.999 | 0.999 | 0.999 | 0.999 | 0.994 | 0.999 | 0.999 | 0.998 | 0.999 |
| MD mFWE p | 0.999 | 0.873 | 0.999 | 0.999 | 0.999 | 0.999 | 0.999 | 0.999 | 0.999 | 0.999 | 0.999 | 0.999 | 0.999 | 0.999 |
| RD | -0.27 | 2.35 | -0.04 | -0.97 | -0.39 | -0.87 | -0.39 | 0.34 | -0.41 | 0.40 | -1.18 | 0.10 | 0.38 | -0.31 |
| RD FWE p | 0.999 | 0.363 | 0.999 | 0.999 | 0.999 | 0.999 | 0.999 | 0.999 | 0.999 | 0.999 | 0.999 | 0.999 | 0.999 | 0.999 |
| RD mFWE p | 0.999 | 0.839 | 0.999 | 0.999 | 0.999 | 0.999 | 0.999 | 0.999 | 0.999 | 0.999 | 0.999 | 0.999 | 0.999 | 0.999 |
| AD | -0.32 | 1.96 | -1.09 | -1.43 | -1.78 | -2.43 | -1.58 | 0.04 | 0.08 | 0.83 | -1.84 | -1.67 | 0.28 | -0.33 |
| AD FWE p | 0.999 | 0.543 | 0.999 | 0.999 | 0.999 | 0.999 | 0.999 | 0.999 | 0.999 | 0.98 | 0.999 | 0.999 | 0.999 | 0.999 |
| AD mFWE p | 0.999 | 0.987 | 0.999 | 0.999 | 0.999 | 0.999 | 0.999 | 0.999 | 0.999 | 0.999 | 0.999 | 0.999 | 0.999 | 0.999 |
| Volume | -1.56 | -0.99 | -1.15 | -1.79 | -0.86 | -3.51 | -3.60 | -3.27 | -2.28 | -2.24 | -0.49 | -4.10 | 0.999 | -3.67 |
| Volume FWE p | 0.964 | 0.997 | 0.994 | 0.919 | 0.999 | 0.077$^{+}$ | 0.058$^{+}$ | 0.150 | 0.720 | 0.739 | 0.999 | 0.009* | 0.999 | 0.046* |
| Volume mFWE p | 0.999 | 0.999 | 0.999 | 0.999 | 0.999 | 0.152 | 0.116 | 0.291 | 0.955 | 0.963 | 0.999 | 0.017* | 0.999 | 0.092$^{+}$ |
| Thickness | -0.02 | -2.06 | -2.35 | 0.95 | -0.51 | -2.17 | -1.43 | -1.38 | 0.24 | -2.68 | -1.94 | -3.57 | -1.95 | -4.00 |
| Thickness FWE p | 0.999 | 0.796 | 0.616 | 0.999 | 0.999 | 0.736 | 0.987 | 0.991 | 0.999 | 0.399 | 0.861 | 0.060$^{+}$ | 0.854 | 0.018* |
| Thickness mFWE p | 0.999 | 0.968 | 0.837 | 0.999 | 0.999 | 0.934 | 0.999 | 0.999 | 0.999 | 0.582 | 0.991 | 0.088$^{+}$ | 0.989 | 0.026* |

Table 3.3 continued

| | Left anterior segment of the circular sulcus of the insula | Left inferior segment of the circular sulcus of the insula | Left superior segment of the circular sulcus of the insula | Left anterior transverse collateral sulcus | Left posterior transverse collateral sulcus | Left inferior frontal sulcus | Left middle frontal sulcus | Left superior frontal sulcus | Left sulcus intermedius primus | Left intraparietal sulcus and transverse parietal sulci | Left middle occipital sulcus and lunatus sulcus | Left superior occipital sulcus and transverse occipital [illegible] | Left anterior occipital sulcus and preoccipital notch | Left lateral occipito temporal sulcus |
|---|---|---|---|---|---|---|---|---|---|---|---|---|---|---|
| **Fisher F** | **32.18** | **12.31** | **20.14** | **3.19** | **11.95** | **10.77** | **11.03** | **13.55** | **22.43** | **12.73** | **17.19** | **16.93** | **7.17** | **14.6** |
| **Fisher FWE p** | **0.331** | **0.998** | **0.871** | **0.999** | **0.999** | **0.999** | **0.999** | **0.994** | **0.781** | **0.997** | **0.952** | **0.957** | **0.999** | **0.987** |
| MD | 0.24 | -0.36 | 0.39 | -2.02 | -0.65 | -0.57 | -1.41 | -0.58 | -0.38 | -0.78 | -0.87 | 0.17 | 0.16 | -0.33 |
| MD FWE p | 0.999 | 0.999 | 0.998 | 0.999 | 0.999 | 0.999 | 0.999 | 0.999 | 0.999 | 0.999 | 0.999 | 0.999 | 0.999 | 0.999 |
| MD mFWE p | 0.999 | 0.999 | 0.999 | 0.999 | 0.999 | 0.999 | 0.999 | 0.999 | 0.999 | 0.999 | 0.999 | 0.999 | 0.999 | 0.999 |
| RD | 0.30 | -0.39 | -0.02 | -1.79 | -0.82 | -0.49 | -1.33 | -0.63 | -0.43 | -0.83 | -0.65 | 0.33 | -0.01 | -0.05 |
| RD FWE p | 0.999 | 0.999 | 0.999 | 0.999 | 0.999 | 0.999 | 0.999 | 0.999 | 0.999 | 0.999 | 0.999 | 0.999 | 0.999 | 0.999 |
| RD mFWE p | 0.999 | 0.999 | 0.999 | 0.999 | 0.999 | 0.999 | 0.999 | 0.999 | 0.999 | 0.999 | 0.999 | 0.999 | 0.999 | 0.999 |
| AD | 0.09 | -0.23 | 1.06 | -1.58 | -0.21 | -0.64 | -1.32 | -0.38 | -0.21 | -0.6 | -1.07 | -0.16 | 0.46 | -0.70 |
| AD FWE p | 0.999 | 0.999 | 0.949 | 0.999 | 0.999 | 0.999 | 0.999 | 0.999 | 0.999 | 0.999 | 0.999 | 0.999 | 0.997 | 0.999 |
| AD mFWE p | 0.999 | 0.999 | 0.999 | 0.999 | 0.999 | 0.999 | 0.999 | 0.999 | 0.999 | 0.999 | 0.999 | 0.999 | 0.999 | 0.999 |
| Volume | -4.05 | 2.29 | -2.33 | -2.37 | 0.16 | -0.98 | 2.04 | -0.31 | 0.35 | -2.73 | -1.33 | -2.82 | -1.28 | -3.36 |
| Volume FWE p | 0.011* | 0.999 | 0.690 | 0.670 | 0.999 | 0.997 | 0.999 | 0.999 | 0.999 | 0.436 | 0.986 | 0.379 | 0.989 | 0.118 |
| Volume mFWE p | 0.022* | 0.999 | 0.940 | 0.930 | 0.999 | 0.999 | 0.999 | 0.999 | 0.999 | 0.725 | 0.999 | 0.655 | 0.999 | 0.231 |
| Thickness | -4.68 | 0.78 | -2.94 | -0.74 | -2.12 | -2.17 | -0.65 | -2.55 | -3.62 | -2.67 | -3.36 | -2.83 | -0.17 | -2.78 |
| Thickness FWE p | 0.002* | 0.999 | 0.256 | 0.999 | 0.764 | 0.735 | 0.999 | 0.479 | $0.053^{+}$ | 0.404 | 0.103 | 0.308 | 0.999 | 0.338 |
| Thickness mFWE p | 0.003* | 0.999 | 0.381 | 0.999 | 0.952 | 0.934 | 0.999 | 0.685 | $0.077^{+}$ | 0.590 | 0.153 | 0.457 | 0.999 | 0.499 |

Table 3.3 continued

| | Left lateral orbital sulcus | Left medial orbital sulcus | Left orbital sulci | Left parieto occipital sulcus | Left pericallosal sulcus | Left postcentral sulcus | Left inferior part of the precentral sulcus | Left superior part of the precentral sulcus | Left suborbital sulcus | Left subparietal sulcus | Left inferior temporal sulcus | Left superior temporal sulcus | Left transverse temporal sulcus | Right fronto marginal gyrus and sulcus |
|---|---|---|---|---|---|---|---|---|---|---|---|---|---|---|
| **Fisher F** | **5.00** | **14.05** | **10.77** | **51.83** | **1.15** | **17.73** | **8.00** | **12.67** | **6.16** | **19.48** | **4.61** | **16.73** | **5.20** | **12.40** |
| **Fisher FWE p** | **0.999** | **0.991** | **0.999** | **0.016*** | **0.999** | **0.941** | **0.999** | **0.997** | **0.999** | **0.893** | **0.999** | **0.961** | **0.999** | **0.998** |
| MD | -1.02 | 0.80 | 0.4 | 1.40 | -1.69 | -0.25 | -0.66 | 0.02 | -0.30 | -0.11 | -0.89 | -0.04 | 0.07 | -0.62 |
| MD FWE p | 0.999 | 0.984 | 0.998 | 0.872 | 0.999 | 0.999 | 0.999 | 0.999 | 0.999 | 0.999 | 0.999 | 0.999 | 0.999 | 0.999 |
| MD mFWE p | 0.999 | 0.999 | 0.999 | 0.999 | 0.999 | 0.999 | 0.999 | 0.999 | 0.999 | 0.999 | 0.999 | 0.999 | 0.999 | 0.999 |
| RD | -0.96 | 1.46 | -0.10 | 1.41 | -1.66 | -0.26 | -0.63 | 0.19 | -0.11 | -0.54 | -0.24 | 0.04 | 0.21 | -0.75 |
| RD FWE p | 0.999 | 0.882 | 0.999 | 0.896 | 0.999 | 0.999 | 0.999 | 0.999 | 0.999 | 0.999 | 0.999 | 0.999 | 0.999 | 0.999 |
| RD mFWE p | 0.999 | 0.999 | 0.999 | 0.999 | 0.999 | 0.999 | 0.999 | 0.999 | 0.999 | 0.999 | 0.999 | 0.999 | 0.999 | 0.999 |
| AD | -0.93 | -0.17 | 1.03 | 1.20 | -1.22 | -0.2 | -0.62 | -0.33 | -0.43 | 0.68 | -1.48 | -0.19 | -0.19 | -0.29 |
| AD FWE p | 0.999 | 0.999 | 0.955 | 0.917 | 0.999 | 0.999 | 0.999 | 0.999 | 0.999 | 0.99 | 0.999 | 0.999 | 0.999 | 0.999 |
| AD mFWE p | 0.999 | 0.999 | 0.999 | 0.999 | 0.999 | 0.999 | 0.999 | 0.999 | 0.999 | 0.999 | 0.999 | 0.999 | 0.999 | 0.999 |
| Volume | -1.13 | -1.60 | -2.46 | -3.06 | -1.99 | -1.84 | -2.78 | -1.84 | -0.86 | -1.41 | -2.62 | -1.49 | -0.93 | -3.31 |
| Volume FWE p | 0.994 | 0.957 | 0.609 | 0.243 | 0.857 | 0.906 | 0.406 | 0.908 | 0.999 | 0.979 | 0.509 | 0.972 | 0.998 | 0.135 |
| Volume mFWE p | 0.999 | 0.999 | 0.891 | 0.452 | 0.994 | 0.998 | 0.689 | 0.998 | 0.999 | 0.999 | 0.804 | 0.999 | 0.999 | 0.262 |
| Thickness | -0.98 | -1.24 | -0.98 | -5.67 | 0.57 | -3.2 | -1.69 | -2.2 | -0.66 | -3.21 | -0.76 | -2.92 | 0.83 | -2.52 |
| Thickness FWE p | 0.999 | 0.997 | 0.999 | < 0.001* | 0.999 | 0.149 | 0.947 | 0.716 | 0.999 | 0.146 | 0.999 | 0.263 | 0.999 | 0.500 |
| Thickness mFWE p | 0.999 | 0.999 | 0.999 | < 0.001* | 0.999 | 0.223 | 0.999 | 0.921 | 0.999 | 0.217 | 0.999 | 0.391 | 0.999 | 0.711 |

Table 3.3 continued

| | Right paracentral lobule and sulcus | Right subcentral gyrus and sulci | Right transverse frontopolar gyri and sulci | Right anterior part of the cingulate gyrus and sulcus | Right middle anterior part of the cingulate gyrus and sulcus | Right middle posterior part of the cingulate gyrus and sulcus | Right posterior dorsal part of the cingulate gyrus | Right posterior ventral part of the cingulate gyrus | Right cuneus | Right opercular part of the inferior frontal gyrus | Right orbital part of the inferior frontal gyrus | Right triangular part of the inferior frontal gyrus | Right middle frontal gyrus | Right superior frontal gyrus |
|---|---|---|---|---|---|---|---|---|---|---|---|---|---|---|
| **Fisher F** | **41.23** | **2.88** | **10.01** | **11.94** | **22.79** | **15.94** | **9.40** | **4.94** | **7.75** | **2.20** | **3.80** | **7.67** | **7.08** | **12.72** |
| **Fisher FWE p** | **0.096** | **0.999** | **0.999** | **0.999** | **0.765** | **0.973** | **0.999** | **0.999** | **0.999** | **0.999** | **0.999** | **0.999** | **0.999** | **0.997** |
| MD | 2.22 | -0.88 | -0.43 | -1.73 | -0.64 | 0.00 | -0.62 | -1.74 | -0.27 | -1.75 | -1.01 | -1.50 | -0.36 | -0.21 |
| MD FWE p | 0.403 | 0.999 | 0.999 | 0.999 | 0.999 | 0.999 | 0.999 | 0.999 | 0.999 | 0.999 | 0.999 | 0.999 | 0.999 | 0.999 |
| MD mFWE p | 0.909 | 0.999 | 0.999 | 0.999 | 0.999 | 0.999 | 0.999 | 0.999 | 0.999 | 0.999 | 0.999 | 0.999 | 0.999 | 0.999 |
| RD | 2.27 | -0.64 | -0.52 | -1.55 | -0.76 | 0.15 | -0.36 | -1.07 | -0.21 | -1.57 | -0.76 | -1.13 | -0.6 | -0.28 |
| RD FWE p | 0.415 | 0.999 | 0.999 | 0.999 | 0.999 | 0.999 | 0.999 | 0.999 | 0.999 | 0.999 | 0.999 | 0.999 | 0.999 | 0.999 |
| RD mFWE p | 0.887 | 0.999 | 0.999 | 0.999 | 0.999 | 0.999 | 0.999 | 0.999 | 0.999 | 0.999 | 0.999 | 0.999 | 0.999 | 0.999 |
| AD | 1.83 | -1.25 | -0.23 | -1.57 | -0.28 | -0.32 | -0.97 | -2.47 | -0.35 | -1.96 | -1.32 | -2.01 | 0.10 | -0.06 |
| AD FWE p | 0.626 | 0.999 | 0.999 | 0.999 | 0.999 | 0.999 | 0.999 | 0.999 | 0.999 | 0.999 | 0.999 | 0.999 | 0.999 | 0.999 |
| AD mFWE p | 0.998 | 0.999 | 0.999 | 0.999 | 0.999 | 0.999 | 0.999 | 0.999 | 0.999 | 0.999 | 0.999 | 0.999 | 0.999 | 0.999 |
| Volume | -1.83 | -2.19 | -3.4 | -1.72 | -1.49 | -1.99 | -3.51 | -0.06 | -1.02 | -0.70 | -2.92 | -1.87 | -0.99 | -3.17 |
| Volume FWE p | 0.909 | 0.767 | 0.106 | 0.936 | 0.972 | 0.858 | 0.076 | 0.999 | 0.997 | 0.999 | 0.318 | 0.898 | 0.997 | 0.191 |
| Volume mFWE p | 0.998 | 0.973 | 0.208 | 0.999 | 0.999 | 0.994 | 0.15 | 0.999 | 0.999 | 0.999 | 0.568 | 0.998 | 0.999 | 0.363 |
| Thickness | -3.51 | -0.13 | -1.97 | -2.73 | -3.98 | -2.8 | -1.99 | -0.85 | -1.23 | 0.00 | -0.67 | -1.91 | -0.99 | -2.35 |
| Thickness FWE p | 0.070$^{+}$ | 0.999 | 0.843 | 0.365 | 0.019* | 0.328 | 0.834 | 0.999 | 0.997 | 0.999 | 0.999 | 0.872 | 0.999 | 0.614 |
| Thickness mFWE p | 0.103 | 0.999 | 0.986 | 0.537 | 0.027* | 0.484 | 0.983 | 0.999 | 0.999 | 0.999 | 0.999 | 0.993 | 0.999 | 0.834 |

Table 3.3 continued

| | Right short insular gyri | Right middle occipital gyrus | Right superior occipital gyrus | Right lateral occipito temporal gyrus | Right lingual gyrus | Right parahippocampal gyrus | Right orbital gyri | Right angular gyrus | Right supramarginal gyrus | Right superior parietal lobule | Right postcentral gyrus | Right precentral gyrus | Right precuneus |
|---|---|---|---|---|---|---|---|---|---|---|---|---|---|
| **Fisher F** | **4.65** | **9.44** | **22.13** | **37.58** | **19.53** | **27.23** | **13.28** | **13.02** | **13.74** | **11.46** | **13.73** | **20.62** | **11.76** |
| **Fisher FWE p** | **0.999** | **0.999** | **0.794** | **0.165** | **0.892** | **0.551** | **0.995** | **0.996** | **0.993** | **0.999** | **0.993** | **0.854** | **0.999** |
| MD | -0.18 | -0.51 | 1.16 | 1.37 | -0.47 | 0.61 | -0.04 | 0.47 | 0.08 | 0.08 | 0.44 | 0.91 | 0.76 |
| MD FWE p | 0.999 | 0.999 | 0.937 | 0.882 | 0.999 | 0.993 | 0.999 | 0.997 | 0.999 | 0.999 | 0.997 | 0.975 | 0.987 |
| MD mFWE p | 0.999 | 0.999 | 0.999 | 0.999 | 0.999 | 0.999 | 0.999 | 0.999 | 0.999 | 0.999 | 0.999 | 0.999 | 0.999 |
| RD | -0.05 | 0.12 | 1.40 | 1.62 | -0.35 | 0.81 | -0.25 | 0.64 | 0.15 | 0.12 | 0.34 | 0.69 | 0.71 |
| RD FWE p | 0.999 | 0.999 | 0.899 | 0.814 | 0.999 | 0.991 | 0.999 | 0.996 | 0.999 | 0.999 | 0.999 | 0.995 | 0.994 |
| RD mFWE p | 0.999 | 0.999 | 0.999 | 0.999 | 0.999 | 0.999 | 0.999 | 0.999 | 0.999 | 0.999 | 0.999 | 0.999 | 0.999 |
| AD | -0.34 | -1.37 | 0.63 | 0.57 | -0.62 | 0.19 | 0.24 | 0.10 | -0.06 | 0.01 | 0.54 | 1.21 | 0.82 |
| AD FWE p | 0.999 | 0.999 | 0.992 | 0.994 | 0.999 | 0.999 | 0.999 | 0.999 | 0.999 | 0.999 | 0.995 | 0.916 | 0.981 |
| AD mFWE p | 0.999 | 0.999 | 0.999 | 0.999 | 0.999 | 0.999 | 0.999 | 0.999 | 0.999 | 0.999 | 0.999 | 0.999 | 0.999 |
| Volume | -3.1 | -2.53 | -1.99 | -1.52 | -0.94 | -3.48 | -3.33 | -1.55 | -2.94 | -4.05 | -2.68 | -3.04 | -3.74 |
| Volume FWE p | 0.223 | 0.564 | 0.859 | 0.969 | 0.998 | 0.083$^{+}$ | 0.129 | 0.965 | 0.307 | 0.011* | 0.469 | 0.253 | 0.037* |
| Volume mFWE p | 0.418 | 0.855 | 0.994 | 0.999 | 0.999 | 0.163 | 0.250 | 0.999 | 0.553 | 0.021* | 0.763 | 0.468 | 0.073$^{+}$ |
| Thickness | 0.06 | -1.86 | -2.5 | -4.39 | -3.52 | -3.89 | -2.31 | -1.73 | -2.34 | -1.87 | -1.89 | -2.48 | -0.66 |
| Thickness FWE p | 0.999 | 0.890 | 0.513 | 0.005* | 0.069$^{+}$ | 0.025* | 0.643 | 0.934 | 0.624 | 0.889 | 0.881 | 0.531 | 0.999 |
| Thickness mFWE p | 0.999 | 0.996 | 0.726 | 0.008* | 0.102 | 0.036* | 0.862 | 0.999 | 0.844 | 0.996 | 0.995 | 0.747 | 0.999 |

Table 3.3 continued

| | Right subcallosal gyrus | Right anterior transverse temporal gyrus | Right lateral aspect of the superior temporal gyrus | Right planum polare of the superior temporal gyrus | Right planum temporale | Right inferior temporal gyrus | Right middle temporal gyrus | Right horizontal ramus of the anterior segment of the lateral sulcus | Right vertical ramus of the anterior segment of the lateral sulcus | Right posterior ramus of the lateral sulcus | Right occipital pole | Right temporal pole | Right calcarine sulcus | Right central sulcus |
|---|---|---|---|---|---|---|---|---|---|---|---|---|---|---|
| **Fisher F** | **5.25** | **20.33** | **8.77** | **2.28** | **13.06** | **14.12** | **11.26** | **7.06** | **0.88** | **11.07** | **21.71** | **7.99** | **15.64** | **7.35** |
| **Fisher FWE p** | **0.999** | **0.865** | **0.999** | **0.999** | **0.996** | **0.991** | **0.999** | **0.999** | **0.999** | **0.999** | **0.811** | **0.999** | **0.977** | **0.999** |
| MD | -1.19 | 1.23 | -0.49 | -0.78 | 0.21 | -1.33 | -1.64 | -0.85 | -1.58 | 0.13 | -0.67 | -1.22 | -0.22 | -0.58 |
| MD FWE p | 0.999 | 0.923 | 0.999 | 0.999 | 0.999 | 0.999 | 0.999 | 0.999 | 0.999 | 0.999 | 0.999 | 0.999 | 0.999 | 0.999 |
| MD mFWE p | 0.999 | 0.999 | 0.999 | 0.999 | 0.999 | 0.999 | 0.999 | 0.999 | 0.999 | 0.999 | 0.999 | 0.999 | 0.999 | 0.999 |
| RD | -1.06 | 1.60 | -0.16 | -0.64 | 0.44 | -0.62 | -0.82 | -0.90 | -1.79 | 0.05 | 0.07 | -0.23 | -0.03 | -0.52 |
| RD FWE p | 0.999 | 0.823 | 0.999 | 0.999 | 0.999 | 0.999 | 0.999 | 0.999 | 0.999 | 0.999 | 0.999 | 0.999 | 0.999 | 0.999 |
| RD mFWE p | 0.999 | 0.999 | 0.999 | 0.999 | 0.999 | 0.999 | 0.999 | 0.999 | 0.999 | 0.999 | 0.999 | 0.999 | 0.999 | 0.999 |
| AD | -1.27 | 0.41 | -1.04 | -0.81 | -0.26 | -2 | -2.49 | -0.61 | -0.85 | 0.28 | -1.62 | -2.28 | -0.51 | -0.67 |
| AD FWE p | 0.999 | 0.998 | 0.999 | 0.999 | 0.999 | 0.999 | 0.999 | 0.999 | 0.999 | 0.999 | 0.999 | 0.999 | 0.999 | 0.999 |
| AD mFWE p | 0.999 | 0.999 | 0.999 | 0.999 | 0.999 | 0.999 | 0.999 | 0.999 | 0.999 | 0.999 | 0.999 | 0.999 | 0.999 | 0.999 |
| Volume | 1.16 | -1.79 | -2.18 | -0.89 | -0.69 | -3.36 | -3.4 | -0.45 | -1.9 | -1.43 | -2.04 | -2.92 | -0.22 | -1.36 |
| Volume FWE p | 0.999 | 0.92 | 0.773 | 0.998 | 0.999 | 0.116 | 0.104 | 0.999 | 0.89 | 0.978 | 0.839 | 0.32 | 0.999 | 0.983 |
| Volume mFWE p | 0.999 | 0.999 | 0.975 | 0.999 | 0.999 | 0.227 | 0.204 | 0.999 | 0.997 | 0.999 | 0.991 | 0.572 | 0.999 | 0.999 |
| Thickness | 1.14 | -2.07 | -1.77 | 1.06 | -1.99 | -3.01 | -2.59 | -1.33 | 1.34 | -1.64 | -3.85 | -1.81 | -2.72 | -1.45 |
| Thickness FWE p | 0.999 | 0.795 | 0.924 | 0.999 | 0.836 | 0.222 | 0.454 | 0.994 | 0.999 | 0.958 | 0.028* | 0.912 | 0.374 | 0.986 |
| Thickness mFWE p | 0.999 | 0.968 | 0.999 | 0.999 | 0.984 | 0.331 | 0.654 | 0.999 | 0.999 | 0.999 | 0.040* | 0.999 | 0.548 | 0.999 |

Table 3.3 continued

| | Right anterior segment of the circular sulcus of the insula | Right inferior segment of the circular sulcus of the insula | Right superior segment of the circular sulcus of the insula | Right anterior transverse collateral sulcus | Right posterior transverse collateral sulcus | Right inferior frontal sulcus | Right middle frontal sulcus | Right superior frontal sulcus | Right sulcus intermedius primus | Right intraparietal sulcus and transverse parietal sulci | Right middle occipital sulcus and lunatus sulcus | Right superior occipital sulcus and transverse occipital sulcus | Right anterior occipital sulcus and preoccipital notch | Right lateral occipito temporal sulcus |
|---|---|---|---|---|---|---|---|---|---|---|---|---|---|---|
| **Fisher F** | **9.94** | **6.73** | **11.46** | **7.97** | **30.62** | **15.81** | **10.43** | **16.02** | **7.83** | **10.10** | **13.91** | **11.18** | **20.49** | **15.84** |
| **Fisher FWE p** | **0.999** | **0.999** | **0.999** | **0.999** | **0.394** | **0.975** | **0.999** | **0.972** | **0.999** | **0.999** | **0.992** | **0.999** | **0.859** | **0.974** |
| MD | -0.58 | -0.18 | -0.22 | -0.57 | 0.77 | -1.32 | -1.25 | -0.39 | 0.10 | 0.02 | -0.91 | -0.23 | 1.15 | -0.35 |
| MD FWE p | 0.999 | 0.999 | 0.999 | 0.999 | 0.986 | 0.999 | 0.999 | 0.999 | 0.999 | 0.999 | 0.999 | 0.999 | 0.941 | 0.999 |
| MD mFWE p | 0.999 | 0.999 | 0.999 | 0.999 | 0.999 | 0.999 | 0.999 | 0.999 | 0.999 | 0.999 | 0.999 | 0.999 | 0.999 | 0.999 |
| RD | -0.35 | 0.11 | -0.72 | -0.04 | 0.44 | -1.59 | -1.51 | -0.54 | -0.01 | -0.03 | -0.63 | 0.18 | 1.30 | 0.15 |
| RD FWE p | 0.999 | 0.999 | 0.999 | 0.999 | 0.999 | 0.999 | 0.999 | 0.999 | 0.999 | 0.999 | 0.999 | 0.999 | 0.927 | 0.999 |
| RD mFWE p | 0.999 | 0.999 | 0.999 | 0.999 | 0.999 | 0.999 | 0.999 | 0.999 | 0.999 | 0.999 | 0.999 | 0.999 | 0.999 | 0.999 |
| AD | -0.80 | -0.63 | 0.76 | -1.1 | 1.14 | -0.62 | -0.56 | -0.02 | 0.31 | 0.12 | -1.23 | -0.99 | 0.56 | -1.06 |
| AD FWE p | 0.999 | 0.999 | 0.985 | 0.999 | 0.932 | 0.999 | 0.999 | 0.999 | 0.999 | 0.999 | 0.999 | 0.999 | 0.995 | 0.999 |
| AD mFWE p | 0.999 | 0.999 | 0.999 | 0.999 | 0.999 | 0.999 | 0.999 | 0.999 | 0.999 | 0.999 | 0.999 | 0.999 | 0.999 | 0.999 |
| Volume | -2.12 | 0.58 | -3.06 | -2.67 | -0.57 | -1.72 | -0.78 | -0.43 | -2.15 | -2.35 | -2.07 | -1.81 | -2.20 | -2.74 |
| Volume FWE p | 0.803 | 0.999 | 0.240 | 0.472 | 0.999 | 0.935 | 0.999 | 0.999 | 0.790 | 0.682 | 0.825 | 0.915 | 0.765 | 0.431 |
| Volume mFWE p | 0.983 | 0.999 | 0.446 | 0.766 | 0.999 | 0.999 | 0.999 | 0.999 | 0.980 | 0.936 | 0.988 | 0.999 | 0.972 | 0.720 |
| Thickness | -2.06 | 0.38 | -1.84 | -1.57 | -3.99 | -3.23 | -2.27 | -2.86 | -0.73 | -1.58 | -2.91 | -2.09 | -2.31 | -2.97 |
| Thickness FWE p | 0.795 | 0.999 | 0.898 | 0.971 | 0.019* | 0.137 | 0.671 | 0.295 | 0.999 | 0.969 | 0.267 | 0.781 | 0.641 | 0.241 |
| Thickness mFWE p | 0.968 | 0.999 | 0.997 | 0.999 | 0.027* | 0.204 | 0.886 | 0.437 | 0.999 | 0.999 | 0.398 | 0.961 | 0.860 | 0.359 |

Table 3.3 continued

| | Right lateral orbital sulcus | Right medial orbital sulcus | Right orbital sulci | Right parieto occipital sulcus | Right pericallosal sulcus | Right postcentral sulcus | Right inferior part of the precentral sulcus | Right superior part of the precentral sulcus | Right suborbital sulcus | Right subparietal sulcus | Right inferior temporal sulcus | Right superior temporal sulcus | Right transverse temporal sulcus |
|---|---|---|---|---|---|---|---|---|---|---|---|---|---|
| **Fisher F** | **4.85** | **3.49** | **11.78** | **38.13** | **3.21** | **17.12** | **17.16** | **11.70** | **6.25** | **22.25** | **11.63** | **19.79** | **12.2** |
| **Fisher FWE p** | **0.999** | **0.999** | **0.999** | **0.152** | **0.999** | **0.953** | **0.953** | **0.999** | **0.999** | **0.789** | **0.999** | **0.883** | **0.998** |
| MD | -1.17 | -1.63 | 0.38 | 1.41 | -2.92 | -0.86 | 0.04 | -0.01 | -0.58 | 0.47 | -1.45 | -0.41 | 0.86 |
| MD FWE p | 0.999 | 0.999 | 0.998 | 0.867 | 0.999 | 0.999 | 0.999 | 0.999 | 0.999 | 0.997 | 0.999 | 0.999 | 0.979 |
| MD mFWE p | 0.999 | 0.999 | 0.999 | 0.999 | 0.999 | 0.999 | 0.999 | 0.999 | 0.999 | 0.999 | 0.999 | 0.999 | 0.999 |
| RD | -1.05 | -1.15 | -0.5 | 1.58 | -2.21 | -0.78 | 0.23 | 0.01 | 0.12 | 0.38 | -0.58 | -0.03 | 1.27 |
| RD FWE p | 0.999 | 0.999 | 0.999 | 0.832 | 0.999 | 0.999 | 0.999 | 0.999 | 0.999 | 0.999 | 0.999 | 0.999 | 0.934 |
| RD mFWE p | 0.999 | 0.999 | 0.999 | 0.999 | 0.999 | 0.999 | 0.999 | 0.999 | 0.999 | 0.999 | 0.999 | 0.999 | 0.999 |
| AD | -1.17 | -1.85 | 1.53 | 0.94 | -2.94 | -0.97 | -0.32 | -0.04 | -1.17 | 0.59 | -2.29 | -1.16 | 0.03 |
| AD FWE p | 0.999 | 0.999 | 0.795 | 0.968 | 0.999 | 0.999 | 0.999 | 0.999 | 0.999 | 0.994 | 0.999 | 0.999 | 0.999 |
| AD mFWE p | 0.999 | 0.999 | 0.999 | 0.999 | 0.999 | 0.999 | 0.999 | 0.999 | 0.999 | 0.999 | 0.999 | 0.999 | 0.999 |
| Volume | -0.48 | -1.73 | -2.9 | -1.81 | 0.83 | -2.90 | -2.46 | -1.06 | -0.86 | -2.58 | -3.47 | -1.92 | -1.07 |
| Volume FWE p | 0.999 | 0.933 | 0.330 | 0.913 | 0.999 | 0.332 | 0.612 | 0.996 | 0.999 | 0.535 | $0.087^{+}$ | 0.881 | 0.996 |
| Volume mFWE p | 0.999 | 0.999 | 0.586 | 0.999 | 0.999 | 0.588 | 0.893 | 0.999 | 0.999 | 0.829 | 0.171 | 0.996 | 0.999 |
| Thickness | -0.86 | -0.75 | -0.91 | -4.35 | 3.63 | -3.38 | -2.96 | -1.94 | -0.87 | -3.31 | -2.61 | -3.58 | -0.61 |
| Thickness FWE p | 0.999 | 0.999 | 0.999 | 0.006 | 0.999 | $0.098^{+}$ | 0.242 | 0.858 | 0.999 | 0.116 | 0.442 | $0.060^{+}$ | 0.999 |
| Thickness mFWE p | 0.999 | 0.999 | 0.999 | 0.009 | 0.999 | 0.144 | 0.360 | 0.990 | 0.999 | 0.173 | 0.639 | 0.087 | 0.999 |

**Table 3.4 Modeling subcortical grey matter volume as a mediator of the effect of asthma on behavior**

Parameter estimates from bootstrapping procedure to test a model where group differences in grey matter (GM) volumes mediate the relationship between asthma history and behavior controlling for age, sex, head motion, and scanner site. Behavioral outcomes that showed a relationship with GM volume in a region of interest were tested for consistency with mediation. *g*, executive functioning, language and memory scores were derived from the NIH Toolbox. Total problems and attention problems are from parent reports on the Child Behavior Checklist (CBCL).

| | Path a (Asthma → brain structure) | Path b (Brain Structure → Behavior) | Path c (Asthma → Behavior; no mediator) | Path c' (Asthma → Behavior with mediator) | Indirect effect (a*b) | % effect mediated |
|---|---|---|---|---|---|---|
| **Right caudate GM Volume** | | | | | | |
| *g* | [-0.187, -0.053] | [0.154, 0.211] | [-0.291, -0.157] | [-0.314, -0.179] | [-0.034, -0.009] | 8.43% |
| Executive Functioning | [-0.186, -0.049] | [0.085, 0.137] | [-0.234, -0.111] | [-0.219, -0.098] | [-0.022, -0.005] | 7.51% |
| Language | [-0.306, -0.171] | [0.192, 0.245] | [-0.185, -0.051] | [-0.277, -0.145] | [-0.041, -0.011] | 10.41% |
| Memory | [ -0.179, -0.045] | [0.102, 0.156] | [-0.306, -0.167] | [ -0.293, -0.155] | [ -0.024, -0.005] | 6.41% |
| Total problems | [-0.197, -0.059] | [-1.552, -0.536] | [1.397, 3.828] | [1.291, 3.708] | [0.053, 0.248] | 5.14% |
| Attention problems | [-0.189, -0.063] | [-0.298, -0.110] | [0.213, 0.679] | [0.187, 0.656] | [0.010, 0.047] | 5.80% |
| Attention problems (Year 3) | [-0.188, -0.012] | [-0.249, -0.042] | [0.114, 0.739] | [0.095, 0.723] | [0.001, 0.034] | 3.36% |
| **Right hippocampus GM volume** | | | | | | |
| *g* | [-0.147, -0.021] | [ 0.180, 0.235] | [-0.312, -0.182] | [-0.291, -0.165] | [-0.031, -0.004] | 7.22% |
| Executive Functioning | [-0.151, -0.025] | [0.103, 0.157] | [-0.238, -0.114] | [-0.223, -0.103] | [-0.020, -0.003] | 6.35% |
| Language | [-0.158, -0.023] | [0.205, 0.262] | [-0.304, -0.172] | [-0.283, -0.151] | [-0.038, -0.005] | 8.71% |
| Memory | [-0.155, -0.023] | [ 0.128, 0.184] | [-0.302, -0.164] | [-0.285, -0.153] | [-0.025, -0.004] | 5.93% |
| Total problems | [-0.170, -0.041] | [-1.612, -0.663] | [1.389, 3.873] | [1.264, 3.729] | [0.037, 0.218] | 4.55% |
| Attention problems | [-0.171, -0.033] | [-0.271, -0.076] | [0.212, 0.664] | [ 0.203, 0.641] | [0.005, 0.035] | 4.04% |

**Table 3.5 Modeling cortical grey matter metrics as a mediator of the effect of asthma on behavior**

Parameter estimates from bootstrapping procedure to test a model where group differences in grey matter (GM) volumes mediate the relationship between asthma history and behavior controlling for age, sex, head motion, and scanner site. Behavioral outcomes that showed a relationship with GM volume in a region of interest were tested for consistency with mediation. *g*, executive functioning, language and memory scores were derived from the NIH Toolbox. Total problems and attention problems are from parent reports on the Child Behavior Checklist (CBCL).

| | Path a (Ashtma → brain strucure) | Path b (Brain Structure → Behavior) | Path c (Asthma → Behavior; no mediator) | Path c' (Asthma → Behavior with mediator) | Indirect effect (a*b) | % effect mediated |
|---|---|---|---|---|---|---|
| **Left anterior insula GM Volume** | | | | | | |
| g | [-0.186, -0.019] | [0.069, 0.129] | [-0.283, -0.135] | [-0.273, -0.125] | [-0.020, -0.002] | 4.67% |
| Executive Functioning | [-0.183, -0.027] | [0.012, 0.070] | [-0.194, -0.047] | [-0.188, -0.042] | [-0.009, -0.001] | 3.42% |
| Language | [-0.186, -0.019] | [0.102, 0.170] | [-0.286, -0.135] | [-0.271, -0.122] | [-0.026, -0.002 | 6.57% |
| Memory | [-0.183, -0.027] | [0.030, 0.097] | [-0.299, -0.135] | [-0.293, -0.128] | [-0.014, -0.001] | 2.76% |
| Total problems | [ -0.193 ,-0.024] | [-1.421, -0.259] | [1.247, 4.011] | [1.137, 3.907] | [0.011, 0.214] | 3.52% |
| Attention problems | [-0.188, -0.032] | [-0.284, -0.040] | [0.126, 0.679] | [0.111, 0.659] | [0.003, 0.039] | 4.56% |
| **Left anterior insula GM thickness** | | | | | | |
| g | [-0.230, -0.048] | [0.042, 0.102] | [ -0.293, -0.140] | [-0.283, -0.130] | [ -0.019, -0.003] | 4.67% |
| Executive Functioning | [-0.229, -0.043] | [ 0.020, 0.074] | [-0.191, -0.046] | [-0.186, -0.041] | [-0.013, -0.002] | 5.13% |
| Language | [-0.230, -0.047] | [0.045, 0.105] | [-0.296, -0.133] | [-0.285, -0.122] | [-0.019, -0.003] | 4.69% |
| Memory | [-0.226, -0.050] | [0.038, 0.098] | [-0.295, -0.137] | [ -0.287, -0.128] | [-0.018, -0.003] | 4.15% |

# CHAPTER 4: CONCLUSION

In the popular imagination, asthma is a transient childhood condition that is isolated to the lung and is only a concern when it causes active symptoms. However, evidence is increasing that youth with asthma have persistent, systemic physiological differences when compared to their unaffected peers (Tattersall et al., 2018), which has implications for more serious lifelong outcomes. The current investigation demonstrates that, at 12 years old, asthma history is associated with decreases in cognitive performance that are related to markers of asthma severity (Chapter 2). In this sample, asthma history was also associated with brain structural differences, notably, smaller GM volumes in the right caudate, the right hippocampus, and salience network regions of the left anterior insula and right anterior middle cingulate (Chapter 3).

The greatest concern arising from these data is that the observed differences in brain structure may portend increased risk for serious health conditions in adulthood. Adults with asthma, particularly severe asthma, suffer from elevated rates of major depressive disorder (MDD; Z. Lu et al., 2018), Alzheimer's disease, and cognitive decline (Li et al., 2023). The structural changes in youth with asthma observed in this sample are consistent with the changes seen in adults with MDD, including decreased GM volumes in the orbital frontal cortex, striatum, anterior cingulate cortex and left insula (Zheng et al., 2021). Further, brain volume decreases, especially in the hippocampus, appear to be predictors of future negative clinical outcomes. For example, reduced hippocampal volume in childhood has been associated with greater risk for emotion dysregulation and more depressive symptoms in adolescents (Barch et al., 2019b). Smaller hippocampal volumes in adults with MDD are associated with less favorable treatment outcomes (for review see Gerlach et al., 2022). Later in life, smaller hippocampal volumes are also associated with an increased likelihood of transitioning from mild cognitive

impairment to Alzheimer's disease (McRae-McKee et al., 2019). Smaller hippocampal volumes are likely not an asthma-specific finding, as they have also been found to be associated with a variety of different kinds of early life chronic stress. Nor are reduced hippocampal volumes specific to MDD or Alzheimer's risk. Instead, smaller hippocampal volume and other structural changes and could represent a general vulnerability factor to difficulties with emotion and cognition that can manifest in a range of conditions across the life span.

The study findings do not assuage the concern that structural brain changes observed in older adults with asthma may be set in motion much earlier in life. The adults with severe asthma who have the greatest risk for psychiatric and neurodegenerative comorbidities often first experience the disease as children. For example, among the adults in the Severe Asthma Research Program, 46% of adults with severe asthma first had symptoms before 12 years old (Moore et al., 2010). A recent analysis from our group found asthma severity-related brain structural changes in adults (with a mean age of 38 years) in several of the same regions where I saw asthma-history-related differences in ABCD, including decreased GM volume in the insula and caudate. In adults with severe asthma, lower insula thickness was associated with higher serum levels of glial fibrillary acidic protein (GFAP), produced by reactive astrocytes and indicative of neuroinflammation. Higher asthma severity was also associated with smaller bilateral dorsal striatal volume (Carrol et al, *in prep*). However, the youth in ABCD study did not show evidence of the widespread white matter microstructural differences observed in this adult sample, where increased MD and RD were associated with greater asthma severity, higher levels of serum GFAP, and slower processing speed (Rosenkranz, Dean, et al., 2022). Understanding the time course of white matter and grey matter changes will be an important next step towards understanding if the patterns seen in ABCD are precursors to the changes observed in adults.

Although youth with severe asthma are uncommon in the general population and rare in the ABCD dataset, some youth with mild disease will experience severe asthma as adults (Izadi et al., 2021). Further, youth with mild asthma may have less pronounced but nonetheless important increases in risk for poor outcomes, because mild, uncontrolled asthma can still be associated with untreated chronic inflammation. If there is a link between chronic inflammation and the observed structural differences, which was supported by the relationships between structural alterations and lifetime asthma attacks, less severe asthma may be associated with more subtle or more slowly emerging behavioral and structural brain differences. It is unknown how permanent or reversible such changes might be. Therefore, understanding the mechanistic pathways that connect asthma, behavior, and brain structure and identifying how or whether early intervention can shape brain structural trajectories has important public health implications for the burden of MDD and Alzheimer's disease, but also for encouraging all youth to achieve their maximal flourishing potential.

While the current project cannot delineate causal mechanistic relationships between asthma, brain structure, and psychological outcomes, it provides justification to design more targeted investigations in animal models across the lifespan that can provide causal inference. Ongoing human observational studies will continue to be an important complement to these experiments. As animal studies refine our understanding of the important cellular and molecular signaling processes linking chronic inflammation and brain integrity, human imaging work will refine our understanding of how the signaling cascades identified in the lab translate outcomes in humans, subject to the complex, interactive contexts influenced by structural and social determinants of health. Identifying efficacious leverage points to shift the multi-factorial relationship between asthma and brain health will likely requiring accounting for the

bidirectional effects of behavioral influences on asthma management. Experimental and observational approaches together will likely be needed to close the gaps in health outcomes seen in youth with asthma.

Outstanding Questions and Future Directions

Future work designed to probe the specific biological mechanisms underlying the brain differences observed in the current investigation will be critical for developing intervention strategies to close the gap in risk for psychological and neurological comorbidities between people with and without asthma. For instance, it is still not clear which aspects of asthma pathophysiology are interacting with the brain, which could include a combination of inflammatory signaling, vascular changes, sleep disruption or medication-related effects. In the current study, I have focused on Type 2 signaling because serum eosinophils are an available biomarker in the ABCD dataset. However, other pathways, including IL-6 and IL-17, are active in asthma, involved in lung-brain communication, and implicated in behavioral modification in animal models of chronic inflammatory disease (Chapter 1). Alternatively, intermittent hypoxia or systemic effects of asthma on the cardiovascular system (Tattersall, 2023) may partially mediate the relationship between ongoing inflammation and long-term increased risk for comorbidities. This is further complicated by the phenotypic heterogeneity of the underlying biological processes active in youth asthma, the phenotypic heterogeneity in the psychological conditions that are more common in youth with asthma (e.g. anxiety, depression, ADHD), and fundamental knowledge gaps in the fields of neuro-immune communication, developmental neurobiology, and biological psychiatry.

The search for the biological mediators of the observed differences in brain structure, cognition, and emotional outcomes will continue to benefit from a biopsychosocial framing as

research continues in both animal models and in humans. Social determinants of health and individual differences in the ability to manage chronic disease (e.g. medication adherence, exacerbation risk reduction) will continue to be important potential moderators, both of inflammatory biology and especially of the efficacy of interventions. For instance, an important candidate process mediating the link between asthma and negative psychological outcomes is asthma-related sleep disruptions. Sleep is critical for cognitive development in adolescence, inflammation is most active at night in part due to low cortisol levels, and more severe asthma is associated with more nighttime awakenings. Understanding how inflammatory signaling in the lung contributes to nighttime awakenings is relevant for preventing negative outcomes associated with this potential mechanism, but so is understanding how psychopathology or stressful psychosocial environments impact sleep hygiene. Testing whether the differences observed between youth with and without asthma are related to sleep-disruption or if a sleep-focused intervention can change psychological symptoms and brain structure may help to determine whether this biologically plausible pathway playing a role in humans. The example also illustrates that human work is important to establish whether behavioral and environmental modifications are relevant interventions.

There are several outstanding questions that human studies can answer to advance the search for mechanisms. One of the barriers to progress in identifying relevant underlying biological mediators between asthma and brain health is phenotypic heterogeneity. Chapter 2 made an initial attempt at characterizing the influence of heterogeneity by examining aspects of asthma severity at a specific developmental period and examining outcomes in the framework of dimensions of cognitive and emotional function that underlie a variety of mental health conditions, rather than relative risk of specific diagnoses. Relatedly, exploring sex differences,

and the interaction between age, puberty, and sex differences will be important next steps for answering questions about heterogeneity of psychological profiles in youth with asthma. The prevalence of internalizing and externalizing symptoms, as well as symptom trajectories from early and mid-adolescence have marked sex differences (Murray et al., 2022). There are sex differences in the prevalence of asthma that reverse during adolescence, in part because of puberty-related changes to airway diameter (Trivedi & Denton, 2019).

The primarily cross-sectional analytic strategy used in the current investigation does not address questions about whether alterations in cognition and emotional symptoms occur within the same individuals over time. For instance, I initially hypothesized that asthma would be related to elevated depressive, anxiety and attentional problems, conceptualizing attentional problems as a salience-network anxiety-related hypervigilance. Instead, in this age range, behavioral differences emerged primarily in the cognitive domain, suggesting that asthma-associated parent-reported attentional problems may be more closely related to other dimensions of psychopathology like externalizing or neurodevelopmental symptoms. An important next step is to establish whether cognitive differences, and potentially differences in externalizing or impulsive behaviors, are a precursor to the stress-related internalizing phenotype our group has explored in the past. In other words, do internalizing and externalizing changes tend to occur in the same individuals or different populations of individuals? Longitudinal observations will help to clarify whether there are sub-groups of elevated cognitive and psychological problems in youth with asthma.

Similarly, longitudinal work in the ABCD sample may additionally clarify whether timing of asthma exposure changes the associated behavioral and neural correlates related to asthma history. In the future, I may be able to compare brain differences between youth who

develop asthma for the first time during the ABCD study to youth who report a history of asthma before age 10, but who have no further asthma symptoms during the 10 years of the study. This comparison would also help to clarify whether there is regional specificity to the observed differences and if that regional specificity depends on the developmental timing of the exposure to asthma. One possibility is that children exposed to asthma earlier in life are more prone to a broad range of neurodevelopmental symptoms because they are exposed to inflammation during the development of more basic thalamic and somatomotor areas. In contrast, youth who are exposed for the first time in adolescence may be vulnerable to more specific emotion regulation difficulties because of the specific inhibitory control circuitry that is developing. In this case, asthma may act on common mechanisms which result in different phenotypes depending on which brain regions are critically sensitive during asthma exposure.

Further, the ABCD sample provides opportunities to test hypotheses about the correspondence between brain structural differences, brain functional differences, and behavioral phenotypes. I hypothesize that differences in orbital-striatal volumes are related to functional differences in those same regions and may be related to differences in reward processing and inhibitory control. In the future, I could, for example, examine the relationship between brain structure and performance in the fMRI monetary incentive-delay task, which probes dopaminergic reward circuitry. The degree of specificity in the hypothesized correspondence between brain structure, brain function, and observed symptoms is not always supported in human studies (Goldstein-Piekarski et al., 2022), so the specific functional implications of findings discussed in Chapter 3 should be rigorously tested.

I would also like to explore whether these behavioral and brain changes are moderated by other pro-inflammatory factors related to chronic stress and structural determinants of health.

Previous work from our group has found that in some populations, asthma accelerates the WM degradation associated with normal aging and cardiovascular risk (Nair et al., 2022, 2023). It is possible that asthma may moderate the effect of other proinflammatory factors on brain structure in youth. For instance, the relationships between asthma and negative behavioral and brain health outcomes may be exacerbated in low-income or Black youth who have been found to have higher circulating levels of inflammatory cytokines (E. Chen et al., 2023; Lam et al., 2022; Mac Giollabhui et al., 2021). It will be difficult to test in the ABCD sample, but it will be important for future studies to track the extent to which differences in asthma control in youth are related to treatment access and adherence issues. If existing immunomodulatory tools (e.g. corticosteroids, immunomodulators) are effective in targeting the relevant biological mediators between asthma and poor brain health, the health disparity-related concerns will likely continue to grow due to the cost of and access to the new, expensive immunomodulatory drugs.

Clinical Implications

Currently, clinical guidelines for asthma management are aimed at reducing the risk of exacerbations, hospitalizations, and the need for more intensive corticosteroids (2020 Focused Updates to the Asthma Management Guidelines, 2020). However, management strategies that reduce asthma exacerbation risk may or may not influence long-term associations between asthma, behavior, and brain health. In adults, there are existing examples of clinical strategies to manage asthma symptoms that do not manage potential long-term systemic consequences of ongoing inflammation. For example, in many of our prior studies, participants classified clinically as having well-controlled, mild to moderate asthma still have elevations in Type-2 lung inflammation, including FeNO > 30 ppb. Elevated FeNO is a predictor of airway remodeling (Scott et al., 2023) which can increase the severity of respiratory problems long-term, but is not

often measured if asthma symptoms are well-managed. In other words, tailoring treatment to prevent potential deleterious airway remodeling is not part of the current asthma management algorithm. We do not know if the markers used to measure asthma control are the same markers that influence brain outcomes. Therefore, the risk of negative cognitive and emotional consequences may be increasing, and neurodegeneration may be accumulating, even in individuals who have clinically well-controlled asthma according to current best-practices.

As the field gathers mechanistic evidence of how asthma is related to changes in extra-pulmonary organs, we may be able to implement management strategies to reduce risk for neurological and psychiatric comorbidities in people with asthma starting at a young age. We can look to other chronic diseases to imagine the far-reaching implications of early disease control that targets biological factors related to brain health rather than solely focusing on symptoms. For example, in the initial management of diabetes, minimizing the neurological symptoms resulting from extreme blood sugar levels is very important. However even when blood sugar is in a range where diabetes is asymptomatic, achieving long-term glucose control early in the disease process is critical to reduce the risk of serious microvascular complications over 10 years later, including diabetic retinopathy (Folz & Laiteerapong, 2021). Diabetic retinopathy, in turn, has been associated with a 34% increase in 5-year risk for Alzheimer's disease (Pedersen et al., 2021). In another example, patients with rheumatoid arthritis, who overall have an increased risk developing Alzheimer's disease, using TNF-alpha targeting treatments lowered risk for Alzheimer's disease below the base rate in the general population, while those with rheumatoid arthritis who achieved symptom control with other treatments remained at elevated risk (Chou et al., 2016). Similar reductions in long-term risk for Alzheimer's disease associated with asthma

may be possible if the risk is related to similar underlying exposure to uncontrolled systemic inflammation.

Modifying current clinical guidelines to target brain-relevant biological pathways will likely require not only identifying the mechanistic pathway or pathways involved in the elevated risk for brain-related conditions in youth with asthma, but also developing a robust indicator of the pathway's activity that can be easily assayed in most medical centers, as well as establishing that accessible interventions can change activity in that pathway. The most persuasive evidence would be a randomized clinical trial demonstrating that targeting the pathway, in addition to treatment as usual, resulted in improved brain-health outcomes such as reduced rates of ADHD or MDD. However, emergence of MDD or Alzheimer's disease may not be a feasible outcome measure in the timeframe of a clinical trial if the intervention is delivered early in life. If there was an established brain structural biomarker that mediated this increased risk, this biomarker may be a more feasible clinical trial endpoint. The translation process may be accelerated by considering these longer-term clinical goals when designing more basic mechanistic studies.

Although many outstanding questions remain, evidence from other chronic conditions suggests that differences in brain health between people with and without asthma likely can be addressed or even prevented. Our data suggests that in asthma, this will need to happen earlier in life. Intervening early in life and promoting brain health in youth with asthma may have cascading positive outcomes for this vulnerable group on a population level.

# REFERENCES

2020 Focused Updates to the Asthma Management Guidelines: A Report from the National Asthma Education and Prevention Program Coordinating Committee Expert Panel Working Group (p. 1217). (2020). National Heart, Lung, and Blood Institute / National Asthma Education and Prevention Program [NHLBI/NAEPP]. https://www.ncbi.nlm.nih.gov/pmc/articles/PMC7924476/

Achenbach, T., & Rescorla, L. (2001). Manual for the ASEBA School-Age Forms & Profiles. University of Vermont, Research Center for Children, Youth, & Families.

Afari, M. E., & Bhat, T. (2016). Neutrophil to lymphocyte ratio (NLR) and cardiovascular diseases: An update. Expert Review of Cardiovascular Therapy, 14(5), 573–577. https://doi.org/10.1586/14779072.2016.1154788

Alloy, L. B., Olino, T., Freed, R. D., & Nusslock, R. (2016). Role of Reward Sensitivity and Processing in Major Depressive and Bipolar Spectrum Disorders. Behavior Therapy, 47(5), 600–621. https://doi.org/10.1016/j.beth.2016.02.014

Andre, J., Picchioni, M., Zhang, R., & Toulopoulou, T. (2016). Working memory circuit as a function of increasing age in healthy adolescence: A systematic review and meta-analyses. NeuroImage: Clinical, 12, 940–948. https://doi.org/10.1016/j.nicl.2015.12.002

Arnsten, A. F. T., Raskind, M. A., Taylor, F. B., & Connor, D. F. (2014). The effects of stress exposure on prefrontal cortex: Translating basic research into successful treatments for post-traumatic stress disorder. Neurobiology of Stress, 1, 89–99. https://doi.org/10.1016/j.ynstr.2014.10.002

Assari, S., Boyce, S., & Jovanovic, T. (2021). Association between Hippocampal Volume and Working Memory in 10,000+ 9–10-Year-Old Children: Sex Differences. Children, 8(5), Article 5. https://doi.org/10.3390/children8050411

Asthma Care Quick Reference (NIH publicaiton No. 12-5075). (2002). National Heart, Lung, and Blood Institute, National Institutes of Health, U.S. Department of Health and Human Services.

Avants, B. B., Tustison, N. J., Wu, J., Cook, P. A., & Gee, J. C. (2011). An Open Source Multivariate Framework for n-Tissue Segmentation with Evaluation on Public Data. Neuroinformatics, 9(4), 381–400. https://doi.org/10.1007/s12021-011-9109-y

Backhausen, L. L., Herting, M. M., Tamnes, C. K., & Vetter, N. C. (2022). Best Practices in Structural Neuroimaging of Neurodevelopmental Disorders. Neuropsychology Review, 32(2), 400–418. https://doi.org/10.1007/s11065-021-09496-2

Barch, D. M., Donohue, M. R., Elsayed, N. M., Gilbert, K., Harms, M. P., Hennefield, L., Herzberg, M., Kandala, S., Karcher, N. R., Jackson, J. J., Luking, K. R., Rappaport, B. I., Sanders, A., Taylor, R., Tillman, R., Vogel, A. C., Whalen, D., & Luby, J. L. (2022). Early Childhood Socioeconomic Status and Cognitive and Adaptive Outcomes at the Transition to Adulthood: The Mediating Role of Gray Matter Development Across Five Scan Waves. Biological Psychiatry: Cognitive Neuroscience and Neuroimaging, 7(1), 34–44. https://doi.org/10.1016/j.bpsc.2021.07.002

Barch, D. M., Harms, M. P., Tillman, R., Hawkey, E., & Luby, J. L. (2019a). Early childhood depression, emotion regulation, episodic memory, and hippocampal development. Journal of Abnormal Psychology, 128(1), 81–95. https://doi.org/10.1037/abn0000392

Barch, D. M., Harms, M. P., Tillman, R., Hawkey, E., & Luby, J. L. (2019b). Early childhood depression, emotion regulation, episodic memory, and hippocampal development. Journal of Abnormal Psychology, 128(1), 81–95. https://doi.org/10.1037/abn0000392

Baron Nelson, M., O'Neil, S. H., Wisnowski, J. L., Hart, D., Sawardekar, S., Rauh, V., Perera, F., Andrews, H. F., Hoepner, L. A., Garcia, W., Algermissen, M., Bansal, R., & Peterson, B. S. (2019). Maturation of Brain Microstructure and Metabolism Associates with Increased Capacity for Self-Regulation during the Transition from Childhood to Adolescence. The Journal of

Neuroscience: The Official Journal of the Society for Neuroscience, 39(42), 8362–8375. https://doi.org/10.1523/JNEUROSCI.2422-18.2019

Bartels, C. M., Chen, Y., Powell, W. R., Rosenkranz, M. A., Bendlin, B. B., Kramer, J., Busse, W. W., & Kind, A. (2024). Alzheimer's Incidence and Prevalence with and without Asthma: A Medicare cohort study. Journal of Allergy and Clinical Immunology. https://doi.org/10.1016/j.jaci.2024.04.008

Basser, P. J., Mattiello, J., & LeBihan, D. (1994). Estimation of the effective self-diffusion tensor from the NMR spin echo. Journal of Magnetic Resonance. Series B, 103(3), 247–254. https://doi.org/10.1006/jmrb.1994.1037

Beauchaine, T. P., & Cicchetti, D. (2019). Emotion dysregulation and emerging psychopathology: A transdiagnostic, transdisciplinary perspective. Development and Psychopathology, 31(3), 799–804. https://doi.org/10.1017/S0954579419000671

Bekhbat, M., Li, Z., Mehta, N. D., Treadway, M. T., Lucido, M. J., Woolwine, B. J., Haroon, E., Miller, A. H., & Felger, J. C. (2022). Functional connectivity in reward circuitry and symptoms of anhedonia as therapeutic targets in depression with high inflammation: Evidence from a dopamine challenge study. Molecular Psychiatry, 27(10), 4113–4121. https://doi.org/10.1038/s41380-022-01715-3

Benear, S. L., Ngo, C. T., & Olson, I. R. (2020). Dissecting the Fornix in Basic Memory Processes and Neuropsychiatric Disease: A Review. Brain Connectivity, 10(7), 331–354. https://doi.org/10.1089/brain.2020.0749

Besteher, B., Gaser, C., & Nenadić, I. (2019). Brain Structure and Subclinical Symptoms: A Dimensional Perspective of Psychopathology in the Depression and Anxiety Spectrum. Neuropsychobiology, 79(4–5), 270–283. https://doi.org/10.1159/000501024

Bilbo, S. D., & Schwarz, J. M. (2009). Early-Life Programming of Later-Life Brain and Behavior: A Critical Role for the Immune System. Frontiers in Behavioral Neuroscience, 3, 14. https://doi.org/10.3389/neuro.08.014.2009

Boyle, C. C., Kuhlman, K. R., Dooley, L. N., Haydon, M. D., Robles, T. F., Ang, Y.-S., Pizzagalli, D. A., & Bower, J. E. (2019). Inflammation and dimensions of reward processing following exposure to the influenza vaccine. Psychoneuroendocrinology, 102, 16–23. https://doi.org/10.1016/j.psyneuen.2018.11.024

Brearly, T. W., Rowland, J. A., Martindale, S. L., Shura, R. D., Curry, D., & Taber, K. H. (2019). Comparability of iPad and Web-Based NIH Toolbox Cognitive Battery Administration in Veterans. Archives of Clinical Neuropsychology, 34(4), 524–530. https://doi.org/10.1093/arclin/acy070

Brenhouse, H. C. (2023). Points of divergence on a bumpy road: Early development of brain and immune threat processing systems following postnatal adversity. Molecular Psychiatry, 28(1), Article 1. https://doi.org/10.1038/s41380-022-01658-9

Brenhouse, H. C., & Schwarz, J. M. (2016). Immunoadolescence: Neuroimmune development and adolescent behavior. Neuroscience and Biobehavioral Reviews, 70, 288–299. https://doi.org/10.1016/j.neubiorev.2016.05.035

Brieant, A. E., Sisk, L. M., & Gee, D. G. (2021). Associations among negative life events, changes in cortico-limbic connectivity, and psychopathology in the ABCD Study. Developmental Cognitive Neuroscience, 52, 101022. https://doi.org/10.1016/j.dcn.2021.101022

Burrows, K., Stewart, J. L., Kuplicki, R., Figueroa-Hall, L., Spechler, P. A., Zheng, H., Guinjoan, S. M., Savitz, J. B., Teague, T. K., & Paulus, M. P. (2021). Elevated peripheral inflammation is associated with attenuated striatal reward anticipation in major depressive disorder. Brain, Behavior, and Immunity, 93, 214–225. https://doi.org/10.1016/j.bbi.2021.01.016

Busse, W. W., Kraft, M., Rabe, K. F., Deniz, Y., Rowe, P. J., Ruddy, M., & Castro, M. (2021). Understanding the key issues in the treatment of uncontrolled persistent asthma with type 2 inflammation. European Respiratory Journal, 58(2). https://doi.org/10.1183/13993003.03393-2020

Calem, M., Bromis, K., McGuire, P., Morgan, C., & Kempton, M. J. (2017). Meta-analysis of associations between childhood adversity and hippocampus and amygdala volume in non-clinical and general population samples. NeuroImage: Clinical, 14, 471–479. https://doi.org/10.1016/j.nicl.2017.02.016

Cao, P., Chen, C., Liu, A., Shan, Q., Zhu, X., Jia, C., Peng, X., Zhang, M., Farzinpour, Z., Zhou, W., Wang, H., Zhou, J.-N., Song, X., Wang, L., Tao, W., Zheng, C., Zhang, Y., Ding, Y.-Q., Jin, Y., … Zhang, Z. (2021). Early-life inflammation promotes depressive symptoms in adolescence via microglial engulfment of dendritic spines. Neuron, 109(16), 2573-2589.e9. https://doi.org/10.1016/j.neuron.2021.06.012

Capuron, L., Pagnoni, G., Drake, D. F., Woolwine, B. J., Spivey, J. R., Crowe, R. J., Votaw, J. R., Goodman, M. M., & Miller, A. H. (2012). Dopaminergic mechanisms of reduced basal ganglia responses to hedonic reward during interferon alfa administration. Archives of General Psychiatry, 69(10), 1044–1053. https://doi.org/10.1001/archgenpsychiatry.2011.2094

Carlson, S. M., Kim, J., Khan, D. A., King, K., Lucarelli, R. T., McColl, R., Peshock, R., & Brown, E. S. (2017). Hippocampal volume in patients with asthma: Results from the Dallas Heart Study. Journal of Asthma, 54(1), 9–16. https://doi.org/10.1080/02770903.2016.1186174

Casey, B. J., Getz, S., & Galvan, A. (2008). The adolescent brain. Developmental Review, 28(1), 62–77. https://doi.org/10.1016/j.dr.2007.08.003

Caspi, A., Houts, R. M., Belsky, D. W., Goldman-Mellor, S. J., Harrington, H., Israel, S., Meier, M. H., Ramrakha, S., Shalev, I., Poulton, R., & Moffitt, T. E. (2014). The p Factor: One General

Psychopathology Factor in the Structure of Psychiatric Disorders? Clinical Psychological Science, 2(2), 119–137. https://doi.org/10.1177/2167702613497473

Catale, C., Gironda, S., Lo Iacono, L., & Carola, V. (2020). Microglial Function in the Effects of Early-Life Stress on Brain and Behavioral Development. Journal of Clinical Medicine, 9(2), 468. https://doi.org/10.3390/jcm9020468

Caulfield, J. I., Caruso, M. J., Michael, K. C., Bourne, R. A., Chirichella, N. R., Klein, L. C., Craig, T., Bonneau, R. H., August, A., & Cavigelli, S. A. (2017). Peri-adolescent asthma symptoms cause adult anxiety-related behavior and neurobiological processes in mice. Behavioural Brain Research, 326, 244–255. https://doi.org/10.1016/j.bbr.2017.02.046

Caulfield, J. I., Ching, A. M., Cover, E. M., August, A., Craig, T., Kamens, H. M., & Cavigelli, S. A. (2021). Inhaled corticosteroids as treatment for adolescent asthma: Effects on adult anxiety-related outcomes in a murine model. Psychopharmacology, 238(1), 165–179. https://doi.org/10.1007/s00213-020-05666-x

Chaku, N., Barry, K., Fowle, J., & Hoyt, L. T. (2022). Understanding patterns of heterogeneity in executive functioning during adolescence: Evidence from population-level data. Developmental Science, 25(6), e13256. https://doi.org/10.1111/desc.13256

Chen, A. P., Chen, L., Kim, T. A., & Xiong, Q. (2021). Integrating the Roles of Midbrain Dopamine Circuits in Behavior and Neuropsychiatric Disease. Biomedicines, 9(6), 647. https://doi.org/10.3390/biomedicines9060647

Chen, E., Yu, T., Brody, G. H., Lam, P. H., Goosby, B. J., & Miller, G. E. (2023). Discrimination and Inflammation in Adolescents of Color. Biological Psychiatry Global Open Science, 3(2), 204–212. https://doi.org/10.1016/j.bpsgos.2022.02.008

Chen, J., Yan, Y., Yuan, F., Cao, J., Li, S., Eickhoff, S. B., & Zhang, J. (2019). Brain grey matter volume reduction and anxiety-like behavior in lipopolysaccharide-induced chronic pulmonary

inflammation rats: A structural MRI study with histological validation. Brain, Behavior, and Immunity, 76, 182–197. https://doi.org/10.1016/j.bbi.2018.11.020

Chen, L., Zeng, X., Zhou, S., Gu, Z., & Pan, J. (2022). Correlation Between Serum High-Sensitivity C-Reactive Protein, Tumor Necrosis Factor-Alpha, Serum Interleukin-6 and White Matter Integrity Before and After the Treatment of Drug-Naïve Patients With Major Depressive Disorder. Frontiers in Neuroscience, 16. https://www.frontiersin.org/articles/10.3389/fnins.2022.948637

Chen, W., Wang, J., Ye, B., Zhou, J., & Wang, W. (2021). The population characteristics of the main leukocyte subsets and their association with chronic diseases in a community-dwelling population: A cross-sectional study. Primary Health Care Research & Development, 22, e18. https://doi.org/10.1017/S1463423621000153

Chiang, J. J., Lam, P. H., Chen, E., & Miller, G. E. (2022). Psychological stress during childhood and adolescence and its association with inflammation across the lifespan: A critical review and meta-analysis. Psychological Bulletin, 148, 27–66. https://doi.org/10.1037/bul0000351

Chou, R. C., Kane, M., Ghimire, S., Gautam, S., & Gui, J. (2016). Treatment for Rheumatoid Arthritis and Risk of Alzheimer's Disease: A Nested Case-Control Analysis. CNS Drugs, 30(11), 1111–1120. https://doi.org/10.1007/s40263-016-0374-z

Chuang, Y.-C., Wang, C.-Y., Huang, W.-L., Wang, L.-J., Kuo, H.-C., Chen, Y.-C., & Huang, Y.-J. (2022). Two meta-analyses of the association between atopic diseases and core symptoms of attention deficit hyperactivity disorder. Scientific Reports, 12(1), 3377. https://doi.org/10.1038/s41598-022-07232-1

Cohen, A. O., Breiner, K., Steinberg, L., Bonnie, R. J., Scott, E. S., Taylor-Thompson, K. A., Rudolph, M. D., Chein, J., Richeson, J. A., Heller, A. S., Silverman, M. R., Dellarco, D. V., Fair, D. A., Galván, A., & Casey, B. J. (2016). When Is an Adolescent an Adult? Assessing Cognitive Control

in Emotional and Nonemotional Contexts. Psychological Science, 27(4), 549–562. https://doi.org/10.1177/0956797615627625

Cohen-Gilbert, J. E., & Thomas, K. M. (2013). Inhibitory control during emotional distraction across adolescence and early adulthood. Child Development, 84(6), 1954–1966. https://doi.org/10.1111/cdev.12085

Colonna, M., & Butovsky, O. (2017). Microglia Function in the Central Nervous System During Health and Neurodegeneration. Annual Review of Immunology, 35(1), 441–468. https://doi.org/10.1146/annurev-immunol-051116-052358

Copeland, W. E., Wolke, D., Shanahan, L., & Costello, E. J. (2015). Adult Functional Outcomes of Common Childhood Psychiatric Problems: A Prospective, Longitudinal Study. JAMA Psychiatry, 72(9), 892–899. https://doi.org/10.1001/jamapsychiatry.2015.0730

Cortés Pascual, A., Moyano Muñoz, N., & Quílez Robres, A. (2019). The Relationship Between Executive Functions and Academic Performance in Primary Education: Review and Meta-Analysis. Frontiers in Psychology, 10. https://www.frontiersin.org/articles/10.3389/fpsyg.2019.01582

Dantzer, R. (2018). Neuroimmune Interactions: From the Brain to the Immune System and Vice Versa. Physiological Reviews, 98(1), 477–504. https://doi.org/10.1152/physrev.00039.2016

Davies, K. A., Cooper, E., Voon, V., Tibble, J., Cercignani, M., & Harrison, N. A. (2021). Interferon and anti-TNF therapies differentially modulate amygdala reactivity which predicts associated bidirectional changes in depressive symptoms. Molecular Psychiatry, 26(9), 5150–5160. https://doi.org/10.1038/s41380-020-0790-9

Davis, J. C., Marra, C. A., Najafzadeh, M., & Liu-Ambrose, T. (2010). The independent contribution of executive functions to health related quality of life in older women. BMC Geriatrics, 10, 16. https://doi.org/10.1186/1471-2318-10-16

Deer, L. K., Hastings, P. D., & Hostinar, C. E. (2020). The Role of Childhood Executive Function in Explaining Income Disparities in Long-Term Academic Achievement. Child Development, 91(5), e1046–e1063. https://doi.org/10.1111/cdev.13383

Dehdar, K., & Raoufy, M. R. (2023a). Brain structural and functional alterations related to anxiety in allergic asthma. Brain Research Bulletin, 202, 110727. https://doi.org/10.1016/j.brainresbull.2023.110727

Dehdar, K., & Raoufy, M. R. (2023b). Effects of inhaled corticosteroids on brain volumetry, depression and anxiety-like behaviors in a rat model of asthma. RESPIRATORY PHYSIOLOGY & NEUROBIOLOGY, 315, 104121. https://doi.org/10.1016/j.resp.2023.104121

Destrieux, C., Fischl, B., Dale, A., & Halgren, E. (2010). Automatic parcellation of human cortical gyri and sulci using standard anatomical nomenclature. NeuroImage, 53(1), 1–15. https://doi.org/10.1016/j.neuroimage.2010.06.010

Dill-McFarland, K. A., Altman, M. C., Esnault, S., Jarjour, N. N., Busse, W. W., & Rosenkranz, M. A. (2024). Molecular pathways underlying lung-brain axis signaling in asthma: Relevance for psychopathology and neuroinflammation. The Journal of Allergy and Clinical Immunology, 153(1), 111–121. https://doi.org/10.1016/j.jaci.2023.07.025

DiPiero, M., Rodrigues, P. G., Gromala, A., & Dean, D. C. (2022). Applications of advanced diffusion MRI in early brain development: A comprehensive review. Brain Structure and Function. https://doi.org/10.1007/s00429-022-02605-8

Dudeney, J., Sharpe, L., Jaffe, A., Jones, E. B., & Hunt, C. (2017). Anxiety in youth with asthma: A meta-analysis. Pediatric Pulmonology, 52(9), 1121–1129. https://doi.org/10.1002/ppul.23689

Ehrlich, K. B., Miller, G. E., & Chen, E. (2015). Family Functioning, Eosinophil Activity, and Symptoms in Children With Asthma. Journal of Pediatric Psychology, 40(8), 781–789. https://doi.org/10.1093/jpepsy/jsv045

Elwenspoek, M. M. C., Kuehn, A., Muller, C. P., & Turner, J. D. (2017). The effects of early life adversity on the immune system. Psychoneuroendocrinology, 82, 140–154. https://doi.org/10.1016/j.psyneuen.2017.05.012

Eng, A. G., Phan, J. M., Shirtcliff, E. A., Eisenlohr-Moul, T. A., Goh, P. K., & Martel, M. M. (2023). Aging and Pubertal Development Differentially Predict Symptoms of ADHD, Depression, and Impairment in Children and Adolescents: An Eight-Year Longitudinal Study. Research on Child and Adolescent Psychopathology, 51(6), 819–832. https://doi.org/10.1007/s10802-023-01030-7

Esmaeilzadeh, H., Nouri, F., Nabavizadeh, S. H., Alyasin, S., & Mortazavi, N. (2021). Can eosinophilia and neutrophil–lymphocyte ratio predict hospitalization in asthma exacerbation? Allergy, Asthma & Clinical Immunology, 17(1), 16. https://doi.org/10.1186/s13223-021-00512-x

Fahy, J. V. (2015). Type 2 inflammation in asthma—Present in most, absent in many. Nature Reviews. Immunology, 15(1), 57–65. https://doi.org/10.1038/nri3786

Felger, J. C. (2018). Imaging the Role of Inflammation in Mood and Anxiety-related Disorders. Current Neuropharmacology, 16(5), 533–558. https://doi.org/10.2174/1570159X15666171123201142

Felger, J. C., & Treadway, M. T. (2017). Inflammation Effects on Motivation and Motor Activity: Role of Dopamine. Neuropsychopharmacology, 42(1), 216–241. https://doi.org/10.1038/npp.2016.143

Ferro, M. A., Gorter, J. W., & Boyle, M. H. (2015). Trajectories of depressive symptoms during the transition to young adulthood: The role of chronic illness. Journal of Affective Disorders, 174, 594–601. https://doi.org/10.1016/j.jad.2014.12.014

Fischl, B., & Dale, A. M. (2000). Measuring the thickness of the human cerebral cortex from magnetic resonance images. Proceedings of the National Academy of Sciences of the United States of America, 97(20), 11050–11055. https://doi.org/10.1073/pnas.200033797

Fischl, B., Salat, D. H., Busa, E., Albert, M., Dieterich, M., Haselgrove, C., van der Kouwe, A., Killiany, R., Kennedy, D., Klaveness, S., Montillo, A., Makris, N., Rosen, B., & Dale, A. M. (2002).

Whole brain segmentation: Automated labeling of neuroanatomical structures in the human brain. Neuron, 33(3), 341–355. https://doi.org/10.1016/s0896-6273(02)00569-x

Fischl, B., Sereno, M. I., & Dale, A. M. (1999). Cortical Surface-Based Analysis: II: Inflation, Flattening, and a Surface-Based Coordinate System. NeuroImage, 9(2), 195–207. https://doi.org/10.1006/nimg.1998.0396

Flouri, E., Papachristou, E., Midouhas, E., Ploubidis, G. B., Lewis, G., & Joshi, H. (2019). Developmental cascades of internalising symptoms, externalising problems and cognitive ability from early childhood to middle adolescence. European Psychiatry, 57, 61–69. https://doi.org/10.1016/j.eurpsy.2018.12.005

Folz, R., & Laiteerapong, N. (2021). The legacy effect in diabetes: Are there long-term benefits? Diabetologia, 64(10), 2131–2137. https://doi.org/10.1007/s00125-021-05539-8

Frodl, T., & Amico, F. (2014). Is there an association between peripheral immune markers and structural/functional neuroimaging findings? Progress in Neuro-Psychopharmacology & Biological Psychiatry, 48, 295–303. https://doi.org/10.1016/j.pnpbp.2012.12.013

Furman, D., Campisi, J., Verdin, E., Carrera-Bastos, P., Targ, S., Franceschi, C., Ferrucci, L., Gilroy, D. W., Fasano, A., Miller, G. W., Miller, A. H., Mantovani, A., Weyand, C. M., Barzilai, N., Goronzy, J. J., Rando, T. A., Effros, R. B., Lucia, A., Kleinstreuer, N., & Slavich, G. M. (2019). Chronic inflammation in the etiology of disease across the life span. Nature Medicine, 25(12), 1822–1832. https://doi.org/10.1038/s41591-019-0675-0

Garavan, H., Bartsch, H., Conway, K., Decastro, A., Goldstein, R. Z., Heeringa, S., Jernigan, T., Potter, A., Thompson, W., & Zahs, D. (2018). Recruiting the ABCD sample: Design considerations and procedures. Developmental Cognitive Neuroscience, 32, 16–22. https://doi.org/10.1016/j.dcn.2018.04.004

Gee, D. G., Bath, K. G., Johnson, C. M., Meyer, H. C., Murty, V. P., van den Bos, W., & Hartley, C. A. (2018). Neurocognitive Development of Motivated Behavior: Dynamic Changes across Childhood and Adolescence. The Journal of Neuroscience, 38(44), 9433–9445. https://doi.org/10.1523/JNEUROSCI.1674-18.2018

Gerlach, A. R., Karim, H. T., Peciña, M., Ajilore, O., Taylor, W. D., Butters, M. A., & Andreescu, C. (2022). MRI predictors of pharmacotherapy response in major depressive disorder. NeuroImage: Clinical, 36, 103157. https://doi.org/10.1016/j.nicl.2022.103157

Goddings, A.-L., Roalf, D., Lebel, C., & Tamnes, C. K. (2021). Development of white matter microstructure and executive functions during childhood and adolescence: A review of diffusion MRI studies. Developmental Cognitive Neuroscience, 51, 101008. https://doi.org/10.1016/j.dcn.2021.101008

Goldsmith, D. R., Bekhbat, M., Mehta, N. D., & Felger, J. C. (2023). Inflammation-Related Functional and Structural Dysconnectivity as a Pathway to Psychopathology. Biological Psychiatry, 93(5), 405–418. https://doi.org/10.1016/j.biopsych.2022.11.003

Goldstein-Piekarski, A. N., Ball, T. M., Samara, Z., Staveland, B. R., Keller, A. S., Fleming, S. L., Grisanzio, K. A., Holt-Gosselin, B., Stetz, P., Ma, J., & Williams, L. M. (2022). Mapping Neural Circuit Biotypes to Symptoms and Behavioral Dimensions of Depression and Anxiety. Biological Psychiatry, 91(6), 561–571. https://doi.org/10.1016/j.biopsych.2021.06.024

Gunnar, M., & Quevedo, K. (2007). The neurobiology of stress and development. Annual Review of Psychology, 58, 145–173. https://doi.org/10.1146/annurev.psych.58.110405.085605

Hagler, D. J., Ahmadi, M. E., Kuperman, J., Holland, D., McDonald, C. R., Halgren, E., & Dale, A. M. (2009). Automated white-matter tractography using a probabilistic diffusion tensor atlas: Application to temporal lobe epilepsy. Human Brain Mapping, 30(5), 1535–1547. https://doi.org/10.1002/hbm.20619

Hagler, D. J., Hatton, S., Cornejo, M. D., Makowski, C., Fair, D. A., Dick, A. S., Sutherland, M. T., Casey, B. J., Barch, D. M., Harms, M. P., Watts, R., Bjork, J. M., Garavan, H. P., Hilmer, L., Pung, C. J., Sicat, C. S., Kuperman, J., Bartsch, H., Xue, F., … Dale, A. M. (2019). Image processing and analysis methods for the Adolescent Brain Cognitive Development Study. NeuroImage, 202, 116091. https://doi.org/10.1016/j.neuroimage.2019.116091

Halse, M., Steinsbekk, S., Hammar, Å., & Wichstrøm, L. (2022). Longitudinal relations between impaired executive function and symptoms of psychiatric disorders in childhood. Journal of Child Psychology and Psychiatry, 63(12), 1574–1582. https://doi.org/10.1111/jcpp.13622

Harrison, N. A., Brydon, L., Walker, C., Gray, M. A., Steptoe, A., & Critchley, H. D. (2009). Inflammation causes mood changes through alterations in subgenual cingulate activity and mesolimbic connectivity. Biological Psychiatry, 66(5), 407–414. https://doi.org/10.1016/j.biopsych.2009.03.015

Heleniak, C., Jenness, J. L., Vander Stoep, A., McCauley, E., & McLaughlin, K. A. (2016). Childhood Maltreatment Exposure and Disruptions in Emotion Regulation: A Transdiagnostic Pathway to Adolescent Internalizing and Externalizing Psychopathology. Cognitive Therapy and Research, 40(3), 394–415. https://doi.org/10.1007/s10608-015-9735-z

Howe, A. S., & Lynch, D. A. (2022). Cytokine alterations in pediatric internalizing disorders: Systematic review and exploratory multi-variate meta-analysis. Brain, Behavior, & Immunity - Health, 24, 100490. https://doi.org/10.1016/j.bbih.2022.100490

Huang, W.-J., Huang, G.-T., Zhan, Q.-M., Chen, J.-L., Luo, W.-T., Wu, L.-H., Wu, L.-Y., Wu, L.-Y., Lu, Z.-N., & Sun, Y.-F. (2020). The neutrophil to lymphocyte ratio as a novel predictor of asthma and its exacerbation: A systematic review and meta-analysis. European Review for Medical and Pharmacological Sciences, 24(22), 11719–11728. https://doi.org/10.26355/eurrev_202011_23819

Husain, S. F., Cremaschi, A., Suaini, N. H. A., De Iorio, M., Loo, E. X. L., Shek, L. P., Goh, A. E. N., Meaney, M. J., Tham, E. H., & Law, E. C. (2024). Maternal asthma symptoms during pregnancy on child behaviour and executive function: A Bayesian phenomics approach. Brain, Behavior, and Immunity, 118, 202–209. https://doi.org/10.1016/j.bbi.2024.02.028

Irani, F., Barbone, J. M., Beausoleil, J., & Gerald, L. (2017). Is asthma associated with cognitive impairments? A meta-analytic review. Journal of Clinical and Experimental Neuropsychology, 39, 965–978.

Izadi, N., Baraghoshi, D., Curran-Everett, D., Zeiger, R. S., Szefler, S. J., Covar, R. A., Williams, P., Lasley, M. V., Chinn, T., Hinatsu, M., Furukawa, C. T., Altman, L. C., Virant, F. S., Kennedy, M. S., Tilles, S., Becker, J. W., Bierman, C. W., Crawford, D., DuHamel, T., … Zeiger, R. (2021). Factors Associated with Persistence of Severe Asthma from Late Adolescence to Early Adulthood. American Journal of Respiratory and Critical Care Medicine, 204(7), 776–787. https://doi.org/10.1164/rccm.202010-3763OC

Jackman, S., Tahk, A., Zeileis, A., Maimone, C., Fearon, J., & Meers, Z. (2024). pscl: Political Science Computational Laboratory (1.5.9) [Computer software]. https://cran.r-project.org/web/packages/pscl/index.html

Jackson-Cowan, L., Cole, E. F., Silverberg, J. I., & Lawley, L. P. (2021). Childhood atopic dermatitis is associated with cognitive dysfunction: A National Health Interview Survey study from 2008 to 2018. Annals of Allergy, Asthma & Immunology, 126(6), 661–665. https://doi.org/10.1016/j.anai.2020.11.008

Jones, S. A., Morales, A. M., Lavine, J. B., & Nagel, B. J. (2017). Convergent neurobiological predictors of emergent psychopathology during adolescence. Birth Defects Research, 109(20), 1613–1622. https://doi.org/10.1002/bdr2.1176

Kaas, T. H., Vinding, R. K., Stokholm, J., Bønnelykke, K., Bisgaard, H., & Chawes, B. L. (2021). Association between childhood asthma and attention deficit hyperactivity or autism spectrum disorders: A systematic review with meta-analysis. Clinical & Experimental Allergy, 51(2), 228–252. https://doi.org/10.1111/cea.13750

Kang, D. H., Coe, C. L., McCarthy, D. O., Jarjour, N. N., Kelly, E. A., Rodriguez, R. R., & Busse, W. W. (1997). Cytokine profiles of stimulated blood lymphocytes in asthmatic and healthy adolescents across the school year. Journal of Interferon & Cytokine Research: The Official Journal of the International Society for Interferon and Cytokine Research, 17(8), 481–487. https://doi.org/10.1089/jir.1997.17.481

Kaplan, A., & Price, D. (2020). Treatment Adherence in Adolescents with Asthma. Journal of Asthma and Allergy, 13, 39–49. https://doi.org/10.2147/JAA.S233268

Kessler, R. C., Berglund, P., Demler, O., Jin, R., Merikangas, K. R., & Walters, E. E. (2005). Lifetime prevalence and age-of-onset distributions of DSM-IV disorders in the National Comorbidity Survey Replication. Archives of General Psychiatry, 62(6), 593–602. https://doi.org/10.1001/archpsyc.62.6.593

Koren, T., Yifa, R., Amer, M., Krot, M., Boshnak, N., Ben-Shaanan, T. L., Azulay-Debby, H., Zalayat, I., Avishai, E., Hajjo, H., Schiller, M., Haykin, H., Korin, B., Farfara, D., Hakim, F., Kobiler, O., Rosenblum, K., & Rolls, A. (2021). Insular cortex neurons encode and retrieve specific immune responses. Cell, 184(24), 5902-5915.e17. https://doi.org/10.1016/j.cell.2021.10.013

Kroll, J. L., & Ritz, T. (2023). Asthma, the central nervous system, and neurocognition: Current findings, potential mechanisms, and treatment implications. Neuroscience & Biobehavioral Reviews, 146, 105063. https://doi.org/10.1016/j.neubiorev.2023.105063

Labrenz, F., Ferri, F., Wrede, K., Forsting, M., Schedlowski, M., Engler, H., Elsenbruch, S., Benson, S., & Costantini, M. (2019). Altered temporal variance and functional connectivity of BOLD signal

is associated with state anxiety during acute systemic inflammation. NeuroImage, 184, 916–924. https://doi.org/10.1016/j.neuroimage.2018.09.056

Lam, P. H., Chen, E., Chiang, J. J., & Miller, G. E. (2022). Socioeconomic disadvantage, chronic stress, and proinflammatory phenotype: An integrative data analysis across the lifecourse. PNAS Nexus, 1(4), pgac219. https://doi.org/10.1093/pnasnexus/pgac219

Larsen, B., Verstynen, T. D., Yeh, F.-C., & Luna, B. (2018). Developmental Changes in the Integration of Affective and Cognitive Corticostriatal Pathways are Associated with Reward-Driven Behavior. Cerebral Cortex (New York, N.Y.: 1991), 28(8), 2834–2845. https://doi.org/10.1093/cercor/bhx162

Leffa, D. T., Caye, A., Santos, I., Matijasevich, A., Menezes, A., Wehrmeister, F. C., Oliveira, I., Vitola, E., Bau, C. H. D., Grevet, E. H., Tovo-Rodrigues, L., & Rohde, L. A. (2021). Attention-deficit/hyperactivity disorder has a state-dependent association with asthma: The role of systemic inflammation in a population-based birth cohort followed from childhood to adulthood. Brain, Behavior, and Immunity, 97, 239–249. https://doi.org/10.1016/j.bbi.2021.08.004

Leonard, S. I., Turi, E. R., Powell, J. S., Usseglio, J., MacDonell, K. K., & Bruzzese, J.-M. (2022). Associations of asthma self-management and mental health in adolescents: A scoping review. Respiratory Medicine, 200, 106897. https://doi.org/10.1016/j.rmed.2022.106897

Li, Q.-Y., Li, X.-M., Hu, H.-Y., Ma, Y.-H., Ou, Y.-N., Wang, A.-Y., Tan, L., & Yu, J.-T. (2023). Associations of Lung Function Decline with Risks of Cognitive Impairment and Dementia: A Meta-Analysis and Systematic Review. Journal of Alzheimer's Disease, 92(3), 853–873. https://doi.org/10.3233/JAD-221136

Licari, A., Castagnoli, R., Brambilla, I., Marseglia, A., Tosca, M. A., Marseglia, G. L., & Ciprandi, G. (2018). Asthma Endotyping and Biomarkers in Childhood Asthma. Pediatric Allergy, Immunology, and Pulmonology, 31(2), 44–55. https://doi.org/10.1089/ped.2018.0886

Lim, J., Sohn, H., Kwon, M.-S., & Kim, B. (2021). White Matter Alterations Associated with Pro-inflammatory Cytokines in Patients with Major Depressive Disorder. Clinical Psychopharmacology and Neuroscience: The Official Scientific Journal of the Korean College of Neuropsychopharmacology, 19(3), 449–458. https://doi.org/10.9758/cpn.2021.19.3.449

Lipner, E., Mac Giollabhui, N., Breen, E. C., Cohn, B. A., Krigbaum, N. Y., Cirillo, P. M., Olino, T. M., Alloy, L. B., & Ellman, L. M. (2024). Sex-Specific Pathways From Prenatal Maternal Inflammation to Adolescent Depressive Symptoms. JAMA Psychiatry, 81(5), 498–505. https://doi.org/10.1001/jamapsychiatry.2023.5458

Lorch, S. A., & Enlow, E. (2016). The role of social determinants in explaining racial/ethnic disparities in perinatal outcomes. Pediatric Research, 79(1), 141–147. https://doi.org/10.1038/pr.2015.199

Lu, Y., Mak, K.-K., van Bever, H. P. S., Ng, T. P., Mak, A., & Ho, R. C.-M. (2012). Prevalence of anxiety and depressive symptoms in adolescents with asthma: A meta-analysis and meta-regression. Pediatric Allergy and Immunology, 23(8), 707–715. https://doi.org/10.1111/pai.12000

Lu, Y., Zhou, S., Fan, C., Li, J., Lian, Y., Shang, Y., & Bi, X. (2022). Higher inflammation and cerebral white matter injury associated with cognitive deficit in asthmatic patients with depression. Journal of Asthma, 59(2), 288–296. https://doi.org/10.1080/02770903.2020.1853155

Lu, Z., Chen, L., Xu, S., Bao, Q., Ma, Y., Guo, L., Zhang, S., Huang, X., Cao, C., & Ruan, L. (2018). Allergic disorders and risk of depression: A systematic review and meta-analysis of 51 large-scale studies. Annals of Allergy, Asthma & Immunology, 120(3), 310-317.e2. https://doi.org/10.1016/j.anai.2017.12.011

Lundholm, C., Brew, B. K., D'Onofrio, B. M., Osvald, E. C., Larsson, H., & Almqvist, C. (2020). Asthma and subsequent school performance at age 15–16 years: A Swedish population-based sibling control study. Scientific Reports, 10, 7661. https://doi.org/10.1038/s41598-020-64633-w

Määttä, H., Honkanen, M., Hurtig, T., Taanila, A., Ebeling, H., & Koivumaa-Honkanen, H. (2022). Childhood chronic condition and subsequent self-reported internalizing and externalizing problems in adolescence: A birth cohort study. European Journal of Pediatrics, 181(9), 3377–3387. https://doi.org/10.1007/s00431-022-04505-9

Mac Giollabhui, N., Alloy, L. B., Swistun, D., Coe, C. L., Ellman, L. M., Moriarity, D. P., Stumper, A. C., & Abramson, L. Y. (2021). Concurrent and Longitudinal Associations of Sex and Race with Inflammatory Biomarkers during Adolescence. Journal of Youth and Adolescence, 50(4), 711–723. https://doi.org/10.1007/s10964-020-01369-w

Mah, A., Geeraert, B., & Lebel, C. (2017). Detailing neuroanatomical development in late childhood and early adolescence using NODDI. PLoS ONE, 12(8). https://doi.org/10.1371/journal.pone.0182340

Marek, S., & Dosenbach, N. U. F. (2018). The frontoparietal network: Function, electrophysiology, and importance of individual precision mapping. Dialogues in Clinical Neuroscience, 20(2), 133–140.

Marek, S., Hwang, K., Foran, W., Hallquist, M. N., & Luna, B. (2015). The Contribution of Network Organization and Integration to the Development of Cognitive Control. PLOS Biology, 13(12), e1002328. https://doi.org/10.1371/journal.pbio.1002328

Markanday, A. (2015). Acute Phase Reactants in Infections: Evidence-Based Review and a Guide for Clinicians. Open Forum Infectious Diseases, 2(3), ofv098. https://doi.org/10.1093/ofid/ofv098

Marrie, R. A., & Bernstein, C. N. (2021). Psychiatric comorbidity in immune-mediated inflammatory diseases. World Psychiatry, 20(2), 298–299. https://doi.org/10.1002/wps.20873

Marsland, A. L., Gianaros, P. J., Abramowitch, S. M., Manuck, S. B., & Hariri, A. R. (2008). Interleukin-6 covaries inversely with hippocampal grey matter volume in middle-aged adults. Biological Psychiatry, 64(6), 484–490. https://doi.org/10.1016/j.biopsych.2008.04.016

McLaughlin, K. A., Garrad, M. C., & Somerville, L. H. (2015). What develops during emotional development? A component process approach to identifying sources of psychopathology risk in adolescence. Dialogues in Clinical Neuroscience, 17(4), 403–410.

McLaughlin, K. A., Hatzenbuehler, M. L., Mennin, D. S., & Nolen-Hoeksema, S. (2011). Emotion Dysregulation and Adolescent Psychopathology: A Prospective Study. Behaviour Research and Therapy, 49(9), 544–554. https://doi.org/10.1016/j.brat.2011.06.003

McLaughlin, K. A., Weissman, D., & Bitrán, D. (2019). Childhood Adversity and Neural Development: A Systematic Review. Annual Review of Developmental Psychology, 1(1), 277–312. https://doi.org/10.1146/annurev-devpsych-121318-084950

McRae-McKee, K., Evans, S., Hadjichrysanthou, C., Wong, M. M., de Wolf, F., & Anderson, R. M. (2019). Combining hippocampal volume metrics to better understand Alzheimer's disease progression in at-risk individuals. Scientific Reports, 9(1), 7499. https://doi.org/10.1038/s41598-019-42632-w

Mehta, N. D., Stevens, J. S., Li, Z., Gillespie, C. F., Fani, N., Michopoulos, V., & Felger, J. C. (2020). Inflammation, reward circuitry and symptoms of anhedonia and PTSD in trauma-exposed women. Social Cognitive and Affective Neuroscience, 15(10), 1046–1055. https://doi.org/10.1093/scan/nsz100

Menon, V., & D'Esposito, M. (2022). The role of PFC networks in cognitive control and executive function. Neuropsychopharmacology, 47(1), Article 1. https://doi.org/10.1038/s41386-021-01152-w

Miller, G. A., & Chapman, J. P. (2001). Misunderstanding analysis of covariance. Journal of Abnormal Psychology, 110(1), 40–48. https://doi.org/10.1037//0021-843x.110.1.40

Miller, G. E., Chen, E., & Parker, K. J. (2011). Psychological stress in childhood and susceptibility to the chronic diseases of aging: Moving toward a model of behavioral and biological mechanisms. Psychological Bulletin, 137(6), 959–997. https://doi.org/10.1037/a0024768

Miller, G. F., Coffield, E., Leroy, Z., & Wallin, R. (2016). Prevalence and Costs of Five Chronic Conditions in Children. The Journal of School Nursing : The Official Publication of the National Association of School Nurses, 32(5), 357–364. https://doi.org/10.1177/1059840516641190

Mills, K. L., & Tamnes, C. K. (2014). Methods and considerations for longitudinal structural brain imaging analysis across development. Developmental Cognitive Neuroscience, 9, 172–190. https://doi.org/10.1016/j.dcn.2014.04.004

Misiak, B., Wójta-Kempa, M., Samochowiec, J., Schiweck, C., Aichholzer, M., Reif, A., Samochowiec, A., & Stańczykiewicz, B. (2022). Peripheral blood inflammatory markers in patients with attention deficit/hyperactivity disorder (ADHD): A systematic review and meta-analysis. Progress in Neuro-Psychopharmacology and Biological Psychiatry, 118, 110581. https://doi.org/10.1016/j.pnpbp.2022.110581

Moore, W. C., Meyers, D. A., Wenzel, S. E., Teague, W. G., Li, H., Li, X., D'Agostino, R., Castro, M., Curran-Everett, D., Fitzpatrick, A. M., Gaston, B., Jarjour, N. N., Sorkness, R., Calhoun, W. J., Chung, K. F., Comhair, S. A. A., Dweik, R. A., Israel, E., Peters, S. P., … Bleecker, E. R. (2010). Identification of Asthma Phenotypes Using Cluster Analysis in the Severe Asthma Research Program. American Journal of Respiratory and Critical Care Medicine, 181(4), 315–323. https://doi.org/10.1164/rccm.200906-0896OC

Most Recent National Asthma Data | CDC. (2021, April 7). https://www.cdc.gov/asthma/most_recent_national_asthma_data.htm

Moura, L. M., Crossley, N. A., Zugman, A., Pan, P. M., Gadelha, A., Del Aquilla, M. a. G., Picon, F. A., Anés, M., Amaro, E., de Jesus Mari, J., Miguel, E. C., Rohde, L. A., Bressan, R. A., McGuire, P.,

Sato, J. R., & Jackowski, A. P. (2017). Coordinated brain development: Exploring the synchrony between changes in grey and white matter during childhood maturation. Brain Imaging and Behavior, 11(3), 808–817. https://doi.org/10.1007/s11682-016-9555-0

Mukherjee, P., Miller, J. H., Shimony, J. S., Philip, J. V., Nehra, D., Snyder, A. Z., Conturo, T. E., Neil, J. J., & McKinstry, R. C. (2002). Diffusion-Tensor MR Imaging of Gray and White Matter Development during Normal Human Brain Maturation. American Journal of Neuroradiology, 23(9), 1445–1456.

Munshi, S., & Rosenkranz, J. A. (2018). Effects of Peripheral Immune Challenge on In Vivo Firing of Basolateral Amygdala Neurons in Adult Male Rats. Neuroscience, 390, 174–186. https://doi.org/10.1016/j.neuroscience.2018.08.017

Murray, A. L., Ushakova, A., Speyer, L., Brown, R., Auyeung, B., & Zhu, X. (2022). Sex/gender differences in individual and joint trajectories of common mental health symptoms in early to middle adolescence. JCPP Advances, 2(1), e12057. https://doi.org/10.1002/jcv2.12057

Nair, A. K., Van Hulle, C. A., Bendlin, B. B., Zetterberg, H., Blennow, K., Wild, N., Kollmorgen, G., Suridjan, I., Busse, W. W., Dean, D. C., & Rosenkranz, M. A. (2023). Impact of asthma on the brain: Evidence from diffusion MRI, CSF biomarkers and cognitive decline. Brain Communications, 5(3), fcad180. https://doi.org/10.1093/braincomms/fcad180

Nair, A. K., Van Hulle, C. A., Bendlin, B. B., Zetterberg, H., Blennow, K., Wild, N., Kollmorgen, G., Suridjan, I., Busse, W. W., & Rosenkranz, M. A. (2022). Asthma amplifies dementia risk: Evidence from CSF biomarkers and cognitive decline. Alzheimer's & Dementia : Translational Research & Clinical Interventions, 8(1), e12315. https://doi.org/10.1002/trc2.12315

Nawijn, L., van Zuiden, M., Frijling, J. L., Koch, S. B. J., Veltman, D. J., & Olff, M. (2015). Reward functioning in PTSD: A systematic review exploring the mechanisms underlying anhedonia.

Neuroscience & Biobehavioral Reviews, 51, 189–204. https://doi.org/10.1016/j.neubiorev.2015.01.019

Nazeri, A., Chakravarty, M. M., Rotenberg, D. J., Rajji, T. K., Rathi, Y., Michailovich, O. V., & Voineskos, A. N. (2015). Functional consequences of neurite orientation dispersion and density in humans across the adult lifespan. The Journal of Neuroscience: The Official Journal of the Society for Neuroscience, 35(4), 1753–1762. https://doi.org/10.1523/JNEUROSCI.3979-14.2015

Nazeri, A., Mulsant, B. H., Rajji, T. K., Levesque, M. L., Pipitone, J., Stefanik, L., Shahab, S., Roostaei, T., Wheeler, A. L., Chavez, S., & Voineskos, A. N. (2017). Gray Matter Neuritic Microstructure Deficits in Schizophrenia and Bipolar Disorder. Biological Psychiatry, 82(10), 726–736. https://doi.org/10.1016/j.biopsych.2016.12.005

Newcombe, E. A., Camats-Perna, J., Silva, M. L., Valmas, N., Huat, T. J., & Medeiros, R. (2018). Inflammation: The link between comorbidities, genetics, and Alzheimer's disease. Journal of Neuroinflammation, 15(1), 276. https://doi.org/10.1186/s12974-018-1313-3

Noble, K. G., & Giebler, M. A. (2020). The neuroscience of socioeconomic inequality. Current Opinion in Behavioral Sciences, 36, 23–28. https://doi.org/10.1016/j.cobeha.2020.05.007

Norbom, L. B., Ferschmann, L., Parker, N., Agartz, I., Andreassen, O. A., Paus, T., Westlye, L. T., & Tamnes, C. K. (2021). New insights into the dynamic development of the cerebral cortex in childhood and adolescence: Integrating macro- and microstructural MRI findings. Progress in Neurobiology, 204, 102109. https://doi.org/10.1016/j.pneurobio.2021.102109

Nusslock, R., & Alloy, L. B. (2017). Reward Processing and Mood-Related Symptoms: An RDoC and Translational Neuroscience Perspective. Journal of Affective Disorders, 216, 3–16. https://doi.org/10.1016/j.jad.2017.02.001

Nusslock, R., Alloy, L. B., Brody, G. H., & Miller, G. E. (2024). Annual Research Review: Neuroimmune network model of depression: a developmental perspective. Journal of Child Psychology and Psychiatry, 65(4), 538–567. https://doi.org/10.1111/jcpp.13961

Ouyang, M., Dubois, J., Yu, Q., Mukherjee, P., & Huang, H. (2019). Delineation of early brain development from fetuses to infants with diffusion MRI and beyond. NEUROIMAGE, 185, 836–850. https://doi.org/10.1016/j.neuroimage.2018.04.017

Oyama, K., Hori, Y., Mimura, K., Nagai, Y., Eldridge, M. A. G., Saunders, R. C., Miyakawa, N., Hirabayashi, T., Hori, Y., Inoue, K.-I., Suhara, T., Takada, M., Higuchi, M., Richmond, B. J., & Minamimoto, T. (2022). Chemogenetic Disconnection between the Orbitofrontal Cortex and the Rostromedial Caudate Nucleus Disrupts Motivational Control of Goal-Directed Action. The Journal of Neuroscience: The Official Journal of the Society for Neuroscience, 42(32), 6267–6275. https://doi.org/10.1523/JNEUROSCI.0229-22.2022

Palmer, C. E., Pecheva, D., Iversen, J. R., Hagler, D. J., Sugrue, L., Nedelec, P., Fan, C. C., Thompson, W. K., Jernigan, T. L., & Dale, A. M. (2022). Microstructural development from 9 to 14 years: Evidence from the ABCD Study. Developmental Cognitive Neuroscience, 53, 101044. https://doi.org/10.1016/j.dcn.2021.101044

Parr, A. C., Calabro, F., Tervo-Clemmens, B., Larsen, B., Foran, W., & Luna, B. (2022). Contributions of dopamine-related basal ganglia neurophysiology to the developmental effects of incentives on inhibitory control. Developmental Cognitive Neuroscience, 54, 101100. https://doi.org/10.1016/j.dcn.2022.101100

Pat, N., Riglin, L., Anney, R., Wang, Y., Barch, D. M., Thapar, A., & Stringaris, A. (2022). Motivation and Cognitive Abilities as Mediators Between Polygenic Scores and Psychopathology in Children. Journal of the American Academy of Child and Adolescent Psychiatry, 61(6), 782-795.e3. https://doi.org/10.1016/j.jaac.2021.08.019

Pat, N., Wang, Y., Anney, R., Riglin, L., Thapar, A., & Stringaris, A. (2022). Longitudinally stable, brain-based predictive models mediate the relationships between childhood cognition and socio-demographic, psychological and genetic factors. Human Brain Mapping, 43(18), 5520–5542. https://doi.org/10.1002/hbm.26027

Pedersen, F., Stokholm, L., Pouwer, F., Rubin, K., Peto, T., Frydkjaer-Olsen, U., Thykjær, A. S., Simó, R., & Grauslund, J. (2021). Diabetic retinopathy independently predicts five-year risk of Alzheimer's disease. Investigative Ophthalmology & Visual Science, 62(8), 1071.

Perez, M. F., & Coutinho, M. T. (2021). An Overview of Health Disparities in Asthma. The Yale Journal of Biology and Medicine, 94(3), 497–507.

Pocket Guide for Asthma Management and Prevention for Adults and Children Older than 5 Years. (2022). Global Initiative for Asthma.

Poon, J. A., Thompson, J. C., & Chaplin, T. M. (2022). Task-Based Functional Connectivity Patterns: Links to Adolescent Emotion Regulation and Psychopathology. Journal of Affective Disorders, 302, 33–40. https://doi.org/10.1016/j.jad.2022.01.092

Ravens-Sieberer, U., Otto, C., Kriston, L., Rothenberger, A., Döpfner, M., Herpertz-Dahlmann, B., Barkmann, C., Schön, G., Hölling, H., Schulte-Markwort, M., Klasen, F., & The BELLA study group. (2015). The longitudinal BELLA study: Design, methods and first results on the course of mental health problems. European Child & Adolescent Psychiatry, 24(6), 651–663. https://doi.org/10.1007/s00787-014-0638-4

Ritz, T., Kroll, J. L., Patel, S. V., Chen, J. R., Yezhuvath, U. S., Aslan, S., Khan, D. A., Pinkham, A. E., Rosenfield, D., & Brown, E. S. (2019). Central nervous system signatures of affect in asthma: Associations with emotion-induced bronchoconstriction, airway inflammation, and asthma control. Journal of Applied Physiology (Bethesda, Md.: 1985), 126(6), 1725–1736. https://doi.org/10.1152/japplphysiol.01018.2018

Rizopoulos, D. (2023). GLMMadaptive: Generalized Linear Mixed Models using Adaptive Gaussian Quadrature. [Computer software]. https://drizopoulos.github.io/GLMMadaptive/;, https://github.com/drizopoulos/GLMMadaptive

Rolls, E. T. (2019). The cingulate cortex and limbic systems for emotion, action, and memory. Brain Structure & Function, 224(9), 3001–3018. https://doi.org/10.1007/s00429-019-01945-2

Rosenberg, M. D., Martinez, S. A., Rapuano, K. M., Conley, M. I., Cohen, A. O., Cornejo, M. D., Hagler, D. J., Meredith, W. J., Anderson, K. M., Wager, T. D., Feczko, E., Earl, E., Fair, D. A., Barch, D. M., Watts, R., & Casey, B. J. (2020). Behavioral and Neural Signatures of Working Memory in Childhood. Journal of Neuroscience, 40(26), 5090–5104. https://doi.org/10.1523/JNEUROSCI.2841-19.2020

Rosenkranz, M. A., Busse, W. W., Johnstone, T., Swenson, C. A., Crisafi, G. M., Jackson, M. M., Bosch, J. A., Sheridan, J. F., & Davidson, R. J. (2005). Neural circuitry underlying the interaction between emotion and asthma symptom exacerbation. Proceedings of the National Academy of Sciences, 102(37), 13319–13324. https://doi.org/10.1073/pnas.0504365102

Rosenkranz, M. A., Busse, W. W., Sheridan, J. F., Crisafi, G. M., & Davidson, R. J. (2012). Are There Neurophenotypes for Asthma? Functional Brain Imaging of the Interaction between Emotion and Inflammation in Asthma. PLOS ONE, 7(8), e40921. https://doi.org/10.1371/journal.pone.0040921

Rosenkranz, M. A., Dean, D. C., Bendlin, B. B., Jarjour, N. N., Esnault, S., Zetterberg, H., Heslegrave, A., Evans, M. D., Davidson, R. J., & Busse, W. W. (2022). Neuroimaging and biomarker evidence of neurodegeneration in asthma. Journal of Allergy and Clinical Immunology, 149(2), 589-598.e6. https://doi.org/10.1016/j.jaci.2021.09.010

Rosenkranz, M. A., Esnault, S., Christian, B. T., Crisafi, G., Gresham, L. K., Higgins, A. T., Moore, M. N., Moore, S. M., Weng, H. Y., Salk, R. H., Busse, W. W., & Davidson, R. J. (2018).

Corrigendum to “Mind-body interactions in the regulation of airway inflammation in asthma: A PET study of acute and chronic stress” [Brain Behav. Immun. 58 (2016) 18-30]. Brain, Behavior, and Immunity, 67, 398–401. https://doi.org/10.1016/j.bbi.2017.08.009

Rosenkranz, M. A., Esnault, S., Gresham, L., Davidson, R. J., Christian, B. T., Jarjour, N. N., & Busse, W. W. (2022). Role of amygdala in stress-induced upregulation of airway IL-1 signaling in asthma. Biological Psychology, 167, 108226. https://doi.org/10.1016/j.biopsycho.2021.108226

Rosseel, Y. (2012). lavaan: An R Package for Structural Equation Modeling. Journal of Statistical Software, 48, 1–36. https://doi.org/10.18637/jss.v048.i02

Saitoh, B., Tanaka, E., Yamamoto, N., Kruining, D. van, Iinuma, K., Nakamuta, Y., Yamaguchi, H., Yamasaki, R., Matsumoto, K., & Kira, J. (2021). Early postnatal allergic airway inflammation induces dystrophic microglia leading to excitatory postsynaptic surplus and autism-like behavior. Brain, Behavior, and Immunity, 95, 362–380. https://doi.org/10.1016/j.bbi.2021.04.008

Schalbetter, S. M., von Arx, A. S., Cruz-Ochoa, N., Dawson, K., Ivanov, A., Mueller, F. S., Lin, H.-Y., Amport, R., Mildenberger, W., Mattei, D., Beule, D., Földy, C., Greter, M., Notter, T., & Meyer, U. (n.d.). Adolescence is a sensitive period for prefrontal microglia to act on cognitive development. Science Advances, 8(9), eabi6672. https://doi.org/10.1126/sciadv.abi6672

Schmidt, L., Lebreton, M., Cléry-Melin, M.-L., Daunizeau, J., & Pessiglione, M. (2012). Neural mechanisms underlying motivation of mental versus physical effort. PLoS Biology, 10(2), e1001266. https://doi.org/10.1371/journal.pbio.1001266

Schramm, E., & Waisman, A. (2022). Microglia as Central Protagonists in the Chronic Stress Response. Neurology - Neuroimmunology Neuroinflammation, 9(6), e200023. https://doi.org/10.1212/NXI.0000000000200023

Schweizer, S., Gotlib, I. H., & Blakemore, S.-J. (2020). The Role of Affective Control in Emotion Regulation During Adolescence. Emotion (Washington, D.C.), 20(1), 80–86. https://doi.org/10.1037/emo0000695

Schweizer, S., Parker, J., Leung, J. T., Griffin, C., & Blakemore, S.-J. (2020). Age-related differences in affective control and its association with mental health difficulties. Development and Psychopathology, 32(1), 329–341. https://doi.org/10.1017/S0954579419000099

Scott, G., Asrat, S., Allinne, J., Keat Lim, W., Nagashima, K., Birchard, D., Srivatsan, S., Ajithdoss, D. K., Oyejide, A., Ben, L.-H., Walls, J., Le Floc'h, A., Yancopoulos, G. D., Murphy, A. J., Sleeman, M. A., & Orengo, J. M. (2023). IL-4 and IL-13, not eosinophils, drive type 2 airway inflammation, remodeling and lung function decline. Cytokine, 162, 156091. https://doi.org/10.1016/j.cyto.2022.156091

Seeley, W. W. (2019). The Salience Network: A Neural System for Perceiving and Responding to Homeostatic Demands. The Journal of Neuroscience: The Official Journal of the Society for Neuroscience, 39(50), 9878–9882. https://doi.org/10.1523/JNEUROSCI.1138-17.2019

Shackman, A. J., Salomons, T. V., Slagter, H. A., Fox, A. S., Winter, J. J., & Davidson, R. J. (2011). The integration of negative affect, pain and cognitive control in the cingulate cortex. Nature Reviews. Neuroscience, 12(3), 154–167. https://doi.org/10.1038/nrn2994

Shero, S. T., Ammary-Risch, N. J., Lomotan, E. A., Mardon, R. E., & Michaels, M. (2023). Creating implementable clinical practice guidelines: The 2020 Focused Updates to the National Heart, Lung, and Blood Institute's Asthma Management Guidelines. Implementation Science Communications, 4(1), 36. https://doi.org/10.1186/s43058-023-00417-3

Simmonds, D. J., Hallquist, M. N., & Luna, B. (2017). Protracted development of executive and mnemonic brain systems underlying working memory in adolescence: A longitudinal fMRI study. NeuroImage, 157, 695–704. https://doi.org/10.1016/j.neuroimage.2017.01.016

Smith, B. L., Laaker, C. J., Lloyd, K. R., Hiltz, A. R., & Reyes, T. M. (2020). Adolescent microglia play a role in executive function in male mice exposed to perinatal high fat diet. Brain, Behavior, and Immunity, 84, 80–89. https://doi.org/10.1016/j.bbi.2019.11.010

Smith, S. M. (2002). Fast robust automated brain extraction. Human Brain Mapping, 17(3), 143–155. https://doi.org/10.1002/hbm.10062

Smith, S. M., Jenkinson, M., Johansen-Berg, H., Rueckert, D., Nichols, T. E., Mackay, C. E., Watkins, K. E., Ciccarelli, O., Cader, M. Z., Matthews, P. M., & Behrens, T. E. J. (2006). Tract-based spatial statistics: Voxelwise analysis of multi-subject diffusion data. NeuroImage, 31(4), 1487–1505. https://doi.org/10.1016/j.neuroimage.2006.02.024

Snyder, H. R. (2013). Major depressive disorder is associated with broad impairments on neuropsychological measures of executive function: A meta-analysis and review. Psychological Bulletin, 139(1), 81–132. https://doi.org/10.1037/a0028727

Solmi, M., Radua, J., Olivola, M., Croce, E., Soardo, L., Salazar de Pablo, G., Il Shin, J., Kirkbride, J. B., Jones, P., Kim, J. H., Kim, J. Y., Carvalho, A. F., Seeman, M. V., Correll, C. U., & Fusar-Poli, P. (2022). Age at onset of mental disorders worldwide: Large-scale meta-analysis of 192 epidemiological studies. Molecular Psychiatry, 27(1), 281–295. https://doi.org/10.1038/s41380-021-01161-7

Sousa, S. S., Amaro, E., Crego, A., Gonçalves, Ó. F., & Sampaio, A. (2018). Developmental trajectory of the prefrontal cortex: A systematic review of diffusion tensor imaging studies. Brain Imaging and Behavior, 12(4), 1197–1210. https://doi.org/10.1007/s11682-017-9761-4

Sugimoto, K., Kakeda, S., Watanabe, K., Katsuki, A., Ueda, I., Igata, N., Igata, R., Abe, O., Yoshimura, R., & Korogi, Y. (2018). Relationship between white matter integrity and serum inflammatory cytokine levels in drug-naive patients with major depressive disorder: Diffusion tensor imaging

study using tract-based spatial statistics. Translational Psychiatry, 8(1), 141. https://doi.org/10.1038/s41398-018-0174-y

Sydnor, V. J., Larsen, B., Bassett, D. S., Alexander-Bloch, A., Fair, D. A., Liston, C., Mackey, A. P., Milham, M. P., Pines, A., Roalf, D. R., Seidlitz, J., Xu, T., Raznahan, A., & Satterthwaite, T. D. (2021). Neurodevelopment of the association cortices: Patterns, mechanisms, and implications for psychopathology. Neuron, 109(18), 2820–2846. https://doi.org/10.1016/j.neuron.2021.06.016

Tattersall, M. C. (2023). Asthma as a Systemic Disease: Cardiovascular Effects Associated with Asthma. In A. R. Brasier & N. N. Jarjour (Eds.), Precision Approaches to Heterogeneity in Asthma (pp. 77–100). Springer International Publishing. https://doi.org/10.1007/978-3-031-32259-4_4

Tattersall, M. C., Evans, M. D., Korcarz, C. E., Mitchell, C., Anderson, E., DaSilva, D. F., Salazar, L. P., Gern, J. E., Jackson, D. J., Jr, R. F. L., & Stein, J. H. (2018). Asthma is associated with carotid arterial injury in children: The Childhood Origins of Asthma (COAST) Cohort. PLOS ONE, 13(9), e0204708. https://doi.org/10.1371/journal.pone.0204708

Tattersall, M. C., Jarjour, N. N., & Busse, P. J. (2024). Systemic Inflammation in Asthma: What Are the Risks and Impacts Outside the Airway? The Journal of Allergy and Clinical Immunology: In Practice, 12(4), 849–862. https://doi.org/10.1016/j.jaip.2024.02.004

Thomas, M., Savitz, J., Zhang, Y., Burrows, K., Smith, R., Figueroa-Hall, L., Kuplicki, R., Khalsa, S. S., Taki, Y., Teague, T. K., Irwin, M. R., Yeh, F.-C., Paulus, M. P., Zheng, H., & On Behalf Of Tulsa Investigators, null. (2021). Elevated Systemic Inflammation Is Associated with Reduced Corticolimbic White Matter Integrity in Depression. Life (Basel, Switzerland), 12(1), 43. https://doi.org/10.3390/life12010043

Thompson, A., & Steinbeis, N. (2020). Sensitive periods in executive function development. Current Opinion in Behavioral Sciences, 36, 98–105. https://doi.org/10.1016/j.cobeha.2020.08.001

Trivedi, M., & Denton, E. (2019). Asthma in Children and Adults—What Are the Differences and What Can They Tell us About Asthma? Frontiers in Pediatrics, 7, 256. https://doi.org/10.3389/fped.2019.00256

Uncontrolled Asthma among Children, 2012–2014. (2019). Centers for Disease Control and Prevention (CDC). https://www.cdc.gov/asthma/asthma_stats/uncontrolled-asthma-children.htm

Usán Supervía, P., & Quílez Robres, A. (2021). Emotional Regulation and Academic Performance in the Academic Context: The Mediating Role of Self-Efficacy in Secondary Education Students. International Journal of Environmental Research and Public Health, 18(11), 5715. https://doi.org/10.3390/ijerph18115715

Vichaya, E. G., & Dantzer, R. (2018). Inflammation-induced motivational changes: Perspective gained by evaluating positive and negative valence systems. Current Opinion in Behavioral Sciences, 22, 90–95. https://doi.org/10.1016/j.cobeha.2018.01.008

Vorona, G. A., & Berman, J. I. (2015). Review of diffusion tensor imaging and its application in children. Pediatric Radiology, 45(3), 375–381. https://doi.org/10.1007/s00247-015-3277-0

Weber, M. D., Godbout, J. P., & Sheridan, J. F. (2017). Repeated Social Defeat, Neuroinflammation, and Behavior: Monocytes Carry the Signal. Neuropsychopharmacology, 42(1), 46–61. https://doi.org/10.1038/npp.2016.102

Weintraub, S., Bauer, P. J., Zelazo, P. D., Wallner-Allen, K., Dikmen, S. S., Heaton, R. K., Tulsky, D. S., Slotkin, J., Blitz, D. L., Carlozzi, N. E., Havlik, R. J., Beaumont, J. L., Mungas, D., Manly, J. J., Borosh, B. G., Nowinski, C. J., & Gershon, R. C. (2013). NIH Toolbox Cognition Battery (CB): Introduction and pediatric data. Monographs of the Society for Research in Child Development, 78(4), 1–15. https://doi.org/10.1111/mono.12031

Westbrook, A., van den Bosch, R., Määttä, J. I., Hofmans, L., Papadopetraki, D., Cools, R., & Frank, M. J. (2020). Dopamine promotes cognitive effort by biasing the benefits versus costs of cognitive work. Science, 367(6484), 1362–1366. https://doi.org/10.1126/science.aaz5891

Whittle, S., Simmons, J. G., Hendriksma, S., Vijayakumar, N., Byrne, M. L., Dennison, M., & Allen, N. B. (2017). Childhood maltreatment, psychopathology, and the development of hippocampal subregions during adolescence. Brain and Behavior, 7(2), e00607. https://doi.org/10.1002/brb3.607

Winkler, A. M., Ridgway, G. R., Webster, M. A., Smith, S. M., & Nichols, T. E. (2014). Permutation inference for the general linear model. NeuroImage, 92, 381–397. https://doi.org/10.1016/j.neuroimage.2014.01.060

Winkler, A. M., Webster, M. A., Vidaurre, D., Nichols, T. E., & Smith, S. M. (2015). Multi-level block permutation. NeuroImage, 123, 253–268. https://doi.org/10.1016/j.neuroimage.2015.05.092

Woodburn, S. C., Bollinger, J. L., & Wohleb, E. S. (2021). The semantics of microglia activation: Neuroinflammation, homeostasis, and stress. Journal of Neuroinflammation, 18(1), 258. https://doi.org/10.1186/s12974-021-02309-6

Xu, X.-F., Li, Y.-J., Sheng, Y.-J., Liu, J.-L., Tang, L.-F., & Chen, Z.-M. (2014). Effect of low birth weight on childhood asthma: A meta-analysis. BMC Pediatrics, 14, 275. https://doi.org/10.1186/1471-2431-14-275

Yamasaki, A., Okazaki, R., & Harada, T. (2022). Neutrophils and Asthma. Diagnostics (Basel, Switzerland), 12(5), 1175. https://doi.org/10.3390/diagnostics12051175

Yang, Y., Shields, G. S., Zhang, Y., Wu, H., Chen, H., & Romer, A. L. (2022). Child executive function and future externalizing and internalizing problems: A meta-analysis of prospective longitudinal studies. Clinical Psychology Review, 97, 102194. https://doi.org/10.1016/j.cpr.2022.102194

Yaple, Z., & Arsalidou, M. (2018). N-back Working Memory Task: Meta-analysis of Normative fMRI Studies With Children. Child Development, 89(6), 2010–2022. https://doi.org/10.1111/cdev.13080

Zhang, H., Schneider, T., Wheeler-Kingshott, C. A., & Alexander, D. C. (2012). NODDI: Practical in vivo neurite orientation dispersion and density imaging of the human brain. NeuroImage, 61(4), 1000–1016. https://doi.org/10.1016/j.neuroimage.2012.03.072

Zheng, R., Zhang, Y., Yang, Z., Han, S., & Cheng, J. (2021). Reduced Brain Gray Matter Volume in Patients With First-Episode Major Depressive Disorder: A Quantitative Meta-Analysis. Frontiers in Psychiatry, 12. https://doi.org/10.3389/fpsyt.2021.671348

Zhu, Y., Womer, F. Y., Leng, H., Chang, M., Yin, Z., Wei, Y., Zhou, Q., Fu, S., Deng, X., Lv, J., Song, Y., Ma, Y., Sun, X., Bao, J., Wei, S., Jiang, X., Tan, S., Tang, Y., & Wang, F. (2019). The Relationship Between Cognitive Dysfunction and Symptom Dimensions Across Schizophrenia, Bipolar Disorder, and Major Depressive Disorder. Frontiers in Psychiatry, 10. https://doi.org/10.3389/fpsyt.2019.00253

Zhu, Z., Zhu, X., Liu, C.-L., Shi, H., Shen, S., Yang, Y., Hasegawa, K., Camargo, C. A., & Liang, L. (2019). Shared genetics of asthma and mental health disorders: A large-scale genome-wide cross-trait analysis. The European Respiratory Journal, 54(6), 1901507. https://doi.org/10.1183/13993003.01507-2019

# APPENDIX A: Classification of Medications Consistent with Asthma History in Adolescent Brain Cognitive Development Study

Youth where classified as taking "asthma-specific medications" if their medication list included one of the specified strings from the following medication classes: short-acting beta-agonists (Albuterol, proventil, vospire, accuneb, ventolin, proair, levalbuterol, xopenex, pirbuterol, terbutaline, maxair), long-acting beta-agonists (foradil, formoterol, salmeterol, serevent, vilanterol), short-acting or long-acting muscarinic-agonists (tiotropium, oxitropium, spiriva, atrovent, combivent, duoneb), mast cell stabilizers (cromolyn, nedocromil, intal, tilade), theophylline (theophylline, quibron, elixophyllin, theochron, uniphyl, slo-bid, theo), medications containing inhaled corticosteroids (advair, aerobid, aerospan, airduo, alvesco, arnuity, armonair, asmanex, azmacort, breo, ciclesonide, dulera, flovent, pulmicort, qvar, symbicort, vanceril, wixela), immunomodulators (benralizumab, cinqair, dupilumab, dupixent, fasenra, mepolizumab, nucala, omalizumab, reslizuma, tezepelumab, tezspire, xolair) or other (daliresp, roflumilast, trelegy, umeclidinium).

Generic inhaled steroids were identified for further analysis when dose and route of administration were unspecified (beclomethasone, budesonide, mometasone, fluticasone, flunisolide, triamcinolone). Steroids were not classified as asthma medications if they were reported as over the counter medications or if they contained one of the following strings: nasal, naso, flonase, nasacort qnasl, nasoflow, clarispray, sinex, topical, paste ointment, triderm, dermasorb, pediaderm, ophthalmic, ciprodex, cyproheptadine, maxidex, urea, neomycin, tobramycin. Steroids were assumed to be asthma-specific inhaled steroids if the participant additionally reported using a rescue inhaler (i.e. short acting beta-agnoistt, combivent, duoneb) and the steroid medication did not contain a disqualifying string (e.g. topical).

Two additional classes of medications were considered asthma-related medications depending on context. Both ipratropium (with an unspecified route of administration) and leukotrienes are prescribed for both asthma and allergic rhinitis (montelukast, singulair, acolate, pranlukast, zafirlukast, zileuton, zyflo). Therefore, participants had to additionally endorse an asthma history or report taking another asthma-related medication for these to be considered asthma-specific medications. Use of either off these medications alone was not sufficient to earn an asthma classification.

# APPENDIX B

## Additional Results

There were no relationships between the Neutrophil-to-Lymphocyte Ratio and cognitive outcomes ($N$ = 531; $g$: $F(1, 316.97) = 0.17$, $p = 0.69$; executive functioning: $F(1, 500.31) = 2.10$, $p = 0.148$; memory: $b = -0.02$, $F(1, 278.0) = 0.07$ , $p = 0.791$; language: $b = 0.004$, $F(1, 390.87) = 0.005$ , $p = 0.943$) or emotional outcomes ($N$ = 518; total problems: $b = 0.075$, $Z = 1.01$, $p = 0.312$; internalizing problems: $b = 0.04$, $Z = 0.43$, $p = 0.670$; anxiety and depressive problems: $b = 0.03$, $Z = 1.34$, $p = 0.179$; attention problems: $b = -0.02$, $Z = -0.25$, $p = 0.806$).

Additionally, there were no relationships between eosinophils and emotional outcomes.

(total problems: $b = 0.16$, SE = 0.32, $Z = 0.52$, 0.607; internalizing problems: $b = 0.06$, SE = 0.36, $Z = -0.18$, $p = 0.857$; anxiety and depressive problems: $b = -0.07$, SE = 0.62, $Z = -0.11$, $p = 0.913$; attention problems: $b = 0.39$, SE = 0.38, $Z = 1.03$, $p = 0.306$).

## Additional Tables

Captions for Additional Tables

Tables B1 to B25 are the statistical results from permutation analyses (PALM) to examine the relationship between brain structure (*i.e.* white matter, subcortical grey matter, cortical grey matter) and behavioral outcome metrics. Behavioral outcome metrics included latent scores from performance on NIH Toolbox metrics (*g*, executive functioning, language, and memory scores) and parent-reported problems for the Child Behavior Checklist (total problems, internalizing problems, anxiety/depressive problems, and attention problems). Table B26 to B28 are similar PALM analyses to examine the correlation between these outcomes and lifetime asthma attacks in youth with asthma.

For each table, the abbreviation FWE indicates *p* statistics with family-wise error correction applied across regions of interest within a modality and mFWE indicates *p* statistics with familywise error correction applied both across regions and across e modalities. FA = fractional anisotropy; MD =mean diffusivity; RD = radial diffusivity; AD = axial diffusivity.

**Table B1 Negative correlations between white matter metrics and *g* scores**

| | Right fornix | Left fornix | Right cingulate bundle (cingulate) | Left cingulate bundle (cingulate) | Right cingulate bundle (PH) | Left cingulate bundle (PH) | Right corticospinal tract | Left corticospinal | Right anterior thalamic radiations | Left anterior thalamic radiations | Right uncinate fasciculus | Left uncinate fasciculus | Right inferior longitudinal fasciculus | Left inferior longitudinal fasciculus |
|---|---|---|---|---|---|---|---|---|---|---|---|---|---|---|
| **Fisher F** | **434.37** | **543.86** | **104.02** | **62.79** | **135.15** | **148.89** | **229.46** | **271.33** | **163.26** | **159.92** | **93.46** | **99.07** | **193.45** | **174.79** |
| **Fisher FWE p** | **0.001** | **< 0.001** | **0.009** | **0.016** | **0.007** | **0.006** | **0.003** | **0.002** | **0.005** | **0.005** | **0.011** | **0.01** | **0.004** | **0.005** |
| FA | 3.5 | 5.68 | -4.04 | -3.25 | 1.77 | 4.13 | 3.63 | 2.8 | 1.93 | 2.12 | -2.22 | -0.85 | 1.22 | 1.7 |
| FA FWE p | 0.001 | < 0.001 | 0.999 | 0.999 | 0.019 | < 0.001 | 0.001 | 0.003 | 0.014 | 0.01 | 0.999 | 0.999 | 0.049 | 0.021 |
| FA mFWE p | 0.121 | 0.028 | 0.999 | 0.999 | 0.999 | 0.064 | 0.1 | 0.999 | 0.999 | 0.999 | 0.999 | 0.999 | 0.999 | 0.999 |
| MD | 2.9 | 2.36 | -0.93 | -1.73 | 0.56 | -0.12 | 2.32 | 1.48 | 0.66 | 0.3 | -2.23 | -2.68 | -0.12 | -0.76 |
| MD FWE p | 0.02 | 0.105 | 0.999 | 0.999 | 0.917 | 0.991 | 0.116 | 0.518 | 0.894 | 0.962 | 0.999 | 0.999 | 0.991 | 0.999 |
| MD mFWE p | 0.999 | 0.999 | 0.999 | 0.999 | 0.999 | 0.999 | 0.999 | 0.999 | 0.999 | 0.999 | 0.999 | 0.999 | 0.999 | 0.999 |
| RD | 5.12 | 6.01 | -3.42 | -3.3 | 1.72 | 2.71 | 4.29 | 2.89 | 1.68 | 1.51 | -2.48 | -1.84 | 0.87 | 0.71 |
| RD FWE p | < 0.001 | < 0.001 | 0.999 | 0.999 | 0.093 | 0.016 | 0.001 | 0.012 | 0.101 | 0.13 | 0.999 | 0.999 | 0.324 | 0.395 |
| RD mFWE p | 0.036 | 0.025 | 0.999 | 0.999 | 0.999 | 0.999 | 0.058 | 0.999 | 0.999 | 0.999 | 0.999 | 0.999 | 0.999 | 0.999 |
| AD | -0.27 | -1.96 | 3.49 | 1.85 | -1.18 | -3.57 | -0.8 | -0.83 | -1.02 | -1.56 | -0.12 | -1.98 | -1.18 | -2.15 |
| AD FWE p | 0.999 | 0.999 | 0.061 | 0.939 | 0.999 | 0.999 | 0.999 | 0.999 | 0.999 | 0.999 | 0.999 | 0.999 | 0.999 | 0.999 |
| AD mFWE p | 0.999 | 0.999 | 0.121 | 0.999 | 0.999 | 0.999 | 0.999 | 0.999 | 0.999 | 0.999 | 0.999 | 0.999 | 0.999 | 0.999 |
| Volume | 19.46 | 21.63 | 9.02 | 7.09 | 10.69 | 10.45 | 13.22 | 15.47 | 11.92 | 11.81 | 9.31 | 9.64 | 13.43 | 12.68 |
| Volume FWE p | < 0.001 | < 0.001 | 0.01 | 0.02 | 0.006 | 0.006 | 0.002 | 0.001 | 0.004 | 0.004 | 0.009 | 0.008 | 0.002 | 0.003 |
| Volume mFWE p | < 0.001 | < 0.001 | 0.008 | 0.016 | 0.005 | 0.005 | 0.002 | 0.001 | 0.004 | 0.004 | 0.008 | 0.007 | 0.002 | 0.003 |

Table B1 Continued

| | Right inferior fronto occipital fasciculus | Left inferior fronto occipital fasciculus | Forceps major | Forceps minor | Corpus callosum | Right SLF | Left SLF | Right temporal SLF | Left temporal SLF | Right parietal SLF | Left parietal SLF | Right superior corticostriate | Left superior corticostriate |
|---|---|---|---|---|---|---|---|---|---|---|---|---|---|
| **Fisher F** | **200.88** | **182.06** | **239.19** | **150.88** | **258.59** | **242.86** | **324.08** | **260.8** | **319.77** | **225.36** | **293.94** | **161.52** | **218.71** |
| **Fisher FWE p** | **0.004** | **0.004** | **0.003** | **0.006** | **0.002** | **0.003** | **0.002** | **0.002** | **0.002** | **0.003** | **0.002** | **0.005** | **0.003** |
| FA | -0.44 | 0.57 | 1.02 | -1.86 | -0.33 | 3.17 | 4.49 | 2.29 | 4.11 | 3.21 | 4.46 | 0.31 | 2.35 |
| FA FWE p | 0.68 | 0.145 | 0.069 | 0.999 | 0.579 | 0.002 | < 0.001 | 0.008 | < 0.001 | 0.001 | < 0.001 | 0.222 | 0.007 |
| FA mFWE p | 0.999 | 0.999 | 0.999 | 0.999 | 0.999 | 0.999 | 0.051 | 0.999 | 0.065 | 0.999 | 0.052 | 0.999 | 0.999 |
| MD | -1.19 | -1.26 | 1.21 | -4.66 | -1.01 | 2.07 | 1.01 | 1.52 | 0.71 | 2.21 | 1.57 | 2.77 | 0.41 |
| MD FWE p | 0.999 | 0.999 | 0.671 | 0.999 | 0.999 | 0.204 | 0.77 | 0.493 | 0.88 | 0.152 | 0.468 | 0.032 | 0.947 |
| MD mFWE p | 0.999 | 0.999 | 0.999 | 0.999 | 0.999 | 0.999 | 0.999 | 0.999 | 0.999 | 0.999 | 0.999 | 0.999 | 0.999 |
| RD | -1.02 | -0.41 | 1.15 | -3.39 | -0.85 | 3.17 | 3.5 | 2.48 | 3.17 | 3.2 | 3.68 | 1.66 | 1.68 |
| RD FWE p | 0.999 | 0.937 | 0.224 | 0.999 | 0.998 | 0.007 | 0.003 | 0.025 | 0.007 | 0.006 | 0.002 | 0.104 | 0.1 |
| RD mFWE p | 0.999 | 0.999 | 0.999 | 0.999 | 0.999 | 0.999 | 0.119 | 0.999 | 0.999 | 0.999 | 0.095 | 0.999 | 0.999 |
| AD | -0.63 | -1.52 | 0.4 | -3.65 | -0.49 | -0.92 | -3.48 | -0.86 | -3.36 | -0.75 | -2.92 | 1.94 | -1.32 |
| AD FWE p | 0.999 | 0.999 | 0.999 | 0.999 | 0.999 | 0.999 | 0.999 | 0.999 | 0.999 | 0.999 | 0.999 | 0.916 | 0.999 |
| AD mFWE p | 0.999 | 0.999 | 0.999 | 0.999 | 0.999 | 0.999 | 0.999 | 0.999 | 0.999 | 0.999 | 0.999 | 0.999 | 0.999 |
| Volume | 13.98 | 13.2 | 14.91 | 12.09 | 15.97 | 14.23 | 16.69 | 15.29 | 16.76 | 13.54 | 15.62 | 11.38 | 14.06 |
| Volume FWE p | 0.002 | 0.002 | 0.001 | 0.003 | 0.001 | 0.002 | 0.001 | 0.001 | 0.001 | 0.002 | 0.001 | 0.004 | 0.002 |
| Volume mFWE p | 0.002 | 0.002 | 0.002 | 0.003 | 0.001 | 0.002 | 0.001 | 0.001 | 0.001 | 0.002 | 0.001 | 0.004 | 0.002 |

Table B1 Continued

| | Right superior corticostriatal | Left superior corticostriatal | Right inferior frontal cortex | Left inferior frontal cortex |
|---|---|---|---|---|
| **Fisher F** | **147.88** | **131.17** | **193.8** | **180.87** |
| **Fisher FWE p** | **0.006** | **0.007** | **0.004** | **0.005** |
| FA | -1.77 | 0.28 | 2.48 | 2.79 |
| FA FWE p | 0.999 | 0.232 | 0.005 | 0.003 |
| FA mFWE p | 0.999 | 0.999 | 0.999 | 0.999 |
| MD | -2.09 | -1.61 | -0.03 | -0.45 |
| MD FWE p | 0.999 | 0.999 | 0.988 | 0.998 |
| MD mFWE p | 0.999 | 0.999 | 0.999 | 0.999 |
| RD | -2.41 | -1.09 | 1.15 | 1.12 |
| RD FWE p | 0.999 | 0.999 | 0.224 | 0.235 |
| RD mFWE p | 0.999 | 0.999 | 0.999 | 0.999 |
| AD | -0.14 | -1.57 | -1.8 | -2.64 |
| AD FWE p | 0.999 | 0.999 | 0.999 | 0.999 |
| AD mFWE p | 0.999 | 0.999 | 0.999 | 0.999 |
| Volume | 11.91 | 11.12 | 13.2 | 12.64 |
| Volume FWE p | 0.004 | 0.005 | 0.002 | 0.003 |
| Volume mFWE p | 0.004 | 0.004 | 0.002 | 0.003 |

**Table B2 Negative correlations between white matter metrics and language scores**

| | Right fornix | Left fornix | Right cingulate bundle (cingulate) | Left cingulate bundle (cingulate) | Right cingulate bundle (PH) | Left cingulate bundle (PH) | Right corticospinal tract | Left corticospinal | Right anterior thalamic radiations | Left anterior thalamic radiations | Right uncinate fasciculus | Left uncinate fasciculus |
|---|---|---|---|---|---|---|---|---|---|---|---|---|
| **Fisher F** | **510.58** | **612.42** | **128.44** | **81.02** | **193.56** | **206.41** | **296.08** | **346.05** | **232.21** | **231.21** | **128.49** | **128.05** |
| **Fisher FWE p** | **0.001** | < 0.001 | **0.008** | **0.014** | **0.005** | **0.004** | **0.002** | **0.002** | **0.004** | **0.004** | **0.008** | **0.008** |
| FA | 3.03 | 5.46 | -4.18 | -3.17 | 2.69 | 4.62 | 3.73 | 2.92 | 1.9 | 1.93 | -1.22 | 0.11 |
| FA FWE p | 0.002 | < 0.001 | 0.999 | 0.999 | 0.003 | < 0.001 | < 0.001 | 0.002 | 0.019 | 0.018 | 0.999 | 0.537 |
| FA mFWE p | 0.999 | 0.032 | 0.999 | 0.999 | 0.999 | 0.049 | 0.122 | 0.999 | 0.999 | 0.999 | 0.999 | 0.999 |
| MD | 2.76 | 2.09 | -0.53 | -1.47 | 1.52 | 0.83 | 3.14 | 2.27 | 0.85 | 0.1 | -1.29 | -1.93 |
| MD FWE p | 0.253 | 0.644 | 0.999 | 0.999 | 0.889 | 0.988 | 0.107 | 0.537 | 0.987 | 0.999 | 0.999 | 0.999 |
| MD mFWE p | 0.999 | 0.999 | 0.999 | 0.999 | 0.999 | 0.999 | 0.999 | 0.999 | 0.999 | 0.999 | 0.999 | 0.999 |
| RD | 4.8 | 5.74 | -3.36 | -3.11 | 3.05 | 3.7 | 4.8 | 3.31 | 1.8 | 1.27 | -1.4 | -0.89 |
| RD FWE p | < 0.001 | < 0.001 | 0.999 | 0.999 | 0.016 | 0.003 | < 0.001 | 0.009 | 0.198 | 0.431 | 0.999 | 0.999 |
| RD mFWE p | 0.044 | 0.028 | 0.999 | 0.999 | 0.999 | 0.132 | 0.044 | 0.999 | 0.999 | 0.999 | 0.999 | 0.999 |
| AD | -0.19 | -2.14 | 4.03 | 1.99 | -1.26 | -3.32 | -0.21 | -0.2 | -0.84 | -1.58 | -0.12 | -2.18 |
| AD FWE p | 0.999 | 0.999 | 0.025 | 0.956 | 0.999 | 0.999 | 0.999 | 0.999 | 0.999 | 0.999 | 0.999 | 0.999 |
| AD mFWE p | 0.999 | 0.999 | 0.077 | 0.999 | 0.999 | 0.999 | 0.999 | 0.999 | 0.999 | 0.999 | 0.999 | 0.999 |
| Volume | 21.65 | 23.48 | 10.07 | 8.23 | 12.59 | 12.42 | 15.24 | 17.6 | 14.56 | 14.66 | 11.02 | 10.99 |
| Volume FWE p | < 0.001 | < 0.001 | 0.008 | 0.014 | 0.004 | 0.004 | 0.002 | 0.001 | 0.002 | 0.002 | 0.006 | 0.006 |
| Volume mFWE p | < 0.001 | < 0.001 | 0.007 | 0.012 | 0.004 | 0.004 | 0.002 | 0.001 | 0.002 | 0.002 | 0.005 | 0.005 |

Table B2 Continued

| | Right inferior longitudinal fasciculus | Left inferior longitudinal fasciculus | Forceps major | Forceps minor | Corpus callosum | Right SLF | Left SLF | Right temporal SLF | Left temporal SLF | Right parietal SLF | Left parietal SLF | Right superior corticostriate | Left superior corticostriate |
|---|---|---|---|---|---|---|---|---|---|---|---|---|---|
| **Fisher F** | **248.56** | **228.57** | **268.8** | **234.74** | **334.95** | **320.05** | **399.05** | **336.82** | **388.12** | **298.96** | **372.77** | **197.87** | **278.36** |
| **Fisher FWE p** | **0.003** | **0.004** | **0.003** | **0.004** | **0.002** | **0.002** | **0.001** | **0.002** | **0.001** | **0.002** | **0.001** | **0.005** | **0.003** |
| FA | 1.32 | 2.1 | 0.38 | -1.17 | -0.74 | 3.69 | 4.89 | 2.58 | 4.37 | 3.78 | 5.03 | 0.37 | 2.88 |
| FA FWE p | 0.063 | 0.012 | 0.356 | 0.999 | 0.999 | < 0.001 | < 0.001 | 0.004 | < 0.001 | < 0.001 | < 0.001 | 0.36 | 0.002 |
| FA mFWE p | 0.999 | 0.999 | 0.999 | 0.999 | 0.999 | 0.135 | 0.042 | 0.999 | 0.058 | 0.108 | 0.039 | 0.999 | 0.999 |
| MD | -0.16 | -0.95 | 1.23 | -4.94 | -1.09 | 1.76 | 0.78 | 1.24 | 0.58 | 1.87 | 1.07 | 2.27 | 0.1 |
| MD FWE p | 0.999 | 0.999 | 0.951 | 0.999 | 0.999 | 0.805 | 0.99 | 0.95 | 0.996 | 0.758 | 0.971 | 0.537 | 0.999 |
| MD mFWE p | 0.999 | 0.999 | 0.999 | 0.999 | 0.999 | 0.999 | 0.999 | 0.999 | 0.999 | 0.999 | 0.999 | 0.999 | 0.999 |
| RD | 0.89 | 0.81 | 0.65 | -3.18 | -1.28 | 3.25 | 3.57 | 2.4 | 3.22 | 3.31 | 3.7 | 1.34 | 1.75 |
| RD FWE p | 0.648 | 0.697 | 0.783 | 0.999 | 0.999 | 0.01 | 0.005 | 0.066 | 0.011 | 0.009 | 0.003 | 0.394 | 0.217 |
| RD mFWE p | 0.999 | 0.999 | 0.999 | 0.999 | 0.999 | 0.999 | 0.999 | 0.999 | 0.999 | 0.999 | 0.133 | 0.999 | 0.999 |
| AD | -1.28 | -2.59 | 0.95 | -4.61 | -0.11 | -1.57 | -4.02 | -1.21 | -3.66 | -1.51 | -3.91 | 1.60 | -1.88 |
| AD FWE p | 0.999 | 0.999 | 0.999 | 0.999 | 0.999 | 0.999 | 0.999 | 0.999 | 0.999 | 0.999 | 0.999 | 0.995 | 0.999 |
| AD mFWE p | 0.999 | 0.999 | 0.999 | 0.999 | 0.999 | 0.999 | 0.999 | 0.999 | 0.999 | 0.999 | 0.999 | 0.999 | 0.999 |
| Volume | 15.4 | 14.64 | 15.97 | 15.25 | 18.32 | 16.75 | 18.81 | 17.71 | 18.73 | 16.02 | 17.96 | 13.12 | 16.03 |
| Volume FWE p | 0.002 | 0.002 | 0.002 | 0.002 | 0.001 | 0.001 | 0.001 | 0.001 | 0.001 | 0.002 | 0.001 | 0.003 | 0.002 |
| Volume mFWE p | 0.002 | 0.002 | 0.002 | 0.002 | 0.001 | 0.001 | 0.001 | 0.001 | 0.001 | 0.002 | 0.001 | 0.003 | 0.002 |

Table B2 Continued

| | Right superior corticostriatal | Left superior corticostriatal | Right inferior frontal cortex | Left inferior frontal cortex |
|---|---|---|---|---|
| **Fisher F** | **215.56** | **191.02** | **258.75** | **250.81** |
| **Fisher FWE p** | **0.004** | **0.005** | **0.003** | **0.003** |
| FA | -0.81 | 1.18 | 2.22 | 2.71 |
| FA FWE p | 0.999 | 0.084 | 0.01 | 0.003 |
| FA mFWE p | 0.999 | 0.999 | 0.999 | 0.999 |
| MD | -1.74 | -1.21 | -0.51 | -0.86 |
| MD FWE p | 0.999 | 0.999 | 0.999 | 0.999 |
| MD mFWE p | 0.999 | 0.999 | 0.999 | 0.999 |
| RD | -1.73 | -0.43 | 0.65 | 0.74 |
| RD FWE p | 0.999 | 0.999 | 0.783 | 0.739 |
| RD mFWE p | 0.999 | 0.999 | 0.999 | 0.999 |
| AD | -0.67 | -1.88 | -1.99 | -2.88 |
| AD FWE p | 0.999 | 0.999 | 0.999 | 0.999 |
| AD mFWE p | 0.999 | 0.999 | 0.999 | 0.999 |
| Volume | 14.54 | 13.48 | 15.65 | 15.3 |
| Volume FWE p | 0.002 | 0.003 | 0.002 | 0.002 |
| Volume mFWE p | 0.002 | 0.003 | 0.002 | 0.002 |

**Table B3 Negative correlations between white matter metrics and executive functioning scores**

| | Right fornix | Left fornix | Right cingulate bundle (cingulate) | Left cingulate bundle (cingulate) | Right cingulate bundle (PH) | Left cingulate bundle (PH) | Right corticospinal tract | Left corticospinal | Right anterior thalamic radiations | Left anterior thalamic radiations | Right uncinate fasciculus | Left uncinate fasciculus | Right inferior longitudinal fasciculus |
|---|---|---|---|---|---|---|---|---|---|---|---|---|---|
| **Fisher F** | **234.87** | **275.04** | **70.23** | **46.28** | **52.67** | **57.07** | **121.05** | **143.73** | **92.56** | **87.31** | **68.56** | **70.71** | **104.27** |
| **Fisher FWE p** | **0.001** | **< 0.001** | **0.013** | **0.024** | **0.02** | **0.018** | **0.004** | **0.003** | **0.008** | **0.009** | **0.013** | **0.012** | **0.006** |
| FA | 1.7 | 2.99 | -2.63 | -3.43 | -0.31 | 1.74 | 1.44 | 0.76 | 1.19 | 0.82 | -2.97 | -1.93 | -0.08 |
| FA FWE p | 0.001 | < 0.001 | 0.999 | 0.999 | 0.158 | 0.001 | 0.002 | 0.014 | 0.004 | 0.012 | 0.999 | 0.937 | 0.099 |
| FA mFWE p | 0.999 | 0.999 | 0.999 | 0.999 | 0.999 | 0.999 | 0.999 | 0.999 | 0.999 | 0.999 | 0.999 | 0.999 | 0.999 |
| MD | 4.03 | 3.74 | 0.37 | -0.73 | 0.999 | 0.58 | 2.65 | 2 | 1.89 | 1.35 | -1 | -1.51 | 0.74 |
| MD FWE p | 0.001 | 0.003 | 0.953 | 0.999 | 0.769 | 0.911 | 0.076 | 0.269 | 0.316 | 0.597 | 0.999 | 0.999 | 0.869 |
| MD mFWE p | 0.073 | 0.101 | 0.999 | 0.999 | 0.999 | 0.999 | 0.999 | 0.999 | 0.999 | 0.999 | 0.999 | 0.999 | 0.999 |
| RD | 4.7 | 5.28 | -1.68 | -2.82 | 0.59 | 1.64 | 2.72 | 1.69 | 2.12 | 1.51 | -2.14 | -1.81 | 0.63 |
| RD FWE p | < 0.001 | < 0.001 | 0.993 | 0.999 | 0.246 | 0.044 | 0.005 | 0.04 | 0.017 | 0.056 | 0.999 | 0.997 | 0.232 |
| RD mFWE p | 0.041 | 0.027 | 0.999 | 0.999 | 0.999 | 0.999 | 0.999 | 0.999 | 0.999 | 0.999 | 0.999 | 0.999 | 0.999 |
| AD | 1.78 | 0.83 | 3.04 | 2.69 | 0.85 | -1.13 | 0.98 | 0.999 | 0.56 | 0.38 | 1.74 | 0.24 | 0.44 |
| AD FWE p | 0.998 | 0.999 | 0.623 | 0.833 | 0.999 | 0.999 | 0.999 | 0.999 | 0.999 | 0.999 | 0.998 | 0.999 | 0.999 |
| Volume | 13.03 | 14.29 | 7.01 | 5.41 | 6.07 | 6.04 | 9.18 | 10.87 | 8.06 | 8.13 | 7.5 | 7.94 | 9.47 |
| Volume FWE p | < 0.001 | < 0.001 | 0.008 | 0.025 | 0.016 | 0.016 | 0.002 | 0.001 | 0.004 | 0.004 | 0.006 | 0.004 | 0.001 |
| Volume mFWE p | < 0.001 | < 0.001 | 0.009 | 0.025 | 0.016 | 0.016 | 0.003 | 0.001 | 0.005 | 0.005 | 0.007 | 0.005 | 0.002 |

Table B3 Continued

| | Left inferior longitudinal fasciculus | Right inferior fronto occipital fasciculus | Forceps major | Forceps minor | Corpus callosum | Right SLF | Left SLF | Right temporal SLF | Left temporal SLF | Right parietal SLF | Left parietal SLF |
|---|---|---|---|---|---|---|---|---|---|---|---|
| **Fisher F** | **94.41** | **96.18** | **146.08** | **57.76** | **133.16** | **127.52** | **162.18** | **128.67** | **158.14** | **121.99** | **145.9** |
| **Fisher FWE p** | **0.007** | **0.007** | **0.003** | **0.017** | **0.004** | **0.004** | **0.002** | **0.004** | **0.002** | **0.004** | **0.003** |
| FA | -0.1 | -1.52 | 0.81 | -2.81 | -0.75 | 1.59 | 2.21 | 1.11 | 2.02 | 1.59 | 2.1 |
| FA FWE p | 0.104 | 0.772 | 0.012 | 0.999 | 0.332 | 0.001 | < 0.001 | 0.005 | < 0.001 | 0.001 | < 0.001 |
| FA mFWE p | 0.999 | 0.999 | 0.999 | 0.999 | 0.999 | 0.999 | 0.999 | 0.999 | 0.999 | 0.999 | 0.999 |
| MD | -0.03 | 0.26 | 2.26 | -2.68 | 0.7 | 2.81 | 1.37 | 2.36 | 0.93 | 2.94 | 2.28 |
| MD FWE p | 0.99 | 0.967 | 0.17 | 0.999 | 0.881 | 0.052 | 0.587 | 0.142 | 0.801 | 0.037 | 0.165 |
| MD mFWE p | 0.999 | 0.999 | 0.999 | 0.999 | 0.999 | 0.999 | 0.999 | 0.999 | 0.999 | 0.999 | 0.999 |
| RD | 0.15 | -0.83 | 1.56 | -2.89 | -0.15 | 2.79 | 2.43 | 2.37 | 2.11 | 2.8 | 2.76 |
| RD FWE p | 0.42 | 0.851 | 0.052 | 0.999 | 0.561 | 0.004 | 0.009 | 0.01 | 0.017 | 0.004 | 0.004 |
| RD mFWE p | 0.999 | 0.999 | 0.999 | 0.999 | 0.999 | 0.999 | 0.999 | 0.999 | 0.999 | 0.999 | 0.999 |
| AD | -0.23 | 1.44 | 1.37 | -0.44 | 1.21 | 0.93 | -1.17 | 0.72 | -1.44 | 1.13 | -0.05 |
| AD FWE p | 0.999 | 0.999 | 0.999 | 0.999 | 0.999 | 0.999 | 0.999 | 0.999 | 0.999 | 0.999 | 0.999 |
| Volume | 9.14 | 9.11 | 10.88 | 7.17 | 10.91 | 9.43 | 11.56 | 9.87 | 11.57 | 9.04 | 10.51 |
| Volume FWE p | 0.002 | 0.002 | 0.001 | 0.007 | 0.001 | 0.001 | < 0.001 | 0.001 | < 0.001 | 0.002 | 0.001 |
| Volume mFWE p | 0.003 | 0.003 | 0.001 | 0.008 | 0.001 | 0.002 | 0.001 | 0.002 | 0.001 | 0.003 | 0.001 |

Table B3 Continued

| | Right superior corticostriate | Left superior corticostriate | Right superior corticostriatal | Left superior corticostriatal | Right inferior frontal cortex | Left inferior frontal cortex |
|---|---|---|---|---|---|---|
| **Fisher F** | **107.11** | **134.22** | **74.56** | **74.94** | **100.19** | **97.75** |
| **Fisher FWE p** | **0.006** | **0.003** | **0.011** | **0.011** | **0.007** | **0.007** |
| FA | -0.23 | 1.13 | -2.51 | -1.22 | 1.27 | 1.44 |
| FA FWE p | 0.136 | 0.005 | 0.998 | 0.601 | 0.003 | 0.002 |
| FA mFWE p | 0.999 | 0.999 | 0.999 | 0.999 | 0.999 | 0.999 |
| MD | 3.7 | 2.24 | -0.99 | -0.38 | 1.57 | 1.23 |
| MD FWE p | 0.004 | 0.177 | 0.999 | 0.998 | 0.481 | 0.658 |
| MD mFWE p | 0.105 | 0.999 | 0.999 | 0.999 | 0.999 | 0.999 |
| RD | 1.84 | 2.13 | -2.03 | -0.94 | 1.54 | 1.62 |
| RD FWE p | 0.03 | 0.017 | 0.999 | 0.887 | 0.054 | 0.046 |
| RD mFWE p | 0.999 | 0.999 | 0.999 | 0.999 | 0.999 | 0.999 |
| AD | 2.97 | 1.04 | 1.71 | 0.85 | 0.77 | 0.02 |
| AD FWE p | 0.671 | 0.999 | 0.999 | 0.999 | 0.999 | 0.999 |
| Volume | 7.9 | 10.19 | 7.89 | 8.04 | 8.7 | 8.67 |
| Volume FWE p | 0.004 | 0.001 | 0.004 | 0.004 | 0.002 | 0.002 |
| Volume mFWE p | 0.005 | 0.002 | 0.005 | 0.005 | 0.003 | 0.004 |

**Table B4 Negative correlations between white matter metrics and memory scores**

| | Right fornix | Left fornix | Right cingulate bundle (cingulate) | Left cingulate bundle (cingulate) | Right cingulate bundle (PH) | Left cingulate bundle (PH) | Right corticospinal tract | Left corticospinal | Right anterior thalamic radiations | Left anterior thalamic radiations | Right uncinate fasciculus | Left uncinate fasciculus | Right inferior longitudinal fasciculus | Left inferior longitudinal fasciculus |
|---|---|---|---|---|---|---|---|---|---|---|---|---|---|---|
| **Fisher F** | **246.36** | **337** | **47.76** | **26.02** | **68.23** | **78.01** | **115.44** | **135.15** | **64.07** | **63.56** | **31.91** | **38.91** | **92.93** | **81.12** |
| **Fisher FWE p** | **0.001** | **< 0.001** | **0.017** | **0.035** | **0.011** | **0.009** | **0.005** | **0.004** | **0.012** | **0.012** | **0.027** | **0.021** | **0.007** | **0.009** |
| FA | 4.04 | 5.72 | -3.37 | -2.2 | 1.24 | 3.57 | 3.63 | 2.96 | 1.8 | 2.45 | -2.36 | -1.16 | 1.46 | 1.7 |
| FA FWE p | < 0.001 | < 0.001 | 0.999 | 0.999 | 0.139 | 0.001 | 0.001 | 0.004 | 0.047 | 0.012 | 0.999 | 0.999 | 0.092 | 0.057 |
| FA mFWE p | 0.074 | 0.025 | 0.999 | 0.999 | 0.999 | 0.106 | 0.101 | 0.191 | 0.999 | 0.999 | 0.999 | 0.999 | 0.999 | 0.999 |
| MD | 1.46 | 1.13 | -1.91 | -2.11 | -1.12 | -1.71 | 0.31 | -0.33 | -0.53 | -0.17 | -3.47 | -3.49 | -0.53 | -0.71 |
| MD FWE p | 0.19 | 0.333 | 0.999 | 0.999 | 0.999 | 0.999 | 0.775 | 0.961 | 0.983 | 0.933 | 0.999 | 0.999 | 0.982 | 0.992 |
| MD mFWE p | 0.999 | 0.999 | 0.999 | 0.999 | 0.999 | 0.999 | 0.999 | 0.999 | 0.999 | 0.999 | 0.999 | 0.999 | 0.999 | 0.999 |
| RD | 4.12 | 4.83 | -3.44 | -2.76 | 0.12 | 1.19 | 3.17 | 2.11 | 0.71 | 1.34 | -3.28 | -2.49 | 0.7 | 0.69 |
| RD FWE p | < 0.001 | < 0.001 | 0.999 | 0.999 | 0.7 | 0.186 | 0.001 | 0.027 | 0.384 | 0.142 | 0.999 | 0.999 | 0.388 | 0.396 |
| RD mFWE p | 0.07 | 0.043 | 0.999 | 0.999 | 0.999 | 0.999 | 0.152 | 0.999 | 0.999 | 0.999 | 0.999 | 0.999 | 0.999 | 0.999 |
| AD | -1.5 | -2.76 | 1.94 | 0.58 | -1.89 | -4.2 | -2.38 | -2.46 | -1.86 | -2.17 | -1.19 | -2.39 | -1.64 | -2.03 |
| AD FWE p | 0.999 | 0.999 | 0.322 | 0.976 | 0.999 | 0.999 | 0.999 | 0.999 | 0.999 | 0.999 | 0.999 | 0.999 | 0.999 | 0.999 |
| AD mFWE p | 0.999 | 0.999 | 0.999 | 0.999 | 0.999 | 0.999 | 0.999 | 0.999 | 0.999 | 0.999 | 0.999 | 0.999 | 0.999 | 0.999 |
| Volume | 13.96 | 16.31 | 5.93 | 4.31 | 7.5 | 7.13 | 8.71 | 10.38 | 6.95 | 6.5 | 5.15 | 5.77 | 8.86 | 8.12 |
| Volume FWE p | < 0.001 | < 0.001 | 0.025 | 0.074 | 0.009 | 0.012 | 0.005 | 0.002 | 0.013 | 0.017 | 0.041 | 0.028 | 0.004 | 0.007 |
| Volume mFWE p | < 0.001 | < 0.001 | 0.022 | 0.061 | 0.009 | 0.011 | 0.005 | 0.002 | 0.013 | 0.016 | 0.035 | 0.024 | 0.005 | 0.007 |

Table B4 continued

| | Right inferior fronto occipital fasciculus | Left inferior fronto occipital fasciculus | Forceps major | Forceps minor | Corpus callosum | Right SLF | Left SLF | Right temporal SLF | Left temporal SLF | Right parietal SLF | Left parietal SLF |
|---|---|---|---|---|---|---|---|---|---|---|---|
| **Fisher F** | **87.26** | **70.58** | **138.49** | **55.41** | **123.21** | **114.53** | **172.35** | **130.79** | **175.23** | **104.17** | **151.55** |
| **Fisher FWE p** | **0.008** | **0.011** | **0.004** | **0.014** | **0.005** | **0.005** | **0.002** | **0.004** | **0.002** | **0.006** | **0.003** |
| FA | -0.42 | 0.41 | 1.64 | -1.61 | 0.57 | 2.42 | 3.88 | 1.88 | 3.68 | 2.4 | 3.67 |
| FA FWE p | 0.984 | 0.515 | 0.064 | 0.999 | 0.417 | 0.012 | < 0.001 | 0.039 | 0.001 | 0.013 | 0.001 |
| FA mFWE p | 0.999 | 0.999 | 0.999 | 0.999 | 0.999 | 0.999 | 0.083 | 0.999 | 0.097 | 0.999 | 0.098 |
| MD | -1.7 | -1.62 | 0.16 | -3.95 | -1.59 | 1.37 | 0.76 | 0.9 | 0.51 | 1.5 | 1.27 |
| MD FWE p | 0.999 | 0.999 | 0.836 | 0.999 | 0.999 | 0.226 | 0.533 | 0.457 | 0.673 | 0.178 | 0.266 |
| MD mFWE p | 0.999 | 0.999 | 0.999 | 0.999 | 0.999 | 0.999 | 0.999 | 0.999 | 0.999 | 0.999 | 0.999 |
| RD | -1.31 | -0.74 | 1.18 | -2.85 | -0.44 | 2.28 | 2.92 | 1.86 | 2.7 | 2.27 | 3.01 |
| RD FWE p | 0.999 | 0.974 | 0.188 | 0.999 | 0.922 | 0.018 | 0.003 | 0.048 | 0.006 | 0.018 | 0.002 |
| RD mFWE p | 0.999 | 0.999 | 0.999 | 0.999 | 0.999 | 0.999 | 0.202 | 0.999 | 0.276 | 0.999 | 0.182 |
| AD | -1.07 | -1.69 | -1.02 | -3.14 | -1.83 | -0.87 | -3.04 | -1.05 | -3.04 | -0.65 | -2.4 |
| AD FWE p | 0.999 | 0.999 | 0.999 | 0.999 | 0.999 | 0.999 | 0.999 | 0.999 | 0.999 | 0.999 | 0.999 |
| AD mFWE p | 0.999 | 0.999 | 0.999 | 0.999 | 0.999 | 0.999 | 0.999 | 0.999 | 0.999 | 0.999 | 0.999 |
| Volume | 8.96 | 7.88 | 11 | 7.05 | 10.7 | 9.22 | 11.49 | 10.38 | 11.77 | 8.6 | 10.5 |
| Volume FWE p | 0.004 | 0.008 | 0.001 | 0.012 | 0.001 | 0.003 | 0.001 | 0.002 | 0.001 | 0.005 | 0.002 |
| Volume mFWE p | 0.004 | 0.008 | 0.002 | 0.012 | 0.002 | 0.004 | 0.001 | 0.002 | 0.001 | 0.005 | 0.002 |

Table B4 continued

| | Right superior corticostriate | Left superior corticostriate | Right superior corticostriatal | Left superior corticostriatal | Right inferior frontal cortex | Left inferior frontal cortex |
|---|---|---|---|---|---|---|
| **Fisher F** | **80.48** | **100.19** | **55.91** | **46.45** | **93.02** | **77.34** |
| **Fisher FWE p** | **0.009** | **0.006** | **0.014** | **0.018** | **0.007** | **0.009** |
| FA | 0.45 | 1.63 | -2 | -0.08 | 2.74 | 2.79 |
| FA FWE p | 0.493 | 0.065 | 0.999 | 0.849 | 0.006 | 0.005 |
| FA mFWE p | 0.999 | 0.999 | 0.999 | 0.999 | 0.26 | 0.239 |
| MD | 1.97 | -0.42 | -2.53 | -2.33 | -0.35 | -0.78 |
| MD FWE p | 0.063 | 0.972 | 0.999 | 0.999 | 0.964 | 0.994 |
| MD mFWE p | 0.999 | 0.999 | 0.999 | 0.999 | 0.999 | 0.999 |
| RD | 1.41 | 0.78 | -2.74 | -1.68 | 1.19 | 0.95 |
| RD FWE p | 0.123 | 0.352 | 0.999 | 0.999 | 0.185 | 0.274 |
| RD mFWE p | 0.999 | 0.999 | 0.999 | 0.999 | 0.999 | 0.999 |
| AD | 1.14 | -1.56 | -0.51 | -2.09 | -2.5 | -3.06 |
| AD FWE p | 0.82 | 0.999 | 0.999 | 0.999 | 0.999 | 0.999 |
| AD mFWE p | 0.999 | 0.999 | 0.999 | 0.999 | 0.999 | 0.999 |
| Volume | 7.49 | 9.2 | 7.04 | 6.3 | 8.41 | 7.47 |
| Volume FWE p | 0.01 | 0.003 | 0.013 | 0.02 | 0.006 | 0.01 |
| Volume mFWE p | 0.009 | 0.004 | 0.012 | 0.018 | 0.006 | 0.009 |

**Table B5 Positive correlations between white matter metrics and parent-reported total problems**

| | Right fornix | Left fornix | Right cingulate bundle (cingulate) | Left cingulate bundle (cingulate) | Right cingulate bundle (PH) | Left cingulate bundle (PH) | Right corticospinal tract | Left corticospinal | Right anterior thalamic radiations | Left anterior thalamic radiations | Right uncinate fasciculus | Left uncinate fasciculus | Right inferior longitudinal fasciculus | Left inferior longitudinal fasciculus |
|---|---|---|---|---|---|---|---|---|---|---|---|---|---|---|
| **Fisher F** | **77.52** | **71.11** | **29.35** | **16.72** | **45.37** | **44.86** | **68.09** | **64.17** | **38.58** | **37.77** | **13.77** | **23.58** | **20.44** | **25.65** |
| **Fisher FWE p** | **0.004** | **0.011** | **0.891** | **0.999** | **0.343** | **0.359** | **0.018** | **0.033** | **0.588** | **0.619** | **0.999** | **0.978** | **0.994** | **0.957** |
| FA | -1.17 | -0.74 | -0.62 | -1.12 | -1.8 | -1.08 | -0.83 | 0.38 | -2.33 | -2.32 | -2.51 | -2.2 | -1.43 | -0.64 |
| FA FWE p | 0.728 | 0.465 | 0.39 | 0.699 | 0.957 | 0.675 | 0.522 | 0.041 | 0.997 | 0.997 | 0.999 | 0.994 | 0.852 | 0.402 |
| FA mFWE p | 0.999 | 0.999 | 0.999 | 0.999 | 0.999 | 0.999 | 0.999 | 0.999 | 0.999 | 0.999 | 0.999 | 0.999 | 0.999 | 0.999 |
| MD | 4.21 | 3.99 | 1.72 | 0.63 | 2.77 | 3.11 | 4.29 | 4.11 | 1.69 | 1.54 | -0.23 | 0.73 | 0.72 | 0.75 |
| MD FWE p | 0.088 | 0.149 | 0.987 | 0.999 | 0.748 | 0.573 | 0.073 | 0.112 | 0.988 | 0.994 | 0.999 | 0.999 | 0.999 | 0.999 |
| MD mFWE p | 0.47 | 0.635 | 0.999 | 0.999 | 0.998 | 0.983 | 0.416 | 0.542 | 0.999 | 0.999 | 0.999 | 0.999 | 0.999 | 0.999 |
| RD | 3.04 | 3.1 | 0.54 | -0.39 | 0.9 | 1.54 | 2.04 | 2.56 | 0 | -0.15 | -1.51 | -0.92 | -0.27 | 0.17 |
| RD FWE p | 0.039 | 0.034 | 0.87 | 0.992 | 0.749 | 0.456 | 0.246 | 0.104 | 0.968 | 0.98 | 0.999 | 0.999 | 0.987 | 0.948 |
| RD mFWE p | 0.989 | 0.985 | 0.999 | 0.999 | 0.999 | 0.999 | 0.999 | 0.999 | 0.999 | 0.999 | 0.999 | 0.999 | 0.999 | 0.999 |
| AD | 3.52 | 3.23 | 1.96 | 1.44 | 3.25 | 2.99 | 3.65 | 2.94 | 2.96 | 3.03 | 2.16 | 2.98 | 1.45 | 1.06 |
| AD FWE p | 0.889 | 0.966 | 0.999 | 0.999 | 0.963 | 0.991 | 0.83 | 0.993 | 0.992 | 0.989 | 0.999 | 0.991 | 0.999 | 0.999 |
| AD mFWE p | 0.897 | 0.969 | 0.999 | 0.999 | 0.966 | 0.992 | 0.842 | 0.994 | 0.993 | 0.989 | 0.999 | 0.992 | 0.999 | 0.999 |
| Volume | 4.43 | 4.08 | 2.91 | 2.04 | 3.3 | 2.79 | 3.77 | 3.55 | 3.67 | 3.62 | 1.17 | 1.91 | 2.67 | 3.48 |
| Volume FWE p | < 0.001 | 0.001 | 0.039 | 0.237 | 0.013 | 0.052 | 0.003 | 0.006 | 0.004 | 0.005 | 0.648 | 0.287 | 0.068 | 0.008 |
| Volume mFWE p | 0.322 | 0.564 | 0.995 | 0.999 | 0.957 | 0.998 | 0.774 | 0.886 | 0.83 | 0.856 | 0.999 | 0.999 | 0.999 | 0.912 |

Table B5 continued

| | Right inferior fronto occipital fasciculus | Left inferior fronto occipital fasciculus | Forceps major | Forceps minor | Corpus callosum | Right SLF | Left SLF | Right temporal SLF | Left temporal SLF | Right parietal SLF | Left parietal SLF | Right superior corticostriate | Left superior corticostriate |
|---|---|---|---|---|---|---|---|---|---|---|---|---|---|
| **Fisher F** | **31.64** | **44.02** | **54.89** | **12.89** | **30.78** | **28.46** | **28.39** | **23.65** | **31.12** | **30.52** | **22.27** | **34.44** | **40.28** |
| **Fisher FWE p** | **0.832** | **0.387** | **0.120** | **0.999** | **0.856** | **0.911** | **0.912** | **0.977** | **0.847** | **0.863** | **0.986** | **0.742** | **0.524** |
| FA | -1.68 | -0.56 | -0.67 | -1.9 | -1.49 | -0.87 | -0.39 | -1.68 | -0.53 | -0.57 | -0.31 | -1.8 | -0.43 |
| FA FWE p | 0.933 | 0.354 | 0.42 | 0.972 | 0.875 | 0.546 | 0.263 | 0.933 | 0.338 | 0.363 | 0.227 | 0.957 | 0.286 |
| FA mFWE p | 0.999 | 0.999 | 0.999 | 0.999 | 0.999 | 0.999 | 0.999 | 0.999 | 0.999 | 0.999 | 0.999 | 0.999 | 0.999 |
| MD | 1.5 | 2.13 | 3.25 | -1.8 | 0.84 | 1.03 | 1.38 | 0.66 | 1.46 | 1.04 | 1.05 | 2.12 | 1.91 |
| MD FWE p | 0.994 | 0.946 | 0.494 | 0.999 | 0.999 | 0.999 | 0.997 | 0.999 | 0.995 | 0.999 | 0.999 | 0.947 | 0.973 |
| MD mFWE p | 0.999 | 0.999 | 0.965 | 0.999 | 0.999 | 0.999 | 0.999 | 0.999 | 0.999 | 0.999 | 0.999 | 0.999 | 0.999 |
| RD | -0.07 | 1.03 | 1.19 | -1.88 | -0.52 | 0.01 | 0.48 | -0.64 | 0.42 | 0.17 | 0.37 | 0.02 | 0.999 |
| RD FWE p | 0.975 | 0.695 | 0.624 | 0.999 | 0.995 | 0.967 | 0.885 | 0.997 | 0.901 | 0.947 | 0.913 | 0.966 | 0.71 |
| RD mFWE p | 0.999 | 0.999 | 0.999 | 0.999 | 0.999 | 0.999 | 0.999 | 0.999 | 0.999 | 0.999 | 0.999 | 0.999 | 0.999 |
| AD | 2.49 | 2.15 | 3.06 | -0.4 | 1.84 | 1.81 | 1.82 | 2.01 | 1.98 | 1.59 | 1.45 | 2.78 | 1.84 |
| AD FWE p | 0.999 | 0.999 | 0.986 | 0.999 | 0.999 | 0.999 | 0.999 | 0.999 | 0.999 | 0.999 | 0.999 | 0.998 | 0.999 |
| AD mFWE p | 0.999 | 0.999 | 0.987 | 0.999 | 0.999 | 0.999 | 0.999 | 0.999 | 0.999 | 0.999 | 0.999 | 0.998 | 0.999 |
| Volume | 3.23 | 4.28 | 4.09 | 2.79 | 3.9 | 3.43 | 3.04 | 2.91 | 3.34 | 3.74 | 2.51 | 2.96 | 4.13 |
| Volume FWE p | 0.016 | < 0.001 | 0.001 | 0.052 | 0.002 | 0.009 | 0.027 | 0.039 | 0.012 | 0.003 | 0.099 | 0.034 | 0.001 |
| Volume mFWE p | 0.969 | 0.424 | 0.558 | 0.998 | 0.695 | 0.927 | 0.989 | 0.995 | 0.95 | 0.793 | 0.999 | 0.993 | 0.527 |

Table B5 continued

| | Right superior corticostriatal | Left superior corticostriatal | Right inferior frontal cortex | Left inferior frontal cortex |
|---|---|---|---|---|
| **Fisher F** | **13.67** | **16.45** | **17.43** | **22.13** |
| **Fisher FWE p** | **0.999** | **0.999** | **0.999** | **0.987** |
| FA | -4.02 | -3.04 | -1.72 | -0.08 |
| FA FWE p | 0.999 | 0.999 | 0.943 | 0.138 |
| FA mFWE p | 0.999 | 0.999 | 0.999 | 0.999 |
| MD | -1.86 | -0.87 | -1.14 | -0.71 |
| MD FWE p | 0.999 | 0.999 | 0.999 | 0.999 |
| MD mFWE p | 0.999 | 0.999 | 0.999 | 0.999 |
| RD | -3.06 | -1.93 | -1.61 | -0.48 |
| RD FWE p | 0.999 | 0.999 | 0.999 | 0.994 |
| RD mFWE p | 0.999 | 0.999 | 0.999 | 0.999 |
| AD | 1.7 | 1.55 | 0.17 | -0.7 |
| AD FWE p | 0.999 | 0.999 | 0.999 | 0.999 |
| AD mFWE p | 0.999 | 0.999 | 0.999 | 0.999 |
| Volume | 1.97 | 2.54 | 3.3 | 3.8 |
| Volume FWE p | 0.265 | 0.093 | 0.013 | 0.003 |
| Volume mFWE p | 0.999 | 0.999 | 0.956 | 0.761 |

**Table B6 Positive correlations between white matter metrics and parent-reported internalizing problems**

| | Right fornix | Left fornix | Right cingulate bundle (cingulate) | Left cingulate bundle (cingulate) | Right cingulate bundle (PH) | Left cingulate bundle (PH) | Right corticospinal tract | Left corticospinal | Right anterior thalamic radiations | Left anterior thalamic radiations | Right uncinate fasciculus | Left uncinate fasciculus | Right inferior longitudinal fasciculus | Left inferior longitudinal fasciculus |
|---|---|---|---|---|---|---|---|---|---|---|---|---|---|---|
| **Fisher F** | **56.72** | **53.26** | **21.43** | **11.76** | **34.52** | **32.34** | **41.11** | **40.87** | **21.57** | **21.24** | **10.22** | **22.19** | **18.17** | **17.6** |
| **Fisher FWE p** | **0.029** | **0.05** | **0.956** | **0.999** | **0.489** | **0.583** | **0.253** | **0.26** | **0.953** | **0.959** | **0.999** | **0.942** | **0.99** | **0.993** |
| FA | -1.24 | -1.14 | 0.51 | -0.3 | -1.66 | -1.34 | -1.68 | -0.6 | -2.33 | -2.44 | -1.93 | -1.96 | -0.76 | -0.78 |
| FA FWE p | 0.878 | 0.84 | 0.049 | 0.329 | 0.976 | 0.914 | 0.978 | 0.521 | 0.999 | 0.999 | 0.994 | 0.995 | 0.623 | 0.636 |
| FA mFWE p | 0.999 | 0.999 | 0.999 | 0.999 | 0.999 | 0.999 | 0.999 | 0.999 | 0.999 | 0.999 | 0.999 | 0.999 | 0.999 | 0.999 |
| MD | 4.17 | 4 | 1.54 | 0.86 | 2.77 | 2.72 | 3.54 | 3.64 | 1.25 | 1.2 | 0.12 | 1.26 | 1.65 | 1.35 |
| MD FWE p | 0.039 | 0.062 | 0.978 | 0.999 | 0.57 | 0.594 | 0.181 | 0.147 | 0.993 | 0.995 | 0.999 | 0.993 | 0.967 | 0.989 |
| MD mFWE p | 0.25 | 0.352 | 0.999 | 0.999 | 0.979 | 0.984 | 0.68 | 0.611 | 0.999 | 0.999 | 0.999 | 0.999 | 0.999 | 0.999 |
| RD | 2.91 | 2.79 | 1.31 | 0.35 | 0.98 | 1.11 | 0.92 | 1.55 | -0.36 | -0.49 | -0.98 | -0.49 | 0.69 | 0.42 |
| RD FWE p | 0.029 | 0.038 | 0.496 | 0.898 | 0.661 | 0.594 | 0.687 | 0.378 | 0.99 | 0.994 | 0.999 | 0.994 | 0.789 | 0.88 |
| RD mFWE p | 0.959 | 0.976 | 0.999 | 0.999 | 0.999 | 0.999 | 0.999 | 0.999 | 0.999 | 0.999 | 0.999 | 0.999 | 0.999 | 0.999 |
| AD | 3.57 | 3.54 | 0.57 | 0.8 | 3.14 | 2.91 | 3.68 | 3.29 | 2.67 | 2.89 | 1.94 | 3.29 | 1.82 | 1.76 |
| AD FWE p | 0.645 | 0.668 | 0.999 | 0.999 | 0.889 | 0.956 | 0.56 | 0.819 | 0.988 | 0.96 | 0.999 | 0.823 | 0.999 | 0.999 |
| AD mFWE p | 0.66 | 0.682 | 0.999 | 0.999 | 0.894 | 0.958 | 0.577 | 0.828 | 0.988 | 0.962 | 0.999 | 0.832 | 0.999 | 0.999 |
| Volume | 1.27 | 0.93 | 1.71 | 0.52 | 1.37 | 1.11 | 0.54 | 0.16 | 1.41 | 0.99 | -0.32 | 0.19 | 0.38 | 0.97 |
| Volume FWE p | 0.405 | 0.575 | 0.215 | 0.758 | 0.356 | 0.486 | 0.752 | 0.877 | 0.34 | 0.545 | 0.961 | 0.87 | 0.809 | 0.552 |
| Volume mFWE p | 0.999 | 0.999 | 0.999 | 0.999 | 0.999 | 0.999 | 0.999 | 0.999 | 0.999 | 0.999 | 0.999 | 0.999 | 0.999 | 0.999 |

Table B6 continued

| | Right inferior fronto occipital fasciculus | Left inferior fronto occipital fasciculus | Forceps major | Forceps minor | Corpus callosum | Right SLF | Left SLF | Right temporal SLF | Left temporal SLF | Right parietal SLF | Left parietal SLF | Right superior corticostriate | Left superior corticostriate |
|---|---|---|---|---|---|---|---|---|---|---|---|---|---|
| **Fisher F** | **21.87** | **29.51** | **37.33** | **5.91** | **16.42** | **15.73** | **14.47** | **14.81** | **17.08** | **15.96** | **9.96** | **21.99** | **21.06** |
| **Fisher FWE p** | **0.948** | **0.705** | **0.378** | **0.999** | **0.997** | **0.998** | **0.999** | **0.999** | **0.995** | **0.998** | **0.999** | **0.946** | **0.961** |
| FA | -1.32 | -0.6 | -0.42 | -1.3 | -1.05 | -0.68 | -0.87 | -1.27 | -0.95 | -0.46 | -0.77 | -2.17 | -1.39 |
| FA FWE p | 0.907 | 0.518 | 0.406 | 0.899 | 0.795 | 0.573 | 0.696 | 0.891 | 0.74 | 0.431 | 0.635 | 0.999 | 0.928 |
| FA mFWE p | 0.999 | 0.999 | 0.999 | 0.999 | 0.999 | 0.999 | 0.999 | 0.999 | 0.999 | 0.999 | 0.999 | 0.999 | 0.999 |
| MD | 1.76 | 2.32 | 3.11 | -0.67 | 1.2 | 1.04 | 1.07 | 0.9 | 1.31 | 0.999 | 0.5 | 1.82 | 1.64 |
| MD FWE p | 0.952 | 0.798 | 0.375 | 0.999 | 0.995 | 0.998 | 0.997 | 0.999 | 0.991 | 0.998 | 0.999 | 0.943 | 0.968 |
| MD mFWE p | 0.999 | 0.999 | 0.904 | 0.999 | 0.999 | 0.999 | 0.999 | 0.999 | 0.999 | 0.999 | 0.999 | 0.999 | 0.999 |
| RD | 0.28 | 1.14 | 1.3 | -1.04 | -0.05 | 0.2 | 0.02 | -0.22 | 0.08 | 0.3 | -0.22 | -0.41 | 0.22 |
| RD FWE p | 0.914 | 0.583 | 0.498 | 0.999 | 0.967 | 0.931 | 0.959 | 0.982 | 0.951 | 0.909 | 0.982 | 0.991 | 0.925 |
| RD mFWE p | 0.999 | 0.999 | 0.999 | 0.999 | 0.999 | 0.999 | 0.999 | 0.999 | 0.999 | 0.999 | 0.999 | 0.999 | 0.999 |
| AD | 2.46 | 2.31 | 2.75 | 0.45 | 1.83 | 1.54 | 1.95 | 1.83 | 2.2 | 1.34 | 1.32 | 2.83 | 2.32 |
| AD FWE p | 0.997 | 0.999 | 0.98 | 0.999 | 0.999 | 0.999 | 0.999 | 0.999 | 0.999 | 0.999 | 0.999 | 0.971 | 0.999 |
| AD mFWE p | 0.997 | 0.999 | 0.981 | 0.999 | 0.999 | 0.999 | 0.999 | 0.999 | 0.999 | 0.999 | 0.999 | 0.972 | 0.999 |
| Volume | 0.89 | 1.76 | 1.7 | 0.58 | 0.99 | 1.12 | 0.03 | 0.89 | 0.29 | 1.32 | -0.05 | 0.47 | 1.09 |
| Volume FWE p | 0.592 | 0.197 | 0.218 | 0.733 | 0.543 | 0.478 | 0.908 | 0.591 | 0.839 | 0.379 | 0.923 | 0.776 | 0.495 |
| Volume mFWE p | 0.999 | 0.999 | 0.999 | 0.999 | 0.999 | 0.999 | 0.999 | 0.999 | 0.999 | 0.999 | 0.999 | 0.999 | 0.999 |

Table B6 Continued

| | Right superior corticostriatal | Left superior corticostriatal | Right inferior frontal cortex | Left inferior frontal cortex |
|---|---|---|---|---|
| **Fisher F** | **4.67** | **7.15** | **5.8** | **5.96** |
| **Fisher FWE p** | **0.999** | **0.999** | **0.999** | **0.999** |
| FA | -2.85 | -2.79 | -2.19 | -0.57 |
| FA FWE p | 0.999 | 0.999 | 0.999 | 0.502 |
| FA mFWE p | 0.999 | 0.999 | 0.999 | 0.999 |
| MD | -1.55 | -0.82 | -0.89 | -0.37 |
| MD FWE p | 0.999 | 0.999 | 0.999 | 0.999 |
| MD mFWE p | 0.999 | 0.999 | 0.999 | 0.999 |
| RD | -2.29 | -1.76 | -1.76 | -0.56 |
| RD FWE p | 0.999 | 0.999 | 0.999 | 0.995 |
| RD mFWE p | 0.999 | 0.999 | 0.999 | 0.999 |
| AD | 0.9 | 1.35 | 0.91 | 0.11 |
| AD FWE p | 0.999 | 0.999 | 0.999 | 0.999 |
| AD mFWE p | 0.999 | 0.999 | 0.999 | 0.999 |
| Volume | -0.18 | 0.21 | 0.27 | 0.42 |
| Volume FWE p | 0.944 | 0.863 | 0.846 | 0.798 |
| Volume mFWE p | 0.999 | 0.999 | 0.999 | 0.999 |

**Table B7. Positive correlations between white matter metrics and parent-reported anxiety and depressive problems**

| | Right fornix | Left fornix | Right cingulate bundle (cingualte) | Left cingulate bundle (cingualte) | Right cingulate bundle (PH) | Left cingulate bundle (PH) | Right corticospinal tract | Left corticospinal | Right anterior thalamic radiations | Left anterior thalamic radiations | Right uncinate fasciculus | Left uncinate fasciculus | Right inferior longitudinal fasciculus | Left inferior longitudinal fasciculus |
|---|---|---|---|---|---|---|---|---|---|---|---|---|---|---|
| **Fisher F** | **45.75** | **45.19** | **25.62** | **20.15** | **34.33** | **42.57** | **32.14** | **32.11** | **21.13** | **21.71** | **12.08** | **31.06** | **18.13** | **22.09** |
| **Fisher FWE p** | **0.012** | **0.014** | **0.357** | **0.639** | **0.1** | **0.023** | **0.142** | **0.142** | **0.584** | **0.553** | **0.971** | **0.167** | **0.748** | **0.532** |
| FA | -1.23 | -1.96 | 0.7 | 0.35 | -1.59 | -1.59 | -1.83 | -0.94 | -2.22 | -2.29 | -1.4 | -1.53 | -0.17 | -0.25 |
| FA FWE p | 0.952 | 0.999 | 0.074 | 0.175 | 0.991 | 0.991 | 0.998 | 0.871 | 0.999 | 0.999 | 0.976 | 0.988 | 0.438 | 0.49 |
| FA mFWE p | 0.999 | 0.999 | 0.999 | 0.999 | 0.999 | 0.999 | 0.999 | 0.999 | 0.999 | 0.999 | 0.999 | 0.999 | 0.999 | 0.999 |
| MD | 3.77 | 3.67 | 1.99 | 1.97 | 3.02 | 3.52 | 2.94 | 3.05 | 1.45 | 1.41 | 0.68 | 2.2 | 1.73 | 1.89 |
| MD FWE p | 0.007 | 0.01 | 0.508 | 0.522 | 0.075 | 0.017 | 0.094 | 0.071 | 0.794 | 0.807 | 0.975 | 0.391 | 0.657 | 0.568 |
| MD mFWE p | 0.07 | 0.094 | 0.966 | 0.97 | 0.42 | 0.143 | 0.482 | 0.406 | 0.999 | 0.999 | 0.999 | 0.917 | 0.992 | 0.98 |
| RD | 2.46 | 1.89 | 1.65 | 1.34 | 1.14 | 1.38 | 0.31 | 0.88 | -0.23 | -0.29 | -0.38 | 0.23 | 1.13 | 1.03 |
| RD FWE p | 0.027 | 0.112 | 0.18 | 0.302 | 0.397 | 0.284 | 0.801 | 0.532 | 0.945 | 0.953 | 0.964 | 0.832 | 0.402 | 0.454 |
| RD mFWE p | 0.809 | 0.98 | 0.995 | 0.999 | 0.999 | 0.999 | 0.999 | 0.999 | 0.999 | 0.999 | 0.999 | 0.999 | 0.999 | 0.999 |
| AD | 3.38 | 3.88 | 0.8 | 1.11 | 3.35 | 3.84 | 3.46 | 3.15 | 2.84 | 2.99 | 2 | 3.84 | 1.43 | 1.89 |
| AD FWE p | 0.201 | 0.047 | 0.999 | 0.999 | 0.217 | 0.054 | 0.166 | 0.328 | 0.544 | 0.435 | 0.959 | 0.054 | 0.999 | 0.975 |
| AD mFWE p | 0.204 | 0.048 | 0.999 | 0.999 | 0.22 | 0.055 | 0.168 | 0.332 | 0.552 | 0.442 | 0.965 | 0.056 | 0.999 | 0.98 |
| Volume | -0.26 | -0.99 | 1.68 | 0.27 | -0.19 | -0.12 | -0.35 | -0.6 | 0.62 | 0.54 | -0.55 | -0.11 | 0 | 0.82 |
| Volume FWE p | 0.92 | 0.989 | 0.178 | 0.778 | 0.906 | 0.89 | 0.935 | 0.965 | 0.635 | 0.671 | 0.96 | 0.889 | 0.862 | 0.544 |
| Volume mFWE p | 0.999 | 0.999 | 0.994 | 0.999 | 0.999 | 0.999 | 0.999 | 0.999 | 0.999 | 0.999 | 0.999 | 0.999 | 0.999 | 0.999 |

Table B7 continued

| | Right inferior fronto occipital | Left inferior fronto occipital | Forceps major | Forceps minor | Corpus callosum | Right SLF | Left SLF | Right temporal SLF | Left temporal SLF | Right parietal SLF | Left parietal SLF | Right superior corticostriate | Left superior corticostriate |
|---|---|---|---|---|---|---|---|---|---|---|---|---|---|
| **Fisher F** | **21.35** | **31.11** | **29.93** | **12.69** | **21.51** | **19.75** | **19.31** | **15.92** | **20.64** | **20.73** | **16.03** | **21.85** | **23.17** |
| **Fisher FWE p** | **0.572** | **0.166** | **0.198** | **0.96** | **0.564** | **0.661** | **0.685** | **0.854** | **0.611** | **0.606** | **0.85** | **0.545** | **0.475** |
| FA | -1.12 | -0.78 | -0.55 | -0.96 | -0.87 | -0.69 | -1.27 | -0.95 | -1.33 | -0.61 | -1.16 | -1.48 | -1.24 |
| FA FWE p | 0.928 | 0.801 | 0.675 | 0.879 | 0.845 | 0.759 | 0.959 | 0.874 | 0.967 | 0.712 | 0.938 | 0.983 | 0.954 |
| FA mFWE p | 0.999 | 0.999 | 0.999 | 0.999 | 0.999 | 0.999 | 0.999 | 0.999 | 0.999 | 0.999 | 0.999 | 0.999 | 0.999 |
| MD | 1.86 | 2.54 | 2.88 | 0.81 | 2.06 | 1.72 | 1.51 | 1.39 | 1.65 | 1.81 | 1.19 | 2.09 | 2.07 |
| MD FWE p | 0.587 | 0.224 | 0.107 | 0.961 | 0.47 | 0.664 | 0.767 | 0.818 | 0.7 | 0.616 | 0.883 | 0.456 | 0.464 |
| MD mFWE p | 0.983 | 0.76 | 0.521 | 0.999 | 0.954 | 0.993 | 0.998 | 0.999 | 0.995 | 0.988 | 0.999 | 0.948 | 0.951 |
| RD | 0.45 | 1.09 | 1.05 | -0.13 | 0.49 | 0.57 | -0.02 | 0.26 | -0.02 | 0.64 | -0.08 | 0.17 | 0.55 |
| RD FWE p | 0.745 | 0.423 | 0.445 | 0.926 | 0.729 | 0.69 | 0.905 | 0.821 | 0.903 | 0.655 | 0.918 | 0.85 | 0.701 |
| RD mFWE p | 0.999 | 0.999 | 0.999 | 0.999 | 0.999 | 0.999 | 0.999 | 0.999 | 0.999 | 0.999 | 0.999 | 0.999 | 0.999 |
| AD | 2.4 | 2.74 | 2.72 | 1.91 | 2.47 | 2.21 | 2.83 | 1.99 | 2.94 | 2.25 | 2.46 | 2.58 | 2.63 |
| AD FWE p | 0.828 | 0.621 | 0.632 | 0.973 | 0.79 | 0.907 | 0.553 | 0.96 | 0.47 | 0.891 | 0.795 | 0.728 | 0.696 |
| AD mFWE p | 0.838 | 0.63 | 0.641 | 0.978 | 0.8 | 0.916 | 0.561 | 0.966 | 0.477 | 0.9 | 0.805 | 0.738 | 0.706 |
| Volume | 0.49 | 1.32 | 0.07 | -0.39 | -0.35 | 0.24 | -1.36 | -0.14 | -1.22 | 0.29 | -1.16 | 0.04 | 0.18 |
| Volume FWE p | 0.692 | 0.313 | 0.843 | 0.941 | 0.934 | 0.791 | 0.997 | 0.895 | 0.995 | 0.771 | 0.993 | 0.853 | 0.811 |
| Volume mFWE p | 0.999 | 0.999 | 0.999 | 0.999 | 0.999 | 0.999 | 0.999 | 0.999 | 0.999 | 0.999 | 0.999 | 0.999 | 0.999 |

Table B7 Continued

| | Right superior corticostriatal | Left superior corticostriatal | Right inferior frontal cortex | Left inferior frontal cortex |
|---|---|---|---|---|
| **Fisher F** | **7.52** | **11.65** | **11.35** | **11.63** |
| **Fisher FWE p** | **0.999** | **0.978** | **0.982** | **0.978** |
| FA | -2.14 | -2.67 | -1.97 | -0.57 |
| FA FWE p | 0.999 | 0.999 | 0.999 | 0.692 |
| FA mFWE p | 0.999 | 0.999 | 0.999 | 0.999 |
| MD | -0.35 | 0.04 | 0.45 | 0.85 |
| MD FWE p | 0.999 | 0.998 | 0.99 | 0.956 |
| MD mFWE p | 0.999 | 0.999 | 0.999 | 0.999 |
| RD | -1.18 | -1.13 | -0.81 | 0.2 |
| RD FWE p | 0.999 | 0.998 | 0.992 | 0.843 |
| RD mFWE p | 0.999 | 0.999 | 0.999 | 0.999 |
| AD | 1.54 | 2.11 | 2.1 | 1.43 |
| AD FWE p | 0.997 | 0.936 | 0.937 | 0.999 |
| AD mFWE p | 0.998 | 0.943 | 0.944 | 0.999 |
| Volume | -0.47 | 0.26 | -0.73 | -0.38 |
| Volume FWE p | 0.952 | 0.783 | 0.975 | 0.94 |
| Volume mFWE p | 0.999 | 0.999 | 0.999 | 0.999 |

**Table B8. Positive correlations between white matter metrics and parent-reported attention problems**

| | Right fornix | Left fornix | Right cingulate bundle (cingualte) | Left cingulate bundle (cingualte) | Right cingulate bundle (PH) | Left cingulate bundle (PH) | Right corticospinal tract | Left corticospinal | Right anterior thalamic radiations | Left anterior thalamic radiations | Right uncinate fasciculus | Left uncinate fasciculus | Right inferior longitudinal fasciculus | Left inferior longitudinal fasciculus |
|---|---|---|---|---|---|---|---|---|---|---|---|---|---|---|
| **Fisher F** | **45.75** | **45.19** | **25.62** | **20.15** | **34.33** | **42.57** | **32.14** | **32.11** | **21.13** | **21.71** | **12.08** | **31.06** | **18.13** | **22.09** |
| **Fisher FWE p** | **0.012** | **0.014** | **0.357** | **0.639** | **0.1** | **0.023** | **0.142** | **0.142** | **0.584** | **0.553** | **0.971** | **0.167** | **0.748** | **0.532** |
| FA | -1.23 | -1.96 | 0.7 | 0.35 | -1.59 | -1.59 | -1.83 | -0.94 | -2.22 | -2.29 | -1.4 | -1.53 | -0.17 | -0.25 |
| FA FWE p | 0.952 | 0.999 | 0.074 | 0.175 | 0.991 | 0.991 | 0.998 | 0.871 | 0.999 | 0.999 | 0.976 | 0.988 | 0.438 | 0.49 |
| FA mFWE p | 0.999 | 0.999 | 0.999 | 0.999 | 0.999 | 0.999 | 0.999 | 0.999 | 0.999 | 0.999 | 0.999 | 0.999 | 0.999 | 0.999 |
| MD | 3.77 | 3.67 | 1.99 | 1.97 | 3.02 | 3.52 | 2.94 | 3.05 | 1.45 | 1.41 | 0.68 | 2.2 | 1.73 | 1.89 |
| MD FWE p | 0.007 | 0.01 | 0.508 | 0.522 | 0.075 | 0.017 | 0.094 | 0.071 | 0.794 | 0.807 | 0.975 | 0.391 | 0.657 | 0.568 |
| MD mFWE p | 0.07 | 0.094 | 0.966 | 0.97 | 0.42 | 0.143 | 0.482 | 0.406 | 0.999 | 0.999 | 0.999 | 0.917 | 0.992 | 0.98 |
| RD | 2.46 | 1.89 | 1.65 | 1.34 | 1.14 | 1.38 | 0.31 | 0.88 | -0.23 | -0.29 | -0.38 | 0.23 | 1.13 | 1.03 |
| RD FWE p | 0.027 | 0.112 | 0.18 | 0.302 | 0.397 | 0.284 | 0.801 | 0.532 | 0.945 | 0.953 | 0.964 | 0.832 | 0.402 | 0.454 |
| RD mFWE p | 0.809 | 0.98 | 0.995 | 0.999 | 0.999 | 0.999 | 0.999 | 0.999 | 0.999 | 0.999 | 0.999 | 0.999 | 0.999 | 0.999 |
| AD | 3.38 | 3.88 | 0.8 | 1.11 | 3.35 | 3.84 | 3.46 | 3.15 | 2.84 | 2.99 | 2 | 3.84 | 1.43 | 1.89 |
| AD FWE p | 0.201 | 0.047 | 0.999 | 0.999 | 0.217 | 0.054 | 0.166 | 0.328 | 0.544 | 0.435 | 0.959 | 0.054 | 0.999 | 0.975 |
| AD mFWE p | 0.204 | 0.048 | 0.999 | 0.999 | 0.22 | 0.055 | 0.168 | 0.332 | 0.552 | 0.442 | 0.965 | 0.056 | 0.999 | 0.98 |
| Volume | -0.26 | -0.99 | 1.68 | 0.27 | -0.19 | -0.12 | -0.35 | -0.6 | 0.62 | 0.54 | -0.55 | -0.11 | 0 | 0.82 |
| Volume FWE p | 0.92 | 0.989 | 0.178 | 0.778 | 0.906 | 0.89 | 0.935 | 0.965 | 0.635 | 0.671 | 0.96 | 0.889 | 0.862 | 0.544 |
| Volume mFWE p | 0.999 | 0.999 | 0.994 | 0.999 | 0.999 | 0.999 | 0.999 | 0.999 | 0.999 | 0.999 | 0.999 | 0.999 | 0.999 | 0.999 |

Table B8 continued

| | Right inferior fronto occipital | Left inferior fronto occipital | Forceps major | Forceps minor | Corpus callosum | Right SLF | Left SLF | Right temporal SLF | Left temporal SLF | Right parietal SLF | Left parietal SLF | Right superior corticostriate | Left superior corticostriate |
|---|---|---|---|---|---|---|---|---|---|---|---|---|---|
| **Fisher F** | **21.35** | **31.11** | **29.93** | **12.69** | **21.51** | **19.75** | **19.31** | **15.92** | **20.64** | **20.73** | **16.03** | **21.85** | **23.17** |
| **Fisher FWE p** | **0.572** | **0.166** | **0.198** | **0.96** | **0.564** | **0.661** | **0.685** | **0.854** | **0.611** | **0.606** | **0.85** | **0.545** | **0.475** |
| FA | -1.12 | -0.78 | -0.55 | -0.96 | -0.87 | -0.69 | -1.27 | -0.95 | -1.33 | -0.61 | -1.16 | -1.48 | -1.24 |
| FA FWE p | 0.928 | 0.801 | 0.675 | 0.879 | 0.845 | 0.759 | 0.959 | 0.874 | 0.967 | 0.712 | 0.938 | 0.983 | 0.954 |
| FA mFWE p | 0.999 | 0.999 | 0.999 | 0.999 | 0.999 | 0.999 | 0.999 | 0.999 | 0.999 | 0.999 | 0.999 | 0.999 | 0.999 |
| MD | 1.86 | 2.54 | 2.88 | 0.81 | 2.06 | 1.72 | 1.51 | 1.39 | 1.65 | 1.81 | 1.19 | 2.09 | 2.07 |
| MD FWE p | 0.587 | 0.224 | 0.107 | 0.961 | 0.47 | 0.664 | 0.767 | 0.818 | 0.7 | 0.616 | 0.883 | 0.456 | 0.464 |
| MD mFWE p | 0.983 | 0.76 | 0.521 | 0.999 | 0.954 | 0.993 | 0.998 | 0.999 | 0.995 | 0.988 | 0.999 | 0.948 | 0.951 |
| RD | 0.45 | 1.09 | 1.05 | -0.13 | 0.49 | 0.57 | -0.02 | 0.26 | -0.02 | 0.64 | -0.08 | 0.17 | 0.55 |
| RD FWE p | 0.745 | 0.423 | 0.445 | 0.926 | 0.729 | 0.69 | 0.905 | 0.821 | 0.903 | 0.655 | 0.918 | 0.85 | 0.701 |
| RD mFWE p | 0.999 | 0.999 | 0.999 | 0.999 | 0.999 | 0.999 | 0.999 | 0.999 | 0.999 | 0.999 | 0.999 | 0.999 | 0.999 |
| AD | 2.4 | 2.74 | 2.72 | 1.91 | 2.47 | 2.21 | 2.83 | 1.99 | 2.94 | 2.25 | 2.46 | 2.58 | 2.63 |
| AD FWE p | 0.828 | 0.621 | 0.632 | 0.973 | 0.79 | 0.907 | 0.553 | 0.96 | 0.47 | 0.891 | 0.795 | 0.728 | 0.696 |
| AD mFWE p | 0.838 | 0.63 | 0.641 | 0.978 | 0.8 | 0.916 | 0.561 | 0.966 | 0.477 | 0.9 | 0.805 | 0.738 | 0.706 |
| Volume | 0.49 | 1.32 | 0.07 | -0.39 | -0.35 | 0.24 | -1.36 | -0.14 | -1.22 | 0.29 | -1.16 | 0.04 | 0.18 |
| Volume FWE p | 0.692 | 0.313 | 0.843 | 0.941 | 0.934 | 0.791 | 0.997 | 0.895 | 0.995 | 0.771 | 0.993 | 0.853 | 0.811 |
| Volume mFWE p | 0.999 | 0.999 | 0.999 | 0.999 | 0.999 | 0.999 | 0.999 | 0.999 | 0.999 | 0.999 | 0.999 | 0.999 | 0.999 |

Table B8 continued

| | Right superior corticostriatal | Left superior corticostriatal | Right inferior frontal cortex | Left inferior frontal cortex |
|---|---|---|---|---|
| **Fisher F** | **7.52** | **11.65** | **11.35** | **11.63** |
| **Fisher FWE p** | **0.999** | **0.978** | **0.982** | **0.978** |
| FA | -2.14 | -2.67 | -1.97 | -0.57 |
| FA FWE p | 0.999 | 0.999 | 0.999 | 0.692 |
| FA mFWE p | 0.999 | 0.999 | 0.999 | 0.999 |
| MD | -0.35 | 0.04 | 0.45 | 0.85 |
| MD FWE p | 0.999 | 0.998 | 0.99 | 0.956 |
| MD mFWE p | 0.999 | 0.999 | 0.999 | 0.999 |
| RD | -1.18 | -1.13 | -0.81 | 0.2 |
| RD FWE p | 0.999 | 0.998 | 0.992 | 0.843 |
| RD mFWE p | 0.999 | 0.999 | 0.999 | 0.999 |
| AD | 1.54 | 2.11 | 2.1 | 1.43 |
| AD FWE p | 0.997 | 0.936 | 0.937 | 0.999 |
| AD mFWE p | 0.998 | 0.943 | 0.944 | 0.999 |
| Volume | -0.47 | 0.26 | -0.73 | -0.38 |
| Volume FWE p | 0.952 | 0.783 | 0.975 | 0.94 |
| Volume mFWE p | 0.999 | 0.999 | 0.999 | 0.999 |

**Table B9 Positive correlations between subcortical grey matter metrics and *g* scores**

| | Left thalamus | Left caudate | Left putamen | Left pallidum | Left hippocampus | Left amygdala | Left accumbens |
|---|---|---|---|---|---|---|---|
| **Fisher F** | **229.04** | **248.76** | **200.74** | **106.63** | **313.22** | **137.92** | **186.54** |
| **Fisher FWE p** | **0.001** | **0.001** | **0.002** | **0.016** | **< 0.001** | **0.008** | **0.003** |
| MD | -0.74 | 3.93 | 3.08 | 0.99 | -1.87 | -0.59 | 4.14 |
| MD FWE p | 0.999 | 0.072 | 0.376 | 0.998 | 0.999 | 0.999 | 0.041 |
| MD mFWE p | 0.999 | 0.099 | 0.999 | 0.999 | 0.999 | 0.999 | 0.081 |
| RD | -1.71 | 3.81 | 4.14 | 2.88 | -2.88 | -0.66 | 3.91 |
| RD FWE p | 0.999 | 0.278 | 0.151 | 0.762 | 0.999 | 0.999 | 0.235 |
| RD mFWE p | 0.999 | 0.113 | 0.081 | 0.999 | 0.999 | 0.999 | 0.101 |
| AD | 0.59 | 3.39 | 1.05 | -2.09 | -0.16 | -0.41 | 3.84 |
| AD FWE p | 0.99 | 0.045 | 0.945 | 0.999 | 0.999 | 0.999 | 0.012 |
| AD mFWE p | 0.999 | 0.263 | 0.999 | 0.999 | 0.999 | 0.999 | 0.11 |
| Volume | 14.95 | 13.78 | 12.52 | 9.21 | 17.72 | 11.44 | 10.96 |
| Volume FWE p | < 0.001 | 0.001 | 0.001 | 0.005 | < 0.001 | 0.002 | 0.002 |
| Volume mFWE p | 0.001 | 0.001 | 0.001 | 0.006 | < 0.001 | 0.002 | 0.003 |

Table B9 continued

| | Right thalamus | Right caudate | Right putamen | Right pallidum | Right hippocampus | Right amygdala | Right accumbens |
|---|---|---|---|---|---|---|---|
| **Fisher F** | **204.87** | **221.54** | **198.61** | **119.75** | **276.01** | **134.09** | **175.68** |
| **Fisher FWE p** | **0.002** | **0.001** | **0.002** | **0.012** | **< 0.001** | **0.008** | **0.003** |
| MD | -0.13 | 1.84 | 2.27 | 0.5 | -2.56 | -1.84 | 4.43 |
| MD FWE p | 0.999 | 0.937 | 0.806 | 0.999 | 0.999 | 0.999 | 0.018 |
| MD mFWE p | 0.999 | 0.999 | 0.999 | 0.999 | 0.999 | 0.999 | 0.065 |
| RD | -0.6 | 1.29 | 3.03 | 2.14 | -3.34 | -1.96 | 4.42 |
| RD FWE p | 0.999 | 0.999 | 0.694 | 0.967 | 0.999 | 0.999 | 0.082 |
| RD mFWE p | 0.999 | 0.999 | 0.999 | 0.999 | 0.999 | 0.999 | 0.065 |
| AD | 0.41 | 2.29 | 0.75 | -1.83 | -1.16 | -1.42 | 3.8 |
| AD FWE p | 0.996 | 0.413 | 0.982 | 0.999 | 0.999 | 0.999 | 0.014 |
| AD mFWE p | 0.999 | 0.999 | 0.999 | 0.999 | 0.999 | 0.999 | 0.114 |
| Volume | 14.06 | 14.06 | 13.01 | 10.18 | 16.6 | 11.35 | 10.12 |
| Volume FWE p | 0.001 | 0.001 | 0.001 | 0.003 | < 0.001 | 0.002 | 0.003 |
| Volume mFWE p | 0.001 | 0.001 | 0.001 | 0.004 | < 0.001 | 0.002 | 0.004 |

**Table B10 Positive correlations between subcortical grey matter metrics and language scores**

| | Left thalamus | Left caudate | Left putamen | Left pallidum | Left hippocampus | Left amygdala | Left accumbens |
|---|---|---|---|---|---|---|---|
| **Fisher F** | **277.43** | **302.5** | **221.22** | **140.63** | **363.95** | **182.93** | **235.9** |
| **Fisher FWE p** | **0.001** | **0.001** | **0.002** | **0.008** | **< 0.001** | **0.004** | **0.002** |
| MD | -1 | 3.65 | 3.07 | 1.04 | -2.46 | -0.61 | 4.55 |
| MD FWE p | 0.978 | 0.087 | 0.27 | 0.989 | 0.516 | 0.994 | 0.007 |
| MD mFWE p | 0.999 | 0.111 | 0.999 | 0.999 | 0.756 | 0.999 | 0.05 |
| RD | -1.63 | 3.59 | 4.02 | 2.98 | -3.64 | -0.81 | 4.28 |
| RD FWE p | 0.672 | 0.327 | 0.158 | 0.646 | 0.014 | 0.932 | 0.092 |
| RD mFWE p | 0.981 | 0.121 | 0.074 | 0.999 | 0.112 | 0.999 | 0.06 |
| AD | -0.01 | 3.07 | 1.21 | -2.13 | -0.42 | -0.26 | 4.24 |
| AD FWE p | 0.995 | 0.055 | 0.8 | 0.881 | 0.999 | 0.999 | 0.001 |
| AD mFWE p | 0.999 | 0.999 | 0.999 | 0.894 | 0.999 | 0.999 | 0.062 |
| Volume | 16.6 | 15.89 | 13.36 | 10.89 | 19.19 | 13.3 | 12.65 |
| Volume FWE p | < 0.001 | 0.001 | 0.001 | 0.003 | < 0.001 | 0.001 | 0.002 |
| Volume m FWE p | 0.001 | 0.001 | 0.002 | 0.004 | < 0.001 | 0.002 | 0.002 |

Table B10 continued

| | Right thalamus | Right caudate | Right putamen | Right pallidum | Right hippocampus | Right amygdala | Right accumbens |
|---|---|---|---|---|---|---|---|
| **Fisher F** | **264.41** | **278.95** | **221.81** | **143.61** | **320.19** | **179.93** | **201.86** |
| **Fisher FWE p** | **0.001** | **0.001** | **0.002** | **0.008** | **0.001** | **0.004** | **0.003** |
| MD | -0.74 | 1.19 | 2.25 | 0.33 | -3.19 | -2.46 | 4.63 |
| MD FWE p | 0.991 | 0.981 | 0.693 | 0.999 | 0.161 | 0.516 | 0.005 |
| MD m FWE p | 0.999 | 0.999 | 0.999 | 0.999 | 0.309 | 0.756 | 0.047 |
| RD | -0.97 | 0.71 | 2.86 | 2.22 | -4.01 | -2.7 | 4.65 |
| RD FWE p | 0.902 | 0.999 | 0.704 | 0.928 | 0.003 | 0.17 | 0.037 |
| RD mFWE p | 0.999 | 0.999 | 0.999 | 0.999 | 0.034 | 0.618 | 0.047 |
| AD | -0.33 | 1.66 | 0.91 | -2.28 | -1.64 | -1.81 | 3.93 |
| AD FWE p | 0.999 | 0.588 | 0.894 | 0.826 | 0.976 | 0.955 | 0.004 |
| AD mFWE p | 0.999 | 0.999 | 0.999 | 0.842 | 0.981 | 0.963 | 0.08 |
| Volume | 16.18 | 16.28 | 13.92 | 11.31 | 17.96 | 13.26 | 11.12 |
| Volume FWE p | < 0.001 | < 0.001 | 0.001 | 0.003 | < 0.001 | 0.001 | 0.003 |
| Volume mFWE p | 0.001 | 0.001 | 0.001 | 0.003 | < 0.001 | 0.002 | 0.003 |

**Table B11 Positive correlations between subcortical grey matter metrics and executive functioning scores**

| | Left thalamus | Left caudate | Left putamen | Left pallidum | Left hippocampus | Left amygdala | Left accumbens |
|---|---|---|---|---|---|---|---|
| **Fisher F** | **121.49** | **100.49** | **108.85** | **43.43** | **146.71** | **58.15** | **74.35** |
| **Fisher FWE p** | **< 0.001** | **0.005** | **0.002** | **0.514** | **< 0.001** | **0.203** | **0.056** |
| MD | 1.82 | -2.35 | -0.75 | 0.93 | 2.04 | 2.25 | -1.03 |
| MD FWE p | 0.322 | 0.999 | 0.999 | 0.774 | 0.222 | 0.145 | 0.999 |
| MD mFWE p | 0.782 | 0.999 | 0.999 | 0.996 | 0.642 | 0.491 | 0.999 |
| RD | 2.33 | -2.15 | -1.76 | -0.76 | 2.19 | 1.89 | -0.93 |
| RD FWE p | 0.084 | 0.999 | 0.999 | 0.988 | 0.11 | 0.191 | 0.993 |
| RD mFWE p | 0.44 | 0.999 | 0.999 | 0.999 | 0.534 | 0.741 | 0.999 |
| AD | 0.76 | -2.23 | 0.75 | 3.02 | 1.43 | 2.33 | -1 |
| AD FWE p | 0.994 | 0.999 | 0.994 | 0.078 | 0.893 | 0.375 | 0.999 |
| AD mFWE p | 0.999 | 0.999 | 0.999 | 0.097 | 0.939 | 0.438 | 0.999 |
| Volume | -10.75 | -8.28 | -9.66 | -5.89 | -11.9 | -7.24 | -7.6 |
| Volume FWE p | < 0.001 | 0.001 | < 0.001 | 0.007 | < 0.001 | 0.002 | 0.001 |
| Volume mFWE p | < 0.001 | 0.002 | < 0.001 | 0.019 | < 0.001 | 0.005 | 0.003 |

Table B11 continued

| | Right thalamus | Right caudate | Right putamen | Right pallidum | Right hippocampus | Right amygdala | Right accumbens |
|---|---|---|---|---|---|---|---|
| **Fisher F** | **97.67** | **86.96** | **108.99** | **78.4** | **136.16** | **56.79** | **70.64** |
| **Fisher FWE p** | **0.006** | **0.018** | **0.002** | **0.039** | **< 0.001** | **0.224** | **0.076** |
| MD | 1.57 | -0.08 | -0.09 | 0.61 | 2.88 | 2.7 | -1.29 |
| MD FWE p | 0.453 | 0.983 | 0.984 | 0.882 | 0.028 | 0.048 | 0.999 |
| MD mFWE p | 0.898 | 0.999 | 0.999 | 0.999 | 0.141 | 0.219 | 0.999 |
| RD | 1.9 | 0.66 | -0.82 | -1.24 | 3.31 | 2.36 | -1.41 |
| RD FWE p | 0.186 | 0.71 | 0.99 | 0.998 | 0.006 | 0.079 | 0.999 |
| RD mFWE p | 0.733 | 0.999 | 0.999 | 0.999 | 0.039 | 0.42 | 0.999 |
| AD | 0.89 | -1.16 | 0.87 | 2.81 | 1.85 | 2.66 | -0.96 |
| AD FWE p | 0.988 | 0.999 | 0.989 | 0.138 | 0.692 | 0.195 | 0.999 |
| AD mFWE p | 0.997 | 0.999 | 0.997 | 0.168 | 0.765 | 0.235 | 0.999 |
| Volume | -9.57 | -8.66 | -9.92 | -8.23 | -11.45 | -7.16 | -7.2 |
| Volume FWE p | < 0.001 | < 0.001 | < 0.001 | 0.001 | < 0.001 | 0.002 | 0.002 |
| Volume mFWE p | < 0.001 | 0.001 | < 0.001 | 0.002 | < 0.001 | 0.005 | 0.005 |

**Table B12 Positive correlations between subcortical grey matter metrics and memory scores**

| | Left thalamus | Left caudate | Left putamen | Left pallidum | Left hippocampus | Left amygdala | Left accumbens |
|---|---|---|---|---|---|---|---|
| **Fisher F** | **123.41** | **158.14** | **133.09** | **62.48** | **186.93** | **74.12** | **117.97** |
| **Fisher FWE p** | **0.002** | **< 0.001** | **0.001** | **0.077** | **< 0.001** | **0.037** | **0.003** |
| MD | 0.48 | 3.96 | 3.48 | 1.75 | -0.4 | 0.61 | 4.12 |
| MD FWE p | 0.999 | 0.055 | 0.189 | 0.946 | 0.999 | 0.999 | 0.033 |
| MD mFWE p | 0.999 | 0.12 | 0.219 | 0.999 | 0.999 | 0.999 | 0.102 |
| RD | -0.9 | 3.86 | 4.38 | 3.09 | -1.37 | 0.47 | 3.94 |
| RD FWE p | 0.999 | 0.199 | 0.061 | 0.579 | 0.999 | 0.999 | 0.17 |
| RD mFWE p | 0.999 | 0.135 | 0.078 | 0.5 | 0.999 | 0.999 | 0.124 |
| AD | 1.98 | 3.4 | 1.59 | -0.82 | 0.97 | 0.68 | 3.75 |
| AD FWE p | 0.668 | 0.046 | 0.841 | 0.999 | 0.97 | 0.989 | 0.013 |
| AD mFWE p | 0.999 | 0.246 | 0.999 | 0.999 | 0.999 | 0.999 | 0.152 |
| Volume | 10.39 | 9.84 | 9.01 | 6.03 | 13.36 | 7.8 | 7.2 |
| Volume FWE p | < 0.001 | 0.001 | 0.001 | 0.011 | < 0.001 | 0.003 | 0.005 |
| Volume mFWE p | 0.001 | 0.001 | 0.002 | 0.019 | < 0.001 | 0.005 | 0.008 |

Table B12 continued

| | Right thalamus | Right caudate | Right putamen | Right pallidum | Right hippocampus | Right amygdala | Right accumbens |
|---|---|---|---|---|---|---|---|
| **Fisher F** | **110.05** | **141.27** | **127.36** | **61.17** | **160.6** | **69.01** | **130.35** |
| **Fisher FWE p** | **0.004** | **0.001** | **0.001** | **0.084** | **< 0.001** | **0.051** | **0.001** |
| MD | 1.55 | 3.14 | 2.86 | 1.23 | -0.73 | 0.07 | 4.59 |
| MD FWE p | 0.971 | 0.346 | 0.508 | 0.991 | 0.999 | 0.999 | 0.005 |
| MD mFWE p | 0.999 | 0.414 | 0.999 | 0.999 | 0.999 | 0.999 | 0.064 |
| RD | 0.84 | 2.8 | 3.56 | 1.86 | -1.41 | -0.13 | 4.47 |
| RD FWE p | 0.999 | 0.73 | 0.326 | 0.974 | 0.999 | 0.999 | 0.048 |
| RD mFWE p | 0.999 | 0.999 | 0.194 | 0.999 | 0.999 | 0.999 | 0.072 |
| AD | 2 | 3.04 | 1.25 | -0.07 | 0.25 | 0.28 | 4.08 |
| AD FWE p | 0.653 | 0.126 | 0.932 | 0.999 | 0.998 | 0.998 | 0.003 |
| AD mFWE p | 0.999 | 0.999 | 0.999 | 0.999 | 0.999 | 0.999 | 0.105 |
| Volume | 9.38 | 9.81 | 9.37 | 6.56 | 12.39 | 7.67 | 7.25 |
| Volume FWE p | 0.001 | 0.001 | 0.001 | 0.008 | < 0.001 | 0.003 | 0.004 |
| Volume mFWE p | 0.002 | 0.001 | 0.002 | 0.012 | < 0.001 | 0.005 | 0.007 |

**Table B13 Negative correlations between subcortical grey matter metrics and total problem scores**

| | Left thalamus | Left caudate | Left putamen | Left pallidum | Left hippocampus | Left amygdala | Left accumbens |
|---|---|---|---|---|---|---|---|
| **Fisher F** | **20.84** | **21.47** | **26.34** | **18.69** | **37.78** | **17.97** | **28.06** |
| **Fisher FWE p** | **0.013** | **0.011** | **0.002** | **0.025** | **< 0.001** | **0.031** | **0.001** |
| MD | -4.41 | -0.45 | -2.18 | -1.76 | -2.58 | -2.01 | -0.31 |
| MD FWE p | 0.999 | 0.597 | 0.994 | 0.976 | 0.999 | 0.99 | 0.519 |
| MD mFWE p | 0.999 | 0.999 | 0.999 | 0.999 | 0.999 | 0.999 | 0.999 |
| RD | -3.99 | 0.48 | -0.76 | -0.7 | -1.78 | -1.57 | 0.03 |
| RD FWE p | 0.999 | 0.499 | 0.954 | 0.946 | 0.999 | 0.998 | 0.726 |
| RD mFWE p | 0.999 | 0.967 | 0.999 | 0.999 | 0.999 | 0.999 | 0.996 |
| AD | -3.78 | -1.83 | -3.67 | -2.63 | -3.14 | -2.22 | -0.69 |
| AD FWE p | 0.999 | 0.837 | 0.999 | 0.987 | 0.999 | 0.944 | 0.247 |
| AD mFWE p | 0.999 | 0.999 | 0.999 | 0.999 | 0.999 | 0.999 | 0.999 |
| Volume | 4.02 | 3.71 | 4.57 | 3.67 | 5.69 | 3.64 | 4.5 |
| Volume FWE p | 0.004 | 0.01 | 0.001 | 0.011 | < 0.001 | 0.012 | 0.001 |
| Volume mFWE p | 0.004 | 0.01 | 0.001 | 0.011 | < 0.001 | 0.012 | 0.001 |

Table B13 continued

| | Right thalamus | Right caudate | Right putamen | Right pallidum | Right hippocampus | Right amygdala | Right accumbens |
|---|---|---|---|---|---|---|---|
| **Fisher F** | **14.84** | **20.6** | **26.21** | **28.03** | **28.31** | **24.14** | **38.56** |
| **Fisher FWE p** | **0.077** | **0.014** | **0.003** | **0.001** | **0.001** | **0.005** | **< 0.001** |
| MD | -3.6 | -1.6 | -2.1 | -1.61 | -3.24 | -1.91 | -0.86 |
| MD FWE p | 0.999 | 0.962 | 0.993 | 0.963 | 0.999 | 0.985 | 0.785 |
| MD mFWE p | 0.999 | 0.999 | 0.999 | 0.999 | 0.999 | 0.999 | 0.999 |
| RD | -2.84 | -1.01 | -0.15 | 0.02 | -2.97 | -1.17 | -0.76 |
| RD FWE p | 0.999 | 0.979 | 0.802 | 0.732 | 0.999 | 0.988 | 0.954 |
| RD mFWE p | 0.999 | 0.999 | 0.999 | 0.997 | 0.999 | 0.999 | 0.999 |
| AD | -3.69 | -2.17 | -4.12 | -3.15 | -3.02 | -2.46 | -0.85 |
| AD FWE p | 0.999 | 0.935 | 0.999 | 0.999 | 0.998 | 0.975 | 0.328 |
| AD mFWE p | 0.999 | 0.999 | 0.999 | 0.999 | 0.999 | 0.999 | 0.999 |
| Volume | 3.24 | 3.93 | 4.49 | 4.64 | 4.83 | 4.36 | 5.65 |
| Volume FWE p | 0.032 | 0.005 | 0.001 | < 0.001 | < 0.001 | 0.001 | < 0.001 |
| Volume mFWE p | 0.032 | 0.005 | 0.001 | 0.001 | < 0.001 | 0.002 | < 0.001 |

**Table B14 Negative correlations between subcortical grey matter metrics and internalizing problem scores**

| | Left thalamus | Left caudate | Left putamen | Left pallidum | Left hippocampus | Left amygdala | Left accumbens |
|---|---|---|---|---|---|---|---|
| **Fisher F** | **3.98** | **5.91** | **7.97** | **6.08** | **8.87** | **5.81** | **11.32** |
| **Fisher FWE p** | **0.818** | **0.561** | **0.316** | **0.538** | **0.236** | **0.575** | **0.097** |
| MD | -3.84 | -0.95 | -2.12 | -1.66 | -2.45 | -1.53 | -0.88 |
| MD FWE p | 0.999 | 0.739 | 0.99 | 0.951 | 0.998 | 0.928 | 0.708 |
| MD mFWE p | 0.999 | 0.999 | 0.999 | 0.999 | 0.999 | 0.999 | 0.999 |
| RD | -3.29 | -0.18 | -0.83 | -0.87 | -1.68 | -1.05 | -0.78 |
| RD FWE p | 0.999 | 0.717 | 0.933 | 0.94 | 0.997 | 0.965 | 0.923 |
| RD mFWE p | 0.999 | 0.995 | 0.999 | 0.999 | 0.999 | 0.999 | 0.999 |
| AD | -3.5 | -1.99 | -3.44 | -2.18 | -2.98 | -1.85 | -0.89 |
| AD FWE p | 0.999 | 0.886 | 0.999 | 0.935 | 0.997 | 0.84 | 0.3 |
| AD mFWE p | 0.999 | 0.999 | 0.999 | 0.999 | 0.999 | 0.999 | 0.999 |
| Volume | 1.1 | 1.21 | 1.98 | 1.53 | 2.24 | 1.47 | 2.47 |
| Volume FWE p | 0.592 | 0.533 | 0.19 | 0.375 | 0.118 | 0.403 | 0.073 |
| Volume mFWE p | 0.658 | 0.593 | 0.202 | 0.413 | 0.122 | 0.446 | 0.074 |

Table B14 continued

| | Right thalamus | Right caudate | Right putamen | Right pallidum | Right hippocampus | Right amygdala | Right accumbens |
|---|---|---|---|---|---|---|---|
| **Fisher F** | **2.74** | **4.91** | **7.49** | **18.89** | **5.81** | **7.07** | **18.79** |
| **Fisher FWE p** | **0.94** | **0.697** | **0.366** | **0.003** | **0.574** | **0.414** | **0.004** |
| MD | -3.45 | -1.91 | -1.64 | -0.89 | -2.64 | -1.43 | -1.31 |
| MD FWE p | 0.999 | 0.979 | 0.948 | 0.712 | 0.999 | 0.908 | 0.876 |
| MD mFWE p | 0.999 | 0.999 | 0.999 | 0.999 | 0.999 | 0.999 | 0.999 |
| RD | -2.91 | -1.35 | -0.05 | 0.8 | -2.21 | -0.77 | -1.21 |
| RD FWE p | 0.999 | 0.988 | 0.654 | 0.235 | 0.999 | 0.92 | 0.98 |
| RD mFWE p | 0.999 | 0.999 | 0.991 | 0.808 | 0.999 | 0.999 | 0.999 |
| AD | -3.33 | -2.36 | -3.29 | -2.78 | -2.72 | -1.97 | -1.25 |
| AD FWE p | 0.999 | 0.964 | 0.999 | 0.993 | 0.991 | 0.88 | 0.518 |
| AD mFWE p | 0.999 | 0.999 | 0.999 | 0.999 | 0.999 | 0.999 | 0.999 |
| Volume | 0.66 | 1.3 | 1.67 | 3.32 | 1.59 | 1.73 | 3.68 |
| Volume FWE p | 0.792 | 0.49 | 0.312 | 0.008 | 0.346 | 0.283 | 0.003 |
| Volume mFWE p | 0.862 | 0.545 | 0.341 | 0.008 | 0.38 | 0.308 | 0.002 |

**Table B15 Positive correlations between subcortical grey matter metrics and anxiety/depressive problem scores**

| | Left thalamus | Left caudate | Left putamen | Left pallidum | Left hippocampus | Left amygdala | Left accumbens |
|---|---|---|---|---|---|---|---|
| **Fisher F** | **48.56** | **22.07** | **33.25** | **21.5** | **32.1** | **16.84** | **23.38** |
| **Fisher FWE p** | **0.03** | **0.857** | **0.348** | **0.876** | **0.397** | **0.975** | **0.808** |
| MD | 3.66 | 1.84 | 2.6 | 2.03 | 2.61 | 1.56 | 2.12 |
| MD FWE p | 0.02 | 0.851 | 0.393 | 0.758 | 0.385 | 0.937 | 0.707 |
| MD mFWE p | 0.044 | 0.977 | 0.635 | 0.939 | 0.625 | 0.996 | 0.912 |
| RD | 3.12 | 1.28 | 1.55 | 1.62 | 1.88 | 1.39 | 2.07 |
| RD FWE p | 0.063 | 0.911 | 0.819 | 0.788 | 0.652 | 0.879 | 0.534 |
| RD mFWE p | 0.241 | 0.999 | 0.996 | 0.994 | 0.971 | 0.999 | 0.927 |
| AD | 3.35 | 2.37 | 3.5 | 1.87 | 3.06 | 1.51 | 1.88 |
| AD FWE p | 0.089 | 0.676 | 0.055 | 0.927 | 0.207 | 0.986 | 0.925 |
| AD mFWE p | 0.128 | 0.79 | 0.08 | 0.972 | 0.283 | 0.997 | 0.971 |
| Volume | -0.34 | -0.14 | -1.26 | -0.35 | -0.52 | -0.51 | -1.07 |
| Volume FWE p | 0.808 | 0.871 | 0.385 | 0.804 | 0.738 | 0.741 | 0.476 |
| Volume mFWE p | 0.929 | 0.967 | 0.488 | 0.926 | 0.875 | 0.878 | 0.6 |

Table B15 continued

| | Right thalamus | Right caudate | Right putamen | Right pallidum | Right hippocampus | Right amygdala | Right accumbens |
|---|---|---|---|---|---|---|---|
| **Fisher F** | **38.08** | **25.31** | **28.17** | **14.68** | **28.84** | **13.1** | **28.98** |
| **Fisher FWE p** | **0.182** | **0.724** | **0.585** | **0.992** | **0.552** | **0.997** | **0.545** |
| MD | 3.03 | 2.21 | 2.26 | 1.26 | 2.43 | 1.18 | 2.52 |
| MD FWE p | 0.158 | 0.65 | 0.623 | 0.981 | 0.508 | 0.987 | 0.444 |
| MD mFWE p | 0.303 | 0.875 | 0.855 | 0.999 | 0.757 | 0.999 | 0.692 |
| RD | 2.46 | 1.89 | 1.05 | 0.21 | 2.1 | 0.83 | 2.69 |
| RD FWE p | 0.3 | 0.647 | 0.958 | 0.999 | 0.52 | 0.982 | 0.191 |
| RD mFWE p | 0.732 | 0.97 | 0.999 | 0.999 | 0.921 | 0.999 | 0.56 |
| AD | 3.03 | 2.26 | 3.27 | 2.17 | 2.42 | 1.4 | 1.95 |
| AD FWE p | 0.223 | 0.749 | 0.116 | 0.805 | 0.642 | 0.992 | 0.902 |
| AD mFWE p | 0.304 | 0.851 | 0.164 | 0.894 | 0.759 | 0.999 | 0.958 |
| Volume | -0.02 | -0.47 | -0.82 | -2.31 | -0.04 | -0.62 | -1.65 |
| Volume FWE p | 0.901 | 0.756 | 0.599 | 0.068 | 0.899 | 0.691 | 0.228 |
| Volume mFWE p | 0.98 | 0.89 | 0.74 | 0.077 | 0.979 | 0.834 | 0.284 |

**Table B16 Positive correlations between subcortical grey matter metrics and attention problem scores**

| | Left thalamus | Left caudate | Left putamen | Left pallidum | Left hippocampus | Left amygdala | Left accumbens |
|---|---|---|---|---|---|---|---|
| **Fisher F** | **48.56** | **22.07** | **33.25** | **21.5** | **32.1** | **16.84** | **23.38** |
| **Fisher FWE p** | **0.03** | **0.857** | **0.348** | **0.876** | **0.397** | **0.975** | **0.808** |
| MD | 3.66 | 1.84 | 2.6 | 2.03 | 2.61 | 1.56 | 2.12 |
| MD FWE p | 0.02 | 0.851 | 0.393 | 0.758 | 0.385 | 0.937 | 0.707 |
| MD mFWE p | 0.044 | 0.977 | 0.635 | 0.939 | 0.625 | 0.996 | 0.912 |
| RD | 3.12 | 1.28 | 1.55 | 1.62 | 1.88 | 1.39 | 2.07 |
| RD FWE p | 0.063 | 0.911 | 0.819 | 0.788 | 0.652 | 0.879 | 0.534 |
| RD mFWE p | 0.241 | 0.999 | 0.996 | 0.994 | 0.971 | 0.999 | 0.927 |
| AD | 3.35 | 2.37 | 3.5 | 1.87 | 3.06 | 1.51 | 1.88 |
| AD FWE p | 0.089 | 0.676 | 0.055 | 0.927 | 0.207 | 0.986 | 0.925 |
| AD mFWE p | 0.128 | 0.79 | 0.08 | 0.972 | 0.283 | 0.997 | 0.971 |
| Volume | -0.34 | -0.14 | -1.26 | -0.35 | -0.52 | -0.51 | -1.07 |
| Volume FWE p | 0.808 | 0.871 | 0.385 | 0.804 | 0.738 | 0.741 | 0.476 |
| Volume mFWE p | 0.929 | 0.967 | 0.488 | 0.926 | 0.875 | 0.878 | 0.6 |

Table B16 continued

| | Right thalamus | Right caudate | Right putamen | Right pallidum | Right hippocampus | Right amygdala | Right accumbens |
|---|---|---|---|---|---|---|---|
| **Fisher F** | **38.08** | **25.31** | **28.17** | **14.68** | **28.84** | **13.1** | **28.98** |
| **Fisher FWE p** | **0.182** | **0.724** | **0.585** | **0.992** | **0.552** | **0.997** | **0.545** |
| MD | 3.03 | 2.21 | 2.26 | 1.26 | 2.43 | 1.18 | 2.52 |
| MD FWE p | 0.158 | 0.65 | 0.623 | 0.981 | 0.508 | 0.987 | 0.444 |
| MD mFWE p | 0.303 | 0.875 | 0.855 | 0.999 | 0.757 | 0.999 | 0.692 |
| RD | 2.46 | 1.89 | 1.05 | 0.21 | 2.1 | 0.83 | 2.69 |
| RD FWE p | 0.3 | 0.647 | 0.958 | 0.999 | 0.52 | 0.982 | 0.191 |
| RD mFWE p | 0.732 | 0.97 | 0.999 | 0.999 | 0.921 | 0.999 | 0.56 |
| AD | 3.03 | 2.26 | 3.27 | 2.17 | 2.42 | 1.4 | 1.95 |
| AD FWE p | 0.223 | 0.749 | 0.116 | 0.805 | 0.642 | 0.992 | 0.902 |
| AD mFWE p | 0.304 | 0.851 | 0.164 | 0.894 | 0.759 | 0.999 | 0.958 |
| Volume | -0.02 | -0.47 | -0.82 | -2.31 | -0.04 | -0.62 | -1.65 |
| Volume FWE p | 0.901 | 0.756 | 0.599 | 0.068 | 0.899 | 0.691 | 0.228 |
| Volume mFWE p | 0.98 | 0.89 | 0.74 | 0.077 | 0.979 | 0.834 | 0.284 |

**Table B17 Positive correlations between cortical grey matter metrics and *g* scores**

| | Left fronto marginal gyrus and sulcus | Left inferior occipital gyrus and sulcus | Left paracentral lobule and sulcus | Left subcentral gyrus and sulci | Left transverse frontopolar gyri and sulci | Left anterior part of the cingulate gyrus and sulcus | Left middle anterior part of the cingulate gyrus and sulcus | Left middle posterior part of the cingulate gyrus and sulcus | Left posterior dorsal part of the cingulate gyrus | Left posterior ventral part of the cingulate gyrus | Left cuneus | Left opercular part of the inferior frontal gyrus | Left orbital part of the inferior frontal gyrus | Left triangular part of the inferior frontal gyrus | Left middle frontal gyrus |
|---|---|---|---|---|---|---|---|---|---|---|---|---|---|---|---|
| **Fisher F** | **215.2** | **137.6** | **102.9** | **172.7** | **157.0** | **219.3** | **104.2** | **104.7** | **120.7** | **19.2** | **116.7** | **124.9** | **109.7** | **73.95** | **169.1** |
| **Fisher FWE p** | **0.003** | **0.014** | **0.031** | **0.007** | **0.009** | **0.003** | **0.03** | **0.03** | **0.02** | **0.999** | **0.022** | **0.019** | **0.026** | **0.076** | **0.007** |
| MD | 3.48 | 0.87 | -3.08 | -1.14 | 4.23 | 4.39 | 1.51 | 0.63 | -0.95 | -3.32 | -1.3 | 2 | 1.24 | 2.85 | 3.23 |
| MD FWE p | 0.614 | 0.999 | 0.999 | 0.999 | 0.193 | 0.138 | 0.999 | 0.999 | 0.999 | 0.999 | 0.999 | 0.998 | 0.999 | 0.907 | 0.757 |
| MD mFWE p | 0.999 | 0.999 | 0.999 | 0.999 | 0.999 | 0.147 | 0.999 | 0.999 | 0.999 | 0.999 | 0.999 | 0.999 | 0.999 | 0.999 | 0.999 |
| RD | 3.82 | -0.11 | -3.28 | -1.77 | 4.38 | 5.37 | 1.96 | 0.64 | -1.05 | -4.06 | -1.54 | 1.95 | 0.83 | 2.98 | 3.33 |
| RD FWE p | 0.282 | 0.999 | 0.999 | 0.999 | 0.081 | 0.003 | 0.995 | 0.999 | 0.999 | 0.999 | 0.999 | 0.995 | 0.999 | 0.781 | 0.578 |
| RD mFWE p | 0.999 | 0.999 | 0.999 | 0.999 | 0.153 | 0.046 | 0.999 | 0.999 | 0.999 | 0.999 | 0.999 | 0.999 | 0.999 | 0.999 | 0.999 |
| AD | 2.26 | 2.08 | -2.28 | 0.22 | 3.22 | 1.92 | 0.43 | 0.47 | -0.59 | -1.53 | -0.81 | 1.9 | 1.78 | 2.34 | 2.7 |
| AD FWE p | 0.996 | 0.999 | 0.999 | 0.999 | 0.839 | 0.999 | 0.999 | 0.999 | 0.999 | 0.999 | 0.999 | 0.999 | 0.999 | 0.994 | 0.968 |
| AD mFWE p | 0.999 | 0.999 | 0.999 | 0.999 | 0.999 | 0.999 | 0.999 | 0.999 | 0.999 | 0.999 | 0.999 | 0.999 | 0.999 | 0.999 | 0.999 |
| Volume | 12.9 | 10.95 | 9.87 | 12.9 | 9.38 | 11.88 | 9.14 | 9.57 | 10.68 | 3.78 | 10.51 | 9.21 | 9.48 | 5.71 | 11 |
| Volume FWE p | 0.002 | 0.003 | 0.005 | 0.002 | 0.007 | 0.002 | 0.007 | 0.006 | 0.004 | 0.999 | 0.004 | 0.007 | 0.006 | 0.042 | 0.003 |
| Volume mFWE p | 0.002 | 0.003 | 0.005 | 0.002 | 0.006 | 0.002 | 0.007 | 0.006 | 0.004 | 0.999 | 0.004 | 0.007 | 0.006 | 0.037 | 0.003 |
| Thickness | 3.53 | 6.51 | 6.08 | 2.96 | -0.41 | -2.09 | 3.29 | 3.8 | 4.31 | 1.36 | 7.04 | -2.88 | 4.41 | -0.09 | -0.02 |
| Thickness FWE p | 0.293 | 0.008 | 0.013 | 0.843 | 0.999 | 0.999 | 0.422 | 0.203 | 0.104 | 0.999 | 0.004 | 0.999 | 0.092 | 0.999 | 0.999 |
| Thickness mFWE p | 0.334 | 0.009 | 0.014 | 0.999 | 0.999 | 0.999 | 0.532 | 0.222 | 0.11 | 0.999 | 0.005 | 0.999 | 0.097 | 0.999 | 0.999 |

Table B17 continued

| | Left long insular gyrus and central sulcus of the insula | Left short insular gyri | Left middle occipital gyrus | Left superior occipital gyrus | Left lateral occipito temporal gyrus | Left lingual gyrus | Left parahippocampal gyrus | Left orbital gyri | Left angular gyrus | Left supramarginal gyrus | Left superior parietal lobule | Left postcentral gyrus | Left precentral gyrus | Left precuneus |
|---|---|---|---|---|---|---|---|---|---|---|---|---|---|---|
| **Fisher F** | **217.3** | **191.3** | **137.1** | **155.07** | **122.6** | **107.1** | **132.4** | **261.5** | **107.4** | **197.4** | **177.1** | **172.0** | **230.7** | **142.8** |
| **Fisher FWE p** | **0.003** | **0.005** | **0.014** | **0.01** | **0.02** | **0.028** | **0.016** | **0.001** | **0.028** | **0.004** | **0.006** | **0.007** | **0.002** | **0.013** |
| MD | 4.19 | 2.55 | 0.74 | -1.15 | -1.23 | -1.36 | -4.38 | 0.84 | 0.67 | -1.28 | 2.26 | -1.17 | 0.18 | -0.62 |
| MD FWE p | 0.211 | 0.969 | 0.999 | 0.999 | 0.999 | 0.999 | 0.999 | 0.999 | 0.999 | 0.999 | 0.992 | 0.999 | 0.999 | 0.999 |
| MD mFWE p | 0.999 | 0.999 | 0.999 | 0.999 | 0.999 | 0.999 | 0.999 | 0.999 | 0.999 | 0.999 | 0.999 | 0.999 | 0.999 | 0.999 |
| RD | 3.41 | 2.08 | -0.85 | -1.9 | -1.89 | -1.59 | -5.26 | 0.94 | -0.17 | -1.82 | 1.93 | -1.65 | 0.07 | -0.39 |
| RD FWE p | 0.526 | 0.99 | 0.999 | 0.999 | 0.999 | 0.999 | 0.999 | 0.999 | 0.999 | 0.999 | 0.996 | 0.999 | 0.999 | 0.999 |
| RD mFWE p | 0.999 | 0.999 | 0.999 | 0.999 | 0.999 | 0.999 | 0.999 | 0.999 | 0.999 | 0.999 | 0.999 | 0.999 | 0.999 | 0.999 |
| AD | 4.77 | 2.97 | 2.65 | 0.07 | 0.12 | -0.87 | -2.22 | 0.55 | 1.92 | -0.08 | 2.68 | -0.27 | 0.38 | -1.02 |
| AD FWE p | 0.092 | 0.919 | 0.975 | 0.999 | 0.999 | 0.999 | 0.999 | 0.999 | 0.999 | 0.999 | 0.971 | 0.999 | 0.999 | 0.999 |
| AD mFWE p | 0.078 | 0.999 | 0.999 | 0.999 | 0.999 | 0.999 | 0.999 | 0.999 | 0.999 | 0.999 | 0.999 | 0.999 | 0.999 | 0.999 |
| Volume | 12.07 | 12.46 | 10.84 | 12.19 | 10.74 | 10.04 | 11.28 | 15.84 | 9.5 | 13.87 | 12.03 | 12.9 | 14.93 | 11.64 |
| Volume FWE p | 0.002 | 0.002 | 0.004 | 0.002 | 0.004 | 0.005 | 0.003 | < 0.001 | 0.006 | 0.001 | 0.002 | 0.002 | 0.001 | 0.003 |
| Volume mFWE p | 0.002 | 0.002 | 0.004 | 0.002 | 0.004 | 0.005 | 0.003 | 0.001 | 0.006 | 0.001 | 0.002 | 0.002 | 0.001 | 0.003 |
| Thickness | 0.44 | 2.55 | 6.51 | 5.42 | 4.87 | 8.39 | 7.87 | 3.43 | 0.66 | 2.73 | 1.11 | 6.38 | 3.22 | 0.82 |
| Thickness FWE p | 0.999 | 0.999 | 0.008 | 0.027 | 0.053 | 0.001 | 0.002 | 0.34 | 0.999 | 0.999 | 0.999 | 0.009 | 0.475 | 0.999 |
| Thickness mFWE p | 0.999 | 0.999 | 0.009 | 0.029 | 0.056 | 0.001 | 0.002 | 0.4 | 0.999 | 0.999 | 0.999 | 0.01 | 0.644 | 0.999 |

Table B17 continued

| | Left subcallosal gyrus | Left anterior transverse temporal gyrus | Left lateral aspect of the superior temporal gyrus | Left planum polare of the superior temporal gyrus | Left planum temporale | Left inferior temporal gyrus | Left middle temporal gyrus | Left horizontal ramus of the anterior segment of the lateral sulcus | Left vertical ramus of the anterior segment of the lateral sulcus | Left posterior ramus of the lateral sulcus | Left occipital pole | Left temporal pole | Left calcarine sulcus | Left central sulcus |
|---|---|---|---|---|---|---|---|---|---|---|---|---|---|---|
| **Fisher F** | **52.7** | **95.3** | **179.3** | **198.8** | **100.8** | **265.2** | **235.6** | **93.6** | **87.4** | **133.0** | **75.2** | **211.6** | **110.7** | **188.2** |
| **Fisher FWE p** | **0.999** | **0.038** | **0.006** | **0.004** | **0.033** | **0.001** | **0.002** | **0.04** | **0.048** | **0.015** | **0.073** | **0.003** | **0.026** | **0.005** |
| MD | -0.44 | -1.92 | -0.5 | 1.3 | -1.89 | 3.76 | 2.06 | 0.97 | 2.4 | -2.35 | -1.05 | -2.11 | -0.68 | -1.23 |
| MD FWE p | 0.999 | 0.999 | 0.999 | 0.999 | 0.999 | 0.438 | 0.997 | 0.999 | 0.984 | 0.999 | 0.999 | 0.999 | 0.999 | 0.999 |
| MD mFWE p | 0.999 | 0.999 | 0.999 | 0.999 | 0.999 | 0.999 | 0.999 | 0.999 | 0.999 | 0.999 | 0.999 | 0.999 | 0.999 | 0.999 |
| RD | -0.94 | -2.23 | -0.89 | 1.43 | -2.03 | 1.59 | 0.81 | 1.04 | 2.23 | -2.24 | -3 | -3.03 | -1.04 | -0.97 |
| RD FWE p | 0.999 | 0.999 | 0.999 | 0.999 | 0.999 | 0.999 | 0.999 | 0.999 | 0.981 | 0.999 | 0.999 | 0.999 | 0.999 | 0.999 |
| RD mFWE p | 0.999 | 0.999 | 0.999 | 0.999 | 0.999 | 0.999 | 0.999 | 0.999 | 0.999 | 0.999 | 0.999 | 0.999 | 0.999 | 0.999 |
| AD | 0.43 | -1.17 | 0.23 | 0.78 | -1.42 | 5.56 | 3.34 | 0.65 | 2.4 | -2.2 | 1.7 | -0.29 | 0.01 | -1.65 |
| AD FWE p | 0.999 | 0.999 | 0.999 | 0.999 | 0.999 | 0.008 | 0.789 | 0.999 | 0.992 | 0.999 | 0.999 | 0.999 | 0.999 | 0.999 |
| AD mFWE p | 0.999 | 0.999 | 0.999 | 0.999 | 0.999 | 0.041 | 0.999 | 0.999 | 0.999 | 0.999 | 0.999 | 0.999 | 0.999 | 0.999 |
| Volume | 6.58 | 9.45 | 13.12 | 13.49 | 9.75 | 14.19 | 14.35 | 8.82 | 7.27 | 11.3 | 7.94 | 14.41 | 10.15 | 13.56 |
| Volume FWE p | 0.025 | 0.006 | 0.001 | 0.001 | 0.006 | 0.001 | 0.001 | 0.008 | 0.018 | 0.003 | 0.013 | 0.001 | 0.005 | 0.001 |
| Volume mFWE p | 0.022 | 0.006 | 0.001 | 0.001 | 0.005 | 0.001 | 0.001 | 0.008 | 0.016 | 0.003 | 0.012 | 0.001 | 0.005 | 0.001 |
| Thickness | 0.7 | 2.26 | 1.78 | 2.71 | 3.09 | 4.11 | 3.83 | 2.17 | 0.24 | 5.66 | 4.15 | 1.95 | 10.89 | 8.83 |
| Thickness FWE p | 0.999 | 0.999 | 0.999 | 0.999 | 0.612 | 0.135 | 0.195 | 0.999 | 0.999 | 0.021 | 0.128 | 0.999 | < 0.001 | 0.001 |
| Thickness mFWE p | 0.999 | 0.999 | 0.999 | 0.999 | 0.999 | 0.144 | 0.212 | 0.999 | 0.999 | 0.022 | 0.136 | 0.999 | < 0.001 | 0.001 |

Table B17 continued

| | Left anterior segment of the circular sulcus of the insula | Left inferior segment of the circular sulcus of the insula | Left superior segment of the circular sulcus of the insula | Left anterior transverse collateral sulcus | Left posterior transverse collateral sulcus | Left inferior frontal sulcus | Left middle frontal sulcus | Left superior frontal sulcus | Left sulcus intermedius primus | Left intraparietal sulcus and transverse parietal sulci | Left middle occipital sulcus and lunatus sulcus | Left superior occipital sulcus and transverse occipital | Left anterior occipital sulcus and preoccipital notch | Left lateral occipito temporal sulcus |
|---|---|---|---|---|---|---|---|---|---|---|---|---|---|---|
| **Fisher F** | **142.08** | **46.44** | **160.52** | **287.44** | **48.46** | **85.6** | **111.69** | **109.43** | **30.48** | **93.06** | **80.79** | **77.91** | **71.03** | **119.46** |
| **Fisher FWE p** | **0.013** | **0.999** | **0.009** | **0.001** | **0.999** | **0.051** | **0.025** | **0.027** | **0.999** | **0.041** | **0.06** | **0.066** | **0.086** | **0.021** |
| MD | 1.11 | 0.81 | 1.64 | 2.34 | -0.23 | 3.13 | 4.53 | 2.69 | -1.08 | -2.2 | -0.86 | -1.33 | 1.11 | 0.04 |
| MD FWE p | 0.999 | 0.999 | 0.999 | 0.987 | 0.999 | 0.801 | 0.099 | 0.946 | 0.999 | 0.999 | 0.999 | 0.999 | 0.999 | 0.999 |
| MD mFWE p | 0.999 | 0.999 | 0.999 | 0.999 | 0.999 | 0.999 | 0.108 | 0.999 | 0.999 | 0.999 | 0.999 | 0.999 | 0.999 | 0.999 |
| RD | 0.72 | 0.44 | 1.68 | 1.18 | -0.05 | 3.5 | 4.48 | 3.05 | -1.27 | -1.96 | -1.61 | -1.73 | 0.46 | -1.17 |
| RD FWE p | 0.999 | 0.999 | 0.999 | 0.999 | 0.999 | 0.471 | 0.061 | 0.743 | 0.999 | 0.999 | 0.999 | 0.999 | 0.999 | 0.999 |
| RD mFWE p | 0.999 | 0.999 | 0.999 | 0.999 | 0.999 | 0.999 | 0.119 | 0.999 | 0.999 | 0.999 | 0.999 | 0.999 | 0.999 | 0.999 |
| AD | 1.51 | 1.22 | 1.11 | 2.93 | -0.49 | 1.92 | 3.84 | 1.53 | -0.46 | -2.5 | 0.66 | -0.37 | 2.12 | 1.94 |
| AD FWE p | 0.999 | 0.999 | 0.999 | 0.929 | 0.999 | 0.999 | 0.504 | 0.999 | 0.999 | 0.999 | 0.999 | 0.999 | 0.998 | 0.999 |
| AD mFWE p | 0.999 | 0.999 | 0.999 | 0.999 | 0.999 | 0.999 | 0.999 | 0.999 | 0.999 | 0.999 | 0.999 | 0.999 | 0.999 | 0.999 |
| Volume | 11.16 | 5.61 | 11.81 | 16.13 | 6.32 | 6.49 | 6.05 | 8.57 | 4.8 | 9.35 | 8.48 | 8.43 | 7.14 | 10.25 |
| Volume FWE p | 0.003 | 0.044 | 0.002 | < 0.001 | 0.029 | 0.026 | 0.034 | 0.009 | 0.079 | 0.007 | 0.01 | 0.01 | 0.019 | 0.005 |
| Volume mFWE p | 0.003 | 0.039 | 0.002 | 0.001 | 0.026 | 0.023 | 0.03 | 0.009 | 0.076 | 0.006 | 0.009 | 0.009 | 0.017 | 0.004 |
| Thickness | 7.55 | 2.63 | 6.92 | 2.75 | 3.77 | 3.27 | 2.06 | 4.12 | 0.16 | 5.28 | 8.28 | 5.53 | 5.52 | 4.22 |
| Thickness FWE p | 0.002 | 0.999 | 0.005 | 0.999 | 0.211 | 0.437 | 0.999 | 0.134 | 0.999 | 0.032 | 0.001 | 0.024 | 0.025 | 0.117 |
| Thickness mFWE p | 0.003 | 0.999 | 0.006 | 0.999 | 0.232 | 0.561 | 0.999 | 0.143 | 0.999 | 0.034 | 0.001 | 0.026 | 0.026 | 0.125 |

Table B17 continued

| | Right paracentral lobule and sulcus | Right subcentral gyrus and sulci | Right transverse frontopolar gyri and sulci | Right anterior part of the cingulate gyrus and sulcus | Right middle anterior part of the cingulate gyrus and sulcus | Right middle posterior part of the cingulate gyrus and sulcus | Right posterior dorsal part of the cingulate gyrus | Right posterior ventral part of the cingulate gyrus | Right cuneus | Right opercular part of the inferior frontal gyrus | Right orbital part of the inferior frontal gyrus | Right triangular part of the inferior frontal gyrus | Right middle frontal gyrus | Right superior frontal gyrus |
|---|---|---|---|---|---|---|---|---|---|---|---|---|---|---|
| **Fisher F** | **81.1** | **185.2** | **214.72** | **251.22** | **147.86** | **134.76** | **146.43** | **16.34** | **106.98** | **118.53** | **88.7** | **70.86** | **162.93** | **241.85** |
| **Fisher FWE p** | **0.059** | **0.005** | **0.003** | **0.002** | **0.011** | **0.015** | **0.012** | **0.999** | **0.028** | **0.021** | **0.046** | **0.087** | **0.008** | **0.002** |
| MD | -2.85 | -1.46 | 4.39 | 4.98 | 1.02 | -0.92 | -0.9 | -4.06 | -1.83 | 1.87 | 2.84 | 3.22 | 4.28 | 1.14 |
| MD FWE p | 0.999 | 0.999 | 0.137 | 0.027 | 0.999 | 0.999 | 0.999 | 0.999 | 0.999 | 0.999 | 0.911 | 0.76 | 0.177 | 0.999 |
| MD mFWE p | 0.999 | 0.999 | 0.146 | 0.063 | 0.999 | 0.999 | 0.999 | 0.999 | 0.999 | 0.999 | 0.999 | 0.999 | 0.999 | 0.999 |
| RD | -3.05 | -2.2 | 4.13 | 5.17 | 1.54 | -0.7 | -0.92 | -4.34 | -2.1 | 1.5 | 2.21 | 3.31 | 4.27 | 1.31 |
| RD FWE p | 0.999 | 0.999 | 0.151 | 0.006 | 0.999 | 0.999 | 0.999 | 0.999 | 0.999 | 0.999 | 0.983 | 0.592 | 0.107 | 0.999 |
| RD mFWE p | 0.999 | 0.999 | 0.999 | 0.054 | 0.999 | 0.999 | 0.999 | 0.999 | 0.999 | 0.999 | 0.999 | 0.999 | 0.999 | 0.999 |
| AD | -2.01 | 0.21 | 4.03 | 3.37 | -0.22 | -1.12 | -0.68 | -2.85 | -1.21 | 2.47 | 3.56 | 2.74 | 3.9 | 0.69 |
| AD FWE p | 0.999 | 0.999 | 0.392 | 0.77 | 0.999 | 0.999 | 0.999 | 0.999 | 0.999 | 0.988 | 0.671 | 0.964 | 0.47 | 0.999 |
| AD mFWE p | 0.999 | 0.999 | 0.999 | 0.999 | 0.999 | 0.999 | 0.999 | 0.999 | 0.999 | 0.999 | 0.999 | 0.999 | 0.999 | 0.999 |
| Volume | 8.68 | 13.39 | 11.96 | 13.02 | 11.51 | 11.33 | 11.84 | 3.45 | 10.06 | 9.35 | 6.72 | 4.74 | 9.5 | 15.09 |
| Volume FWE p | 0.009 | 0.001 | 0.002 | 0.001 | 0.003 | 0.003 | 0.002 | 0.999 | 0.005 | 0.007 | 0.023 | 0.083 | 0.006 | 0.001 |
| Volume mFWE p | 0.008 | 0.001 | 0.002 | 0.002 | 0.003 | 0.003 | 0.002 | 0.999 | 0.005 | 0.006 | 0.021 | 0.081 | 0.006 | 0.001 |
| Thickness | 6.13 | 2.88 | 1.5 | 1.91 | 6.27 | 5.41 | 2.76 | 2.81 | 8.07 | -0.85 | 1.67 | -0.29 | 0.17 | 1.23 |
| Thickness FWE p | 0.012 | 0.999 | 0.999 | 0.999 | 0.01 | 0.028 | 0.999 | 0.999 | 0.001 | 0.999 | 0.999 | 0.999 | 0.999 | 0.999 |
| Thickness mFWE p | 0.013 | 0.999 | 0.999 | 0.999 | 0.011 | 0.03 | 0.999 | 0.999 | 0.002 | 0.999 | 0.999 | 0.999 | 0.999 | 0.999 |

Table B17 continued

| | Right short insular gyri | Right middle occipital gyrus | Right superior occipital gyrus | Right lateral occipito temporal gyrus | Right lingual gyrus | Right parahippocampal gyrus | Right orbital gyri | Right angular gyrus | Right supramarginal gyrus | Right superior parietal lobule | Right postcentral gyrus | Right precentral gyrus | Right precuneus |
|---|---|---|---|---|---|---|---|---|---|---|---|---|---|
| **Fisher F** | **156.07** | **141.35** | **128.98** | **89.63** | **113.71** | **94.57** | **245.81** | **118.11** | **145.15** | **137.64** | **120.33** | **197.15** | **143.25** |
| **Fisher FWE p** | **0.01** | **0.013** | **0.017** | **0.045** | **0.024** | **0.039** | **0.002** | **0.022** | **0.012** | **0.014** | **0.021** | **0.004** | **0.012** |
| MD | 2.65 | 0.6 | -1.62 | -2.52 | -2.83 | -4.39 | 0.62 | 0.21 | -0.74 | 1.45 | 0.42 | -1.31 | -1.4 |
| MD FWE p | 0.954 | 0.999 | 0.999 | 0.999 | 0.999 | 0.999 | 0.999 | 0.999 | 0.999 | 0.999 | 0.999 | 0.999 | 0.999 |
| MD mFWE p | 0.999 | 0.999 | 0.999 | 0.999 | 0.999 | 0.999 | 0.999 | 0.999 | 0.999 | 0.999 | 0.999 | 0.999 | 0.999 |
| RD | 2 | -0.78 | -2.65 | -2.72 | -2.88 | -5.03 | 0.12 | -0.22 | -1.39 | 1.17 | 0.02 | -1.58 | -1.21 |
| RD FWE p | 0.994 | 0.999 | 0.999 | 0.999 | 0.999 | 0.999 | 0.999 | 0.999 | 0.999 | 0.999 | 0.999 | 0.999 | 0.999 |
| RD mFWE p | 0.999 | 0.999 | 0.999 | 0.999 | 0.999 | 0.999 | 0.999 | 0.999 | 0.999 | 0.999 | 0.999 | 0.999 | 0.999 |
| AD | 3.19 | 2.55 | 0.24 | -1.45 | -2.49 | -2.53 | 1.15 | 0.99 | 0.57 | 1.87 | 1.13 | -0.61 | -1.68 |
| AD FWE p | 0.848 | 0.983 | 0.999 | 0.999 | 0.999 | 0.999 | 0.999 | 0.999 | 0.999 | 0.999 | 0.999 | 0.999 | 0.999 |
| AD mFWE p | 0.999 | 0.999 | 0.999 | 0.999 | 0.999 | 0.999 | 0.999 | 0.999 | 0.999 | 0.999 | 0.999 | 0.999 | 0.999 |
| Volume | 10.66 | 11.08 | 11.04 | 9.16 | 10.41 | 9.43 | 15.35 | 10.29 | 11.71 | 10.73 | 10.36 | 13.88 | 11.68 |
| Volume FWE p | 0.004 | 0.003 | 0.003 | 0.007 | 0.004 | 0.006 | 0.001 | 0.004 | 0.002 | 0.004 | 0.004 | 0.001 | 0.002 |
| Volume mFWE p | 0.004 | 0.003 | 0.003 | 0.007 | 0.004 | 0.006 | 0.001 | 0.004 | 0.003 | 0.004 | 0.004 | 0.001 | 0.003 |
| Thickness | -1.11 | 3.88 | 6.65 | 5.3 | 9.07 | 6.03 | 4.06 | 0.94 | 2.68 | 0.33 | 3.98 | 4.63 | 0 |
| Thickness FWE p | 0.999 | 0.183 | 0.007 | 0.032 | < 0.001 | 0.014 | 0.143 | 0.999 | 0.999 | 0.999 | 0.159 | 0.071 | 0.999 |
| Thickness mFWE p | 0.999 | 0.198 | 0.007 | 0.033 | 0.001 | 0.015 | 0.153 | 0.999 | 0.999 | 0.999 | 0.171 | 0.075 | 0.999 |

Table B17 continued

| | Right subcallosal gyrus | Right anterior transverse temporal gyrus | Right lateral aspect of the superior temporal gyrus | Right planum polare of the superior temporal gyrus | Right planum temporale | Right inferior temporal gyrus | Right middle temporal gyrus | Right horizontal ramus of the anterior segment of the lateral | Right vertical ramus of the anterior segment of the lateral | Right posterior ramus of the lateral sulcus | Right occipital pole | Right temporal pole | Right calcarine sulcus | Right central sulcus |
|---|---|---|---|---|---|---|---|---|---|---|---|---|---|---|
| **Fisher F** | **50.41** | **119.1** | **224.34** | **103.63** | **55.1** | **220.36** | **362.38** | **39.38** | **71.19** | **60.16** | **155.72** | **172.22** | **94.64** | **117.71** |
| **Fisher FWE p** | **0.999** | **0.021** | **0.003** | **0.031** | **0.999** | **0.003** | **< 0.001** | **0.999** | **0.085** | **0.162** | **0.01** | **0.007** | **0.039** | **0.022** |
| MD | 0.62 | -3.17 | -0.12 | -1.08 | -2.95 | 1.33 | 2.61 | 0.5 | 1.71 | -3.23 | -1.86 | -0.91 | -2.7 | -0.98 |
| MD FWE p | 0.999 | 0.999 | 0.999 | 0.999 | 0.999 | 0.999 | 0.96 | 0.999 | 0.999 | 0.999 | 0.999 | 0.999 | 0.999 | 0.999 |
| MD mFWE p | 0.999 | 0.999 | 0.999 | 0.999 | 0.999 | 0.999 | 0.999 | 0.999 | 0.999 | 0.999 | 0.999 | 0.999 | 0.999 | 0.999 |
| RD | -0.28 | -3.66 | -0.43 | -1 | -2.9 | -0.53 | 1.15 | 0.2 | 1.16 | -2.74 | -3.04 | -1.83 | -3.03 | -0.87 |
| RD FWE p | 0.999 | 0.999 | 0.999 | 0.999 | 0.999 | 0.999 | 0.999 | 0.999 | 0.999 | 0.999 | 0.999 | 0.999 | 0.999 | 0.999 |
| RD mFWE p | 0.999 | 0.999 | 0.999 | 0.999 | 0.999 | 0.999 | 0.999 | 0.999 | 0.999 | 0.999 | 0.999 | 0.999 | 0.999 | 0.999 |
| AD | 1.95 | -1.95 | 0.47 | -0.96 | -2.76 | 3.87 | 4.22 | 1.02 | 2.39 | -3.76 | 0.24 | 0.46 | -1.87 | -1.13 |
| AD FWE p | 0.999 | 0.999 | 0.999 | 0.999 | 0.999 | 0.486 | 0.289 | 0.999 | 0.992 | 0.999 | 0.999 | 0.999 | 0.999 | 0.999 |
| AD mFWE p | 0.999 | 0.999 | 0.999 | 0.999 | 0.999 | 0.999 | 0.999 | 0.999 | 0.999 | 0.999 | 0.999 | 0.999 | 0.999 | 0.999 |
| Volume | 5.83 | 10.67 | 14.74 | 9.85 | 7.04 | 13.85 | 18.1 | 5.13 | 6.73 | 7.39 | 12.21 | 12.81 | 9.43 | 10.55 |
| Volume FWE p | 0.039 | 0.004 | 0.001 | 0.005 | 0.02 | 0.001 | < 0.001 | 0.061 | 0.023 | 0.017 | 0.002 | 0.002 | 0.006 | 0.004 |
| Volume mFWE p | 0.034 | 0.004 | 0.001 | 0.005 | 0.018 | 0.001 | < 0.001 | 0.056 | 0.021 | 0.015 | 0.002 | 0.002 | 0.006 | 0.004 |
| Thickness | 1.43 | 4.8 | 4.1 | 2.45 | 4.05 | 4.35 | 3.98 | 1.39 | 0.78 | 5.95 | 8.36 | 0.17 | 11.34 | 7.27 |
| Thickness FWE p | 0.999 | 0.058 | 0.137 | 0.999 | 0.145 | 0.1 | 0.159 | 0.999 | 0.999 | 0.015 | 0.001 | 0.999 | < 0.001 | 0.003 |
| Thickness mFWE p | 0.999 | 0.061 | 0.146 | 0.999 | 0.156 | 0.106 | 0.171 | 0.999 | 0.999 | 0.016 | 0.001 | 0.999 | < 0.001 | 0.004 |

Table B17 continued

| | Right anterior segment of the circular sulcus of the insula | Right inferior segment of the circular sulcus of the insula | Right superior segment of the circular sulcus of the insula | Right anterior transverse collateral sulcus | Right posterior transverse collateral sulcus | Right inferior frontal sulcus | Right middle frontal sulcus | Right superior frontal sulcus | Right sulcus intermedius primus | Right intraparietal sulcus and transverse parietal sulci | Right middle occipital sulcus and lunatus sulcus | Right superior occipital sulcus and transverse occipital sulcus | Right anterior occipital sulcus and preoccipital notch | Right lateral occipito temporal sulcus |
|---|---|---|---|---|---|---|---|---|---|---|---|---|---|---|
| **Fisher F** | **101.0** | **58.3** | **158.1** | **191.77** | **70.6** | **89.24** | **112.39** | **109.34** | **61.38** | **105.44** | **123.93** | **81.33** | **116.38** | **172.92** |
| **Fisher FWE p** | **0.033** | **0.203** | **0.009** | **0.005** | **0.088** | **0.046** | **0.025** | **0.027** | **0.146** | **0.029** | **0.019** | **0.059** | **0.023** | **0.007** |
| MD | 1.18 | -1.81 | 1.96 | 1.33 | -0.46 | 2.92 | 4.06 | 2.03 | 0.22 | -1.84 | -0.14 | -2.09 | -0.13 | -0.85 |
| MD FWE p | 0.999 | 0.999 | 0.999 | 0.999 | 0.999 | 0.888 | 0.274 | 0.998 | 0.999 | 0.999 | 0.999 | 0.999 | 0.999 | 0.999 |
| MD mFWE p | 0.999 | 0.999 | 0.999 | 0.999 | 0.999 | 0.999 | 0.999 | 0.999 | 0.999 | 0.999 | 0.999 | 0.999 | 0.999 | 0.999 |
| RD | 1.2 | -2.32 | 2.21 | 0.69 | -0.12 | 3.33 | 4.06 | 2.51 | 0.0 | -1.87 | -0.09 | -2.22 | -0.2 | -2.14 |
| RD FWE p | 0.999 | 0.999 | 0.982 | 0.999 | 0.999 | 0.575 | 0.176 | 0.943 | 0.999 | 0.999 | 0.999 | 0.999 | 0.999 | 0.999 |
| RD mFWE p | 0.999 | 0.999 | 0.999 | 0.999 | 0.999 | 0.999 | 0.999 | 0.999 | 0.999 | 0.999 | 0.999 | 0.999 | 0.999 | 0.999 |
| AD | 0.77 | -0.53 | 0.96 | 1.64 | -0.93 | 1.7 | 3.37 | 0.7 | 0.61 | -1.65 | -0.22 | -1.54 | 0.04 | 1.81 |
| AD FWE p | 0.999 | 0.999 | 0.999 | 0.999 | 0.999 | 0.999 | 0.771 | 0.999 | 0.999 | 0.999 | 0.999 | 0.999 | 0.999 | 0.999 |
| AD mFWE p | 0.999 | 0.999 | 0.999 | 0.999 | 0.999 | 0.999 | 0.999 | 0.999 | 0.999 | 0.999 | 0.999 | 0.999 | 0.999 | 0.999 |
| Volume | 9.15 | 7.2 | 11.56 | 13.18 | 7.91 | 7.02 | 6.98 | 9.11 | 7.07 | 9.99 | 10.73 | 8.69 | 10.36 | 12.7 |
| Volume FWE p | 0.007 | 0.018 | 0.003 | 0.001 | 0.013 | 0.02 | 0.02 | 0.007 | 0.02 | 0.005 | 0.004 | 0.009 | 0.004 | 0.002 |
| Volume mFWE p | 0.007 | 0.016 | 0.003 | 0.001 | 0.012 | 0.018 | 0.018 | 0.007 | 0.017 | 0.005 | 0.004 | 0.008 | 0.004 | 0.002 |
| Thickness | 6.59 | 3.1 | 6.34 | 0.92 | 3.8 | 3.32 | 4.14 | 3.9 | 1.47 | 3.12 | 6.73 | 5.21 | 7.5 | 6.79 |
| Thickness FWE p | 0.007 | 0.597 | 0.01 | 0.999 | 0.204 | 0.402 | 0.129 | 0.177 | 0.999 | 0.573 | 0.006 | 0.035 | 0.003 | 0.006 |
| Thickness mFWE p | 0.008 | 0.999 | 0.01 | 0.999 | 0.222 | 0.497 | 0.137 | 0.192 | 0.999 | 0.999 | 0.007 | 0.037 | 0.003 | 0.006 |

Table B17 continued

| | Right lateral orbital sulcus | Right medial orbital sulcus | Right orbital sulci | Right parieto occipital sulcus | Right pericallosal sulcus | Right postcentral sulcus | Right inferior part of the precentral sulcus | Right superior part of the precentral sulcus | Right suborbital sulcus | Right subparietal sulcus | Right inferior temporal sulcus | Right superior temporal sulcus | Right transverse temporal sulcus |
|---|---|---|---|---|---|---|---|---|---|---|---|---|---|
| **Fisher F** | **55.75** | **105.62** | **196.14** | **143.93** | **105.38** | **81.48** | **133.94** | **48.51** | **49.24** | **102** | **193.36** | **202.5** | **73.88** |
| **Fisher FWE p** | **0.999** | **0.029** | **0.004** | **0.012** | **0.029** | **0.058** | **0.015** | **0.999** | **0.999** | **0.032** | **0.005** | **0.004** | **0.077** |
| MD | 2.17 | 1.92 | 0.87 | -3.9 | 3.13 | -2.46 | 0.58 | -0.67 | 1.77 | -2.57 | 2.88 | -0.82 | -5.44 |
| MD FWE p | 0.995 | 0.999 | 0.999 | 0.999 | 0.804 | 0.999 | 0.999 | 0.999 | 0.999 | 0.999 | 0.899 | 0.999 | 0.999 |
| MD mFWE p | 0.999 | 0.999 | 0.999 | 0.999 | 0.999 | 0.999 | 0.999 | 0.999 | 0.999 | 0.999 | 0.999 | 0.999 | 0.999 |
| RD | 1.89 | 1.03 | 1.72 | -4.46 | 3.22 | -2.28 | 0.44 | 0.0 | 1.05 | -2.39 | 1.38 | -1.11 | -5.26 |
| RD FWE p | 0.997 | 0.999 | 0.999 | 0.999 | 0.644 | 0.999 | 0.999 | 0.999 | 0.999 | 0.999 | 0.999 | 0.999 | 0.999 |
| RD mFWE p | 0.999 | 0.999 | 0.999 | 0.999 | 0.999 | 0.999 | 0.999 | 0.999 | 0.999 | 0.999 | 0.999 | 0.999 | 0.999 |
| AD | 2.27 | 2.58 | -0.58 | -2.43 | 2.1 | -2.66 | 0.77 | -1.9 | 2.09 | -2.57 | 4.16 | -0.05 | -5.01 |
| AD FWE p | 0.996 | 0.981 | 0.999 | 0.999 | 0.998 | 0.999 | 0.999 | 0.999 | 0.999 | 0.999 | 0.324 | 0.999 | 0.999 |
| AD mFWE p | 0.999 | 0.999 | 0.999 | 0.999 | 0.999 | 0.999 | 0.999 | 0.999 | 0.999 | 0.999 | 0.999 | 0.999 | 0.999 |
| Volume | 5.13 | 8.69 | 13.49 | 11.79 | 5.89 | 8.71 | 11 | 6.41 | 4.45 | 9.82 | 12.22 | 14.04 | 8.26 |
| Volume FWE p | 0.061 | 0.009 | 0.001 | 0.002 | 0.037 | 0.009 | 0.003 | 0.028 | 0.109 | 0.005 | 0.002 | 0.001 | 0.011 |
| Volume mFWE p | 0.056 | 0.008 | 0.001 | 0.002 | 0.033 | 0.008 | 0.003 | 0.024 | 0.125 | 0.005 | 0.002 | 0.001 | 0.01 |
| Thickness | 4.69 | -0.73 | 2.36 | 6.36 | -4.84 | 7.32 | 5.73 | 4.7 | -1.7 | 2.11 | 3.55 | 5.26 | 1.9 |
| Thickness FWE p | 0.066 | 0.999 | 0.999 | 0.009 | 0.999 | 0.003 | 0.019 | 0.065 | 0.999 | 0.999 | 0.286 | 0.033 | 0.999 |
| Thickness mFWE p | 0.069 | 0.999 | 0.999 | 0.01 | 0.999 | 0.004 | 0.021 | 0.068 | 0.999 | 0.999 | 0.326 | 0.035 | 0.999 |

**Table B18 Positive correlations between cortical grey matter metrics and language scores**

| | Left fronto marginal gyrus and sulcus | Left inferior occipital gyrus and sulcus | Left paracentral lobule and sulcus | Left subcentral gyrus and sulci | Left transverse frontopolar gyri and sulci | Left anterior part of the cingulate gyrus and sulcus | Left middle anterior part of the cingulate gyrus and | Left middle posterior part of the cingulate gyrus and | Left posterior dorsal part of the cingulate gyrus | Left posterior ventral part of the cingulate gyrus | Left cuneus | Left opercular part of the inferior frontal gyrus | Left orbital part of the inferior frontal gyrus | Left triangular part of the inferior frontal gyrus | Left middle frontal gyrus |
|---|---|---|---|---|---|---|---|---|---|---|---|---|---|---|---|
| **Fisher F** | **266.6** | **158.9** | **126.3** | **238.6** | **208.7** | **331.5** | **160.6** | **146.8** | **152** | **26.2** | **123.3** | **184.1** | **145.2** | **105.0** | **268.1** |
| **Fisher FWE p** | **0.002** | **0.012** | **0.022** | **0.003** | **0.005** | **0.001** | **0.012** | **0.015** | **0.013** | **0.999** | **0.023** | **0.008** | **0.015** | **0.035** | **0.002** |
| MD | 3.54 | 0.79 | -2.09 | -0.54 | 4.82 | 5.74 | 2.57 | 1.49 | 0.38 | -2.5 | -0.4 | 3.28 | 2.16 | 3.79 | 4.44 |
| MD FWE p | 0.756 | 0.999 | 0.999 | 0.999 | 0.116 | 0.005 | 0.983 | 0.999 | 0.999 | 0.999 | 0.999 | 0.858 | 0.997 | 0.628 | 0.263 |
| MD mFWE p | 0.999 | 0.999 | 0.999 | 0.999 | 0.081 | 0.037 | 0.999 | 0.999 | 0.999 | 0.999 | 0.999 | 0.999 | 0.999 | 0.999 | 0.999 |
| RD | 3.88 | 0.14 | -2.16 | -1.11 | 5.04 | 6.78 | 3.08 | 1.81 | 0.45 | -2.99 | -0.42 | 3.24 | 1.72 | 3.96 | 4.55 |
| RD FWE p | 0.648 | 0.999 | 0.999 | 0.999 | 0.086 | < 0.001 | 0.95 | 0.999 | 0.999 | 0.999 | 0.999 | 0.916 | 0.999 | 0.601 | 0.259 |
| RD mFWE p | 0.999 | 0.999 | 0.999 | 0.999 | 0.063 | 0.021 | 0.999 | 0.999 | 0.999 | 0.999 | 0.999 | 0.999 | 0.999 | 0.999 | 0.147 |
| AD | 2.32 | 1.54 | -1.6 | 0.66 | 3.58 | 2.92 | 1.2 | 0.57 | 0.18 | -1.27 | -0.34 | 3.03 | 2.62 | 3.08 | 3.78 |
| AD FWE p | 0.983 | 0.999 | 0.999 | 0.999 | 0.542 | 0.878 | 0.999 | 0.999 | 0.999 | 0.999 | 0.999 | 0.839 | 0.949 | 0.815 | 0.416 |
| AD mFWE p | 0.999 | 0.999 | 0.999 | 0.999 | 0.999 | 0.999 | 0.999 | 0.999 | 0.999 | 0.999 | 0.999 | 0.999 | 0.999 | 0.999 | 0.999 |
| Volume | 14.77 | 11.99 | 10.99 | 15.26 | 11.21 | 14.82 | 11.26 | 11.27 | 11.88 | 4.55 | 10.74 | 11.2 | 10.69 | 6.71 | 13.93 |
| Volume FWE p | 0.001 | 0.003 | 0.004 | 0.001 | 0.004 | 0.001 | 0.004 | 0.004 | 0.003 | 0.106 | 0.005 | 0.004 | 0.005 | 0.026 | 0.001 |
| Volume mFWE p | 0.001 | 0.003 | 0.004 | 0.001 | 0.004 | 0.001 | 0.004 | 0.004 | 0.003 | 0.148 | 0.004 | 0.004 | 0.005 | 0.022 | 0.002 |
| Thickness | 3.29 | 7.14 | 5.74 | 4.23 | -0.27 | -1.87 | 3.73 | 3.61 | 4.68 | 1.12 | 7.56 | -2.47 | 4.62 | 0.02 | -0.02 |
| Thickness FWE p | 0.454 | 0.005 | 0.023 | 0.127 | 0.999 | 0.999 | 0.238 | 0.281 | 0.075 | 0.999 | 0.004 | 0.999 | 0.08 | 0.999 | 0.999 |
| Thickness mFWE p | 0.546 | 0.006 | 0.024 | 0.13 | 0.999 | 0.999 | 0.251 | 0.302 | 0.077 | 0.999 | 0.004 | 0.999 | 0.081 | 0.999 | 0.999 |

Table B18 continued

| | Left long insular gyrus and central sulcus of the insula | Left short insular gyri | Left middle occipital gyrus | Left superior occipital gyrus | Left lateral occipito temporal gyrus | Left lingual gyrus | Left parahippocampal gyrus | Left orbital gyri | Left angular gyrus | Left supramarginal gyrus | Left superior parietal lobule | Left postcentral gyrus | Left precentral gyrus | Left precuneus |
|---|---|---|---|---|---|---|---|---|---|---|---|---|---|---|
| **Fisher F** | **259.8** | **252.5** | **174.6** | **179.9** | **161.7** | **133.0** | **151.8** | **344.1** | **133.2** | **228.8** | **206.4** | **206.9** | **291.6** | **174.1** |
| **Fisher FWE p** | **0.002** | **0.003** | **0.009** | **0.008** | **0.011** | **0.019** | **0.014** | **0.001** | **0.019** | **0.004** | **0.005** | **0.005** | **0.001** | **0.009** |
| MD | 5.14 | 4.05 | 1.12 | -0.3 | -0.8 | -0.82 | -3.82 | 0.35 | 1.43 | -0.12 | 3.14 | -0.61 | 1.59 | 0.57 |
| MD FWE p | 0.048 | 0.477 | 0.999 | 0.999 | 0.999 | 0.999 | 0.999 | 0.999 | 0.999 | 0.999 | 0.9 | 0.999 | 0.999 | 0.999 |
| MD mFWE p | 0.058 | 0.999 | 0.999 | 0.999 | 0.999 | 0.999 | 0.999 | 0.999 | 0.999 | 0.999 | 0.999 | 0.999 | 0.999 | 0.999 |
| RD | 4.28 | 3.63 | -0.17 | -0.77 | -1.16 | -0.83 | -4.41 | 0.65 | 0.83 | -0.54 | 3 | -1.04 | 1.57 | 0.97 |
| RD FWE p | 0.405 | 0.78 | 0.999 | 0.999 | 0.999 | 0.999 | 0.999 | 0.999 | 0.999 | 0.999 | 0.962 | 0.999 | 0.999 | 0.999 |
| RD mFWE p | 0.999 | 0.999 | 0.999 | 0.999 | 0.999 | 0.999 | 0.999 | 0.999 | 0.999 | 0.999 | 0.999 | 0.999 | 0.999 | 0.999 |
| AD | 5.65 | 4.15 | 2.6 | 0.42 | -0.02 | -0.73 | -2.19 | -0.15 | 2.17 | 0.72 | 3.15 | 0.18 | 1.5 | -0.24 |
| AD FWE p | 0.001 | 0.21 | 0.953 | 0.999 | 0.999 | 0.999 | 0.999 | 0.999 | 0.991 | 0.999 | 0.787 | 0.999 | 0.999 | 0.999 |
| AD mFWE p | 0.039 | 0.999 | 0.999 | 0.999 | 0.999 | 0.999 | 0.999 | 0.999 | 0.999 | 0.999 | 0.999 | 0.999 | 0.999 | 0.999 |
| Volume | 12.76 | 13.71 | 12.41 | 13.12 | 12.45 | 11.25 | 12.13 | 18.48 | 10.52 | 14.88 | 12.66 | 14.18 | 16.57 | 12.75 |
| Volume FWE p | 0.002 | 0.002 | 0.003 | 0.002 | 0.003 | 0.004 | 0.003 | < 0.001 | 0.005 | 0.001 | 0.002 | 0.001 | 0.001 | 0.002 |
| Volume mFWE p | 0.002 | 0.002 | 0.003 | 0.002 | 0.003 | 0.004 | 0.003 | < 0.001 | 0.005 | 0.001 | 0.002 | 0.001 | 0.001 | 0.002 |
| Thickness | 0.52 | 2.43 | 7.23 | 6.38 | 5.26 | 8.92 | 7.71 | 3.24 | 0.99 | 2.94 | 1.65 | 7.03 | 3.13 | 1.31 |
| Thickness FWE p | 0.999 | 0.999 | 0.005 | 0.012 | 0.039 | 0.001 | 0.003 | 0.492 | 0.999 | 0.999 | 0.999 | 0.006 | 0.617 | 0.999 |
| Thickness mFWE p | 0.999 | 0.999 | 0.005 | 0.013 | 0.04 | 0.001 | 0.003 | 0.62 | 0.999 | 0.999 | 0.999 | 0.007 | 0.999 | 0.999 |

Table B18 continued

| | Left subcallosal gyrus | Left anterior transverse temporal gyrus | Left lateral aspect of the superior temporal gyrus | Left planum polare of the superior temporal gyrus | Left planum temporale | Left inferior temporal gyrus | Left middle temporal gyrus | Left horizontal ramus of the anterior segment of the lateral sulcus | Left vertical ramus of the anterior segment of the lateral sulcus | Left posterior ramus of the lateral sulcus | Left occipital pole | Left temporal pole | Left calcarine sulcus | Left central sulcus |
|---|---|---|---|---|---|---|---|---|---|---|---|---|---|---|
| **Fisher F** | **72.0** | **134.1** | **247.5** | **252.3** | **122.7** | **272.2** | **276.3** | **125.5** | **112.6** | **153.3** | **100.5** | **250.1** | **131.1** | **233.6** |
| **Fisher FWE p** | **0.1** | **0.019** | **0.003** | **0.003** | **0.024** | **0.002** | **0.002** | **0.022** | **0.03** | **0.013** | **0.039** | **0.003** | **0.02** | **0.003** |
| MD | 0.16 | -1.75 | 0.61 | 0.83 | -1.16 | 3.28 | 2.02 | 2.05 | 3.28 | -1.57 | -0.85 | -1.7 | 0.95 | -0.1 |
| MD FWE p | 0.999 | 0.999 | 0.999 | 0.999 | 0.999 | 0.861 | 0.998 | 0.998 | 0.858 | 0.999 | 0.999 | 0.999 | 0.999 | 0.999 |
| MD mFWE p | 0.999 | 0.999 | 0.999 | 0.999 | 0.999 | 0.999 | 0.999 | 0.999 | 0.999 | 0.999 | 0.999 | 0.999 | 0.999 | 0.999 |
| RD | -0.18 | -2 | 0.2 | 0.54 | -1.23 | 1.67 | 1.03 | 2.29 | 3.09 | -1.28 | -2.33 | -2.26 | 0.74 | 0.26 |
| RD FWE p | 0.999 | 0.999 | 0.999 | 0.999 | 0.999 | 0.999 | 0.999 | 0.998 | 0.948 | 0.999 | 0.999 | 0.999 | 0.999 | 0.999 |
| RD mFWE p | 0.999 | 0.999 | 0.999 | 0.999 | 0.999 | 0.999 | 0.999 | 0.999 | 0.999 | 0.999 | 0.999 | 0.999 | 0.999 | 0.999 |
| AD | 0.71 | -1.11 | 1.29 | 1.07 | -0.89 | 4.47 | 2.96 | 1.22 | 3.21 | -1.89 | 1.26 | -0.48 | 1.22 | -0.78 |
| AD FWE p | 0.999 | 0.999 | 0.999 | 0.999 | 0.999 | 0.096 | 0.863 | 0.999 | 0.755 | 0.999 | 0.999 | 0.999 | 0.999 | 0.999 |
| AD mFWE p | 0.999 | 0.999 | 0.999 | 0.999 | 0.999 | 0.999 | 0.999 | 0.999 | 0.999 | 0.999 | 0.999 | 0.999 | 0.999 | 0.999 |
| Volume | 7.74 | 11.34 | 15.38 | 15.53 | 10.8 | 14.96 | 15.83 | 9.94 | 7.86 | 12.17 | 9.49 | 15.73 | 10.72 | 15.09 |
| Volume FWE p | 0.016 | 0.004 | 0.001 | 0.001 | 0.005 | 0.001 | 0.001 | 0.006 | 0.015 | 0.003 | 0.008 | 0.001 | 0.005 | 0.001 |
| Volume mFWE p | 0.014 | 0.004 | 0.001 | 0.001 | 0.004 | 0.001 | 0.001 | 0.006 | 0.013 | 0.003 | 0.007 | 0.001 | 0.004 | 0.001 |
| Thickness | 0.4 | 3.3 | 2.18 | 3.39 | 3.13 | 4.26 | 4.01 | 2.44 | -0.16 | 5.47 | 5.41 | 1.4 | 11.32 | 9.31 |
| Thickness FWE p | 0.999 | 0.446 | 0.999 | 0.388 | 0.612 | 0.122 | 0.165 | 0.999 | 0.999 | 0.031 | 0.033 | 0.999 | < 0.001 | 0.001 |
| Thickness mFWE p | 0.999 | 0.531 | 0.999 | 0.442 | 0.999 | 0.125 | 0.171 | 0.999 | 0.999 | 0.032 | 0.034 | 0.999 | < 0.001 | 0.001 |

Table B18 continued

| | Left anterior segment of the circular sulcus of the insula | Left inferior segment of the circular sulcus of the insula | Left superior segment of the circular sulcus of the insula | Left anterior transverse collateral sulcus | Left posterior transverse collateral sulcus | Left inferior frontal sulcus | Left middle frontal sulcus | Left superior frontal sulcus | Left sulcus intermedius primus | Left intraparietal sulcus and transverse parietal sulci | Left middle occipital sulcus and lunatus sulcus | Left superior occipital sulcus and transverse occipital sulcus | Left anterior occipital sulcus and preoccipital notch | Left lateral occipito temporal sulcus |
|---|---|---|---|---|---|---|---|---|---|---|---|---|---|---|
| **Fisher F** | **195.7** | **82.6** | **219.2** | **314.3** | **71.6** | **136.4** | **163.4** | **166.9** | **29.4** | **105.7** | **105.6** | **94.6** | **99.3** | **149.9** |
| **Fisher FWE p** | **0.006** | **0.065** | **0.004** | **0.001** | **0.102** | **0.018** | **0.011** | **0.01** | **0.999** | **0.035** | **0.035** | **0.046** | **0.04** | **0.014** |
| MD | 1.9 | 0.74 | 2.76 | 1.92 | 0.9 | 4.17 | 5.22 | 3.88 | -0.32 | -0.89 | -0.11 | -0.57 | 2.52 | 0.76 |
| MD FWE p | 0.999 | 0.999 | 0.968 | 0.999 | 0.999 | 0.405 | 0.037 | 0.578 | 0.999 | 0.999 | 0.999 | 0.999 | 0.986 | 0.999 |
| MD mFWE p | 0.999 | 0.999 | 0.999 | 0.999 | 0.999 | 0.999 | 0.054 | 0.999 | 0.999 | 0.999 | 0.999 | 0.999 | 0.999 | 0.999 |
| RD | 1.68 | 0.16 | 2.98 | 1.24 | 1.04 | 4.66 | 5.17 | 4.34 | -0.27 | -0.47 | -0.68 | -0.94 | 2 | -0.3 |
| RD FWE p | 0.999 | 0.999 | 0.964 | 0.999 | 0.999 | 0.21 | 0.06 | 0.372 | 0.999 | 0.999 | 0.999 | 0.999 | 0.999 | 0.999 |
| RD mFWE p | 0.999 | 0.999 | 0.999 | 0.999 | 0.999 | 0.106 | 0.056 | 0.999 | 0.999 | 0.999 | 0.999 | 0.999 | 0.999 | 0.999 |
| AD | 1.8 | 1.53 | 1.51 | 2.07 | 0.41 | 2.56 | 4.42 | 2.31 | -0.36 | -1.71 | 0.93 | 0.2 | 3.03 | 2.23 |
| AD FWE p | 0.998 | 0.999 | 0.999 | 0.994 | 0.999 | 0.959 | 0.107 | 0.984 | 0.999 | 0.999 | 0.999 | 0.999 | 0.837 | 0.988 |
| AD mFWE p | 0.999 | 0.999 | 0.999 | 0.999 | 0.999 | 0.999 | 0.999 | 0.999 | 0.999 | 0.999 | 0.999 | 0.999 | 0.999 | 0.999 |
| Volume | 13.1 | 8.18 | 13.61 | 17.19 | 7.53 | 8.45 | 8.31 | 10.44 | 4.54 | 9.95 | 9.74 | 9.28 | 7.91 | 11.5 |
| Volume FWE p | 0.002 | 0.013 | 0.002 | < 0.001 | 0.017 | 0.012 | 0.012 | 0.005 | 0.108 | 0.006 | 0.007 | 0.008 | 0.015 | 0.004 |
| Volume mFWE p | 0.002 | 0.011 | 0.002 | 0.001 | 0.015 | 0.01 | 0.011 | 0.005 | 0.166 | 0.006 | 0.006 | 0.007 | 0.013 | 0.003 |
| Thickness | 7.63 | 4.37 | 7.42 | 3 | 4.53 | 3.53 | 2.08 | 4 | 0.17 | 5.72 | 9.16 | 6.22 | 5.34 | 4.13 |
| Thickness FWE p | 0.003 | 0.108 | 0.004 | 0.999 | 0.089 | 0.311 | 0.999 | 0.168 | 0.999 | 0.024 | 0.001 | 0.014 | 0.036 | 0.143 |
| Thickness mFWE p | 0.004 | 0.11 | 0.004 | 0.999 | 0.091 | 0.338 | 0.999 | 0.174 | 0.999 | 0.025 | 0.001 | 0.015 | 0.037 | 0.147 |

Table B18 continued

| | Left lateral orbital sulcus | Left medial orbital sulcus | Left orbital sulci | Left parieto occipital sulcus | Left pericallosal sulcus | Left postcentral sulcus | Left inferior part of the precentral sulcus | Left superior part of the precentral sulcus | Left suborbital sulcus | Left subparietal sulcus | Left inferior temporal sulcus | Left superior temporal sulcus | Left transverse temporal sulcus | Right fronto marginal gyrus and sulcus |
|---|---|---|---|---|---|---|---|---|---|---|---|---|---|---|
| **Fisher F** | **117.6** | **144.7** | **259.4** | **118.1** | **161.5** | **114.2** | **232.1** | **70.3** | **88.1** | **112.8** | **211.9** | **212.6** | **85.5** | **237.8** |
| **Fisher FWE p** | **0.026** | **0.015** | **0.002** | **0.026** | **0.011** | **0.029** | **0.004** | **0.11** | **0.055** | **0.029** | **0.005** | **0.005** | **0.059** | **0.003** |
| MD | 4.69 | 1.45 | 1.66 | -0.86 | 3.58 | -0.18 | 1.95 | 1.6 | 2.42 | 0.36 | 3.78 | 0.89 | -1.95 | 3.86 |
| MD FWE p | 0.157 | 0.999 | 0.999 | 0.999 | 0.736 | 0.999 | 0.999 | 0.999 | 0.991 | 0.999 | 0.633 | 0.999 | 0.999 | 0.588 |
| MD mFWE p | 0.099 | 0.999 | 0.999 | 0.999 | 0.999 | 0.999 | 0.999 | 0.999 | 0.999 | 0.999 | 0.999 | 0.999 | 0.999 | 0.999 |
| RD | 4.73 | 1.69 | 2.8 | -1.15 | 4.45 | 0.42 | 1.62 | 2.23 | 3.01 | 0.78 | 2.45 | 0.63 | -0.97 | 3.94 |
| RD FWE p | 0.183 | 0.999 | 0.982 | 0.999 | 0.314 | 0.999 | 0.999 | 0.999 | 0.961 | 0.999 | 0.996 | 0.999 | 0.999 | 0.615 |
| RD mFWE p | 0.093 | 0.999 | 0.999 | 0.999 | 0.999 | 0.999 | 0.999 | 0.999 | 0.999 | 0.999 | 0.999 | 0.999 | 0.999 | 0.999 |
| AD | 3.84 | 0.74 | -0.46 | -0.2 | 1.33 | -1.5 | 2.3 | 0.07 | 1.15 | -0.43 | 4.43 | 1.25 | -3.28 | 2.84 |
| AD FWE p | 0.381 | 0.999 | 0.999 | 0.999 | 0.999 | 0.999 | 0.984 | 0.999 | 0.999 | 0.999 | 0.106 | 0.999 | 0.999 | 0.9 |
| AD mFWE p | 0.999 | 0.999 | 0.999 | 0.999 | 0.999 | 0.999 | 0.999 | 0.999 | 0.999 | 0.999 | 0.999 | 0.999 | 0.999 | 0.999 |
| Volume | 6.2 | 11.05 | 15.26 | 10.54 | 10.11 | 10.26 | 14.38 | 6.98 | 6.33 | 10.07 | 12.41 | 14.1 | 8.23 | 13.49 |
| Volume FWE p | 0.033 | 0.004 | 0.001 | 0.005 | 0.006 | 0.006 | 0.001 | 0.023 | 0.031 | 0.006 | 0.003 | 0.001 | 0.013 | 0.002 |
| Volume mFWE p | 0.028 | 0.004 | 0.001 | 0.005 | 0.006 | 0.005 | 0.001 | 0.019 | 0.026 | 0.006 | 0.003 | 0.001 | 0.011 | 0.002 |
| Thickness | 1.55 | -0.8 | -1.58 | 7.28 | -1.89 | 8.22 | 5.32 | 4.34 | -3.34 | 4.31 | 4.76 | 5.11 | -2.76 | 5.25 |
| Thickness FWE p | 0.999 | 0.999 | 0.999 | 0.005 | 0.999 | 0.002 | 0.037 | 0.111 | 0.999 | 0.116 | 0.069 | 0.046 | 0.999 | 0.04 |
| Thickness mFWE p | 0.999 | 0.999 | 0.999 | 0.005 | 0.999 | 0.002 | 0.038 | 0.114 | 0.999 | 0.118 | 0.07 | 0.047 | 0.999 | 0.041 |

Table B18 continued

| | Right paracentral lobule and sulcus | Right subcentral gyrus and sulci | Right transverse frontopolar gyri and sulci | Right anterior part of the cingulate gyrus and sulcus | Right middle anterior part of the cingulate gyrus and sulcus | Right middle posterior part of the cingulate gyrus and sulcus | Right posterior dorsal part of the cingulate gyrus | Right posterior ventral part of the cingulate gyrus | Right cuneus | Right opercular part of the inferior frontal gyrus | Right orbital part of the inferior frontal gyrus | Right triangular part of the inferior frontal gyrus | Right middle frontal gyrus | Right superior frontal gyrus |
|---|---|---|---|---|---|---|---|---|---|---|---|---|---|---|
| **Fisher F** | **83.4** | **250.7** | **251.6** | **350.0** | **202.7** | **168.1** | **183.3** | **25.1** | **123.8** | **155.2** | **111.0** | **95.7** | **245.5** | **322.7** |
| **Fisher FWE p** | **0.064** | **0.003** | **0.003** | **0.001** | **0.006** | **0.01** | **0.008** | **0.999** | **0.023** | **0.013** | **0.031** | **0.044** | **0.003** | **0.001** |
| MD | -1.83 | -0.53 | 4.69 | 6.18 | 2.02 | -0.35 | 0.11 | -3.84 | -1.5 | 3.07 | 3.43 | 4.06 | 5.22 | 2.5 |
| MD FWE p | 0.999 | 0.999 | 0.158 | 0.001 | 0.998 | 0.999 | 0.999 | 0.999 | 0.999 | 0.916 | 0.803 | 0.468 | 0.037 | 0.987 |
| MD mFWE p | 0.999 | 0.999 | 0.1 | 0.029 | 0.999 | 0.999 | 0.999 | 0.999 | 0.999 | 0.999 | 0.999 | 0.999 | 0.054 | 0.999 |
| RD | -1.87 | -1.22 | 4.61 | 6.52 | 2.73 | 0.24 | 0.25 | -3.85 | -1.59 | 2.63 | 2.97 | 4.19 | 5.3 | 2.75 |
| RD FWE p | 0.999 | 0.999 | 0.233 | < 0.001 | 0.986 | 0.999 | 0.999 | 0.999 | 0.999 | 0.991 | 0.966 | 0.46 | 0.041 | 0.986 |
| RD mFWE p | 0.999 | 0.999 | 0.12 | 0.024 | 0.999 | 0.999 | 0.999 | 0.999 | 0.999 | 0.999 | 0.999 | 0.999 | 0.051 | 0.999 |
| AD | -1.32 | 0.95 | 4 | 4.01 | 0.2 | -1.41 | -0.17 | -3.1 | -1.21 | 3.71 | 3.77 | 3.42 | 4.61 | 1.75 |
| AD FWE p | 0.999 | 0.999 | 0.287 | 0.278 | 0.999 | 0.999 | 0.999 | 0.999 | 0.999 | 0.458 | 0.418 | 0.639 | 0.062 | 0.999 |
| AD mFWE p | 0.999 | 0.999 | 0.999 | 0.999 | 0.999 | 0.999 | 0.999 | 0.999 | 0.999 | 0.999 | 0.999 | 0.999 | 0.119 | 0.999 |
| Volume | 8.8 | 15.64 | 13.17 | 15.35 | 13.34 | 12.68 | 13.22 | 4.49 | 10.86 | 10.2 | 7.57 | 5.35 | 12.15 | 17.16 |
| Volume FWE p | 0.01 | 0.001 | 0.002 | 0.001 | 0.002 | 0.002 | 0.002 | 0.114 | 0.005 | 0.006 | 0.017 | 0.055 | 0.003 | < 0.001 |
| Volume mFWE p | 0.009 | 0.001 | 0.002 | 0.001 | 0.002 | 0.002 | 0.002 | 0.999 | 0.004 | 0.005 | 0.015 | 0.048 | 0.003 | 0.001 |
| Thickness | 5.43 | 3.73 | 0.96 | 1.8 | 5.77 | 5.25 | 2.14 | 2.25 | 8.71 | -0.66 | 2.13 | -0.42 | 0.04 | 0.34 |
| Thickness FWE p | 0.033 | 0.239 | 0.999 | 0.999 | 0.023 | 0.04 | 0.999 | 0.999 | 0.001 | 0.999 | 0.999 | 0.999 | 0.999 | 0.999 |
| Thickness mFWE p | 0.033 | 0.252 | 0.999 | 0.999 | 0.024 | 0.041 | 0.999 | 0.999 | 0.001 | 0.999 | 0.999 | 0.999 | 0.999 | 0.999 |

Table B18 continued

| | Right short insular gyri | Right middle occipital gyrus | Right superior occipital gyrus | Right lateral occipito temporal gyrus | Right lingual gyrus | Right parahippocampal gyrus | Right orbital gyri | Right angular gyrus | Right supramarginal gyrus | Right superior parietal lobule | Right postcentral gyrus | Right precentral gyrus | Right precuneus |
|---|---|---|---|---|---|---|---|---|---|---|---|---|---|
| **Fisher F** | **211.0** | **185.7** | **159.5** | **137.3** | **132.2** | **123.0** | **321.9** | **146.9** | **198.5** | **178.0** | **156.0** | **252.4** | **184.5** |
| **Fisher FWE p** | **0.005** | **0.008** | **0.012** | **0.018** | **0.02** | **0.024** | **0.001** | **0.015** | **0.006** | **0.009** | **0.013** | **0.003** | **0.008** |
| MD | 3.97 | 1.51 | -0.64 | -2.3 | -2.21 | -3.62 | 0.03 | 1.34 | 0.43 | 2.51 | 1.28 | -0.42 | -0.32 |
| MD FWE p | 0.523 | 0.999 | 0.999 | 0.999 | 0.999 | 0.999 | 0.999 | 0.999 | 0.999 | 0.987 | 0.999 | 0.999 | 0.999 |
| MD mFWE p | 0.999 | 0.999 | 0.999 | 0.999 | 0.999 | 0.999 | 0.999 | 0.999 | 0.999 | 0.999 | 0.999 | 0.999 | 0.999 |
| RD | 3.42 | 0.34 | -1.52 | -2.06 | -2.07 | -4.03 | -0.16 | 1.02 | -0.1 | 2.41 | 0.98 | -0.62 | -0.03 |
| RD FWE p | 0.863 | 0.999 | 0.999 | 0.999 | 0.999 | 0.999 | 0.999 | 0.999 | 0.999 | 0.997 | 0.999 | 0.999 | 0.999 |
| RD mFWE p | 0.999 | 0.999 | 0.999 | 0.999 | 0.999 | 0.999 | 0.999 | 0.999 | 0.999 | 0.999 | 0.999 | 0.999 | 0.999 |
| AD | 4.1 | 3 | 0.84 | -1.93 | -2.26 | -2.26 | 0.28 | 1.79 | 1.41 | 2.51 | 1.78 | 0.06 | -0.89 |
| AD FWE p | 0.236 | 0.851 | 0.999 | 0.999 | 0.999 | 0.999 | 0.999 | 0.999 | 0.999 | 0.966 | 0.999 | 0.999 | 0.999 |
| AD mFWE p | 0.999 | 0.999 | 0.999 | 0.999 | 0.999 | 0.999 | 0.999 | 0.999 | 0.999 | 0.999 | 0.999 | 0.999 | 0.999 |
| Volume | 12.02 | 12.67 | 12.28 | 11.5 | 11.27 | 10.85 | 17.88 | 11.24 | 13.65 | 11.92 | 11.67 | 15.75 | 13.29 |
| Volume FWE p | 0.003 | 0.002 | 0.003 | 0.004 | 0.004 | 0.005 | < 0.001 | 0.004 | 0.002 | 0.003 | 0.003 | 0.001 | 0.002 |
| Volume mFWE p | 0.003 | 0.002 | 0.003 | 0.003 | 0.004 | 0.004 | < 0.001 | 0.004 | 0.002 | 0.003 | 0.003 | 0.001 | 0.002 |
| Thickness | -0.99 | 4.54 | 7.43 | 6.07 | 9.51 | 6.19 | 3.46 | 0.999 | 3.27 | 0.28 | 3.57 | 4.8 | 0.14 |
| Thickness FWE p | 0.999 | 0.088 | 0.004 | 0.017 | < 0.001 | 0.015 | 0.347 | 0.999 | 0.47 | 0.999 | 0.295 | 0.066 | 0.999 |
| Thickness mFWE p | 0.999 | 0.09 | 0.004 | 0.017 | 0.001 | 0.015 | 0.384 | 0.999 | 0.575 | 0.999 | 0.319 | 0.067 | 0.999 |

Table B18 continued

| | Right subcallosal gyrus | Right anterior transverse temporal gyrus | Right lateral aspect of the superior temporal gyrus | Right planum polare of the superior temporal gyrus | Right planum temporale | Right inferior temporal gyrus | Right middle temporal gyrus | Right horizontal ramus of the anterior segment of the lateral sulcus | Right vertical ramus of the anterior segment of the lateral sulcus | Right posterior ramus of the lateral sulcus | Right occipital pole | Right temporal pole | Right calcarine sulcus | Right central sulcus |
|---|---|---|---|---|---|---|---|---|---|---|---|---|---|---|
| **Fisher F** | **67.4** | **159.0** | **291.4** | **145.3** | **81.4** | **256.7** | **414.1** | **61.7** | **88.7** | **87.6** | **196.3** | **203.5** | **115.1** | **142.9** |
| **Fisher FWE p** | **0.132** | **0.012** | **0.001** | **0.015** | **0.068** | **0.002** | **< 0.001** | **0.999** | **0.054** | **0.056** | **0.006** | **0.006** | **0.028** | **0.016** |
| MD | 0.77 | -2.98 | 0.96 | -0.84 | -2.23 | 1.36 | 2.88 | 1.64 | 2.54 | -1.84 | -1.18 | -0.42 | -1.61 | 0.43 |
| MD FWE p | 0.999 | 0.999 | 0.999 | 0.999 | 0.999 | 0.999 | 0.953 | 0.999 | 0.985 | 0.999 | 0.999 | 0.999 | 0.999 | 0.999 |
| MD mFWE p | 0.999 | 0.999 | 0.999 | 0.999 | 0.999 | 0.999 | 0.999 | 0.999 | 0.999 | 0.999 | 0.999 | 0.999 | 0.999 | 0.999 |
| RD | 0.09 | -3.37 | 0.71 | -0.94 | -2.25 | -0.03 | 1.55 | 1.59 | 1.92 | -1.27 | -2.05 | -1.1 | -1.85 | 0.56 |
| RD FWE p | 0.999 | 0.999 | 0.999 | 0.999 | 0.999 | 0.999 | 0.999 | 0.999 | 0.999 | 0.999 | 0.999 | 0.999 | 0.999 | 0.999 |
| RD mFWE p | 0.999 | 0.999 | 0.999 | 0.999 | 0.999 | 0.999 | 0.999 | 0.999 | 0.999 | 0.999 | 0.999 | 0.999 | 0.999 | 0.999 |
| AD | 1.75 | -1.96 | 1.32 | -0.51 | -1.97 | 3.11 | 4.25 | 1.48 | 3.17 | -2.76 | 0.32 | 0.55 | -1.03 | 0.16 |
| AD FWE p | 0.999 | 0.999 | 0.999 | 0.999 | 0.999 | 0.804 | 0.168 | 0.999 | 0.777 | 0.999 | 0.999 | 0.999 | 0.999 | 0.999 |
| AD mFWE p | 0.999 | 0.999 | 0.999 | 0.999 | 0.999 | 0.999 | 0.999 | 0.999 | 0.999 | 0.999 | 0.999 | 0.999 | 0.999 | 0.999 |
| Volume | 7.12 | 12.43 | 16.74 | 11.78 | 8.7 | 15.31 | 19.47 | 6.26 | 7.15 | 9.04 | 13.8 | 13.96 | 10.45 | 11.47 |
| Volume FWE p | 0.021 | 0.003 | 0.001 | 0.003 | 0.011 | 0.001 | < 0.001 | 0.032 | 0.021 | 0.009 | 0.002 | 0.001 | 0.005 | 0.004 |
| Volume mFWE p | 0.018 | 0.003 | 0.001 | 0.003 | 0.009 | 0.001 | < 0.001 | 0.028 | 0.018 | 0.008 | 0.002 | 0.002 | 0.005 | 0.003 |
| Thickness | 1.52 | 5.23 | 4.26 | 2.79 | 4.52 | 4.62 | 3.68 | 1.77 | 1.67 | 6.42 | 9.51 | -0.08 | 12.08 | 7.2 |
| Thickness FWE p | 0.999 | 0.041 | 0.122 | 0.999 | 0.09 | 0.081 | 0.254 | 0.999 | 0.999 | 0.011 | < 0.001 | 0.999 | < 0.001 | 0.005 |
| Thickness mFWE p | 0.999 | 0.042 | 0.125 | 0.999 | 0.092 | 0.082 | 0.269 | 0.999 | 0.999 | 0.012 | 0.001 | 0.999 | < 0.001 | 0.006 |

Table B18 continued

| | Right anterior segment of the circular sulcus of the insula | Right inferior segment of the circular sulcus of the insula | Right superior segment of the circular sulcus of the insula | Right anterior transverse collateral sulcus | Right posterior transverse collateral sulcus | Right inferior frontal sulcus | Right middle frontal sulcus | Right superior frontal sulcus | Right sulcus intermedius primus | Right intraparietal sulcus and transverse parietal sulci | Right middle occipital sulcus and lunatus sulcus | Right superior occipital sulcus and transverse occipital sulcus | Right anterior occipital sulcus and preoccipital notch | Right lateral occipito temporal sulcus |
|---|---|---|---|---|---|---|---|---|---|---|---|---|---|---|
| **Fisher F** | **141.1** | **83.9** | **213.1** | **240.8** | **73.0** | **128.0** | **145.7** | **150.7** | **88.5** | **132.0** | **145.5** | **93.2** | **161.3** | **223.0** |
| **Fisher FWE p** | **0.016** | **0.062** | **0.005** | **0.003** | **0.095** | **0.021** | **0.015** | **0.014** | **0.054** | **0.02** | **0.015** | **0.047** | **0.011** | **0.004** |
| MD | 2.29 | -1.43 | 3.4 | 1.76 | 0.46 | 3.86 | 4.78 | 3 | 1.12 | -0.4 | 0.83 | -1.02 | 1.48 | 0.11 |
| MD FWE p | 0.995 | 0.999 | 0.817 | 0.999 | 0.999 | 0.589 | 0.128 | 0.931 | 0.999 | 0.999 | 0.999 | 0.999 | 0.999 | 0.999 |
| MD mFWE p | 0.999 | 0.999 | 0.999 | 0.999 | 0.999 | 0.999 | 0.086 | 0.999 | 0.999 | 0.999 | 0.999 | 0.999 | 0.999 | 0.999 |
| RD | 2.51 | -1.92 | 3.77 | 1.29 | 0.69 | 4.34 | 4.81 | 3.56 | 0.999 | -0.31 | 1.05 | -1.12 | 1.59 | -0.95 |
| RD FWE p | 0.995 | 0.999 | 0.709 | 0.999 | 0.999 | 0.371 | 0.153 | 0.811 | 0.999 | 0.999 | 0.999 | 0.999 | 0.999 | 0.999 |
| RD mFWE p | 0.999 | 0.999 | 0.999 | 0.999 | 0.999 | 0.999 | 0.082 | 0.999 | 0.999 | 0.999 | 0.999 | 0.999 | 0.999 | 0.999 |
| AD | 1.19 | -0.28 | 1.8 | 1.59 | -0.07 | 2.38 | 3.92 | 1.35 | 1.22 | -0.56 | 0.22 | -0.68 | 0.94 | 1.93 |
| AD FWE p | 0.999 | 0.999 | 0.998 | 0.999 | 0.999 | 0.979 | 0.329 | 0.999 | 0.999 | 0.999 | 0.999 | 0.999 | 0.999 | 0.997 |
| AD mFWE p | 0.999 | 0.999 | 0.999 | 0.999 | 0.999 | 0.999 | 0.999 | 0.999 | 0.999 | 0.999 | 0.999 | 0.999 | 0.999 | 0.999 |
| Volume | 10.59 | 8.78 | 12.94 | 14.87 | 7.81 | 8.35 | 8 | 10.49 | 8.4 | 11.15 | 11.48 | 9.3 | 11.91 | 14.52 |
| Volume FWE p | 0.005 | 0.01 | 0.002 | 0.001 | 0.015 | 0.012 | 0.014 | 0.005 | 0.012 | 0.004 | 0.004 | 0.008 | 0.003 | 0.001 |
| Volume mFWE p | 0.005 | 0.009 | 0.002 | 0.001 | 0.013 | 0.011 | 0.012 | 0.005 | 0.01 | 0.004 | 0.003 | 0.007 | 0.003 | 0.001 |
| Thickness | 6.41 | 4.54 | 6.93 | 1.03 | 4.73 | 3.14 | 4.03 | 3.8 | 1.48 | 3.28 | 8.19 | 6.12 | 7.93 | 7.78 |
| Thickness FWE p | 0.012 | 0.088 | 0.007 | 0.999 | 0.071 | 0.602 | 0.162 | 0.218 | 0.999 | 0.464 | 0.002 | 0.016 | 0.002 | 0.003 |
| Thickness mFWE p | 0.012 | 0.09 | 0.007 | 0.999 | 0.072 | 0.999 | 0.167 | 0.228 | 0.999 | 0.564 | 0.002 | 0.016 | 0.003 | 0.003 |

Table B18 continued

| | Right lateral orbital sulcus | Right medial orbital sulcus | Right orbital sulci | Right parieto occipital sulcus | Right pericallosal sulcus | Right postcentral sulcus | Right inferior part of the precentral sulcus | Right superior part of the precentral sulcus | Right suborbital sulcus | Right subparietal sulcus | Right inferior temporal sulcus | Right superior temporal sulcus | Right transverse temporal sulcus |
|---|---|---|---|---|---|---|---|---|---|---|---|---|---|
| **Fisher F** | **86.4** | **127.1** | **249.8** | **168.9** | **139.9** | **106.1** | **168.9** | **65.0** | **47.6** | **121.5** | **219.1** | **250.2** | **97.5** |
| **Fisher FWE p** | **0.058** | **0.022** | **0.003** | **0.01** | **0.017** | **0.034** | **0.01** | **0.166** | **0.999** | **0.024** | **0.004** | **0.003** | **0.042** |
| MD | 3.01 | 2.08 | 1.28 | -2.99 | 4.02 | -1.07 | 1.66 | 0.31 | 0.64 | -1.53 | 2.99 | 0.54 | -4.41 |
| MD FWE p | 0.93 | 0.998 | 0.999 | 0.999 | 0.492 | 0.999 | 0.999 | 0.999 | 0.999 | 0.999 | 0.934 | 0.999 | 0.999 |
| MD mFWE p | 0.999 | 0.999 | 0.999 | 0.999 | 0.999 | 0.999 | 0.999 | 0.999 | 0.999 | 0.999 | 0.999 | 0.999 | 0.999 |
| RD | 2.83 | 1.5 | 2.38 | -3.45 | 4.6 | -0.78 | 1.37 | 1.07 | 0.23 | -1.35 | 1.94 | 0.33 | -4.22 |
| RD FWE p | 0.98 | 0.999 | 0.997 | 0.999 | 0.239 | 0.999 | 0.999 | 0.999 | 0.999 | 0.999 | 0.999 | 0.999 | 0.999 |
| RD mFWE p | 0.999 | 0.999 | 0.999 | 0.999 | 0.124 | 0.999 | 0.999 | 0.999 | 0.999 | 0.999 | 0.999 | 0.999 | 0.999 |
| AD | 2.81 | 2.32 | -0.63 | -1.79 | 2.15 | -1.59 | 1.99 | -1.23 | 0.91 | -1.66 | 3.53 | 0.93 | -4.16 |
| AD FWE p | 0.91 | 0.983 | 0.999 | 0.999 | 0.992 | 0.999 | 0.996 | 0.999 | 0.999 | 0.999 | 0.573 | 0.999 | 0.999 |
| AD mFWE p | 0.999 | 0.999 | 0.999 | 0.999 | 0.999 | 0.999 | 0.999 | 0.999 | 0.999 | 0.999 | 0.999 | 0.999 | 0.999 |
| Volume | 6.6 | 9.74 | 15.26 | 12.83 | 7.35 | 9.99 | 12.07 | 7.31 | 5.12 | 10.76 | 13.33 | 15.51 | 9.59 |
| Volume FWE p | 0.027 | 0.007 | 0.001 | 0.002 | 0.019 | 0.006 | 0.003 | 0.019 | 0.064 | 0.005 | 0.002 | 0.001 | 0.007 |
| Volume mFWE p | 0.023 | 0.006 | 0.001 | 0.002 | 0.016 | 0.006 | 0.003 | 0.017 | 0.058 | 0.004 | 0.002 | 0.001 | 0.007 |
| Thickness | 4.64 | -1.15 | 1.39 | 6.55 | -4.48 | 7.24 | 6.25 | 4.89 | -2.17 | 2.41 | 4.07 | 5.76 | 1.64 |
| Thickness FWE p | 0.079 | 0.999 | 0.999 | 0.01 | 0.999 | 0.005 | 0.014 | 0.059 | 0.999 | 0.999 | 0.155 | 0.023 | 0.999 |
| Thickness mFWE p | 0.08 | 0.999 | 0.999 | 0.011 | 0.999 | 0.005 | 0.014 | 0.06 | 0.999 | 0.999 | 0.16 | 0.024 | 0.999 |

**Table B19 Positive correlations between cortical grey matter metrics and executive functioning scores**

| | Left fronto marginal gyrus and sulcus | Left inferior occipital gyrus and sulcus | Left paracentral lobule and sulcus | Left subcentral gyrus and sulci | Left transverse frontopolar gyri and sulci | Left anterior part of the cingulate gyrus and sulcus | Left middle anterior part of the cingulate gyrus and sulcus | Left middle posterior part of the cingulate gyrus and sulcus | Left posterior dorsal part of the cingulate gyrus | Left posterior ventral part of the cingulate gyrus | Left cuneus | Left opercular part of the inferior frontal gyrus | Left orbital part of the inferior frontal gyrus | Left triangular part of the inferior frontal gyrus | Left middle frontal gyrus |
|---|---|---|---|---|---|---|---|---|---|---|---|---|---|---|---|
| **Fisher F** | **108.73** | **84.68** | **41.08** | **72.36** | **82.53** | **85.35** | **36.12** | **40.07** | **53.25** | **14.41** | **75.55** | **52.94** | **52.06** | **40.14** | **63.51** |
| **Fisher FWE p** | **0.021** | **0.139** | **0.999** | **0.325** | **0.163** | **0.133** | **0.999** | **0.999** | **0.848** | **0.999** | **0.264** | **0.856** | **0.878** | **0.999** | **0.545** |
| MD | 3.46 | 2.17 | -2.47 | -1.44 | 3.41 | 1.71 | -0.36 | -0.81 | -2.01 | -2.18 | -0.11 | 0.64 | 0.06 | 1.67 | 2.37 |
| MD FWE p | 0.742 | 0.997 | 0.999 | 0.999 | 0.766 | 0.999 | 0.999 | 0.999 | 0.999 | 0.999 | 0.999 | 0.999 | 0.999 | 0.999 | 0.992 |
| MD mFWE p | 0.999 | 0.999 | 0.999 | 0.999 | 0.999 | 0.999 | 0.999 | 0.999 | 0.999 | 0.999 | 0.999 | 0.999 | 0.999 | 0.999 | 0.999 |
| RD | 3.37 | 0.94 | -3.11 | -2.16 | 2.92 | 2.38 | 0.17 | -1.15 | -2.36 | -3.38 | -0.71 | 0.49 | -0.18 | 1.54 | 2.31 |
| RD FWE p | 0.444 | 0.999 | 0.999 | 0.999 | 0.701 | 0.916 | 0.999 | 0.999 | 0.999 | 0.999 | 0.999 | 0.999 | 0.999 | 0.998 | 0.933 |
| RD mFWE p | 0.999 | 0.999 | 0.999 | 0.999 | 0.999 | 0.999 | 0.999 | 0.999 | 0.999 | 0.999 | 0.999 | 0.999 | 0.999 | 0.999 | 0.999 |
| AD | 2.88 | 3.42 | -1.06 | 0.14 | 3.49 | 0.28 | -1.25 | -0.01 | -0.98 | 0.14 | 0.88 | 0.86 | 0.47 | 1.73 | 2.24 |
| AD FWE p | 0.999 | 0.989 | 0.999 | 0.999 | 0.984 | 0.999 | 0.999 | 0.999 | 0.999 | 0.999 | 0.999 | 0.999 | 0.999 | 0.999 | 0.999 |
| AD mFWE p | 0.999 | 0.999 | 0.999 | 0.999 | 0.999 | 0.999 | 0.999 | 0.999 | 0.999 | 0.999 | 0.999 | 0.999 | 0.999 | 0.999 | 0.999 |
| Volume | 7.65 | 7.15 | 5.95 | 8.05 | 5.45 | 6.85 | 5.25 | 5.72 | 6.88 | 2.9 | 8.05 | 5.45 | 6.46 | 3.87 | 5.22 |
| Volume FWE p | 0.003 | 0.005 | 0.02 | 0.002 | 0.038 | 0.007 | 0.048 | 0.027 | 0.007 | 0.999 | 0.002 | 0.038 | 0.011 | 0.281 | 0.05 |
| Volume mFWE p | 0.006 | 0.013 | 0.07 | 0.004 | 0.143 | 0.019 | 0.192 | 0.098 | 0.019 | 0.999 | 0.004 | 0.144 | 0.034 | 0.999 | 0.202 |
| Thickness | 2.07 | 3.22 | 3.32 | 1.64 | -0.41 | -3.3 | 0.67 | 2.16 | 2.2 | 1.43 | 4.32 | -2.43 | 2.24 | -0.59 | -1.05 |
| Thickness FWE p | 0.994 | 0.45 | 0.384 | 0.999 | 0.999 | 0.999 | 0.999 | 0.987 | 0.981 | 0.999 | 0.048 | 0.999 | 0.974 | 0.999 | 0.999 |
| Thickness mFWE p | 0.999 | 0.762 | 0.69 | 0.999 | 0.999 | 0.999 | 0.999 | 0.999 | 0.999 | 0.999 | 0.119 | 0.999 | 0.999 | 0.999 | 0.999 |

Table B19 continued

| | Left long insular gyrus and central sulcus of the insula | Left short insular gyri | Left middle occipital gyrus | Left superior occipital gyrus | Left lateral occipito temporal gyrus | Left lingual gyrus | Left parahippocampal gyrus | Left orbital gyri | Left angular gyrus | Left supramarginal gyrus | Left superior parietal lobule | Left postcentral gyrus | Left precentral gyrus | Left precuneus |
|---|---|---|---|---|---|---|---|---|---|---|---|---|---|---|
| **Fisher F** | **122.2** | **95.13** | **72.16** | **73.34** | **63.57** | **47.36** | **63.45** | **98.72** | **54.97** | **90.42** | **71.25** | **76.68** | **105.55** | **55.74** |
| **Fisher FWE p** | **0.007** | **0.063** | **0.33** | **0.306** | **0.544** | **0.97** | **0.547** | **0.047** | **0.8** | **0.091** | **0.349** | **0.245** | **0.027** | **0.777** |
| MD | 2.77 | 0.79 | 1.11 | -0.42 | -0.95 | -0.16 | -3.76 | 1.72 | -0.11 | -1.43 | 1.29 | -0.15 | -1.49 | -0.91 |
| MD FWE p | 0.959 | 0.999 | 0.999 | 0.999 | 0.999 | 0.999 | 0.999 | 0.999 | 0.999 | 0.999 | 0.999 | 0.999 | 0.999 | 0.999 |
| MD mFWE p | 0.999 | 0.999 | 0.999 | 0.999 | 0.999 | 0.999 | 0.999 | 0.999 | 0.999 | 0.999 | 0.999 | 0.999 | 0.999 | 0.999 |
| RD | 2.04 | 0.34 | -0.77 | -1.44 | -2.25 | -0.87 | -5.05 | 1.12 | -1.12 | -2.06 | 0.75 | -0.62 | -1.72 | -1.12 |
| RD FWE p | 0.974 | 0.999 | 0.999 | 0.999 | 0.999 | 0.999 | 0.999 | 0.999 | 0.999 | 0.999 | 0.999 | 0.999 | 0.999 | 0.999 |
| RD mFWE p | 0.999 | 0.999 | 0.999 | 0.999 | 0.999 | 0.999 | 0.999 | 0.999 | 0.999 | 0.999 | 0.999 | 0.999 | 0.999 | 0.999 |
| AD | 3.57 | 1.48 | 3.35 | 1.11 | 1.25 | 1.01 | -1.12 | 2.24 | 1.55 | -0.07 | 2.17 | 0.7 | -0.92 | -0.45 |
| AD FWE p | 0.977 | 0.999 | 0.993 | 0.999 | 0.999 | 0.999 | 0.999 | 0.999 | 0.999 | 0.999 | 0.999 | 0.999 | 0.999 | 0.999 |
| AD mFWE p | 0.999 | 0.999 | 0.999 | 0.999 | 0.999 | 0.999 | 0.999 | 0.999 | 0.999 | 0.999 | 0.999 | 0.999 | 0.999 | 0.999 |
| Volume | 8.9 | 8.89 | 6.82 | 7.91 | 7.29 | 6.06 | 7.59 | 8.6 | 6.29 | 9.09 | 6.86 | 8.15 | 9.97 | 6.93 |
| Volume FWE p | 0.001 | 0.001 | 0.007 | 0.002 | 0.004 | 0.018 | 0.003 | 0.001 | 0.014 | < 0.001 | 0.007 | 0.001 | < 0.001 | 0.006 |
| Volume mFWE p | 0.001 | 0.001 | 0.02 | 0.004 | 0.01 | 0.06 | 0.007 | 0.002 | 0.043 | 0.001 | 0.019 | 0.003 | < 0.001 | 0.017 |
| Thickness | 0.67 | 2.18 | 2.94 | 1.73 | 3.26 | 4.3 | 5.27 | 1.7 | -0.71 | 0.53 | -0.64 | 2.76 | 1.76 | 0.47 |
| Thickness FWE p | 0.999 | 0.984 | 0.639 | 0.999 | 0.425 | 0.051 | 0.003 | 0.999 | 0.999 | 0.999 | 0.999 | 0.761 | 0.999 | 0.999 |
| Thickness mFWE p | 0.999 | 0.999 | 0.911 | 0.999 | 0.736 | 0.124 | 0.008 | 0.999 | 0.999 | 0.999 | 0.999 | 0.966 | 0.999 | 0.999 |

Table B19 continued

| | Left subcallosal gyrus | Left anterior transverse temporal gyrus | Left lateral aspect of the superior temporal gyrus | Left planum polare of the superior temporal gyrus | Left planum temporale | Left inferior temporal gyrus | Left middle temporal gyrus | Left horizontal ramus of the anterior segment of the lateral [illegible] | Left vertical ramus of the anterior segment of the lateral sulcus | Left posterior ramus of the lateral sulcus | Left occipital pole | Left temporal pole | Left calcarine sulcus | Left central sulcus |
|---|---|---|---|---|---|---|---|---|---|---|---|---|---|---|
| **Fisher F** | **24.1** | **44.47** | **80.01** | **108.57** | **49.7** | **169.93** | **116.92** | **35.35** | **35.64** | **62.31** | **39.46** | **109.99** | **48.32** | **107.35** |
| **Fisher FWE p** | **0.999** | **0.996** | **0.195** | **0.021** | **0.931** | **< 0.001** | **0.01** | **0.999** | **0.999** | **0.58** | **0.999** | **0.019** | **0.956** | **0.023** |
| MD | -1.14 | -0.45 | -0.67 | 2.14 | -0.77 | 3.85 | 2.24 | -0.51 | 0.68 | -1.88 | 0.91 | -0.58 | -1.01 | -1.46 |
| MD FWE p | 0.999 | 0.999 | 0.999 | 0.998 | 0.999 | 0.529 | 0.996 | 0.999 | 0.999 | 0.999 | 0.999 | 0.999 | 0.999 | 0.999 |
| MD mFWE p | 0.999 | 0.999 | 0.999 | 0.999 | 0.999 | 0.999 | 0.999 | 0.999 | 0.999 | 0.999 | 0.999 | 0.999 | 0.999 | 0.999 |
| RD | -1.87 | -0.84 | -1.06 | 3.03 | -1.05 | 1.43 | 0.92 | -0.65 | 0.47 | -2.26 | -1.2 | -2.18 | -1.62 | -1.41 |
| RD FWE p | 0.999 | 0.999 | 0.999 | 0.645 | 0.999 | 0.999 | 0.999 | 0.999 | 0.999 | 0.999 | 0.999 | 0.999 | 0.999 | 0.999 |
| RD mFWE p | 0.999 | 0.999 | 0.999 | 0.999 | 0.999 | 0.999 | 0.999 | 0.999 | 0.999 | 0.999 | 0.999 | 0.999 | 0.999 | 0.999 |
| AD | 0.17 | 0.31 | 0.11 | 0.25 | -0.15 | 5.95 | 3.6 | -0.13 | 0.999 | -0.81 | 3.44 | 1.87 | 0.13 | -1.47 |
| AD FWE p | 0.999 | 0.999 | 0.999 | 0.999 | 0.999 | 0.04 | 0.974 | 0.999 | 0.999 | 0.999 | 0.988 | 0.999 | 0.999 | 0.999 |
| AD mFWE p | 0.999 | 0.999 | 0.999 | 0.999 | 0.999 | 0.07 | 0.999 | 0.999 | 0.999 | 0.999 | 0.999 | 0.999 | 0.999 | 0.999 |
| Volume | 4.09 | 5.95 | 8.44 | 8.9 | 6.49 | 9.95 | 9.03 | 5.2 | 4.5 | 7.49 | 3.7 | 9.82 | 6.39 | 10.07 |
| Volume FWE p | 0.209 | 0.02 | 0.001 | 0.001 | 0.011 | < 0.001 | < 0.001 | 0.051 | 0.124 | 0.003 | 0.35 | < 0.001 | 0.012 | < 0.001 |
| Volume mFWE p | 0.999 | 0.07 | 0.002 | 0.001 | 0.032 | < 0.001 | 0.001 | 0.207 | 0.61 | 0.008 | 0.999 | < 0.001 | 0.037 | < 0.001 |
| Thickness | 0.59 | 0.71 | 0.59 | 0.93 | 1.54 | 1.53 | 1.4 | 0.61 | -0.23 | 4.51 | 0.07 | 0.88 | 5.6 | 5 |
| Thickness FWE p | 0.999 | 0.999 | 0.999 | 0.999 | 0.999 | 0.999 | 0.999 | 0.999 | 0.999 | 0.029 | 0.999 | 0.999 | 0.001 | 0.008 |
| Thickness mFWE p | 0.999 | 0.999 | 0.999 | 0.999 | 0.999 | 0.999 | 0.999 | 0.999 | 0.999 | 0.073 | 0.999 | 0.999 | 0.003 | 0.018 |

Table B19 continued

| | Left anterior segment of the circular sulcus of the insula | Left inferior segment of the circular sulcus of the insula | Left superior segment of the circular sulcus of the insula | Left anterior transverse collateral sulcus | Left posterior transverse collateral sulcus | Left inferior frontal sulcus | Left middle frontal sulcus | Left superior frontal sulcus | Left sulcus intermedius primus | Left intraparietal sulcus and transverse parietal sulci | Left middle occipital sulcus and lunatus sulcus | Left superior occipital sulcus and transverse occipital sulcus | Left anterior occipital sulcus and preoccipital notch | Left lateral occipito temporal sulcus |
|---|---|---|---|---|---|---|---|---|---|---|---|---|---|---|
| **Fisher F** | **50.12** | **27.73** | **60.41** | **159.86** | **13.33** | **30.4** | **59.2** | **38.09** | **28.4** | **41.38** | **39.3** | **41.87** | **30.7** | **54.74** |
| **Fisher FWE p** | **0.923** | **0.999** | **0.637** | **< 0.001** | **0.999** | **0.999** | **0.673** | **0.999** | **0.999** | **0.999** | **0.999** | **0.999** | **0.999** | **0.806** |
| MD | 0.25 | 1.19 | -0.07 | 2.55 | -1.13 | 1.53 | 3.42 | 0.71 | -1.43 | -2.28 | -0.45 | -0.56 | -0.49 | -0.43 |
| MD FWE p | 0.999 | 0.999 | 0.999 | 0.982 | 0.999 | 0.999 | 0.76 | 0.999 | 0.999 | 0.999 | 0.999 | 0.999 | 0.999 | 0.999 |
| MD mFWE p | 0.999 | 0.999 | 0.999 | 0.999 | 0.999 | 0.999 | 0.999 | 0.999 | 0.999 | 0.999 | 0.999 | 0.999 | 0.999 | 0.999 |
| RD | -0.39 | 1.03 | -0.42 | 0.25 | -1.03 | 1.68 | 3.2 | 0.87 | -1.98 | -2.52 | -1.51 | -1.26 | -1.34 | -1.91 |
| RD FWE p | 0.999 | 0.999 | 0.999 | 0.999 | 0.999 | 0.995 | 0.543 | 0.999 | 0.999 | 0.999 | 0.999 | 0.999 | 0.999 | 0.999 |
| RD mFWE p | 0.999 | 0.999 | 0.999 | 0.999 | 0.999 | 0.999 | 0.999 | 0.999 | 0.999 | 0.999 | 0.999 | 0.999 | 0.999 | 0.999 |
| AD | 1.29 | 1.18 | 0.65 | 4.51 | -1.02 | 1.01 | 3.26 | 0.25 | < 0.001 | -1.54 | 1.53 | 0.82 | 1.21 | 2.04 |
| AD FWE p | 0.999 | 0.999 | 0.999 | 0.63 | 0.999 | 0.999 | 0.996 | 0.999 | 0.999 | 0.999 | 0.999 | 0.999 | 0.999 | 0.999 |
| AD mFWE p | 0.999 | 0.999 | 0.999 | 0.601 | 0.999 | 0.999 | 0.999 | 0.999 | 0.999 | 0.999 | 0.999 | 0.999 | 0.999 | 0.999 |
| Volume | 6.12 | 3.29 | 7.08 | 10.82 | 2.86 | 3.24 | 2.85 | 5 | 4.41 | 5.99 | 5.26 | 5.7 | 4.53 | 6.38 |
| Volume FWE p | 0.017 | 0.642 | 0.005 | < 0.001 | 0.999 | 0.691 | 0.999 | 0.066 | 0.139 | 0.02 | 0.048 | 0.028 | 0.119 | 0.012 |
| Volume mFWE p | 0.055 | 0.999 | 0.014 | < 0.001 | 0.999 | 0.999 | 0.999 | 0.278 | 0.711 | 0.066 | 0.189 | 0.099 | 0.579 | 0.038 |
| Thickness | 4.71 | 1.12 | 3.61 | 2 | 1.79 | 1.33 | 0.08 | 2.57 | -0.58 | 2.11 | 4.65 | 2.47 | 3.93 | 2.07 |
| Thickness FWE p | 0.017 | 0.999 | 0.233 | 0.997 | 0.999 | 0.999 | 0.999 | 0.868 | 0.999 | 0.991 | 0.021 | 0.912 | 0.12 | 0.994 |
| Thickness mFWE p | 0.042 | 0.999 | 0.48 | 0.999 | 0.999 | 0.999 | 0.999 | 0.992 | 0.999 | 0.999 | 0.051 | 0.997 | 0.275 | 0.999 |

Table B19 continued

| | Left lateral orbital sulcus | Left medial orbital sulcus | Left orbital sulci | Left parieto occipital sulcus | Left pericallosal sulcus | Left postcentral sulcus | Left inferior part of the precentral sulcus | Left superior part of the precentral sulcus | Left suborbital sulcus | Left subparietal sulcus | Left inferior temporal sulcus | Left superior temporal sulcus | Left transverse temporal sulcus | Right fronto marginal gyrus and sulcus |
|---|---|---|---|---|---|---|---|---|---|---|---|---|---|---|
| **Fisher F** | **71.21** | **70.2** | **68.15** | **49.82** | **61.77** | **30.86** | **69.89** | **26.99** | **66.06** | **33.02** | **149.86** | **55.55** | **49.04** | **102.52** |
| **Fisher FWE p** | **0.35** | **0.372** | **0.421** | **0.929** | **0.596** | **0.999** | **0.379** | **0.999** | **0.475** | **0.999** | **< 0.001** | **0.783** | **0.944** | **0.035** |
| MD | 3.85 | 1.95 | 1.85 | -2.04 | 1.61 | -1.83 | -0.44 | -1.77 | 3.01 | -2.7 | 4.58 | -0.79 | -1.63 | 3.72 |
| MD FWE p | 0.53 | 0.999 | 0.999 | 0.999 | 0.999 | 0.999 | 0.999 | 0.999 | 0.911 | 0.999 | 0.167 | 0.999 | 0.999 | 0.605 |
| MD mFWE p | 0.999 | 0.999 | 0.999 | 0.999 | 0.999 | 0.999 | 0.999 | 0.999 | 0.999 | 0.999 | 0.533 | 0.999 | 0.999 | 0.999 |
| RD | 3.84 | 0.33 | 1.95 | -2.97 | 1.56 | -1.89 | -0.58 | -1.37 | 2.28 | -2.87 | 2.44 | -1.31 | -1.08 | 3.01 |
| RD FWE p | 0.21 | 0.999 | 0.982 | 0.999 | 0.997 | 0.999 | 0.999 | 0.999 | 0.94 | 0.999 | 0.902 | 0.999 | 0.999 | 0.655 |
| RD mFWE p | 0.999 | 0.999 | 0.999 | 0.999 | 0.999 | 0.999 | 0.999 | 0.999 | 0.999 | 0.999 | 0.999 | 0.999 | 0.999 | 0.999 |
| AD | 3.2 | 3.1 | 1.2 | 0.02 | 1.18 | -1.5 | -0.09 | -2.3 | 3.02 | -2.05 | 6.03 | 0.39 | -2.28 | 3.84 |
| AD FWE p | 0.997 | 0.999 | 0.999 | 0.999 | 0.999 | 0.999 | 0.999 | 0.999 | 0.999 | 0.999 | 0.032 | 0.999 | 0.999 | 0.932 |
| AD mFWE p | 0.999 | 0.999 | 0.999 | 0.999 | 0.999 | 0.999 | 0.999 | 0.999 | 0.999 | 0.999 | 0.062 | 0.999 | 0.999 | 0.999 |
| Volume | 3.07 | 6.32 | 6.11 | 6.55 | 6.04 | 5.05 | 7.85 | 4.67 | 2.32 | 5.27 | 8.12 | 6.87 | 5.76 | 6.79 |
| Volume FWE p | 0.973 | 0.013 | 0.017 | 0.01 | 0.018 | 0.062 | 0.002 | 0.1 | 0.999 | 0.047 | 0.001 | 0.007 | 0.026 | 0.007 |
| Volume mFWE p | 0.999 | 0.041 | 0.056 | 0.03 | 0.061 | 0.259 | 0.005 | 0.466 | 0.999 | 0.187 | 0.003 | 0.019 | 0.091 | 0.021 |
| Thickness | -1.16 | -0.15 | -1.87 | 4.6 | -1.14 | 4.02 | 2.94 | 4.19 | -4.08 | 2.25 | 0.38 | 1.97 | -2.49 | 3.29 |
| Thickness FWE p | 0.999 | 0.999 | 0.999 | 0.023 | 0.999 | 0.099 | 0.64 | 0.067 | 0.999 | 0.974 | 0.999 | 0.998 | 0.999 | 0.407 |
| Thickness mFWE p | 0.999 | 0.999 | 0.999 | 0.058 | 0.999 | 0.232 | 0.911 | 0.161 | 0.999 | 0.999 | 0.999 | 0.999 | 0.999 | 0.716 |

Table B19 continued

| | Right paracentral lobule and sulcus | Right subcentral gyrus and sulci | Right transverse frontopolar gyri and sulci | Right anterior part of the cingulate gyrus and sulcus | Right middle anterior part of the cingulate gyrus and sulcus | Right middle posterior part of the cingulate gyrus and sulcus | Right posterior dorsal part of the cingulate gyrus | Right posterior ventral part of the cingulate gyrus | Right cuneus | Right opercular part of the inferior frontal gyrus | Right orbital part of the inferior frontal gyrus | Right triangular part of the inferior frontal gyrus | Right middle frontal gyrus | Right superior frontal gyrus |
|---|---|---|---|---|---|---|---|---|---|---|---|---|---|---|
| **Fisher F** | **42.57** | **73.35** | **116.77** | **107.12** | **64.97** | **64.83** | **56.65** | **8.12** | **49.99** | **50.43** | **61.63** | **47.62** | **82.85** | **98.27** |
| **Fisher FWE p** | **0.999** | **0.305** | **0.01** | **0.024** | **0.504** | **0.508** | **0.751** | **0.999** | **0.925** | **0.916** | **0.6** | **0.967** | **0.159** | **0.049** |
| MD | -2.47 | -2.04 | 4.02 | 2.49 | -0.63 | -1.61 | -1.57 | -3.29 | -0.35 | 0.64 | 2.5 | 2.31 | 3.46 | -0.33 |
| MD FWE p | 0.999 | 0.999 | 0.428 | 0.987 | 0.999 | 0.999 | 0.999 | 0.999 | 0.999 | 0.999 | 0.986 | 0.994 | 0.744 | 0.999 |
| MD mFWE p | 0.999 | 0.999 | 0.999 | 0.999 | 0.999 | 0.999 | 0.999 | 0.999 | 0.999 | 0.999 | 0.999 | 0.999 | 0.999 | 0.999 |
| RD | -3.15 | -2.85 | 3.21 | 2.08 | -0.59 | -2.14 | -2.07 | -4.16 | -0.9 | 0.27 | 1.67 | 2.13 | 3.15 | -0.53 |
| RD FWE p | 0.999 | 0.999 | 0.537 | 0.97 | 0.999 | 0.999 | 0.999 | 0.999 | 0.999 | 0.999 | 0.995 | 0.964 | 0.577 | 0.999 |
| RD mFWE p | 0.999 | 0.999 | 0.999 | 0.999 | 0.999 | 0.999 | 0.999 | 0.999 | 0.999 | 0.999 | 0.999 | 0.999 | 0.999 | 0.999 |
| AD | -0.92 | -0.18 | 4.58 | 2.51 | -0.58 | -0.17 | -0.3 | -1.3 | 0.61 | 1.36 | 3.64 | 2.42 | 3.69 | 0.08 |
| AD FWE p | 0.999 | 0.999 | 0.587 | 0.999 | 0.999 | 0.999 | 0.999 | 0.999 | 0.999 | 0.999 | 0.969 | 0.999 | 0.961 | 0.999 |
| AD mFWE p | 0.999 | 0.999 | 0.537 | 0.999 | 0.999 | 0.999 | 0.999 | 0.999 | 0.999 | 0.999 | 0.999 | 0.999 | 0.999 | 0.999 |
| Volume | 6.07 | 8.16 | 7.02 | 8.53 | 7.58 | 7.61 | 7.07 | 2.06 | 6.38 | 5.73 | 4.69 | 3.69 | 4.93 | 9.45 |
| Volume FWE p | 0.018 | 0.001 | 0.006 | 0.001 | 0.003 | 0.003 | 0.005 | 0.999 | 0.012 | 0.027 | 0.097 | 0.359 | 0.072 | < 0.001 |
| Volume mFWE p | 0.059 | 0.003 | 0.015 | 0.002 | 0.007 | 0.007 | 0.014 | 0.999 | 0.038 | 0.095 | 0.451 | 0.999 | 0.312 | < 0.001 |
| Thickness | 3.91 | 2.36 | 0.75 | 0.78 | 4.82 | 3.8 | 2.6 | 1.8 | 4.04 | -0.69 | 0.58 | -0.54 | -1.33 | 1.19 |
| Thickness FWE p | 0.126 | 0.95 | 0.999 | 0.999 | 0.013 | 0.161 | 0.855 | 0.999 | 0.094 | 0.999 | 0.999 | 0.999 | 0.999 | 0.999 |
| Thickness mFWE p | 0.287 | 0.999 | 0.999 | 0.999 | 0.031 | 0.355 | 0.99 | 0.999 | 0.222 | 0.999 | 0.999 | 0.999 | 0.999 | 0.999 |

Table B19 continued

| | Right short insular gyri | Right middle occipital gyrus | Right superior occipital gyrus | Right lateral occipito temporal gyrus | Right lingual gyrus | Right parahippocampal gyrus | Right orbital gyri | Right angular gyrus | Right supramarginal gyrus | Right superior parietal lobule | Right postcentral gyrus | Right precentral gyrus | Right precuneus |
|---|---|---|---|---|---|---|---|---|---|---|---|---|---|
| **Fisher F** | **73.27** | **64.12** | **59.3** | **35.82** | **45.65** | **34.52** | **102.07** | **67.68** | **61.82** | **58.3** | **59.39** | **79.21** | **52.91** |
| **Fisher FWE p** | **0.307** | **0.528** | **0.67** | **0.999** | **0.988** | **0.999** | **0.036** | **0.433** | **0.595** | **0.701** | **0.668** | **0.206** | **0.857** |
| MD | 0.4 | 0.84 | -1.16 | -1.91 | -1.9 | -4.58 | 1.29 | -0.03 | -0.89 | 0.93 | 1.08 | -1.54 | -1.74 |
| MD FWE p | 0.999 | 0.999 | 0.999 | 0.999 | 0.999 | 0.999 | 0.999 | 0.999 | 0.999 | 0.999 | 0.999 | 0.999 | 0.999 |
| MD mFWE p | 0.999 | 0.999 | 0.999 | 0.999 | 0.999 | 0.999 | 0.999 | 0.999 | 0.999 | 0.999 | 0.999 | 0.999 | 0.999 |
| RD | -0.48 | -0.55 | -2.21 | -3.21 | -2.41 | -5.81 | 0.18 | -0.79 | -1.76 | 0.29 | 0.47 | -1.99 | -1.86 |
| RD FWE p | 0.999 | 0.999 | 0.999 | 0.999 | 0.999 | 0.999 | 0.999 | 0.999 | 0.999 | 0.999 | 0.999 | 0.999 | 0.999 |
| RD mFWE p | 0.999 | 0.999 | 0.999 | 0.999 | 0.999 | 0.999 | 0.999 | 0.999 | 0.999 | 0.999 | 0.999 | 0.999 | 0.999 |
| AD | 1.75 | 2.76 | 0.66 | 0.57 | -0.88 | -1.79 | 2.5 | 1.38 | 0.87 | 2.05 | 2.09 | -0.51 | -1.35 |
| AD FWE p | 0.999 | 0.999 | 0.999 | 0.999 | 0.999 | 0.999 | 0.999 | 0.999 | 0.999 | 0.999 | 0.999 | 0.999 | 0.999 |
| AD mFWE p | 0.999 | 0.999 | 0.999 | 0.999 | 0.999 | 0.999 | 0.999 | 0.999 | 0.999 | 0.999 | 0.999 | 0.999 | 0.999 |
| Volume | 7.26 | 6.55 | 7.12 | 5.3 | 6.3 | 5.41 | 8.94 | 7.14 | 7.1 | 5.99 | 6.3 | 8.52 | 6.7 |
| Volume FWE p | 0.004 | 0.01 | 0.005 | 0.045 | 0.013 | 0.04 | 0.001 | 0.005 | 0.005 | 0.019 | 0.013 | 0.001 | 0.008 |
| Volume mFWE p | 0.011 | 0.03 | 0.013 | 0.179 | 0.042 | 0.153 | 0.001 | 0.013 | 0.014 | 0.065 | 0.042 | 0.002 | 0.024 |
| Thickness | -1.55 | 1.31 | 3.35 | 2.72 | 4.7 | 3.38 | 2.49 | -1.19 | -0.39 | -1.06 | 1.68 | 1.95 | -0.43 |
| Thickness FWE p | 0.999 | 0.999 | 0.367 | 0.789 | 0.018 | 0.353 | 0.903 | 0.999 | 0.999 | 0.999 | 0.999 | 0.999 | 0.999 |
| Thickness mFWE p | 0.999 | 0.999 | 0.67 | 0.975 | 0.044 | 0.653 | 0.996 | 0.999 | 0.999 | 0.999 | 0.999 | 0.999 | 0.999 |

Table B19 continued

| | Right subcallosal gyrus | Right anterior transverse temporal gyrus | Right lateral aspect of the superior temporal gyrus | Right planum polare of the superior temporal gyrus | Right planum temporale | Right inferior temporal gyrus | Right middle temporal gyrus | Right horizontal ramus of the anterior segment of the lateral sulcus | Right vertical ramus of the anterior segment of the lateral sulcus | Right posterior ramus of the lateral sulcus | Right occipital pole | Right temporal pole | Right calcarine sulcus | Right central sulcus |
|---|---|---|---|---|---|---|---|---|---|---|---|---|---|---|
| **Fisher F** | **32.68** | **79.52** | **111.39** | **54.67** | **30.55** | **111.73** | **173.32** | **15.72** | **39.33** | **32.9** | **63.23** | **72** | **40.31** | **69.46** |
| **Fisher FWE p** | **0.999** | **0.202** | **0.017** | **0.809** | **0.999** | **0.016** | **< 0.001** | **0.999** | **0.999** | **0.999** | **0.553** | **0.333** | **0.999** | **0.389** |
| MD | -0.24 | -1.77 | -0.37 | -0.65 | -1.48 | 0.79 | 2.53 | -1.21 | -0.29 | -3.97 | -0.17 | -0.67 | -2.48 | -1.62 |
| MD FWE p | 0.999 | 0.999 | 0.999 | 0.999 | 0.999 | 0.999 | 0.984 | 0.999 | 0.999 | 0.999 | 0.999 | 0.999 | 0.999 | 0.999 |
| MD mFWE p | 0.999 | 0.999 | 0.999 | 0.999 | 0.999 | 0.999 | 0.999 | 0.999 | 0.999 | 0.999 | 0.999 | 0.999 | 0.999 | 0.999 |
| RD | -1.32 | -2.33 | -0.94 | -0.53 | -1.53 | -1.43 | 0.95 | -1.68 | -0.81 | -3.95 | -1.47 | -1.89 | -3.09 | -1.67 |
| RD FWE p | 0.999 | 0.999 | 0.999 | 0.999 | 0.999 | 0.999 | 0.999 | 0.999 | 0.999 | 0.999 | 0.999 | 0.999 | 0.999 | 0.999 |
| RD mFWE p | 0.999 | 0.999 | 0.999 | 0.999 | 0.999 | 0.999 | 0.999 | 0.999 | 0.999 | 0.999 | 0.999 | 0.999 | 0.999 | 0.999 |
| AD | 1.45 | -0.55 | 0.71 | -0.68 | -1.21 | 4.14 | 4.33 | -0.04 | 0.75 | -3.38 | 1.76 | 1.05 | -1.21 | -1.45 |
| AD FWE p | 0.999 | 0.999 | 0.999 | 0.999 | 0.999 | 0.829 | 0.733 | 0.999 | 0.999 | 0.999 | 0.999 | 0.999 | 0.999 | 0.999 |
| AD mFWE p | 0.999 | 0.999 | 0.999 | 0.999 | 0.999 | 0.999 | 0.812 | 0.999 | 0.999 | 0.999 | 0.999 | 0.999 | 0.999 | 0.999 |
| Volume | 4.61 | 8.55 | 10.09 | 6.87 | 4.99 | 9 | 11.44 | 2.85 | 5.14 | 5.27 | 7.07 | 7.67 | 5.89 | 7.97 |
| Volume FWE p | 0.108 | 0.001 | < 0.001 | 0.007 | 0.067 | 0.001 | < 0.001 | 0.999 | 0.055 | 0.047 | 0.005 | 0.003 | 0.022 | 0.002 |
| Volume mFWE p | 0.511 | 0.002 | < 0.001 | 0.019 | 0.285 | 0.001 | < 0.001 | 0.999 | 0.226 | 0.188 | 0.014 | 0.006 | 0.076 | 0.004 |
| Thickness | 1.84 | 4.14 | 2.48 | 1.88 | 1.62 | 2.92 | 2.19 | -0.26 | -0.89 | 3.44 | 3.48 | -0.79 | 6.69 | 4.34 |
| Thickness FWE p | 0.999 | 0.074 | 0.908 | 0.999 | 0.999 | 0.653 | 0.983 | 0.999 | 0.999 | 0.317 | 0.296 | 0.999 | < 0.001 | 0.045 |
| Thickness mFWE p | 0.999 | 0.178 | 0.997 | 0.999 | 0.999 | 0.919 | 0.999 | 0.999 | 0.999 | 0.605 | 0.575 | 0.999 | < 0.001 | 0.112 |

Table B19 continued

| | Right anterior segment of the circular sulcus of the insula | Right inferior segment of the circular sulcus of the insula | Right superior segment of the circular sulcus of the insula | Right anterior transverse collateral sulcus | Right posterior transverse collateral sulcus | Right inferior frontal sulcus | Right middle frontal sulcus | Right superior frontal sulcus | Right sulcus intermedius primus | Right intraparietal sulcus and transverse parietal sulci | Right middle occipital sulcus and lunatus sulcus | Right superior occipital sulcus and transverse occipital sulcus | Right anterior occipital sulcus and preoccipital notch | Right lateral occipito temporal sulcus |
|---|---|---|---|---|---|---|---|---|---|---|---|---|---|---|
| **Fisher F** | **38.73** | **42.06** | **64.08** | **82.17** | **47.06** | **32.9** | **52.38** | **43.86** | **24.93** | **47.81** | **57.7** | **46.02** | **38.5** | **63.6** |
| **Fisher FWE p** | **0.999** | **0.999** | **0.529** | **0.167** | **0.974** | **0.999** | **0.87** | **0.998** | **0.999** | **0.964** | **0.719** | **0.985** | **0.999** | **0.543** |
| MD | -0.12 | -1.75 | -0.74 | 0.41 | -1.13 | 0.999 | 2.58 | 0.07 | -1.37 | -2.73 | -0.06 | -1.39 | -2.08 | -2.19 |
| MD FWE p | 0.999 | 0.999 | 0.999 | 0.999 | 0.999 | 0.999 | 0.98 | 0.999 | 0.999 | 0.999 | 0.999 | 0.999 | 0.999 | 0.999 |
| MD mFWE p | 0.999 | 0.999 | 0.999 | 0.999 | 0.999 | 0.999 | 0.999 | 0.999 | 0.999 | 0.999 | 0.999 | 0.999 | 0.999 | 0.999 |
| RD | -0.31 | -2.15 | -0.77 | -1.11 | -1.07 | 1.14 | 2.38 | 0.16 | -1.62 | -3.07 | -0.53 | -1.79 | -2.31 | -3.57 |
| RD FWE p | 0.999 | 0.999 | 0.999 | 0.999 | 0.999 | 0.999 | 0.918 | 0.999 | 0.999 | 0.999 | 0.999 | 0.999 | 0.999 | 0.999 |
| RD mFWE p | 0.999 | 0.999 | 0.999 | 0.999 | 0.999 | 0.999 | 0.999 | 0.999 | 0.999 | 0.999 | 0.999 | 0.999 | 0.999 | 0.999 |
| AD | 0.24 | -0.68 | -0.48 | 2.52 | -0.9 | 0.6 | 2.55 | -0.12 | -0.69 | -1.82 | 0.86 | -0.41 | -1.12 | 1.25 |
| AD FWE p | 0.999 | 0.999 | 0.999 | 0.999 | 0.999 | 0.999 | 0.999 | 0.999 | 0.999 | 0.999 | 0.999 | 0.999 | 0.999 | 0.999 |
| AD mFWE p | 0.999 | 0.999 | 0.999 | 0.999 | 0.999 | 0.999 | 0.999 | 0.999 | 0.999 | 0.999 | 0.999 | 0.999 | 0.999 | 0.999 |
| Volume | 5.44 | 6 | 7.53 | 7.91 | 6.37 | 4.2 | 4.13 | 5.85 | 4.07 | 6.43 | 6.85 | 6.29 | 5.73 | 7.31 |
| Volume FWE p | 0.038 | 0.019 | 0.003 | 0.002 | 0.012 | 0.18 | 0.199 | 0.023 | 0.214 | 0.011 | 0.007 | 0.014 | 0.027 | 0.004 |
| Volume mFWE p | 0.146 | 0.065 | 0.007 | 0.004 | 0.038 | 0.999 | 0.999 | 0.081 | 0.999 | 0.035 | 0.019 | 0.043 | 0.095 | 0.01 |
| Thickness | 4.61 | 2.43 | 3.24 | 0.07 | 1.63 | 1.99 | 1.81 | 2.38 | -0.68 | 0.32 | 2.7 | 2.14 | 4.55 | 3.01 |
| Thickness FWE p | 0.023 | 0.928 | 0.44 | 0.999 | 0.999 | 0.997 | 0.999 | 0.943 | 0.999 | 0.999 | 0.796 | 0.988 | 0.027 | 0.594 |
| Thickness mFWE p | 0.056 | 0.998 | 0.752 | 0.999 | 0.999 | 0.999 | 0.999 | 0.999 | 0.999 | 0.999 | 0.977 | 0.999 | 0.066 | 0.883 |

Table B19 continued

| | Right lateral orbital sulcus | Right medial orbital sulcus | Right orbital sulci | Right parieto occipital sulcus | Right pericallosal sulcus | Right postcentral sulcus | Right inferior part of the precentral sulcus | Right superior part of the precentral sulcus | Right suborbital sulcus | Right subparietal sulcus | Right inferior temporal sulcus | Right superior temporal sulcus | Right transverse temporal sulcus |
|---|---|---|---|---|---|---|---|---|---|---|---|---|---|
| **Fisher F** | **18.11** | **62.81** | **82.37** | **57.96** | **48.53** | **32.08** | **54.32** | **26.44** | **47.69** | **37.4** | **90.15** | **102.01** | **29.23** |
| **Fisher FWE p** | **0.999** | **0.566** | **0.165** | **0.711** | **0.953** | **0.999** | **0.818** | **0.999** | **0.966** | **0.999** | **0.093** | **0.036** | **0.999** |
| MD | 1.05 | 0.85 | 0.44 | -2.74 | 1.33 | -3.14 | -1.02 | -2.55 | 2.87 | -2.7 | 1.09 | -2.02 | -4.28 |
| MD FWE p | 0.999 | 0.999 | 0.999 | 0.999 | 0.999 | 0.999 | 0.999 | 0.999 | 0.943 | 0.999 | 0.999 | 0.999 | 0.999 |
| MD mFWE p | 0.999 | 0.999 | 0.999 | 0.999 | 0.999 | 0.999 | 0.999 | 0.999 | 0.999 | 0.999 | 0.999 | 0.999 | 0.999 |
| RD | 0.86 | -0.35 | 0.54 | -3.46 | 0.79 | -3.34 | -1.05 | -2.03 | 1.43 | -2.79 | -0.69 | -2.45 | -4.22 |
| RD FWE p | 0.999 | 0.999 | 0.999 | 0.999 | 0.999 | 0.999 | 0.999 | 0.999 | 0.999 | 0.999 | 0.999 | 0.999 | 0.999 |
| RD mFWE p | 0.999 | 0.999 | 0.999 | 0.999 | 0.999 | 0.999 | 0.999 | 0.999 | 0.999 | 0.999 | 0.999 | 0.999 | 0.999 |
| AD | 1.21 | 2.11 | 0.17 | -1.09 | 1.6 | -2.5 | -0.84 | -3.23 | 3.68 | -2.18 | 3.46 | -0.76 | -3.81 |
| AD FWE p | 0.999 | 0.999 | 0.999 | 0.999 | 0.999 | 0.999 | 0.999 | 0.999 | 0.963 | 0.999 | 0.987 | 0.999 | 0.999 |
| AD mFWE p | 0.999 | 0.999 | 0.999 | 0.999 | 0.999 | 0.999 | 0.999 | 0.999 | 0.999 | 0.999 | 0.999 | 0.999 | 0.999 |
| Volume | 1.79 | 6.45 | 8.39 | 7.22 | 3.02 | 5.19 | 6.91 | 4.63 | 2.09 | 5.63 | 7.96 | 9.79 | 4.86 |
| Volume FWE p | 0.999 | 0.011 | 0.001 | 0.004 | 0.999 | 0.052 | 0.006 | 0.104 | 0.999 | 0.03 | 0.002 | < 0.001 | 0.078 |
| Volume mFWE p | 0.999 | 0.034 | 0.002 | 0.011 | 0.999 | 0.211 | 0.018 | 0.492 | 0.999 | 0.111 | 0.004 | < 0.001 | 0.343 |
| Thickness | 2.22 | -0.93 | 2.27 | 3.73 | -4.1 | 3.57 | 3.5 | 3.27 | -1.12 | 0.8 | 1.52 | 2.11 | 0.71 |
| Thickness FWE p | 0.978 | 0.999 | 0.97 | 0.182 | 0.999 | 0.251 | 0.285 | 0.415 | 0.999 | 0.999 | 0.999 | 0.991 | 0.999 |
| Thickness mFWE p | 0.999 | 0.999 | 0.999 | 0.394 | 0.999 | 0.51 | 0.56 | 0.726 | 0.999 | 0.999 | 0.999 | 0.999 | 0.999 |

**Table B20 Positive correlations between cortical grey matter metrics and memory scores**

| | Left fronto marginal gyrus and sulcus | Left inferior occipital gyrus and sulcus | Left paracentral lobule and sulcus | Left subcentral gyrus and sulci | Left transverse frontopolar gyri and sulci | Left anterior part of the cingulate gyrus and sulcus | Left middle anterior part of the cingulate gyrus and sulcus | Left middle posterior part of the cingulate gyrus and sulcus | Left posterior dorsal part of the cingulate gyrus | Left posterior ventral part of the cingulate gyrus | Left cuneus | Left opercular part of the inferior frontal gyrus | Left orbital part of the inferior frontal gyrus | Left triangular part of the inferior frontal gyrus | Left middle frontal gyrus |
|---|---|---|---|---|---|---|---|---|---|---|---|---|---|---|---|
| **Fisher F** | **118.45** | **80.42** | **62.09** | **79.93** | **76.57** | **94.9** | **46.91** | **53.7** | **68.41** | **8.24** | **73.21** | **58.62** | **56.13** | **33.58** | **68.27** |
| **Fisher FWE p** | **0.008** | **0.044** | **0.116** | **0.045** | **0.054** | **0.022** | **0.322** | **0.194** | **0.082** | **0.999** | **0.064** | **0.142** | **0.165** | **0.999** | **0.082** |
| MD | 2.28 | -0.07 | -3.73 | -1.38 | 2.59 | 2.8 | 0.75 | 0.17 | -1.74 | -3.97 | -2.76 | 0.51 | 0.35 | 1.43 | 1.12 |
| MD FWE p | 0.889 | 0.999 | 0.999 | 0.999 | 0.769 | 0.661 | 0.999 | 0.999 | 0.999 | 0.999 | 0.999 | 0.999 | 0.999 | 0.996 | 0.999 |
| MD mFWE p | 0.999 | 0.999 | 0.999 | 0.999 | 0.999 | 0.999 | 0.999 | 0.999 | 0.999 | 0.999 | 0.999 | 0.999 | 0.999 | 0.999 | 0.999 |
| RD | 2.78 | -1.02 | -3.77 | -1.8 | 2.96 | 3.58 | 0.94 | -0.02 | -1.87 | -4.52 | -2.98 | 0.52 | 0.01 | 1.59 | 1.27 |
| RD FWE p | 0.437 | 0.999 | 0.999 | 0.999 | 0.327 | 0.08 | 0.998 | 0.999 | 0.999 | 0.999 | 0.999 | 0.999 | 0.999 | 0.961 | 0.989 |
| RD mFWE p | 0.999 | 0.999 | 0.999 | 0.999 | 0.999 | 0.999 | 0.999 | 0.999 | 0.999 | 0.999 | 0.999 | 0.999 | 0.999 | 0.999 | 0.999 |
| AD | 1.08 | 1.31 | -3.14 | -0.37 | 1.54 | 0.98 | 0.29 | 0.49 | -1.17 | -2.37 | -2.17 | 0.44 | 0.9 | 0.98 | 0.72 |
| AD FWE p | 0.999 | 0.999 | 0.999 | 0.999 | 0.999 | 0.999 | 0.999 | 0.999 | 0.999 | 0.999 | 0.999 | 0.999 | 0.999 | 0.999 | 0.999 |
| AD mFWE p | 0.999 | 0.999 | 0.999 | 0.999 | 0.999 | 0.999 | 0.999 | 0.999 | 0.999 | 0.999 | 0.999 | 0.999 | 0.999 | 0.999 | 0.999 |
| Volume | 9.39 | 8.28 | 7.52 | 8.54 | 6.3 | 7.27 | 5.77 | 6.55 | 7.9 | 2.08 | 8.22 | 5.9 | 6.62 | 3.64 | 7.11 |
| Volume FWE p | 0.002 | 0.005 | 0.009 | 0.004 | 0.02 | 0.01 | 0.03 | 0.017 | 0.007 | 0.999 | 0.005 | 0.027 | 0.016 | 0.249 | 0.011 |
| Volume mFWE p | 0.003 | 0.005 | 0.009 | 0.005 | 0.02 | 0.01 | 0.03 | 0.017 | 0.007 | 0.999 | 0.006 | 0.027 | 0.016 | 0.999 | 0.011 |
| Thickness | 3.57 | 5.54 | 6.17 | 1.14 | -0.46 | -0.98 | 3.22 | 3.79 | 3.69 | 1.19 | 5.68 | -2.74 | 4 | 0.09 | 0.59 |
| Thickness FWE p | 0.236 | 0.014 | 0.005 | 0.999 | 0.999 | 0.999 | 0.381 | 0.175 | 0.2 | 0.999 | 0.011 | 0.999 | 0.13 | 0.999 | 0.999 |
| Thickness mFWE p | 0.285 | 0.016 | 0.006 | 0.999 | 0.999 | 0.999 | 0.485 | 0.207 | 0.239 | 0.999 | 0.013 | 0.999 | 0.151 | 0.999 | 0.999 |

Table B20 continued

| | Left long insular gyrus and central sulcus of the insula | Left short insular gyri | Left middle occipital gyrus | Left superior occipital gyrus | Left lateral occipito temporal gyrus | Left lingual gyrus | Left parahippocampal gyrus | Left orbital gyri | Left angular gyrus | Left supramarginal gyrus | Left superior parietal lobule | Left postcentral gyrus | Left precentral gyrus | Left precuneus |
|---|---|---|---|---|---|---|---|---|---|---|---|---|---|---|
| **Fisher F** | **118.51** | **94.75** | **70.54** | **96.5** | **56.86** | **63.01** | **81.01** | **147.15** | **60.69** | **122.57** | **124.1** | **102.46** | **124.75** | **91.84** |
| **Fisher FWE p** | **0.008** | **0.022** | **0.073** | **0.021** | **0.158** | **0.11** | **0.043** | **0.002** | **0.126** | **0.006** | **0.006** | **0.016** | **0.006** | **0.026** |
| MD | 2.45 | 0.82 | -0.23 | -2.32 | -1.57 | -2.33 | -4.05 | 0.69 | -0.08 | -2.27 | 0.96 | -2.13 | -0.71 | -1.78 |
| MD FWE p | 0.831 | 0.999 | 0.999 | 0.999 | 0.999 | 0.999 | 0.999 | 0.999 | 0.999 | 0.999 | 0.999 | 0.999 | 0.999 | 0.999 |
| MD mFWE p | 0.999 | 0.999 | 0.999 | 0.999 | 0.999 | 0.999 | 0.999 | 0.999 | 0.999 | 0.999 | 0.999 | 0.999 | 0.999 | 0.999 |
| RD | 1.99 | 0.45 | -1.5 | -3.03 | -2.01 | -2.49 | -4.78 | 0.9 | -0.86 | -2.75 | 0.62 | -2.52 | -0.84 | -1.58 |
| RD FWE p | 0.865 | 0.999 | 0.999 | 0.999 | 0.999 | 0.999 | 0.999 | 0.998 | 0.999 | 0.999 | 0.999 | 0.999 | 0.999 | 0.999 |
| RD mFWE p | 0.999 | 0.999 | 0.999 | 0.999 | 0.999 | 0.999 | 0.999 | 0.999 | 0.999 | 0.999 | 0.999 | 0.999 | 0.999 | 0.999 |
| AD | 2.79 | 1.38 | 1.44 | -1.02 | -0.41 | -1.89 | -2.19 | 0.27 | 1.18 | -1.11 | 1.51 | -1.34 | -0.41 | -2.03 |
| AD FWE p | 0.82 | 0.999 | 0.999 | 0.999 | 0.999 | 0.999 | 0.999 | 0.999 | 0.999 | 0.999 | 0.999 | 0.999 | 0.999 | 0.999 |
| AD mFWE p | 0.999 | 0.999 | 0.999 | 0.999 | 0.999 | 0.999 | 0.999 | 0.999 | 0.999 | 0.999 | 0.999 | 0.999 | 0.999 | 0.999 |
| Volume | 9.07 | 8.87 | 7.65 | 9.52 | 7.09 | 7.57 | 8.68 | 11.58 | 6.98 | 10.82 | 10.33 | 9.84 | 10.85 | 9.21 |
| Volume FWE p | 0.003 | 0.003 | 0.008 | 0.002 | 0.011 | 0.008 | 0.004 | 0.001 | 0.012 | 0.001 | 0.001 | 0.002 | 0.001 | 0.003 |
| Volume mFWE p | 0.003 | 0.004 | 0.008 | 0.003 | 0.012 | 0.008 | 0.004 | 0.001 | 0.012 | 0.001 | 0.002 | 0.002 | 0.001 | 0.003 |
| Thickness | 0.05 | 2.08 | 5.59 | 4.62 | 3.73 | 7.41 | 7.06 | 3.59 | 0.84 | 2.88 | 1.09 | 5.61 | 3.17 | 0.12 |
| Thickness FWE p | 0.999 | 0.999 | 0.013 | 0.053 | 0.191 | 0.001 | 0.001 | 0.23 | 0.999 | 0.592 | 0.999 | 0.012 | 0.409 | 0.999 |
| Thickness mFWE p | 0.999 | 0.999 | 0.015 | 0.06 | 0.227 | 0.001 | 0.002 | 0.277 | 0.999 | 0.827 | 0.999 | 0.014 | 0.527 | 0.999 |

Table B20 continued

| | Left subcallosal gyrus | Left anterior transverse temporal gyrus | Left lateral aspect of the superior temporal gyrus | Left planum polare of the superior temporal gyrus | Left planum temporale | Left inferior temporal gyrus | Left middle temporal gyrus | Left horizontal ramus of the anterior segment of the lateral sulcus | Left vertical ramus of the anterior segment of the lateral sulcus | Left posterior ramus of the lateral sulcus | Left occipital pole | Left temporal pole | Left calcarine sulcus | Left central sulcus |
|---|---|---|---|---|---|---|---|---|---|---|---|---|---|---|
| **Fisher F** | **27.31** | **42.2** | **82.15** | **100.34** | **56.63** | **173.65** | **140.92** | **54.62** | **54.87** | **81.98** | **42.87** | **119.21** | **74.88** | **90.19** |
| **Fisher FWE p** | **0.999** | **0.558** | **0.041** | **0.017** | **0.16** | **0.001** | **0.003** | **0.182** | **0.179** | **0.041** | **0.5** | **0.007** | **0.058** | **0.028** |
| MD | -0.65 | -2.4 | -1.69 | 0.99 | -2.9 | 3.12 | 1.32 | 0.13 | 1.49 | -2.89 | -2.13 | -2.88 | -2.37 | -2.16 |
| MD FWE p | 0.999 | 0.999 | 0.999 | 0.999 | 0.999 | 0.477 | 0.997 | 0.999 | 0.994 | 0.999 | 0.999 | 0.999 | 0.999 | 0.999 |
| MD mFWE p | 0.999 | 0.999 | 0.999 | 0.999 | 0.999 | 0.999 | 0.999 | 0.999 | 0.999 | 0.999 | 0.999 | 0.999 | 0.999 | 0.999 |
| RD | -1.06 | -2.62 | -1.9 | 1.17 | -2.99 | 1.07 | 0.21 | 0.1 | 1.43 | -2.75 | -3.96 | -3.54 | -2.66 | -1.98 |
| RD FWE p | 0.999 | 0.999 | 0.999 | 0.993 | 0.999 | 0.996 | 0.999 | 0.999 | 0.978 | 0.999 | 0.999 | 0.999 | 0.999 | 0.999 |
| RD mFWE p | 0.999 | 0.999 | 0.999 | 0.999 | 0.999 | 0.999 | 0.999 | 0.999 | 0.999 | 0.999 | 0.999 | 0.999 | 0.999 | 0.999 |
| AD | 0.08 | -1.76 | -1.14 | 0.47 | -2.4 | 4.95 | 2.58 | 0.17 | 1.4 | -2.71 | 0.69 | -1.24 | -1.63 | -2.36 |
| AD FWE p | 0.999 | 0.999 | 0.999 | 0.999 | 0.999 | 0.012 | 0.897 | 0.999 | 0.999 | 0.999 | 0.999 | 0.999 | 0.999 | 0.999 |
| AD mFWE p | 0.999 | 0.999 | 0.999 | 0.999 | 0.999 | 0.058 | 0.999 | 0.999 | 0.999 | 0.999 | 0.999 | 0.999 | 0.999 | 0.999 |
| Volume | 4.43 | 6.04 | 8.71 | 9.2 | 7.15 | 11 | 10.89 | 6.65 | 5.8 | 8.74 | 5.89 | 10.66 | 8.31 | 9.19 |
| Volume FWE p | 0.095 | 0.025 | 0.004 | 0.003 | 0.011 | 0.001 | 0.001 | 0.016 | 0.029 | 0.004 | 0.028 | 0.001 | 0.005 | 0.003 |
| Volume mFWE p | 0.097 | 0.024 | 0.004 | 0.003 | 0.011 | 0.001 | 0.001 | 0.016 | 0.029 | 0.004 | 0.027 | 0.001 | 0.005 | 0.003 |
| Thickness | 0.94 | 1.09 | 1.38 | 2.01 | 2.95 | 4.1 | 3.79 | 2.05 | 0.96 | 4.74 | 3.6 | 2.68 | 9.91 | 7.6 |
| Thickness FWE p | 0.999 | 0.999 | 0.999 | 0.999 | 0.542 | 0.112 | 0.175 | 0.999 | 0.999 | 0.044 | 0.228 | 0.749 | < 0.001 | 0.001 |
| Thickness mFWE p | 0.999 | 0.999 | 0.999 | 0.999 | 0.739 | 0.13 | 0.207 | 0.999 | 0.999 | 0.051 | 0.275 | 0.999 | < 0.001 | 0.001 |

Table B20 continued

| | Left anterior segment of the circular sulcus of the insula | Left inferior segment of the circular sulcus of the insula | Left superior segment of the circular sulcus of the insula | Left anterior transverse collateral sulcus | Left posterior transverse collateral sulcus | Left inferior frontal sulcus | Left middle frontal sulcus | Left superior frontal sulcus | Left sulcus intermedius primus | Left intraparietal sulcus and transverse parietal sulci | Left middle occipital sulcus and lunatus sulcus | Left superior occipital sulcus and transverse occipital sulcus | Left anterior occipital sulcus and preoccipital notch | Left lateral occipito temporal sulcus |
|---|---|---|---|---|---|---|---|---|---|---|---|---|---|---|
| **Fisher F** | **76.11** | **14.14** | **85.07** | **182.6** | **28.66** | **36.44** | **46.76** | **50** | **20.64** | **62.06** | **42.32** | **44.04** | **39.18** | **67.3** |
| **Fisher FWE p** | **0.055** | **0.999** | **0.035** | **< 0.001** | **0.999** | **0.999** | **0.326** | **0.251** | **0.999** | **0.116** | **0.546** | **0.429** | **0.999** | **0.087** |
| MD | 0.24 | 0.41 | 0.69 | 2 | -1.08 | 1.73 | 2.81 | 1.46 | -1.5 | -3.14 | -1.78 | -2.33 | -0.13 | -0.64 |
| MD FWE p | 0.999 | 0.999 | 0.999 | 0.953 | 0.999 | 0.983 | 0.656 | 0.995 | 0.999 | 0.999 | 0.999 | 0.999 | 0.999 | 0.999 |
| MD mFWE p | 0.999 | 0.999 | 0.999 | 0.999 | 0.999 | 0.999 | 0.999 | 0.999 | 0.999 | 0.999 | 0.999 | 0.999 | 0.999 | 0.999 |
| RD | -0.11 | 0.32 | 0.69 | 1.27 | -0.86 | 1.95 | 2.88 | 1.69 | -1.74 | -2.93 | -2.35 | -2.48 | -0.6 | -1.48 |
| RD FWE p | 0.999 | 0.999 | 0.999 | 0.989 | 0.999 | 0.879 | 0.374 | 0.946 | 0.999 | 0.999 | 0.999 | 0.999 | 0.999 | 0.999 |
| RD mFWE p | 0.999 | 0.999 | 0.999 | 0.999 | 0.999 | 0.999 | 0.999 | 0.999 | 0.999 | 0.999 | 0.999 | 0.999 | 0.999 | 0.999 |
| AD | 0.77 | 0.46 | 0.49 | 2.16 | -1.2 | 1.02 | 2.19 | 0.78 | -0.71 | -3.29 | -0.41 | -1.71 | 0.8 | 0.86 |
| AD FWE p | 0.999 | 0.999 | 0.999 | 0.976 | 0.999 | 0.999 | 0.973 | 0.999 | 0.999 | 0.999 | 0.999 | 0.999 | 0.999 | 0.999 |
| AD mFWE p | 0.999 | 0.999 | 0.999 | 0.999 | 0.999 | 0.999 | 0.999 | 0.999 | 0.999 | 0.999 | 0.999 | 0.999 | 0.999 | 0.999 |
| Volume | 8.03 | 1.87 | 8.46 | 12.55 | 4.76 | 3.8 | 3.09 | 5.51 | 3.81 | 7.51 | 6 | 6.21 | 5.39 | 7.6 |
| Volume FWE p | 0.006 | 0.999 | 0.005 | < 0.001 | 0.07 | 0.196 | 0.999 | 0.037 | 0.192 | 0.009 | 0.025 | 0.022 | 0.041 | 0.008 |
| Volume mFWE p | 0.006 | 0.999 | 0.005 | < 0.001 | 0.069 | 0.291 | 0.999 | 0.036 | 0.275 | 0.009 | 0.025 | 0.021 | 0.04 | 0.008 |
| Thickness | 6.68 | 0.42 | 5.99 | 1.99 | 2.73 | 3.03 | 2.54 | 3.85 | 0.52 | 4.9 | 6.61 | 4.66 | 4.9 | 4.23 |
| Thickness FWE p | 0.002 | 0.999 | 0.007 | 0.999 | 0.704 | 0.491 | 0.871 | 0.161 | 0.999 | 0.035 | 0.003 | 0.05 | 0.035 | 0.093 |
| Thickness mFWE p | 0.003 | 0.999 | 0.008 | 0.999 | 0.999 | 0.654 | 0.999 | 0.19 | 0.999 | 0.04 | 0.003 | 0.057 | 0.04 | 0.107 |

Table B20 continued

| | Left lateral orbital sulcus | Left medial orbital sulcus | Left orbital sulci | Left parieto occipital sulcus | Left pericallosal sulcus | Left postcentral sulcus | Left inferior part of the precentral sulcus | Left superior part of the precentral sulcus | Left suborbital sulcus | Left subparietal sulcus | Left inferior temporal sulcus | Left superior temporal sulcus | Left transverse temporal sulcus | Right fronto marginal gyrus and sulcus |
|---|---|---|---|---|---|---|---|---|---|---|---|---|---|---|
| **Fisher F** | **43.84** | **53.95** | **88.13** | **56.81** | **75.14** | **56.79** | **117.06** | **31.58** | **48.61** | **57.57** | **155.11** | **76.05** | **37.77** | **110.61** |
| **Fisher FWE p** | **0.44** | **0.19** | **0.03** | **0.159** | **0.058** | **0.159** | **0.008** | **0.999** | **0.279** | **0.151** | **0.002** | **0.055** | **0.999** | **0.011** |
| MD | 2.91 | 1.1 | 0.79 | -2.99 | 2.6 | -2.53 | -0.39 | -0.25 | 1.99 | -1.7 | 4.75 | -1.25 | -3.43 | 2.82 |
| MD FWE p | 0.598 | 0.999 | 0.999 | 0.999 | 0.763 | 0.999 | 0.999 | 0.999 | 0.954 | 0.999 | 0.01 | 0.999 | 0.999 | 0.649 |
| MD mFWE p | 0.999 | 0.999 | 0.999 | 0.999 | 0.999 | 0.999 | 0.999 | 0.999 | 0.999 | 0.999 | 0.07 | 0.999 | 0.999 | 0.999 |
| RD | 3.45 | 0.5 | 1.48 | -3.49 | 2.26 | -2.2 | -0.52 | 0.06 | 2.03 | -1.4 | 2.85 | -1.7 | -2.56 | 3 |
| RD FWE p | 0.115 | 0.999 | 0.974 | 0.999 | 0.745 | 0.999 | 0.999 | 0.999 | 0.849 | 0.999 | 0.39 | 0.999 | 0.999 | 0.306 |
| RD mFWE p | 0.999 | 0.999 | 0.999 | 0.999 | 0.999 | 0.999 | 0.999 | 0.999 | 0.999 | 0.999 | 0.999 | 0.999 | 0.999 | 0.999 |
| AD | 1.53 | 1.41 | -0.46 | -1.66 | 2.24 | -2.97 | -0.06 | -0.84 | 1.42 | -2.02 | 5.84 | -0.11 | -4.3 | 1.91 |
| AD FWE p | 0.999 | 0.999 | 0.999 | 0.999 | 0.967 | 0.999 | 0.999 | 0.999 | 0.999 | 0.999 | < 0.001 | 0.999 | 0.999 | 0.992 |
| AD mFWE p | 0.999 | 0.999 | 0.999 | 0.999 | 0.999 | 0.999 | 0.999 | 0.999 | 0.999 | 0.999 | 0.028 | 0.999 | 0.999 | 0.999 |
| Volume | 2.3 | 6.01 | 8.29 | 7.15 | 5.48 | 7.16 | 10.43 | 4.86 | 4.05 | 7.19 | 8.39 | 8.3 | 4.18 | 8.52 |
| Volume FWE p | 0.999 | 0.025 | 0.005 | 0.011 | 0.038 | 0.011 | 0.001 | 0.064 | 0.142 | 0.011 | 0.005 | 0.005 | 0.123 | 0.004 |
| Volume mFWE p | 0.999 | 0.025 | 0.005 | 0.011 | 0.037 | 0.011 | 0.001 | 0.063 | 0.159 | 0.011 | 0.005 | 0.005 | 0.132 | 0.005 |
| Thickness | 1.24 | 0.18 | -1.29 | 7.23 | -2.72 | 7.21 | 4.29 | 4.6 | -1.9 | 3.77 | 3.23 | 3.61 | -3.34 | 4.78 |
| Thickness FWE p | 0.999 | 0.999 | 0.999 | 0.001 | 0.999 | 0.001 | 0.085 | 0.055 | 0.999 | 0.179 | 0.378 | 0.226 | 0.999 | 0.042 |
| Thickness mFWE p | 0.999 | 0.999 | 0.999 | 0.001 | 0.999 | 0.001 | 0.098 | 0.063 | 0.999 | 0.212 | 0.48 | 0.271 | 0.999 | 0.048 |

Table B20 continued

| | Right paracentral lobule and sulcus | Right subcentral gyrus and sulci | Right transverse frontopolar gyri and sulci | Right anterior part of the cingulate gyrus and sulcus | Right middle anterior part of the cingulate gyrus and sulcus | Right middle posterior part of the cingulate gyrus and sulcus | Right posterior dorsal part of the cingulate gyrus | Right posterior ventral part of the cingulate gyrus | Right cuneus | Right opercular part of the inferior frontal gyrus | Right orbital part of the inferior frontal gyrus | Right triangular part of the inferior frontal gyrus | Right middle frontal gyrus | Right superior frontal gyrus |
|---|---|---|---|---|---|---|---|---|---|---|---|---|---|---|
| **Fisher F** | **58.11** | **91.95** | **127.17** | **117.01** | **71.33** | **72.4** | **87.47** | **6.73** | **68.34** | **69.83** | **42.84** | **31.26** | **62.36** | **125.98** |
| **Fisher FWE p** | **0.146** | **0.025** | **0.005** | **0.008** | **0.07** | **0.066** | **0.031** | **0.999** | **0.082** | **0.076** | **0.502** | **0.999** | **0.114** | **0.006** |
| MD | -3.48 | -1.86 | 2.79 | 3.31 | 0.38 | -0.96 | -1.52 | -3.47 | -2.55 | 0.44 | 1.35 | 1.62 | 2.16 | -0.12 |
| MD FWE p | 0.999 | 0.999 | 0.666 | 0.37 | 0.999 | 0.999 | 0.999 | 0.999 | 0.999 | 0.999 | 0.997 | 0.989 | 0.922 | 0.999 |
| MD mFWE p | 0.999 | 0.999 | 0.999 | 0.999 | 0.999 | 0.999 | 0.999 | 0.999 | 0.999 | 0.999 | 0.999 | 0.999 | 0.999 | 0.999 |
| RD | -3.53 | -2.38 | 2.7 | 3.6 | 0.77 | -0.84 | -1.44 | -3.66 | -2.8 | 0.29 | 0.83 | 1.79 | 2.23 | 0.13 |
| RD FWE p | 0.999 | 0.999 | 0.484 | 0.077 | 0.999 | 0.999 | 0.999 | 0.999 | 0.999 | 0.999 | 0.999 | 0.924 | 0.764 | 0.999 |
| RD mFWE p | 0.999 | 0.999 | 0.999 | 0.999 | 0.999 | 0.999 | 0.999 | 0.999 | 0.999 | 0.999 | 0.999 | 0.999 | 0.999 | 0.999 |
| AD | -2.89 | -0.6 | 2.45 | 1.97 | -0.47 | -0.95 | -1.34 | -2.52 | -1.9 | 0.72 | 2.08 | 1.16 | 1.83 | -0.55 |
| AD FWE p | 0.999 | 0.999 | 0.932 | 0.99 | 0.999 | 0.999 | 0.999 | 0.999 | 0.999 | 0.999 | 0.983 | 0.999 | 0.995 | 0.999 |
| AD mFWE p | 0.999 | 0.999 | 0.999 | 0.999 | 0.999 | 0.999 | 0.999 | 0.999 | 0.999 | 0.999 | 0.999 | 0.999 | 0.999 | 0.999 |
| Volume | 7.25 | 9.24 | 9.41 | 8.44 | 7.74 | 8.1 | 9.02 | 1.81 | 7.92 | 7.34 | 4.65 | 3.02 | 5.75 | 10.83 |
| Volume FWE p | 0.01 | 0.003 | 0.002 | 0.005 | 0.007 | 0.006 | 0.003 | 0.999 | 0.006 | 0.01 | 0.077 | 0.999 | 0.031 | 0.001 |
| Volume mFWE p | 0.01 | 0.003 | 0.003 | 0.005 | 0.008 | 0.006 | 0.003 | 0.999 | 0.007 | 0.01 | 0.077 | 0.999 | 0.03 | 0.001 |
| Thickness | 6.37 | 1.16 | 2.17 | 2.11 | 5.73 | 4.81 | 2.76 | 3.21 | 7.01 | -0.92 | 1.18 | 0.12 | 1.17 | 2 |
| Thickness FWE p | 0.004 | 0.999 | 0.999 | 0.999 | 0.01 | 0.04 | 0.678 | 0.386 | 0.001 | 0.999 | 0.999 | 0.999 | 0.999 | 0.999 |
| Thickness mFWE p | 0.005 | 0.999 | 0.999 | 0.999 | 0.012 | 0.046 | 0.999 | 0.493 | 0.002 | 0.999 | 0.999 | 0.999 | 0.999 | 0.999 |

Table B20 continued

| | Right short insular gyri | Right middle occipital gyrus | Right superior occipital gyrus | Right lateral occipito temporal gyrus | Right lingual gyrus | Right parahippocampal gyrus | Right orbital gyri | Right angular gyrus | Right supramarginal gyrus | Right superior parietal lobule | Right postcentral gyrus | Right precentral gyrus | Right precuneus |
|---|---|---|---|---|---|---|---|---|---|---|---|---|---|
| **Fisher F** | **79.28** | **75.25** | **72.5** | **35.38** | **74.94** | **53.51** | **132.83** | **63.98** | **72.14** | **82.25** | **65.66** | **107.95** | **83.49** |
| **Fisher FWE p** | **0.047** | **0.057** | **0.066** | **0.999** | **0.058** | **0.196** | **0.004** | **0.104** | **0.067** | **0.04** | **0.095** | **0.012** | **0.038** |
| MD | 1.42 | -0.91 | -2.63 | -2.36 | -3.27 | -3.86 | 0.78 | -1.18 | -1.93 | -0.08 | -1.22 | -1.89 | -2.15 |
| MD FWE p | 0.996 | 0.999 | 0.999 | 0.999 | 0.999 | 0.999 | 0.999 | 0.999 | 0.999 | 0.999 | 0.999 | 0.999 | 0.999 |
| MD mFWE p | 0.999 | 0.999 | 0.999 | 0.999 | 0.999 | 0.999 | 0.999 | 0.999 | 0.999 | 0.999 | 0.999 | 0.999 | 0.999 |
| RD | 0.99 | -2.13 | -3.53 | -2.42 | -3.29 | -4.23 | 0.41 | -1.43 | -2.38 | -0.29 | -1.49 | -2.08 | -1.97 |
| RD FWE p | 0.997 | 0.999 | 0.999 | 0.999 | 0.999 | 0.999 | 0.999 | 0.999 | 0.999 | 0.999 | 0.999 | 0.999 | 0.999 |
| RD mFWE p | 0.999 | 0.999 | 0.999 | 0.999 | 0.999 | 0.999 | 0.999 | 0.999 | 0.999 | 0.999 | 0.999 | 0.999 | 0.999 |
| AD | 1.85 | 1.02 | -0.87 | -1.54 | -2.94 | -2.5 | 1.1 | -0.59 | -0.88 | 0.32 | -0.64 | -1.34 | -2.34 |
| AD FWE p | 0.994 | 0.999 | 0.999 | 0.999 | 0.999 | 0.999 | 0.999 | 0.999 | 0.999 | 0.999 | 0.999 | 0.999 | 0.999 |
| AD mFWE p | 0.999 | 0.999 | 0.999 | 0.999 | 0.999 | 0.999 | 0.999 | 0.999 | 0.999 | 0.999 | 0.999 | 0.999 | 0.999 |
| Volume | 7.44 | 8.09 | 8.15 | 5.48 | 8.33 | 6.93 | 10.88 | 7.57 | 8.13 | 8.49 | 7.69 | 10.11 | 8.75 |
| Volume FWE p | 0.009 | 0.006 | 0.006 | 0.038 | 0.005 | 0.013 | 0.001 | 0.008 | 0.006 | 0.004 | 0.008 | 0.002 | 0.004 |
| Volume mFWE p | 0.009 | 0.006 | 0.006 | 0.037 | 0.005 | 0.013 | 0.001 | 0.008 | 0.006 | 0.005 | 0.008 | 0.002 | 0.004 |
| Thickness | -0.66 | 3.28 | 5.45 | 4.12 | 8.14 | 5.46 | 4.46 | 1.82 | 2.88 | 1.12 | 4.59 | 4.5 | 0.07 |
| Thickness FWE p | 0.999 | 0.351 | 0.016 | 0.109 | < 0.001 | 0.015 | 0.067 | 0.999 | 0.594 | 0.999 | 0.056 | 0.064 | 0.999 |
| Thickness mFWE p | 0.999 | 0.442 | 0.018 | 0.126 | < 0.001 | 0.018 | 0.076 | 0.999 | 0.83 | 0.999 | 0.063 | 0.073 | 0.999 |

Table B20 continued

| | Right subcallosal gyrus | Right anterior transverse temporal gyrus | Right lateral aspect of the superior temporal gyrus | Right planum polare of the superior temporal gyrus | Right planum temporale | Right inferior temporal gyrus | Right middle temporal gyrus | Right horizontal ramus of the anterior segment of the lateral | Right vertical ramus of the anterior segment of the lateral | Right posterior ramus of the lateral sulcus | Right occipital pole | Right temporal pole | Right calcarine sulcus | Right central sulcus |
|---|---|---|---|---|---|---|---|---|---|---|---|---|---|---|
| **Fisher F** | **25.09** | **43.65** | **108.1** | **41.46** | **19.36** | **132.36** | **224.7** | **20.64** | **44.01** | **21.78** | **91.27** | **110.4** | **56.66** | **61.09** |
| **Fisher FWE p** | **0.999** | **0.45** | **0.012** | **0.662** | **0.999** | **0.004** | **< 0.001** | **0.999** | **0.43** | **0.999** | **0.026** | **0.011** | **0.16** | **0.123** |
| MD | 0.73 | -3.22 | -1.33 | -1.29 | -3.81 | 1.18 | 1.46 | -0.14 | 1.26 | -3.55 | -3.13 | -1.41 | -3.38 | -2.1 |
| MD FWE p | 0.999 | 0.999 | 0.999 | 0.999 | 0.999 | 0.999 | 0.995 | 0.999 | 0.998 | 0.999 | 0.999 | 0.999 | 0.999 | 0.999 |
| MD mFWE p | 0.999 | 0.999 | 0.999 | 0.999 | 0.999 | 0.999 | 0.999 | 0.999 | 0.999 | 0.999 | 0.999 | 0.999 | 0.999 | 0.999 |
| RD | -0.06 | -3.64 | -1.47 | -1.02 | -3.62 | -0.48 | 0.38 | -0.55 | 0.95 | -3.04 | -4.29 | -2.15 | -3.55 | -1.96 |
| RD FWE p | 0.999 | 0.999 | 0.999 | 0.999 | 0.999 | 0.999 | 0.999 | 0.999 | 0.998 | 0.999 | 0.999 | 0.999 | 0.999 | 0.999 |
| RD mFWE p | 0.999 | 0.999 | 0.999 | 0.999 | 0.999 | 0.999 | 0.999 | 0.999 | 0.999 | 0.999 | 0.999 | 0.999 | 0.999 | 0.999 |
| AD | 1.89 | -2.13 | -0.93 | -1.4 | -3.8 | 3.45 | 2.76 | 0.73 | 1.57 | -4.07 | -0.83 | -0.16 | -2.74 | -2.26 |
| AD FWE p | 0.993 | 0.999 | 0.999 | 0.999 | 0.999 | 0.454 | 0.834 | 0.999 | 0.999 | 0.999 | 0.999 | 0.999 | 0.999 | 0.999 |
| AD mFWE p | 0.999 | 0.999 | 0.999 | 0.999 | 0.999 | 0.999 | 0.999 | 0.999 | 0.999 | 0.999 | 0.999 | 0.999 | 0.999 | 0.999 |
| Volume | 3 | 6.18 | 10.1 | 5.94 | 3.84 | 10.28 | 14.23 | 3.36 | 4.93 | 4.13 | 9.23 | 10.16 | 7.15 | 7.44 |
| Volume FWE p | 0.999 | 0.022 | 0.002 | 0.026 | 0.185 | 0.001 | < 0.001 | 0.999 | 0.06 | 0.13 | 0.003 | 0.001 | 0.011 | 0.009 |
| Volume mFWE p | 0.999 | 0.022 | 0.002 | 0.026 | 0.252 | 0.002 | < 0.001 | 0.999 | 0.059 | 0.142 | 0.003 | 0.002 | 0.011 | 0.009 |
| Thickness | 0.6 | 3.07 | 3.51 | 1.55 | 3.57 | 3.43 | 4.14 | 1.42 | 0.36 | 4.9 | 7.06 | 1.02 | 9.45 | 6.73 |
| Thickness FWE p | 0.999 | 0.465 | 0.258 | 0.999 | 0.238 | 0.288 | 0.106 | 0.999 | 0.999 | 0.035 | 0.001 | 0.999 | < 0.001 | 0.002 |
| Thickness mFWE p | 0.999 | 0.612 | 0.314 | 0.999 | 0.288 | 0.354 | 0.123 | 0.999 | 0.999 | 0.04 | 0.002 | 0.999 | < 0.001 | 0.003 |

Table B20 continued

| | Right anterior segment of the circular sulcus of the insula | Right inferior segment of the circular sulcus of the insula | Right superior segment of the circular sulcus of the insula | Right anterior transverse collateral sulcus | Right posterior transverse collateral sulcus | Right inferior frontal sulcus | Right middle frontal sulcus | Right superior frontal sulcus | Right sulcus intermedius primus | Right intraparietal sulcus and transverse parietal sulci | Right middle occipital sulcus and lunatus sulcus | Right superior occipital sulcus and transverse occipital sulcus | Right anterior occipital sulcus and preoccipital notch | Right lateral occipito temporal sulcus |
|---|---|---|---|---|---|---|---|---|---|---|---|---|---|---|
| **Fisher F** | **52.9** | **18.5** | **86.41** | **111.42** | **47.08** | **46.45** | **61.79** | **57.62** | **32.67** | **59.36** | **79.4** | **47.61** | **66.67** | **99.51** |
| **Fisher FWE p** | **0.204** | **0.999** | **0.033** | **0.01** | **0.317** | **0.336** | **0.118** | **0.151** | **0.999** | **0.136** | **0.047** | **0.303** | **0.09** | **0.018** |
| MD | 0.12 | -1.74 | 1.06 | 0.9 | -1.1 | 1.89 | 2.68 | 1.27 | -0.09 | -2.58 | -1.41 | -3.21 | -1.03 | -1.03 |
| MD FWE p | 0.999 | 0.999 | 0.999 | 0.999 | 0.999 | 0.968 | 0.728 | 0.998 | 0.999 | 0.999 | 0.999 | 0.999 | 0.999 | 0.999 |
| MD mFWE p | 0.999 | 0.999 | 0.999 | 0.999 | 0.999 | 0.999 | 0.999 | 0.999 | 0.999 | 0.999 | 0.999 | 0.999 | 0.999 | 0.999 |
| RD | 0.01 | -2.18 | 1.26 | 0.76 | -0.56 | 2.25 | 2.77 | 1.73 | -0.33 | -2.57 | -1.27 | -3.18 | -1.2 | -2.14 |
| RD FWE p | 0.999 | 0.999 | 0.99 | 0.999 | 0.999 | 0.75 | 0.443 | 0.937 | 0.999 | 0.999 | 0.999 | 0.999 | 0.999 | 0.999 |
| RD mFWE p | 0.999 | 0.999 | 0.999 | 0.999 | 0.999 | 0.999 | 0.999 | 0.999 | 0.999 | 0.999 | 0.999 | 0.999 | 0.999 | 0.999 |
| AD | 0.29 | -0.6 | 0.42 | 0.66 | -1.75 | 0.92 | 2.06 | 0.12 | 0.38 | -2.43 | -1.37 | -2.81 | -0.44 | 1.4 |
| AD FWE p | 0.999 | 0.999 | 0.999 | 0.999 | 0.999 | 0.999 | 0.985 | 0.999 | 0.999 | 0.999 | 0.999 | 0.999 | 0.999 | 0.999 |
| AD mFWE p | 0.999 | 0.999 | 0.999 | 0.999 | 0.999 | 0.999 | 0.999 | 0.999 | 0.999 | 0.999 | 0.999 | 0.999 | 0.999 | 0.999 |
| Volume | 6.52 | 3.56 | 8.38 | 9.82 | 6.37 | 4.71 | 5.09 | 6.3 | 4.83 | 7.33 | 8.56 | 6.49 | 7.73 | 9.41 |
| Volume FWE p | 0.017 | 0.294 | 0.005 | 0.002 | 0.019 | 0.073 | 0.052 | 0.02 | 0.065 | 0.01 | 0.004 | 0.018 | 0.007 | 0.002 |
| Volume mFWE p | 0.017 | 0.999 | 0.005 | 0.002 | 0.019 | 0.072 | 0.051 | 0.02 | 0.064 | 0.01 | 0.005 | 0.017 | 0.008 | 0.003 |
| Thickness | 5.85 | 0.63 | 5.38 | 0.98 | 2.64 | 3.28 | 4.33 | 3.67 | 2.27 | 3.57 | 5.06 | 4.17 | 6.25 | 5.55 |
| Thickness FWE p | 0.008 | 0.999 | 0.017 | 0.999 | 0.781 | 0.354 | 0.081 | 0.207 | 0.999 | 0.238 | 0.028 | 0.102 | 0.005 | 0.013 |
| Thickness mFWE p | 0.01 | 0.999 | 0.02 | 0.999 | 0.999 | 0.446 | 0.092 | 0.248 | 0.999 | 0.287 | 0.032 | 0.118 | 0.006 | 0.015 |

Table B20 continued

| | Right lateral orbital sulcus | Right medial orbital sulcus | Right orbital sulci | Right parieto occipital sulcus | Right pericallosal sulcus | Right postcentral sulcus | Right inferior part of the precentral sulcus | Right superior part of the precentral sulcus | Right suborbital sulcus | Right subparietal sulcus | Right inferior temporal sulcus | Right superior temporal sulcus | Right transverse temporal sulcus |
|---|---|---|---|---|---|---|---|---|---|---|---|---|---|
| **Fisher F** | **28.95** | **59.53** | **108.19** | **92.14** | **61.93** | **45.29** | **80.79** | **24.54** | **41.03** | **68.02** | **130.34** | **106.9** | **39.88** |
| **Fisher FWE p** | **0.999** | **0.134** | **0.012** | **0.025** | **0.117** | **0.375** | **0.043** | **0.999** | **0.834** | **0.084** | **0.005** | **0.013** | **0.999** |
| MD | 1.04 | 1.74 | 0.31 | -4.51 | 2.03 | -3.06 | -0.04 | -0.62 | 2 | -3 | 2.86 | -1.61 | -5.68 |
| MD FWE p | 0.999 | 0.982 | 0.999 | 0.999 | 0.947 | 0.999 | 0.999 | 0.999 | 0.953 | 0.999 | 0.628 | 0.999 | 0.999 |
| MD mFWE p | 0.999 | 0.999 | 0.999 | 0.999 | 0.999 | 0.999 | 0.999 | 0.999 | 0.999 | 0.999 | 0.999 | 0.999 | 0.999 |
| RD | 0.69 | 0.9 | 1.01 | -4.91 | 1.85 | -2.85 | -0.01 | -0.19 | 1.54 | -2.71 | 1.44 | -1.83 | -5.53 |
| RD FWE p | 0.999 | 0.998 | 0.997 | 0.999 | 0.908 | 0.999 | 0.999 | 0.999 | 0.967 | 0.999 | 0.978 | 0.999 | 0.999 |
| RD mFWE p | 0.999 | 0.999 | 0.999 | 0.999 | 0.999 | 0.999 | 0.999 | 0.999 | 0.999 | 0.999 | 0.999 | 0.999 | 0.999 |
| AD | 1.47 | 2.36 | -0.77 | -3.27 | 1.66 | -3.28 | -0.1 | -1.37 | 1.99 | -3.16 | 4.03 | -0.89 | -5.19 |
| AD FWE p | 0.999 | 0.949 | 0.999 | 0.999 | 0.998 | 0.999 | 0.999 | 0.999 | 0.989 | 0.999 | 0.165 | 0.999 | 0.999 |
| AD mFWE p | 0.999 | 0.999 | 0.999 | 0.999 | 0.999 | 0.999 | 0.999 | 0.999 | 0.999 | 0.999 | 0.166 | 0.999 | 0.999 |
| Volume | 3.54 | 5.83 | 9.82 | 9.3 | 3.81 | 6.31 | 8.44 | 4.22 | 3.54 | 7.89 | 9.29 | 10.04 | 5.88 |
| Volume FWE p | 0.303 | 0.029 | 0.002 | 0.003 | 0.193 | 0.02 | 0.005 | 0.117 | 0.304 | 0.007 | 0.003 | 0.002 | 0.028 |
| Volume mFWE p | 0.999 | 0.028 | 0.002 | 0.003 | 0.28 | 0.02 | 0.005 | 0.124 | 0.999 | 0.007 | 0.003 | 0.002 | 0.027 |
| Thickness | 4.7 | 0.19 | 2.92 | 5.6 | -4.18 | 7.29 | 4.51 | 3.78 | -0.89 | 1.82 | 2.94 | 4.79 | 2.34 |
| Thickness FWE p | 0.047 | 0.999 | 0.565 | 0.012 | 0.999 | 0.001 | 0.062 | 0.177 | 0.999 | 0.999 | 0.547 | 0.041 | 0.999 |
| Thickness mFWE p | 0.054 | 0.999 | 0.778 | 0.014 | 0.999 | 0.001 | 0.071 | 0.21 | 0.999 | 0.999 | 0.748 | 0.047 | 0.999 |

**Table B21 Positive correlations between cortical grey matter metrics and total problems**

| | Left fronto marginal gyrus and sulcus | Left inferior occipital gyrus and sulcus | Left paracentral lobule and sulcus | Left subcentral gyrus and sulci | Left transverse frontopolar gyri and sulci | Left anterior part of the cingulate gyrus and sulcus | Left middle anterior part of the cingulate gyrus and | Left middle posterior part of the cingulate gyrus and | Left posterior dorsal part of the cingulate gyrus | Left posterior ventral part of the cingulate gyrus | Left cuneus | Left opercular part of the inferior frontal gyrus | Left orbital part of the inferior frontal gyrus | Left triangular part of the inferior frontal gyrus | Left middle frontal gyrus |
|---|---|---|---|---|---|---|---|---|---|---|---|---|---|---|---|
| **Fisher F** | **11.91** | **5.2** | **5.98** | **6.85** | **5.18** | **9.44** | **4.12** | **5.39** | **5** | **13** | **5.75** | **7.8** | **10.63** | **9.03** | **4.12** |
| **Fisher FWE p** | **0.976** | **0.999** | **0.999** | **0.999** | **0.999** | **0.999** | **0.999** | **0.999** | **0.999** | **0.947** | **0.999** | **0.999** | **0.993** | **0.999** | **0.999** |
| MD | 0.55 | -2.37 | -0.33 | -1.04 | -1.26 | -0.06 | -1.14 | -0.36 | -1.97 | 0.87 | -0.93 | -0.36 | 0.03 | -0.38 | -0.69 |
| MD FWE p | 0.876 | 0.999 | 0.996 | 0.999 | 0.999 | 0.985 | 0.999 | 0.997 | 0.999 | 0.732 | 0.999 | 0.997 | 0.979 | 0.997 | 0.999 |
| MD mFWE p | 0.999 | 0.999 | 0.999 | 0.999 | 0.999 | 0.999 | 0.999 | 0.999 | 0.999 | 0.999 | 0.999 | 0.999 | 0.999 | 0.999 | 0.999 |
| RD | -0.02 | -2.55 | -0.53 | -1.1 | -1.84 | -0.4 | -1.57 | -0.43 | -1.8 | 1.25 | -1.01 | -0.53 | -0.6 | -0.65 | -1.06 |
| RD FWE p | 0.989 | 0.999 | 0.999 | 0.999 | 0.999 | 0.998 | 0.999 | 0.999 | 0.999 | 0.557 | 0.999 | 0.999 | 0.999 | 0.999 | 0.999 |
| RD mFWE p | 0.999 | 0.999 | 0.999 | 0.999 | 0.999 | 0.999 | 0.999 | 0.999 | 0.999 | 0.999 | 0.999 | 0.999 | 0.999 | 0.999 | 0.999 |
| AD | 1.27 | -1.53 | 0.05 | -0.8 | -0.15 | 0.51 | -0.17 | -0.15 | -1.92 | 0.11 | -0.74 | 0.02 | 1.1 | 0.14 | 0.07 |
| AD FWE p | 0.506 | 0.999 | 0.985 | 0.999 | 0.994 | 0.908 | 0.995 | 0.994 | 0.999 | 0.98 | 0.999 | 0.987 | 0.62 | 0.977 | 0.983 |
| AD mFWE p | 0.999 | 0.999 | 0.999 | 0.999 | 0.999 | 0.999 | 0.999 | 0.999 | 0.999 | 0.999 | 0.999 | 0.999 | 0.999 | 0.999 | 0.999 |
| Volume | 0.28 | 0.84 | -0.13 | 1.19 | 0.53 | -0.98 | 0.39 | -1.37 | 0.87 | 0.42 | 1.25 | 0.64 | 1.21 | 1.26 | -0.76 |
| Volume FWE p | 0.999 | 0.999 | 0.999 | 0.996 | 0.999 | 0.999 | 0.999 | 0.999 | 0.999 | 0.999 | 0.995 | 0.999 | 0.996 | 0.994 | 0.999 |
| Volume mFWE p | 0.999 | 0.999 | 0.999 | 0.999 | 0.999 | 0.999 | 0.999 | 0.999 | 0.999 | 0.999 | 0.999 | 0.999 | 0.999 | 0.999 | 0.999 |
| Thickness | -0.15 | -0.25 | -0.18 | -0.05 | 0.04 | -1.27 | 0.81 | -0.5 | -0.09 | -0.05 | 2.25 | -0.38 | 1.28 | -0.01 | 0.1 |
| Thickness FWE p | 0.999 | 0.999 | 0.999 | 0.999 | 0.999 | 0.999 | 0.999 | 0.999 | 0.999 | 0.999 | 0.751 | 0.999 | 0.998 | 0.999 | 0.999 |
| Thickness mFWE p | 0.999 | 0.999 | 0.999 | 0.999 | 0.999 | 0.999 | 0.999 | 0.999 | 0.999 | 0.999 | 0.987 | 0.999 | 0.999 | 0.999 | 0.999 |

Table B21 continued

| | Left long insular gyrus and central sulcus of the insula | Left short insular gyri | Left middle occipital gyrus | Left superior occipital gyrus | Left lateral occipito temporal gyrus | Left lingual gyrus | Left parahippocampal gyrus | Left orbital gyri | Left angular gyrus | Left supramarginal gyrus | Left superior parietal lobule | Left postcentral gyrus | Left precentral gyrus | Left precuneus |
|---|---|---|---|---|---|---|---|---|---|---|---|---|---|---|
| **Fisher F** | **11.74** | **5.47** | **3.88** | **5.01** | **3.04** | **7.11** | **6.66** | **10.32** | **3.33** | **3.92** | **7.89** | **4.31** | **11.94** | **9.27** |
| **Fisher FWE p** | **0.979** | **0.999** | **0.999** | **0.999** | **0.999** | **0.999** | **0.999** | **0.996** | **0.999** | **0.999** | **0.999** | **0.999** | **0.975** | **0.999** |
| MD | 0.32 | -0.67 | -2.14 | -1.68 | -1.46 | -1.22 | -0.64 | -0.16 | -1.64 | -1.82 | -0.33 | -1.34 | -1.47 | -0.63 |
| MD FWE p | 0.938 | 0.999 | 0.999 | 0.999 | 0.999 | 0.999 | 0.999 | 0.991 | 0.999 | 0.999 | 0.996 | 0.999 | 0.999 | 0.999 |
| MD mFWE p | 0.999 | 0.999 | 0.999 | 0.999 | 0.999 | 0.999 | 0.999 | 0.999 | 0.999 | 0.999 | 0.999 | 0.999 | 0.999 | 0.999 |
| RD | 0.36 | -0.88 | -2.43 | -2 | -1.03 | -1.03 | -0.61 | -0.49 | -1.88 | -1.76 | -0.55 | -1.39 | -1.64 | -0.57 |
| RD FWE p | 0.948 | 0.999 | 0.999 | 0.999 | 0.999 | 0.999 | 0.999 | 0.999 | 0.999 | 0.999 | 0.999 | 0.999 | 0.999 | 0.999 |
| RD mFWE p | 0.999 | 0.999 | 0.999 | 0.999 | 0.999 | 0.999 | 0.999 | 0.999 | 0.999 | 0.999 | 0.999 | 0.999 | 0.999 | 0.999 |
| AD | 0.16 | -0.17 | -1.41 | -1.02 | -1.59 | -1.44 | -0.56 | 0.34 | -0.99 | -1.74 | 0.1 | -1.18 | -1 | -0.69 |
| AD FWE p | 0.975 | 0.995 | 0.999 | 0.999 | 0.999 | 0.999 | 0.999 | 0.948 | 0.999 | 0.999 | 0.98 | 0.999 | 0.999 | 0.999 |
| AD mFWE p | 0.999 | 0.999 | 0.999 | 0.999 | 0.999 | 0.999 | 0.999 | 0.999 | 0.999 | 0.999 | 0.999 | 0.999 | 0.999 | 0.999 |
| Volume | 0.87 | 0.78 | 0.79 | -0.08 | -0.45 | 1.72 | 1.27 | 1.04 | -0.28 | -0.13 | 0.96 | 0.5 | 2.65 | 1.14 |
| Volume FWE p | 0.999 | 0.999 | 0.999 | 0.999 | 0.999 | 0.957 | 0.994 | 0.998 | 0.999 | 0.999 | 0.999 | 0.999 | 0.568 | 0.997 |
| Volume mFWE p | 0.999 | 0.999 | 0.999 | 0.999 | 0.999 | 0.995 | 0.999 | 0.999 | 0.999 | 0.999 | 0.999 | 0.999 | 0.686 | 0.999 |
| Thickness | -0.68 | 1.12 | 0.66 | -0.86 | -0.16 | 1.81 | 1.39 | -0.61 | -0.25 | -0.56 | 0.16 | 0.03 | 1.06 | -0.87 |
| Thickness FWE p | 0.999 | 0.999 | 0.999 | 0.999 | 0.999 | 0.948 | 0.996 | 0.999 | 0.999 | 0.999 | 0.999 | 0.999 | 0.999 | 0.999 |
| Thickness mFWE p | 0.999 | 0.999 | 0.999 | 0.999 | 0.999 | 0.999 | 0.999 | 0.999 | 0.999 | 0.999 | 0.999 | 0.999 | 0.999 | 0.999 |

Table B21 continued

| | Left subcallosal gyrus | Left anterior transverse temporal gyrus | Left lateral aspect of the superior temporal gyrus | Left planum polare of the superior temporal gyrus | Left planum temporale | Left inferior temporal gyrus | Left middle temporal gyrus | Left horizontal ramus of the anterior segment of the lateral sulcus | Left vertical ramus of the anterior segment of the lateral sulcus | Left posterior ramus of the lateral sulcus | Left occipital pole | Left temporal pole | Left calcarine sulcus | Left central sulcus |
|---|---|---|---|---|---|---|---|---|---|---|---|---|---|---|
| **Fisher F** | **4.09** | **9.28** | **2.6** | **6.7** | **5.08** | **4.02** | **5.18** | **20.04** | **18.68** | **4.58** | **3.45** | **4.77** | **3.9** | **6.25** |
| **Fisher FWE p** | **0.999** | **0.999** | **0.999** | **0.999** | **0.999** | **0.999** | **0.999** | **0.512** | **0.609** | **0.999** | **0.999** | **0.999** | **0.999** | **0.999** |
| MD | -0.45 | -0.89 | -1.59 | -0.09 | -0.64 | -1.32 | -0.88 | 1.18 | 0.72 | -2.4 | -1.95 | -1.03 | -0.93 | -1.04 |
| MD FWE p | 0.998 | 0.999 | 0.999 | 0.987 | 0.999 | 0.999 | 0.999 | 0.545 | 0.807 | 0.999 | 0.999 | 0.999 | 0.999 | 0.999 |
| MD mFWE p | 0.999 | 0.999 | 0.999 | 0.999 | 0.999 | 0.999 | 0.999 | 0.999 | 0.999 | 0.999 | 0.999 | 0.999 | 0.999 | 0.999 |
| RD | -0.41 | -0.87 | -1.8 | -0.11 | -0.91 | -1.36 | -1.52 | 0.81 | 0.67 | -2.3 | -2.12 | -0.99 | -0.74 | -1.18 |
| RD FWE p | 0.999 | 0.999 | 0.999 | 0.993 | 0.999 | 0.999 | 0.999 | 0.807 | 0.866 | 0.999 | 0.999 | 0.999 | 0.999 | 0.999 |
| RD mFWE p | 0.999 | 0.999 | 0.999 | 0.999 | 0.999 | 0.999 | 0.999 | 0.999 | 0.999 | 0.999 | 0.999 | 0.999 | 0.999 | 0.999 |
| AD | -0.49 | -0.84 | -1.05 | -0.04 | -0.05 | -0.88 | 0.17 | 1.73 | 0.73 | -2.2 | -1.31 | -0.85 | -1.15 | -0.71 |
| AD FWE p | 0.999 | 0.999 | 0.999 | 0.99 | 0.99 | 0.999 | 0.974 | 0.227 | 0.828 | 0.999 | 0.999 | 0.999 | 0.999 | 0.999 |
| AD mFWE p | 0.999 | 0.999 | 0.999 | 0.999 | 0.999 | 0.999 | 0.999 | 0.995 | 0.999 | 0.999 | 0.999 | 0.999 | 0.999 | 0.999 |
| Volume | -0.36 | 1.43 | -0.14 | 0.46 | -1.07 | 0.36 | 0.42 | 1.41 | 1.8 | 0.84 | 0.69 | -0.07 | 0.61 | 1.32 |
| Volume FWE p | 0.999 | 0.987 | 0.999 | 0.999 | 0.999 | 0.999 | 0.999 | 0.988 | 0.943 | 0.999 | 0.999 | 0.999 | 0.999 | 0.992 |
| Volume mFWE p | 0.999 | 0.999 | 0.999 | 0.999 | 0.999 | 0.999 | 0.999 | 0.999 | 0.991 | 0.999 | 0.999 | 0.999 | 0.999 | 0.999 |
| Thickness | 0.42 | -0.7 | 0.33 | 0.6 | -0.55 | 0.15 | 0.45 | 0.11 | -0.93 | 0.05 | 1.01 | -0.52 | 1.62 | 0.94 |
| Thickness FWE p | 0.999 | 0.999 | 0.999 | 0.999 | 0.999 | 0.999 | 0.999 | 0.999 | 0.999 | 0.999 | 0.999 | 0.999 | 0.981 | 0.999 |
| Thickness mFWE p | 0.999 | 0.999 | 0.999 | 0.999 | 0.999 | 0.999 | 0.999 | 0.999 | 0.999 | 0.999 | 0.999 | 0.999 | 0.999 | 0.999 |

Table B21 continued

| | Left anterior segment of the circular sulcus of the insula | Left inferior segment of the circular sulcus of the insula | Left superior segment of the circular sulcus of the insula | Left anterior transverse collateral sulcus | Left posterior transverse collateral sulcus | Left inferior frontal sulcus | Left middle frontal sulcus | Left superior frontal sulcus | Left sulcus intermedius primus | Left intraparietal sulcus and transverse parietal sulci | Left middle occipital sulcus and lunatus sulcus | Left superior occipital sulcus and transverse occipital sulcus | Left anterior occipital sulcus and preoccipital notch | Left lateral occipito temporal sulcus |
|---|---|---|---|---|---|---|---|---|---|---|---|---|---|---|
| **Fisher F** | **13.06** | **3.28** | **8.94** | **11.83** | **4.24** | **6.75** | **4.73** | **11.61** | **4.34** | **3.63** | **3.25** | **2.71** | **5.71** | **5.03** |
| **Fisher FWE p** | **0.945** | **0.999** | **0.999** | **0.977** | **0.999** | **0.999** | **0.999** | **0.981** | **0.999** | **0.999** | **0.999** | **0.999** | **0.999** | **0.999** |
| MD | 0.84 | -0.78 | -0.28 | -1.53 | -1.52 | -0.25 | -0.99 | 0.02 | -1.45 | -1.8 | -1.75 | -1.54 | -0.74 | -1.61 |
| MD FWE p | 0.752 | 0.999 | 0.995 | 0.999 | 0.999 | 0.994 | 0.999 | 0.98 | 0.999 | 0.999 | 0.999 | 0.999 | 0.999 | 0.999 |
| MD mFWE p | 0.999 | 0.999 | 0.999 | 0.999 | 0.999 | 0.999 | 0.999 | 0.999 | 0.999 | 0.999 | 0.999 | 0.999 | 0.999 | 0.999 |
| RD | 0.26 | -0.91 | -0.51 | -0.71 | -1.43 | -0.62 | -1.6 | -0.67 | -1.82 | -1.87 | -1.8 | -1.83 | -1.06 | -1.32 |
| RD FWE p | 0.964 | 0.999 | 0.999 | 0.999 | 0.999 | 0.999 | 0.999 | 0.999 | 0.999 | 0.999 | 0.999 | 0.999 | 0.999 | 0.999 |
| RD mFWE p | 0.999 | 0.999 | 0.999 | 0.999 | 0.999 | 0.999 | 0.999 | 0.999 | 0.999 | 0.999 | 0.999 | 0.999 | 0.999 | 0.999 |
| AD | 1.62 | -0.38 | 0.26 | -1.97 | -1.31 | 0.56 | 0.32 | 1.45 | -0.38 | -1.47 | -1.34 | -0.79 | < 0.001 | -1.62 |
| AD FWE p | 0.286 | 0.998 | 0.961 | 0.999 | 0.999 | 0.893 | 0.952 | 0.39 | 0.999 | 0.999 | 0.999 | 0.999 | 0.988 | 0.999 |
| AD mFWE p | 0.998 | 0.999 | 0.999 | 0.999 | 0.999 | 0.999 | 0.999 | 0.999 | 0.999 | 0.999 | 0.999 | 0.999 | 0.999 | 0.999 |
| Volume | 0.36 | -0.11 | 1.17 | 2.63 | -0.24 | 0.53 | 0.3 | -0.16 | 0.42 | 0.07 | 0.58 | -0.25 | 0.23 | -1.28 |
| Volume FWE p | 0.999 | 0.999 | 0.996 | 0.579 | 0.999 | 0.999 | 0.999 | 0.999 | 0.999 | 0.999 | 0.999 | 0.999 | 0.999 | 0.999 |
| Volume mFWE p | 0.999 | 0.999 | 0.999 | 0.698 | 0.999 | 0.999 | 0.999 | 0.999 | 0.999 | 0.999 | 0.999 | 0.999 | 0.999 | 0.999 |
| Thickness | 1.82 | 1.07 | 0.17 | 1.39 | -0.65 | 1.35 | 0.95 | -0.85 | 0.21 | -0.26 | 0.94 | 0.27 | -0.19 | -1.22 |
| Thickness FWE p | 0.946 | 0.999 | 0.999 | 0.996 | 0.999 | 0.997 | 0.999 | 0.999 | 0.999 | 0.999 | 0.999 | 0.999 | 0.999 | 0.999 |
| Thickness mFWE p | 0.999 | 0.999 | 0.999 | 0.999 | 0.999 | 0.999 | 0.999 | 0.999 | 0.999 | 0.999 | 0.999 | 0.999 | 0.999 | 0.999 |

Table B21 continued

| | Left lateral orbital sulcus | Left medial orbital sulcus | Left orbital sulci | Left parieto occipital sulcus | Left pericallosal sulcus | Left postcentral sulcus | Left inferior part of the precentral sulcus | Left superior part of the precentral sulcus | Left suborbital sulcus | Left subparietal sulcus | Left inferior temporal sulcus | Left superior temporal sulcus | Left transverse temporal sulcus | Right fronto marginal gyrus and sulcus |
|---|---|---|---|---|---|---|---|---|---|---|---|---|---|---|
| **Fisher F** | **13.37** | **7.49** | **13.27** | **3.38** | **6.45** | **9.22** | **12.53** | **8.99** | **8.34** | **5.85** | **5.18** | **2.33** | **10.55** | **9.64** |
| **Fisher FWE p** | **0.934** | **0.999** | **0.937** | **0.999** | **0.999** | **0.999** | **0.961** | **0.999** | **0.999** | **0.999** | **0.999** | **0.999** | **0.994** | **0.999** |
| MD | 0.42 | -1.48 | 0.76 | -0.89 | -0.88 | -0.59 | -1.64 | -0.05 | 0.2 | -0.91 | -1.18 | -1.31 | -1.35 | 0.49 |
| MD FWE p | 0.915 | 0.999 | 0.789 | 0.999 | 0.999 | 0.999 | 0.999 | 0.985 | 0.959 | 0.999 | 0.999 | 0.999 | 0.999 | 0.896 |
| MD mFWE p | 0.999 | 0.999 | 0.999 | 0.999 | 0.999 | 0.999 | 0.999 | 0.999 | 0.999 | 0.999 | 0.999 | 0.999 | 0.999 | 0.999 |
| RD | -0.1 | -1.44 | 0.38 | -0.72 | -0.74 | -0.71 | -1.94 | -0.37 | 0.11 | -0.92 | -1.74 | -1.46 | -1.13 | 0.24 |
| RD FWE p | 0.992 | 0.999 | 0.945 | 0.999 | 0.999 | 0.999 | 0.999 | 0.998 | 0.98 | 0.999 | 0.999 | 0.999 | 0.999 | 0.967 |
| RD mFWE p | 0.999 | 0.999 | 0.999 | 0.999 | 0.999 | 0.999 | 0.999 | 0.999 | 0.999 | 0.999 | 0.999 | 0.999 | 0.999 | 0.999 |
| AD | 1.21 | -1.05 | 1.12 | -1.11 | -0.79 | -0.26 | -0.82 | 0.59 | 0.25 | -0.77 | -0.16 | -0.79 | -1.49 | 0.71 |
| AD FWE p | 0.55 | 0.999 | 0.609 | 0.999 | 0.999 | 0.997 | 0.999 | 0.881 | 0.964 | 0.999 | 0.995 | 0.999 | 0.999 | 0.835 |
| AD mFWE p | 0.999 | 0.999 | 0.999 | 0.999 | 0.999 | 0.999 | 0.999 | 0.999 | 0.999 | 0.999 | 0.999 | 0.999 | 0.999 | 0.999 |
| Volume | 1.2 | 0.29 | 1.07 | 0.23 | 1.25 | 0.84 | 2.74 | 0.78 | -0.05 | 0.61 | 0.48 | -0.7 | 0.45 | 0.45 |
| Volume FWE p | 0.996 | 0.999 | 0.998 | 0.999 | 0.994 | 0.999 | 0.512 | 0.999 | 0.999 | 0.999 | 0.999 | 0.999 | 0.999 | 0.999 |
| Volume mFWE p | 0.999 | 0.999 | 0.999 | 0.999 | 0.999 | 0.999 | 0.622 | 0.999 | 0.999 | 0.999 | 0.999 | 0.999 | 0.999 | 0.999 |
| Thickness | 0.05 | -1.38 | 1.24 | 0.98 | 0.75 | -1.04 | 0.99 | 0.12 | -0.29 | -0.31 | < 0.001 | 0.31 | -2.03 | 0.92 |
| Thickness FWE p | 0.999 | 0.999 | 0.999 | 0.999 | 0.999 | 0.999 | 0.999 | 0.999 | 0.999 | 0.999 | 0.999 | 0.999 | 0.999 | 0.999 |
| Thickness mFWE p | 0.999 | 0.999 | 0.999 | 0.999 | 0.999 | 0.999 | 0.999 | 0.999 | 0.999 | 0.999 | 0.999 | 0.999 | 0.999 | 0.999 |

Table B21 continued

| | Right paracentral lobule and sulcus | Right subcentral gyrus and sulci | Right transverse frontopolar gyri and sulci | Right anterior part of the cingulate gyrus and sulcus | Right middle anterior part of the cingulate gyrus and sulcus | Right middle posterior part of the cingulate gyrus and sulcus | Right posterior dorsal part of the cingulate gyrus | Right posterior ventral part of the cingulate gyrus | Right cuneus | Right opercular part of the inferior frontal gyrus | Right orbital part of the inferior frontal gyrus | Right triangular part of the inferior frontal gyrus | Right middle frontal gyrus | Right superior frontal gyrus |
|---|---|---|---|---|---|---|---|---|---|---|---|---|---|---|
| **Fisher F** | **10.89** | **6.82** | **8.92** | **9.37** | **8.06** | **7.14** | **4.68** | **5.28** | **4.86** | **7.93** | **6.49** | **8** | **11.82** | **9.28** |
| **Fisher FWE p** | **0.991** | **0.999** | **0.999** | **0.999** | **0.999** | **0.999** | **0.999** | **0.999** | **0.999** | **0.999** | **0.999** | **0.999** | **0.978** | **0.999** |
| MD | 0.36 | -0.77 | -0.18 | 0.24 | -0.57 | -0.11 | -1.85 | -0.74 | -1.84 | -0.9 | -0.32 | -0.95 | 0.05 | -0.4 |
| MD FWE p | 0.929 | 0.999 | 0.992 | 0.952 | 0.999 | 0.988 | 0.999 | 0.999 | 0.999 | 0.999 | 0.996 | 0.999 | 0.977 | 0.997 |
| MD mFWE p | 0.999 | 0.999 | 0.999 | 0.999 | 0.999 | 0.999 | 0.999 | 0.999 | 0.999 | 0.999 | 0.999 | 0.999 | 0.999 | 0.999 |
| RD | -0.12 | -0.9 | -0.49 | -0.03 | -1.14 | -0.34 | -1.62 | -0.53 | -1.98 | -1.05 | -0.68 | -1.09 | -0.33 | -0.86 |
| RD FWE p | 0.993 | 0.999 | 0.999 | 0.989 | 0.999 | 0.998 | 0.999 | 0.999 | 0.999 | 0.999 | 0.999 | 0.999 | 0.998 | 0.999 |
| RD mFWE p | 0.999 | 0.999 | 0.999 | 0.999 | 0.999 | 0.999 | 0.999 | 0.999 | 0.999 | 0.999 | 0.999 | 0.999 | 0.999 | 0.999 |
| AD | 1.13 | -0.42 | 0.32 | 0.63 | 0.68 | 0.37 | -1.88 | -0.93 | -1.44 | -0.52 | 0.38 | -0.6 | 0.71 | 0.51 |
| AD FWE p | 0.602 | 0.999 | 0.953 | 0.866 | 0.849 | 0.942 | 0.999 | 0.999 | 0.999 | 0.999 | 0.94 | 0.999 | 0.837 | 0.909 |
| AD mFWE p | 0.999 | 0.999 | 0.999 | 0.999 | 0.999 | 0.999 | 0.999 | 0.999 | 0.999 | 0.999 | 0.999 | 0.999 | 0.999 | 0.999 |
| Volume | 0.11 | 0.81 | 0.09 | -0.25 | -0.07 | -0.52 | 0.72 | 0.53 | 1.26 | 0.32 | 0.27 | 1.62 | -0.06 | -0.51 |
| Volume FWE p | 0.999 | 0.999 | 0.999 | 0.999 | 0.999 | 0.999 | 0.999 | 0.999 | 0.994 | 0.999 | 0.999 | 0.971 | 0.999 | 0.999 |
| Volume mFWE p | 0.999 | 0.999 | 0.999 | 0.999 | 0.999 | 0.999 | 0.999 | 0.999 | 0.999 | 0.999 | 0.999 | 0.998 | 0.999 | 0.999 |
| Thickness | -0.32 | -0.32 | -0.96 | -0.57 | -0.79 | -0.44 | -0.09 | 0.09 | 1.85 | -1.26 | 0.25 | 0.44 | -1.47 | -1.36 |
| Thickness FWE p | 0.999 | 0.999 | 0.999 | 0.999 | 0.999 | 0.999 | 0.999 | 0.999 | 0.938 | 0.999 | 0.999 | 0.999 | 0.999 | 0.999 |
| Thickness mFWE p | 0.999 | 0.999 | 0.999 | 0.999 | 0.999 | 0.999 | 0.999 | 0.999 | 0.999 | 0.999 | 0.999 | 0.999 | 0.999 | 0.999 |

Table B21 continued

| | Right short insular gyri | Right middle occipital gyrus | Right superior occipital gyrus | Right lateral occipito temporal gyrus | Right lingual gyrus | Right parahippocampal gyrus | Right orbital gyri | Right angular gyrus | Right supramarginal gyrus | Right superior parietal lobule | Right postcentral gyrus | Right precentral gyrus | Right precuneus |
|---|---|---|---|---|---|---|---|---|---|---|---|---|---|
| **Fisher F** | **4.97** | **3.73** | **4.37** | **4.25** | **7.16** | **2.38** | **3.19** | **4.98** | **6.42** | **12.11** | **8.54** | **6.81** | **10.24** |
| **Fisher FWE p** | **0.999** | **0.999** | **0.999** | **0.999** | **0.999** | **0.999** | **0.999** | **0.999** | **0.999** | **0.972** | **0.999** | **0.999** | **0.996** |
| MD | -0.78 | -1.09 | -0.88 | -0.89 | -2.53 | -1.37 | -1.07 | -0.64 | -1.15 | -0.27 | -0.79 | -0.94 | -0.63 |
| MD FWE p | 0.999 | 0.999 | 0.999 | 0.999 | 0.999 | 0.999 | 0.999 | 0.999 | 0.999 | 0.994 | 0.999 | 0.999 | 0.999 |
| MD mFWE p | 0.999 | 0.999 | 0.999 | 0.999 | 0.999 | 0.999 | 0.999 | 0.999 | 0.999 | 0.999 | 0.999 | 0.999 | 0.999 |
| RD | -0.96 | -1.44 | -1.37 | -0.8 | -2.37 | -1.29 | -0.8 | -0.9 | -1.33 | -0.62 | -0.91 | -1.32 | -0.82 |
| RD FWE p | 0.999 | 0.999 | 0.999 | 0.999 | 0.999 | 0.999 | 0.999 | 0.999 | 0.999 | 0.999 | 0.999 | 0.999 | 0.999 |
| RD mFWE p | 0.999 | 0.999 | 0.999 | 0.999 | 0.999 | 0.999 | 0.999 | 0.999 | 0.999 | 0.999 | 0.999 | 0.999 | 0.999 |
| AD | -0.34 | -0.39 | < 0.001 | -0.75 | -2.56 | -1.21 | -1.18 | -0.11 | -0.7 | 0.41 | -0.5 | -0.19 | -0.21 |
| AD FWE p | 0.998 | 0.999 | 0.988 | 0.999 | 0.999 | 0.999 | 0.999 | 0.993 | 0.999 | 0.933 | 0.999 | 0.995 | 0.996 |
| AD mFWE p | 0.999 | 0.999 | 0.999 | 0.999 | 0.999 | 0.999 | 0.999 | 0.999 | 0.999 | 0.999 | 0.999 | 0.999 | 0.999 |
| Volume | 0.61 | 0.01 | 0.26 | -0.78 | 1.9 | 0.18 | 0.12 | -0.96 | 1.21 | 1.24 | 1.16 | 1.22 | 1.04 |
| Volume FWE p | 0.999 | 0.999 | 0.999 | 0.999 | 0.92 | 0.999 | 0.999 | 0.999 | 0.996 | 0.995 | 0.997 | 0.995 | 0.998 |
| Volume mFWE p | 0.999 | 0.999 | 0.999 | 0.999 | 0.983 | 0.999 | 0.999 | 0.999 | 0.999 | 0.999 | 0.999 | 0.999 | 0.999 |
| Thickness | 0.67 | 0.25 | 0.71 | -0.51 | 3.14 | 1.92 | 0.69 | -0.51 | 0.24 | -1.06 | -0.66 | 0.49 | -1.19 |
| Thickness FWE p | 0.999 | 0.999 | 0.999 | 0.999 | 0.179 | 0.915 | 0.999 | 0.999 | 0.999 | 0.999 | 0.999 | 0.999 | 0.999 |
| Thickness mFWE p | 0.999 | 0.999 | 0.999 | 0.999 | 0.637 | 0.999 | 0.999 | 0.999 | 0.999 | 0.999 | 0.999 | 0.999 | 0.999 |

Table B21 continued

| | Right subcallosal gyrus | Right anterior transverse temporal gyrus | Right lateral aspect of the superior temporal gyrus | Right planum polare of the superior temporal gyrus | Right planum temporale | Right inferior temporal gyrus | Right middle temporal gyrus | Right horizontal ramus of the anterior segment of the lateral sulcus | Right vertical ramus of the anterior segment of the lateral sulcus | Right posterior ramus of the lateral sulcus | Right occipital pole | Right temporal pole | Right calcarine sulcus | Right central sulcus |
|---|---|---|---|---|---|---|---|---|---|---|---|---|---|---|
| **Fisher F** | **2.55** | **6.99** | **4.89** | **3.73** | **10.22** | **8.09** | **4.13** | **10.51** | **8.57** | **7.78** | **8.43** | **3.43** | **4.3** | **7.28** |
| **Fisher FWE p** | **0.999** | **0.999** | **0.999** | **0.999** | **0.996** | **0.999** | **0.999** | **0.994** | **0.999** | **0.999** | **0.999** | **0.999** | **0.999** | **0.999** |
| MD | -1.35 | -1.6 | -1.52 | -0.75 | -1.09 | -0.69 | -0.97 | 0.48 | -0.36 | -1.85 | -2.23 | -1.71 | -1.47 | -0.13 |
| MD FWE p | 0.999 | 0.999 | 0.999 | 0.999 | 0.999 | 0.999 | 0.999 | 0.898 | 0.997 | 0.999 | 0.999 | 0.999 | 0.999 | 0.989 |
| MD mFWE p | 0.999 | 0.999 | 0.999 | 0.999 | 0.999 | 0.999 | 0.999 | 0.999 | 0.999 | 0.999 | 0.999 | 0.999 | 0.999 | 0.999 |
| RD | -1.36 | -1.77 | -1.68 | -1.01 | -1.29 | -1.35 | -1.43 | -0.04 | -0.42 | -2.05 | -2.28 | -1.5 | -1.42 | -0.34 |
| RD FWE p | 0.999 | 0.999 | 0.999 | 0.999 | 0.999 | 0.999 | 0.999 | 0.99 | 0.999 | 0.999 | 0.999 | 0.999 | 0.999 | 0.998 |
| RD mFWE p | 0.999 | 0.999 | 0.999 | 0.999 | 0.999 | 0.999 | 0.999 | 0.999 | 0.999 | 0.999 | 0.999 | 0.999 | 0.999 | 0.999 |
| AD | -1.19 | -1.13 | -1.05 | -0.19 | -0.58 | 0.67 | -0.09 | 1.46 | -0.18 | -1.13 | -1.72 | -1.62 | -1.41 | 0.27 |
| AD FWE p | 0.999 | 0.999 | 0.999 | 0.995 | 0.999 | 0.854 | 0.992 | 0.379 | 0.995 | 0.999 | 0.999 | 0.999 | 0.999 | 0.96 |
| AD mFWE p | 0.999 | 0.999 | 0.999 | 0.999 | 0.999 | 0.999 | 0.999 | 0.999 | 0.999 | 0.999 | 0.999 | 0.999 | 0.999 | 0.999 |
| Volume | 0.28 | 1.58 | 0.84 | 0.03 | -0.13 | -0.27 | 0.14 | -0.46 | 0.45 | 1.85 | 2.1 | 0.42 | 1.03 | 0.5 |
| Volume FWE p | 0.999 | 0.975 | 0.999 | 0.999 | 0.999 | 0.999 | 0.999 | 0.999 | 0.999 | 0.932 | 0.858 | 0.999 | 0.998 | 0.999 |
| Volume mFWE p | 0.999 | 0.998 | 0.999 | 0.999 | 0.999 | 0.999 | 0.999 | 0.999 | 0.999 | 0.988 | 0.952 | 0.999 | 0.999 | 0.999 |
| Thickness | 1.93 | 0.45 | 0.17 | 1.02 | -2.06 | -0.97 | 0.5 | 0.42 | -0.94 | 0.75 | 1.23 | 0.35 | 1.9 | 0.32 |
| Thickness FWE p | 0.91 | 0.999 | 0.999 | 0.999 | 0.999 | 0.999 | 0.999 | 0.999 | 0.999 | 0.999 | 0.999 | 0.999 | 0.922 | 0.999 |
| Thickness mFWE p | 0.999 | 0.999 | 0.999 | 0.999 | 0.999 | 0.999 | 0.999 | 0.999 | 0.999 | 0.999 | 0.999 | 0.999 | 0.999 | 0.999 |

Table B21 continued

| | Right anterior segment of the circular sulcus of the insula | Right inferior segment of the circular sulcus of the insula | Right superior segment of the circular sulcus of the insula | Right anterior transverse collateral sulcus | Right posterior transverse collateral sulcus | Right inferior frontal sulcus | Right middle frontal sulcus | Right superior frontal sulcus | Right sulcus intermedius primus | Right intraparietal sulcus and transverse parietal sulci | Right middle occipital sulcus and lunatus sulcus | Right superior occipital sulcus and transverse occipital sulcus | Right anterior occipital sulcus and preoccipital notch | Right lateral occipito temporal sulcus |
|---|---|---|---|---|---|---|---|---|---|---|---|---|---|---|
| **Fisher F** | **5.23** | **5.03** | **8.31** | **6.9** | **6.97** | **7.11** | **6.82** | **10.08** | **2.33** | **8.23** | **3.63** | **4.78** | **3.66** | **2.83** |
| **Fisher FWE p** | **0.999** | **0.999** | **0.999** | **0.999** | **0.999** | **0.999** | **0.999** | **0.997** | **0.999** | **0.999** | **0.999** | **0.999** | **0.999** | **0.999** |
| MD | -0.35 | -0.42 | -0.39 | -0.29 | -2.17 | -0.1 | -0.86 | -0.08 | -1.58 | -0.22 | -2.09 | -0.79 | -0.48 | -1.52 |
| MD FWE p | 0.996 | 0.998 | 0.997 | 0.995 | 0.999 | 0.988 | 0.999 | 0.987 | 0.999 | 0.993 | 0.999 | 0.999 | 0.998 | 0.999 |
| MD mFWE p | 0.999 | 0.999 | 0.999 | 0.999 | 0.999 | 0.999 | 0.999 | 0.999 | 0.999 | 0.999 | 0.999 | 0.999 | 0.999 | 0.999 |
| RD | -0.62 | -0.84 | -0.71 | 0.04 | -1.73 | -0.38 | -1.32 | -0.54 | -1.71 | -0.32 | -2.22 | -0.9 | -0.71 | -1.25 |
| RD FWE p | 0.999 | 0.999 | 0.999 | 0.986 | 0.999 | 0.998 | 0.999 | 0.999 | 0.999 | 0.998 | 0.999 | 0.999 | 0.999 | 0.999 |
| RD mFWE p | 0.999 | 0.999 | 0.999 | 0.999 | 0.999 | 0.999 | 0.999 | 0.999 | 0.999 | 0.999 | 0.999 | 0.999 | 0.999 | 0.999 |
| AD | 0.24 | 0.39 | 0.3 | -0.62 | -2.32 | 0.47 | 0.16 | 0.9 | -1.1 | < 0.001 | -1.4 | -0.47 | 0.09 | -1.28 |
| AD FWE p | 0.965 | 0.938 | 0.956 | 0.999 | 0.999 | 0.92 | 0.974 | 0.74 | 0.999 | 0.988 | 0.999 | 0.999 | 0.982 | 0.999 |
| AD mFWE p | 0.999 | 0.999 | 0.999 | 0.999 | 0.999 | 0.999 | 0.999 | 0.999 | 0.999 | 0.999 | 0.999 | 0.999 | 0.999 | 0.999 |
| Volume | 0.26 | 0.03 | 0.65 | 0.72 | 1.83 | 0.16 | 1.03 | 0.57 | 0.25 | 0.26 | 0.76 | -0.33 | -1.33 | -0.34 |
| Volume FWE p | 0.999 | 0.999 | 0.999 | 0.999 | 0.936 | 0.999 | 0.998 | 0.999 | 0.999 | 0.999 | 0.999 | 0.999 | 0.999 | 0.999 |
| Volume mFWE p | 0.999 | 0.999 | 0.999 | 0.999 | 0.989 | 0.999 | 0.999 | 0.999 | 0.999 | 0.999 | 0.999 | 0.999 | 0.999 | 0.999 |
| Thickness | 1.97 | 1.27 | -0.47 | 0.3 | 2.12 | 0.21 | 0.48 | -0.44 | 2.58 | -0.76 | 0.91 | -0.43 | 0.61 | 0.02 |
| Thickness FWE p | 0.896 | 0.999 | 0.999 | 0.999 | 0.826 | 0.999 | 0.999 | 0.999 | 0.52 | 0.999 | 0.999 | 0.999 | 0.999 | 0.999 |
| Thickness mFWE p | 0.998 | 0.999 | 0.999 | 0.999 | 0.995 | 0.999 | 0.999 | 0.999 | 0.933 | 0.999 | 0.999 | 0.999 | 0.999 | 0.999 |

Table B21 continued

| | Right lateral orbital sulcus | Right medial orbital sulcus | Right orbital sulci | Right parieto occipital sulcus | Right pericallosal sulcus | Right postcentral sulcus | Right inferior part of the precentral sulcus | Right superior part of the precentral sulcus | Right suborbital sulcus | Right subparietal sulcus | Right inferior temporal sulcus | Right superior temporal sulcus | Right transverse temporal sulcus |
|---|---|---|---|---|---|---|---|---|---|---|---|---|---|
| **Fisher F** | **3.99** | **3.86** | **8.75** | **3.65** | **12.69** | **8.3** | **15.57** | **5.63** | **7.51** | **6.35** | **7.01** | **3.63** | **5.69** |
| **Fisher FWE p** | **0.999** | **0.999** | **0.999** | **0.999** | **0.956** | **0.999** | **0.824** | **0.999** | **0.999** | **0.999** | **0.999** | **0.999** | **0.999** |
| MD | -0.47 | -0.71 | 0.34 | -1.25 | 0.46 | -0.38 | -0.86 | -0.51 | 0.25 | -0.83 | -0.47 | -0.83 | -1.97 |
| MD FWE p | 0.998 | 0.999 | 0.934 | 0.999 | 0.903 | 0.997 | 0.999 | 0.998 | 0.951 | 0.999 | 0.998 | 0.999 | 0.999 |
| MD mFWE p | 0.999 | 0.999 | 0.999 | 0.999 | 0.999 | 0.999 | 0.999 | 0.999 | 0.999 | 0.999 | 0.999 | 0.999 | 0.999 |
| RD | -0.66 | -0.57 | 0.29 | -1.31 | -0.28 | -0.52 | -1.54 | -0.94 | 0.26 | -0.86 | -0.7 | -1 | -2.04 |
| RD FWE p | 0.999 | 0.999 | 0.961 | 0.999 | 0.997 | 0.999 | 0.999 | 0.999 | 0.964 | 0.999 | 0.999 | 0.999 | 0.999 |
| RD mFWE p | 0.999 | 0.999 | 0.999 | 0.999 | 0.999 | 0.999 | 0.999 | 0.999 | 0.999 | 0.999 | 0.999 | 0.999 | 0.999 |
| AD | -0.06 | -0.72 | 0.32 | -1.02 | 1.24 | -0.07 | 0.54 | 0.42 | 0.18 | -0.67 | 0.06 | -0.31 | -1.58 |
| AD FWE p | 0.991 | 0.999 | 0.952 | 0.999 | 0.529 | 0.991 | 0.898 | 0.932 | 0.973 | 0.999 | 0.983 | 0.998 | 0.999 |
| AD mFWE p | 0.999 | 0.999 | 0.999 | 0.999 | 0.999 | 0.999 | 0.999 | 0.999 | 0.999 | 0.999 | 0.999 | 0.999 | 0.999 |
| Volume | -0.23 | 0.33 | 0.34 | 0.68 | -0.03 | 1.02 | 1.93 | 0.15 | -0.93 | -0.04 | -0.09 | 0.02 | 1.06 |
| Volume FWE p | 0.999 | 0.999 | 0.999 | 0.999 | 0.999 | 0.999 | 0.912 | 0.999 | 0.999 | 0.999 | 0.999 | 0.999 | 0.998 |
| Volume mFWE p | 0.999 | 0.999 | 0.999 | 0.999 | 0.999 | 0.999 | 0.98 | 0.999 | 0.999 | 0.999 | 0.999 | 0.999 | 0.999 |
| Thickness | 1.09 | 1.56 | 0.37 | 1.64 | -0.99 | -0.18 | -1.48 | 0.53 | -0.21 | -0.96 | -0.74 | 0.82 | -0.13 |
| Thickness FWE p | 0.999 | 0.987 | 0.999 | 0.979 | 0.999 | 0.999 | 0.999 | 0.999 | 0.999 | 0.999 | 0.999 | 0.999 | 0.999 |
| Thickness mFWE p | 0.999 | 0.999 | 0.999 | 0.999 | 0.999 | 0.999 | 0.999 | 0.999 | 0.999 | 0.999 | 0.999 | 0.999 | 0.999 |

**Table B22 Positive correlations between cortical grey matter metrics and internalizing problems**

| | Left fronto marginal gyrus and sulcus | Left inferior occipital gyrus and sulcus | Left paracentral lobule and sulcus | Left subcentral gyrus and sulci | Left transverse frontopolar gyri and sulci | Left anterior part of the cingulate gyrus and sulcus | Left middle anterior part of the cingulate gyrus and | Left middle posterior part of the cingulate gyrus and | Left posterior dorsal part of the cingulate gyrus | Left posterior ventral part of the cingulate gyrus | Left cuneus | Left opercular part of the inferior frontal gyrus | Left orbital part of the inferior frontal gyrus | Left triangular part of the inferior frontal gyrus | Left middle frontal gyrus |
|---|---|---|---|---|---|---|---|---|---|---|---|---|---|---|---|
| **Fisher F** | **7.93** | **7.57** | **9.76** | **3.78** | **4.67** | **8.77** | **5.7** | **11.15** | **6.24** | **18.26** | **3.94** | **4.62** | **4.14** | **6.07** | **4.85** |
| **Fisher FWE p** | **0.999** | **0.999** | **0.999** | **0.999** | **0.999** | **0.999** | **0.999** | **0.981** | **0.999** | **0.513** | **0.999** | **0.999** | **0.999** | **0.999** | **0.999** |
| MD | -0.47 | -2.61 | -0.1 | -1.77 | -2.02 | -1.04 | -1.42 | -0.84 | -3.08 | 1.41 | -0.77 | -1.13 | -0.98 | -1.54 | -1.58 |
| MD FWE p | 0.989 | 0.999 | 0.956 | 0.999 | 0.999 | 0.999 | 0.999 | 0.998 | 0.999 | 0.253 | 0.998 | 0.999 | 0.999 | 0.999 | 0.999 |
| MD mFWE p | 0.999 | 0.999 | 0.999 | 0.999 | 0.999 | 0.999 | 0.999 | 0.999 | 0.999 | 0.999 | 0.999 | 0.999 | 0.999 | 0.999 | 0.999 |
| RD | -1.25 | -3.09 | -0.3 | -1.67 | -2.86 | -1.64 | -2.11 | -1.06 | -2.82 | 1.88 | -0.98 | -1.34 | -1.65 | -1.76 | -2.06 |
| RD FWE p | 0.999 | 0.999 | 0.978 | 0.999 | 0.999 | 0.999 | 0.999 | 0.999 | 0.999 | 0.053 | 0.999 | 0.999 | 0.999 | 0.999 | 0.999 |
| RD mFWE p | 0.999 | 0.999 | 0.999 | 0.999 | 0.999 | 0.999 | 0.999 | 0.999 | 0.999 | 0.994 | 0.999 | 0.999 | 0.999 | 0.999 | 0.999 |
| AD | 0.78 | -1.27 | 0.24 | -1.75 | -0.39 | 0.13 | 0.06 | -0.22 | -2.98 | 0.4 | -0.36 | -0.58 | 0.29 | -0.99 | -0.52 |
| AD FWE p | 0.751 | 0.999 | 0.943 | 0.999 | 0.997 | 0.962 | 0.971 | 0.992 | 0.999 | 0.904 | 0.996 | 0.999 | 0.931 | 0.999 | 0.999 |
| AD mFWE p | 0.999 | 0.999 | 0.999 | 0.999 | 0.999 | 0.999 | 0.999 | 0.999 | 0.999 | 0.999 | 0.999 | 0.999 | 0.999 | 0.999 | 0.999 |
| Volume | -0.49 | -0.06 | -1.75 | 0.33 | -0.63 | -2.5 | -1.31 | -2.37 | -0.18 | 0.35 | 0.39 | 0.01 | -0.12 | 1.29 | -2.1 |
| Volume FWE p | 0.999 | 0.999 | 0.999 | 0.999 | 0.999 | 0.999 | 0.999 | 0.999 | 0.999 | 0.999 | 0.999 | 0.999 | 0.999 | 0.998 | 0.999 |
| Volume mFWE p | 0.999 | 0.999 | 0.999 | 0.999 | 0.999 | 0.999 | 0.999 | 0.999 | 0.999 | 0.999 | 0.999 | 0.999 | 0.999 | 0.999 | 0.999 |
| Thickness | -0.81 | -1.66 | -1.57 | -0.09 | -0.82 | -1.82 | -1.05 | -2.35 | -1.42 | -0.36 | 1.8 | -0.38 | 0.69 | 0.37 | -1.08 |
| Thickness FWE p | 0.999 | 0.999 | 0.999 | 0.999 | 0.999 | 0.999 | 0.999 | 0.999 | 0.999 | 0.999 | 0.919 | 0.999 | 0.999 | 0.999 | 0.999 |
| Thickness mFWE p | 0.999 | 0.999 | 0.999 | 0.999 | 0.999 | 0.999 | 0.999 | 0.999 | 0.999 | 0.999 | 0.999 | 0.999 | 0.999 | 0.999 | 0.999 |

Table B22 continued

| | Left long insular gyrus and central sulcus of the insula | Left short insular gyri | Left middle occipital gyrus | Left superior occipital gyrus | Left lateral occipito temporal gyrus | Left lingual gyrus | Left parahippocampal gyrus | Left orbital gyri | Left angular gyrus | Left supramarginal gyrus | Left superior parietal lobule | Left postcentral gyrus | Left precentral gyrus | Left precuneus |
|---|---|---|---|---|---|---|---|---|---|---|---|---|---|---|
| **Fisher F** | **5.75** | **1.95** | **3.96** | **10.42** | **7.38** | **4.68** | **5.2** | **5.87** | **4.11** | **5.21** | **3.48** | **3** | **4.96** | **7.77** |
| **Fisher FWE p** | **0.999** | **0.999** | **0.999** | **0.994** | **0.999** | **0.999** | **0.999** | **0.999** | **0.999** | **0.999** | **0.999** | **0.999** | **0.999** | **0.999** |
| MD | -0.77 | -1.26 | -2.28 | -1.28 | -1.02 | -1.8 | -0.39 | -1.01 | -2.03 | -2.29 | -1.21 | -1.61 | -1.44 | -0.97 |
| MD FWE p | 0.998 | 0.999 | 0.999 | 0.999 | 0.999 | 0.999 | 0.985 | 0.999 | 0.999 | 0.999 | 0.999 | 0.999 | 0.999 | 0.999 |
| MD mFWE p | 0.999 | 0.999 | 0.999 | 0.999 | 0.999 | 0.999 | 0.999 | 0.999 | 0.999 | 0.999 | 0.999 | 0.999 | 0.999 | 0.999 |
| RD | -0.85 | -1.57 | -2.69 | -1.72 | -0.9 | -1.61 | -0.48 | -1.59 | -2.47 | -2.32 | -1.53 | -1.73 | -1.67 | -0.99 |
| RD FWE p | 0.998 | 0.999 | 0.999 | 0.999 | 0.999 | 0.999 | 0.99 | 0.999 | 0.999 | 0.999 | 0.999 | 0.999 | 0.999 | 0.999 |
| RD mFWE p | 0.999 | 0.999 | 0.999 | 0.999 | 0.999 | 0.999 | 0.999 | 0.999 | 0.999 | 0.999 | 0.999 | 0.999 | 0.999 | 0.999 |
| AD | -0.46 | -0.49 | -1.38 | -0.49 | -0.85 | -1.98 | -0.18 | 0.03 | -1.01 | -1.99 | -0.51 | -1.32 | -0.86 | -0.86 |
| AD FWE p | 0.998 | 0.999 | 0.999 | 0.999 | 0.999 | 0.999 | 0.99 | 0.975 | 0.999 | 0.999 | 0.999 | 0.999 | 0.999 | 0.999 |
| AD mFWE p | 0.999 | 0.999 | 0.999 | 0.999 | 0.999 | 0.999 | 0.999 | 0.999 | 0.999 | 0.999 | 0.999 | 0.999 | 0.999 | 0.999 |
| Volume | 0.28 | -0.63 | -0.06 | -1.54 | -1.23 | 1.14 | 0.14 | -0.23 | -1.57 | -1.54 | -0.73 | -0.95 | 0.73 | 0.2 |
| Volume FWE p | 0.999 | 0.999 | 0.999 | 0.999 | 0.999 | 0.999 | 0.999 | 0.999 | 0.999 | 0.999 | 0.999 | 0.999 | 0.999 | 0.999 |
| Volume mFWE p | 0.999 | 0.999 | 0.999 | 0.999 | 0.999 | 0.999 | 0.999 | 0.999 | 0.999 | 0.999 | 0.999 | 0.999 | 0.999 | 0.999 |
| Thickness | -0.4 | 1.19 | -0.55 | -2.33 | -1.64 | 1.03 | 0.39 | -0.73 | -0.97 | -1.39 | -0.26 | -0.45 | 0.01 | -1.36 |
| Thickness FWE p | 0.999 | 0.994 | 0.999 | 0.999 | 0.999 | 0.997 | 0.999 | 0.999 | 0.999 | 0.999 | 0.999 | 0.999 | 0.999 | 0.999 |
| Thickness mFWE p | 0.999 | 0.999 | 0.999 | 0.999 | 0.999 | 0.999 | 0.999 | 0.999 | 0.999 | 0.999 | 0.999 | 0.999 | 0.999 | 0.999 |

Table B22 continued

| | Left subcallosal gyrus | Left anterior transverse temporal gyrus | Left lateral aspect of the superior temporal gyrus | Left planum polare of the superior temporal gyrus | Left planum temporale | Left inferior temporal gyrus | Left middle temporal gyrus | Left horizontal ramus of the anterior segment of the lateral sulcus | Left vertical ramus of the anterior segment of the lateral sulcus | Left posterior ramus of the lateral sulcus | Left occipital pole | Left temporal pole | Left calcarine sulcus | Left central sulcus |
|---|---|---|---|---|---|---|---|---|---|---|---|---|---|---|
| **Fisher F** | **2.48** | **8.07** | **2.53** | **3.83** | **9.14** | **5.29** | **2.81** | **15.08** | **14.98** | **4.79** | **3.44** | **2.74** | **3.74** | **4.94** |
| **Fisher FWE p** | **0.999** | **0.999** | **0.999** | **0.999** | **0.999** | **0.999** | **0.999** | **0.768** | **0.776** | **0.999** | **0.999** | **0.999** | **0.999** | **0.999** |
| MD | -0.66 | -0.92 | -2.17 | -0.83 | -0.55 | -1.17 | -1.83 | 0.69 | 0.47 | -2.7 | -1.85 | -1.71 | -0.84 | -1.02 |
| MD FWE p | 0.996 | 0.999 | 0.999 | 0.998 | 0.993 | 0.999 | 0.999 | 0.67 | 0.78 | 0.999 | 0.999 | 0.999 | 0.998 | 0.999 |
| MD mFWE p | 0.999 | 0.999 | 0.999 | 0.999 | 0.999 | 0.999 | 0.999 | 0.999 | 0.999 | 0.999 | 0.999 | 0.999 | 0.999 | 0.999 |
| RD | -0.71 | -0.95 | -2.28 | -0.85 | -0.93 | -1.55 | -2.54 | 0.32 | 0.47 | -2.73 | -2.1 | -2.02 | -0.81 | -1.32 |
| RD FWE p | 0.996 | 0.999 | 0.999 | 0.998 | 0.999 | 0.999 | 0.999 | 0.84 | 0.771 | 0.999 | 0.999 | 0.999 | 0.998 | 0.999 |
| RD mFWE p | 0.999 | 0.999 | 0.999 | 0.999 | 0.999 | 0.999 | 0.999 | 0.999 | 0.999 | 0.999 | 0.999 | 0.999 | 0.999 | 0.999 |
| AD | -0.52 | -0.8 | -1.74 | -0.58 | 0.23 | -0.33 | -0.48 | 1.32 | 0.42 | -2.21 | -1.1 | -0.88 | -0.82 | -0.37 |
| AD FWE p | 0.999 | 0.999 | 0.999 | 0.999 | 0.944 | 0.996 | 0.998 | 0.446 | 0.898 | 0.999 | 0.999 | 0.999 | 0.999 | 0.997 |
| AD mFWE p | 0.999 | 0.999 | 0.999 | 0.999 | 0.999 | 0.999 | 0.999 | 0.999 | 0.999 | 0.999 | 0.999 | 0.999 | 0.999 | 0.999 |
| Volume | -0.75 | 0.57 | -1.57 | -0.57 | -1.47 | -0.86 | -0.37 | 1.31 | 0.7 | 0.08 | -0.76 | -1.74 | -0.24 | 0.26 |
| Volume FWE p | 0.999 | 0.999 | 0.999 | 0.999 | 0.999 | 0.999 | 0.999 | 0.997 | 0.999 | 0.999 | 0.999 | 0.999 | 0.999 | 0.999 |
| Volume mFWE p | 0.999 | 0.999 | 0.999 | 0.999 | 0.999 | 0.999 | 0.999 | 0.999 | 0.999 | 0.999 | 0.999 | 0.999 | 0.999 | 0.999 |
| Thickness | 1.6 | -1.2 | -0.47 | -0.13 | -1.68 | -0.96 | 0.2 | 0.39 | -1.5 | -0.85 | -0.58 | -0.39 | 0.04 | -0.17 |
| Thickness FWE p | 0.961 | 0.999 | 0.999 | 0.999 | 0.999 | 0.999 | 0.999 | 0.999 | 0.999 | 0.999 | 0.999 | 0.999 | 0.999 | 0.999 |
| Thickness mFWE p | 0.999 | 0.999 | 0.999 | 0.999 | 0.999 | 0.999 | 0.999 | 0.999 | 0.999 | 0.999 | 0.999 | 0.999 | 0.999 | 0.999 |

Table B22 continued

| | Left anterior segment of the circular sulcus of the insula | Left inferior segment of the circular sulcus of the insula | Left superior segment of the circular sulcus of the insula | Left anterior transverse collateral sulcus | Left posterior transverse collateral sulcus | Left inferior frontal sulcus | Left middle frontal sulcus | Left superior frontal sulcus | Left sulcus intermedius primus | Left intraparietal sulcus and transverse parietal sulci | Left middle occipital sulcus and lunatus sulcus | Left superior occipital sulcus and transverse occipital sulcus | Left anterior occipital sulcus and preoccipital notch | Left lateral occipito temporal sulcus |
|---|---|---|---|---|---|---|---|---|---|---|---|---|---|---|
| **Fisher F** | **8.36** | **3.03** | **4.74** | **4.97** | **6.98** | **4.93** | **2.61** | **10.02** | **5.26** | **2.55** | **4.21** | **4.79** | **5.63** | **7.66** |
| **Fisher FWE p** | **0.999** | **0.999** | **0.999** | **0.999** | **0.999** | **0.999** | **0.999** | **0.997** | **0.999** | **0.999** | **0.999** | **0.999** | **0.999** | **0.999** |
| MD | 0.36 | -0.71 | -0.74 | -2.35 | -2.17 | -1.03 | -2.16 | -0.88 | -1.54 | -2.22 | -1.99 | -1.31 | -0.92 | -1.28 |
| MD FWE p | 0.828 | 0.997 | 0.997 | 0.999 | 0.999 | 0.999 | 0.999 | 0.999 | 0.999 | 0.999 | 0.999 | 0.999 | 0.999 | 0.999 |
| MD mFWE p | 0.999 | 0.999 | 0.999 | 0.999 | 0.999 | 0.999 | 0.999 | 0.999 | 0.999 | 0.999 | 0.999 | 0.999 | 0.999 | 0.999 |
| RD | -0.29 | -0.92 | -1.1 | -1.77 | -2.25 | -1.53 | -2.79 | -1.65 | -2.02 | -2.29 | -2.26 | -1.73 | -1.44 | -1.31 |
| RD FWE p | 0.977 | 0.999 | 0.999 | 0.999 | 0.999 | 0.999 | 0.999 | 0.999 | 0.999 | 0.999 | 0.999 | 0.999 | 0.999 | 0.999 |
| RD mFWE p | 0.999 | 0.999 | 0.999 | 0.999 | 0.999 | 0.999 | 0.999 | 0.999 | 0.999 | 0.999 | 0.999 | 0.999 | 0.999 | 0.999 |
| AD | 1.4 | -0.21 | 0.17 | -2.19 | -1.5 | 0.14 | -0.61 | 0.86 | -0.27 | -1.84 | -1.14 | -0.35 | 0.25 | -0.87 |
| AD FWE p | 0.401 | 0.992 | 0.955 | 0.999 | 0.999 | 0.96 | 0.999 | 0.71 | 0.994 | 0.999 | 0.999 | 0.996 | 0.941 | 0.999 |
| AD mFWE p | 0.999 | 0.999 | 0.999 | 0.999 | 0.999 | 0.999 | 0.999 | 0.999 | 0.999 | 0.999 | 0.999 | 0.999 | 0.999 | 0.999 |
| Volume | -1.49 | -0.94 | -0.11 | 1.32 | -0.42 | 0.22 | -0.73 | -1.28 | -0.03 | -1.36 | -0.32 | -0.44 | -0.32 | -1.82 |
| Volume FWE p | 0.999 | 0.999 | 0.999 | 0.997 | 0.999 | 0.999 | 0.999 | 0.999 | 0.999 | 0.999 | 0.999 | 0.999 | 0.999 | 0.999 |
| Volume mFWE p | 0.999 | 0.999 | 0.999 | 0.999 | 0.999 | 0.999 | 0.999 | 0.999 | 0.999 | 0.999 | 0.999 | 0.999 | 0.999 | 0.999 |
| Thickness | 1.49 | 0.6 | 0.23 | 1.7 | -1.64 | 0.21 | -0.02 | -1.65 | -0.67 | -0.45 | -0.73 | -0.68 | -0.49 | -1.82 |
| Thickness FWE p | 0.975 | 0.999 | 0.999 | 0.942 | 0.999 | 0.999 | 0.999 | 0.999 | 0.999 | 0.999 | 0.999 | 0.999 | 0.999 | 0.999 |
| Thickness mFWE p | 0.999 | 0.999 | 0.999 | 0.999 | 0.999 | 0.999 | 0.999 | 0.999 | 0.999 | 0.999 | 0.999 | 0.999 | 0.999 | 0.999 |

Table B22 continued

| | Left lateral orbital sulcus | Left medial orbital sulcus | Left orbital sulci | Left parieto occipital sulcus | Left pericallosal sulcus | Left postcentral sulcus | Left inferior part of the precentral sulcus | Left superior part of the precentral sulcus | Left suborbital sulcus | Left subparietal sulcus | Left inferior temporal sulcus | Left superior temporal sulcus | Left transverse temporal sulcus | Right fronto marginal gyrus and sulcus |
|---|---|---|---|---|---|---|---|---|---|---|---|---|---|---|
| **Fisher F** | **6.42** | **4.75** | **10.27** | **5.22** | **4.42** | **10.92** | **8.75** | **8.73** | **6.92** | **7.54** | **4.31** | **2.09** | **12.25** | **6.35** |
| **Fisher FWE p** | **0.999** | **0.999** | **0.995** | **0.999** | **0.999** | **0.986** | **0.999** | **0.999** | **0.999** | **0.999** | **0.999** | **0.999** | **0.945** | **0.999** |
| MD | -0.97 | -1.79 | 0.52 | -0.59 | -1.25 | -0.91 | -2.43 | -0.39 | -0.12 | -1.19 | -2.07 | -1.91 | -0.56 | -0.37 |
| MD FWE p | 0.999 | 0.999 | 0.758 | 0.994 | 0.999 | 0.999 | 0.999 | 0.985 | 0.959 | 0.999 | 0.999 | 0.999 | 0.993 | 0.984 |
| MD mFWE p | 0.999 | 0.999 | 0.999 | 0.999 | 0.999 | 0.999 | 0.999 | 0.999 | 0.999 | 0.999 | 0.999 | 0.999 | 0.999 | 0.999 |
| RD | -1.46 | -2.11 | -0.23 | -0.46 | -1.56 | -1.13 | -2.83 | -0.91 | -0.46 | -1.27 | -2.89 | -2.13 | -0.55 | -0.99 |
| RD FWE p | 0.999 | 0.999 | 0.971 | 0.989 | 0.999 | 0.999 | 0.999 | 0.999 | 0.989 | 0.999 | 0.999 | 0.999 | 0.993 | 0.999 |
| RD mFWE p | 0.999 | 0.999 | 0.999 | 0.999 | 0.999 | 0.999 | 0.999 | 0.999 | 0.999 | 0.999 | 0.999 | 0.999 | 0.999 | 0.999 |
| AD | 0.01 | -0.88 | 1.48 | -0.77 | -0.45 | -0.32 | -1.29 | 0.73 | 0.27 | -0.89 | -0.49 | -1.13 | -0.48 | 0.57 |
| AD FWE p | 0.977 | 0.999 | 0.359 | 0.999 | 0.998 | 0.996 | 0.999 | 0.778 | 0.935 | 0.999 | 0.999 | 0.999 | 0.998 | 0.845 |
| AD mFWE p | 0.999 | 0.999 | 0.999 | 0.999 | 0.999 | 0.999 | 0.999 | 0.999 | 0.999 | 0.999 | 0.999 | 0.999 | 0.999 | 0.999 |
| Volume | 0.95 | 0.22 | -0.36 | -0.84 | 0.18 | -0.48 | 1.85 | 0.02 | -1.45 | -0.95 | -0.42 | -1.41 | -0.41 | -1.07 |
| Volume FWE p | 0.999 | 0.999 | 0.999 | 0.999 | 0.999 | 0.999 | 0.945 | 0.999 | 0.999 | 0.999 | 0.999 | 0.999 | 0.999 | 0.999 |
| Volume mFWE p | 0.999 | 0.999 | 0.999 | 0.999 | 0.999 | 0.999 | 0.995 | 0.999 | 0.999 | 0.999 | 0.999 | 0.999 | 0.999 | 0.999 |
| Thickness | 0.29 | -0.54 | 0.66 | -0.7 | -0.12 | -2.2 | -0.14 | -0.82 | -0.73 | -1.72 | -0.64 | -0.1 | -2.34 | -0.48 |
| Thickness FWE p | 0.999 | 0.999 | 0.999 | 0.999 | 0.999 | 0.999 | 0.999 | 0.999 | 0.999 | 0.999 | 0.999 | 0.999 | 0.999 | 0.999 |
| Thickness mFWE p | 0.999 | 0.999 | 0.999 | 0.999 | 0.999 | 0.999 | 0.999 | 0.999 | 0.999 | 0.999 | 0.999 | 0.999 | 0.999 | 0.999 |

Table B22 continued

| | Right paracentral lobule and sulcus | Right subcentral gyrus and sulci | Right transverse frontopolar gyri and sulci | Right anterior part of the cingulate gyrus and sulcus | Right middle anterior part of the cingulate gyrus and sulcus | Right middle posterior part of the cingulate gyrus and sulcus | Right posterior dorsal part of the cingulate gyrus | Right posterior ventral part of the cingulate gyrus | Right cuneus | Right opercular part of the inferior frontal gyrus | Right orbital part of the inferior frontal gyrus | Right triangular part of the inferior frontal gyrus | Right middle frontal gyrus | Right superior frontal gyrus |
|---|---|---|---|---|---|---|---|---|---|---|---|---|---|---|
| **Fisher F** | **20.73** | **2.49** | **8.2** | **6.48** | **9.66** | **7.39** | **3.23** | **5.68** | **3.12** | **6.74** | **2.67** | **8.38** | **8.97** | **7.8** |
| **Fisher FWE p** | **0.341** | **0.999** | **0.999** | **0.999** | **0.999** | **0.999** | **0.999** | **0.999** | **0.999** | **0.999** | **0.999** | **0.999** | **0.999** | **0.999** |
| MD | 0.93 | -1.8 | -1.32 | -0.98 | -1.23 | -0.44 | -2.88 | -0.33 | -1.21 | -1.81 | -1.53 | -2.3 | -0.85 | -1.64 |
| MD FWE p | 0.525 | 0.999 | 0.999 | 0.999 | 0.999 | 0.988 | 0.999 | 0.981 | 0.999 | 0.999 | 0.999 | 0.999 | 0.998 | 0.999 |
| MD mFWE p | 0.999 | 0.999 | 0.999 | 0.999 | 0.999 | 0.999 | 0.999 | 0.999 | 0.999 | 0.999 | 0.999 | 0.999 | 0.999 | 0.999 |
| RD | 0.49 | -1.79 | -1.88 | -1.4 | -1.91 | -0.76 | -2.54 | -0.09 | -1.48 | -1.89 | -1.98 | -2.53 | -1.3 | -2.12 |
| RD FWE p | 0.762 | 0.999 | 0.999 | 0.999 | 0.999 | 0.997 | 0.999 | 0.953 | 0.999 | 0.999 | 0.999 | 0.999 | 0.999 | 0.999 |
| RD mFWE p | 0.999 | 0.999 | 0.999 | 0.999 | 0.999 | 0.999 | 0.999 | 0.999 | 0.999 | 0.999 | 0.999 | 0.999 | 0.999 | 0.999 |
| AD | 1.57 | -1.63 | -0.24 | -0.04 | 0.37 | 0.29 | -2.91 | -0.64 | -0.66 | -1.48 | -0.52 | -1.65 | 0.01 | -0.54 |
| AD FWE p | 0.316 | 0.999 | 0.993 | 0.981 | 0.912 | 0.931 | 0.999 | 0.999 | 0.999 | 0.999 | 0.999 | 0.999 | 0.976 | 0.999 |
| AD mFWE p | 0.999 | 0.999 | 0.999 | 0.999 | 0.999 | 0.999 | 0.999 | 0.999 | 0.999 | 0.999 | 0.999 | 0.999 | 0.999 | 0.999 |
| Volume | -2.03 | -0.66 | -1.62 | -1.99 | -1.5 | -1.42 | -0.09 | 0.01 | -0.02 | -0.75 | -0.93 | 1.85 | -1.42 | -2.06 |
| Volume FWE p | 0.999 | 0.999 | 0.999 | 0.999 | 0.999 | 0.999 | 0.999 | 0.999 | 0.999 | 0.999 | 0.999 | 0.945 | 0.999 | 0.999 |
| Volume mFWE p | 0.999 | 0.999 | 0.999 | 0.999 | 0.999 | 0.999 | 0.999 | 0.999 | 0.999 | 0.999 | 0.999 | 0.995 | 0.999 | 0.999 |
| Thickness | -2.33 | -0.15 | -1.83 | -1.28 | -1.92 | -1.11 | -0.32 | -0.07 | 0.45 | -1.64 | < 0.001 | 0.02 | -1.82 | -1.86 |
| Thickness FWE p | 0.999 | 0.999 | 0.999 | 0.999 | 0.999 | 0.999 | 0.999 | 0.999 | 0.999 | 0.999 | 0.999 | 0.999 | 0.999 | 0.999 |
| Thickness mFWE p | 0.999 | 0.999 | 0.999 | 0.999 | 0.999 | 0.999 | 0.999 | 0.999 | 0.999 | 0.999 | 0.999 | 0.999 | 0.999 | 0.999 |

Table B22 continued

| | Right short insular gyri | Right middle occipital gyrus | Right superior occipital gyrus | Right lateral occipito temporal gyrus | Right lingual gyrus | Right parahippocampal gyrus | Right orbital gyri | Right angular gyrus | Right supramarginal gyrus | Right superior parietal lobule | Right postcentral gyrus | Right precentral gyrus | Right precuneus |
|---|---|---|---|---|---|---|---|---|---|---|---|---|---|
| **Fisher F** | **4.14** | **4.29** | **7.19** | **5.84** | **3.79** | **2.25** | **1.73** | **4.11** | **3.08** | **5.92** | **4.64** | **4** | **9.34** |
| **Fisher FWE p** | **0.999** | **0.999** | **0.999** | **0.999** | **0.999** | **0.999** | **0.999** | **0.999** | **0.999** | **0.999** | **0.999** | **0.999** | **0.999** |
| MD | -1.03 | -1.65 | -0.29 | -1.04 | -2.44 | -0.91 | -1.66 | -1.48 | -1.7 | -0.81 | -1.19 | -1.47 | -0.45 |
| MD FWE p | 0.999 | 0.999 | 0.978 | 0.999 | 0.999 | 0.999 | 0.999 | 0.999 | 0.999 | 0.998 | 0.999 | 0.999 | 0.988 |
| MD mFWE p | 0.999 | 0.999 | 0.999 | 0.999 | 0.999 | 0.999 | 0.999 | 0.999 | 0.999 | 0.999 | 0.999 | 0.999 | 0.999 |
| RD | -1.65 | -1.81 | -0.72 | -1.26 | -2.24 | -1.03 | -1.7 | -1.75 | -1.84 | -1.25 | -1.31 | -1.8 | -0.77 |
| RD FWE p | 0.999 | 0.999 | 0.997 | 0.999 | 0.999 | 0.999 | 0.999 | 0.999 | 0.999 | 0.999 | 0.999 | 0.999 | 0.997 |
| RD mFWE p | 0.999 | 0.999 | 0.999 | 0.999 | 0.999 | 0.999 | 0.999 | 0.999 | 0.999 | 0.999 | 0.999 | 0.999 | 0.999 |
| AD | 0.16 | -1.15 | 0.43 | -0.39 | -2.56 | -0.55 | -1.21 | -0.81 | -1.29 | 0.06 | -0.9 | -0.76 | 0.25 |
| AD FWE p | 0.956 | 0.999 | 0.893 | 0.997 | 0.999 | 0.999 | 0.999 | 0.999 | 0.999 | 0.97 | 0.999 | 0.999 | 0.94 |
| AD mFWE p | 0.999 | 0.999 | 0.999 | 0.999 | 0.999 | 0.999 | 0.999 | 0.999 | 0.999 | 0.999 | 0.999 | 0.999 | 0.999 |
| Volume | -0.31 | 0.32 | -0.5 | -1.1 | 1.01 | -0.83 | -0.75 | -2.12 | -0.87 | -0.76 | -0.51 | 0.12 | -0.52 |
| Volume FWE p | 0.999 | 0.999 | 0.999 | 0.999 | 0.999 | 0.999 | 0.999 | 0.999 | 0.999 | 0.999 | 0.999 | 0.999 | 0.999 |
| Volume mFWE p | 0.999 | 0.999 | 0.999 | 0.999 | 0.999 | 0.999 | 0.999 | 0.999 | 0.999 | 0.999 | 0.999 | 0.999 | 0.999 |
| Thickness | 0.2 | -0.28 | -0.66 | -1.15 | 2.36 | 0.94 | 0.46 | -0.9 | -0.47 | -0.85 | -0.78 | -0.17 | -1.52 |
| Thickness FWE p | 0.999 | 0.999 | 0.999 | 0.999 | 0.665 | 0.998 | 0.999 | 0.999 | 0.999 | 0.999 | 0.999 | 0.999 | 0.999 |
| Thickness mFWE p | 0.999 | 0.999 | 0.999 | 0.999 | 0.999 | 0.999 | 0.999 | 0.999 | 0.999 | 0.999 | 0.999 | 0.999 | 0.999 |

Table B22 continued

| | Right subcallosal gyrus | Right anterior transverse temporal gyrus | Right lateral aspect of the superior temporal gyrus | Right planum polare of the superior temporal gyrus | Right planum temporale | Right inferior temporal gyrus | Right middle temporal gyrus | Right horizontal ramus of the anterior segment of the lateral | Right vertical ramus of the anterior segment of the lateral sulcus | Right posterior ramus of the lateral sulcus | Right occipital pole | Right temporal pole | Right calcarine sulcus | Right central sulcus |
|---|---|---|---|---|---|---|---|---|---|---|---|---|---|---|
| **Fisher F** | **1.47** | **3.37** | **3.69** | **2.06** | **12.3** | **11.68** | **2.27** | **7.4** | **7.68** | **5.71** | **4.77** | **1.55** | **3.58** | **7.97** |
| **Fisher FWE p** | **0.999** | **0.999** | **0.999** | **0.999** | **0.943** | **0.966** | **0.999** | **0.999** | **0.999** | **0.999** | **0.999** | **0.999** | **0.999** | **0.999** |
| MD | -1.26 | -1.92 | -2.42 | -1.15 | -1.32 | -1.5 | -2.02 | 0.02 | -1.19 | -2.23 | -2.16 | -2.8 | -0.92 | -0.01 |
| MD FWE p | 0.999 | 0.999 | 0.999 | 0.999 | 0.999 | 0.999 | 0.999 | 0.934 | 0.999 | 0.999 | 0.999 | 0.999 | 0.999 | 0.939 |
| MD mFWE p | 0.999 | 0.999 | 0.999 | 0.999 | 0.999 | 0.999 | 0.999 | 0.999 | 0.999 | 0.999 | 0.999 | 0.999 | 0.999 | 0.999 |
| RD | -1.29 | -2.1 | -2.5 | -1.4 | -1.52 | -2.26 | -2.44 | -0.37 | -1.16 | -2.52 | -2.21 | -2.76 | -0.89 | -0.34 |
| RD FWE p | 0.999 | 0.999 | 0.999 | 0.999 | 0.999 | 0.999 | 0.999 | 0.984 | 0.999 | 0.999 | 0.999 | 0.999 | 0.999 | 0.982 |
| RD mFWE p | 0.999 | 0.999 | 0.999 | 0.999 | 0.999 | 0.999 | 0.999 | 0.999 | 0.999 | 0.999 | 0.999 | 0.999 | 0.999 | 0.999 |
| AD | -1.09 | -1.41 | -2.01 | -0.53 | -0.78 | 0.34 | -0.98 | 0.8 | -0.98 | -1.26 | -1.67 | -2.29 | -0.88 | 0.62 |
| AD FWE p | 0.999 | 0.999 | 0.999 | 0.999 | 0.999 | 0.92 | 0.999 | 0.741 | 0.999 | 0.999 | 0.999 | 0.999 | 0.999 | 0.824 |
| AD mFWE p | 0.999 | 0.999 | 0.999 | 0.999 | 0.999 | 0.999 | 0.999 | 0.999 | 0.999 | 0.999 | 0.999 | 0.999 | 0.999 | 0.999 |
| Volume | -0.5 | 0.68 | -1 | -0.55 | -1.06 | -1.77 | -0.98 | -0.74 | 0.61 | 0.84 | 0.43 | -0.54 | -0.21 | -0.13 |
| Volume FWE p | 0.999 | 0.999 | 0.999 | 0.999 | 0.999 | 0.999 | 0.999 | 0.999 | 0.999 | 0.999 | 0.999 | 0.999 | 0.999 | 0.999 |
| Volume mFWE p | 0.999 | 0.999 | 0.999 | 0.999 | 0.999 | 0.999 | 0.999 | 0.999 | 0.999 | 0.999 | 0.999 | 0.999 | 0.999 | 0.999 |
| Thickness | 2.6 | 1.03 | -0.86 | 1.23 | -2.67 | -2.37 | -0.07 | -0.06 | -1.16 | -0.45 | -0.53 | 0.42 | 0.08 | -0.26 |
| Thickness FWE p | 0.513 | 0.997 | 0.999 | 0.992 | 0.999 | 0.999 | 0.999 | 0.999 | 0.999 | 0.999 | 0.999 | 0.999 | 0.999 | 0.999 |
| Thickness mFWE p | 0.995 | 0.999 | 0.999 | 0.999 | 0.999 | 0.999 | 0.999 | 0.999 | 0.999 | 0.999 | 0.999 | 0.999 | 0.999 | 0.999 |

T

able B22 continued

| | Right anterior segment of the circular sulcus of the insula | Right inferior segment of the circular sulcus of the insula | Right superior segment of the circular sulcus of the insula | Right anterior transverse collateral sulcus | Right posterior transverse collateral sulcus | Right inferior frontal sulcus | Right middle frontal sulcus | Right superior frontal sulcus | Right sulcus intermedius primus | Right intraparietal sulcus and transverse parietal sulci | Right middle occipital sulcus and lunatus sulcus | Right superior occipital sulcus and transverse occipital sulcus | Right anterior occipital sulcus and preoccipital notch | Right lateral occipito temporal sulcus |
|---|---|---|---|---|---|---|---|---|---|---|---|---|---|---|
| **Fisher F** | **4.55** | **4.71** | **5.73** | **2.39** | **4.13** | **5.93** | **6.45** | **9.83** | **0.76** | **6.32** | **3.81** | **6.22** | **4.76** | **3.78** |
| **Fisher FWE p** | **0.999** | **0.999** | **0.999** | **0.999** | **0.999** | **0.999** | **0.999** | **0.998** | **0.999** | **0.999** | **0.999** | **0.999** | **0.999** | **0.999** |
| MD | -0.54 | -0.41 | -1.2 | -1.36 | -2.11 | -1.1 | -2 | -1.02 | -2.44 | -0.28 | -2.47 | -0.69 | -0.69 | -1.92 |
| MD FWE p | 0.992 | 0.987 | 0.999 | 0.999 | 0.999 | 0.999 | 0.999 | 0.999 | 0.999 | 0.977 | 0.999 | 0.996 | 0.996 | 0.999 |
| MD mFWE p | 0.999 | 0.999 | 0.999 | 0.999 | 0.999 | 0.999 | 0.999 | 0.999 | 0.999 | 0.999 | 0.999 | 0.999 | 0.999 | 0.999 |
| RD | -1.16 | -0.95 | -1.44 | -1.26 | -1.73 | -1.56 | -2.77 | -1.7 | -2.47 | -0.48 | -2.85 | -0.94 | -1.04 | -1.81 |
| RD FWE p | 0.999 | 0.999 | 0.999 | 0.999 | 0.999 | 0.999 | 0.999 | 0.999 | 0.999 | 0.99 | 0.999 | 0.999 | 0.999 | 0.999 |
| RD mFWE p | 0.999 | 0.999 | 0.999 | 0.999 | 0.999 | 0.999 | 0.999 | 0.999 | 0.999 | 0.999 | 0.999 | 0.999 | 0.999 | 0.999 |
| AD | 0.71 | 0.61 | -0.44 | -0.85 | -2.18 | -0.07 | -0.2 | 0.57 | -2.07 | 0.14 | -1.22 | -0.11 | 0.18 | -1.24 |
| AD FWE p | 0.784 | 0.831 | 0.998 | 0.999 | 0.999 | 0.984 | 0.992 | 0.844 | 0.999 | 0.959 | 0.999 | 0.986 | 0.954 | 0.999 |
| AD mFWE p | 0.999 | 0.999 | 0.999 | 0.999 | 0.999 | 0.999 | 0.999 | 0.999 | 0.999 | 0.999 | 0.999 | 0.999 | 0.999 | 0.999 |
| Volume | -0.73 | -0.56 | 0.13 | -0.43 | 0.98 | -0.72 | 0.34 | -0.42 | -0.57 | -0.94 | 0.18 | 0.06 | -1.13 | -1.18 |
| Volume FWE p | 0.999 | 0.999 | 0.999 | 0.999 | 0.999 | 0.999 | 0.999 | 0.999 | 0.999 | 0.999 | 0.999 | 0.999 | 0.999 | 0.999 |
| Volume mFWE p | 0.999 | 0.999 | 0.999 | 0.999 | 0.999 | 0.999 | 0.999 | 0.999 | 0.999 | 0.999 | 0.999 | 0.999 | 0.999 | 0.999 |
| Thickness | 1.37 | 1.25 | -0.73 | 0.5 | 0.97 | -1.01 | -0.87 | -1.66 | 2.28 | -0.59 | -0.27 | -0.59 | -0.29 | -0.83 |
| Thickness FWE p | 0.985 | 0.991 | 0.999 | 0.999 | 0.998 | 0.999 | 0.999 | 0.999 | 0.717 | 0.999 | 0.999 | 0.999 | 0.999 | 0.999 |
| Thickness mFWE p | 0.999 | 0.999 | 0.999 | 0.999 | 0.999 | 0.999 | 0.999 | 0.999 | 0.999 | 0.999 | 0.999 | 0.999 | 0.999 | 0.999 |

Table B22 continued

| | Right lateral orbital sulcus | Right medial orbital sulcus | Right orbital sulci | Right parieto occipital sulcus | Right pericallosal sulcus | Right postcentral sulcus | Right inferior part of the precentral sulcus | Right superior part of the precentral sulcus | Right suborbital sulcus | Right subparietal sulcus | Right inferior temporal sulcus | Right superior temporal sulcus | Right transverse temporal sulcus |
|---|---|---|---|---|---|---|---|---|---|---|---|---|---|
| **Fisher F** | **2.59** | **2.07** | **9.6** | **4.41** | **10.65** | **7.87** | **10.16** | **4.66** | **6.65** | **8.75** | **5.51** | **3.1** | **4.9** |
| **Fisher FWE p** | **0.999** | **0.999** | **0.999** | **0.999** | **0.99** | **0.999** | **0.996** | **0.999** | **0.999** | **0.999** | **0.999** | **0.999** | **0.999** |
| MD | -1.63 | -0.92 | 0.44 | -0.63 | 0.34 | -0.43 | -1.72 | -0.92 | 0.04 | -1.08 | -0.96 | -1.4 | -2.16 |
| MD FWE p | 0.999 | 0.999 | 0.797 | 0.995 | 0.837 | 0.988 | 0.999 | 0.999 | 0.93 | 0.999 | 0.999 | 0.999 | 0.999 |
| MD mFWE p | 0.999 | 0.999 | 0.999 | 0.999 | 0.999 | 0.999 | 0.999 | 0.999 | 0.999 | 0.999 | 0.999 | 0.999 | 0.999 |
| RD | -1.98 | -0.99 | -0.11 | -0.77 | -0.38 | -0.72 | -2.53 | -1.6 | -0.17 | -1.26 | -1.46 | -1.6 | -2.21 |
| RD FWE p | 0.999 | 0.999 | 0.956 | 0.997 | 0.985 | 0.997 | 0.999 | 0.999 | 0.965 | 0.999 | 0.999 | 0.999 | 0.999 |
| RD mFWE p | 0.999 | 0.999 | 0.999 | 0.999 | 0.999 | 0.999 | 0.999 | 0.999 | 0.999 | 0.999 | 0.999 | 0.999 | 0.999 |
| AD | -0.75 | -0.62 | 1.09 | -0.31 | 1.13 | 0.21 | 0.02 | 0.56 | 0.24 | -0.62 | 0.16 | -0.76 | -1.78 |
| AD FWE p | 0.999 | 0.999 | 0.58 | 0.995 | 0.557 | 0.948 | 0.975 | 0.851 | 0.942 | 0.999 | 0.957 | 0.999 | 0.999 |
| AD mFWE p | 0.999 | 0.999 | 0.999 | 0.999 | 0.999 | 0.999 | 0.999 | 0.999 | 0.999 | 0.999 | 0.999 | 0.999 | 0.999 |
| Volume | -0.4 | -0.65 | -0.41 | 0.26 | -0.19 | -0.72 | 0.63 | -0.72 | -1.51 | -1.19 | -0.44 | -0.86 | 0.66 |
| Volume FWE p | 0.999 | 0.999 | 0.999 | 0.999 | 0.999 | 0.999 | 0.999 | 0.999 | 0.999 | 0.999 | 0.999 | 0.999 | 0.999 |
| Volume mFWE p | 0.999 | 0.999 | 0.999 | 0.999 | 0.999 | 0.999 | 0.999 | 0.999 | 0.999 | 0.999 | 0.999 | 0.999 | 0.999 |
| Thickness | 0.21 | 1.62 | 0.01 | 0.79 | -0.59 | -1.17 | -1.64 | 0.17 | -0.4 | -1.96 | -0.58 | -0.28 | -0.35 |
| Thickness FWE p | 0.999 | 0.956 | 0.999 | 0.999 | 0.999 | 0.999 | 0.999 | 0.999 | 0.999 | 0.999 | 0.999 | 0.999 | 0.999 |
| Thickness mFWE p | 0.999 | 0.999 | 0.999 | 0.999 | 0.999 | 0.999 | 0.999 | 0.999 | 0.999 | 0.999 | 0.999 | 0.999 | 0.999 |

**Table B23 Positive correlations between cortical grey matter metrics and anxiety/depressive problems**

| | Left fronto marginal gyrus and sulcus | Left inferior occipital gyrus and sulcus | Left paracentral lobule and sulcus | Left subcentral gyrus and sulci | Left transverse frontopolar gyri and sulci | Left anterior part of the cingulate gyrus and sulcus | Left middle anterior part of the cingulate gyrus and sulcus | Left middle posterior part of the cingulate gyrus and sulcus | Left posterior dorsal part of the cingulate gyrus | Left posterior ventral part of the cingulate gyrus | Left cuneus | Left opercular part of the inferior frontal gyrus | Left orbital part of the inferior frontal gyrus | Left triangular part of the inferior frontal gyrus | Left middle frontal gyrus |
|---|---|---|---|---|---|---|---|---|---|---|---|---|---|---|---|
| **Fisher F** | **11.91** | **5.2** | **5.98** | **6.85** | **5.18** | **9.44** | **4.12** | **5.39** | **5** | **13** | **5.75** | **7.8** | **10.63** | **9.03** | **4.12** |
| **Fisher FWE p** | **0.976** | **0.999** | **0.999** | **0.999** | **0.999** | **0.999** | **0.999** | **0.999** | **0.999** | **0.947** | **0.999** | **0.999** | **0.993** | **0.999** | **0.999** |
| MD | 0.55 | -2.37 | -0.33 | -1.04 | -1.26 | -0.06 | -1.14 | -0.36 | -1.97 | 0.87 | -0.93 | -0.36 | 0.03 | -0.38 | -0.69 |
| MD FWE p | 0.876 | 0.999 | 0.996 | 0.999 | 0.999 | 0.985 | 0.999 | 0.997 | 0.999 | 0.732 | 0.999 | 0.997 | 0.979 | 0.997 | 0.999 |
| MD mFWE p | 0.999 | 0.999 | 0.999 | 0.999 | 0.999 | 0.999 | 0.999 | 0.999 | 0.999 | 0.999 | 0.999 | 0.999 | 0.999 | 0.999 | 0.999 |
| RD | -0.02 | -2.55 | -0.53 | -1.1 | -1.84 | -0.4 | -1.57 | -0.43 | -1.8 | 1.25 | -1.01 | -0.53 | -0.6 | -0.65 | -1.06 |
| RD FWE p | 0.989 | 0.999 | 0.999 | 0.999 | 0.999 | 0.998 | 0.999 | 0.999 | 0.999 | 0.557 | 0.999 | 0.999 | 0.999 | 0.999 | 0.999 |
| RD mFWE p | 0.999 | 0.999 | 0.999 | 0.999 | 0.999 | 0.999 | 0.999 | 0.999 | 0.999 | 0.999 | 0.999 | 0.999 | 0.999 | 0.999 | 0.999 |
| AD | 1.27 | -1.53 | 0.05 | -0.8 | -0.15 | 0.51 | -0.17 | -0.15 | -1.92 | 0.11 | -0.74 | 0.02 | 1.1 | 0.14 | 0.07 |
| AD FWE p | 0.506 | 0.999 | 0.985 | 0.999 | 0.994 | 0.908 | 0.995 | 0.994 | 0.999 | 0.98 | 0.999 | 0.987 | 0.62 | 0.977 | 0.983 |
| AD mFWE p | 0.999 | 0.999 | 0.999 | 0.999 | 0.999 | 0.999 | 0.999 | 0.999 | 0.999 | 0.999 | 0.999 | 0.999 | 0.999 | 0.999 | 0.999 |
| Volume | 0.28 | 0.84 | -0.13 | 1.19 | 0.53 | -0.98 | 0.39 | -1.37 | 0.87 | 0.42 | 1.25 | 0.64 | 1.21 | 1.26 | -0.76 |
| Volume FWE p | 0.999 | 0.999 | 0.999 | 0.996 | 0.999 | 0.999 | 0.999 | 0.999 | 0.999 | 0.999 | 0.995 | 0.999 | 0.996 | 0.994 | 0.999 |
| Volume mFWE p | 0.999 | 0.999 | 0.999 | 0.999 | 0.999 | 0.999 | 0.999 | 0.999 | 0.999 | 0.999 | 0.999 | 0.999 | 0.999 | 0.999 | 0.999 |
| Thickness | -0.15 | -0.25 | -0.18 | -0.05 | 0.04 | -1.27 | 0.81 | -0.5 | -0.09 | -0.05 | 2.25 | -0.38 | 1.28 | -0.01 | 0.1 |
| Thickness FWE p | 0.999 | 0.999 | 0.999 | 0.999 | 0.999 | 0.999 | 0.999 | 0.999 | 0.999 | 0.999 | 0.751 | 0.999 | 0.998 | 0.999 | 0.999 |
| Thickness mFWE p | 0.999 | 0.999 | 0.999 | 0.999 | 0.999 | 0.999 | 0.999 | 0.999 | 0.999 | 0.999 | 0.987 | 0.999 | 0.999 | 0.999 | 0.999 |

Table 23 continued

| | Left long insular gyrus and central sulcus of the insula | Left short insular gyri | Left middle occipital gyrus | Left superior occipital gyrus | Left lateral occipito temporal gyrus | Left lingual gyrus | Left parahippocampal gyrus | Left orbital gyri | Left angular gyrus | Left supramarginal gyrus | Left superior parietal lobule | Left postcentral gyrus | Left precentral gyrus | Left precuneus |
|---|---|---|---|---|---|---|---|---|---|---|---|---|---|---|
| **Fisher F** | **11.74** | **5.47** | **3.88** | **5.01** | **3.04** | **7.11** | **6.66** | **10.32** | **3.33** | **3.92** | **7.89** | **4.31** | **11.94** | **9.27** |
| **Fisher FWE p** | **0.979** | **0.999** | **0.999** | **0.999** | **0.999** | **0.999** | **0.999** | **0.996** | **0.999** | **0.999** | **0.999** | **0.999** | **0.975** | **0.999** |
| MD | 0.32 | -0.67 | -2.14 | -1.68 | -1.46 | -1.22 | -0.64 | -0.16 | -1.64 | -1.82 | -0.33 | -1.34 | -1.47 | -0.63 |
| MD FWE p | 0.938 | 0.999 | 0.999 | 0.999 | 0.999 | 0.999 | 0.999 | 0.991 | 0.999 | 0.999 | 0.996 | 0.999 | 0.999 | 0.999 |
| MD mFWE p | 0.999 | 0.999 | 0.999 | 0.999 | 0.999 | 0.999 | 0.999 | 0.999 | 0.999 | 0.999 | 0.999 | 0.999 | 0.999 | 0.999 |
| RD | 0.36 | -0.88 | -2.43 | -2 | -1.03 | -1.03 | -0.61 | -0.49 | -1.88 | -1.76 | -0.55 | -1.39 | -1.64 | -0.57 |
| RD FWE p | 0.948 | 0.999 | 0.999 | 0.999 | 0.999 | 0.999 | 0.999 | 0.999 | 0.999 | 0.999 | 0.999 | 0.999 | 0.999 | 0.999 |
| RD mFWE p | 0.999 | 0.999 | 0.999 | 0.999 | 0.999 | 0.999 | 0.999 | 0.999 | 0.999 | 0.999 | 0.999 | 0.999 | 0.999 | 0.999 |
| AD | 0.16 | -0.17 | -1.41 | -1.02 | -1.59 | -1.44 | -0.56 | 0.34 | -0.99 | -1.74 | 0.1 | -1.18 | -1 | -0.69 |
| AD FWE p | 0.975 | 0.995 | 0.999 | 0.999 | 0.999 | 0.999 | 0.999 | 0.948 | 0.999 | 0.999 | 0.98 | 0.999 | 0.999 | 0.999 |
| AD mFWE p | 0.999 | 0.999 | 0.999 | 0.999 | 0.999 | 0.999 | 0.999 | 0.999 | 0.999 | 0.999 | 0.999 | 0.999 | 0.999 | 0.999 |
| Volume | 0.87 | 0.78 | 0.79 | -0.08 | -0.45 | 1.72 | 1.27 | 1.04 | -0.28 | -0.13 | 0.96 | 0.5 | 2.65 | 1.14 |
| Volume FWE p | 0.999 | 0.999 | 0.999 | 0.999 | 0.999 | 0.957 | 0.994 | 0.998 | 0.999 | 0.999 | 0.999 | 0.999 | 0.568 | 0.997 |
| Volume mFWE p | 0.999 | 0.999 | 0.999 | 0.999 | 0.999 | 0.995 | 0.999 | 0.999 | 0.999 | 0.999 | 0.999 | 0.999 | 0.686 | 0.999 |
| Thickness | -0.68 | 1.12 | 0.66 | -0.86 | -0.16 | 1.81 | 1.39 | -0.61 | -0.25 | -0.56 | 0.16 | 0.03 | 1.06 | -0.87 |
| Thickness FWE p | 0.999 | 0.999 | 0.999 | 0.999 | 0.999 | 0.948 | 0.996 | 0.999 | 0.999 | 0.999 | 0.999 | 0.999 | 0.999 | 0.999 |
| Thickness mFWE p | 0.999 | 0.999 | 0.999 | 0.999 | 0.999 | 0.999 | 0.999 | 0.999 | 0.999 | 0.999 | 0.999 | 0.999 | 0.999 | 0.999 |

Table 23 continued

| | Left subcallosal gyrus | Left anterior transverse temporal gyrus | Left lateral aspect of the superior temporal gyrus | Left planum polare of the superior temporal gyrus | Left planum temporale | Left inferior temporal gyrus | Left middle temporal gyrus | Left horizontal ramus of the anterior segment of the lateral | Left vertical ramus of the anterior segment of the lateral sulcus | Left posterior ramus of the lateral sulcus | Left occipital pole | Left temporal pole | Left calcarine sulcus | Left central sulcus |
|---|---|---|---|---|---|---|---|---|---|---|---|---|---|---|
| **Fisher F** | **4.09** | **9.28** | **2.6** | **6.7** | **5.08** | **4.02** | **5.18** | **20.04** | **18.68** | **4.58** | **3.45** | **4.77** | **3.9** | **6.25** |
| **Fisher FWE p** | **0.999** | **0.999** | **0.999** | **0.999** | **0.999** | **0.999** | **0.999** | **0.512** | **0.609** | **0.999** | **0.999** | **0.999** | **0.999** | **0.999** |
| MD | -0.45 | -0.89 | -1.59 | -0.09 | -0.64 | -1.32 | -0.88 | 1.18 | 0.72 | -2.4 | -1.95 | -1.03 | -0.93 | -1.04 |
| MD FWE p | 0.998 | 0.999 | 0.999 | 0.987 | 0.999 | 0.999 | 0.999 | 0.545 | 0.807 | 0.999 | 0.999 | 0.999 | 0.999 | 0.999 |
| MD mFWE p | 0.999 | 0.999 | 0.999 | 0.999 | 0.999 | 0.999 | 0.999 | 0.999 | 0.999 | 0.999 | 0.999 | 0.999 | 0.999 | 0.999 |
| RD | -0.41 | -0.87 | -1.8 | -0.11 | -0.91 | -1.36 | -1.52 | 0.81 | 0.67 | -2.3 | -2.12 | -0.99 | -0.74 | -1.18 |
| RD FWE p | 0.999 | 0.999 | 0.999 | 0.993 | 0.999 | 0.999 | 0.999 | 0.807 | 0.866 | 0.999 | 0.999 | 0.999 | 0.999 | 0.999 |
| RD mFWE p | 0.999 | 0.999 | 0.999 | 0.999 | 0.999 | 0.999 | 0.999 | 0.999 | 0.999 | 0.999 | 0.999 | 0.999 | 0.999 | 0.999 |
| AD | -0.49 | -0.84 | -1.05 | -0.04 | -0.05 | -0.88 | 0.17 | 1.73 | 0.73 | -2.2 | -1.31 | -0.85 | -1.15 | -0.71 |
| AD FWE p | 0.999 | 0.999 | 0.999 | 0.99 | 0.99 | 0.999 | 0.974 | 0.227 | 0.828 | 0.999 | 0.999 | 0.999 | 0.999 | 0.999 |
| AD mFWE p | 0.999 | 0.999 | 0.999 | 0.999 | 0.999 | 0.999 | 0.999 | 0.995 | 0.999 | 0.999 | 0.999 | 0.999 | 0.999 | 0.999 |
| Volume | -0.36 | 1.43 | -0.14 | 0.46 | -1.07 | 0.36 | 0.42 | 1.41 | 1.8 | 0.84 | 0.69 | -0.07 | 0.61 | 1.32 |
| Volume FWE p | 0.999 | 0.987 | 0.999 | 0.999 | 0.999 | 0.999 | 0.999 | 0.988 | 0.943 | 0.999 | 0.999 | 0.999 | 0.999 | 0.992 |
| Volume mFWE p | 0.999 | 0.999 | 0.999 | 0.999 | 0.999 | 0.999 | 0.999 | 0.999 | 0.991 | 0.999 | 0.999 | 0.999 | 0.999 | 0.999 |
| Thickness | 0.42 | -0.7 | 0.33 | 0.6 | -0.55 | 0.15 | 0.45 | 0.11 | -0.93 | 0.05 | 1.01 | -0.52 | 1.62 | 0.94 |
| Thickness FWE p | 0.999 | 0.999 | 0.999 | 0.999 | 0.999 | 0.999 | 0.999 | 0.999 | 0.999 | 0.999 | 0.999 | 0.999 | 0.981 | 0.999 |
| Thickness mFWE p | 0.999 | 0.999 | 0.999 | 0.999 | 0.999 | 0.999 | 0.999 | 0.999 | 0.999 | 0.999 | 0.999 | 0.999 | 0.999 | 0.999 |

Table 23 continued

| | Left anterior segment of the circular sulcus of the insula | Left inferior segment of the circular sulcus of the insula | Left superior segment of the circular sulcus of the insula | Left anterior transverse collateral sulcus | Left posterior transverse collateral sulcus | Left inferior frontal sulcus | Left middle frontal sulcus | Left superior frontal sulcus | Left sulcus intermedius primus | Left intraparietal sulcus and transverse parietal sulci | Left middle occipital sulcus and lunatus sulcus | Left superior occipital sulcus and transverse occipital sulcus | Left anterior occipital sulcus and preoccipital notch | Left lateral occipito temporal sulcus |
|---|---|---|---|---|---|---|---|---|---|---|---|---|---|---|
| **Fisher F** | **13.06** | **3.28** | **8.94** | **11.83** | **4.24** | **6.75** | **4.73** | **11.61** | **4.34** | **3.63** | **3.25** | **2.71** | **5.71** | **5.03** |
| **Fisher FWE p** | **0.945** | **0.999** | **0.999** | **0.977** | **0.999** | **0.999** | **0.999** | **0.981** | **0.999** | **0.999** | **0.999** | **0.999** | **0.999** | **0.999** |
| MD | 0.84 | -0.78 | -0.28 | -1.53 | -1.52 | -0.25 | -0.99 | 0.02 | -1.45 | -1.8 | -1.75 | -1.54 | -0.74 | -1.61 |
| MD FWE p | 0.752 | 0.999 | 0.995 | 0.999 | 0.999 | 0.994 | 0.999 | 0.98 | 0.999 | 0.999 | 0.999 | 0.999 | 0.999 | 0.999 |
| MD mFWE p | 0.999 | 0.999 | 0.999 | 0.999 | 0.999 | 0.999 | 0.999 | 0.999 | 0.999 | 0.999 | 0.999 | 0.999 | 0.999 | 0.999 |
| RD | 0.26 | -0.91 | -0.51 | -0.71 | -1.43 | -0.62 | -1.6 | -0.67 | -1.82 | -1.87 | -1.8 | -1.83 | -1.06 | -1.32 |
| RD FWE p | 0.964 | 0.999 | 0.999 | 0.999 | 0.999 | 0.999 | 0.999 | 0.999 | 0.999 | 0.999 | 0.999 | 0.999 | 0.999 | 0.999 |
| RD mFWE p | 0.999 | 0.999 | 0.999 | 0.999 | 0.999 | 0.999 | 0.999 | 0.999 | 0.999 | 0.999 | 0.999 | 0.999 | 0.999 | 0.999 |
| AD | 1.62 | -0.38 | 0.26 | -1.97 | -1.31 | 0.56 | 0.32 | 1.45 | -0.38 | -1.47 | -1.34 | -0.79 | 0.0 | -1.62 |
| AD FWE p | 0.286 | 0.998 | 0.961 | 0.999 | 0.999 | 0.893 | 0.952 | 0.39 | 0.999 | 0.999 | 0.999 | 0.999 | 0.988 | 0.999 |
| AD mFWE p | 0.998 | 0.999 | 0.999 | 0.999 | 0.999 | 0.999 | 0.999 | 0.999 | 0.999 | 0.999 | 0.999 | 0.999 | 0.999 | 0.999 |
| Volume | 0.36 | -0.11 | 1.17 | 2.63 | -0.24 | 0.53 | 0.3 | -0.16 | 0.42 | 0.07 | 0.58 | -0.25 | 0.23 | -1.28 |
| Volume FWE p | 0.999 | 0.999 | 0.996 | 0.579 | 0.999 | 0.999 | 0.999 | 0.999 | 0.999 | 0.999 | 0.999 | 0.999 | 0.999 | 0.999 |
| Volume mFWE p | 0.999 | 0.999 | 0.999 | 0.698 | 0.999 | 0.999 | 0.999 | 0.999 | 0.999 | 0.999 | 0.999 | 0.999 | 0.999 | 0.999 |
| Thickness | 1.82 | 1.07 | 0.17 | 1.39 | -0.65 | 1.35 | 0.95 | -0.85 | 0.21 | -0.26 | 0.94 | 0.27 | -0.19 | -1.22 |
| Thickness FWE p | 0.946 | 0.999 | 0.999 | 0.996 | 0.999 | 0.997 | 0.999 | 0.999 | 0.999 | 0.999 | 0.999 | 0.999 | 0.999 | 0.999 |
| Thickness mFWE p | 0.999 | 0.999 | 0.999 | 0.999 | 0.999 | 0.999 | 0.999 | 0.999 | 0.999 | 0.999 | 0.999 | 0.999 | 0.999 | 0.999 |

Table 23 continued

| | Left lateral orbital sulcus | Left medial orbital sulcus | Left orbital sulci | Left parieto occipital sulcus | Left pericallosal sulcus | Left postcentral sulcus | Left inferior part of the precentral sulcus | Left superior part of the precentral sulcus | Left suborbital sulcus | Left subparietal sulcus | Left inferior temporal sulcus | Left superior temporal sulcus | Left transverse temporal sulcus | Right fronto marginal gyrus and sulcus |
|---|---|---|---|---|---|---|---|---|---|---|---|---|---|---|
| **Fisher F** | **13.37** | **7.49** | **13.27** | **3.38** | **6.45** | **9.22** | **12.53** | **8.99** | **8.34** | **5.85** | **5.18** | **2.33** | **10.55** | **9.64** |
| **Fisher FWE p** | **0.934** | **0.999** | **0.937** | **0.999** | **0.999** | **0.999** | **0.961** | **0.999** | **0.999** | **0.999** | **0.999** | **0.999** | **0.994** | **0.999** |
| MD | 0.42 | -1.48 | 0.76 | -0.89 | -0.88 | -0.59 | -1.64 | -0.05 | 0.2 | -0.91 | -1.18 | -1.31 | -1.35 | 0.49 |
| MD FWE p | 0.915 | 0.999 | 0.789 | 0.999 | 0.999 | 0.999 | 0.999 | 0.985 | 0.959 | 0.999 | 0.999 | 0.999 | 0.999 | 0.896 |
| MD mFWE p | 0.999 | 0.999 | 0.999 | 0.999 | 0.999 | 0.999 | 0.999 | 0.999 | 0.999 | 0.999 | 0.999 | 0.999 | 0.999 | 0.999 |
| RD | -0.1 | -1.44 | 0.38 | -0.72 | -0.74 | -0.71 | -1.94 | -0.37 | 0.11 | -0.92 | -1.74 | -1.46 | -1.13 | 0.24 |
| RD FWE p | 0.992 | 0.999 | 0.945 | 0.999 | 0.999 | 0.999 | 0.999 | 0.998 | 0.98 | 0.999 | 0.999 | 0.999 | 0.999 | 0.967 |
| RD mFWE p | 0.999 | 0.999 | 0.999 | 0.999 | 0.999 | 0.999 | 0.999 | 0.999 | 0.999 | 0.999 | 0.999 | 0.999 | 0.999 | 0.999 |
| AD | 1.21 | -1.05 | 1.12 | -1.11 | -0.79 | -0.26 | -0.82 | 0.59 | 0.25 | -0.77 | -0.16 | -0.79 | -1.49 | 0.71 |
| AD FWE p | 0.55 | 0.999 | 0.609 | 0.999 | 0.999 | 0.997 | 0.999 | 0.881 | 0.964 | 0.999 | 0.995 | 0.999 | 0.999 | 0.835 |
| AD mFWE p | 0.999 | 0.999 | 0.999 | 0.999 | 0.999 | 0.999 | 0.999 | 0.999 | 0.999 | 0.999 | 0.999 | 0.999 | 0.999 | 0.999 |
| Volume | 1.2 | 0.29 | 1.07 | 0.23 | 1.25 | 0.84 | 2.74 | 0.78 | -0.05 | 0.61 | 0.48 | -0.7 | 0.45 | 0.45 |
| Volume FWE p | 0.996 | 0.999 | 0.998 | 0.999 | 0.994 | 0.999 | 0.512 | 0.999 | 0.999 | 0.999 | 0.999 | 0.999 | 0.999 | 0.999 |
| Volume mFWE p | 0.999 | 0.999 | 0.999 | 0.999 | 0.999 | 0.999 | 0.622 | 0.999 | 0.999 | 0.999 | 0.999 | 0.999 | 0.999 | 0.999 |
| Thickness | 0.05 | -1.38 | 1.24 | 0.98 | 0.75 | -1.04 | 0.99 | 0.12 | -0.29 | -0.31 | 0.000 | 0.31 | -2.03 | 0.92 |
| Thickness FWE p | 0.999 | 0.999 | 0.999 | 0.999 | 0.999 | 0.999 | 0.999 | 0.999 | 0.999 | 0.999 | 0.999 | 0.999 | 0.999 | 0.999 |
| Thickness mFWE p | 0.999 | 0.999 | 0.999 | 0.999 | 0.999 | 0.999 | 0.999 | 0.999 | 0.999 | 0.999 | 0.999 | 0.999 | 0.999 | 0.999 |

Table 23 continued

| | Right paracentral lobule and sulcus | Right subcentral gyrus and sulci | Right transverse frontopolar gyri and sulci | Right anterior part of the cingulate gyrus and sulcus | Right middle anterior part of the cingulate gyrus and sulcus | Right middle posterior part of the cingulate gyrus and sulcus | Right posterior dorsal part of the cingulate gyrus | Right posterior ventral part of the cingulate gyrus | Right cuneus | Right opercular part of the inferior frontal gyrus | Right orbital part of the inferior frontal gyrus | Right triangular part of the inferior frontal gyrus | Right middle frontal gyrus | Right superior frontal gyrus |
|---|---|---|---|---|---|---|---|---|---|---|---|---|---|---|
| **Fisher F** | **10.89** | **6.82** | **8.92** | **9.37** | **8.06** | **7.14** | **4.68** | **5.28** | **4.86** | **7.93** | **6.49** | **8** | **11.82** | **9.28** |
| **Fisher FWE p** | **0.991** | **0.999** | **0.999** | **0.999** | **0.999** | **0.999** | **0.999** | **0.999** | **0.999** | **0.999** | **0.999** | **0.999** | **0.978** | **0.999** |
| MD | 0.36 | -0.77 | -0.18 | 0.24 | -0.57 | -0.11 | -1.85 | -0.74 | -1.84 | -0.9 | -0.32 | -0.95 | 0.05 | -0.4 |
| MD FWE p | 0.929 | 0.999 | 0.992 | 0.952 | 0.999 | 0.988 | 0.999 | 0.999 | 0.999 | 0.999 | 0.996 | 0.999 | 0.977 | 0.997 |
| MD mFWE p | 0.999 | 0.999 | 0.999 | 0.999 | 0.999 | 0.999 | 0.999 | 0.999 | 0.999 | 0.999 | 0.999 | 0.999 | 0.999 | 0.999 |
| RD | -0.12 | -0.9 | -0.49 | -0.03 | -1.14 | -0.34 | -1.62 | -0.53 | -1.98 | -1.05 | -0.68 | -1.09 | -0.33 | -0.86 |
| RD FWE p | 0.993 | 0.999 | 0.999 | 0.989 | 0.999 | 0.998 | 0.999 | 0.999 | 0.999 | 0.999 | 0.999 | 0.999 | 0.998 | 0.999 |
| RD mFWE p | 0.999 | 0.999 | 0.999 | 0.999 | 0.999 | 0.999 | 0.999 | 0.999 | 0.999 | 0.999 | 0.999 | 0.999 | 0.999 | 0.999 |
| AD | 1.13 | -0.42 | 0.32 | 0.63 | 0.68 | 0.37 | -1.88 | -0.93 | -1.44 | -0.52 | 0.38 | -0.6 | 0.71 | 0.51 |
| AD FWE p | 0.602 | 0.999 | 0.953 | 0.866 | 0.849 | 0.942 | 0.999 | 0.999 | 0.999 | 0.999 | 0.94 | 0.999 | 0.837 | 0.909 |
| AD mFWE p | 0.999 | 0.999 | 0.999 | 0.999 | 0.999 | 0.999 | 0.999 | 0.999 | 0.999 | 0.999 | 0.999 | 0.999 | 0.999 | 0.999 |
| Volume | 0.11 | 0.81 | 0.09 | -0.25 | -0.07 | -0.52 | 0.72 | 0.53 | 1.26 | 0.32 | 0.27 | 1.62 | -0.06 | -0.51 |
| Volume FWE p | 0.999 | 0.999 | 0.999 | 0.999 | 0.999 | 0.999 | 0.999 | 0.999 | 0.994 | 0.999 | 0.999 | 0.971 | 0.999 | 0.999 |
| Volume mFWE p | 0.999 | 0.999 | 0.999 | 0.999 | 0.999 | 0.999 | 0.999 | 0.999 | 0.999 | 0.999 | 0.999 | 0.998 | 0.999 | 0.999 |
| Thickness | -0.32 | -0.32 | -0.96 | -0.57 | -0.79 | -0.44 | -0.09 | 0.09 | 1.85 | -1.26 | 0.25 | 0.44 | -1.47 | -1.36 |
| Thickness FWE p | 0.999 | 0.999 | 0.999 | 0.999 | 0.999 | 0.999 | 0.999 | 0.999 | 0.938 | 0.999 | 0.999 | 0.999 | 0.999 | 0.999 |
| Thickness mFWE p | 0.999 | 0.999 | 0.999 | 0.999 | 0.999 | 0.999 | 0.999 | 0.999 | 0.999 | 0.999 | 0.999 | 0.999 | 0.999 | 0.999 |

Table 23 continued

| | Right short insular gyri | Right middle occipital gyrus | Right superior occipital gyrus | Right lateral occipito temporal gyrus | Right lingual gyrus | Right parahippocampal gyrus | Right orbital gyri | Right angular gyrus | Right supramarginal gyrus | Right superior parietal lobule | Right postcentral gyrus | Right precentral gyrus | Right precuneus |
|---|---|---|---|---|---|---|---|---|---|---|---|---|---|
| **Fisher F** | **4.97** | **3.73** | **4.37** | **4.25** | **7.16** | **2.38** | **3.19** | **4.98** | **6.42** | **12.11** | **8.54** | **6.81** | **10.24** |
| **Fisher FWE p** | **0.999** | **0.999** | **0.999** | **0.999** | **0.999** | **0.999** | **0.999** | **0.999** | **0.999** | **0.972** | **0.999** | **0.999** | **0.996** |
| MD | -0.78 | -1.09 | -0.88 | -0.89 | -2.53 | -1.37 | -1.07 | -0.64 | -1.15 | -0.27 | -0.79 | -0.94 | -0.63 |
| MD FWE p | 0.999 | 0.999 | 0.999 | 0.999 | 0.999 | 0.999 | 0.999 | 0.999 | 0.999 | 0.994 | 0.999 | 0.999 | 0.999 |
| MD mFWE p | 0.999 | 0.999 | 0.999 | 0.999 | 0.999 | 0.999 | 0.999 | 0.999 | 0.999 | 0.999 | 0.999 | 0.999 | 0.999 |
| RD | -0.96 | -1.44 | -1.37 | -0.8 | -2.37 | -1.29 | -0.8 | -0.9 | -1.33 | -0.62 | -0.91 | -1.32 | -0.82 |
| RD FWE p | 0.999 | 0.999 | 0.999 | 0.999 | 0.999 | 0.999 | 0.999 | 0.999 | 0.999 | 0.999 | 0.999 | 0.999 | 0.999 |
| RD mFWE p | 0.999 | 0.999 | 0.999 | 0.999 | 0.999 | 0.999 | 0.999 | 0.999 | 0.999 | 0.999 | 0.999 | 0.999 | 0.999 |
| AD | -0.34 | -0.39 | 0.0 | -0.75 | -2.56 | -1.21 | -1.18 | -0.11 | -0.7 | 0.41 | -0.5 | -0.19 | -0.21 |
| AD FWE p | 0.998 | 0.999 | 0.988 | 0.999 | 0.999 | 0.999 | 0.999 | 0.993 | 0.999 | 0.933 | 0.999 | 0.995 | 0.996 |
| AD mFWE p | 0.999 | 0.999 | 0.999 | 0.999 | 0.999 | 0.999 | 0.999 | 0.999 | 0.999 | 0.999 | 0.999 | 0.999 | 0.999 |
| Volume | 0.61 | 0.01 | 0.26 | -0.78 | 1.9 | 0.18 | 0.12 | -0.96 | 1.21 | 1.24 | 1.16 | 1.22 | 1.04 |
| Volume FWE p | 0.999 | 0.999 | 0.999 | 0.999 | 0.92 | 0.999 | 0.999 | 0.999 | 0.996 | 0.995 | 0.997 | 0.995 | 0.998 |
| Volume mFWE p | 0.999 | 0.999 | 0.999 | 0.999 | 0.983 | 0.999 | 0.999 | 0.999 | 0.999 | 0.999 | 0.999 | 0.999 | 0.999 |
| Thickness | 0.67 | 0.25 | 0.71 | -0.51 | 3.14 | 1.92 | 0.69 | -0.51 | 0.24 | -1.06 | -0.66 | 0.49 | -1.19 |
| Thickness FWE p | 0.999 | 0.999 | 0.999 | 0.999 | 0.179 | 0.915 | 0.999 | 0.999 | 0.999 | 0.999 | 0.999 | 0.999 | 0.999 |
| Thickness mFWE p | 0.999 | 0.999 | 0.999 | 0.999 | 0.637 | 0.999 | 0.999 | 0.999 | 0.999 | 0.999 | 0.999 | 0.999 | 0.999 |

Table 23 continued

| | Right subcallosal gyrus | Right anterior transverse temporal gyrus | Right lateral aspect of the superior temporal gyrus | Right planum polare of the superior temporal gyrus | Right planum temporale | Right inferior temporal gyrus | Right middle temporal gyrus | Right horizontal ramus of the anterior segment of the lateral sulcus | Right vertical ramus of the anterior segment of the lateral sulcus | Right posterior ramus of the lateral sulcus | Right occipital pole | Right temporal pole | Right calcarine sulcus | Right central sulcus |
|---|---|---|---|---|---|---|---|---|---|---|---|---|---|---|
| **Fisher F** | **2.55** | **6.99** | **4.89** | **3.73** | **10.22** | **8.09** | **4.13** | **10.51** | **8.57** | **7.78** | **8.43** | **3.43** | **4.3** | **7.28** |
| **Fisher FWE p** | **0.999** | **0.999** | **0.999** | **0.999** | **0.996** | **0.999** | **0.999** | **0.994** | **0.999** | **0.999** | **0.999** | **0.999** | **0.999** | **0.999** |
| MD | -1.35 | -1.6 | -1.52 | -0.75 | -1.09 | -0.69 | -0.97 | 0.48 | -0.36 | -1.85 | -2.23 | -1.71 | -1.47 | -0.13 |
| MD FWE p | 0.999 | 0.999 | 0.999 | 0.999 | 0.999 | 0.999 | 0.999 | 0.898 | 0.997 | 0.999 | 0.999 | 0.999 | 0.999 | 0.989 |
| MD mFWE p | 0.999 | 0.999 | 0.999 | 0.999 | 0.999 | 0.999 | 0.999 | 0.999 | 0.999 | 0.999 | 0.999 | 0.999 | 0.999 | 0.999 |
| RD | -1.36 | -1.77 | -1.68 | -1.01 | -1.29 | -1.35 | -1.43 | -0.04 | -0.42 | -2.05 | -2.28 | -1.5 | -1.42 | -0.34 |
| RD FWE p | 0.999 | 0.999 | 0.999 | 0.999 | 0.999 | 0.999 | 0.999 | 0.99 | 0.999 | 0.999 | 0.999 | 0.999 | 0.999 | 0.998 |
| RD mFWE p | 0.999 | 0.999 | 0.999 | 0.999 | 0.999 | 0.999 | 0.999 | 0.999 | 0.999 | 0.999 | 0.999 | 0.999 | 0.999 | 0.999 |
| AD | -1.19 | -1.13 | -1.05 | -0.19 | -0.58 | 0.67 | -0.09 | 1.46 | -0.18 | -1.13 | -1.72 | -1.62 | -1.41 | 0.27 |
| AD FWE p | 0.999 | 0.999 | 0.999 | 0.995 | 0.999 | 0.854 | 0.992 | 0.379 | 0.995 | 0.999 | 0.999 | 0.999 | 0.999 | 0.96 |
| AD mFWE p | 0.999 | 0.999 | 0.999 | 0.999 | 0.999 | 0.999 | 0.999 | 0.999 | 0.999 | 0.999 | 0.999 | 0.999 | 0.999 | 0.999 |
| Volume | 0.28 | 1.58 | 0.84 | 0.03 | -0.13 | -0.27 | 0.14 | -0.46 | 0.45 | 1.85 | 2.1 | 0.42 | 1.03 | 0.5 |
| Volume FWE p | 0.999 | 0.975 | 0.999 | 0.999 | 0.999 | 0.999 | 0.999 | 0.999 | 0.999 | 0.932 | 0.858 | 0.999 | 0.998 | 0.999 |
| Volume mFWE p | 0.999 | 0.998 | 0.999 | 0.999 | 0.999 | 0.999 | 0.999 | 0.999 | 0.999 | 0.988 | 0.952 | 0.999 | 0.999 | 0.999 |
| Thickness | 1.93 | 0.45 | 0.17 | 1.02 | -2.06 | -0.97 | 0.5 | 0.42 | -0.94 | 0.75 | 1.23 | 0.35 | 1.9 | 0.32 |
| Thickness FWE p | 0.91 | 0.999 | 0.999 | 0.999 | 0.999 | 0.999 | 0.999 | 0.999 | 0.999 | 0.999 | 0.999 | 0.999 | 0.922 | 0.999 |
| Thickness mFWE p | 0.999 | 0.999 | 0.999 | 0.999 | 0.999 | 0.999 | 0.999 | 0.999 | 0.999 | 0.999 | 0.999 | 0.999 | 0.999 | 0.999 |

Table 23 continued

| | Right anterior segment of the circular sulcus of the insula | Right inferior segment of the circular sulcus of the insula | Right superior segment of the circular sulcus of the insula | Right anterior transverse collateral sulcus | Right posterior transverse collateral sulcus | Right inferior frontal sulcus | Right middle frontal sulcus | Right superior frontal sulcus | Right sulcus intermedius primus | Right intraparietal sulcus and transverse parietal sulci | Right middle occipital sulcus and lunatus sulcus | Right superior occipital sulcus and transverse occipital sulcus | Right anterior occipital sulcus and preoccipital notch | Right lateral occipito temporal sulcus |
|---|---|---|---|---|---|---|---|---|---|---|---|---|---|---|
| **Fisher F** | **5.23** | **5.03** | **8.31** | **6.9** | **6.97** | **7.11** | **6.82** | **10.08** | **2.33** | **8.23** | **3.63** | **4.78** | **3.66** | **2.83** |
| **Fisher FWE p** | **0.999** | **0.999** | **0.999** | **0.999** | **0.999** | **0.999** | **0.999** | **0.997** | **0.999** | **0.999** | **0.999** | **0.999** | **0.999** | **0.999** |
| MD | -0.35 | -0.42 | -0.39 | -0.29 | -2.17 | -0.1 | -0.86 | -0.08 | -1.58 | -0.22 | -2.09 | -0.79 | -0.48 | -1.52 |
| MD FWE p | 0.996 | 0.998 | 0.997 | 0.995 | 0.999 | 0.988 | 0.999 | 0.987 | 0.999 | 0.993 | 0.999 | 0.999 | 0.998 | 0.999 |
| MD mFWE p | 0.999 | 0.999 | 0.999 | 0.999 | 0.999 | 0.999 | 0.999 | 0.999 | 0.999 | 0.999 | 0.999 | 0.999 | 0.999 | 0.999 |
| RD | -0.62 | -0.84 | -0.71 | 0.04 | -1.73 | -0.38 | -1.32 | -0.54 | -1.71 | -0.32 | -2.22 | -0.9 | -0.71 | -1.25 |
| RD FWE p | 0.999 | 0.999 | 0.999 | 0.986 | 0.999 | 0.998 | 0.999 | 0.999 | 0.999 | 0.998 | 0.999 | 0.999 | 0.999 | 0.999 |
| RD mFWE p | 0.999 | 0.999 | 0.999 | 0.999 | 0.999 | 0.999 | 0.999 | 0.999 | 0.999 | 0.999 | 0.999 | 0.999 | 0.999 | 0.999 |
| AD | 0.24 | 0.39 | 0.3 | -0.62 | -2.32 | 0.47 | 0.16 | 0.9 | -1.1 | 0,0 | -1.4 | -0.47 | 0.09 | -1.28 |
| AD FWE p | 0.965 | 0.938 | 0.956 | 0.999 | 0.999 | 0.92 | 0.974 | 0.74 | 0.999 | 0.988 | 0.999 | 0.999 | 0.982 | 0.999 |
| AD mFWE p | 0.999 | 0.999 | 0.999 | 0.999 | 0.999 | 0.999 | 0.999 | 0.999 | 0.999 | 0.999 | 0.999 | 0.999 | 0.999 | 0.999 |
| Volume | 0.26 | 0.03 | 0.65 | 0.72 | 1.83 | 0.16 | 1.03 | 0.57 | 0.25 | 0.26 | 0.76 | -0.33 | -1.33 | -0.34 |
| Volume FWE p | 0.999 | 0.999 | 0.999 | 0.999 | 0.936 | 0.999 | 0.998 | 0.999 | 0.999 | 0.999 | 0.999 | 0.999 | 0.999 | 0.999 |
| Volume mFWE p | 0.999 | 0.999 | 0.999 | 0.999 | 0.989 | 0.999 | 0.999 | 0.999 | 0.999 | 0.999 | 0.999 | 0.999 | 0.999 | 0.999 |
| Thickness | 1.97 | 1.27 | -0.47 | 0.3 | 2.12 | 0.21 | 0.48 | -0.44 | 2.58 | -0.76 | 0.91 | -0.43 | 0.61 | 0.02 |
| Thickness FWE p | 0.896 | 0.999 | 0.999 | 0.999 | 0.826 | 0.999 | 0.999 | 0.999 | 0.52 | 0.999 | 0.999 | 0.999 | 0.999 | 0.999 |
| Thickness mFWE p | 0.998 | 0.999 | 0.999 | 0.999 | 0.995 | 0.999 | 0.999 | 0.999 | 0.933 | 0.999 | 0.999 | 0.999 | 0.999 | 0.999 |

Table 23 continued

| | Right lateral orbital sulcus | Right medial orbital sulcus | Right orbital sulci | Right parieto occipital sulcus | Right pericallosal sulcus | Right postcentral sulcus | Right inferior part of the precentral sulcus | Right superior part of the precentral sulcus | Right suborbital sulcus | Right subparietal sulcus | Right inferior temporal sulcus | Right superior temporal sulcus | Right transverse temporal sulcus |
|---|---|---|---|---|---|---|---|---|---|---|---|---|---|
| **Fisher F** | **3.99** | **3.86** | **8.75** | **3.65** | **12.69** | **8.3** | **15.57** | **5.63** | **7.51** | **6.35** | **7.01** | **3.63** | **5.69** |
| **Fisher FWE p** | **0.999** | **0.999** | **0.999** | **0.999** | **0.956** | **0.999** | **0.824** | **0.999** | **0.999** | **0.999** | **0.999** | **0.999** | **0.999** |
| MD | -0.47 | -0.71 | 0.34 | -1.25 | 0.46 | -0.38 | -0.86 | -0.51 | 0.25 | -0.83 | -0.47 | -0.83 | -1.97 |
| MD FWE p | 0.998 | 0.999 | 0.934 | 0.999 | 0.903 | 0.997 | 0.999 | 0.998 | 0.951 | 0.999 | 0.998 | 0.999 | 0.999 |
| MD mFWE p | 0.999 | 0.999 | 0.999 | 0.999 | 0.999 | 0.999 | 0.999 | 0.999 | 0.999 | 0.999 | 0.999 | 0.999 | 0.999 |
| RD | -0.66 | -0.57 | 0.29 | -1.31 | -0.28 | -0.52 | -1.54 | -0.94 | 0.26 | -0.86 | -0.7 | -1 | -2.04 |
| RD FWE p | 0.999 | 0.999 | 0.961 | 0.999 | 0.997 | 0.999 | 0.999 | 0.999 | 0.964 | 0.999 | 0.999 | 0.999 | 0.999 |
| RD mFWE p | 0.999 | 0.999 | 0.999 | 0.999 | 0.999 | 0.999 | 0.999 | 0.999 | 0.999 | 0.999 | 0.999 | 0.999 | 0.999 |
| AD | -0.06 | -0.72 | 0.32 | -1.02 | 1.24 | -0.07 | 0.54 | 0.42 | 0.18 | -0.67 | 0.06 | -0.31 | -1.58 |
| AD FWE p | 0.991 | 0.999 | 0.952 | 0.999 | 0.529 | 0.991 | 0.898 | 0.932 | 0.973 | 0.999 | 0.983 | 0.998 | 0.999 |
| AD mFWE p | 0.999 | 0.999 | 0.999 | 0.999 | 0.999 | 0.999 | 0.999 | 0.999 | 0.999 | 0.999 | 0.999 | 0.999 | 0.999 |
| Volume | -0.23 | 0.33 | 0.34 | 0.68 | -0.03 | 1.02 | 1.93 | 0.15 | -0.93 | -0.04 | -0.09 | 0.02 | 1.06 |
| Volume FWE p | 0.999 | 0.999 | 0.999 | 0.999 | 0.999 | 0.999 | 0.912 | 0.999 | 0.999 | 0.999 | 0.999 | 0.999 | 0.998 |
| Volume mFWE p | 0.999 | 0.999 | 0.999 | 0.999 | 0.999 | 0.999 | 0.98 | 0.999 | 0.999 | 0.999 | 0.999 | 0.999 | 0.999 |
| Thickness | 1.09 | 1.56 | 0.37 | 1.64 | -0.99 | -0.18 | -1.48 | 0.53 | -0.21 | -0.96 | -0.74 | 0.82 | -0.13 |
| Thickness FWE p | 0.999 | 0.987 | 0.999 | 0.979 | 0.999 | 0.999 | 0.999 | 0.999 | 0.999 | 0.999 | 0.999 | 0.999 | 0.999 |
| Thickness mFWE p | 0.999 | 0.999 | 0.999 | 0.999 | 0.999 | 0.999 | 0.999 | 0.999 | 0.999 | 0.999 | 0.999 | 0.999 | 0.999 |

**Table B24 Positive correlations between cortical grey matter metrics and attention problems**

| | Left fronto marginal gyrus and sulcus | Left inferior occipital gyrus and sulcus | Left paracentral lobule and sulcus | Left subcentral gyrus and sulci | Left transverse frontopolar gyri and sulci | Left anterior part of the cingulate gyrus and sulcus | Left middle anterior part of the cingulate gyrus and sulcus | Left middle posterior part of the cingulate gyrus and sulcus | Left posterior dorsal part of the cingulate gyrus | Left posterior ventral part of the cingulate gyrus | Left cuneus | Left opercular part of the inferior frontal gyrus | Left orbital part of the inferior frontal gyrus | Left triangular part of the inferior frontal gyrus | Left middle frontal gyrus |
|---|---|---|---|---|---|---|---|---|---|---|---|---|---|---|---|
| **Fisher F** | **4.03** | **6.08** | **11.56** | **0.28** | **0.19** | **6.45** | **19.05** | **16.8** | **5.85** | **7.46** | **0.44** | **2.93** | **3.36** | **2.65** | **1.84** |
| **Fisher FWE p** | **0.999** | **0.999** | **0.958** | **0.999** | **0.999** | **0.999** | **0.423** | **0.597** | **0.999** | **0.999** | **0.999** | **0.999** | **0.999** | **0.999** | **0.999** |
| MD | -0.63 | -2.5 | -0.6 | -2.34 | -3.71 | -0.71 | -1.54 | -0.89 | -2.43 | 0.22 | -1.63 | -0.91 | -1.73 | -2.71 | -2.03 |
| MD FWE p | 0.998 | 0.999 | 0.998 | 0.999 | 0.999 | 0.999 | 0.999 | 0.999 | 0.999 | 0.884 | 0.999 | 0.999 | 0.999 | 0.999 | 0.999 |
| MD mFWE p | 0.999 | 0.999 | 0.999 | 0.999 | 0.999 | 0.999 | 0.999 | 0.999 | 0.999 | 0.999 | 0.999 | 0.999 | 0.999 | 0.999 | 0.999 |
| RD | -1.41 | -2.45 | -0.62 | -2.45 | -4.31 | -1.64 | -1.9 | -0.91 | -1.89 | 0.72 | -1.49 | -1.39 | -1.94 | -3.05 | -2.56 |
| RD FWE p | 0.999 | 0.999 | 0.995 | 0.999 | 0.999 | 0.999 | 0.999 | 0.999 | 0.999 | 0.609 | 0.999 | 0.999 | 0.999 | 0.999 | 0.999 |
| RD mFWE p | 0.999 | 0.999 | 0.999 | 0.999 | 0.999 | 0.999 | 0.999 | 0.999 | 0.999 | 0.999 | 0.999 | 0.999 | 0.999 | 0.999 | 0.999 |
| AD | 0.64 | -1.97 | -0.57 | -1.86 | -2.11 | 0.94 | -0.62 | -0.68 | -2.98 | -0.64 | -1.75 | 0.15 | -1.14 | -1.82 | -0.84 |
| AD FWE p | 0.831 | 0.999 | 0.999 | 0.999 | 0.999 | 0.682 | 0.999 | 0.999 | 0.999 | 0.999 | 0.999 | 0.967 | 0.999 | 0.999 | 0.999 |
| AD mFWE p | 0.999 | 0.999 | 0.999 | 0.999 | 0.999 | 0.999 | 0.999 | 0.999 | 0.999 | 0.999 | 0.999 | 0.999 | 0.999 | 0.999 | 0.999 |
| Volume | -3.22 | -3.33 | -2.39 | -2.48 | -1.85 | -3.69 | -4.71 | -4.66 | -3.73 | -0.34 | -2 | -0.96 | -1.88 | 0.59 | -4.16 |
| Volume FWE p | 0.999 | 0.999 | 0.999 | 0.999 | 0.999 | 0.999 | 0.999 | 0.999 | 0.999 | 0.999 | 0.999 | 0.999 | 0.999 | 0.999 | 0.999 |
| Volume mFWE p | 0.999 | 0.999 | 0.999 | 0.999 | 0.999 | 0.999 | 0.999 | 0.999 | 0.999 | 0.999 | 0.999 | 0.999 | 0.999 | 0.999 | 0.999 |
| Thickness | 0.7 | -1.65 | -2.4 | 1.39 | 1.74 | -0.48 | -3.7 | -3.32 | -1.59 | 0.06 | 1.83 | 0.99 | -0.72 | 2.68 | 0.03 |
| Thickness FWE p | 0.999 | 0.999 | 0.999 | 0.986 | 0.938 | 0.999 | 0.999 | 0.999 | 0.999 | 0.999 | 0.912 | 0.999 | 0.999 | 0.409 | 0.999 |
| Thickness mFWE p | 0.999 | 0.999 | 0.999 | 0.999 | 0.999 | 0.999 | 0.999 | 0.999 | 0.999 | 0.999 | 0.999 | 0.999 | 0.999 | 0.999 | 0.999 |

Table 24 continued

| | Left long insular gyrus and central sulcus of the insula | Left short insular gyri | Left middle occipital gyrus | Left superior occipital gyrus | Left lateral occipito temporal gyrus | Left lingual gyrus | Left parahippocampal gyrus | Left orbital gyri | Left angular gyrus | Left supramarginal gyrus | Left superior parietal lobule | Left postcentral gyrus | Left precentral gyrus | Left precuneus |
|---|---|---|---|---|---|---|---|---|---|---|---|---|---|---|
| **Fisher F** | **0.44** | **2.88** | **3.66** | **2.51** | **1.22** | **1.36** | **8.06** | **3.09** | **1.18** | **1.43** | **0.75** | **3.45** | **11.53** | **0.55** |
| **Fisher FWE p** | **0.999** | **0.999** | **0.999** | **0.999** | **0.999** | **0.999** | **0.999** | **0.999** | **0.999** | **0.999** | **0.999** | **0.999** | **0.959** | **0.999** |
| MD | -2.09 | -0.67 | -1.25 | -1.5 | -1.83 | -1.74 | -0.06 | -1.06 | -1.37 | -1.74 | -2.4 | -2 | 0.15 | -2.57 |
| MD FWE p | 0.999 | 0.998 | 0.999 | 0.999 | 0.999 | 0.999 | 0.956 | 0.999 | 0.999 | 0.999 | 0.999 | 0.999 | 0.906 | 0.999 |
| MD mFWE p | 0.999 | 0.999 | 0.999 | 0.999 | 0.999 | 0.999 | 0.999 | 0.999 | 0.999 | 0.999 | 0.999 | 0.999 | 0.999 | 0.999 |
| RD | -1.88 | -1.13 | -1.44 | -1.63 | -1.51 | -1.26 | 0.06 | -1.53 | -1.71 | -1.93 | -2.51 | -1.86 | 0.06 | -2.45 |
| RD FWE p | 0.999 | 0.999 | 0.999 | 0.999 | 0.999 | 0.999 | 0.921 | 0.999 | 0.999 | 0.999 | 0.999 | 0.999 | 0.92 | 0.999 |
| RD mFWE p | 0.999 | 0.999 | 0.999 | 0.999 | 0.999 | 0.999 | 0.999 | 0.999 | 0.999 | 0.999 | 0.999 | 0.999 | 0.999 | 0.999 |
| AD | -2.04 | 0.28 | -0.8 | -1.12 | -1.68 | -2.39 | -0.23 | -0.19 | -0.62 | -1.19 | -2 | -2.14 | 0.32 | -2.64 |
| AD FWE p | 0.999 | 0.946 | 0.999 | 0.999 | 0.999 | 0.999 | 0.995 | 0.994 | 0.999 | 0.999 | 0.999 | 0.999 | 0.937 | 0.999 |
| AD mFWE p | 0.999 | 0.999 | 0.999 | 0.999 | 0.999 | 0.999 | 0.999 | 0.999 | 0.999 | 0.999 | 0.999 | 0.999 | 0.999 | 0.999 |
| Volume | -2.43 | -3.45 | -2.58 | -2.76 | -2.12 | -2.31 | -2.06 | -4.3 | -3.31 | -3.1 | -1.87 | -3.67 | -3.58 | -1.65 |
| Volume FWE p | 0.999 | 0.999 | 0.999 | 0.999 | 0.999 | 0.999 | 0.999 | 0.999 | 0.999 | 0.999 | 0.999 | 0.999 | 0.999 | 0.999 |
| Volume mFWE p | 0.999 | 0.999 | 0.999 | 0.999 | 0.999 | 0.999 | 0.999 | 0.999 | 0.999 | 0.999 | 0.999 | 0.999 | 0.999 | 0.999 |
| Thickness | 1.12 | 1.49 | -0.68 | -0.33 | 0.36 | 0.26 | -1.16 | -0.09 | 1.12 | 0.24 | 0.63 | -0.87 | -1.75 | 0.88 |
| Thickness FWE p | 0.997 | 0.978 | 0.999 | 0.999 | 0.999 | 0.999 | 0.999 | 0.999 | 0.997 | 0.999 | 0.999 | 0.999 | 0.999 | 0.999 |
| Thickness mFWE p | 0.999 | 0.999 | 0.999 | 0.999 | 0.999 | 0.999 | 0.999 | 0.999 | 0.999 | 0.999 | 0.999 | 0.999 | 0.999 | 0.999 |

Table 24 continued

| | Left subcallosal gyrus | Left anterior transverse temporal gyrus | Left lateral aspect of the superior temporal gyrus | Left planum polare of the superior temporal gyrus | Left planum temporale | Left inferior temporal gyrus | Left middle temporal gyrus | Left horizontal ramus of the anterior segment of the lateral sulcus | Left vertical ramus of the anterior segment of the lateral sulcus | Left posterior ramus of the lateral sulcus | Left occipital pole | Left temporal pole | Left calcarine sulcus | Left central sulcus |
|---|---|---|---|---|---|---|---|---|---|---|---|---|---|---|
| **Fisher F** | **1.47** | **1.29** | **0.1** | **7.54** | **11.48** | **1.11** | **0.44** | **6.31** | **5.01** | **7.2** | **6.41** | **1.58** | **5.01** | **1.88** |
| **Fisher FWE p** | **0.999** | **0.999** | **0.999** | **0.999** | **0.961** | **0.999** | **0.999** | **0.999** | **0.999** | **0.999** | **0.999** | **0.999** | **0.999** | **0.999** |
| MD | -0.93 | -1.28 | -2.81 | 0.28 | 0.01 | -1.7 | -2.8 | -0.18 | -1.09 | -1.67 | -0.92 | -1.16 | -1.68 | -1.91 |
| MD FWE p | 0.999 | 0.999 | 0.999 | 0.861 | 0.942 | 0.999 | 0.999 | 0.974 | 0.999 | 0.999 | 0.999 | 0.999 | 0.999 | 0.999 |
| MD mFWE p | 0.999 | 0.999 | 0.999 | 0.999 | 0.999 | 0.999 | 0.999 | 0.999 | 0.999 | 0.999 | 0.999 | 0.999 | 0.999 | 0.999 |
| RD | -1.01 | -0.97 | -2.78 | 0.08 | 0.0 | -1.56 | -3.27 | -0.56 | -1.41 | -1.78 | -0.9 | -1.15 | -1.36 | -2.01 |
| RD FWE p | 0.999 | 0.999 | 0.999 | 0.917 | 0.936 | 0.999 | 0.999 | 0.994 | 0.999 | 0.999 | 0.999 | 0.999 | 0.999 | 0.999 |
| RD mFWE p | 0.999 | 0.999 | 0.999 | 0.999 | 0.999 | 0.999 | 0.999 | 0.999 | 0.999 | 0.999 | 0.999 | 0.999 | 0.999 | 0.999 |
| AD | -0.74 | -1.72 | -2.56 | 0.51 | 0.04 | -1.39 | -1.55 | 0.64 | -0.33 | -1.18 | -0.74 | -0.9 | -2.07 | -1.61 |
| AD FWE p | 0.999 | 0.999 | 0.999 | 0.882 | 0.98 | 0.999 | 0.999 | 0.833 | 0.997 | 0.999 | 0.999 | 0.999 | 0.999 | 0.999 |
| AD mFWE p | 0.999 | 0.999 | 0.999 | 0.999 | 0.999 | 0.999 | 0.999 | 0.999 | 0.999 | 0.999 | 0.999 | 0.999 | 0.999 | 0.999 |
| Volume | -2.16 | -2.28 | -2.61 | -2.31 | -3.06 | -2.37 | -1.63 | -0.9 | -0.62 | -1.87 | -3.53 | -4.48 | -3.19 | -2.8 |
| Volume FWE p | 0.999 | 0.999 | 0.999 | 0.999 | 0.999 | 0.999 | 0.999 | 0.999 | 0.999 | 0.999 | 0.999 | 0.999 | 0.999 | 0.999 |
| Volume mFWE p | 0.999 | 0.999 | 0.999 | 0.999 | 0.999 | 0.999 | 0.999 | 0.999 | 0.999 | 0.999 | 0.999 | 0.999 | 0.999 | 0.999 |
| Thickness | 1.33 | 0.64 | 1.81 | -0.21 | -1.93 | 0.54 | 1.3 | -0.02 | -0.77 | -1.81 | -1.42 | 0.6 | -1.31 | -0.16 |
| Thickness FWE p | 0.99 | 0.999 | 0.918 | 0.999 | 0.999 | 0.999 | 0.991 | 0.999 | 0.999 | 0.999 | 0.999 | 0.999 | 0.999 | 0.999 |
| Thickness mFWE p | 0.999 | 0.999 | 0.999 | 0.999 | 0.999 | 0.999 | 0.999 | 0.999 | 0.999 | 0.999 | 0.999 | 0.999 | 0.999 | 0.999 |

Table 24 continued

| | Left anterior segment of the circular sulcus of the insula | Left inferior segment of the circular sulcus of the insula | Left superior segment of the circular sulcus of the insula | Left anterior transverse collateral sulcus | Left posterior transverse collateral sulcus | Left inferior frontal sulcus | Left middle frontal sulcus | Left superior frontal sulcus | Left sulcus intermedius primus | Left intraparietal sulcus and transverse parietal sulci | Left middle occipital sulcus and lunatus sulcus | Left superior occipital sulcus and transverse occipital sulcus | Left anterior occipital sulcus and preoccipital notch | Left lateral occipito temporal sulcus |
|---|---|---|---|---|---|---|---|---|---|---|---|---|---|---|
| **Fisher F** | **8.25** | **5.98** | **9.3** | **0.03** | **2.75** | **1.94** | **1.05** | **6.87** | **2.49** | **1.26** | **2.94** | **3.24** | **2.51** | **2.24** |
| **Fisher FWE p** | **0.999** | **0.999** | **0.999** | **0.999** | **0.999** | **0.999** | **0.999** | **0.999** | **0.999** | **0.999** | **0.999** | **0.999** | **0.999** | **0.999** |
| MD | -0.61 | -0.11 | -0.53 | -3.66 | -2.13 | -2.63 | -3.39 | -1.99 | -0.91 | -2.58 | -1.73 | -0.69 | -1.3 | -2.38 |
| MD FWE p | 0.998 | 0.964 | 0.996 | 0.999 | 0.999 | 0.999 | 0.999 | 0.999 | 0.999 | 0.999 | 0.999 | 0.999 | 0.999 | 0.999 |
| MD mFWE p | 0.999 | 0.999 | 0.999 | 0.999 | 0.999 | 0.999 | 0.999 | 0.999 | 0.999 | 0.999 | 0.999 | 0.999 | 0.999 | 0.999 |
| RD | -1.27 | -0.11 | -1.38 | -2.98 | -1.88 | -3.24 | -3.78 | -2.69 | -0.99 | -2.46 | -1.61 | -0.43 | -1.45 | -1.87 |
| RD FWE p | 0.999 | 0.956 | 0.999 | 0.999 | 0.999 | 0.999 | 0.999 | 0.999 | 0.999 | 0.999 | 0.999 | 0.989 | 0.999 | 0.999 |
| RD mFWE p | 0.999 | 0.999 | 0.999 | 0.999 | 0.999 | 0.999 | 0.999 | 0.999 | 0.999 | 0.999 | 0.999 | 0.999 | 0.999 | 0.999 |
| AD | 0.68 | -0.08 | 1.29 | -3.12 | -2.07 | -0.99 | -2.09 | -0.21 | -0.56 | -2.58 | -1.63 | -1.07 | -0.79 | -2.52 |
| AD FWE p | 0.817 | 0.989 | 0.467 | 0.999 | 0.999 | 0.999 | 0.999 | 0.995 | 0.999 | 0.999 | 0.999 | 0.999 | 0.999 | 0.999 |
| AD mFWE p | 0.999 | 0.999 | 0.999 | 0.999 | 0.999 | 0.999 | 0.999 | 0.999 | 0.999 | 0.999 | 0.999 | 0.999 | 0.999 | 0.999 |
| Volume | -3.93 | -2.99 | -2.27 | -3.52 | -2.22 | -0.67 | -2.08 | -3.19 | -0.59 | -3.25 | -1.65 | -2.13 | -1 | -1.77 |
| Volume FWE p | 0.999 | 0.999 | 0.999 | 0.999 | 0.999 | 0.999 | 0.999 | 0.999 | 0.999 | 0.999 | 0.999 | 0.999 | 0.999 | 0.999 |
| Volume mFWE p | 0.999 | 0.999 | 0.999 | 0.999 | 0.999 | 0.999 | 0.999 | 0.999 | 0.999 | 0.999 | 0.999 | 0.999 | 0.999 | 0.999 |
| Thickness | -1.29 | -0.47 | -1.02 | 2.22 | -0.6 | 0.27 | 0.29 | -1.58 | 0.9 | 0.11 | -0.58 | -0.08 | 0.04 | -0.37 |
| Thickness FWE p | 0.999 | 0.999 | 0.999 | 0.732 | 0.999 | 0.999 | 0.999 | 0.999 | 0.999 | 0.999 | 0.999 | 0.999 | 0.999 | 0.999 |
| Thickness mFWE p | 0.999 | 0.999 | 0.999 | 0.999 | 0.999 | 0.999 | 0.999 | 0.999 | 0.999 | 0.999 | 0.999 | 0.999 | 0.999 | 0.999 |

Table 24 continued

| | Left lateral orbital sulcus | Left medial orbital sulcus | Left orbital sulci | Left parieto occipital sulcus | Left pericallosal sulcus | Left postcentral sulcus | Left inferior part of the precentral sulcus | Left superior part of the precentral sulcus | Left suborbital sulcus | Left subparietal sulcus | Left inferior temporal sulcus | Left superior temporal sulcus | Left transverse temporal sulcus | Right fronto marginal gyrus and sulcus |
|---|---|---|---|---|---|---|---|---|---|---|---|---|---|---|
| **Fisher F** | **1.57** | **5.66** | **4.75** | **4.29** | **3.31** | **4.81** | **7.32** | **7.2** | **1.12** | **3.37** | **6.77** | **0.47** | **11.01** | **2.52** |
| **Fisher FWE p** | **0.999** | **0.999** | **0.999** | **0.999** | **0.999** | **0.999** | **0.999** | **0.999** | **0.999** | **0.999** | **0.999** | **0.999** | **0.975** | **0.999** |
| MD | -2.77 | -2.61 | -0.96 | -1.26 | -1.22 | -1.87 | -2.09 | -0.62 | -1.16 | -1.84 | -3.62 | -2.11 | 0.57 | -1.65 |
| MD FWE p | 0.999 | 0.999 | 0.999 | 0.999 | 0.999 | 0.999 | 0.999 | 0.998 | 0.999 | 0.999 | 0.999 | 0.999 | 0.714 | 0.999 |
| MD mFWE p | 0.999 | 0.999 | 0.999 | 0.999 | 0.999 | 0.999 | 0.999 | 0.999 | 0.999 | 0.999 | 0.999 | 0.999 | 0.999 | 0.999 |
| RD | -3.42 | -2.78 | -2.02 | -0.89 | -1.76 | -1.92 | -2.44 | -1.03 | -1.12 | -1.45 | -4.12 | -2.29 | 0.53 | -2.37 |
| RD FWE p | 0.999 | 0.999 | 0.999 | 0.999 | 0.999 | 0.999 | 0.999 | 0.999 | 0.999 | 0.999 | 0.999 | 0.999 | 0.725 | 0.999 |
| RD mFWE p | 0.999 | 0.999 | 0.999 | 0.999 | 0.999 | 0.999 | 0.999 | 0.999 | 0.999 | 0.999 | 0.999 | 0.999 | 0.999 | 0.999 |
| AD | -1.24 | -1.6 | 0.87 | -1.84 | -0.13 | -1.55 | -1.09 | 0.32 | -0.89 | -2.3 | -2.02 | -1.38 | 0.53 | -0.25 |
| AD FWE p | 0.999 | 0.999 | 0.719 | 0.999 | 0.992 | 0.999 | 0.999 | 0.937 | 0.999 | 0.999 | 0.999 | 0.999 | 0.876 | 0.996 |
| AD mFWE p | 0.999 | 0.999 | 0.999 | 0.999 | 0.999 | 0.999 | 0.999 | 0.999 | 0.999 | 0.999 | 0.999 | 0.999 | 0.999 | 0.999 |
| Volume | -0.66 | -3.93 | -3.77 | -3.24 | -3.42 | -1.8 | -2.04 | -1.35 | -2.18 | -2.5 | -2.04 | -3.52 | -2.61 | -3.35 |
| Volume FWE p | 0.999 | 0.999 | 0.999 | 0.999 | 0.999 | 0.999 | 0.999 | 0.999 | 0.999 | 0.999 | 0.999 | 0.999 | 0.999 | 0.999 |
| Volume mFWE p | 0.999 | 0.999 | 0.999 | 0.999 | 0.999 | 0.999 | 0.999 | 0.999 | 0.999 | 0.999 | 0.999 | 0.999 | 0.999 | 0.999 |
| Thickness | 0.49 | -1.53 | 0.25 | -0.97 | -0.24 | -1.25 | -1.86 | -1.13 | 1.5 | -0.8 | -1.81 | 1.21 | -0.98 | 0.01 |
| Thickness FWE p | 0.999 | 0.999 | 0.999 | 0.999 | 0.999 | 0.999 | 0.999 | 0.999 | 0.976 | 0.999 | 0.999 | 0.995 | 0.999 | 0.999 |
| Thickness mFWE p | 0.999 | 0.999 | 0.999 | 0.999 | 0.999 | 0.999 | 0.999 | 0.999 | 0.999 | 0.999 | 0.999 | 0.999 | 0.999 | 0.999 |

Table 24 continued

| | Right paracentral lobule and sulcus | Right subcentral gyrus and sulci | Right transverse frontopolar gyri and sulci | Right anterior part of the cingulate gyrus and sulcus | Right middle anterior part of the cingulate gyrus and sulcus | Right middle posterior part of the cingulate gyrus and sulcus | Right posterior dorsal part of the cingulate gyrus | Right posterior ventral part of the cingulate gyrus | Right cuneus | Right opercular part of the inferior frontal gyrus | Right orbital part of the inferior frontal gyrus | Right triangular part of the inferior frontal gyrus | Right middle frontal gyrus | Right superior frontal gyrus |
|---|---|---|---|---|---|---|---|---|---|---|---|---|---|---|
| **Fisher F** | **7.24** | **0.15** | **2** | **1.85** | **2.44** | **5.16** | **1.55** | **3.11** | **0.95** | **1.54** | **2.98** | **3.62** | **1.02** | **1.64** |
| **Fisher FWE p** | **0.999** | **0.999** | **0.999** | **0.999** | **0.999** | **0.999** | **0.999** | **0.999** | **0.999** | **0.999** | **0.999** | **0.999** | **0.999** | **0.999** |
| MD | -1.06 | -2.6 | -2.05 | -2.53 | -3.1 | -1.44 | -2.21 | -1.08 | -1.63 | -2.36 | -2.73 | -3.51 | -2.19 | -2.07 |
| MD FWE p | 0.999 | 0.999 | 0.999 | 0.999 | 0.999 | 0.999 | 0.999 | 0.999 | 0.999 | 0.999 | 0.999 | 0.999 | 0.999 | 0.999 |
| MD mFWE p | 0.999 | 0.999 | 0.999 | 0.999 | 0.999 | 0.999 | 0.999 | 0.999 | 0.999 | 0.999 | 0.999 | 0.999 | 0.999 | 0.999 |
| RD | -1.11 | -2.62 | -2.76 | -3.15 | -3.51 | -1.66 | -1.56 | -0.93 | -1.46 | -2.42 | -3.16 | -3.75 | -2.7 | -2.4 |
| RD FWE p | 0.999 | 0.999 | 0.999 | 0.999 | 0.999 | 0.999 | 0.999 | 0.999 | 0.999 | 0.999 | 0.999 | 0.999 | 0.999 | 0.999 |
| RD mFWE p | 0.999 | 0.999 | 0.999 | 0.999 | 0.999 | 0.999 | 0.999 | 0.999 | 0.999 | 0.999 | 0.999 | 0.999 | 0.999 | 0.999 |
| AD | -0.98 | -2.28 | -0.61 | -0.86 | -1.61 | -0.62 | -2.96 | -1.1 | -1.79 | -2.02 | -1.58 | -2.72 | -1.09 | -1.2 |
| AD FWE p | 0.999 | 0.999 | 0.999 | 0.999 | 0.999 | 0.999 | 0.999 | 0.999 | 0.999 | 0.999 | 0.999 | 0.999 | 0.999 | 0.999 |
| AD mFWE p | 0.999 | 0.999 | 0.999 | 0.999 | 0.999 | 0.999 | 0.999 | 0.999 | 0.999 | 0.999 | 0.999 | 0.999 | 0.999 | 0.999 |
| Volume | -1.39 | -3.12 | -3.23 | -3.5 | -4.41 | -3.5 | -2.79 | 0.28 | -1.76 | -0.72 | -3.21 | 0.97 | -2.27 | -3.76 |
| Volume FWE p | 0.999 | 0.999 | 0.999 | 0.999 | 0.999 | 0.999 | 0.999 | 0.999 | 0.999 | 0.999 | 0.999 | 0.996 | 0.999 | 0.999 |
| Volume mFWE p | 0.999 | 0.999 | 0.999 | 0.999 | 0.999 | 0.999 | 0.999 | 0.999 | 0.999 | 0.999 | 0.999 | 0.999 | 0.999 | 0.999 |
| Thickness | -1.67 | 1.61 | 0.04 | -0.01 | -0.49 | -1.19 | -0.01 | 1.19 | 0.72 | 0.33 | -0.7 | 2.36 | 0.57 | 0.03 |
| Thickness FWE p | 0.999 | 0.963 | 0.999 | 0.999 | 0.999 | 0.999 | 0.999 | 0.995 | 0.999 | 0.999 | 0.999 | 0.641 | 0.999 | 0.999 |
| Thickness mFWE p | 0.999 | 0.999 | 0.999 | 0.999 | 0.999 | 0.999 | 0.999 | 0.999 | 0.999 | 0.999 | 0.999 | 0.999 | 0.999 | 0.999 |

Table 24 continued

| | Right short insular gyri | Right middle occipital gyrus | Right superior occipital gyrus | Right lateral occipito temporal gyrus | Right lingual gyrus | Right parahippocampal gyrus | Right orbital gyri | Right angular gyrus | Right supramarginal gyrus | Right superior parietal lobule | Right postcentral gyrus | Right precentral gyrus | Right precuneus |
|---|---|---|---|---|---|---|---|---|---|---|---|---|---|
| **Fisher F** | **2.31** | **1.57** | **3.25** | **0.88** | **0.27** | **1.78** | **1.15** | **0.82** | **1.29** | **1.59** | **2.29** | **16.52** | **0.7** |
| **Fisher FWE p** | **0.999** | **0.999** | **0.999** | **0.999** | **0.999** | **0.999** | **0.999** | **0.999** | **0.999** | **0.999** | **0.999** | **0.62** | **0.999** |
| MD | -0.85 | -1.36 | -0.71 | -2.02 | -3.03 | -1.75 | -1.57 | -1.72 | -2.84 | -1.84 | -2.45 | 0.26 | -1.81 |
| MD FWE p | 0.999 | 0.999 | 0.999 | 0.999 | 0.999 | 0.999 | 0.999 | 0.999 | 0.999 | 0.999 | 0.999 | 0.867 | 0.999 |
| MD mFWE p | 0.999 | 0.999 | 0.999 | 0.999 | 0.999 | 0.999 | 0.999 | 0.999 | 0.999 | 0.999 | 0.999 | 0.999 | 0.999 |
| RD | -1.31 | -1.01 | -0.69 | -1.98 | -2.53 | -1.55 | -1.9 | -1.83 | -3.05 | -1.92 | -2.44 | 0.24 | -1.95 |
| RD FWE p | 0.999 | 0.999 | 0.997 | 0.999 | 0.999 | 0.999 | 0.999 | 0.999 | 0.999 | 0.999 | 0.999 | 0.866 | 0.999 |
| RD mFWE p | 0.999 | 0.999 | 0.999 | 0.999 | 0.999 | 0.999 | 0.999 | 0.999 | 0.999 | 0.999 | 0.999 | 0.999 | 0.999 |
| AD | 0.06 | -1.67 | -0.65 | -1.47 | -3.6 | -1.7 | -0.75 | -1.33 | -2.16 | -1.56 | -2.37 | 0.27 | -1.39 |
| AD FWE p | 0.978 | 0.999 | 0.999 | 0.999 | 0.999 | 0.999 | 0.999 | 0.999 | 0.999 | 0.999 | 0.999 | 0.947 | 0.999 |
| AD mFWE p | 0.999 | 0.999 | 0.999 | 0.999 | 0.999 | 0.999 | 0.999 | 0.999 | 0.999 | 0.999 | 0.999 | 0.999 | 0.999 |
| Volume | -2.43 | -2.26 | -1.35 | -2.88 | -1.27 | -2.38 | -4.73 | -3.51 | -3.8 | -2.5 | -2.8 | -3.68 | -3.73 |
| Volume FWE p | 0.999 | 0.999 | 0.999 | 0.999 | 0.999 | 0.999 | 0.999 | 0.999 | 0.999 | 0.999 | 0.999 | 0.999 | 0.999 |
| Volume mFWE p | 0.999 | 0.999 | 0.999 | 0.999 | 0.999 | 0.999 | 0.999 | 0.999 | 0.999 | 0.999 | 0.999 | 0.999 | 0.999 |
| Thickness | 1.4 | 0.33 | 0.02 | 0.6 | 2.02 | -0.05 | 0.83 | 0.81 | 0.09 | 0.03 | -0.45 | -2.65 | 0.91 |
| Thickness FWE p | 0.985 | 0.999 | 0.999 | 0.999 | 0.841 | 0.999 | 0.999 | 0.999 | 0.999 | 0.999 | 0.999 | 0.999 | 0.999 |
| Thickness mFWE p | 0.999 | 0.999 | 0.999 | 0.999 | 0.999 | 0.999 | 0.999 | 0.999 | 0.999 | 0.999 | 0.999 | 0.999 | 0.999 |

Table 24 continued

| | Right subcallosal gyrus | Right anterior transverse temporal gyrus | Right lateral aspect of the superior temporal gyrus | Right planum polare of the superior temporal gyrus | Right planum temporale | Right inferior temporal gyrus | Right middle temporal gyrus | Right horizontal ramus of the anterior segment of the lateral sulcus | Right vertical ramus of the anterior segment of the lateral sulcus | Right posterior ramus of the lateral sulcus | Right occipital pole | Right temporal pole | Right calcarine sulcus | Right central sulcus |
|---|---|---|---|---|---|---|---|---|---|---|---|---|---|---|
| **Fisher F** | **0.35** | **0.29** | **1.03** | **1.41** | **7.86** | **3.82** | **0.24** | **5.59** | **4.81** | **2.29** | **7.42** | **0.48** | **1.97** | **0.73** |
| **Fisher FWE p** | **0.999** | **0.999** | **0.999** | **0.999** | **0.999** | **0.999** | **0.999** | **0.999** | **0.999** | **0.999** | **0.999** | **0.999** | **0.999** | **0.999** |
| MD | -2.18 | -2.21 | -3.24 | -0.96 | -1.54 | -2.74 | -3.73 | -0.91 | -1.49 | -1.79 | -0.54 | -1.81 | -1.22 | -2.34 |
| MD FWE p | 0.999 | 0.999 | 0.999 | 0.999 | 0.999 | 0.999 | 0.999 | 0.999 | 0.999 | 0.999 | 0.996 | 0.999 | 0.999 | 0.999 |
| MD mFWE p | 0.999 | 0.999 | 0.999 | 0.999 | 0.999 | 0.999 | 0.999 | 0.999 | 0.999 | 0.999 | 0.999 | 0.999 | 0.999 | 0.999 |
| RD | -1.99 | -2.19 | -3.32 | -0.92 | -1.42 | -2.6 | -4.3 | -1.35 | -1.72 | -1.97 | -0.03 | -1.45 | -1.01 | -2.37 |
| RD FWE p | 0.999 | 0.999 | 0.999 | 0.999 | 0.999 | 0.999 | 0.999 | 0.999 | 0.999 | 0.999 | 0.943 | 0.999 | 0.999 | 0.999 |
| RD mFWE p | 0.999 | 0.999 | 0.999 | 0.999 | 0.999 | 0.999 | 0.999 | 0.999 | 0.999 | 0.999 | 0.999 | 0.999 | 0.999 | 0.999 |
| AD | -2.26 | -2.05 | -2.75 | -0.8 | -1.63 | -1.89 | -2.11 | 0.14 | -0.71 | -1.12 | -1.17 | -1.91 | -1.42 | -2.19 |
| AD FWE p | 0.999 | 0.999 | 0.999 | 0.999 | 0.999 | 0.999 | 0.999 | 0.969 | 0.999 | 0.999 | 0.999 | 0.999 | 0.999 | 0.999 |
| AD mFWE p | 0.999 | 0.999 | 0.999 | 0.999 | 0.999 | 0.999 | 0.999 | 0.999 | 0.999 | 0.999 | 0.999 | 0.999 | 0.999 | 0.999 |
| Volume | -1.7 | -1.87 | -2.68 | -2.77 | -2.7 | -3.67 | -2.8 | 0.12 | -0.84 | -0.59 | -3.31 | -4.02 | -2.5 | -1.79 |
| Volume FWE p | 0.999 | 0.999 | 0.999 | 0.999 | 0.999 | 0.999 | 0.999 | 0.999 | 0.999 | 0.999 | 0.999 | 0.999 | 0.999 | 0.999 |
| Volume mFWE p | 0.999 | 0.999 | 0.999 | 0.999 | 0.999 | 0.999 | 0.999 | 0.999 | 0.999 | 0.999 | 0.999 | 0.999 | 0.999 | 0.999 |
| Thickness | 1.43 | 1.54 | 0.26 | 1.41 | -1.98 | -1.02 | 1.31 | -0.23 | -0.97 | 0.1 | -1.43 | 1.32 | 0.11 | 0.66 |
| Thickness FWE p | 0.984 | 0.972 | 0.999 | 0.985 | 0.999 | 0.999 | 0.991 | 0.999 | 0.999 | 0.999 | 0.999 | 0.99 | 0.999 | 0.999 |
| Thickness mFWE p | 0.999 | 0.999 | 0.999 | 0.999 | 0.999 | 0.999 | 0.999 | 0.999 | 0.999 | 0.999 | 0.999 | 0.999 | 0.999 | 0.999 |

Table 24 continued

| | Right anterior segment of the circular sulcus of the insula | Right inferior segment of the circular sulcus of the insula | Right superior segment of the circular sulcus of the insula | Right anterior transverse collateral sulcus | Right posterior transverse collateral sulcus | Right inferior frontal sulcus | Right middle frontal sulcus | Right superior frontal sulcus | Right sulcus intermedius primus | Right intraparietal sulcus and transverse parietal sulci | Right middle occipital sulcus and lunatus sulcus | Right superior occipital sulcus and transverse occipital sulcus | Right anterior occipital sulcus and preoccipital notch | Right lateral occipito temporal sulcus |
|---|---|---|---|---|---|---|---|---|---|---|---|---|---|---|
| **Fisher F** | **5.08** | **3.74** | **10.32** | **0.13** | **3.26** | **1.46** | **2.17** | **6.43** | **0.06** | **1.47** | **4.07** | **4.13** | **6.25** | **4.58** |
| **Fisher FWE p** | **0.999** | **0.999** | **0.989** | **0.999** | **0.999** | **0.999** | **0.999** | **0.999** | **0.999** | **0.999** | **0.999** | **0.999** | **0.999** | **0.999** |
| MD | -0.57 | -0.9 | -0.74 | -3.41 | -0.97 | -2.11 | -3.13 | -2.25 | -2.9 | -1.38 | -1.29 | -0.55 | -1.05 | -2.44 |
| MD FWE p | 0.997 | 0.999 | 0.999 | 0.999 | 0.999 | 0.999 | 0.999 | 0.999 | 0.999 | 0.999 | 0.999 | 0.997 | 0.999 | 0.999 |
| MD mFWE p | 0.999 | 0.999 | 0.999 | 0.999 | 0.999 | 0.999 | 0.999 | 0.999 | 0.999 | 0.999 | 0.999 | 0.999 | 0.999 | 0.999 |
| RD | -1.15 | -0.78 | -1.28 | -3.28 | -0.25 | -2.65 | -3.73 | -2.85 | -2.78 | -1.35 | -1.34 | -0.44 | -0.84 | -2.03 |
| RD FWE p | 0.999 | 0.998 | 0.999 | 0.999 | 0.975 | 0.999 | 0.999 | 0.999 | 0.999 | 0.999 | 0.999 | 0.989 | 0.999 | 0.999 |
| RD mFWE p | 0.999 | 0.999 | 0.999 | 0.999 | 0.999 | 0.999 | 0.999 | 0.999 | 0.999 | 0.999 | 0.999 | 0.999 | 0.999 | 0.999 |
| AD | 0.62 | -0.91 | 0.46 | -1.94 | -1.96 | -0.77 | -1.48 | -0.63 | -2.77 | -1.33 | -0.91 | -0.7 | -1.25 | -2.04 |
| AD FWE p | 0.84 | 0.999 | 0.899 | 0.999 | 0.999 | 0.999 | 0.999 | 0.999 | 0.999 | 0.999 | 0.999 | 0.999 | 0.999 | 0.999 |
| AD mFWE p | 0.999 | 0.999 | 0.999 | 0.999 | 0.999 | 0.999 | 0.999 | 0.999 | 0.999 | 0.999 | 0.999 | 0.999 | 0.999 | 0.999 |
| Volume | -2.59 | -2.26 | -1.51 | -4.06 | -0.75 | -1.44 | -1.63 | -2.97 | -3.44 | -2.85 | -2.67 | -1.71 | -3.45 | -3 |
| Volume FWE p | 0.999 | 0.999 | 0.999 | 0.999 | 0.999 | 0.999 | 0.999 | 0.999 | 0.999 | 0.999 | 0.999 | 0.999 | 0.999 | 0.999 |
| Volume mFWE p | 0.999 | 0.999 | 0.999 | 0.999 | 0.999 | 0.999 | 0.999 | 0.999 | 0.999 | 0.999 | 0.999 | 0.999 | 0.999 | 0.999 |
| Thickness | -0.06 | -0.53 | -1.92 | 1.76 | 0.05 | 0.48 | -0.3 | -1.59 | 2.05 | 0.34 | -0.86 | -0.33 | -1.46 | -1.24 |
| Thickness FWE p | 0.999 | 0.999 | 0.999 | 0.931 | 0.999 | 0.999 | 0.999 | 0.999 | 0.828 | 0.999 | 0.999 | 0.999 | 0.999 | 0.999 |
| Thickness mFWE p | 0.999 | 0.999 | 0.999 | 0.999 | 0.999 | 0.999 | 0.999 | 0.999 | 0.999 | 0.999 | 0.999 | 0.999 | 0.999 | 0.999 |

Table 24 continued

| | Right lateral orbital sulcus | Right medial orbital sulcus | Right orbital sulci | Right parieto occipital sulcus | Right pericallosal sulcus | Right postcentral sulcus | Right inferior part of the precentral sulcus | Right superior part of the precentral sulcus | Right suborbital sulcus | Right subparietal sulcus | Right inferior temporal sulcus | Right superior temporal sulcus | Right transverse temporal sulcus |
|---|---|---|---|---|---|---|---|---|---|---|---|---|---|
| **Fisher F** | **0.74** | **0.34** | **7.01** | **1.22** | **4.61** | **4.99** | **8.4** | **8.94** | **1.37** | **2.71** | **3.01** | **1.95** | **0.61** |
| **Fisher FWE p** | **0.999** | **0.999** | **0.999** | **0.999** | **0.999** | **0.999** | **0.999** | **0.999** | **0.999** | **0.999** | **0.999** | **0.999** | **0.999** |
| MD | -2.82 | -1.92 | -0.22 | -1.36 | -2.18 | -1.67 | -1.35 | -0.83 | -1.91 | -1.67 | -2.02 | -1.74 | -2.27 |
| MD FWE p | 0.999 | 0.999 | 0.979 | 0.999 | 0.999 | 0.999 | 0.999 | 0.999 | 0.999 | 0.999 | 0.999 | 0.999 | 0.999 |
| MD mFWE p | 0.999 | 0.999 | 0.999 | 0.999 | 0.999 | 0.999 | 0.999 | 0.999 | 0.999 | 0.999 | 0.999 | 0.999 | 0.999 |
| RD | -3.5 | -1.93 | -1.01 | -1.11 | -3.53 | -1.74 | -1.84 | -1.34 | -2.09 | -1.66 | -2.54 | -1.91 | -2.2 |
| RD FWE p | 0.999 | 0.999 | 0.999 | 0.999 | 0.999 | 0.999 | 0.999 | 0.999 | 0.999 | 0.999 | 0.999 | 0.999 | 0.999 |
| RD mFWE p | 0.999 | 0.999 | 0.999 | 0.999 | 0.999 | 0.999 | 0.999 | 0.999 | 0.999 | 0.999 | 0.999 | 0.999 | 0.999 |
| AD | -1.16 | -1.47 | 0.94 | -1.68 | 0.12 | -1.42 | -0.26 | 0.3 | -1.26 | -1.45 | -0.49 | -1.11 | -2.09 |
| AD FWE p | 0.999 | 0.999 | 0.679 | 0.999 | 0.971 | 0.999 | 0.996 | 0.942 | 0.999 | 0.999 | 0.999 | 0.999 | 0.999 |
| AD mFWE p | 0.999 | 0.999 | 0.999 | 0.999 | 0.999 | 0.999 | 0.999 | 0.999 | 0.999 | 0.999 | 0.999 | 0.999 | 0.999 |
| Volume | -1.45 | -2.3 | -4.29 | -2.35 | -3.09 | -3.08 | -2.31 | -1.77 | -2.28 | -2.21 | -3.15 | -2.04 | -1.95 |
| Volume FWE p | 0.999 | 0.999 | 0.999 | 0.999 | 0.999 | 0.999 | 0.999 | 0.999 | 0.999 | 0.999 | 0.999 | 0.999 | 0.999 |
| Volume mFWE p | 0.999 | 0.999 | 0.999 | 0.999 | 0.999 | 0.999 | 0.999 | 0.999 | 0.999 | 0.999 | 0.999 | 0.999 | 0.999 |
| Thickness | 1.06 | 1.87 | -0.38 | 0.61 | -0.76 | -1.29 | -1.9 | -1.72 | 0.24 | -0.49 | -0.44 | -0.06 | 0.81 |
| Thickness FWE p | 0.998 | 0.902 | 0.999 | 0.999 | 0.999 | 0.999 | 0.999 | 0.999 | 0.999 | 0.999 | 0.999 | 0.999 | 0.999 |
| Thickness mFWE p | 0.999 | 0.999 | 0.999 | 0.999 | 0.999 | 0.999 | 0.999 | 0.999 | 0.999 | 0.999 | 0.999 | 0.999 | 0.999 |

**Table B25 Negative correlations between white matter metrics and lifetime asthma attacks**

| | Right fornix | Left fornix | Right cingulate bundle (cingualte) | Left cingulate bundle (cingualte) | Right cingulate bundle (parahippoccampal) | Left cingulate bundle (parahippoccampal) | Right corticospinal tract | Left corticospinal | Right anterior thalamic radiations | Left anterior thalamic radiations | Right uncinate fasciculus | Left uncinate fasciculus | Right inferior longitudinal fasciculus |
|---|---|---|---|---|---|---|---|---|---|---|---|---|---|
| **Fisher F** | **10.17** | **10.83** | **6.7** | **21.31** | **13.66** | **16.07** | **7.59** | **7.04** | **5.34** | **11.92** | **10.02** | **11.77** | **10.62** |
| **Fisher FWE p** | **0.971** | **0.95** | **0.999** | **0.284** | **0.795** | **0.618** | **0.999** | **0.999** | **0.999** | **0.902** | **0.975** | **0.909** | **0.958** |
| FA | -1.35 | -1.47 | -0.5 | -2.32 | -1.53 | -1.74 | -0.33 | -0.4 | -0.45 | -1.59 | -1.07 | -1.08 | -1.43 |
| FA FWEp | 0.744 | 0.689 | 0.967 | 0.238 | 0.656 | 0.544 | 0.981 | 0.976 | 0.972 | 0.628 | 0.855 | 0.851 | 0.711 |
| FA mFWEp | 0.928 | 0.888 | 0.999 | 0.358 | 0.86 | 0.747 | 0.999 | 0.999 | 0.999 | 0.834 | 0.984 | 0.983 | 0.905 |
| MD | 0 | 0.06 | -0.3 | 0.79 | 0.43 | 0.74 | 0.22 | 0.1 | -0.45 | 0.07 | 0.23 | 0.56 | -0.09 |
| MD FWEp | 0.741 | 0.714 | 0.845 | 0.385 | 0.553 | 0.41 | 0.648 | 0.699 | 0.884 | 0.714 | 0.642 | 0.491 | 0.776 |
| MD mFWEp | 0.999 | 0.999 | 0.999 | 0.998 | 0.999 | 0.999 | 0.999 | 0.999 | 0.999 | 0.999 | 0.999 | 0.999 | 0.999 |
| RD | 0.57 | 0.68 | 0 | 1.95 | 1.06 | 1.41 | 0.23 | 0.26 | -0.33 | 0.73 | 0.66 | 0.93 | 0.65 |
| RD FWEp | 0.761 | 0.713 | 0.939 | 0.138 | 0.517 | 0.341 | 0.885 | 0.876 | 0.979 | 0.689 | 0.721 | 0.588 | 0.727 |
| RD mFWEp | 0.999 | 0.999 | 0.999 | 0.608 | 0.985 | 0.911 | 0.999 | 0.999 | 0.999 | 0.999 | 0.999 | 0.994 | 0.999 |
| AD | -0.57 | -0.57 | -0.56 | -0.81 | -0.39 | -0.23 | 0.17 | -0.04 | -0.52 | -0.72 | -0.32 | -0.01 | -0.82 |
| AD FWEp | 0.822 | 0.822 | 0.82 | 0.888 | 0.76 | 0.695 | 0.518 | 0.615 | 0.807 | 0.865 | 0.733 | 0.602 | 0.891 |
| AD mFWEp | 0.999 | 0.999 | 0.999 | 0.999 | 0.999 | 0.999 | 0.999 | 0.999 | 0.999 | 0.999 | 0.999 | 0.999 | 0.999 |
| Volume | 0.5 | 0.66 | 0.03 | 0.09 | 0.13 | 0.62 | 0.96 | 1.31 | 0.57 | 0.11 | 0.58 | 0.74 | 0.2 |
| Volume FWEp | 0.988 | 0.993 | 0.954 | 0.961 | 0.964 | 0.992 | 0.997 | 0.999 | 0.99 | 0.962 | 0.991 | 0.994 | 0.971 |
| Volume mFWEp | 0.999 | 0.999 | 0.999 | 0.999 | 0.999 | 0.999 | 0.999 | 0.999 | 0.999 | 0.999 | 0.999 | 0.999 | 0.999 |

Table B25 continued

| | Left inferior longitudinal fasciculus | Right inferior fronto occipital fasciculus | Forceps major | Forceps minor | Corpus callosum | Right superior longitudinal fasciculus | Left superior longitudinal fasciculus | Right temporal superior longitduinal fasciculus | Left temporal superior longitduinal fasciculus | Right parietal superior logitduinal fasciculus | Left parietal superior logitduinal fasciculus | Right superior corticostriate | Left superior corticostriate |
|---|---|---|---|---|---|---|---|---|---|---|---|---|---|
| **Fisher F** | **9.07** | **9.97** | **3.92** | **10.18** | **6.48** | **11.63** | **8.49** | **9.58** | **9.34** | **12.46** | **6.5** | **8.64** | **7.02** |
| **Fisher FWE p** | **0.992** | **0.976** | **0.999** | **0.971** | **0.999** | **0.916** | **0.997** | **0.985** | **0.989** | **0.872** | **0.999** | **0.996** | **0.999** |
| FA | -0.81 | -1.34 | 0.1 | -1.04 | -0.25 | -1.27 | -0.7 | -1.15 | -0.94 | -1.31 | -0.19 | -0.8 | -0.46 |
| FA FWEp | 0.92 | 0.75 | 0.996 | 0.864 | 0.986 | 0.781 | 0.941 | 0.825 | 0.891 | 0.763 | 0.988 | 0.923 | 0.971 |
| FA mFWEp | 0.998 | 0.933 | 0.999 | 0.987 | 0.999 | 0.951 | 0.999 | 0.973 | 0.993 | 0.941 | 0.999 | 0.998 | 0.999 |
| MD | 0.27 | -0.09 | -0.48 | 0.33 | 0.05 | 0.08 | -0.28 | -0.18 | -0.28 | 0.19 | -0.29 | 0.1 | -0.04 |
| MD FWEp | 0.624 | 0.774 | 0.89 | 0.601 | 0.722 | 0.708 | 0.839 | 0.804 | 0.837 | 0.662 | 0.842 | 0.699 | 0.757 |
| MD mFWEp | 0.999 | 0.999 | 0.999 | 0.999 | 0.999 | 0.999 | 0.999 | 0.999 | 0.999 | 0.999 | 0.999 | 0.999 | 0.999 |
| RD | 0.54 | 0.64 | -0.47 | 0.78 | 0.08 | 0.75 | 0.29 | 0.52 | 0.46 | 0.84 | -0.1 | 0.44 | 0.12 |
| RD FWEp | 0.775 | 0.732 | 0.988 | 0.663 | 0.923 | 0.679 | 0.868 | 0.784 | 0.805 | 0.631 | 0.954 | 0.816 | 0.914 |
| RD mFWEp | 0.999 | 0.999 | 0.999 | 0.998 | 0.999 | 0.999 | 0.999 | 0.999 | 0.999 | 0.997 | 0.999 | 0.999 | 0.999 |
| AD | -0.06 | -0.82 | -0.32 | -0.33 | 0.01 | -0.68 | -0.87 | -0.89 | -1.04 | -0.59 | -0.47 | -0.23 | -0.2 |
| AD FWEp | 0.62 | 0.89 | 0.735 | 0.738 | 0.591 | 0.855 | 0.902 | 0.906 | 0.932 | 0.827 | 0.789 | 0.698 | 0.683 |
| AD mFWEp | 0.999 | 0.999 | 0.999 | 0.999 | 0.999 | 0.999 | 0.999 | 0.999 | 0.999 | 0.999 | 0.999 | 0.999 | 0.999 |
| Volume | 1.05 | 0.47 | 1.24 | 0.86 | 1.11 | -0.35 | -0.5 | -0.06 | -0.46 | -0.41 | -0.24 | 0.52 | 0.48 |
| Volume FWEp | 0.998 | 0.986 | 0.999 | 0.996 | 0.999 | 0.891 | 0.854 | 0.942 | 0.865 | 0.876 | 0.914 | 0.989 | 0.987 |
| Volume mFWEp | 0.999 | 0.999 | 0.999 | 0.999 | 0.999 | 0.999 | 0.999 | 0.999 | 0.999 | 0.999 | 0.999 | 0.999 | 0.999 |

Table B25 continued

| | Right superior corticostriatal | Left superior corticostriatal | Right inferior frontal cortex | Left inferior frontal cortex |
|---|---|---|---|---|
| **Fisher F** | **8.01** | **9.41** | **7.64** | **6.14** |
| **Fisher FWE p** | **0.999** | **0.988** | **0.999** | **0.999** |
| FA | -0.77 | -0.93 | -0.63 | -0.22 |
| FA FWEp | 0.928 | 0.893 | 0.951 | 0.987 |
| FA mFWEp | 0.998 | 0.994 | 0.999 | 0.999 |
| MD | 0.06 | 0.17 | -0.04 | -0.04 |
| MD FWEp | 0.717 | 0.67 | 0.755 | 0.755 |
| MD mFWEp | 0.999 | 0.999 | 0.999 | 0.999 |
| RD | 0.35 | 0.45 | 0.11 | -0.11 |
| RD FWEp | 0.848 | 0.809 | 0.917 | 0.957 |
| RD mFWEp | 0.999 | 0.999 | 0.999 | 0.999 |
| AD | -0.33 | -0.22 | -0.19 | 0.05 |
| AD FWEp | 0.738 | 0.691 | 0.679 | 0.571 |
| AD mFWEp | 0.999 | 0.999 | 0.999 | 0.999 |
| Volume | 0.71 | 0.33 | 0.3 | 0.97 |
| Volume FWEp | 0.994 | 0.979 | 0.977 | 0.998 |
| Volume mFWEp | 0.999 | 0.999 | 0.999 | 0.999 |

**Table B26 Negative correlations between subcortical grey matter metrics and lifetime asthma attacks**

| | Left thalamus | Left caudate | Left putamen | Left pallidum | Left hippocampus | Left amygdala | Left accumbens |
|---|---|---|---|---|---|---|---|
| **Fisher F** | **6.83** | **7.49** | **6.56** | **10.93** | **8.81** | **5.04** | **10.55** |
| **Fisher FWE p** | **0.548** | **0.5** | **0.568** | **0.302** | **0.414** | **0.693** | **0.32** |
| MD | -0.46 | 0.41 | 0.17 | 0.67 | 0.08 | -0.03 | 0.29 |
| MD FWE p | 0.798 | 0.427 | 0.536 | 0.314 | 0.576 | 0.627 | 0.48 |
| MD mFWE p | 0.977 | 0.774 | 0.861 | 0.653 | 0.886 | 0.914 | 0.82 |
| RD | -0.45 | 0.51 | 0.33 | 1.59 | 0.01 | 0.08 | 0.24 |
| RD FWE p | 0.87 | 0.484 | 0.568 | 0.1 | 0.715 | 0.681 | 0.61 |
| RD mFWE p | 0.976 | 0.728 | 0.803 | 0.205 | 0.906 | 0.885 | 0.836 |
| AD | -0.43 | 0.22 | -0.09 | -0.75 | 0.19 | -0.19 | 0.34 |
| AD FWE p | 0.766 | 0.476 | 0.622 | 0.87 | 0.49 | 0.67 | 0.421 |
| AD mFWE p | 0.974 | 0.843 | 0.926 | 0.993 | 0.853 | 0.945 | 0.8 |
| Volume | 1.24 | -0.13 | 0.15 | 0.28 | 1.16 | -0.21 | 1.35 |
| Volume FWE p | 0.255 | 0.848 | 0.752 | 0.7 | 0.288 | 0.872 | 0.215 |
| Volume mFWE p | 0.358 | 0.934 | 0.866 | 0.824 | 0.397 | 0.949 | 0.307 |

Table B26 continued

| | Right thalamus | Right caudate | Right putamen | Right pallidum | Right hippocampus | Right amygdala | Right accumbens |
|---|---|---|---|---|---|---|---|
| **Fisher F** | **5.28** | **4.55** | **7.92** | **11.56** | **7.89** | **8.09** | **4.99** |
| **Fisher FWE p** | **0.672** | **0.735** | **0.471** | **0.274** | **0.473** | **0.46** | **0.697** |
| MD | -0.16 | -0.47 | 0.19 | 0.75 | 0.03 | -0.25 | -0.29 |
| MD FWE p | 0.682 | 0.804 | 0.524 | 0.282 | 0.602 | 0.721 | 0.737 |
| MD mFWE p | 0.939 | 0.978 | 0.852 | 0.612 | 0.901 | 0.954 | 0.959 |
| RD | 0.1 | -0.79 | 0.34 | 1.88 | 0.11 | -0.2 | -0.27 |
| RD FWE p | 0.674 | 0.941 | 0.566 | 0.055 | 0.668 | 0.792 | 0.817 |
| RD mFWE p | 0.881 | 0.994 | 0.801 | 0.117 | 0.877 | 0.946 | 0.957 |
| AD | -0.46 | 0.05 | -0.03 | -0.86 | -0.1 | -0.31 | -0.31 |
| AD FWE p | 0.779 | 0.559 | 0.594 | 0.897 | 0.629 | 0.721 | 0.718 |
| AD mFWE p | 0.977 | 0.895 | 0.913 | 0.995 | 0.929 | 0.962 | 0.961 |
| Volume | 0.23 | 0.26 | 0.7 | -0.16 | 0.99 | 1.4 | 0.36 |
| Volume FWE p | 0.718 | 0.708 | 0.498 | 0.857 | 0.36 | 0.196 | 0.661 |
| Volume mFWE p | 0.839 | 0.83 | 0.634 | 0.939 | 0.483 | 0.283 | 0.791 |

**Table B27 Positive correlations between cortical grey matter metrics and lifetime asthma attacks**

| | Left fronto marginal gyrus and sulcus | Left inferior occipital gyrus and sulcus | Left paracentral lobule and sulcus | Left subcentral gyrus and sulci | Left transverse frontopolar gyri and sulci | Left anterior part of the cingulate gyrus and sulcus | Left middle anterior part of the cingulate gyrus and sulcus | Left middle posterior part of the cingulate gyrus and sulcus | Left posterior dorsal part of the cingulate gyrus | Left posterior ventral part of the cingulate gyrus | Left cuneus | Left opercular part of the inferior frontal gyrus | Left orbital part of the inferior frontal gyrus | Left triangular part of the inferior frontal gyrus | Left middle frontal gyrus |
|---|---|---|---|---|---|---|---|---|---|---|---|---|---|---|---|
| **Fisher F** | **7.75** | **14.24** | **9.27** | **13.92** | **10.92** | **5.84** | **8.64** | **9.5** | **6.56** | **8.19** | **7.34** | **11.72** | **11.16** | **10.59** | **10.6** |
| **Fisher FWE p** | **0.98** | **0.684** | **0.93** | **0.701** | **0.856** | **0.999** | **0.954** | **0.921** | **0.999** | **0.968** | **0.988** | **0.816** | **0.845** | **0.872** | **0.872** |
| MD | -0.13 | 0.76 | 0.09 | 0.34 | 0.48 | 0.05 | 0.09 | 0.34 | -0.3 | 0.31 | -0.26 | 0.53 | -0.48 | 0.22 | 0.48 |
| MD FWE p | 0.97 | 0.726 | 0.94 | 0.883 | 0.838 | 0.947 | 0.939 | 0.884 | 0.985 | 0.892 | 0.982 | 0.821 | 0.993 | 0.914 | 0.839 |
| MD mFWE p | 0.999 | 0.998 | 0.999 | 0.999 | 0.999 | 0.999 | 0.999 | 0.999 | 0.999 | 0.999 | 0.999 | 0.999 | 0.999 | 0.999 | 0.999 |
| RD | -0.44 | 0.59 | 0.05 | 0.08 | 0.09 | 0.1 | 0.28 | 0.41 | -0.4 | 0.17 | -0.41 | 0.43 | -0.51 | 0.11 | 0.28 |
| RD FWE p | 0.984 | 0.756 | 0.924 | 0.917 | 0.916 | 0.914 | 0.867 | 0.824 | 0.982 | 0.897 | 0.982 | 0.817 | 0.988 | 0.912 | 0.867 |
| RD mFWE p | 0.999 | 0.999 | 0.999 | 0.999 | 0.999 | 0.999 | 0.999 | 0.999 | 0.999 | 0.999 | 0.999 | 0.999 | 0.999 | 0.999 | 0.999 |
| AD | 0.36 | 0.94 | 0.16 | 0.77 | 1.03 | -0.04 | -0.22 | 0.19 | -0.12 | 0.49 | -0.01 | 0.68 | -0.39 | 0.4 | 0.81 |
| AD FWE p | 0.953 | 0.766 | 0.98 | 0.841 | 0.722 | 0.992 | 0.997 | 0.977 | 0.995 | 0.928 | 0.991 | 0.873 | 0.999 | 0.947 | 0.825 |
| AD mFWE p | 0.999 | 0.993 | 0.999 | 0.998 | 0.988 | 0.999 | 0.999 | 0.999 | 0.999 | 0.999 | 0.999 | 0.999 | 0.999 | 0.999 | 0.997 |
| Volume | 0.44 | 0.96 | 0.74 | 1.64 | 0.64 | -0.22 | 0.78 | 0.24 | -0.06 | 0 | 0.13 | 1.04 | 1.66 | 0.75 | 0.4 |
| Volume FWE p | 0.998 | 0.971 | 0.989 | 0.756 | 0.993 | 0.999 | 0.987 | 0.999 | 0.999 | 0.999 | 0.999 | 0.96 | 0.746 | 0.988 | 0.998 |
| Volume mFWE p | 0.999 | 0.992 | 0.998 | 0.847 | 0.999 | 0.999 | 0.998 | 0.999 | 0.999 | 0.999 | 0.999 | 0.988 | 0.839 | 0.998 | 0.999 |
| Thickness | 0.06 | 0.13 | 0.16 | 0.01 | -0.64 | -0.88 | -0.19 | 0.25 | 0.46 | -0.39 | 0.58 | -0.75 | 0.68 | 0.42 | -0.16 |
| Thickness FWE p | 0.995 | 0.993 | 0.991 | 0.996 | 0.999 | 0.999 | 0.999 | 0.986 | 0.964 | 0.999 | 0.945 | 0.999 | 0.922 | 0.97 | 0.999 |
| Thickness mFWE p | 0.999 | 0.999 | 0.999 | 0.999 | 0.999 | 0.999 | 0.999 | 0.999 | 0.999 | 0.999 | 0.999 | 0.999 | 0.999 | 0.999 | 0.999 |

Table B27 continued

| | Left long insular gyrus and central sulcus of the insula | Left short insular gyri | Left middle occipital gyrus | Left superior occipital gyrus | Left lateral occipito temporal gyrus | Left lingual gyrus | Left parahippocampal gyrus | Left orbital gyri | Left angular gyrus | Left supramarginal gyrus | Left superior parietal lobule | Left postcentral gyrus | Left precentral gyrus | Left precuneus |
|---|---|---|---|---|---|---|---|---|---|---|---|---|---|---|
| **Fisher F** | **13.08** | **20.83** | **7.11** | **8.63** | **8.09** | **10.35** | **8.29** | **15.79** | **8.46** | **12.03** | **9.96** | **7.92** | **12.38** | **7.59** |
| **Fisher FWE p** | **0.745** | **0.38** | **0.992** | **0.954** | **0.971** | **0.884** | **0.965** | **0.604** | **0.959** | **0.8** | **0.901** | **0.975** | **0.782** | **0.983** |
| MD | 0.37 | 0.63 | -0.48 | -0.49 | 0.09 | 0.73 | 0.35 | 0.55 | -0.01 | 0.1 | 0.07 | -0.03 | 0.08 | -0.21 |
| MD FWE p | 0.876 | 0.783 | 0.993 | 0.993 | 0.939 | 0.743 | 0.879 | 0.814 | 0.955 | 0.937 | 0.943 | 0.958 | 0.942 | 0.978 |
| MD mFWE p | 0.999 | 0.999 | 0.999 | 0.999 | 0.999 | 0.999 | 0.999 | 0.999 | 0.999 | 0.999 | 0.999 | 0.999 | 0.999 | 0.999 |
| RD | 0.45 | 0.46 | -0.66 | -0.64 | 0.02 | 0.59 | 0.19 | 0.25 | 0.02 | 0.08 | 0.04 | 0 | 0 | -0.29 |
| RD FWE p | 0.812 | 0.808 | 0.994 | 0.993 | 0.931 | 0.757 | 0.892 | 0.877 | 0.93 | 0.918 | 0.926 | 0.934 | 0.934 | 0.973 |
| RD mFWE p | 0.999 | 0.999 | 0.999 | 0.999 | 0.999 | 0.999 | 0.999 | 0.999 | 0.999 | 0.999 | 0.999 | 0.999 | 0.999 | 0.999 |
| AD | 0.21 | 0.88 | -0.17 | -0.23 | 0.21 | 0.91 | 0.56 | 0.92 | -0.05 | 0.14 | 0.12 | -0.06 | 0.22 | -0.07 |
| AD FWE p | 0.975 | 0.796 | 0.997 | 0.997 | 0.974 | 0.781 | 0.908 | 0.777 | 0.993 | 0.981 | 0.983 | 0.993 | 0.974 | 0.993 |
| AD mFWE p | 0.999 | 0.995 | 0.999 | 0.999 | 0.999 | 0.994 | 0.999 | 0.994 | 0.999 | 0.999 | 0.999 | 0.999 | 0.999 | 0.999 |
| Volume | 1.7 | 2.67 | 0.5 | 0.9 | -0.12 | -0.93 | -0.56 | 1.94 | 0.91 | 1.43 | 1.37 | 0.59 | 1.59 | 0.61 |
| Volume FWE p | 0.723 | 0.152 | 0.997 | 0.977 | 0.999 | 0.999 | 0.999 | 0.573 | 0.976 | 0.856 | 0.877 | 0.995 | 0.781 | 0.994 |
| Volume mFWE p | 0.819 | 0.227 | 0.999 | 0.995 | 0.999 | 0.999 | 0.999 | 0.682 | 0.994 | 0.924 | 0.939 | 0.999 | 0.867 | 0.999 |
| Thickness | -0.42 | 0.04 | 0.47 | 0.69 | 0.43 | -0.21 | -0.02 | -0.45 | -0.31 | 0.43 | -0.77 | -0.03 | 0.31 | 0.15 |
| Thickness FWE p | 0.999 | 0.995 | 0.962 | 0.917 | 0.969 | 0.999 | 0.997 | 0.999 | 0.999 | 0.969 | 0.999 | 0.997 | 0.981 | 0.992 |
| Thickness mFWE p | 0.999 | 0.999 | 0.999 | 0.999 | 0.999 | 0.999 | 0.999 | 0.999 | 0.999 | 0.999 | 0.999 | 0.999 | 0.999 | 0.999 |

Table B27 continued

| | Left subcallosal gyrus | Left anterior transverse temporal gyrus | Left lateral aspect of the superior temporal gyrus | Left planum polare of the superior temporal gyrus | Left planum temporale | Left inferior temporal gyrus | Left middle temporal gyrus | Left horizontal ramus of the anterior segment of the lateral sulcus | Left vertical ramus of the anterior segment of the lateral sulcus | Left posterior ramus of the lateral sulcus | Left occipital pole | Left temporal pole | Left calcarine sulcus | Left central sulcus |
|---|---|---|---|---|---|---|---|---|---|---|---|---|---|---|
| **Fisher F** | **14.59** | **13.36** | **11.67** | **16.04** | **12.7** | **10.4** | **13.94** | **16.19** | **8.59** | **13.63** | **12.58** | **10.43** | **6.84** | **9.26** |
| **Fisher FWE p** | **0.665** | **0.73** | **0.819** | **0.591** | **0.765** | **0.881** | **0.7** | **0.584** | **0.955** | **0.716** | **0.771** | **0.88** | **0.996** | **0.93** |
| MD | 0.7 | 0.45 | 0.49 | 0.11 | -0.06 | -0.27 | -0.15 | 0.73 | 0.45 | -0.16 | 0.58 | 0.42 | -0.02 | 0.1 |
| MD FWE p | 0.756 | 0.85 | 0.838 | 0.936 | 0.963 | 0.982 | 0.973 | 0.742 | 0.849 | 0.974 | 0.805 | 0.858 | 0.957 | 0.938 |
| MD mFWE p | 0.999 | 0.999 | 0.999 | 0.999 | 0.999 | 0.999 | 0.999 | 0.998 | 0.999 | 0.999 | 0.999 | 0.999 | 0.999 | 0.999 |
| RD | 0.56 | 0.41 | 0.32 | 0.29 | -0.22 | -0.67 | -0.49 | 0.57 | 0.36 | -0.18 | -0.11 | 0.06 | -0.09 | -0.08 |
| RD FWE p | 0.767 | 0.826 | 0.856 | 0.864 | 0.966 | 0.994 | 0.987 | 0.766 | 0.841 | 0.961 | 0.952 | 0.923 | 0.949 | 0.948 |
| RD mFWE p | 0.999 | 0.999 | 0.999 | 0.999 | 0.999 | 0.999 | 0.999 | 0.999 | 0.999 | 0.999 | 0.999 | 0.999 | 0.999 | 0.999 |
| AD | 0.87 | 0.5 | 0.75 | -0.18 | 0.21 | 0.37 | 0.38 | 0.97 | 0.58 | -0.12 | 1.44 | 0.97 | 0.1 | 0.43 |
| AD FWE p | 0.8 | 0.926 | 0.847 | 0.997 | 0.974 | 0.953 | 0.95 | 0.754 | 0.905 | 0.995 | 0.496 | 0.753 | 0.985 | 0.94 |
| AD mFWE p | 0.996 | 0.999 | 0.998 | 0.999 | 0.999 | 0.999 | 0.999 | 0.992 | 0.999 | 0.999 | 0.921 | 0.992 | 0.999 | 0.999 |
| Volume | 1.18 | 1.7 | 0.99 | 2.47 | 1.53 | 1.21 | 1.64 | 1.48 | 0.1 | 2.02 | 0.51 | 0.11 | -0.63 | 0.62 |
| Volume FWE p | 0.932 | 0.726 | 0.966 | 0.246 | 0.814 | 0.925 | 0.758 | 0.833 | 0.999 | 0.517 | 0.997 | 0.999 | 0.999 | 0.994 |
| Volume mFWE p | 0.974 | 0.821 | 0.991 | 0.338 | 0.893 | 0.97 | 0.849 | 0.907 | 0.999 | 0.627 | 0.999 | 0.999 | 0.999 | 0.999 |
| Thickness | 0.19 | -0.86 | -0.47 | 0.06 | 0.79 | 0.52 | 1.1 | 0.26 | -1.31 | 0.56 | -0.08 | 0.13 | 0.37 | 0.13 |
| Thickness FWE p | 0.99 | 0.999 | 0.999 | 0.995 | 0.889 | 0.954 | 0.766 | 0.985 | 0.999 | 0.948 | 0.998 | 0.993 | 0.975 | 0.992 |
| Thickness mFWE p | 0.999 | 0.999 | 0.999 | 0.999 | 0.997 | 0.999 | 0.983 | 0.999 | 0.999 | 0.999 | 0.999 | 0.999 | 0.999 | 0.999 |

Table B27 continued

| | Left anterior segment of the circular sulcus of the insula | Left inferior segment of the circular sulcus of the insula | Left superior segment of the circular sulcus of the insula | Left anterior transverse collateral sulcus | Left posterior transverse collateral sulcus | Left inferior frontal sulcus | Left middle frontal sulcus | Left superior frontal sulcus | Left sulcus intermedius primus | Left intraparietal sulcus and transverse parietal sulci | Left middle occipital sulcus and lunatus sulcus | Left superior occipital sulcus and transverse occipital sulcus | Left anterior occipital sulcus and preoccipital notch | Left lateral occipito temporal sulcus |
|---|---|---|---|---|---|---|---|---|---|---|---|---|---|---|
| **Fisher F** | **21.94** | **18.21** | **12.86** | **15.17** | **18.46** | **10.58** | **8.6** | **6.5** | **11.91** | **7.5** | **7.72** | **8.23** | **5.24** | **10.38** |
| **Fisher FWE p** | **0.341** | **0.488** | **0.757** | **0.635** | **0.477** | **0.873** | **0.955** | **0.999** | **0.806** | **0.985** | **0.98** | **0.967** | **0.999** | **0.882** |
| MD | -0.31 | 0.16 | 0.25 | 0.36 | 1.31 | 0.25 | 0.11 | -0.16 | 0 | -0.1 | -0.23 | -0.4 | -0.44 | 0.19 |
| MD FWE p | 0.985 | 0.926 | 0.907 | 0.876 | 0.457 | 0.908 | 0.936 | 0.973 | 0.955 | 0.968 | 0.979 | 0.99 | 0.991 | 0.92 |
| MD mFWE p | 0.999 | 0.999 | 0.999 | 0.999 | 0.954 | 0.999 | 0.999 | 0.999 | 0.999 | 0.999 | 0.999 | 0.999 | 0.999 | 0.999 |
| RD | -0.41 | -0.21 | 0.01 | -0.02 | 1.26 | -0.11 | -0.17 | -0.36 | -0.4 | -0.15 | -0.42 | -0.61 | -0.62 | 0.22 |
| RD FWE p | 0.982 | 0.965 | 0.933 | 0.938 | 0.435 | 0.951 | 0.96 | 0.979 | 0.981 | 0.958 | 0.983 | 0.992 | 0.992 | 0.884 |
| RD mFWE p | 0.999 | 0.999 | 0.999 | 0.999 | 0.963 | 0.999 | 0.999 | 0.999 | 0.999 | 0.999 | 0.999 | 0.999 | 0.999 | 0.999 |
| AD | -0.11 | 0.75 | 0.63 | 0.9 | 1.25 | 0.86 | 0.59 | 0.21 | 0.68 | -0.01 | 0.12 | -0.02 | -0.1 | 0.13 |
| AD FWE p | 0.995 | 0.849 | 0.889 | 0.783 | 0.603 | 0.804 | 0.9 | 0.975 | 0.873 | 0.991 | 0.983 | 0.991 | 0.995 | 0.982 |
| AD mFWE p | 0.999 | 0.998 | 0.999 | 0.995 | 0.964 | 0.996 | 0.999 | 0.999 | 0.999 | 0.999 | 0.999 | 0.999 | 0.999 | 0.999 |
| Volume | 3.49 | 2.42 | 1.3 | 1.5 | 0.42 | 0.45 | -0.07 | -0.17 | 1.31 | 0.68 | 0.74 | 0.7 | -0.41 | 0.89 |
| Volume FWE p | 0.01 | 0.268 | 0.901 | 0.824 | 0.998 | 0.998 | 0.999 | 0.999 | 0.898 | 0.992 | 0.989 | 0.991 | 0.999 | 0.978 |
| Volume mFWE p | 0.025 | 0.364 | 0.955 | 0.901 | 0.999 | 0.999 | 0.999 | 0.999 | 0.953 | 0.999 | 0.998 | 0.999 | 0.999 | 0.995 |
| Thickness | 0.49 | 0.68 | 0.48 | 0.74 | 0.59 | 0.36 | 0.36 | 0.11 | 0.43 | -0.3 | -0.05 | 0.59 | 0.21 | 0.3 |
| Thickness FWE p | 0.959 | 0.92 | 0.961 | 0.904 | 0.941 | 0.977 | 0.976 | 0.993 | 0.969 | 0.999 | 0.998 | 0.942 | 0.988 | 0.982 |
| Thickness mFWE p | 0.999 | 0.999 | 0.999 | 0.998 | 0.999 | 0.999 | 0.999 | 0.999 | 0.999 | 0.999 | 0.999 | 0.999 | 0.999 | 0.999 |

Table B27 continued

| | Left lateral orbital sulcus | Left medial orbital sulcus | Left orbital sulci | Left parieto occipital sulcus | Left pericallosal sulcus | Left postcentral sulcus | Left inferior part of the precentral sulcus | Left superior part of the precentral sulcus | Left suborbital sulcus | Left subparietal sulcus | Left inferior temporal sulcus | Left superior temporal sulcus | Left transverse temporal sulcus | Right fronto marginal gyrus and sulcus |
|---|---|---|---|---|---|---|---|---|---|---|---|---|---|---|
| **Fisher F** | **7.73** | **19.42** | **11.96** | **8.99** | **9.71** | **7.66** | **11.83** | **10.3** | **11.65** | **5.33** | **10.1** | **17.18** | **9.12** | **7.81** |
| **Fisher FWE p** | **0.98** | **0.436** | **0.804** | **0.941** | **0.912** | **0.982** | **0.811** | **0.886** | **0.82** | **0.999** | **0.895** | **0.536** | **0.936** | **0.978** |
| MD | -0.8 | 0.79 | 0.25 | -0.64 | 0.63 | -0.4 | 0.15 | -0.61 | 0.18 | -0.04 | -0.22 | 0.21 | -1.14 | -0.23 |
| MD FWE p | 0.999 | 0.716 | 0.907 | 0.997 | 0.784 | 0.989 | 0.928 | 0.996 | 0.923 | 0.959 | 0.978 | 0.916 | 0.999 | 0.979 |
| MD mFWE p | 0.999 | 0.998 | 0.999 | 0.999 | 0.999 | 0.999 | 0.999 | 0.999 | 0.999 | 0.999 | 0.999 | 0.999 | 0.999 | 0.999 |
| RD | -1.09 | 0.11 | 0.11 | -0.77 | 0.75 | -0.46 | -0.04 | -0.82 | 0.29 | -0.04 | -0.43 | 0.01 | -1.01 | -0.42 |
| RD FWE p | 0.999 | 0.911 | 0.912 | 0.996 | 0.684 | 0.985 | 0.941 | 0.997 | 0.866 | 0.941 | 0.984 | 0.932 | 0.999 | 0.983 |
| RD mFWE p | 0.999 | 0.999 | 0.999 | 0.999 | 0.998 | 0.999 | 0.999 | 0.999 | 0.999 | 0.999 | 0.999 | 0.999 | 0.999 | 0.999 |
| AD | -0.22 | 1.44 | 0.43 | -0.38 | 0.35 | -0.26 | 0.48 | -0.2 | 0.01 | -0.03 | 0.13 | 0.54 | -1.27 | 0.09 |
| AD FWE p | 0.997 | 0.499 | 0.94 | 0.999 | 0.956 | 0.998 | 0.93 | 0.997 | 0.99 | 0.992 | 0.982 | 0.916 | 0.999 | 0.985 |
| AD mFWE p | 0.999 | 0.922 | 0.999 | 0.999 | 0.999 | 0.999 | 0.999 | 0.999 | 0.999 | 0.999 | 0.999 | 0.999 | 0.999 | 0.999 |
| Volume | 0.46 | 1.51 | 1.29 | 0.54 | -0.48 | 0.52 | 1.41 | 1.77 | 1.24 | -0.78 | 1.08 | 2.15 | 2 | 0.68 |
| Volume FWE p | 0.997 | 0.819 | 0.904 | 0.996 | 0.999 | 0.996 | 0.863 | 0.684 | 0.917 | 0.999 | 0.952 | 0.435 | 0.534 | 0.992 |
| Volume mFWE p | 0.999 | 0.897 | 0.957 | 0.999 | 0.999 | 0.999 | 0.93 | 0.784 | 0.965 | 0.999 | 0.984 | 0.544 | 0.643 | 0.999 |
| Thickness | 0.98 | 1.15 | 0.21 | 1.27 | -0.06 | 0.62 | 0.06 | 0.13 | 0.44 | -0.4 | 0.64 | 0.88 | -0.5 | 0.13 |
| Thickness FWE p | 0.817 | 0.74 | 0.989 | 0.675 | 0.998 | 0.936 | 0.995 | 0.993 | 0.968 | 0.999 | 0.931 | 0.861 | 0.999 | 0.992 |
| Thickness mFWE p | 0.991 | 0.978 | 0.999 | 0.96 | 0.999 | 0.999 | 0.999 | 0.999 | 0.999 | 0.999 | 0.999 | 0.996 | 0.999 | 0.999 |

Table B27 continued

| | Right paracentral lobule and sulcus | Right subcentral gyrus and sulci | Right transverse frontopolar gyri and sulci | Right anterior part of the cingulate gyrus and sulcus | Right middle anterior part of the cingulate gyrus and sulcus | Right middle posterior part of the cingulate gyrus and sulcus | Right posterior dorsal part of the cingulate gyrus | Right posterior ventral part of the cingulate gyrus | Right cuneus | Right opercular part of the inferior frontal gyrus | Right orbital part of the inferior frontal gyrus | Right triangular part of the inferior frontal gyrus | Right middle frontal gyrus | Right superior frontal gyrus |
|---|---|---|---|---|---|---|---|---|---|---|---|---|---|---|
| **Fisher F** | **7.76** | **14.4** | **10.72** | **11.66** | **8.84** | **10.63** | **15.79** | **7.7** | **3.15** | **8.22** | **18.35** | **15.84** | **8.09** | **12.19** |
| **Fisher FWE p** | **0.979** | **0.675** | **0.866** | **0.819** | **0.946** | **0.87** | **0.604** | **0.981** | **0.999** | **0.967** | **0.482** | **0.601** | **0.971** | **0.792** |
| MD | -0.53 | 0.61 | 0.53 | 0.41 | -0.02 | 0.06 | -0.23 | -0.14 | -0.97 | 0.5 | 0.3 | 0.58 | 0.56 | 0.35 |
| MD FWE p | 0.994 | 0.791 | 0.823 | 0.863 | 0.957 | 0.945 | 0.979 | 0.971 | 0.999 | 0.831 | 0.894 | 0.803 | 0.813 | 0.88 |
| MD mFWE p | 0.999 | 0.999 | 0.999 | 0.999 | 0.999 | 0.999 | 0.999 | 0.999 | 0.999 | 0.999 | 0.999 | 0.999 | 0.999 | 0.999 |
| RD | -0.45 | 0.52 | 0.32 | 0.09 | -0.14 | -0.01 | -0.45 | -0.44 | -1.11 | 0.48 | 0.3 | 0.44 | 0.51 | 0.13 |
| RD FWE p | 0.985 | 0.785 | 0.856 | 0.916 | 0.956 | 0.936 | 0.985 | 0.984 | 0.999 | 0.798 | 0.86 | 0.815 | 0.788 | 0.908 |
| RD mFWE p | 0.999 | 0.999 | 0.999 | 0.999 | 0.999 | 0.999 | 0.999 | 0.999 | 0.999 | 0.999 | 0.999 | 0.999 | 0.999 | 0.999 |
| AD | -0.61 | 0.75 | 0.8 | 0.89 | 0.19 | 0.17 | 0.15 | 0.36 | -0.68 | 0.52 | 0.27 | 0.8 | 0.61 | 0.71 |
| AD FWE p | 0.999 | 0.849 | 0.828 | 0.788 | 0.977 | 0.979 | 0.981 | 0.955 | 0.999 | 0.92 | 0.968 | 0.829 | 0.896 | 0.862 |
| AD mFWE p | 0.999 | 0.998 | 0.997 | 0.995 | 0.999 | 0.999 | 0.999 | 0.999 | 0.999 | 0.999 | 0.999 | 0.997 | 0.999 | 0.999 |
| Volume | 0.78 | 1.37 | 0.54 | 0.28 | 0.15 | 0.59 | 1.93 | -0.32 | -0.85 | -1.38 | 2.52 | 1.77 | -1.35 | 0.91 |
| Volume FWE p | 0.986 | 0.876 | 0.996 | 0.999 | 0.999 | 0.995 | 0.582 | 0.999 | 0.999 | 0.999 | 0.219 | 0.679 | 0.999 | 0.975 |
| Volume mFWE p | 0.998 | 0.939 | 0.999 | 0.999 | 0.999 | 0.999 | 0.69 | 0.999 | 0.999 | 0.999 | 0.307 | 0.78 | 0.999 | 0.994 |
| Thickness | 0.59 | 0.07 | -0.44 | 0.66 | 0.75 | 0.96 | 1.42 | 0.66 | 0.06 | -0.29 | 0.52 | 0.04 | -0.84 | 0.46 |
| Thickness FWE p | 0.942 | 0.995 | 0.999 | 0.926 | 0.903 | 0.829 | 0.592 | 0.925 | 0.995 | 0.999 | 0.956 | 0.996 | 0.999 | 0.964 |
| Thickness mFWE p | 0.999 | 0.999 | 0.999 | 0.999 | 0.998 | 0.992 | 0.927 | 0.999 | 0.999 | 0.999 | 0.999 | 0.999 | 0.999 | 0.999 |

Table B27 continued

| | Right short insular gyri | Right middle occipital gyrus | Right superior occipital gyrus | Right lateral occipito temporal gyrus | Right lingual gyrus | Right parahippocampal gyrus | Right orbital gyri | Right angular gyrus | Right supramarginal gyrus | Right superior parietal lobule | Right postcentral gyrus | Right precentral gyrus | Right precuneus |
|---|---|---|---|---|---|---|---|---|---|---|---|---|---|
| **Fisher F** | **15.94** | **7.67** | **10.14** | **21.49** | **8.23** | **8.57** | **13.78** | **10.88** | **9.81** | **19.87** | **18.75** | **20.85** | **9.04** |
| **Fisher FWE p** | **0.596** | **0.982** | **0.893** | **0.356** | **0.967** | **0.956** | **0.708** | **0.858** | **0.908** | **0.418** | **0.464** | **0.38** | **0.939** |
| MD | 0.71 | -0.11 | -0.66 | 0.16 | 0.41 | 0.19 | -0.24 | -0.32 | -0.31 | 0.1 | 1.44 | -0.56 | -0.36 |
| MD FWE p | 0.75 | 0.968 | 0.997 | 0.926 | 0.863 | 0.92 | 0.98 | 0.985 | 0.985 | 0.938 | 0.393 | 0.995 | 0.987 |
| MD mFWE p | 0.999 | 0.999 | 0.999 | 0.999 | 0.999 | 0.999 | 0.999 | 0.999 | 0.999 | 0.999 | 0.922 | 0.999 | 0.999 |
| RD | 0.51 | -0.39 | -0.86 | -0.02 | 0.37 | -0.15 | -0.3 | -0.3 | -0.38 | 0.09 | 1.58 | -0.66 | -0.34 |
| RD FWE p | 0.789 | 0.981 | 0.998 | 0.938 | 0.84 | 0.958 | 0.974 | 0.974 | 0.981 | 0.917 | 0.288 | 0.994 | 0.977 |
| RD mFWE p | 0.999 | 0.999 | 0.999 | 0.999 | 0.999 | 0.999 | 0.999 | 0.999 | 0.999 | 0.999 | 0.873 | 0.999 | 0.999 |
| AD | 0.96 | 0.33 | -0.29 | 0.43 | 0.46 | 0.7 | -0.12 | -0.32 | -0.19 | 0.12 | 1.12 | -0.35 | -0.37 |
| AD FWE p | 0.759 | 0.959 | 0.998 | 0.94 | 0.935 | 0.865 | 0.995 | 0.999 | 0.997 | 0.983 | 0.674 | 0.999 | 0.999 |
| AD mFWE p | 0.992 | 0.999 | 0.999 | 0.999 | 0.999 | 0.999 | 0.999 | 0.999 | 0.999 | 0.999 | 0.981 | 0.999 | 0.999 |
| Volume | 1.9 | 0.09 | 1.23 | 2.69 | -1.16 | 0.05 | 2.33 | 1.88 | 1.4 | 3.09 | 0.98 | 2.71 | 1.2 |
| Volume FWE p | 0.602 | 0.999 | 0.921 | 0.147 | 0.999 | 0.999 | 0.323 | 0.612 | 0.866 | 0.044 | 0.967 | 0.139 | 0.929 |
| Volume mFWE p | 0.709 | 0.999 | 0.967 | 0.221 | 0.999 | 0.999 | 0.424 | 0.719 | 0.932 | 0.083 | 0.991 | 0.211 | 0.972 |
| Thickness | -1.76 | 0.38 | 1.01 | 1.4 | 0.07 | 0 | -0.01 | -0.24 | 0.27 | 0.01 | -1.37 | 1.95 | 0.35 |
| Thickness FWE p | 0.999 | 0.975 | 0.804 | 0.599 | 0.995 | 0.997 | 0.997 | 0.999 | 0.985 | 0.996 | 0.999 | 0.3 | 0.977 |
| Thickness mFWE p | 0.999 | 0.999 | 0.989 | 0.931 | 0.999 | 0.999 | 0.999 | 0.999 | 0.999 | 0.999 | 0.999 | 0.675 | 0.999 |

Table B27 continued

| | Right subcallosal gyrus | Right anterior transverse temporal gyrus | Right lateral aspect of the superior temporal gyrus | Right planum polare of the superior temporal gyrus | Right planum temporale | Right inferior temporal gyrus | Right middle temporal gyrus | Right horizontal ramus of the anterior segment of the lateral sulcus | Right vertical ramus of the anterior segment of the lateral sulcus | Right posterior ramus of the lateral sulcus | Right occipital pole | Right temporal pole | Right calcarine sulcus | Right central sulcus |
|---|---|---|---|---|---|---|---|---|---|---|---|---|---|---|
| **Fisher F** | **11.56** | **11.35** | **13.44** | **15.45** | **9.9** | **15.19** | **11.43** | **14.51** | **8.61** | **14.86** | **8.89** | **14.84** | **5.9** | **12.19** |
| **Fisher FWE p** | **0.824** | **0.835** | **0.726** | **0.621** | **0.904** | **0.635** | **0.831** | **0.67** | **0.954** | **0.651** | **0.945** | **0.652** | **0.999** | **0.792** |
| MD | 0.46 | 0.47 | 0.63 | 0.59 | 0.17 | -0.2 | 0.1 | 0.78 | -0.09 | -0.31 | 0.35 | 0.5 | -0.43 | 0.73 |
| MD FWE p | 0.848 | 0.844 | 0.783 | 0.799 | 0.925 | 0.977 | 0.937 | 0.717 | 0.966 | 0.985 | 0.879 | 0.833 | 0.991 | 0.742 |
| MD mFWE p | 0.999 | 0.999 | 0.999 | 0.999 | 0.999 | 0.999 | 0.999 | 0.998 | 0.999 | 0.999 | 0.999 | 0.999 | 0.999 | 0.998 |
| RD | 0.19 | 0.24 | 0.42 | 0.49 | 0.16 | -0.55 | -0.19 | 0.87 | -0.13 | -0.26 | 0.08 | 0 | -0.62 | 0.63 |
| RD FWE p | 0.894 | 0.879 | 0.822 | 0.796 | 0.9 | 0.99 | 0.962 | 0.627 | 0.955 | 0.971 | 0.919 | 0.935 | 0.992 | 0.738 |
| RD mFWE p | 0.999 | 0.999 | 0.999 | 0.999 | 0.999 | 0.999 | 0.999 | 0.996 | 0.999 | 0.999 | 0.999 | 0.999 | 0.999 | 0.999 |
| AD | 0.83 | 0.84 | 0.96 | 0.7 | 0.17 | 0.39 | 0.56 | 0.56 | -0.01 | -0.36 | 0.72 | 1.25 | -0.1 | 0.88 |
| AD FWE p | 0.814 | 0.812 | 0.756 | 0.868 | 0.978 | 0.948 | 0.91 | 0.911 | 0.991 | 0.999 | 0.858 | 0.603 | 0.995 | 0.795 |
| AD mFWE p | 0.997 | 0.997 | 0.992 | 0.999 | 0.999 | 0.999 | 0.999 | 0.999 | 0.999 | 0.999 | 0.999 | 0.963 | 0.999 | 0.995 |
| Volume | 1.18 | 0.63 | 0.95 | 1.45 | 1.02 | 2.23 | 1.33 | 1.18 | 1.22 | 1.93 | -0.07 | 1.4 | -0.39 | 0.79 |
| Volume FWE p | 0.933 | 0.993 | 0.971 | 0.849 | 0.963 | 0.383 | 0.892 | 0.932 | 0.924 | 0.582 | 0.999 | 0.868 | 0.999 | 0.986 |
| Volume mFWE p | 0.974 | 0.999 | 0.993 | 0.919 | 0.989 | 0.489 | 0.95 | 0.974 | 0.969 | 0.691 | 0.999 | 0.933 | 0.999 | 0.998 |
| Thickness | -1.44 | 0 | 0.07 | 0.57 | -0.16 | 0.61 | 0.08 | 0.01 | -0.89 | 1.34 | -0.15 | 0.13 | 0.51 | -1.26 |
| Thickness FWE p | 0.999 | 0.997 | 0.995 | 0.945 | 0.999 | 0.938 | 0.994 | 0.996 | 0.999 | 0.639 | 0.999 | 0.993 | 0.956 | 0.999 |
| Thickness mFWE p | 0.999 | 0.999 | 0.999 | 0.999 | 0.999 | 0.999 | 0.999 | 0.999 | 0.999 | 0.947 | 0.999 | 0.999 | 0.999 | 0.999 |

Table B27 continued

| | Right anterior segment of the circular sulcus of the insula | Right inferior segment of the circular sulcus of the insula | Right superior segment of the circular sulcus of the insula | Right anterior transverse collateral sulcus | Right posterior transverse collateral sulcus | Right inferior frontal sulcus | Right middle frontal sulcus | Right superior frontal sulcus | Right sulcus intermedius primus | Right intraparietal sulcus and transverse parietal sulci | Right middle occipital sulcus and lunatus sulcus | Right superior occipital sulcus and transverse occipital sulcus | Right anterior occipital sulcus and preoccipital notch | Right lateral occipito temporal sulcus |
|---|---|---|---|---|---|---|---|---|---|---|---|---|---|---|
| **Fisher F** | **26.35** | **18.53** | **11.29** | **18.37** | **11.77** | **6.18** | **6.96** | **7.07** | **7.85** | **24.25** | **11.39** | **9.06** | **7.59** | **14.1** |
| **Fisher FWE p** | **0.214** | **0.474** | **0.838** | **0.481** | **0.814** | **0.999** | **0.995** | **0.993** | **0.977** | **0.268** | **0.833** | **0.938** | **0.983** | **0.691** |
| MD | -0.08 | 0.39 | -0.1 | 0.32 | 0.71 | -0.16 | -0.26 | 0.07 | 0.16 | -0.14 | -0.29 | -0.6 | -0.52 | -0.4 |
| MD FWE p | 0.965 | 0.868 | 0.968 | 0.889 | 0.752 | 0.974 | 0.982 | 0.944 | 0.927 | 0.971 | 0.984 | 0.996 | 0.994 | 0.989 |
| MD mFWE p | 0.999 | 0.999 | 0.999 | 0.999 | 0.999 | 0.999 | 0.999 | 0.999 | 0.999 | 0.999 | 0.999 | 0.999 | 0.999 | 0.999 |
| RD | 0.27 | 0.18 | -0.15 | 0.03 | 0.93 | -0.13 | -0.45 | 0.03 | 0.07 | -0.25 | -0.48 | -0.88 | -0.52 | -0.7 |
| RD FWE p | 0.871 | 0.895 | 0.958 | 0.928 | 0.599 | 0.956 | 0.985 | 0.928 | 0.92 | 0.969 | 0.986 | 0.998 | 0.988 | 0.995 |
| RD mFWE p | 0.999 | 0.999 | 0.999 | 0.999 | 0.994 | 0.999 | 0.999 | 0.999 | 0.999 | 0.999 | 0.999 | 0.999 | 0.999 | 0.999 |
| AD | -0.64 | 0.72 | -0.01 | 0.68 | 0.25 | -0.2 | 0.09 | 0.13 | 0.3 | 0.06 | 0.06 | -0.06 | -0.5 | 0.19 |
| AD FWE p | 0.999 | 0.859 | 0.991 | 0.873 | 0.97 | 0.997 | 0.985 | 0.983 | 0.963 | 0.987 | 0.987 | 0.993 | 0.999 | 0.977 |
| AD mFWE p | 0.999 | 0.999 | 0.999 | 0.999 | 0.999 | 0.999 | 0.999 | 0.999 | 0.999 | 0.999 | 0.999 | 0.999 | 0.999 | 0.999 |
| Volume | 4.16 | 2.46 | 1.14 | 2.28 | 0.49 | -0.16 | 0.09 | -0.6 | 0.48 | 3.71 | 1.27 | 0.69 | 1.29 | 2.24 |
| Volume FWE p | < 0.001 | 0.246 | 0.942 | 0.351 | 0.997 | 0.999 | 0.999 | 0.999 | 0.997 | 0.004 | 0.909 | 0.991 | 0.902 | 0.374 |
| Volume mFWE p | 0.002 | 0.338 | 0.979 | 0.455 | 0.999 | 0.999 | 0.999 | 0.999 | 0.999 | 0.012 | 0.96 | 0.999 | 0.956 | 0.48 |
| Thickness | -0.62 | 0.29 | 0.91 | 0.85 | -0.05 | 0.14 | 0.38 | 0.28 | -0.82 | 0.47 | 0.97 | 1.07 | -0.47 | 0.45 |
| Thickness FWE p | 0.999 | 0.983 | 0.846 | 0.87 | 0.998 | 0.992 | 0.975 | 0.984 | 0.999 | 0.962 | 0.821 | 0.779 | 0.999 | 0.966 |
| Thickness mFWE p | 0.999 | 0.999 | 0.994 | 0.996 | 0.999 | 0.999 | 0.999 | 0.999 | 0.999 | 0.999 | 0.992 | 0.985 | 0.999 | 0.999 |

Table B27 continued

| | Right lateral orbital sulcus | Right medial orbital sulcus | Right orbital sulci | Right parieto occipital sulcus | Right pericallosal sulcus | Right postcentral sulcus | Right inferior part of the precentral sulcus | Right superior part of the precentral sulcus | Right suborbital sulcus | Right subparietal sulcus | Right inferior temporal sulcus | Right superior temporal sulcus | Right transverse temporal sulcus |
|---|---|---|---|---|---|---|---|---|---|---|---|---|---|
| **Fisher F** | **21.88** | **12.61** | **12.55** | **5.79** | **16.8** | **14.53** | **6.32** | **18.04** | **17.5** | **7.49** | **12.48** | **7.72** | **8.43** |
| **Fisher FWE p** | **0.343** | **0.77** | **0.773** | **0.999** | **0.554** | **0.669** | **0.999** | **0.496** | **0.521** | **0.985** | **0.777** | **0.98** | **0.96** |
| MD | 0.06 | 0.74 | -0.67 | -0.99 | 1.15 | -0.24 | -0.51 | -1.14 | 0.93 | -0.45 | -0.09 | -0.22 | 0.02 |
| MD FWE p | 0.945 | 0.736 | 0.997 | 0.999 | 0.534 | 0.98 | 0.994 | 0.999 | 0.647 | 0.991 | 0.966 | 0.979 | 0.951 |
| MD mFWE p | 0.999 | 0.998 | 0.999 | 0.999 | 0.977 | 0.999 | 0.999 | 0.999 | 0.994 | 0.999 | 0.999 | 0.999 | 0.999 |
| RD | 0.08 | 0.81 | -0.6 | -1.24 | 1.1 | -0.18 | -0.51 | -1.33 | 0.49 | -0.53 | -0.22 | -0.31 | -0.43 |
| RD FWE p | 0.917 | 0.659 | 0.992 | 0.999 | 0.51 | 0.961 | 0.988 | 0.999 | 0.797 | 0.989 | 0.966 | 0.975 | 0.983 |
| RD mFWE p | 0.999 | 0.997 | 0.999 | 0.999 | 0.982 | 0.999 | 0.999 | 0.999 | 0.999 | 0.999 | 0.999 | 0.999 | 0.999 |
| AD | 0.02 | 0.55 | -0.66 | -0.51 | 1.06 | -0.34 | -0.48 | -0.74 | 1.29 | -0.28 | 0.13 | -0.06 | 0.8 |
| AD FWE p | 0.99 | 0.913 | 0.999 | 0.999 | 0.706 | 0.999 | 0.999 | 0.999 | 0.584 | 0.998 | 0.982 | 0.993 | 0.828 |
| AD mFWE p | 0.999 | 0.999 | 0.999 | 0.999 | 0.986 | 0.999 | 0.999 | 0.999 | 0.958 | 0.999 | 0.999 | 0.999 | 0.997 |
| Volume | 3 | 0.999 | 2.01 | 0.45 | -0.1 | 2.12 | -0.03 | 1.25 | 1.04 | 0.91 | 1.66 | 0.43 | 0.13 |
| Volume FWE p | 0.06 | 0.965 | 0.53 | 0.998 | 0.999 | 0.456 | 0.999 | 0.915 | 0.96 | 0.976 | 0.748 | 0.998 | 0.999 |
| Volume mFWE p | 0.105 | 0.99 | 0.64 | 0.999 | 0.999 | 0.565 | 0.999 | 0.964 | 0.988 | 0.995 | 0.84 | 0.999 | 0.999 |
| Thickness | 1.18 | -0.91 | 0.82 | 0.45 | 0.95 | 0.88 | 0.67 | 2.9 | 0.87 | 0.13 | 0.57 | 0.44 | 0.06 |
| Thickness FWE p | 0.723 | 0.999 | 0.88 | 0.966 | 0.833 | 0.86 | 0.923 | 0.042 | 0.863 | 0.993 | 0.945 | 0.967 | 0.995 |
| Thickness mFWE p | 0.974 | 0.999 | 0.997 | 0.999 | 0.993 | 0.995 | 0.999 | 0.134 | 0.996 | 0.999 | 0.999 | 0.999 | 0.999 |

# APPENDIX C: Controlling for Group Demographic Differences

As noted in the main text, compared to youth without an asthma history, youth with asthma in the ABCD sample were more likely to be from a family with a lower total income, less likely to have a parent with a college education or advanced degree, and more likely to be Black/African American. Primary analyses were repeated controlling for these demographic variables as well as birthweight (Xu et al., 2014).

## Differences in Cognitive Function

When controlling for family income, parental education, birthweight, Black/African American race, age, and sex, the pattern of relationships between asthma history and cognitive function largely mirrored those reported in the main text. Youth with asthma had more total problems ($b$ = 0.13, SE = 0.03, Z = 3.73, $p$ = 0.0002), higher rates of internalizing symptoms ($b$ = 0.13, $Z$ = 3.38, $p$ = 0.000720)--although this was not reflected in more anxiety-depressive symptoms ($b$ = 0.065, $Z$ = 1.38, $p$ = 0.169)--and trended towards having higher levels of inattentive symptoms ($b$ = 0.072, $Z$ = 1.73, $p$ = 0.083).

### *Lifetime Asthma Attacks*

Within youth with asthma, when controlling for additional covariates, there were no longer significant relationships between number of lifetime asthma attacks and parent-reported problems (total problems: $b$ = 0.009, $SE$ = 0.01, $Z$ = 0.86, $p$ = 0.388; internalizing problems: $b$ = 0.003, $SE$ = 0.01, $Z$ =0.25, $p$ = 0.806; anxiety and depressive problems: $b$ = 0.009, $SE$ = 0.01, $Z$ = 0.66, $p$ = 0.508; attention problems: $b$ = 0.003, $SE$ = 0.01, $Z$ = 0.31, $p$ = 0.753).

### *Asthma Severity*

Within youth with asthma, when controlling for additional covariates, higher cumulative asthma severity scores were associated with lower $g$ scores ($b$ = -0.20, F(1, 95.501) = 6.26, $p$ =

0.014), marginally lower executive functioning scores ($b$ = -0.18, $F$(1, 95.75) = 4.54, $p$ = 0.036), lower memory scores ($b$ = -0.22, $F$(1, 138.59) = 4.52, $p$ = 0.035), and marginally lower language scores ($b$ = -0.15, $F$(1, 95.23) = 3.60, $p$ = 0.061).

*Eosinophils*

Across all individuals, when controlling for asthma status, family income, parental education, birthweight, Black/African American race and when outliers were removed, higher eosinophils counts were consistently trending towards a relationship with lower cognitive scores (g: $N$ = 375, $b$ = -0.44, $F$(1, 275.93) = 2.93, $p$ = 0.09; memory: $N$ = 374, $b$ = -0.43, $F$(1, 305.17) = 2.39, $p$ = 0.12; language: $N$ = 380, $b$ = -0.43, $F$(1, 324.54) = 2.74, $p$ = 0.10).

Differences in Emotional Function

When controlling for additional covariates, the pattern of relationships between asthma history and emotional function were largely unchanged from the main text. Youth with asthma had higher numbers of parent reported total problems ($N$ = 5037, $b$ = 0.13, SE = 0.03, $Z$ = 3.73, $p$ = 0.0002) and internalizing problems ($N$= 5435, $b$ = 0.13, SE = 0.04, $Z$ = 3.38, $p$ = 0.0007), but had no difference in number of anxiety problems ($N$ = 5435, $b$ = 0.07, SE = 0.05, $Z$ = 1.38, $p$ = 0.169). With additional covariates in the model, the relationship between asthma history and attention problems was only marginally significant ($N$ = 5435, $b$ = 0.07, SE = 0.04, $Z$ = 1.73, $p$ = 0.083).

*Lifetime Asthma Attacks*

When controlling for additional covariates, there were no longer significant relationships between number of lifetime asthma attacks and CBCL parent-reported problems (total problems: $b$ = 0.009, $SE$ = 0.01, $Z$ = 0.86, $p$ = 0.388; internalizing problems: $b$ = 0.003, $SE$ = 0.01, $Z$ =0.25,

$p = 0.806$; anxiety and depressive problems: $b = 0.009$, $SE = 0.01$, $Z = 0.66$, $p = 0.508$; attention problems: $b = 0.003$, $SE = 0.01$, $Z = 0.31$, $p = 0.753$).

*Asthma Severity*

As in the main text, when controlling for additional covariates, higher levels of cumulative asthma severity were associated with *lower* levels of internalizing problems ($b = -0.21$, $SE = 0.10$, $Z = -2.13$, $p = 0.033$) and anxiety/depressive problems ($b = -0.29$, $SE = 0.12$, $Z = -2.43$, $p = 0.015$), but there was no relationship between severity and number off total problems ($b = -0.05$, $SE = 0.08$, $Z = -0.67$, $p = 0.506$) or number of attention problems ($b = 0.05$, $SE = 0.10$, $Z = 0.57$, $p = 0.568$).

*Eosinophils*

When additional covariates were included in the model, *lower* numbers of eosinophils were associated with higher numbers of internalizing problems ($b = -0.91$, SE = 0.397, $Z = -2.29$, $p = 0.022$) and higher numbers of anxiety-depressive problems ($b = -1.15$, SE = 0.52, $Z = -2.21$, $p = 0.027$). Again, there was no relationship between eosinophil count and number of total problem ($b = -0.37$, SE = 0.34, $Z = -1.09$, $p = 0.278$) or attention problems ($b = -0.21$, SE = 0.44, $Z = -0.48$, $p = 0.629$).

Differences in Brain Structure Between Youth With and Without An Asthma History

*White Matter*

When controlling for additional covariates, the WM in the right striatal inferior frontal cortex had lower integrity in youth with an asthma history compared to youth without an asthma history (Fisher $F = 4.29$, $p = 0.042$), specifically higher MD (FWE $p = 0.041$) and higher RD (FWE $p = 0.039$). No other regional differences survived correction for multiple comparisons. However, due to my hypotheses about frontoparietal tracts, it is worth noting that at the less

stringent correction threshold, youth with an asthma history had lower volumes of the right parietal superior longitudinal fasciculus (FWE $p = 0.030$) and were trending towards having lower volumes in the right inferior longitudinal fasciculus (FWE $p = 0.095$) and higher AD in left superior longitudinal fasciculus (FWE $p = 0.074$).

*Subcortical Grey Matter*

When controlling for additional covariates, there were no subcortical grey matter regions that showed group differences in microstructure.

*Cortical Grey Matter*

When controlling for additional covariates, youth with asthma had more organized microstructure in left superior parietal lobule (Fisher $F = 57.43$, $p = 0.033$) with marginally lower MD (FWE $p = 0.059$), AD (FWE $p = 0.066$) and RD (FWE $p = 0.069$). This was trending in the same direction for the left intraparietal sulcus and transverse parietal sulci ($F = 54.64$, $p = 0.051$), driven by increased MD (FWE $p = 0.062$), AD (FWE $p = 0.073$), and RD (FWE $p = 0.074$).